Comportement macroscopique et statistiques des champs dans les composites viscoplastiques.

Martin Idiart

THÈSE présentée pour l'obtention du grade
de Docteur de l'École Polytechnique
Discipline : Mécanique et Matériaux

Sujet de thèse

COMPORTEMENT MACROSCOPIQUE ET STATISTIQUES DES CHAMPS DANS LES COMPOSITES VISCOPLASTIQUES

MACROSCOPIC BEHAVIOR AND FIELD STATISTICS IN VISCOPLASTIC COMPOSITES

par

Martín Ignacio IDIART

Soutenue le 23 Octobre 2006, devant le jury composé de :

Président:	M. Jean-Baptiste LEBLOND
Rapporteurs:	M. Olivier CASTELNAU
	M. Pierre GILORMINI
Examinateurs:	M. Michel BORNERT
	M. Pierre SUQUET
Directeur de thèse:	M. Pedro PONTE CASTAÑEDA

À ma famille

RÉSUMÉ

COMPORTEMENT MACROSCOPIQUE ET STATISTIQUES DES CHAMPS DANS LES COMPOSITES VISCOPLASTIQUES

Martín Ignacio Idiart

Pedro Ponte Castañeda

La plus part des matériaux présentant un intérêt en ingénierie et sciences physiques sont intrinsèquement hétérogènes, comme par example les composites renforcés, les matériaux poreux, et les solides polycristallins (e.g., métaux, glace, plusieurs roches). Un problème fondamental en mécanique des matériaux réside dans l'estimation de la réponse macroscopique de tels matériaux hétérogènes à partir des propriétés et de l'arrangement géométrique (microstructure) de leurs constituants. En plus, l'incorporation de l'effet des processus locaux (*e.g.*, évolution de la microstructure, endommagement, ecruisage, recristallisation) sur la réponse macroscopique exige des connaissances statistiques sur la distribution spatiale des champs locaux dans le matériau.

À cet effet, nous avons développé des méthodes non-linéaires d'homogénéisation capables de fournir des estimations non seulement du comportement macroscopique mais également des statistiques des champs dans les composites viscoplastiques. Ces méthodes sont basées sur des principes variationnels convenablement conçus, qui se servent d'un 'composite linéaire de comparaison' choisi de façon optimale, permettant une conversion directe des estimations linéaires aux estimations correspondantes pour les potentiels effectifs des composites non-linéaires. Afin d'extraire des estimations des statistiques des champs à partir de ces méthodes, nous proposons une nouvelle procédure basée sur l'utilisation de potentiels effectifs convenablement perturbés. Au moyen de cette procédure sont obtenues des estimations pour les premiers moments des champs locaux dans chaque phase, qui sont conformes aux estimations correspondantes pour le comportement effectif. De plus, contrairement aux approches précédantes, cette procédure n'est pas limité aux premiers et seconds moments, et peut être employée pour estimer les moments d'ordre supérieur, aussi bien que la moyenne par phase des fonctions (convexes) plus générales des champs.

Des résultats sont donnés pour des composites biphasés à microstructures particulaires et aléatoires, isotropes transverse ou isotropes. La pertinence de ces résultats est évaluée en les comparant aux résultats exacts correspondant à des matériaux stratifiés séquentiels non-linéaires. Les estimations obtenues s'avèrent en bon accord avec les résultats exacts, même pour des non-linéarités élevées pour lesquelles les champs de déformation sont fortement hétérogènes.

ABSTRACT

MACROSCOPIC BEHAVIOR AND FIELD STATISTICS IN VISCOPLASTIC COMPOSITES

Martín Ignacio Idiart

Pedro Ponte Castañeda

Most man-made as well as natural materials of interest in engineering and physical sciences are intrinsically heterogeneous. Common examples are particle-reinforced composites, porous materials, and polycrystalline solids such as metals, ice, and many rocks. A fundamental problem in mechanics of materials is the estimation of the macroscopic response of such heterogeneous materials from the properties and geometrical arrangement (microstructure) of their constituents. In addition, incorporating the effect of local processes (*e.g.*, microstructure evolution, damage, work hardening, recrystallization) on the macroscopic response requires statistical information about spatial distribution of the local fields within the material.

To this end, we have developed nonlinear homogenization methods capable of delivering estimates not only for the macroscopic behavior but also for the field statistics in viscoplastic composites. These methods are based on suitably designed variational principles, which make use of an optimally chosen 'linear comparison composite', allowing direct conversion of linear estimates into corresponding estimates for the effective potentials of nonlinear composites. In order to extract estimates for the field statistics from these methods, a novel procedure is proposed, making use of suitably perturbed effective potentials. By means of this procedure, we obtain estimates for the first moments of the local fields in each phase that are entirely consistent with the corresponding estimates for the effective behavior. In addition, unlike earlier approaches, this procedure is not limited to first and second moments, and can be used to estimate higher-order moments as well as the phase average of more general convex functions of the fields.

Sample results are given for two-phase composites with random 'particulate' microstructures exhibiting overall transversely isotropic and isotropic symmetry. Their accuracy is assessed by confronting them with corresponding exact results for nonlinear sequential laminates. Homogenization estimates are found to be in good agreement with the exact results, even for high nonlinearities, when the strain-rate fields are found to become strongly heterogeneous.

Acknowledgments

Many people have contributed in different ways to the completion of this work, and I would like to take this opportunity to express my sincere gratitude to them.

First and foremost, I would like to express my profound gratitude and appreciation to my thesis adviser, Prof. P. Ponte Castañeda, for the countless hours he has dedicated to me, even in the midst of his busy schedule, which have been an invaluable source of knowledge and inspiration that will perdure throughout my career.

I am also grateful to my collegue and friend, Oscar Lopez Pamies, for his constant support and companionship, and the many insightful and enriching –though sometimes endless– discussions which have strongly influenced this work.

Many thanks also go to Kostas Danas, for many valuable discussions and comments. I would also like to acknowledge fruitful interactions with P. Suquet, H. Moulinec, F. Willot, and Y. P. Pellegrini.

Because learning is a gradual process, it would be unfair not to acknowledge here the many teachers that were in charge of my earlier instruction, in particular, Profs. A. E. Scarabino, M. D. Actis and M. D'Amato. I also wish to thank Prof. H. Sosa, for encouraging me to pursue my doctoral studies with Prof. P. Ponte Castañeda.

I would like to thank Profs. P. Gilormini and O. Castelnau for having accepted the tedious task of reading this dissertation in detail and reporting on it, and Profs. M. Bornert, J. B. Leblond, P. Ponte Castañeda, and P. Suquet for serving on my Dissertation Committee as 'examinateurs'.

I would also like to extend my gratitude to all members of the Laboratoire de Mécanique des Solides, for providing me with a very friendly and interactive environment.

Financial support of the National Science Foundation (U.S.A.), through Grants CMS-02-01454 and OISE-02-31867, is also gratefully acknowledged.

But above all, I am greatly indebted to my family, for their unconditional support, encouragement and guidance over all these years, and for inculcating in me the value of Education. This work is dedicated to them. Finally, I would be remiss if I did not express my deepest gratitude to my girlfriend, Diana Gasparini. This work would not have been possible without her extraordinary patience, understanding, strength, and optimism.

Contents

Chapter 1

Introduction

Most engineering and natural materials are intrinsically heterogeneous. Metals, like iron, aluminum or titanium, are aggregates of randomly oriented single-crystal grains, whose sizes are typically of the order of a few micrometers. Many geological materials, such as olivine, granite or ice[1], also exhibit polycrystalline structures, with grain sizes ranging from the millimeter to even larger length scales. A random distribution of pores can be found in a wide variety of materials, like sintered, metallic powders and human bone, in sizes as small as a few micrometers. In the last forty years, man-made composite materials, sometimes called 'advanced composites', have been increasingly used in many industrial applications, and a trend towards even more prevalent use of composite materials is expected, their main advantage being the possibility to tailor their properties (mechanical, electrical, etc.), which could not be achieved by either of the constituent materials acting alone. Examples of such applications include polymer matrix composites reinforced with ceramic, glass or Kevlar fibers, used in cars and boat hulls, and metal matrix composites with ceramic particles or short fibers, mainly used by the aerospace industry for high-temperature applications. Because of their universality, understanding the behavior of heterogeneous materials is of paramount importance in engineering as well as in scientific research.

In most structural problems of interest, the length scales involved are of the order of milimeters or larger, so that the size of the heterogeneities (*e.g.*, particles, pores, grains, etc.) in the materials is very small compared to the size of the structural components. This 'separation' of length scales is even more marked in geology, where the 'structure' (*e.g.*, glaciers, tectonic plates, etc.) can span several kilometers. Thus, the ratio of the size of the typical heterogeneity to the size of the structure is often small. In this case, it is common practice when carrying out analysis at the structural level, to replace the highly heterogeneous material by an 'equivalent' homogeneous one, characterized by certain 'homogenized' macroscopic behavior, which should accurately represent the behavior of the composite. The macroscopic response of a composite depends on the properties of its constituents as well as on their spatial distribution, *i.e.*, the microstructure. In most composite materials, the microstructure is extremely complicated and only a partial statistical description of it is possible in practice. Consequently, the macroscopic response cannot be determined exactly in general, but it can

[1] In fact, the Greek root 'krustallos' for the word 'crystal' means 'clear ice'.

be estimated. A means of estimating the macroscopic response of composite materials making use of the available statistical information about their microstructures is provided by the so-called 'homogenization' methods, which serve to establish a link between microscopic and macroscopic scales. The main goal of this work is to develop *reliable* and *efficient* homogenization estimates for composite materials, whose constituent phases exhibit a *nonlinear* mechanical behavior, with emphasis in those exhibiting *viscoplastic* behavior. The efficient character of these estimates should make them extremely valuable in the context of structural design and analysis, allowing their straightforward implementation in standard finite-element packages. In engineering, this is particularly useful to carry out numerical simulations of metal forming processes (*e.g.*, forging, extrusion), in order to analyse the effect of the various operating parameters on the properties of the final piece without the need for extensive (and expensive) experimentation. Applications in this context can be found, for instance, in Dawson & Marin (1998) and Aravas & Ponte Castañeda (2004). In geology, homogenization estimates are being used to model a variety of phenomena, like the movement of the Earth's mantle (*e.g.*, Dawson & Wenk 2000) and inner core (*e.g.*, Wenk *et al.* 2000), or the dynamics of glaciers due to the viscoplastic flow of ice (*e.g.*, Castelnau *et al.* 1996, 1997).

For *linear* constitutive response, there are well-established methods to estimate the effective or overall behavior of composite materials, which improve on the classical estimates of Voigt (1889) and Reuss (1929) by incorporating higher-order statistical information on the microstructure. These homogenization methods include the variational estimates proposed by Hashin & Shtrikman (1962, 1963), which can be used to bound the effective modulus tensor of linear composites with random microstructures. There is also the so-called self-consistent (SC) approximation, introduced by Hershey (1954) and Kröner (1958) in the context of elastic polycrystals, and by Budiansky (1965) and Hill (1965b) for other types of elastic composites. A generalization and rigorous derivation of these two types of estimates in terms of two-point statistics were later provided by Willis (1977, 1978, 1981, 1983). For linear composites with periodic microstructures, estimates of the Hashin-Shtrikman type have been derived by Nemat-Nasser *et al.* (1982) and Suquet (1990). A comprehensive review of this and other works on linear composites can be found, for example, in the monographs by Milton (2002), Torquato (2001), and Nemat-Nasser & Hori (1993).

On the other hand, for *nonlinear* (*e.g.*, plastic, viscoplastic, etc.) composites, rigorous methods have not been available until more recently, even though efforts along these lines have been going on for some time, particularly in the context of ductile polycrystals. In an attempt to improve on the classical models of Taylor (1938) and Sachs (1928), Hill (1965a) proposed an 'incremental' version of the linear self-consistent approximation, which has been extensively applied in the context of elastoplastic polycrystals (*e.g.*, Hill 1965b; Hutchinson 1970), as well as fiber-reinforced composites (*e.g.*, Dvorak & Bahei-En-Din 1979; Lagoudas *et al.* 1991). Hutchinson (1976, 1977) made use of this 'incremental' method in the context of viscoplastic polycrystals, and obtained a simplification of the procedure for power-law viscous materials, which was later proposed by Berveiller & Zaoui (1979)

for more general types of composites, and has come to be known as the (classical) 'secant' method. More recently, Molinari *et al.* (1987) proposed another modification of the 'incremental' method, also for power-law composites, which corresponds to a 'tangent' rather than a 'secant' procedure. A further modification of Hill's 'incremental' method was provided by Nemat Nasser & Obata (1986) for elasto-viscoplastic polycrystals undergoing finite deformations. However, from these and other related works, it has been recognized that the 'incremental' method and its 'secant' version lead to estimates for the effective behavior that are usually too stiff, and even violate rigorous upper bounds (see, for example, Gilormini 1995, 1996; Suquet 1996), while its 'tangent' version is generally too soft (see, for example, Lebensohn & Tomé 1993). In spite of this, the 'incremental' method is still being extensively used in the literature, as can be seen in several recent works (see, for example, Pettermann *et al.* 1999; González & LLorca 2000; Doghri & Ouaar 2003; Chaboche *et al.* 2005). There is also the so-called 'transformation field analysis' (TFA) scheme originally proposed by Dvorak & Rao (1976), and later formalized by Dvorak and co-workers (1992, 1994). As the 'incremental' procedure, this method allows the extension of linear homogenization estimates to nonlinear composites, and has been extensively used in conjuction with the self-consistent and Mori-Tanaka estimates (see, for example, Dvorak *et al.* 1994; Fish *et al.* 1997; Kamiński & Figel 2001; Chaboche *et al.* 2005). However, it has been recognized by Dvorak himself, and confirmed by others (Suquet 1997; Michel *et al.* 2000; Chaboche *et al.* 2005), that the TFA method gives extremely stiff predictions for the macroscopic behavior. A refinement of this method has been proposed by Michel & Suquet (2003), but this approach requires identifying and pre-computing certain eigenstrain modes, which depend on the particular microstructure and loading conditions considered. Even though the interest in this work is on homogenization methods that can be applied to a fairly general class of materials, it should also be mentioned that there is a wide range of micromechanics-based models for nonlinear composites with specific microstructures, notably porous and particle-reinforced materials. The pioneering work of McClintock (1968), Tracey & Rice (1969), and Budiansky *et al.* (1982) in plastic and viscoplastic porous materials spawned a large body of work based on *dilute* approximations in porous (*e.g.*, Duva & Hutchinson 1984; Fleck & Hutchinson 1986; Lee & Mear 1992; Gilormini & Michel 1998; Briottet *et al.* 1999) as well as rigidly-reinforced (*e.g.*, He 1990; Lee & Mear 1992) materials. For *non-dilute* porous materials, there is the popular Gurson (1977) model and its generalization proposed by Leblond *et al.* (1994), which are based on approximate solutions of the hollow sphere problem.

The homogenization methods mentioned above are based mainly on intuitive, *ad hoc* formulations. However, there is a second class of nonlinear homogenization methods, which are based on exact variational principles, and have therefore the virtue of mathematical rigor. These methods originated from the seminal work of Willis (1983), which lead to the first generalization by Talbot & Willis (1985) of the celebrated linear variational HS principles/estimates to the nonlinear realm. These estimates, which make use of a 'homogeneous comparison medium', were applied to composites with isotropic as well as anisotropic (*e.g.*, polycrystals) nonlinear phases by Ponte Castañeda & Willis (1988), Dendievel *et al.* (1991), and Willis (1994).

A more general class of nonlinear homogenization methods has been introduced by Ponte Castañeda (1991, 1996, 2002a), making use of '*linear comparison composites*' (LCCs) with the same microstructure as the nonlinear composite, whose phase potentials are identified with appropriate linearizations of the nonlinear ones. Use can then be made of the various estimates available for linear composites, such as the HS and SC estimates, to generate corresponding estimates for the effective potentials of the nonlinear composites. While the idea of using linear composites to estimate the effective behavior of nonlinear ones had already been introduced in Hill's (1965a) 'incremental' method, the key feature in these novel LCC-based methods is the use of suitably designed variational principles to determine the best possible choice of the LCC of a given type. Thus, within the context of the 'variational' method of Ponte Castañeda (1991), where the LCC is taken to be purely elastic (viscous), the optimal linearization is given by the 'secant' moduli (or viscosities) evaluated at the second moments of the local fields in each phase of the LCC (Suquet 1995). The connections between this method and the Talbot-Willis procedure were explored by Willis (1991, 1992) and Talbot & Willis (1992).

Alternatively, within the context of the 'tangent second-order' method of Ponte Castañeda (1996), where the LCC is a more general 'thermoelastic' comparison composite, the work of Ponte Castañeda & Willis (1999) shows that the optimal choice of certain 'reference' tensors defining the polarizations is given by the phase averages (or first moments) of the local fields in the LCC, while an 'inflection-point' condition requires identifying the tensor of moduli with the tangent moduli of the phases evaluated at these 'reference' tensors. Finally, the optimal linearization in the more recent 'second-order' method of Ponte Castañeda (2002a), which improves on the previous methods, corresponds to certain 'generalized-secant' moduli of the phases, that depend on both, the first and second moments of the local fields, also in a 'thermoelastic' comparison composite. The 'tangent second-order' and 'second-order' methods have the distinguishing capability of reproducing exactly the small-contrast expansion of Suquet & Ponte Castañeda (1993) (see also Ponte Castañeda & Suquet 1995) to second order. These and other works (see, for example, Ponte Castañeda & Suquet 1998, 2001; Bornert *et al.* 2001; Ponte Castañeda 2002b) have shown that the LCC-based methods lead to estimates that are, in general, much more accurate than those resulting from the earlier methodologies mentioned above. Part of this work is concerned with improving and generalizing these LCC-based methods in the context of viscoplastic composites with isotropic and anisotropic constituents.

Because viscoplastic composites may undergo finite deformations of unrestricted extent, their microstructure generally evolves in time during a deformation process. Therefore, since the characterization of the (instantaneous) effective behavior in the above-mentioned methodologies makes use of an *Eulerian* description of the kinematics, it is necessary to complement it with a characterization of the evolution of the microstructure in time. In principle, the solution of the boundary value problem for the (instantaneous) velocity field in the viscoplastic composite contains all the information that is required to determine this microstructure evolution. In practice, however, full-field

solutions are generally not available, and therefore, only approximate descriptions for the microstructure evolution must be adopted, by making use of low-order statistical information about the spatial distribution of the strain-rate and vorticity fields within the composite, which can be extracted from homogenization estimates. Approximate descriptions of this sort have been proposed, for instance, by Ponte Castañeda & Zaidman (1994) and Kailasam & Ponte Castañeda (1998), which make use of the averages (*i.e.*, *first* moments) of the strain-rate and vorticity fields in each phase (see also Gologanu *et al.* 1993, 1994, for an alternative approach in the context of Gurson-type models). It is expected that such descriptions should become more accurate by incorporating higher-order information, such as the *second* moments of the fields, especially in situations where field fluctuations are known to be large (*e.g.*, strong nonlinearity, percolation).

The effective behavior of viscoplastic composites may also be strongly affected by the nucleation and evolution of damage within the material, often in the form of debonding between phases and formation of microvoids or microcracks (see, for instance, Babout *et al.* 2001, Maire *et al.* 2005). These phenomena are typically driven by the stress concentration due to mistmatches between constituent properties, and therefore, accounting for them, at least approximately, requires certain knowledge about the spatial distribution of the stress field within the composite. In fact, incorporating the effect of local processes in general (*e.g.*, work hardening, recrystallization) into homogenization estimates requires statistical information about the local fields. Thus, in addition to developing estimates for the effective behavior, a second objective of this work is to develop reliable homogenization estimates for the statistics of the local fields in viscoplastic random composites. In this connection, it should be emphasized that homogenization methods are *not* expected to be capable of predicting the full field distributions, since this would require a complete description of the random microstructure which is not available in practice. (There are very special classes of random composites for which the full field distributions can be obtained, but such distributions have been found to be unrealistic (see Bornert *et al.* 1994, Cule & Torquato 1998).) In contrast, the goal here is to estimate low-order statistics, such as the first and second moments of the fields in each constituent phase, in the hope that they are sufficient to capture the main features of the desired local effect.

Field statistics, up to second order, in *linear* composites have been studied by Bobeth & Diener (1986, 1987), Kreher (1990), Parton & Buryachenko (1990), and Buryachenko & Kreher (1995), among others. These works were mainly concerned with the distribution of (residual) stresses in random composites and polycrystals, driven by the need to predict the macroscopic toughness and strength of such materials. In contrast, most theoretical studies on field statistics in *nonlinear* composites are very recent, and have appeared during the course of this dissertation work. Following Suquet (1995), Bornert (1996) made use of the 'variational' method to extract the isotropic trace of the second moments of the strain in two-phase, elasto-plastic composites, and compared the predictions with experimental results. Following Ponte Castañeda (2002b), Idiart & Ponte Castañeda (2003) made use of the 'second-order' homogenization method to generate estimates for the phase

average and phase covariance tensors of the local fields in two-phase, fiber composites under in-plane loadings. The 'second-order' estimates for the strain-rate fluctuations were found to increase and to become progressively more anisotropic with increasing nonlinearity, and it was conjectured that this nonlinearity-induced anisotropy could be related to the localization of the strain-rate field. Field statistics in this class of composites were also studied by Moulinec & Suquet (2003, 2004) by means of full-field numerical simulations based on a fast-fourier transform (FFT) algorithm, as well as of the 'variational' method. The strain fluctuations in the numerical simulations were found to increase and to become progressively more anisotropic with increasing nonlinearity, in agreement with the observations of Idiart & Ponte Castañeda (2003). Furthermore, the comparisons provided in these works showed that the 'variational' method underestimates significantly the second moments of the strain-rate field. More recently, Idiart *et al.* (2006) have provided comparisons between the FFT simulations and the more sophisticated 'tangent second-order' and 'second-order' methods, and found that the 'second-order' method improves, often in qualitative terms, on the earlier 'variational' and 'tangent second-order' methods. In addition, it was found that the nonlinearity-induced anisotropy of the strain-rate fluctuations is indeed due to the localization of the strain-rate field in bands, running across the composite along certain preferred orientations determined by the loading conditions. Brenner *et al.* (2004) made use of the 'affine' method, which is a simplified but less accurate version of the 'tangent second-order' method, as well as of the 'classical secant' approach, to study field fluctuations in FCC viscoplastic polycrystals. It was found that both methods can give first and second moments of resolved shear stresses that are inconsistent with the bounding character of the flow stress in the ideally-plastic limit, and are therefore unrealistic. More accurate estimates for field statistics in two- and three-dimensional viscoplastic polycrystals were obtained by Liu & Ponte Castañeda (2004a, 2004b) by means of an approximate extension of the 'second-order' method to polycrystalline materials proposed by Liu & Ponte Castañeda (2004a). The 'second-order' estimates for the phase averages and fluctuations of the stress and strain-rate fields were found to depend strongly on nonlinearity and grain anisotropy. In particular, the stress and strain-rate fluctuations were found to grow and become strongly anisotropic with increasing values of the nonlinearity and grain anisotropy parameters. The accuracy of these estimates was demonstrated by comparisons with FFT numerical simulations (Lebensohn *et al.* 2004a, 2004b), which also showed the superiority of the 'second-order' method over earlier homogenization methods. However, in all these works, the homogenization estimates for the field statistics were obtained by making use of various *ad hoc* assumptions based on the conjecture that the first and second moments of the local fields in the relevant linear comparison composite (LCC) constitute reasonable approximations for the corresponding nonlinear quantities. In this dissertation, an *exact* procedure for determining the field statistics in nonlinear composites is proposed, and it is applied in the context of LCC-based homogenization methods to generate *rigorous* homogenization estimates for the first and second moments of the local fields in each constituent phase. An additional advantage of this procedure over the previous approaches, is that it is not limited to first and second moments, and can be used to generate homogenization

estimates for higher-order moments, as well as other types of statistical quantities.

Even though this dissertation is devoted to theoretical methods, it should be mentioned that several experimental techniques have been developed and utilized to measure full-field distributions in composite materials (for recent reviews, see François 2003, Grédiac 2004). *Elastic* strains within composite materials and polycrystals can be determined, for instance, using X-ray and neutron diffraction techniques (see, for example, Hutchings *et al.* 2005, Letouzé *et al.* 2002). An optical experimental technique particularly suitable for characterizing the local strain field in *elasto-plastic* composites has been introduced by Allais *et al.* (1994), which makes use of scanning electron microscopic, microelectrolithography and image analysis. Recent advances in this technique (Doumalin *et al.* 2003) allow to measure deformations below 0.2%, at a resolution of $5\mu m$.

This dissertation is organized as follows. Chapters 2 and 3 constitute the first part, which deals with exact relations for the effective behavior and field statistics in viscoplastic composites. Thus, Chapter 2 is concerned with general aspects of the theory of composites. Basic notions such as 'representative volume element', 'separation of length scales' hypothesis are introduced, leading to a definition of 'effective behavior' and its characterization by means of effective potentials. In addition, the classical bounds of the Voigt- and Reuss-type for the effective potentials are recalled, along with well-known relations for the effective behavior and field statistics in linear composites. Also, this chapter contains the relevant formulae for the generalized Hashin-Shtrikman estimates of Willis (1977, 1981) for two-phase, linear composites, which are used in the context of the LCC-based nonlinear homogenization methods to obtain the results provided in Chapters 5 and 7. In Chapter 3, an exact procedure for determining the field statistics in nonlinear composites is proposed, making use of suitably defined effective potentials. More precisely, this procedure consists in perturbing the local potentials with a term that contains a parameter, generally a tensor, such that the derivative of the perturbed effective potential with respect to that parameter, evaluated at the parameter equal to zero, yields the average of the desired quantity in the unperturbed problem. The usefulness of such relations is that they allow the determination of rigorous homogenization estimates for the field statistics from corresponding estimates for the effective potentials, exactly in the same way as estimates for the effective behavior are generated. The contents of this chapter have appeared in ref. 5 of the list of publications given below.

Chapters 4 and 5 constitute the second part of the dissertation, devoted to the LCC-based homogenization methods in the context of viscoplastic composites with *isotropic* constituents. In Chapter 4, the formulations of the 'variational', 'tangent second-order' and 'second-order' homogenization methods are recalled, and the corresponding estimates for the effective behavior and field statistics are derived, making use of the procedure introduced in Chapter 3. In the context of the 'second-order' method, modified linearization schemes are proposed, in an attempt to eliminate certain inconsistencies associated with the original formulation of the method. The objective of Chapter 5 is to evaluate the accuracy and relative merits of the different LCC-based homogenization methods in predicting the

effective behavior and field statistics in viscoplastic composites. To this end, the methods are applied to two-phase, random composites with 'particulate' microstructures exhibiting overall isotropic and transversely isotropic symmetry. The constituents are assumed to exhibit an isotropic, power-law behavior, which has linear and rigid-ideally plastic behaviors as limiting cases. The accuracy of the homogenization estimates is assessed by confronting them against corresponding exact results for sequentially laminated composites that have been generated in this work (see below). The effect of nonlinearity, inclusion concentration and heterogeneity contrast are all considered. The contents of Chapters 4 and 5 have appeared in refs. 5 and 6, respectively.

The third and final part of this dissertation, including Chapters 6 and 7, concentrates on viscoplastic composites with *anisotropic* constituents (*e.g.*, polycrystals). Chapter 6 is concerned with the development of bounds for nonlinear composites with anisotropic phases by means of an appropriate generalization of the 'variational' method, originally introduced for composites with isotropic constituents by Ponte Castañeda (1991). The bounds can be expressed in terms of a convex (concave) optimization problem, requiring the computation of certain 'corrector' functions that, in turn, depend on the solution of a non-concave/non-convex optimization problem. A simple formula is derived for the overall stress-strain relation of the composite associated with the bound, and special, simpler forms are provided for power-law materials, as well as for ideally plastic materials, where the computation of the 'corrector' functions simplifies dramatically. It is shown that this generalization has the capability to give improved bounds relative to the earlier generalizations provided by deBotton & Ponte Castañeda (1995) in the specific context of viscoplastic polycrystals, and the further generalization of Suquet (see Ponte Castañeda & Suquet 1998) for more general anisotropies, but at the expense of introducing more complex computations. In Chapter 7, the special but very important case of viscoplastic composites with crystalline constituents is considered. The improvement of the 'variational' bounds proposed in Chapter 6 over the earlier bounds of deBotton & Ponte Castañeda (1995) is put into evidence in the context of a model, two-dimensional, porous composite with a power-law, crystalline matrix phase. The contents of Chapters 6 and 7 have appeared in refs. 7 and 8, respectively.

Finally, the main findings of this work are summarized in Chapter 8, and prospects for future work are proposed. In addition, this dissertation contains six appendices, which have not been included as chapters in order to maintain the integrity of the presentation. Of those six, the first four appendices are publications provided in its original published form, mainly concerned with the development of the 'second-order' method.

Thus, Appendix A corresponds to ref. 1 in the list of publications given below, where the first 'second-order' estimates for field fluctuations were obtained, in the context of two-phase, fiber composites with isotropic constituents. Those estimates followed from the use of the phase averages of the local fields as certain 'reference' tensors in the 'second-order' method, as originally proposed in Ponte Castañeda (2002a), and the assumption that field statistics in the LCC represent the corresponding

nonlinear quantities. The 'second-order' method was found to deliver sensible estimates for the field fluctuations, which were found to increase and become progressively more *anisotropic* with increasing nonlinearity. However, it was later found in ref. 2, which is given here as Appendix B, that the choice of the phase averages as 'reference' tensors in the context of the 'second-order' method could lead to inconsistent results for sufficiently strong nonlinearities. Identifying the 'reference' tensors with the macroscopic stress was found to solve this inconsistency, at least for the case considered (i.e., three-dimensional, two-phase composites with power-law phases), and consequently this alternate choice was recommended. The choice was further explored in ref. 4, which is included in Appendix D, and supported by comparisons with exact results.

A thorough study of the effective behavior and field fluctuations in two-phase, viscoplastic composites was then carried out in ref. 3, provided here as Appendix C, making use not only of the improved 'second-order' method, but also of the earlier 'variational' and 'tangent second-order' methods, as well as of the full-field numerical simulations of Moulinec & Suquet (2003, 2004). Again, all homogenization estimates for the field statistics reported in that work were obtained directly from the LCC, as in Appendix A. However, it was realized that in the context of the 'second-order' method, the so-called *duality gap* was leading to 'second-order' estimates for the phase averages of the strain-rate and stress fields that were not consistent with the corresponding macroscopic averages, and so an alternative scheme for computing 'second-order' field statistics, based on the 'closing' of the duality gap, was proposed. In general, the 'second-order' estimates were found to be in good agreement with the numerical simulations, even for high nonlinearities, and to improve, often in qualitative terms, on the earlier homogenization estimates. The numerical simulations provided in this work confirmed the conjecture (Ponte Castañeda 2002b, Idiart & Ponte Castañeda 2003) that the nonlinearity-induced anisotropy of the field fluctuations is due to the localization of the strain-rate field in bands, running across the composite along certain preferred orientations determined by the loading conditions. The numerical simulations also allowed the study of the full field distributions, which showed that the distributions become progressively disorted away from Gaussian with increasing nonlinearity, precisely because of the above-mentioned localization phenomenon. Such knowledge about the full field distributions can be very useful in the context of recent homogenization methods (Pellegrini 2000, 2001) in which a particular form of the field distribution is assumed.

Finally, Appendix E is concerned with a very special class of two-phase, nonlinear, random composites called 'sequential laminates' (see, for example, deBotton & Hariton 2002). These composites are of high theoretical value because their effective potentials can be computed exactly, making them ideal test cases to evaluate the accuracy of approximate homogenization methods like the ones of interest here. Starting with the exact result for a simple rank-1 laminate, exact expressions for the effective potential and field statistics in rank-M laminates are derived following an iterative procedure. Then, making use of a differential scheme as in deBotton (2005), the limit of infinite rank is evaluated, which allows to consider microstructures exhibiting overall (transversely) isotropic symmetry. This is

particularly useful in this work because, in the *linear* case, sequential laminates with such microstructures can be shown to reproduce exactly the effective behavior predicted by the Hashin-Shtrikman (HS) estimates, for *any* value of the modulus tensors of the constituents. Then, when LCC-based homogenization methods are used in the *nonlinear* case, in conjuction with the linear HS estimates for the LCC, the effective behaviour of the LCC is being computed exactly, and therefore there is only one level of approximation involved, namely, at the linearization stage. Thus, 'sequential laminates' allow us to evaluate the accuracy of the different linearization schemes utilized in the homogenization methods, without the need to resort to more involved numerical procedures to homogenize exactly the LCC, as has been recently proposed by Rekik *et al.* (2005) (see also Moulinec & Suquet 2004).

List of publications resulted from this dissertation work

1. Idiart, M. & Ponte Castañeda, P. (2003) Field fluctuations and macroscopic properties in nonlinear composites. *Int. J. Solids Struct.* **40**, 7015–7033.

2. Idiart, M. & Ponte Castañeda, P. (2005) Second-order estimates for nonlinear isotropic composites with spherical pores and rigid particles. *C. R. Mecanique* **333**, 147–154.

3. Idiart, M. I., Moulinec H., Ponte Castañeda P. & Suquet P. (2006) Macroscopic behavior and field fluctuations in viscoplastic composites: second-order estimates vs full-field simulations. *J. Mech. Phys. Solids* **54**, 1029–1063.

4. Idiart, M. I., Danas, K. & Ponte Castañeda, P. (2006) Second-order theory for nonlinear composites and application to isotropic constituents. *C. R. Mecanique* **334**, 575–581.

5. Idiart, M. I. & Ponte Castañeda P. (2007) Field statistics in nonlinear composites. I. Theory. *Proc. R. Soc. Lond. A* **463**, 183–202.

6. Idiart, M. I. & Ponte Castañeda P. (2007) Field statistics in nonlinear composites. II. Applications. *Proc. R. Soc. Lond. A* **463**, 203–222.

7. Idiart, M. I. & Ponte Castañeda, P. (2007) Variational linear comparison bounds for nonlinear composites with anisotropic phases. I. General results. *Proc. R. Soc. Lond. A*, in press.

8. Idiart, M. I. & Ponte Castañeda, P. (2007) Variational linear comparison bounds for nonlinear composites with anisotropic phases. II. Crystalline materials. *Proc. R. Soc. Lond. A*, in press.

9. Idiart, M. I. & Ponte Castañeda, P. (2007) Two-phase, nonlinear sequential laminates. In preparation.

Chapter 2

Effective behavior of viscoplastic composites

2.1 General considerations and effective potentials

The subject of this chapter is the characterization of the effective constitutive behavior of heterogeneous, viscoplastic materials. The definition of 'effective behavior' requires first introducing the notions of separation of length scales and representative volume element. Typically, in many heterogeneous materials of interest, the size of the inhomogeneities (e.g., pores, particles, grains) is much smaller than the size of the specimen. In that case, we can identify three distinct length scales in the problem:

- the *microscopic* length scale ℓ, which characterizes the typical size of the inhomogeneities in the heterogeneous material defining the *microstructure*;
- the *macroscopic* length scale L, which characterizes the size of the specimen;
- the *mesoscopic* length scale l, which characterizes the size of regions within the heterogeneous material where the microstructure is essentially (statistically) uniform.

Hypothesis 2.1.1. (Separation of length scales) *In this work, we assume that the three length scales defined above are such that*

$$\ell << l << L.$$

We refer to the special class of heterogeneous materials satisfying this hypothesis as composite materials, or *composites*, for short.

The regions of size l in a composite, where the microstructure is statistically uniform are called *representative volume elements* (RVEs), first introduced by Hill (1963, 1967), and can be used to define the effective behavior of the composite, which can then vary at the larger length scale L. Thus, under the hypothesis 2.1.1, we can identify an RVE in the heterogeneous material, occupying a region Ω with boundary $\partial\Omega$, containing, in general, N different homogeneous constituents, or *phases*,

occupying disjoint regions $\Omega^{(r)}$, $r = 1, ..., N$ ($\cup_{r=1}^{N} \Omega^{(r)} = \Omega$), whose distribution is characterized by indicator functions $\chi^{(r)}$, such that

$$\chi^{(r)}(\mathbf{x}) = \begin{cases} 1 & \text{if } \mathbf{x} \in \Omega^{(r)}, \\ 0 & \text{otherwise.} \end{cases} \tag{2.1}$$

While for some material systems the distribution of the phases may be known completely, it is only known partially in most common cases. Thus, for composites with *periodic* microstructures, everything is known once the unit cell is described, and consequently, the effective behavior can be determined exactly, at least in principle. On the other hand, for composites with *random* microstructures, only partial information about the distribution of the phases is available, such as the volume fractions or the two-point correlation functions. Consequently, the effective behavior of these materials can be characterized only partially, to an extent determined by the amount of microstructural information that is accounted for.

In this work, the focus will be on *random* composites whose constituent phases exhibit *viscoplastic* behavior, undergoing steady creep. The constitutive behavior of the phases is assumed to be characterized by *convex* dissipation (or strain-rate) potentials $w^{(r)}$ ($r = 1, ..., N$), such that the local Cauchy stress $\boldsymbol{\sigma}$ and Eulerian strain rate $\boldsymbol{\varepsilon}$ are related by

$$\boldsymbol{\sigma} = \partial_{\boldsymbol{\varepsilon}} w(\mathbf{x}, \boldsymbol{\varepsilon}), \quad w(\mathbf{x}, \boldsymbol{\varepsilon}) = \sum_{r=1}^{N} \chi^{(r)}(\mathbf{x})\ w^{(r)}(\boldsymbol{\varepsilon}), \tag{2.2}$$

where $\partial_{\boldsymbol{\varepsilon}}$ denotes differentiation with respect to $\boldsymbol{\varepsilon}$. It is noted that this constitutive relation can also be used within the context of the deformation theory of plasticity, where $\boldsymbol{\sigma}$ and $\boldsymbol{\varepsilon}$ represent the infinitesimal stress and strain, respectively. In practice, the local potentials can be assumed to be differentiable for most material models of interest, except in some special cases, including the ideally plastic materials, where the potentials are not differentiable, but are still convex (although not strictly so). In this case, it is most natural to work with the subdifferential of convex analysis (Ekeland & Temam 1999). Here, for simplicity, the distinction will not be made between standard (Gateaux) derivatives and subdifferentials, except when it becomes necessary, or convenient to do so.

Due to the presence of the inhomogeneities, the local fields $\boldsymbol{\varepsilon}(\mathbf{x})$ and $\boldsymbol{\sigma}(\mathbf{x})$ exhibit strong spatial variations within the RVE. In the sequel, $\langle\cdot\rangle$ and $\langle\cdot\rangle^{(r)}$ are used to denote volume averages over Ω and $\Omega^{(r)}$, respectively. The macroscopic or *effective behavior* of the composite is defined as the relation between the average stress $\overline{\boldsymbol{\sigma}} = \langle\boldsymbol{\sigma}\rangle$ and the average strain rate $\overline{\boldsymbol{\varepsilon}} = \langle\boldsymbol{\varepsilon}\rangle$ over the RVE. The local fields are the solution to the *local problem* consisting of the constitutive equations, the compatibility conditions satisfied by $\boldsymbol{\varepsilon}$, the equilibrium conditions satisfied by $\boldsymbol{\sigma}$ (with zero body force), and appropriate boundary conditions. A variational representation of this problem is provided by the principle of minimum dissipation energy, which can be used to define the *effective strain-rate potential* $\widetilde{W}$ of the composite, via

$$\widetilde{W}(\overline{\boldsymbol{\varepsilon}}) = \inf_{\boldsymbol{\varepsilon} \in \mathcal{K}(\overline{\boldsymbol{\varepsilon}})} \langle w(\mathbf{x}, \boldsymbol{\varepsilon})\rangle = \inf_{\boldsymbol{\varepsilon} \in \mathcal{K}(\overline{\boldsymbol{\varepsilon}})} \sum_{r=1}^{N} c^{(r)}\ \langle w^{(r)}(\boldsymbol{\varepsilon})\rangle^{(r)}, \tag{2.3}$$

where $c^{(r)} = \langle \chi^{(r)}(\mathbf{x}) \rangle$ denotes the volume fraction of phase r, and $\mathcal{K}(\overline{\boldsymbol{\varepsilon}})$ is the set of kinematically admissible strain-rate fields, defined by

$$\mathcal{K}(\overline{\boldsymbol{\varepsilon}}) = \left\{ \boldsymbol{\varepsilon} \mid \text{there is } \mathbf{v} \text{ with } \boldsymbol{\varepsilon} = \frac{1}{2}\left[\nabla \mathbf{v} + (\nabla \mathbf{v})^T\right] \text{ in } \Omega,\ \mathbf{v} = \overline{\boldsymbol{\varepsilon}}\mathbf{x} \text{ on } \partial\Omega \right\}, \tag{2.4}$$

where $\mathbf{v}$ is a velocity field, and $\overline{\boldsymbol{\varepsilon}}$ is a constant second order tensor. Physically, $\widetilde{W}$ corresponds to the energy dissipated in the composite when subjected to affine velocities on the boundary, with prescribed average strain rate $\overline{\boldsymbol{\varepsilon}} = \langle \boldsymbol{\varepsilon} \rangle$. The reason for making use of this particular type of boundary conditions in the definition (2.3) of $\widetilde{W}$ is that the effective stress-strain-rate relation, or effective behavior, of the composite is then given by (Hill 1967, Hutchinson 1976)

$$\overline{\boldsymbol{\sigma}} = \partial_{\overline{\boldsymbol{\varepsilon}}} \widetilde{W}(\overline{\boldsymbol{\varepsilon}}). \tag{2.5}$$

Alternatively, the behavior of the phases can be characterized by *convex* stress potentials $u^{(r)}$, which are the Legendre-Fenchel transforms of $w^{(r)}$, i.e.,

$$u^{(r)}(\boldsymbol{\sigma}) = (w^{(r)})^*(\boldsymbol{\sigma}) = \sup_{\boldsymbol{\varepsilon}} \left[\boldsymbol{\sigma} \cdot \boldsymbol{\varepsilon} - w^{(r)}(\boldsymbol{\varepsilon}) \right]. \tag{2.6}$$

Then, the local stress and strain-rate tensors are related by

$$\boldsymbol{\varepsilon} = \partial_{\boldsymbol{\sigma}} u(\boldsymbol{\sigma}), \quad u(\mathbf{x}, \boldsymbol{\sigma}) = \sum_{r=1}^{N} \chi^{(r)}(\mathbf{x})\ u^{(r)}(\boldsymbol{\sigma}), \tag{2.7}$$

and the effective behavior can be described in terms of the *effective stress potential*, which, using the minimum complementary-energy principle, can be written as

$$\widetilde{U}(\overline{\boldsymbol{\sigma}}) = \inf_{\boldsymbol{\sigma} \in \mathcal{S}(\overline{\boldsymbol{\sigma}})} \langle u(\mathbf{x}, \boldsymbol{\sigma}) \rangle = \inf_{\boldsymbol{\sigma} \in \mathcal{S}(\overline{\boldsymbol{\sigma}})} \sum_{r=1}^{N} c^{(r)}\ \langle u^{(r)}(\boldsymbol{\sigma}) \rangle^{(r)}, \tag{2.8}$$

where $\mathcal{S}(\overline{\boldsymbol{\sigma}})$ is the set of self-equilibrated stresses such that $\overline{\boldsymbol{\sigma}} = \langle \boldsymbol{\sigma} \rangle$. The effective stress-strain-rate relation of the composite is then given by (Hill 1967, Hutchinson 1976)

$$\overline{\boldsymbol{\varepsilon}} = \partial_{\overline{\boldsymbol{\sigma}}} \widetilde{U}(\overline{\boldsymbol{\sigma}}). \tag{2.9}$$

It is recalled that (strict) convexity of the local potentials in the local variables $\boldsymbol{\varepsilon}$ and $\boldsymbol{\sigma}$ implies (strict) convexity of the effective potentials in the macroscopic variables $\overline{\boldsymbol{\varepsilon}}$ and $\overline{\boldsymbol{\sigma}}$ (Ponte Castañeda & Willis 1988). Under Hypothesis 2.1.1, the variational formulations (2.3) and (2.8) can be shown to be completely equivalent, in the sense that the functions $\widetilde{W}$ and $\widetilde{U}$ are Legendre duals of each other, i.e. $\widetilde{U} = \widetilde{W}^*$, and therefore the effective constitutive relations (2.5) and (2.9) must also be equivalent (Suquet 1986; Willis 1989).

Thus, the problem of computing the effective behavior of the composite is equivalent to that of computing the effective potentials $\widetilde{W}$ or $\widetilde{U}$. However, solving the minimization problems (2.3) and (2.8) is in general a formidable task, since they require the solution to sets of nonlinear partial differential equations with randomly oscillatory coefficients. For this reason, the idea is to develop

approximate methods that deliver *estimates* for these effective potentials, so that corresponding estimates for the effective behavior of the composite may then be generated by differentiation, according to relations (2.5) and (2.9).

It should be emphasized that, while the definition of effective behavior provided here is based on intuitive, physically motivated notions, a rigorous derivation has been provided by the mathematical theory of *homogenization*[1], which amounts to evaluating the limit $\epsilon = \ell/l \to 0$ (see Hypothesis 2.1.1) in the variational problems (2.3) and (2.8). This limit involves rapidly oscillating fields (with 'period' $\sim \epsilon$) whose *average* converge to a 'homogenized' limit, even though the fields themselves do not. The mathematical theory of homogenization originated from the works of Sanchez-Palencia (1970) and Bensoussan *et al.* (1978) in the context of *linear* composites with *periodic* microstructures, later formalized and generalized by Marcellini (1978) to *nonlinear* composites with *strictly* convex local potentials $w(\mathbf{x}, \boldsymbol{\varepsilon})$ satisfying appropriate growth conditions in $\boldsymbol{\varepsilon}$ at infinity. The limiting case of rigid-ideally plastic composites, for which the potentials are convex but *not* strictly so, was considered by Suquet (1983) and Bouchitte & Suquet (1991). Finally, the notion of Γ-convergence introduced by De Giorgi (1975) allowed the generalization of the theory of homogenization to nonlinear composites with *random* microstructures (refer to Jikov *et al.* 1991).

2.2 Classical bounds of the Voigt and Reuss type

Rigorous bounds for the effective potentials $\widetilde{W}$ and $\widetilde{U}$ may be obtained by making use of trial fields for $\boldsymbol{\varepsilon}$ and $\boldsymbol{\sigma}$ in expressions (2.3) and (2.8), respectively. This was first recognized by Bishop & Hill (1951) in the context of rigid-ideally plastic polycrystals. The simplest trial fields that belong to the sets $\mathcal{K}$ and $\mathcal{S}$ are the uniform fields $\boldsymbol{\varepsilon}(\mathbf{x}) = \overline{\boldsymbol{\varepsilon}}$ and $\boldsymbol{\sigma}(\mathbf{x}) = \overline{\boldsymbol{\sigma}}$, respectively, which lead to the rigorous bounds

$$\widetilde{W}(\overline{\boldsymbol{\varepsilon}}) \leq \sum_{r=1}^{N} c^{(r)} w^{(r)}(\overline{\boldsymbol{\varepsilon}}), \tag{2.10}$$

and

$$\widetilde{U}(\overline{\boldsymbol{\sigma}}) \leq \sum_{r=1}^{N} c^{(r)} u^{(r)}(\overline{\boldsymbol{\sigma}}), \tag{2.11}$$

or, equivalently,

$$\begin{aligned} \left(\sum_{r=1}^{N} c^{(r)} u^{(r)}\right)^{*}(\overline{\boldsymbol{\varepsilon}}) \leq \quad & \widetilde{W}(\overline{\boldsymbol{\varepsilon}}) \quad \leq \sum_{r=1}^{N} c^{(r)} w^{(r)}(\overline{\boldsymbol{\varepsilon}}), \\ \left(\sum_{r=1}^{N} c^{(r)} w^{(r)}\right)^{*}(\overline{\boldsymbol{\sigma}}) \leq \quad & \widetilde{U}(\overline{\boldsymbol{\sigma}}) \quad \leq \sum_{r=1}^{N} c^{(r)} u^{(r)}(\overline{\boldsymbol{\sigma}}). \end{aligned} \tag{2.12}$$

These bounds were first proposed by Voigt (1889) and Reuss (1929) in the context of linear composites, and for that reason they are generally referred to as the classical bounds of Voigt and Reuss. In the context of polycrystals, they are often referred to as the Taylor (1938) and Sachs (1928) bounds, respectively. It can be shown that these upper and lower bounds coincide to first order in the

[1] This name seems to have been introduced by Babŭska (1975).

heterogeneity contrast (see, for instance, Ponte Castañeda & Suquet 1998), and since the exact solution should be in between the two, this implies that they are exact in that case. However, it should be noted that the only microstructural information appearing in expressions (2.10) and (2.11) is the volume fraction of the phases $c^{(r)}$, and therefore these bounds cannot account for the way the phases are distributed in the composite. Because of this, they are not very useful in general, particularly when the contrast between the phases is large. Part of the present work is concerned with the development of bounds and estimates for viscoplastic composites, which have the capability of improving on the classical bounds, by incorporating additional statistical information about the microstructure, like, for instance, information about the two-point correlation function of the distribution of the phases.

2.3 Linear composites

Because the methods for nonlinear composites that will be considered in this work make use of available results for linear composites, it is pertinent here to recall certain relations for linear systems, which will be useful in the sequel.

The most general potentials for linear materials are of the form

$$w^{(r)}(\boldsymbol{\varepsilon}) = \frac{1}{2}\boldsymbol{\varepsilon}\cdot\mathbf{L}^{(r)}\boldsymbol{\varepsilon} + \boldsymbol{\tau}^{(r)}\cdot\boldsymbol{\varepsilon} + f^{(r)}, \tag{2.13}$$

where $\mathbf{L}^{(r)}$ is a fully symmetric, fourth-order, positive-definite, viscosity tensor, and $\boldsymbol{\tau}^{(r)}$ is a symmetric, second-order, polarization tensor, so that the stress and strain-rate tensors are linearly related by

$$\boldsymbol{\sigma} = \partial_{\boldsymbol{\varepsilon}} w^{(r)}(\boldsymbol{\varepsilon}) = \mathbf{L}^{(r)}\boldsymbol{\varepsilon} + \boldsymbol{\tau}^{(r)}. \tag{2.14}$$

Note that the particular case of $\boldsymbol{\tau}^{(r)} = \mathbf{0}$ and $f^{(r)} = 0$ corresponds to a purely viscous (Newtonian) material.

If all the phases in a composite are characterized by potentials of the form (2.13), it follows from the linearity of the problem that the effective potential of the composite is also of that form, and can be written as

$$\widetilde{W}(\overline{\boldsymbol{\varepsilon}}) = \frac{1}{2}\overline{\boldsymbol{\varepsilon}}\cdot\widetilde{\mathbf{L}}\overline{\boldsymbol{\varepsilon}} + \widetilde{\boldsymbol{\tau}}\cdot\overline{\boldsymbol{\varepsilon}} + \widetilde{f}, \tag{2.15}$$

where $\widetilde{\mathbf{L}}$ denotes the effective viscosity tensor of the composite, and $\widetilde{\boldsymbol{\tau}}$ is an effective polarization. The effective stress-strain-rate relation of the composite is then given in terms of these effective tensors by

$$\overline{\boldsymbol{\sigma}} = \partial_{\overline{\boldsymbol{\varepsilon}}}\widetilde{W}(\overline{\boldsymbol{\varepsilon}}) = \widetilde{\mathbf{L}}\overline{\boldsymbol{\varepsilon}} + \widetilde{\boldsymbol{\tau}}. \tag{2.16}$$

It also follows from the linearity of the problem that the average of the strain rate over phase r, $\overline{\boldsymbol{\varepsilon}}^{(r)} = \langle\boldsymbol{\varepsilon}\rangle^{(r)}$, may be written in terms of the macroscopic strain rate $\overline{\boldsymbol{\varepsilon}}$ by means of two strain-rate-concentration tensors $\mathbf{A}^{(r)}$ and $\mathbf{a}^{(r)}$, via (Laws 1973, Willis 1981)

$$\overline{\boldsymbol{\varepsilon}}^{(r)} = \mathbf{A}^{(r)}\overline{\boldsymbol{\varepsilon}} + \mathbf{a}^{(r)}. \tag{2.17}$$

Here, $\mathbf{A}^{(r)}$ is a fourth-order tensor exhibiting minor symmetry, but not necessarily major symmetry, and $\mathbf{a}^{(r)}$ is a symmetric, second-order tensor. It should be noted that the tensors $\mathbf{A}^{(r)}$ depend only on the viscosity tensors $\mathbf{L}^{(s)}$, $s = 1, ..., N$, while the $\mathbf{a}^{(r)}$ depend not only on the viscosities $\mathbf{L}^{(s)}$ but also on the polarizations $\boldsymbol{\tau}^{(s)}$.

Since the phase averages (2.17) must satisfy the relation

$$\overline{\boldsymbol{\varepsilon}} = \sum_{r=1}^{N} c^{(r)} \overline{\boldsymbol{\varepsilon}}^{(r)}, \tag{2.18}$$

the concentration tensors $\mathbf{A}^{(r)}$ and $\mathbf{a}^{(r)}$ should be such that

$$\sum_{r=1}^{N} c^{(r)} \mathbf{A}^{(r)} = \mathbf{I}, \quad \sum_{r=1}^{N} c^{(r)} \mathbf{a}^{(r)} = \mathbf{0}. \tag{2.19}$$

In addition, the constitutive relations (2.14) imply that the phase averages of the stress $\overline{\boldsymbol{\sigma}}^{(r)}$ are given by

$$\overline{\boldsymbol{\sigma}}^{(r)} = \mathbf{L}^{(r)} \overline{\boldsymbol{\varepsilon}}^{(r)} + \boldsymbol{\tau}^{(r)}, \tag{2.20}$$

and since these quantities must satisfy the relation

$$\overline{\boldsymbol{\sigma}} = \sum_{r=1}^{N} c^{(r)} \overline{\boldsymbol{\sigma}}^{(r)}, \tag{2.21}$$

it follows that the concentration tensors $\mathbf{A}^{(r)}$ and $\mathbf{a}^{(r)}$ are related to the effective properties appearing in (2.16) by (Laws 1973)

$$\widetilde{\mathbf{L}} = \sum_{r=1}^{N} c^{(r)} \mathbf{L}^{(r)} \mathbf{A}^{(r)}, \tag{2.22}$$

$$\widetilde{\boldsymbol{\tau}} = \sum_{r=1}^{N} c^{(r)} (\mathbf{A}^{(r)})^T \, \boldsymbol{\tau}^{(r)}, \tag{2.23}$$

$$\widetilde{f} = \sum_{r=1}^{N} c^{(r)} \left(f^{(r)} + \frac{1}{2} \boldsymbol{\tau}^{(r)} \cdot \mathbf{a}^{(r)} \right). \tag{2.24}$$

It should be noted that the effective tensors $\widetilde{\mathbf{L}}$ and $\widetilde{\boldsymbol{\tau}}$ depend only on the concentration tensors $\mathbf{A}^{(s)}$, and consequently can be deduced directly from the purely viscous problem (i.e., $\boldsymbol{\tau}^{(s)} = \mathbf{0}$ and $f^{(s)} = 0$).

Relations (2.22)-(2.24) simplify considerably in the case of two-phase ($N = 2$) composites. This is because relations (2.19) and (2.22) can be used in this case to express the strain-rate-concentration tensors in terms of the phase properties $\mathbf{L}^{(r)}$ and $\boldsymbol{\tau}^{(r)}$, and the effective viscosity tensor $\widetilde{\mathbf{L}}$. For instance, in phase 1, these relations are

$$c^{(1)} \left(\mathbf{A}^{(1)} - \mathbf{I} \right)^T = -\left(\widetilde{\mathbf{L}} - \overline{\mathbf{L}} \right) (\Delta \mathbf{L})^{-1}, \tag{2.25}$$

$$c^{(1)} \mathbf{a}^{(1)} = -(\Delta \mathbf{L})^{-1} \left(\widetilde{\mathbf{L}} - \overline{\mathbf{L}} \right) (\Delta \mathbf{L})^{-1} (\Delta \boldsymbol{\tau}), \tag{2.26}$$

where $\Delta \mathbf{L} = \mathbf{L}^{(2)} - \mathbf{L}^{(1)}$ and $\Delta \boldsymbol{\tau} = \boldsymbol{\tau}^{(2)} - \boldsymbol{\tau}^{(1)}$, and the overbar denotes volume average over the composite (e.g., $\overline{\mathbf{L}} = c^{(1)} \mathbf{L}^{(1)} + c^{(2)} \mathbf{L}^{(2)}$). Using these relations in (2.23) and (2.24), it follows that

(Rosen & Hashin 1970)

$$\widetilde{\boldsymbol{\tau}} = \overline{\boldsymbol{\tau}} + \left(\widetilde{\mathbf{L}} - \overline{\mathbf{L}}\right)(\Delta\mathbf{L})^{-1}(\Delta\boldsymbol{\tau}), \tag{2.27}$$

$$\widetilde{f} = \overline{f} + \frac{1}{2}(\Delta\boldsymbol{\tau})(\Delta\mathbf{L})^{-1}\left(\widetilde{\mathbf{L}} - \overline{\mathbf{L}}\right)(\Delta\mathbf{L})^{-1}(\Delta\boldsymbol{\tau}). \tag{2.28}$$

Thus, the effective potential (2.15) of a two-phase composite is completely determined by the effective viscosity tensor $\widetilde{\mathbf{L}}$. These relations were first derived by Levin (1967) for composites with isotropic phases, and for this reason they are commonly known as the 'Levin' relations.

Completely analogous expressions may be derived in terms of the dual, stress potentials $u^{(r)}$, which can be written as

$$u^{(r)}(\boldsymbol{\sigma}) = \frac{1}{2}\boldsymbol{\sigma}\cdot\mathbf{M}^{(r)}\boldsymbol{\sigma} + \boldsymbol{\eta}^{(r)}\cdot\boldsymbol{\sigma} + g^{(r)}, \tag{2.29}$$

where $\mathbf{M}^{(r)}$ is a fully symmetric, positive-definite, fourth-order tensor of compliances, and $\boldsymbol{\eta}^{(r)}$ is a symmetric, second-order, polarization tensor. The effective stress potential of a linear composite is also of this form, and can be written as

$$\widetilde{U}(\overline{\boldsymbol{\sigma}}) = \frac{1}{2}\overline{\boldsymbol{\sigma}}\cdot\widetilde{\mathbf{M}}\overline{\boldsymbol{\sigma}} + \widetilde{\boldsymbol{\eta}}\cdot\overline{\boldsymbol{\sigma}} + \widetilde{g}, \tag{2.30}$$

where $\widetilde{\mathbf{M}}$ and $\widetilde{\boldsymbol{\eta}}$ are the effective compliance and polarization tensors, respectively. The effective stress-strain-rate relation of the composite is then given by

$$\overline{\boldsymbol{\varepsilon}} = \partial_{\overline{\boldsymbol{\sigma}}}\widetilde{U}(\overline{\boldsymbol{\sigma}}) = \widetilde{\mathbf{M}}\overline{\boldsymbol{\sigma}} + \widetilde{\boldsymbol{\eta}}. \tag{2.31}$$

In a completely analogous fashion, stress-concentration tensors $\mathbf{B}^{(r)}$ and $\mathbf{b}^{(r)}$ can be introduced, such that the average of the stress over phase r is given by

$$\overline{\boldsymbol{\sigma}}^{(r)} = \mathbf{B}^{(r)}\overline{\boldsymbol{\sigma}} + \mathbf{b}^{(r)}. \tag{2.32}$$

These stress-concentration tensors should satisfy the relations

$$\sum_{r=1}^{N} c^{(r)}\mathbf{B}^{(r)} = \mathbf{I}, \quad \sum_{r=1}^{N} c^{(r)}\mathbf{b}^{(r)} = \mathbf{0}. \tag{2.33}$$

In addition, the phase averages of the strain rate $\overline{\boldsymbol{\varepsilon}}^{(r)}$ are related to the $\overline{\boldsymbol{\sigma}}^{(r)}$ by

$$\overline{\boldsymbol{\varepsilon}}^{(r)} = \mathbf{M}^{(r)}\overline{\boldsymbol{\sigma}}^{(r)} + \boldsymbol{\eta}^{(r)}, \tag{2.34}$$

and since the quantities $\overline{\boldsymbol{\sigma}}^{(r)}$ and $\overline{\boldsymbol{\varepsilon}}^{(r)}$ should satisfy the relations (2.18), (2.21) and (2.31), it follows that the effective properties appearing in (2.30) are given in terms of the stress-concentration tensors by

$$\widetilde{\mathbf{M}} = \sum_{r=1}^{N} c^{(r)}\mathbf{M}^{(r)}\mathbf{B}^{(r)}, \tag{2.35}$$

$$\widetilde{\boldsymbol{\eta}} = \sum_{r=1}^{N} c^{(r)}(\mathbf{B}^{(r)})^{T}\,\boldsymbol{\eta}^{(r)}, \tag{2.36}$$

$$\widetilde{g} = \sum_{r=1}^{N} c^{(r)}\left(g^{(r)} + \frac{1}{2}\boldsymbol{\eta}^{(r)}\cdot\mathbf{b}^{(r)}\right). \tag{2.37}$$

Once again, it is noted that the tensors $\widetilde{\mathbf{M}}$ and $\widetilde{\boldsymbol{\eta}}$ depend only on the concentration tensors $\mathbf{B}^{(r)}$, and are independent of the tensors $\mathbf{b}^{(r)}$.

Finally, in the case of two-phase composites, the stress-concentration tensors in, say, phase 1 can be expressed in terms of the effective compliance tensor $\widetilde{\mathbf{M}}$ as

$$c^{(1)}\left(\mathbf{B}^{(1)}-\mathbf{I}\right)^{T} = -\left(\widetilde{\mathbf{M}}-\overline{\mathbf{M}}\right)(\Delta\mathbf{M})^{-1}, \tag{2.38}$$

$$c^{(1)}\mathbf{b}^{(1)} = -(\Delta\mathbf{M})^{-1}\left(\widetilde{\mathbf{M}}-\overline{\mathbf{M}}\right)(\Delta\mathbf{M})^{-1}(\Delta\boldsymbol{\eta}), \tag{2.39}$$

so that the Levin relations for the effective properties are given by

$$\widetilde{\boldsymbol{\eta}} = \overline{\boldsymbol{\eta}}+\left(\widetilde{\mathbf{M}}-\overline{\mathbf{M}}\right)(\Delta\mathbf{M})^{-1}(\Delta\boldsymbol{\eta}), \tag{2.40}$$

$$\widetilde{g} = \overline{g}+\frac{1}{2}(\Delta\boldsymbol{\eta})(\Delta\mathbf{M})^{-1}\left(\widetilde{\mathbf{M}}-\overline{\mathbf{M}}\right)(\Delta\mathbf{M})^{-1}(\Delta\boldsymbol{\eta}). \tag{2.41}$$

Expressions (2.17) and (2.32) relate the phase averages (first moments) of the local fields to the macroscopic averages $\overline{\boldsymbol{\varepsilon}}$ and $\overline{\boldsymbol{\sigma}}$ by means of concentration tensors. It is also possible to relate the phase averages to the macroscopic averages directly through the effective potentials (2.15) and (2.30), by making use of the following identities, first given by Kreher (1990) in the context of thermoelastic composites:

$$\overline{\boldsymbol{\varepsilon}}^{(r)}=\frac{1}{c^{(r)}}\partial_{\boldsymbol{\tau}^{(r)}}\widetilde{W}\left(\overline{\boldsymbol{\varepsilon}};\boldsymbol{\tau}^{(s)},\mathbf{L}^{(s)}\right), \quad \overline{\boldsymbol{\sigma}}^{(r)}=\frac{1}{c^{(r)}}\partial_{\boldsymbol{\eta}^{(r)}}\widetilde{U}\left(\overline{\boldsymbol{\sigma}};\boldsymbol{\eta}^{(s)},\mathbf{M}^{(s)}\right). \tag{2.42}$$

A proof of these identities will be given in a more general setting in the next chapter. The advantage of having this type of relations over those involving concentration tensors is that they allow the generation of estimates for the phase averages directly from homogenization estimates for the effective potentials, and they can be generalized to nonlinear composites, as will be seen in the next chapter. It is worth noting that in the linear case, the effective potentials being of the form (2.15) and (2.30), these expressions can be written as

$$\overline{\boldsymbol{\varepsilon}}^{(r)}=\frac{1}{c^{(r)}}\left[\overline{\boldsymbol{\varepsilon}}\cdot\partial_{\boldsymbol{\tau}^{(r)}}\widetilde{\boldsymbol{\tau}}+\partial_{\boldsymbol{\tau}^{(r)}}\widetilde{f}\right], \quad \overline{\boldsymbol{\sigma}}^{(r)}=\frac{1}{c^{(r)}}\left[\overline{\boldsymbol{\sigma}}\cdot\partial_{\boldsymbol{\eta}^{(r)}}\widetilde{\boldsymbol{\eta}}+\partial_{\boldsymbol{\eta}^{(r)}}\widetilde{g}\right], \tag{2.43}$$

where use has been made of the fact that the effective viscosity and compliance tensors are independent of the polarization tensors, and the notation $\mathbf{a}\cdot\partial_{\mathbf{c}}\mathbf{b}$ has been used to denote second-order tensors with ij^{th} components $a_{kl}\partial b_{kl}/\partial c_{ij}$. Then, these relations, together with (2.17) and (2.32), imply that the concentration tensors and the derivatives appearing above are related by

$$\mathbf{A}^{(r)} = \frac{1}{c^{(r)}}\partial_{\boldsymbol{\tau}^{(r)}}\widetilde{\boldsymbol{\tau}}, \quad \mathbf{a}^{(r)}=\frac{1}{c^{(r)}}\partial_{\boldsymbol{\tau}^{(r)}}\widetilde{f}, \tag{2.44}$$

$$\mathbf{B}^{(r)} = \frac{1}{c^{(r)}}\partial_{\boldsymbol{\eta}^{(r)}}\widetilde{\boldsymbol{\eta}}, \quad \mathbf{b}^{(r)}=\frac{1}{c^{(r)}}\partial_{\boldsymbol{\eta}^{(r)}}\widetilde{g}. \tag{2.45}$$

Identities analogous to (2.42) can be derived (see next chapter) for the phase averages of the second moments of the local fields, by differentiating the effective potentials (2.15) and (2.30) with respect to the viscosity and compliance tensors instead of the polarizations. These identities can be written as

$$\langle\boldsymbol{\varepsilon}\otimes\boldsymbol{\varepsilon}\rangle^{(r)}=\frac{2}{c^{(r)}}\partial_{\mathbf{L}^{(r)}}\widetilde{W}\left(\overline{\boldsymbol{\varepsilon}};\boldsymbol{\tau}^{(s)},\mathbf{L}^{(s)}\right), \quad \langle\boldsymbol{\sigma}\otimes\boldsymbol{\sigma}\rangle^{(r)}=\frac{2}{c^{(r)}}\partial_{\mathbf{M}^{(r)}}\widetilde{U}\left(\overline{\boldsymbol{\sigma}};\boldsymbol{\eta}^{(s)},\mathbf{M}^{(s)}\right). \tag{2.46}$$

Relations of this type for the second moments were first provided by Bergman (1978) in the context of linear electrostatics, and were later derived for thermoelastic composites at various levels of generality by Bobeth & Diener (1986), Kreher (1990), and Parton & Buryachenko (1990). In the next chapter, these relations will be generalized to nonlinear composites, and will be extended to moments of order higher than two.

2.4 Generalized Hashin-Shtrikman estimates for two-phase, linear composites

Hashin & Shtrikman (1962, 1963) made use of a variational procedure to generate estimates the effective behavior of linear composites with statistically isotropic, random microstructures, which improve on the classical bounds of Voigt and Reuss. A generalization and elegant derivation of these estimates in terms of two-point statistics has been provided by Willis (1977, 1978, 1980, 1983). These generalized Hashin-Shtrikman (HS) estimates are given below for the specific case of two-phase, linear-elastic composites. It is recalled, however, that such results can then be applied to the more general class of two-phase, thermoelastic composites by making use of the Levin relations given in Section 2.3.

The effective elasticity tensor $\widetilde{\mathbf{L}}$ of a two-phase composite can be written in terms of strain-concentration tensors $\mathbf{A}^{(r)}$ as

$$\widetilde{\mathbf{L}} = c^{(1)}\mathbf{L}^{(1)}\mathbf{A}^{(1)} + c^{(2)}\mathbf{L}^{(2)}\mathbf{A}^{(2)}, \tag{2.47}$$

where the $c^{(r)}$ denote the volume fractions of each phase r, and the tensors $\mathbf{A}^{(r)}$ satisfy the constraint

$$c^{(1)}\mathbf{A}^{(1)} + c^{(2)}\mathbf{A}^{(2)} = \mathbf{I}. \tag{2.48}$$

We consider the special case of two-phase composites with random, 'particulate' microstructures, *i.e.*, with a discontinuous (inclusion) phase embedded in a continuous (matrix) phase. Let the matrix and inclusion phases be identified with $r = 1$ and $r = 2$, respectively. In that case, the generalized HS estimates of Willis lead to the following expression for the strain-concentration tensor of the inclusion phase:

$$\mathbf{A}^{(2)} = \left[\mathbf{I} + c^{(1)}\mathbf{P}^{(1)}\Delta\mathbf{L}\right]^{-1}, \tag{2.49}$$

where $\Delta\mathbf{L} = \mathbf{L}^{(2)} - \mathbf{L}^{(1)}$. In this expression, $\mathbf{P}^{(1)}$ denotes a microstructural tensor, given by

$$\mathbf{P}^{(1)} = \frac{1}{4\pi \det \mathbf{Z}} \int_{|\boldsymbol{\xi}|=1} \mathbf{H}^{(1)}(\boldsymbol{\xi}) \left|\mathbf{Z}^{-1}\boldsymbol{\xi}\right|^{-3} \, dS(\boldsymbol{\xi}), \tag{2.50}$$

where the second-order tensor $\mathbf{Z}$ serves to characterize the 'shape' of the assumed 'ellipsoidal' two-point correlation function, and the fourth-order tensor $\mathbf{H}^{(1)}$ is given in terms of the elasticity tensor $\mathbf{L}^{(1)}$ of the matrix phase by

$$H^{(1)}_{ijkl}(\boldsymbol{\xi}) = N^{(1)}_{ik}\xi_j\xi_h|_{(ij)(kh)}, \quad \mathbf{N}^{(1)} = \mathbf{K}^{(1)^{-1}}, \quad K^{(1)}_{ik} = L^{(1)}_{ijkh}\xi_j\xi_h. \tag{2.51}$$

Here, $\mathbf{K}^{(1)}$ is the so-called accoustic tensor (of phase 1) and the superscript (1) has been used to emphasize the dependence on $\mathbf{L}^{(1)}$. The strain-concentration tensor of the matrix phase can then be obtained from the constraint (2.48).

For microstructures exhibiting overall *isotropic* symmetry, the tensor $\mathbf{Z}$ should be set equal to the identity, in which case expression (2.50) simplifies to (Willis 1982)

$$\mathbf{P}^{(1)} = \frac{1}{4\pi} \int_{|\boldsymbol{\xi}|=1} \mathbf{H}^{(1)}(\boldsymbol{\xi})\ dS(\boldsymbol{\xi}). \tag{2.52}$$

For composites with microstructures exhibiting *cylindrical* symmetry, such as fiber composites, the tensor $\mathbf{Z}$ should be set equal to $\mathrm{diag}(1,1,0)$, in which case expression (2.50) simplifies to (Willis 1982)

$$\mathbf{P}^{(1)} = \frac{1}{2\pi} \int_{\xi_1^2+\xi_2^2=1} \mathbf{H}^{(1)}(\xi_1,\xi_2,0)\ ds(\boldsymbol{\xi}), \tag{2.53}$$

where the x_3-axis has been taken as the axis of symmetry.

Analogous expressions can be derived for the effective compliance tensor $\widetilde{\mathbf{M}}$, in terms of the compliance tensors $\mathbf{M}^{(r)} = (\mathbf{L}^{(r)})^{-1}$. For a two-phase composite, we have that

$$\widetilde{\mathbf{M}} = c^{(1)}\mathbf{M}^{(1)}\mathbf{B}^{(1)} + c^{(2)}\mathbf{M}^{(2)}\mathbf{B}^{(2)}, \tag{2.54}$$

where the stress-concentration tensors $\mathbf{B}^{(r)}$ satisfy the constraint

$$c^{(1)}\mathbf{B}^{(1)} + c^{(2)}\mathbf{B}^{(2)} = \mathbf{I}. \tag{2.55}$$

The generalized HS estimates lead to the following expression for the stress-concentration tensor of the inclusion phase:

$$\mathbf{B}^{(2)} = \left[\mathbf{I} + c^{(1)}\mathbf{Q}^{(1)}\Delta\mathbf{M}\right]^{-1}. \tag{2.56}$$

where $\Delta\mathbf{M} = \mathbf{M}^{(2)} - \mathbf{M}^{(1)}$. In this expression, the microstructural tensor $\mathbf{Q}^{(1)}$ is given in terms of the viscosity tensor $\mathbf{L}^{(1)}$ of the matrix phase and the tensor $\mathbf{P}^{(1)}$ by

$$\mathbf{Q}^{(1)} = \mathbf{L}^{(1)} - \mathbf{L}^{(1)}\mathbf{P}^{(1)}\mathbf{L}^{(1)}. \tag{2.57}$$

Finally, the stress-concentration tensor of the matrix phase can be obtained from the constraint (2.55).

The HS estimates can be shown to be exact to second order in the heterogeneity contrast, and to first order in the inclusion concentration. In addition, they are known to be quite accurate up to moderate concentrations of the inclusion phase. The main difficulty in their computation lies in the evaluation of the integral in the tensor $\mathbf{P}^{(1)}$, which can be carried out analytically in some cases.

Rigid inclusions. This case corresponds to an elasticity tensor $\mathbf{L}^{(2)}$ with infinite eigenvalues. Then, the HS estimates for the effective tensors can be written as

$$\widetilde{\mathbf{L}} = \mathbf{L}^{(1)} + \frac{c^{(2)}}{c^{(1)}}(\mathbf{P}^{(1)})^{-1}, \tag{2.58}$$

$$\widetilde{\mathbf{M}} = \mathbf{M}^{(1)} - c^{(2)}\left[(\mathbf{M}^{(1)})^{-1} - c^{(1)}\mathbf{Q}^{(1)}\right]^{-1}. \tag{2.59}$$

Voids. This case corresponds to an elasticity tensor $\mathbf{L}^{(2)}$ with zero eigenvalues. Then, the HS estimates for the effective tensors can be written as

$$\widetilde{\mathbf{L}} = \mathbf{L}^{(1)} - c^{(2)} \left[(\mathbf{L}^{(1)})^{-1} - c^{(1)} \mathbf{P}^{(1)} \right]^{-1}, \tag{2.60}$$

$$\widetilde{\mathbf{M}} = \mathbf{M}^{(1)} + \frac{c^{(2)}}{c^{(1)}} (\mathbf{Q}^{(1)})^{-1}. \tag{2.61}$$

The concentration tensors (2.49) and (2.56) can be used in relations (2.17) and (2.32) to obtain HS estimates for the phase averages (first moments) of the local fields. In addition, HS estimates for the second moments may be obtained by making use of expressions (2.46), with $\widetilde{\mathbf{L}}$ given by (2.47). Thus, in the matrix phase, it can be verified that

$$\begin{aligned} \langle \boldsymbol{\varepsilon} \otimes \boldsymbol{\varepsilon} \rangle^{(1)} &= \frac{1}{c^{(1)}} \partial_{\mathbf{L}^{(1)}} \left(\overline{\boldsymbol{\varepsilon}} \cdot \widetilde{\mathbf{L}} \overline{\boldsymbol{\varepsilon}} \right) = \left(\mathbf{A}^{(1)} \overline{\boldsymbol{\varepsilon}} \right) \otimes \left(\mathbf{A}^{(1)} \overline{\boldsymbol{\varepsilon}} \right) - ... \\ &\quad ... - c^{(2)} \left(\Delta \mathbf{L} \ \mathbf{A}^{(2)} \overline{\boldsymbol{\varepsilon}} \right) \cdot \partial_{\mathbf{L}^{(1)}} \mathbf{P}^{(1)} \left(\Delta \mathbf{L} \ \mathbf{A}^{(2)} \overline{\boldsymbol{\varepsilon}} \right), \end{aligned} \tag{2.62}$$

while in the inclusion phase, we have that

$$\langle \boldsymbol{\varepsilon} \otimes \boldsymbol{\varepsilon} \rangle^{(2)} = \frac{1}{c^{(2)}} \partial_{\mathbf{L}^{(2)}} \left(\overline{\boldsymbol{\varepsilon}} \cdot \widetilde{\mathbf{L}} \overline{\boldsymbol{\varepsilon}} \right) = \left(\mathbf{A}^{(2)} \overline{\boldsymbol{\varepsilon}} \right) \otimes \left(\mathbf{A}^{(2)} \overline{\boldsymbol{\varepsilon}} \right). \tag{2.63}$$

Recalling the identity $\overline{\boldsymbol{\varepsilon}}^{(r)} = \mathbf{A}^{(r)} \overline{\boldsymbol{\varepsilon}}$ for linearly-elastic composites, these expressions can be written as

$$\langle \boldsymbol{\varepsilon} \otimes \boldsymbol{\varepsilon} \rangle^{(1)} = \overline{\boldsymbol{\varepsilon}}^{(1)} \otimes \overline{\boldsymbol{\varepsilon}}^{(1)} - c^{(2)} (\Delta \mathbf{L} \overline{\boldsymbol{\varepsilon}}^{(2)}) \cdot \partial_{\mathbf{L}^{(1)}} \mathbf{P}^{(1)} \ (\Delta \mathbf{L} \overline{\boldsymbol{\varepsilon}}^{(2)}), \tag{2.64}$$

$$\langle \boldsymbol{\varepsilon} \otimes \boldsymbol{\varepsilon} \rangle^{(2)} = \overline{\boldsymbol{\varepsilon}}^{(2)} \otimes \overline{\boldsymbol{\varepsilon}}^{(2)}. \tag{2.65}$$

Similarly, the HS estimates for the second moments of the stress can be written as

$$\langle \boldsymbol{\sigma} \otimes \boldsymbol{\sigma} \rangle^{(1)} = \overline{\boldsymbol{\sigma}}^{(1)} \otimes \overline{\boldsymbol{\sigma}}^{(1)} - c^{(2)} (\Delta \mathbf{M} \overline{\boldsymbol{\sigma}}^{(2)}) \cdot \partial_{\mathbf{M}^{(1)}} \mathbf{Q}^{(1)} \ (\Delta \mathbf{M} \overline{\boldsymbol{\sigma}}^{(2)}), \tag{2.66}$$

$$\langle \boldsymbol{\sigma} \otimes \boldsymbol{\sigma} \rangle^{(2)} = \overline{\boldsymbol{\sigma}}^{(2)} \otimes \overline{\boldsymbol{\sigma}}^{(2)}. \tag{2.67}$$

Expressions (2.65) and (2.67) imply vanishing phase covariance tensors in the inclusion phase. Thus, the HS estimates predict field fluctuations in the matrix phase ($r = 1$), but *not* in the inclusion phase ($r = 2$). In other words, the HS estimates are consistent with *uniform* fields inside the inclusion phase. It is recalled that this is in precise agreement with the exact solution of Eshelby (1957) for a dilute concentration of inclusions.

Chapter 3

Field statistics in viscoplastic composites

3.1 Introduction

The previous chapter was concerned with the characterization of the effective behavior of viscoplastic composites, in terms of the behavior of their constituents and prescribed statistical information about their microstructure. However, as has been pointed out in the Introduction, it is also important to characterize the statistics of the spatial distribution of the local fields within these materials, and this is the subject of the present chapter.

In the context of *linear* composites, there are already the exact formulas (2.42) and (2.46) expressing the first and second moments of the local fields in the phases, in terms of the effective potentials. Such formulas are useful for they allow to extract estimates for the statistics of the local fields from homogenization estimates for the effective potentials. In this chapter, an exact procedure is proposed, which relates the statistics of the local fields in *nonlinear* composites with suitably perturbed effective potentials. The procedure is quite general, and can be used to generate relations for moments of order higher than two, as well as other types of statistical quantities. The relations derived here will be used in the next chapter, in the context of nonlinear homogenization methods, to generate rigorous homogenization estimates for the statistics of the fields in viscoplastic composites.

In the next section, use will be made of the following lemma. Its proof has been given by Ponte Castañeda & Suquet (1998) (see Appendix B in that reference) for a scalar parameter t, but the proof applies *mutatis mutandis* when t is a tensor. It is a simple consequence of the chain rule, plus the fact that the effective potentials $\widetilde{W}_t$ and $\widetilde{U}_t$ are stationary with respect to $\boldsymbol{\varepsilon}_t$ and $\boldsymbol{\sigma}_t$, respectively.

Lemma 3.1.1. *Consider convex local potentials w_t and u_t depending on a parameter t. Then, the corresponding effective potentials $\widetilde{W}_t$ and $\widetilde{U}_t$ also depend on t, and assuming these potentials are differentiable with respect to this parameter, their derivatives with respect to t are given by*

$$\frac{\partial \widetilde{W}_t}{\partial t}(\overline{\boldsymbol{\varepsilon}}) = \left\langle \frac{\partial w_t}{\partial t}(\mathbf{x}, \boldsymbol{\varepsilon}_t) \right\rangle, \quad \frac{\partial \widetilde{U}_t}{\partial t}(\overline{\boldsymbol{\sigma}}) = \left\langle \frac{\partial u_t}{\partial t}(\mathbf{x}, \boldsymbol{\sigma}_t) \right\rangle, \tag{3.1}$$

where the local fields $\boldsymbol{\varepsilon}_t$ and $\boldsymbol{\sigma}_t$ are the solutions to the minimization problems (2.3)$_2$ and (2.8)$_2$, respectively, with w and u given by w_t and u_t. (The derivatives are taken with $\overline{\boldsymbol{\varepsilon}}$ and $\overline{\boldsymbol{\sigma}}$ held fixed.)

Thus, even though the local fields $\boldsymbol{\varepsilon}_t$ and $\boldsymbol{\sigma}_t$ depend on the parameter t, their derivatives with respect to t do not contribute to those of the effective potentials.

In what follows, it will be assumed for simplicity that the effective potentials are differentiable with respect to the relevant parameter t. While this is expected to hold in most cases of interest, it may not hold if the local potentials are not strictly convex, as in the ideally plastic limit, since the strain-rate field may not be unique in that case. However, if the nonsmooth effective potentials are convex/concave functions of t, which is generally case, relations similar to those derived below, which might involve inclusions rather than equalities, may also be obtained by making use of subdifferentials.

3.2 Exact relations for the statistics of the local fields

In this section, a methodology is provided for extracting, at least theoretically, the statistics of the strain-rate and stress fields, from the knowledge of the effective potentials of suitably perturbed problems. In general, the statistical information of interest corresponds to the first, second and higher moments of the fields in each phase. This is accomplished through the following propositions.

Proposition 3.2.1. *Consider a composite with local potential (2.2). The first moment, or phase average, of the strain rate in phase r is given by*

$$\overline{\boldsymbol{\varepsilon}}^{(r)} = \langle \boldsymbol{\varepsilon} \rangle^{(r)} = \frac{1}{c^{(r)}} \, \partial_{\boldsymbol{\tau}^{(r)}} \widetilde{W}_\tau \Big|_{\boldsymbol{\tau}^{(r)}=\mathbf{0}}, \tag{3.2}$$

where $\boldsymbol{\tau}^{(r)}$ is a constant, symmetric, second-order tensor, and $\widetilde{W}_\tau$ denotes the effective potential of a composite with (perturbed) local potential

$$w_\tau(\mathbf{x}, \boldsymbol{\varepsilon}) = \sum_{s=1}^{N} \chi^{(s)}(\mathbf{x}) \, w^{(s)}(\boldsymbol{\varepsilon}) + \chi^{(r)}(\mathbf{x}) \, \boldsymbol{\tau}^{(r)} \cdot \boldsymbol{\varepsilon}. \tag{3.3}$$

Proof. The local potential (3.3) is convex for any value of the parameter $\boldsymbol{\tau}^{(r)}$, and so the corresponding effective potential $\widetilde{W}_\tau$, which depends on $\boldsymbol{\tau}^{(r)}$, is well defined. It then follows from Lemma 3.1.1 that

$$\partial_{\boldsymbol{\tau}^{(r)}} \widetilde{W}_\tau(\overline{\boldsymbol{\varepsilon}}) = \langle \partial_{\boldsymbol{\tau}^{(r)}} w_\tau(\mathbf{x}, \boldsymbol{\varepsilon}_\tau) \rangle = \langle \, \chi^{(r)}(\mathbf{x}) \, \boldsymbol{\varepsilon}_\tau \rangle = c^{(r)} \langle \, \boldsymbol{\varepsilon}_\tau \rangle^{(r)}, \tag{3.4}$$

where $\boldsymbol{\varepsilon}_\tau$ is the solution to the minimization problem $(2.3)_2$ with a local potential given by (3.3), and the subscript τ has been used to emphasize that it depends on the parameter $\boldsymbol{\tau}^{(r)}$. In particular, for $\boldsymbol{\tau}^{(r)} = \mathbf{0}$, $\boldsymbol{\varepsilon}_\tau$ reduces to the strain rate field in a composite with local potential $(2.2)_2$, and so relation (3.2) follows.

□

Proposition 3.2.2. *Consider a composite with local potential (2.2). The even moments of order $2K$ ($K = 1, 2, 3, ...$) of the strain rate field in phase r are given by*

$$\langle \underbrace{\boldsymbol{\varepsilon} \otimes \boldsymbol{\varepsilon} \otimes ... \otimes \boldsymbol{\varepsilon}}_{2K \text{times}} \rangle^{(r)} = \frac{2K}{c^{(r)}} \, \partial_{\mathbf{t}^{(r)}} \widetilde{W}_t \Big|_{\mathbf{t}^{(r)}=\mathbf{0}}, \tag{3.5}$$

where $\mathbf{t}^{(r)}$ *is a constant, completely symmetric, positive semi-definite tensor of order* $4K$ *(from the space of* $2K$*-th tensors to the space of* $2K$*-th tensors), and* $\widetilde{W}_t$ *is the effective strain-rate potential of a composite with (perturbed) local potential*

$$w_t(\mathbf{x},\boldsymbol{\varepsilon}) = \sum_{s=1}^{N} \chi^{(s)}(\mathbf{x})\, w^{(s)}(\boldsymbol{\varepsilon}) + \chi^{(r)}(\mathbf{x})\, \frac{1}{2K} t^{(r)}_{ijkl\ldots} \underbrace{(\varepsilon_{ij}\varepsilon_{kl}\ldots)}_{2K\,\text{times}}. \tag{3.6}$$

Proof. Since $\mathbf{t}^{(r)}$ is a positive semi-definite tensor, the local potential (3.6) is convex, and so the corresponding effective potential $\widetilde{W}_t$ is well defined. Then, it follows from Lemma 3.1.1 that

$$\begin{aligned} \partial_{\mathbf{t}^{(r)}} \widetilde{W}_t(\overline{\boldsymbol{\varepsilon}}) = \langle \partial_{\mathbf{t}^{(r)}} w_t(\mathbf{x},\boldsymbol{\varepsilon}_t)\rangle &= \frac{1}{2K} \langle\, \chi^{(r)}(\mathbf{x})\, \underbrace{\boldsymbol{\varepsilon}_t \otimes \boldsymbol{\varepsilon}_t \otimes \ldots \otimes \boldsymbol{\varepsilon}_t}_{2K\,\text{times}} \rangle \\ &= \frac{c^{(r)}}{2K} \langle \underbrace{\boldsymbol{\varepsilon}_t \otimes \boldsymbol{\varepsilon}_t \otimes \ldots \otimes \boldsymbol{\varepsilon}_t}_{2K\,\text{times}} \rangle^{(r)}, \end{aligned} \tag{3.7}$$

where $\boldsymbol{\varepsilon}_t$ is the solution to the minimization problem $(2.3)_2$ with a local potential given by (3.6). For $\mathbf{t}^{(r)} = \mathbf{0}$, $\boldsymbol{\varepsilon}_t$ reduces to the strain-rate field in a composite with local potential $(2.2)_2$, and so relation (3.5) follows.

□

Thus, we have obtained identities expressing the phase averages and even moments of the strain-rate field in terms of suitably perturbed effective potentials. In the next chapter, the focus will be on moments up to second order, and it is then useful to consider the following corollary of Proposition 3.2.2 ($K = 1$).

Corollary 3.2.3. *Consider a composite with local potential (2.2). The second moments of the strain rate in phase* r *are given by*

$$\langle \boldsymbol{\varepsilon} \otimes \boldsymbol{\varepsilon} \rangle^{(r)} = \frac{2}{c^{(r)}}\, \partial_{\boldsymbol{\lambda}^{(r)}} \widetilde{W}_\lambda \Big|_{\boldsymbol{\lambda}^{(r)}=\mathbf{0}}, \tag{3.8}$$

where $\boldsymbol{\lambda}^{(r)}$ *is a constant, symmetric, positive semi-definite, fourth-order tensor, and* $\widetilde{W}_\lambda$ *denotes the effective potential of a composite with (perturbed) local potential*

$$w_\lambda(\boldsymbol{\varepsilon}) = \sum_{s=1}^{N} \chi^{(s)}(\mathbf{x}) w^{(s)}(\boldsymbol{\varepsilon}) + \chi^{(r)}(\mathbf{x})\, \frac{1}{2} \boldsymbol{\varepsilon} \cdot \boldsymbol{\lambda}^{(r)} \boldsymbol{\varepsilon}. \tag{3.9}$$

It is noted that the phase covariance tensors $\mathbf{C}^{(r)}_{\boldsymbol{\varepsilon}}$, which provide a measure of the intraphase field fluctuations, can be written in terms of $(3.2)_1$ and $(3.8)_1$:

$$\mathbf{C}^{(r)}_{\boldsymbol{\varepsilon}} \doteq \left\langle \left(\boldsymbol{\varepsilon} - \overline{\boldsymbol{\varepsilon}}^{(r)}\right) \otimes \left(\boldsymbol{\varepsilon} - \overline{\boldsymbol{\varepsilon}}^{(r)}\right) \right\rangle^{(r)} = \langle \boldsymbol{\varepsilon} \otimes \boldsymbol{\varepsilon} \rangle^{(r)} - \overline{\boldsymbol{\varepsilon}}^{(r)} \otimes \overline{\boldsymbol{\varepsilon}}^{(r)}. \tag{3.10}$$

When the potentials $w^{(r)}$ are quadratic, expressions (3.2) and (3.8) reduce to the well-known formulas $(2.42)_1$ and $(2.46)_1$ for linear composites. Of course, it is possible to obtain by completely analogous means corresponding expressions for the statistics of the stress field $\boldsymbol{\sigma}$ in terms of suitably perturbed *stress* potentials. For completeness, these expressions are spelled out next without proof.

Proposition 3.2.4. *Consider a composite with local potential (2.7). The first moment, or phase average, of the stress in phase r is given by*

$$\overline{\boldsymbol{\sigma}}^{(r)} = \langle \boldsymbol{\sigma} \rangle^{(r)} = \frac{1}{c^{(r)}} \, \partial_{\boldsymbol{\eta}^{(r)}} \widetilde{U}_\eta \Big|_{\boldsymbol{\eta}^{(r)}=\mathbf{0}} , \tag{3.11}$$

where $\boldsymbol{\eta}^{(r)}$ *is a constant, symmetric, second-order tensor, and* $\widetilde{U}_\eta$ *denotes the effective potential of a composite with (perturbed) local potential*

$$u_\eta(\mathbf{x}, \boldsymbol{\sigma}) = \sum_{s=1}^{N} \chi^{(s)}(\mathbf{x}) \, u^{(s)}(\boldsymbol{\sigma}) + \chi^{(r)}(\mathbf{x}) \, \boldsymbol{\eta}^{(r)} \cdot \boldsymbol{\sigma}. \tag{3.12}$$

Proposition 3.2.5. *Consider a composite with local potential (2.7). The even moments of order* $2K$ *(*$K = 1, 2, 3, ...$*) of the stress field in phase r are given by*

$$\langle \underbrace{\boldsymbol{\sigma} \otimes \boldsymbol{\sigma} \otimes ... \otimes \boldsymbol{\sigma}}_{2K \text{times}} \rangle^{(r)} = \frac{2K}{c^{(r)}} \, \partial_{\mathbf{t}^{(r)}} \widetilde{U}_t \Big|_{\mathbf{t}^{(r)}=\mathbf{0}} , \tag{3.13}$$

where $\mathbf{t}^{(r)}$ *is a constant, completely symmetric, positive semi-definite tensor of order* $4K$ *(from the space of* $2K$*-th tensors to the space of* $2K$*-th tensors), and* $\widetilde{U}_t$ *is the effective strain-rate potential of a composite with (perturbed) local potential*

$$u_t(\mathbf{x}, \boldsymbol{\sigma}) = \sum_{s=1}^{N} \chi^{(s)}(\mathbf{x}) \, u^{(s)}(\boldsymbol{\sigma}) + \chi^{(r)}(\mathbf{x}) \, \frac{1}{2K} t^{(r)}_{ijkl...} \underbrace{(\sigma_{ij}\sigma_{kl}...)}_{2K \text{times}} . \tag{3.14}$$

Corollary 3.2.6. *Consider a composite with local potential (2.7). The second moments of the stress in phase r are given by*

$$\langle \boldsymbol{\sigma} \otimes \boldsymbol{\sigma} \rangle^{(r)} = \frac{2}{c^{(r)}} \, \partial_{\boldsymbol{\mu}^{(r)}} \widetilde{U}_\mu \Big|_{\boldsymbol{\mu}^{(r)}=\mathbf{0}} , \tag{3.15}$$

where $\boldsymbol{\mu}^{(r)}$ *is a constant, symmetric, positive semi-definite, fourth-order tensor, and* $\widetilde{U}_\mu$ *denotes the effective potential of a composite with (perturbed) local potential*

$$u_\mu(\boldsymbol{\sigma}) = \sum_{s=1}^{N} \chi^{(s)}(\mathbf{x}) u^{(s)}(\boldsymbol{\sigma}) + \chi^{(r)}(\mathbf{x}) \, \frac{1}{2} \boldsymbol{\sigma} \cdot \boldsymbol{\mu}^{(r)} \boldsymbol{\sigma}. \tag{3.16}$$

Next, it is shown how the statistics of the *stress* field may be obtained in terms of suitably perturbed *strain-rate* potentials, which may be more useful in some cases.

Proposition 3.2.7. *Consider a composite with local potential (2.2). The first moment, or phase average, of the stress in phase r is given by*

$$\overline{\boldsymbol{\sigma}}^{(r)} = \langle \boldsymbol{\sigma} \rangle^{(r)} = -\frac{1}{c^{(r)}} \, \partial_{\boldsymbol{\eta}^{(r)}} \widetilde{W}_\eta \Big|_{\boldsymbol{\eta}^{(r)}=\mathbf{0}} , \tag{3.17}$$

where $\boldsymbol{\eta}^{(r)}$ *is a constant, symmetric, second-order tensor, and* $\widetilde{W}_\eta$ *denotes the effective potential of a composite with (perturbed) local potential* w_η *given by the Legendre transform of* u_η*,* $w_\eta = u^*_\eta$ *, where*

$$u_\eta(\mathbf{x}, \boldsymbol{\sigma}) = \sum_{s=1}^{N} \chi^{(s)}(\mathbf{x}) \, u^{(s)}(\boldsymbol{\sigma}) + \chi^{(r)}(\mathbf{x}) \, \boldsymbol{\eta}^{(r)} \cdot \boldsymbol{\sigma}. \tag{3.18}$$

Remark 3.2.8. *It is noted (van Tiel 1984) that w_η can be written in terms of the (unperturbed) potentials $w^{(r)}$ as*

$$w_\eta(\mathbf{x},\boldsymbol{\varepsilon}) = \sum_{\substack{s=1\\ s\neq r}}^{N} \chi^{(s)}(\mathbf{x})\, w^{(s)}(\boldsymbol{\varepsilon}) + \chi^{(r)}(\mathbf{x})\, w^{(r)}(\boldsymbol{\varepsilon}-\boldsymbol{\eta}^{(r)}). \tag{3.19}$$

Proof. The local potential (3.19) is convex for any value of the parameter $\boldsymbol{\eta}^{(r)}$, and so the corresponding effective potential $\widetilde{W}_\eta$, which depends on $\boldsymbol{\eta}^{(r)}$, is well defined. Then, it follows from Lemma 3.1.1 that

$$\begin{aligned} \partial_{\boldsymbol{\eta}^{(r)}} \widetilde{W}_\eta(\overline{\boldsymbol{\varepsilon}}) &= \Big\langle \partial_{\boldsymbol{\eta}^{(r)}} w_\eta(\mathbf{x},\boldsymbol{\varepsilon}_\eta) \Big\rangle \\ &= -\Big\langle \chi^{(r)}(\mathbf{x})\, \partial_{\boldsymbol{\varepsilon}} w^{(r)}(\boldsymbol{\varepsilon}_\eta - \boldsymbol{\eta}^{(r)}) \Big\rangle = -c^{(r)} \langle \boldsymbol{\sigma}_\eta \rangle^{(r)}, \end{aligned} \tag{3.20}$$

where $\boldsymbol{\varepsilon}_\eta$ is the solution to the minimization problem $(2.3)_2$ with a local potential given by (3.19), and $\boldsymbol{\sigma}_\eta = \partial_{\boldsymbol{\varepsilon}} w^{(r)}(\boldsymbol{\varepsilon}_\eta - \boldsymbol{\eta}^{(r)})$ is the corresponding stress. Relation (3.20) is valid for any value of $\boldsymbol{\eta}^{(r)}$. In particular, for $\boldsymbol{\eta}^{(r)} = \mathbf{0}$, $\boldsymbol{\varepsilon}_\eta$ and $\boldsymbol{\sigma}_\eta$ reduce to the strain and stress fields in a composite with local potential $(2.2)_2$, and so relation (3.17) follows.

□

Proposition 3.2.9. *Consider a composite with local potential (2.2). The even moments of order $2K$ ($K = 1, 2, 3, ...$) of the stress field in phase r are given by*

$$\langle \underbrace{\boldsymbol{\sigma}\otimes\boldsymbol{\sigma}\otimes ...\otimes\boldsymbol{\sigma}}_{2K\text{times}} \rangle^{(r)} = -\frac{2K}{c^{(r)}}\, \partial_{\mathbf{t}^{(r)}} \widetilde{W}_t\Big|_{\mathbf{t}^{(r)}=\mathbf{0}}, \tag{3.21}$$

where $\mathbf{t}^{(r)}$ is a constant, completely symmetric, positive semi-definite tensor of order $4K$, and $\widetilde{W}_t$ is the effective strain potential of a composite with a local potential w_t given by the Legendre transform of u_t, $w_t = w_t^*$, where

$$u_t(\mathbf{x},\boldsymbol{\sigma}) = \sum_{s=1}^{N} \chi^{(s)}(\mathbf{x})\, u^{(s)}(\boldsymbol{\sigma}) + \chi^{(r)}(\mathbf{x})\, \frac{1}{2K}\, t^{(r)}_{ijkl...} \underbrace{(\sigma_{ij}\sigma_{kl}...)}_{K\text{times}}. \tag{3.22}$$

Proof. Let $\widetilde{U}_t$ denote the effective stress potential of a composite with local potential (3.22). Since $\mathbf{t}^{(r)}$ is positive semi-definite, the potential (3.22) is convex, and so $\widetilde{U}_t$ is well defined. Let the strain potential w_t be the Legendre dual of (3.22), i.e., $w_t = u_t^*$, and let $\widetilde{W}_t$ be the corresponding effective strain potential. Then, $\widetilde{W}_t = \widetilde{U}_t^*$, or

$$\widetilde{W}_t(\overline{\boldsymbol{\varepsilon}}) = \sup_{\overline{\boldsymbol{\sigma}}} \Big[\overline{\boldsymbol{\sigma}} \cdot \overline{\boldsymbol{\varepsilon}} - \widetilde{U}_t(\overline{\boldsymbol{\sigma}}) \Big]. \tag{3.23}$$

Assuming the supremum over $\overline{\boldsymbol{\sigma}}$ in (3.23) is attained at a stationary point, and differentiating with respect to $\mathbf{t}^{(r)}$, we obtain

$$\partial_{\mathbf{t}^{(r)}} \widetilde{W}_t\Big|_{\mathbf{t}^{(r)}=\mathbf{0}} = -\,\partial_{\mathbf{t}^{(r)}} \widetilde{U}_t\Big|_{\mathbf{t}^{(r)}=\mathbf{0}} = -\frac{c^{(r)}}{2K} \langle \underbrace{\boldsymbol{\sigma}\otimes\boldsymbol{\sigma}\otimes ...\otimes\boldsymbol{\sigma}}_{2K\text{times}} \rangle^{(r)}, \tag{3.24}$$

where the last identity follows from the dual version of Proposition 3.2.2. Relation (3.21) follows immediately. □

In the next chapter, use is made of the following corollary of Proposition 3.2.9 ($K = 1$), for the second moments of the stress.

Corollary 3.2.10. *Consider a composite with local potential (2.2). The second moments of the stress in phase r are given by*

$$\langle \boldsymbol{\sigma} \otimes \boldsymbol{\sigma} \rangle^{(r)} = -\frac{2}{c^{(r)}}\, \partial_{\boldsymbol{\mu}^{(r)}} \widetilde{W}_\mu \Big|_{\boldsymbol{\mu}^{(r)}=\mathbf{0}}, \tag{3.25}$$

where $\boldsymbol{\mu}^{(r)}$ is a constant, symmetric, positive semi-definite, fourth-order tensor, and $\widetilde{W}_\mu$ denotes the effective potential of a composite with (perturbed) local potential w_μ given by the Legendre transform of u_μ, $w_\mu = u_\mu^*$, where

$$u_\mu(\boldsymbol{\sigma}) = \sum_{s=1}^{N} \chi^{(s)}(\mathbf{x})\, u^{(s)}(\boldsymbol{\sigma}) + \chi^{(r)}(\mathbf{x})\, \frac{1}{2}\boldsymbol{\sigma} \cdot \boldsymbol{\mu}^{(r)} \boldsymbol{\sigma}. \tag{3.26}$$

It is straightforward to verify that relations (3.2) and (3.17) for the phase averages are consistent with the macroscopic averages $(2.3)_1$ and $(2.8)_1$, so that

$$\overline{\boldsymbol{\varepsilon}} = \sum_{r=1}^{N} c^{(r)} \overline{\boldsymbol{\varepsilon}}^{(r)}, \quad \overline{\boldsymbol{\sigma}} = \sum_{r=1}^{N} c^{(r)} \overline{\boldsymbol{\sigma}}^{(r)}. \tag{3.27}$$

Once again, exactly analogous arguments can be used to derive expressions relating the statistics of the local strain-rate field and the effective stress potential $\widetilde{U}$. For completeness, these expressions are spelled out next without proof.

Proposition 3.2.11. *Consider a composite with local potential (2.7). The first moment, or phase average, of the strain rate in phase r is given by*

$$\overline{\boldsymbol{\varepsilon}}^{(r)} = \langle \boldsymbol{\varepsilon} \rangle^{(r)} = -\frac{1}{c^{(r)}}\, \partial_{\boldsymbol{\tau}^{(r)}} \widetilde{U}_\tau \Big|_{\boldsymbol{\tau}^{(r)}=\mathbf{0}}, \tag{3.28}$$

where $\boldsymbol{\tau}^{(r)}$ is a constant, symmetric, second-order tensor, and $\widetilde{U}_\tau$ denotes the effective potential of a composite with (perturbed) local potential u_τ given by the Legendre transform of w_τ, $u_\tau = w_\tau^*$, where

$$w_\tau(\mathbf{x}, \boldsymbol{\varepsilon}) = \sum_{s=1}^{N} \chi^{(s)}(\mathbf{x})\, w^{(s)}(\boldsymbol{\varepsilon}) + \chi^{(r)}(\mathbf{x})\, \boldsymbol{\tau}^{(r)} \cdot \boldsymbol{\varepsilon}. \tag{3.29}$$

Proposition 3.2.12. *Consider a composite with local potential (2.7). The even moments of order $2K$ $(K = 1, 2, 3, ...)$ of the strain-rate field in phase r are given by*

$$\langle \underbrace{\boldsymbol{\varepsilon} \otimes \boldsymbol{\varepsilon} \otimes ... \otimes \boldsymbol{\varepsilon}}_{2K\text{times}} \rangle^{(r)} = -\frac{2K}{c^{(r)}}\, \partial_{\mathbf{t}^{(r)}} \widetilde{U}_t \Big|_{\mathbf{t}^{(r)}=\mathbf{0}}, \tag{3.30}$$

where $\mathbf{t}^{(r)}$ is a constant, completely symmetric, positive semi-definite tensor of order $4K$, and $\widetilde{U}_t$ is the effective strain-rate potential of a composite with a local potential u_t given by the Legendre transform of w_t, $u_t = w_t^*$, where

$$w_t(\mathbf{x}, \boldsymbol{\varepsilon}) = \sum_{s=1}^{N} \chi^{(s)}(\mathbf{x})\, w^{(s)}(\boldsymbol{\varepsilon}) + \chi^{(r)}(\mathbf{x})\, \frac{1}{2K}\, t^{(r)}_{ijkl...} \underbrace{(\varepsilon_{ij}\varepsilon_{kl}...)}_{K\text{times}}. \tag{3.31}$$

3.3 Concluding remarks

We conclude this chapter by noting that the procedure presented here is by no means restricted to first and even moments, but can also be used to relate the average of more general functions of the local fields to the effective potentials. For instance, by considering perturbed phase potentials of the form $w_t^{(r)}(\boldsymbol{\varepsilon}) = w^{(r)}(\boldsymbol{\varepsilon}) + t\ \hat{w}^{(r)}(\boldsymbol{\varepsilon})$, with $t \geq 0$ and $\hat{w}^{(r)}$ denoting any convex function of $\boldsymbol{\varepsilon}$, it is possible to prove in a completely analogous fashion that the relation $\langle \hat{w}^{(r)}(\boldsymbol{\varepsilon}) \rangle^{(r)} = \partial_t\ \widetilde{W}_t|_{t=0}$ holds, where $\widetilde{W}_t$ denotes the corresponding perturbed effective potential. On the other hand, if the relevant perturbation term is not a convex function of the local fields, the problem can be mathematically more involved. For instance, relations for the odd moments (higher than one) of the local fields require the use of perturbed phase potentials that are non-convex and unbounded from below, and consequently the effective potentials must be appropriately re-defined. Similarly, relations for the K^{th} moments of the spin or vorticity tensor field $\omega(\mathbf{x})$, which are necessary to describe the evolution of the microstructure, require the use of pertubed phase potentials that depend on the full velocity gradient tensor $\nabla \mathbf{v}$, and so, again, appropriate re-definitions of the effective potentials are necessary.

Chapter 4

Homogenization estimates for viscoplastic composites with isotropic constituents

4.1 Introduction

The relations provided in the previous two chapters allow us to derive the effective behavior as well as the field statistics in viscoplastic composites, from suitably defined effective potentials. However, as has already been mentioned, these potentials are very difficult to compute exactly, and so there is a need to resort to approximate methods to *estimate* them. This is the subject of the present chapter.

In this work, the nonlinear homogenization methods of Ponte Castañeda (1991, 1996, 2002a) are considered. It is recalled that these methods are based on rigorous variational procedures, making use of the notion of 'linear comparison composite' (LCC), which has the same microstructure as the nonlinear composite, but whose phases are identified with appropriate linearizations of the nonlinear ones. In the following, the 'variational' (Ponte Castañeda 1991), 'tangent second-order' (Ponte Castañeda 1996) and 'second-order' (Ponte Castañeda 2002a) formulations are recalled, and the corresponding estimates for the effective behavior and the statistics of the local fields are derived. In this connection, it is emphasized that these LCC-based homogenization methods deliver estimates that are rigorous *only* for the effective potentials. Corresponding estimates for the effective behavior and field statistics must then be obtained by differentiation of these approximate potentials with respect to the relevant parameters. It is recalled, however, that Ponte Castañeda & Zaidman (1994) conjectured that the 'variational' estimates for the phase averages of the local fields in the nonlinear composite are given by the corresponding quantities in the associated LCC. Later, Kailasam and Ponte Castañeda (1998) demonstrated that this conjecture was indeed consistent with the *exact* version of the 'variational' method (Ponte Castañeda 1992a). In the context of the 'tangent second-order' and 'second-order' methods, Ponte Castañeda (2002a) (see also Idiart *et al.* 2006) suggested that the first as well as the second moments of the local fields in each phase of the LCC constitute reasonable approximations for the corresponding nonlinear estimates, even though the averaged sum of the phase averages of the dual variable does not coincide, in general, with the macroscopic average. As will be seen next, it follows from the exact relations derived in the previous chapter that the use of the field statistics

of the LCC as the nonlinear estimate is strictly valid only in the context of the 'variational' method, and does not hold in the context of the 'tangent second-order' and 'second-order' methods, where terms 'correcting' the field statistics of the LCC arise.

Finally, some modifications to the linearization scheme utilized in the context of the 'second-order' method are explored. In this connection, it is emphasized that, while the 'variational' and 'tangent second-order' methods have been fully optimized, the more recent 'second-order' method remains subject of on-going research, as is discussed below.

In the following, we restrict the analysis to composites made of *isotropic* phases, characterized by potentials of the form

$$w^{(r)}(\boldsymbol{\varepsilon}) = \frac{9}{2}\kappa^{(r)}\,\varepsilon_m^2 + \phi^{(r)}(\varepsilon_e), \quad u^{(r)}(\boldsymbol{\sigma}) = \frac{1}{2\kappa^{(r)}}\sigma_m^2 + \psi^{(r)}(\sigma_e), \tag{4.1}$$

where $\varepsilon_m = (1/3)\,\mathrm{tr}(\boldsymbol{\varepsilon})$ and $\sigma_m = (1/3)\,\mathrm{tr}(\boldsymbol{\sigma})$ denote the hydrostatic components of the strain-rate and stress tensors, and the von Mises equivalent strain rate and stress are given in terms of the deviatoric strain rate and stress tensors by $\varepsilon_e = \sqrt{(2/3)\boldsymbol{\varepsilon}_d \cdot \boldsymbol{\varepsilon}_d}$ and $\sigma_e = \sqrt{(3/2)\boldsymbol{\sigma}_d \cdot \boldsymbol{\sigma}_d}$. A particular example of potentials $\phi^{(r)}$ and $\psi^{(r)}$ is that corresponding to power-law behavior,

$$\phi^{(r)}(\varepsilon_e) = \frac{\sigma_0^{(r)}\varepsilon_0}{1+m}\left(\frac{\varepsilon_e}{\varepsilon_0}\right)^{1+m} \quad \text{and} \quad \psi^{(r)}(\sigma_e) = \frac{\sigma_0^{(r)}\varepsilon_0}{1+n}\left(\frac{\sigma_e}{\sigma_0^{(r)}}\right)^{1+n}, \tag{4.2}$$

where $m = 1/n$ is a strain-rate sensitivity, such that $0 \le m \le 1$, $\sigma_0^{(r)}$ is the flow stress of phase r, and ε_0 is a reference strain rate. This model is commonly used, for instance, to characterize the high-temperature steady creep of metals. The more general case of anisotropic constituents will be considered in Chapter 6.

4.2 'Variational' estimates

In this section, the so-called 'variational' method introduced by Ponte Castañeda (1991, 1992a) is considered. First, the 'variational' estimates for the effective potentials are recalled, and then, the corresponding estimates for the effective behavior and the field statistics are derived, making use of the exact relations provided in the previous chapters.

4.2.1 Effective potentials

The 'variational' method is based on the identity (Ponte Castañeda 1992a)

$$w^{(r)}(\boldsymbol{\varepsilon}) = \inf_{\mu_0^{(r)}>0}\left\{w_L^{(r)}(\boldsymbol{\varepsilon};\mu_0^{(r)}) + V^{(r)}(\mu_0^{(r)})\right\}, \tag{4.3}$$

which assumes that the isotropic potentials $(4.1)_1$ are *square concave* in ε_e, i.e., concave in ε_e^2. Also in this relation, $w_L^{(r)}$ denotes the phase potential of an isotropic linear material given by

$$w_L^{(r)}(\boldsymbol{\varepsilon};\mu_0^{(r)}) = \frac{1}{2}\boldsymbol{\varepsilon}\cdot\mathbf{L}_0^{(r)}\boldsymbol{\varepsilon}, \quad \mathbf{L}_0^{(r)} = 3\kappa^{(r)}\mathbf{J} + 2\mu_0^{(r)}\mathbf{K}, \tag{4.4}$$

and the function $V^{(r)}$ is defined by

$$\begin{aligned} V^{(r)}(\mu_0^{(r)}) &= \sup_{\boldsymbol{\varepsilon}^{(r)}} \left\{ w^{(r)}(\boldsymbol{\varepsilon}^{(r)}) - w_L^{(r)}(\boldsymbol{\varepsilon}^{(r)}; \mu_0^{(r)}) \right\} \\ &= \sup_{\varepsilon_e^{(r)}} \left\{ \phi^{(r)}(\varepsilon_e^{(r)}) - \frac{3}{2}\mu_0^{(r)}(\varepsilon_e^{(r)})^2 \right\}. \end{aligned} \tag{4.5}$$

In expression (4.4), $\mathbf{J}$ and $\mathbf{K}$ denote the standard fourth-order, isotropic, hydrostatic and shear projection tensors, and $\kappa^{(r)}$ are the same as those appearing in (4.1). From the square concavity hypothesis on the potentials $w^{(r)}$, or $\phi^{(r)}$, it follows that the term inside the curly brackets in (4.5) is concave in the variable $(\varepsilon_e^{(r)})$, and therefore the optimality condition in (4.5) is given by the 'secant' condition

$$\partial_{\boldsymbol{\varepsilon}} w^{(r)}(\hat{\boldsymbol{\varepsilon}}^{(r)}) = \mathbf{L}_0^{(r)} \hat{\boldsymbol{\varepsilon}}^{(r)}, \tag{4.6}$$

or equivalently,

$$\phi^{(r)\prime}(\hat{\varepsilon}_e^{(r)}) = 3\mu_0^{(r)} \hat{\varepsilon}_e^{(r)}, \tag{4.7}$$

where $\hat{\boldsymbol{\varepsilon}}^{(r)}$ denotes the optimal value of $\boldsymbol{\varepsilon}^{(r)}$ in (4.5).

Now, making use of the identity (4.3) in the definition (2.3) for the effective potential, and interchanging the infima over $\boldsymbol{\varepsilon}$ and $\mu_0^{(r)}$, an alternative, exact expression for $\widetilde{W}$ results. Then, an estimate for the effective potential $\widetilde{W}$ may be obtained by restricting the variables $\mu_0^{(r)}$ to be constant per phase. The estimate is a rigorous *upper* bound for $\widetilde{W}$, due to Ponte Castañeda (1991):

$$\widetilde{W}(\overline{\boldsymbol{\varepsilon}}) \leq \inf_{\mu_0^{(s)}>0} \left\{ \widetilde{W}_L(\overline{\boldsymbol{\varepsilon}}; \mu_0^{(s)}) + \sum_{r=1}^{N} c^{(r)}\, V^{(r)}(\mu_0^{(r)}) \right\}, \tag{4.8}$$

where $\widetilde{W}_L = (1/2)\overline{\boldsymbol{\varepsilon}} \cdot \widetilde{\mathbf{L}}_0 \overline{\boldsymbol{\varepsilon}}$ is the effective strain-rate potential of an LCC with phase potentials (4.4). In the following, equality will be used instead of the inequality, which is to be understood in the sense of a variational approximation. Thus, linear homogenization estimates are required for the effective viscosity tensor $\widetilde{\mathbf{L}}_0$ of the LCC to compute $\widetilde{W}_L$, such as the Hashin-Shtrikman estimates provided in Section 2.4. Then, the optimality conditions in (4.8) generate a system of algebraic nonlinear equations for the optimal values $\hat{\mu}_0^{(r)}$ of the variables $\mu_0^{(r)}$, which can be written as

$$\frac{1}{2c^{(r)}} \overline{\boldsymbol{\varepsilon}} \cdot \partial_{\mu_0^{(r)}} \widetilde{\mathbf{L}}_0(\hat{\mu}_0^{(s)}) \overline{\boldsymbol{\varepsilon}} + \partial_{\mu_0^{(r)}} V^{(r)}(\hat{\mu}_0^{(r)}) = 0. \tag{4.9}$$

Suquet (1995) remarked that the first term in this expression is nothing more than the second moment of the equivalent strain rate $\langle \varepsilon_{Le}^2 \rangle^{(r)}$ over phase r in the LCC, while it can be deduced from (4.5) that the second term is precisely $(\hat{\varepsilon}_e^{(r)})^2$ in the secant condition (4.7), and so it follows that

$$(\hat{\varepsilon}_e^{(r)})^2 = \frac{1}{3\ c^{(r)}}\ \overline{\boldsymbol{\varepsilon}} \cdot \partial_{\mu_0^{(r)}} \widetilde{\mathbf{L}}_0 \left(\hat{\mu}_0^{(s)} \right) \overline{\boldsymbol{\varepsilon}} = \langle \varepsilon_{Le}^2 \rangle^{(r)}, \tag{4.10}$$

and that the optimal viscosities $\hat{\mu}_0^{(s)}$ for the nonlinear composite can be given the interpretation of *secant* viscosities evaluated at the second moments of the strain-rate field, as depicted in figure 4.1. In addition, taking the hydrostatic part of the optimal tensors $\hat{\boldsymbol{\varepsilon}}^{(r)}$ to be given by

$$(\hat{\varepsilon}_m^{(r)})^2 = \frac{1}{9\ c^{(r)}}\ \overline{\boldsymbol{\varepsilon}} \cdot \partial_{\kappa^{(r)}} \widetilde{\mathbf{L}}_0 \left(\hat{\mu}_0^{(s)} \right) \overline{\boldsymbol{\varepsilon}} = \langle \varepsilon_{Lm}^2 \rangle^{(r)}, \tag{4.11}$$

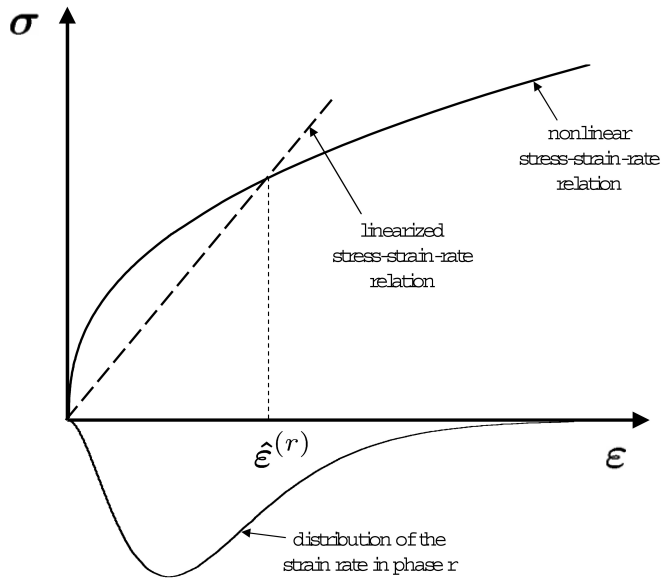

Figure 4.1: One-dimensional sketch of the nonlinear stress-strain-rate relation and the 'secant' linearization used by the 'variational' method.

it also follows that the estimate (4.8) for the effective potential can be written in the simpler form

$$\widetilde{W}(\overline{\boldsymbol{\varepsilon}}) = \sum_{r=1}^{N} c^{(r)} w^{(r)}(\hat{\boldsymbol{\varepsilon}}^{(r)}). \tag{4.12}$$

Alternate derivations of this result were provided independently by Suquet (1993) and Hu (1996) for the special class of power-law materials, and by Olson (1994) for the more specific case of ideally plastic materials.

'Variational' estimates for the dual potential $\widetilde{U}$ follow from exactly analogous expressions in terms of stress potentials $(4.1)_2$. The result is a rigorous *lower* bound for $\widetilde{U}$ (Ponte Castañeda 1991):

$$\widetilde{U}(\overline{\boldsymbol{\sigma}}) \geq \sup_{\mu_0^{(s)}>0} \left\{ \widetilde{U}_L(\overline{\boldsymbol{\sigma}}; \mu_0^{(s)}) - \sum_{r=1}^{N} c^{(r)}\, V^{(r)}(\mu_0^{(r)}) \right\}, \tag{4.13}$$

where $\widetilde{U}_L = (1/2)\overline{\boldsymbol{\sigma}} \cdot \widetilde{\mathbf{M}}_0 \overline{\boldsymbol{\sigma}}$ is the effective stress potential of an LCC with phase potentials

$$u_L^{(r)}(\boldsymbol{\sigma}; \mu_0^{(r)}) = \frac{1}{2}\boldsymbol{\sigma} \cdot \mathbf{M}_0^{(r)} \boldsymbol{\sigma}, \quad \mathbf{M}_0^{(r)} = \frac{1}{3\kappa^{(r)}}\mathbf{J} + \frac{1}{2\mu_0^{(r)}}\mathbf{K}, \tag{4.14}$$

and the function $V^{(r)}$ is defined by

$$\begin{aligned} V^{(r)}(\mu_0^{(r)}) &= \sup_{\boldsymbol{\sigma}^{(r)}} \left\{ u_L^{(r)}(\boldsymbol{\sigma}^{(r)}; \mu_0^{(r)}) - u^{(r)}(\boldsymbol{\sigma}^{(r)}) \right\} \\ &= \sup_{\sigma_e^{(r)}} \left\{ \frac{1}{6\mu_0^{(r)}} (\sigma_e^{(r)})^2 - \psi^{(r)}(\sigma_e^{(r)}) \right\}. \end{aligned} \tag{4.15}$$

These estimates assume that the potentials $\psi^{(r)}$ are *square convex* in σ_e, i.e., convex in the variable σ_e^2. Then, the term inside curly brackets in (4.15) being convex in σ_e^2, the optimality conditions in

(4.15) is given by the 'secant' condition

$$\partial_{\boldsymbol{\sigma}} u^{(r)}(\hat{\boldsymbol{\sigma}}^{(r)}) = \mathbf{M}_0^{(r)} \hat{\boldsymbol{\sigma}}^{(r)}, \tag{4.16}$$

or equivalently,

$$\psi^{(r)'}(\hat{\sigma}_e^{(r)}) = \frac{1}{6\mu_0^{(r)}} \hat{\sigma}_e^{(r)}, \tag{4.17}$$

where $\hat{\boldsymbol{\sigma}}^{(r)}$ denotes the optimal value of $\boldsymbol{\sigma}^{(r)}$ in (4.5). In addition, the optimality conditions in (4.13) for the variables $\mu_0^{(r)}$ are given by

$$\frac{1}{2c^{(r)}} \overline{\boldsymbol{\sigma}} \cdot \partial_{(\mu_0^{(r)})^{-1}} \widetilde{\mathbf{M}}_0(\hat{\mu}_0^{(s)}) \overline{\boldsymbol{\sigma}} + \partial_{(\mu_0^{(r)})^{-1}} V^{(r)}(\hat{\mu}_0^{(r)}) = 0. \tag{4.18}$$

Finally, taking the hydrostatic part of the optimal tensors $\hat{\boldsymbol{\sigma}}^{(r)}$ to be given by

$$(\hat{\sigma}_m^{(r)})^2 = \frac{2}{c^{(r)}} \, \overline{\boldsymbol{\sigma}} \cdot \partial_{(\kappa^{(r)})^{-1}} \widetilde{\mathbf{M}}_0 \left(\hat{\mu}_0^{(s)} \right) \overline{\boldsymbol{\sigma}} = \langle \sigma_{Lm}^2 \rangle^{(r)}, \tag{4.19}$$

the conditions (4.18) can be used to simplify the estimate (4.13) for the effective potential to

$$\widetilde{U}(\overline{\boldsymbol{\sigma}}) = \sum_{r=1}^{N} c^{(r)} u^{(r)}(\hat{\boldsymbol{\sigma}}^{(r)}). \tag{4.20}$$

The 'variational' estimates (4.8) and (4.13) can be shown (Ponte Castañeda 1992a) to be exactly equivalent, in the sense that they are Legendre duals of each other, i.e. $\widetilde{W} = \widetilde{U}^*$ and $\widetilde{U} = \widetilde{W}^*$. In addition, the optimal LCC's associated with each of these estimates are also equivalent to each other, i.e. $u_L^{(r)} = (w_L^{(r)})^*$ and $w_L^{(r)} = (u_L^{(r)})^*$. In other words, the 'variational' estimates exhibit no *duality gap*. In turn, this implies that the 'variational' estimates for the effective potentials are convex, since $\widetilde{W}^{**} = \widetilde{U}^* = \widetilde{W}$, and similarly, $\widetilde{U}^{**} = \widetilde{W}^* = \widetilde{U}$, in agreement with the exact solution.

4.2.2 Effective behavior and field statistics

The 'variational' estimate for the effective behavior of the viscoplastic composite is obtained by differentiation of (4.8) with respect to $\overline{\boldsymbol{\varepsilon}}$. This is made more explicit in the following result, due to deBotton & Ponte Castañeda (1993).

Result 4.2.1. *Since the estimate (4.8) is stationary with respect to the variables $\mu_0^{(r)}$, it follows that the 'variational' estimate for the effective behavior is given by*

$$\overline{\boldsymbol{\sigma}} = \partial_{\overline{\boldsymbol{\varepsilon}}} \widetilde{W}(\overline{\boldsymbol{\varepsilon}}) = \partial_{\overline{\boldsymbol{\varepsilon}}} \widetilde{W}_L(\overline{\boldsymbol{\varepsilon}}; \hat{\mu}_0^{(s)}) = \widetilde{\mathbf{L}}_0(\hat{\mu}_0^{(s)}) \overline{\boldsymbol{\varepsilon}} = \overline{\boldsymbol{\sigma}}_L, \tag{4.21}$$

where $\widetilde{\mathbf{L}}_0$ is evaluated at the optimal values $\hat{\mu}_0^{(r)}$ from equations (4.9), and the notation $\overline{\boldsymbol{\sigma}}_L$ has been used to emphasize that it corresponds to the macroscopic stress in the LCC.

Thus, the 'variational' estimate for the macroscopic stress in the nonlinear composite *coincides* with that in the LCC evaluated at the $\hat{\mu}_0^{(r)}$. It is emphasized, however, that the stress-strain-rate relation (4.21) is nonlinear, as it should be, since the moduli $\hat{\mu}_0^{(r)}$, and therefore $\widetilde{\mathbf{L}}_0$, depend on $\overline{\boldsymbol{\varepsilon}}$. In

fact, recalling that the $\hat{\mu}_0^{(r)}$ can be identified with secant moduli evaluated at the second moments of the strain-rate field (in the LCC), the 'variational' estimate (4.21) can be given the interpretation of a 'modified secant' estimate for the effective stress-strain-rate relation.

In order to obtain corresponding 'variational' estimates for the phase averages of the strain rate, we consider a composite with (perturbed) phase potentials $w_\tau^{(r)}$ given by (3.3), where $w^{(r)}$ is given by $(4.1)_1$, and we evaluate the derivative (3.2) with $\widetilde{W}_\tau$ given by the 'variational' procedure described above. Similarly, 'variational' estimates for the second moments of the strain rate, as well as the first and second moments of the stress, can be obtained by considering (perturbed) potentials (3.9), (3.19) and (3.26), and differentiating the 'variational' estimates for the corresponding effective potentials with respect to the perturbation parameters. These estimates are spelled out in the following result.

Result 4.2.2. *The 'variational' estimates for the first and second moments of the local fields are given by*

$$\overline{\boldsymbol{\varepsilon}}^{(r)} = \overline{\boldsymbol{\varepsilon}}_L^{(r)}, \qquad \langle \boldsymbol{\varepsilon} \otimes \boldsymbol{\varepsilon} \rangle^{(r)} = \langle \boldsymbol{\varepsilon}_L \otimes \boldsymbol{\varepsilon}_L \rangle^{(r)}, \tag{4.22}$$

$$\overline{\boldsymbol{\sigma}}^{(r)} = \overline{\boldsymbol{\sigma}}_L^{(r)}, \qquad \langle \boldsymbol{\sigma} \otimes \boldsymbol{\sigma} \rangle^{(r)} = \langle \boldsymbol{\sigma}_L \otimes \boldsymbol{\sigma}_L \rangle^{(r)}, \tag{4.23}$$

where, again, the subscript L has been used to denote quantities in the LCC associated with the 'variational' estimate (4.8).

Proof. We begin by proving the identity $(4.22)_1$ for the phase averages of the strain rate. In order to make use of proposition 3.2.1, we consider a composite with perturbed local potential (3.3), where the unperturbed phase potentials $w^{(s)}$ are given by $(4.1)_1$. Thus, phase r in this composite is characterized by

$$w_\tau^{(r)}(\boldsymbol{\varepsilon}) = w^{(r)}(\boldsymbol{\varepsilon}) + \boldsymbol{\tau}^{(r)} \cdot \boldsymbol{\varepsilon}. \tag{4.24}$$

Making use of the identity (4.3) for $w^{(r)}$, this potential can be written as

$$w_\tau^{(r)}(\boldsymbol{\varepsilon}) = \inf_{\mu_0^{(r)} > 0} \left\{ w_{L\tau}^{(r)}(\boldsymbol{\varepsilon}; \mu_0^{(r)}) + V^{(r)}(\mu_0^{(r)}) \right\}. \tag{4.25}$$

where $w_{L\tau}^{(r)}$ denotes the phase potential of a perturbed (anisotropic) LCC, given in terms of (4.4) by

$$w_{L\tau}^{(r)}(\boldsymbol{\varepsilon}; \mu_0^{(r)}) = w_L^{(r)}(\boldsymbol{\varepsilon}; \mu_0^{(r)}) + \boldsymbol{\tau}^{(r)} \cdot \boldsymbol{\varepsilon}. \tag{4.26}$$

The 'variational' estimate for the perturbed effective potential $\widetilde{W}_\tau$ is then obtained by following the procedure described in the context of expression (4.8). The resulting expression for $\widetilde{W}_\tau$ is in fact (4.8), but with $\widetilde{W}_L$ replaced by $\widetilde{W}_{L\tau}$, the effective potential of the perturbed LCC with phase r characterized by (4.26). Then, recalling that the 'variational' estimate for $\widetilde{W}_\tau$ is stationary with respect to the variables $\mu_0^{(r)}$, and that the functions $V^{(r)}$ do not depend explicitly on the parameters $\boldsymbol{\tau}^{(r)}$, it follows from proposition 3.2.1 that the 'variational' estimate for the average of the strain rate in phase r is given by

$$\overline{\boldsymbol{\varepsilon}}^{(r)} = \frac{1}{c^{(r)}} \, \partial_{\boldsymbol{\tau}^{(r)}} \widetilde{W}_\tau \Big|_{\boldsymbol{\tau}^{(r)} = \mathbf{0}} = \frac{1}{c^{(r)}} \, \partial_{\boldsymbol{\tau}^{(r)}} \widetilde{W}_{L\tau} \Big|_{\boldsymbol{\tau}^{(r)} = \mathbf{0}} = \overline{\boldsymbol{\varepsilon}}_L^{(r)}, \tag{4.27}$$

where $\overline{\boldsymbol{\varepsilon}}_L^{(r)}$ denotes the average strain rate in phase r in the LCC associated with the estimate (4.8) for the unperturbed effective potential $\widetilde{W}$, and the last identity follows also from proposition 3.2.1.

The remaining estimates in result 4.2.2 can be derived in a completely analogous fashion, by making use of proposition 3.2.7 and corollaries 3.2.3 and 3.2.10, and identities for the relevant perturbed phase potentials analogous to (4.25) with perturbed (anisotropic) LCC phase potentials given in terms of (4.4) by

$$w_{L\lambda}^{(r)}(\boldsymbol{\varepsilon};\mu_0^{(r)}) = w_L^{(r)}(\boldsymbol{\varepsilon};\mu_0^{(r)}) + \frac{1}{2}\boldsymbol{\varepsilon}\cdot\boldsymbol{\lambda}^{(r)}\boldsymbol{\varepsilon}, \tag{4.28}$$

$$w_{L\eta}^{(r)}(\boldsymbol{\varepsilon};\mu_0^{(r)}) = w_L^{(r)}(\boldsymbol{\varepsilon}-\boldsymbol{\eta}^{(r)};\mu_0^{(r)}), \tag{4.29}$$

$$w_{L\mu}^{(r)}(\boldsymbol{\varepsilon};\mu_0^{(r)}) = \inf_{\boldsymbol{\varepsilon}_1+\boldsymbol{\varepsilon}_2=\boldsymbol{\varepsilon}}\left[w_L^{(r)}(\boldsymbol{\varepsilon}_1;\mu_0^{(r)}) + \frac{1}{2}\boldsymbol{\varepsilon}_2\cdot(\boldsymbol{\mu}^{(r)})^{-1}\boldsymbol{\varepsilon}_2\right]. \tag{4.30}$$

□

Thus, the 'variational' estimates for the first and second moments of the local fields *coincide* with those in the LCC. This result is in exact agreement with the conjecture of Ponte Castañeda & Zaidman (1994). It is also worth noting that the nonlinear estimates for the phase averages are consistent with the corresponding estimates for the macroscopic behavior (4.21), in the sense that they satisfy the relations

$$\overline{\boldsymbol{\varepsilon}} = \sum_{r=1}^{N} c^{(r)}\overline{\boldsymbol{\varepsilon}}^{(r)}, \quad \overline{\boldsymbol{\sigma}} = \sum_{r=1}^{N} c^{(r)}\overline{\boldsymbol{\sigma}}^{(r)}. \tag{4.31}$$

(This is so provided the linear estimates used in the context of the LCC are themselves consistent.) It is useful to recall here that the phase averages and second moments of the strain rate and stress fields in the LCC can be computed from (see Chapter 2)

$$\overline{\boldsymbol{\varepsilon}}_L^{(r)} = \mathbf{A}_0^{(r)}\overline{\boldsymbol{\varepsilon}}, \quad \langle\boldsymbol{\varepsilon}_L\otimes\boldsymbol{\varepsilon}_L\rangle^{(r)} = \frac{2}{c^{(r)}}\partial_{\mathbf{L}_0^{(r)}}\widetilde{W}_L, \tag{4.32}$$

$$\overline{\boldsymbol{\sigma}}_L^{(r)} = \mathbf{L}_0^{(r)}\overline{\boldsymbol{\varepsilon}}_L^{(r)}, \quad \langle\boldsymbol{\sigma}_L\otimes\boldsymbol{\sigma}_L\rangle^{(r)} = \mathbf{L}_0^{(r)}\,\langle\boldsymbol{\varepsilon}_L\otimes\boldsymbol{\varepsilon}_L\rangle^{(r)}\,\mathbf{L}_0^{(r)}, \tag{4.33}$$

where $\mathbf{A}_0^{(r)}$ are the strain-rate-concentration tensors, which depend on the linear homogenization method utilized, and the $\mathbf{L}_0^{(r)}$ are evaluated at the optimal $\hat{\mu}_0^{(r)}$.

Following exactly similar arguments, it can be shown that the field statistics arising from the 'variational' estimates for the stress potential $\widetilde{U}$ also coincide with those in the associated LCC. Thus, the identities (4.22)-(4.23) also hold for the dual version of the method, and are, of course, entirely consistent with those resulting from the potential $\widetilde{W}$.

Finally, it is noted that a similar procedure can be used with proposition 3.2.2 to generalize the above results to higher-order moments.

Remark 4.2.3. *The 'variational' estimates for the 2K moments of the local fields in the nonlinear composite are given by*

$$\langle\underbrace{\boldsymbol{\varepsilon}\otimes\boldsymbol{\varepsilon}\otimes\ldots\otimes\boldsymbol{\varepsilon}}_{2K\text{times}}\rangle^{(r)} = \langle\underbrace{\boldsymbol{\varepsilon}_L\otimes\boldsymbol{\varepsilon}_L\otimes\ldots\otimes\boldsymbol{\varepsilon}_L}_{2K\text{times}}\rangle^{(r)}, \tag{4.34}$$

$$\langle\underbrace{\boldsymbol{\sigma}\otimes\boldsymbol{\sigma}\otimes\ldots\otimes\boldsymbol{\sigma}}_{2K\text{times}}\rangle^{(r)} = \langle\underbrace{\boldsymbol{\sigma}_L\otimes\boldsymbol{\sigma}_L\otimes\ldots\otimes\boldsymbol{\sigma}_L}_{2K\text{times}}\rangle^{(r)}. \tag{4.35}$$

Unfortunately, these results are not very useful, because there are no simple formulas to extract the moments of order higher than 2 in linear composites. This suggests making use of the variational method itself to estimate these higher order moments, which can be shown to yield estimates for the higher-order moments of the nonlinear composite depending only on the second-order moments of the field in the LCC. While such estimates would be easily computed, it is unlikely that they would be very accurate.

4.3 'Tangent second-order' estimates

The 'variational' method considered in the previous section delivers estimates for the effective potentials that are exact only to first order in the heterogeneity contrast. In this section we consider the so-called 'tangent second-order' method introduced by Ponte Castañeda (1996), which delivers estimates for the effective potentials that are exact to second order in the heterogeneity contrast, and are therefore expected to be more accurate in general.

4.3.1 Effective potentials

The 'tangent second-order' method makes use of the following identity for the phase potentials $w^{(r)}$ (Ponte Castañeda & Willis 1999):

$$w^{(r)}(\boldsymbol{\varepsilon}) = \underset{\check{\boldsymbol{\varepsilon}}^{(r)}}{\text{stat}} \left\{ w_L^{(r)}(\boldsymbol{\varepsilon}; \check{\boldsymbol{\varepsilon}}^{(r)}, \mathbf{L}_0^{(r)}) \right\}, \tag{4.36}$$

where the stat*ionary* operation consists in setting the partial derivative of the argument with respect to the variable equal to zero, and $w_L^{(r)}$ is the potential of a linear *thermoelastic* comparison composite defined in terms of a reference strain rate tensor $\check{\boldsymbol{\varepsilon}}^{(r)}$ and a tensor of moduli $\mathbf{L}_0^{(r)}$ by

$$w_L^{(r)}(\boldsymbol{\varepsilon}; \check{\boldsymbol{\varepsilon}}^{(r)}, \mathbf{L}_0^{(r)}) = w^{(r)}(\check{\boldsymbol{\varepsilon}}^{(r)}) + \partial_{\boldsymbol{\varepsilon}} w^{(r)}(\check{\boldsymbol{\varepsilon}}^{(r)}) \cdot (\boldsymbol{\varepsilon} - \check{\boldsymbol{\varepsilon}}^{(r)}) + \frac{1}{2}(\boldsymbol{\varepsilon} - \check{\boldsymbol{\varepsilon}}^{(r)}) \cdot \mathbf{L}_0^{(r)}(\boldsymbol{\varepsilon} - \check{\boldsymbol{\varepsilon}}^{(r)}). \tag{4.37}$$

Note that the identity (4.36) is valid for any $\mathbf{L}_0^{(r)}$. The 'tangent second-order' estimates for the effective potential $\widetilde{W}$ is then obtained by introducing (4.36) into (2.3), interchanging the optimization operations over $\boldsymbol{\varepsilon}(\mathbf{x})$ and $\check{\boldsymbol{\varepsilon}}^{(r)}$, and restricting the latter to be constant per phase. The result of this calculation is the approximation

$$\widetilde{W}(\overline{\boldsymbol{\varepsilon}}) = \underset{\check{\boldsymbol{\varepsilon}}^{(s)}}{\text{stat}} \left\{ \widetilde{W}_L(\overline{\boldsymbol{\varepsilon}}; \check{\boldsymbol{\varepsilon}}^{(s)}, \mathbf{L}_0^{(s)}) \right\}, \tag{4.38}$$

where $\widetilde{W}_L$ is the effective strain rate potential of the thermoelastic LCC with phase potentials (4.37). The stationary operation in (4.38) leads to the conditions:

$$\check{\boldsymbol{\varepsilon}}^{(r)} = \overline{\boldsymbol{\varepsilon}}_L^{(r)}, \tag{4.39}$$

where the $\overline{\boldsymbol{\varepsilon}}_L^{(r)}$ denote the averages of the strain rate in phase r of the associated LCC, which depends on the $\check{\boldsymbol{\varepsilon}}^{(s)}$ and $\mathbf{L}_0^{(s)}$ according to the homogenization procedure utilized (see expression (4.48) below). Given this choice for the variables $\check{\boldsymbol{\varepsilon}}^{(r)}$, it is not possible to make the resulting estimate stationary with

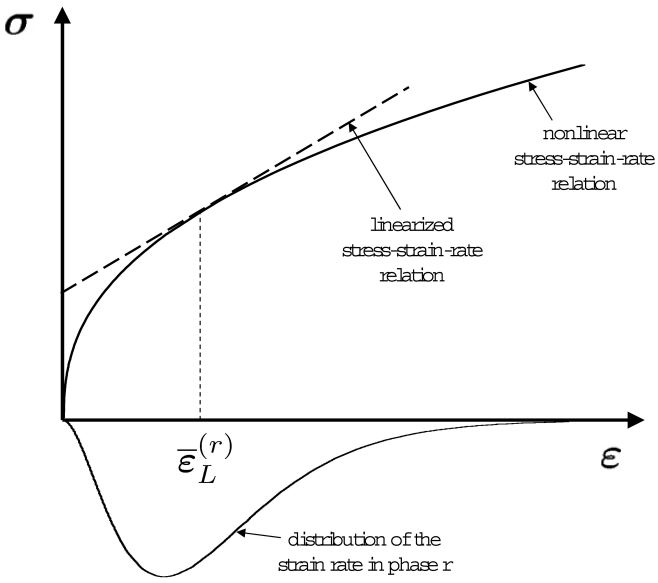

Figure 4.2: One-dimensional sketch of the nonlinear stress-strain-rate relation and the 'secant' linearization used by the 'tangent second-order' method.

respect to the tensors $\mathbf{L}_0^{(r)}$. For this reason, the following physically motivated choice was proposed (Ponte Castañeda 1996) for these tensors:

$$\mathbf{L}_0^{(r)} = \mathbf{L}_t^{(r)}(\check{\boldsymbol{\varepsilon}}^{(r)}) \doteq \partial^2_{\boldsymbol{\varepsilon}\boldsymbol{\varepsilon}} w^{(r)}(\check{\boldsymbol{\varepsilon}}^{(r)}), \tag{4.40}$$

which identifies the tensors $\mathbf{L}_0^{(r)}$ with the tangent viscosity tensors. For potentials $w^{(r)}$ of the form $(4.1)_1$, the tangent viscosity tensors are of the form

$$\mathbf{L}_t^{(r)}(\check{\boldsymbol{\varepsilon}}^{(r)}) = 3\kappa^{(r)}\mathbf{J} + \phi^{(r)\prime\prime}(\check{\varepsilon}_e^{(r)})\ \mathbf{E}^{(r)} + \frac{2}{3}\frac{\phi^{(r)\prime}(\check{\varepsilon}_e^{(r)})}{\check{\varepsilon}_e^{(r)}}\ \mathbf{F}^{(r)}, \tag{4.41}$$

with the projection tensors $\mathbf{E}^{(r)}$ and $\mathbf{F}^{(r)}$ given by

$$\mathbf{E}^{(r)} = \frac{2}{3}\frac{\check{\boldsymbol{\varepsilon}}_d^{(r)}}{\check{\varepsilon}_e^{(r)}} \otimes \frac{\check{\boldsymbol{\varepsilon}}_d^{(r)}}{\check{\varepsilon}_e^{(r)}}, \quad \mathbf{F}^{(r)} = \mathbf{K} - \mathbf{E}^{(r)}. \tag{4.42}$$

Thus, the relations (4.39) and (4.40) serve to specify the variables $\check{\boldsymbol{\varepsilon}}^{(r)}$ and $\mathbf{L}_0^{(r)}$ defining the phase potentials (4.37) of the LCC in terms of the phase averages of the strain-rate field in the phases of the LCC, itself. Figure 4.2 shows a sketch of this linearization scheme, which should be compared with figure 4.1.

Finally, the conditions (4.39) and (4.40) for the reference strain rates $\check{\boldsymbol{\varepsilon}}^{(r)}$ and viscosity tensors $\mathbf{L}_0^{(r)}$ can be used to simplify the expression for the effective potential (4.38) to

$$\widetilde{W}(\overline{\boldsymbol{\varepsilon}}) = \sum_{r=1}^{N} c^{(r)} \left[w^{(r)}(\overline{\boldsymbol{\varepsilon}}_L^{(r)}) + \frac{1}{2}\mathbf{C}_{\boldsymbol{\varepsilon}_L}^{(r)} \cdot \mathbf{L}_t^{(r)}(\overline{\boldsymbol{\varepsilon}}_L^{(r)}) \right], \tag{4.43}$$

where the $\mathbf{C}_{\boldsymbol{\varepsilon}_L}^{(r)}$ denote the phase covariance tensors of the strain rate in the LCC (see below). Further simplification results from the use of the Euler-Lagrange equations of the LCC problem, so that this

expression can be written in terms of the $\overline{\boldsymbol{\varepsilon}}_L^{(r)}$ only (Nebozhyn & Ponte Castañeda 1998, Ponte Castañeda & Suquet 1998):

$$\widetilde{W}(\overline{\boldsymbol{\varepsilon}}) = \sum_{r=1}^{N} c^{(r)} \left[w^{(r)}(\overline{\boldsymbol{\varepsilon}}_L^{(r)}) + \frac{1}{2}\partial_{\boldsymbol{\varepsilon}} w^{(r)}(\overline{\boldsymbol{\varepsilon}}_L^{(r)}) \cdot \left(\overline{\boldsymbol{\varepsilon}} - \overline{\boldsymbol{\varepsilon}}_L^{(r)} \right) \right]. \tag{4.44}$$

Thus, it is seen that the determination of the effective potential for the nonlinear composite requires the computation of the phase averages and phase covariance tensors of the strain-rate field in the LCC defined by the phase potentials (4.37). In addition, the corresponding estimates for the effective behavior and field statistics derived in the next subsection, require the computation of the phase averages and phase covariance tensors of the stress field in the LCC. The phase potentials (4.37) of this 'thermoelastic' LCC may be rewritten in the form

$$w_L^{(r)}(\boldsymbol{\varepsilon}; \check{\boldsymbol{\varepsilon}}^{(r)}, \mathbf{L}_0^{(r)}) = \frac{1}{2}\boldsymbol{\varepsilon} \cdot \mathbf{L}_0^{(r)} \boldsymbol{\varepsilon} + \boldsymbol{\tau}_0^{(r)} \cdot \boldsymbol{\varepsilon} + f_0^{(r)}, \tag{4.45}$$

where the 'thermal stress' $\boldsymbol{\tau}_0^{(r)}$ and 'specific heat' $f_0^{(r)}$ are defined in terms of $\check{\boldsymbol{\varepsilon}}^{(r)}$ and $\mathbf{L}_0^{(r)}$ via

$$\boldsymbol{\tau}_0^{(r)} = \partial_{\boldsymbol{\varepsilon}} w^{(r)}(\check{\boldsymbol{\varepsilon}}^{(r)}) - \mathbf{L}_0^{(r)} \check{\boldsymbol{\varepsilon}}^{(r)}, \quad f_0^{(r)} = w^{(r)}(\check{\boldsymbol{\varepsilon}}^{(r)}) - \boldsymbol{\tau}_0^{(r)} \cdot \check{\boldsymbol{\varepsilon}}^{(r)} - \frac{1}{2}\check{\boldsymbol{\varepsilon}}^{(r)} \cdot \mathbf{L}_0^{(r)} \check{\boldsymbol{\varepsilon}}^{(r)}. \tag{4.46}$$

The effective potential of this LCC can thus be written as (see Chapter 2)

$$\widetilde{W}_L(\overline{\boldsymbol{\varepsilon}}) = \frac{1}{2}\overline{\boldsymbol{\varepsilon}} \cdot \widetilde{\mathbf{L}}_0 \overline{\boldsymbol{\varepsilon}} + \widetilde{\boldsymbol{\tau}}_0 \cdot \overline{\boldsymbol{\varepsilon}} + \widetilde{f}_0, \tag{4.47}$$

where $\widetilde{\mathbf{L}}_0$, $\widetilde{\boldsymbol{\tau}}_0$ and $\widetilde{f}_0$ depend on the linear homogenization estimates utilized. Then, the phase averages and second moments of the local fields in the LCC can be extracted from the relations provided in Chapter 2, namely,

$$\overline{\boldsymbol{\varepsilon}}_L^{(r)} = \mathbf{A}_0^{(r)} \overline{\boldsymbol{\varepsilon}} + \mathbf{a}_0^{(r)}, \qquad \langle \boldsymbol{\varepsilon}_L \otimes \boldsymbol{\varepsilon}_L \rangle^{(r)} = \mathbf{C}_{\boldsymbol{\varepsilon}_L}^{(r)} + \overline{\boldsymbol{\varepsilon}}_L^{(r)} \otimes \overline{\boldsymbol{\varepsilon}}_L^{(r)}, \tag{4.48}$$

$$\overline{\boldsymbol{\sigma}}_L^{(r)} = \mathbf{L}_0^{(r)} \overline{\boldsymbol{\varepsilon}}_L^{(r)} + \boldsymbol{\tau}_0^{(r)}, \quad \langle \boldsymbol{\sigma}_L \otimes \boldsymbol{\sigma}_L \rangle^{(r)} = \overline{\boldsymbol{\sigma}}_L^{(r)} \otimes \overline{\boldsymbol{\sigma}}_L^{(r)} + \mathbf{L}_0^{(r)} \mathbf{C}_{\boldsymbol{\varepsilon}_L}^{(r)} \mathbf{L}_0^{(r)}, \tag{4.49}$$

where the $\mathbf{A}_0^{(r)}$ and $\mathbf{a}_0^{(r)}$ are strain-rate-concentration tensors that depend on the linear homogenization method utilized, and the phase covariance tensors $\mathbf{C}_{\boldsymbol{\varepsilon}_L}^{(r)}$ are given by

$$\mathbf{C}_{\boldsymbol{\varepsilon}_L}^{(r)} \doteq \left\langle (\boldsymbol{\varepsilon}_L - \overline{\boldsymbol{\varepsilon}}_L^{(r)}) \otimes (\boldsymbol{\varepsilon}_L - \overline{\boldsymbol{\varepsilon}}_L^{(r)}) \right\rangle^{(r)} = \frac{2}{c^{(r)}} \partial_{\mathbf{L}_0^{(r)}} \widetilde{W}_L. \tag{4.50}$$

In this last relation, the derivatives should be taken with the $\check{\boldsymbol{\varepsilon}}^{(r)}$ held fixed.

'Tangent second-order' estimates for the dual potential $\widetilde{U}$ follow from exactly analogous expressions in terms of stress potentials $u^{(r)}$ and $u_L^{(r)}$. The result is the approximation

$$\widetilde{U}(\overline{\boldsymbol{\sigma}}) = \underset{\check{\boldsymbol{\sigma}}^{(s)}}{\text{stat}} \left\{ \widetilde{U}_L(\overline{\boldsymbol{\sigma}}; \check{\boldsymbol{\sigma}}^{(s)}, \mathbf{M}_0^{(s)}) \right\}, \tag{4.51}$$

where $\widetilde{U}_L$ is the effective stress potential of an LCC with phase potentials

$$\begin{aligned} u_L^{(r)}(\boldsymbol{\sigma}; \check{\boldsymbol{\sigma}}^{(r)}, \mathbf{M}_0^{(r)}) &= u^{(r)}(\check{\boldsymbol{\sigma}}^{(r)}) + \partial_{\boldsymbol{\sigma}} u^{(r)}(\check{\boldsymbol{\sigma}}^{(r)}) \cdot (\boldsymbol{\sigma} - \check{\boldsymbol{\sigma}}^{(r)}) + ... \\ &\quad ... + \frac{1}{2}(\boldsymbol{\sigma} - \check{\boldsymbol{\sigma}}^{(r)}) \cdot \mathbf{M}_0^{(r)} (\boldsymbol{\sigma} - \check{\boldsymbol{\sigma}}^{(r)}). \end{aligned} \tag{4.52}$$

In this case, the stationarity condition in (4.51) leads to the conditions

$$\check{\boldsymbol{\sigma}}^{(r)} = \overline{\boldsymbol{\sigma}}_L^{(r)}, \tag{4.53}$$

where the $\overline{\boldsymbol{\sigma}}_L^{(r)}$ denote the averages of the stress in phase r of the associated LCC, while the compliance tensors $\mathbf{M}^{(r)}$ are taken to be the tangent compliances of the phases:

$$\mathbf{M}_0^{(r)} = \mathbf{M}_t^{(r)}(\check{\boldsymbol{\sigma}}^{(r)}) \doteq \partial^2_{\boldsymbol{\sigma}\boldsymbol{\sigma}} u^{(r)}(\check{\boldsymbol{\sigma}}^{(r)}), \tag{4.54}$$

For potentials $u^{(r)}$ of the form $(4.1)_2$, the tangent compliance tensors are of the form

$$\mathbf{M}_t^{(r)}(\check{\boldsymbol{\sigma}}^{(r)}) = \frac{1}{3\kappa^{(r)}}\mathbf{J} + \psi^{(r)''}(\check{\sigma}_e^{(r)})\ \mathbf{E}^{(r)} + \frac{3}{2}\frac{\psi^{(r)'}(\check{\sigma}_e^{(r)})}{\check{\sigma}_e^{(r)}}\ \mathbf{F}^{(r)}, \tag{4.55}$$

with the projection tensors $\mathbf{E}^{(r)}$ and $\mathbf{F}^{(r)}$ given by

$$\mathbf{E}^{(r)} = \frac{3}{2}\frac{\check{\boldsymbol{\sigma}}_d^{(r)}}{\check{\sigma}_e^{(r)}} \otimes \frac{\check{\boldsymbol{\sigma}}_d^{(r)}}{\check{\sigma}_e^{(r)}}, \quad \mathbf{F}^{(r)} = \mathbf{K} - \mathbf{E}^{(r)}. \tag{4.56}$$

The LCC being a 'thermoelastic' composite, with phase polarizations $\boldsymbol{\eta}_0^{(r)} = \partial_{\boldsymbol{\sigma}} u^{(r)}(\check{\boldsymbol{\sigma}}^{(r)}) - \mathbf{M}_0^{(r)}\check{\boldsymbol{\sigma}}^{(r)}$, the phase averages and second moments of the fields in each phase can be computed from the relations provided in Chapter 2, namely,

$$\overline{\boldsymbol{\sigma}}_L^{(r)} = \mathbf{B}_0^{(r)}\overline{\boldsymbol{\sigma}} + \mathbf{b}_0^{(r)}, \qquad \langle \boldsymbol{\sigma}_L \otimes \boldsymbol{\sigma}_L \rangle^{(r)} = \mathbf{C}^{(r)}_{\boldsymbol{\sigma}_L} + \overline{\boldsymbol{\sigma}}_L^{(r)} \otimes \overline{\boldsymbol{\sigma}}_L^{(r)}, \tag{4.57}$$

$$\overline{\boldsymbol{\varepsilon}}_L^{(r)} = \mathbf{M}_0^{(r)}\overline{\boldsymbol{\sigma}}_L^{(r)} + \boldsymbol{\eta}_0^{(r)}, \quad \langle \boldsymbol{\varepsilon}_L \otimes \boldsymbol{\varepsilon}_L \rangle^{(r)} = \overline{\boldsymbol{\varepsilon}}_L^{(r)} \otimes \overline{\boldsymbol{\varepsilon}}_L^{(r)} + \mathbf{M}_0^{(r)}\mathbf{C}^{(r)}_{\boldsymbol{\sigma}_L}\mathbf{M}_0^{(r)}, \tag{4.58}$$

where the $\mathbf{B}_0^{(r)}$ and $\mathbf{b}_0^{(r)}$ are stress-concentration tensors that depend on the linear homogenization method utilized, and the phase covariance tensors $\mathbf{C}^{(r)}_{\boldsymbol{\sigma}_L}$ are given by

$$\mathbf{C}^{(r)}_{\boldsymbol{\sigma}_L} \doteq \left\langle (\boldsymbol{\sigma}_L - \overline{\boldsymbol{\sigma}}_L^{(r)}) \otimes (\boldsymbol{\sigma}_L - \overline{\boldsymbol{\sigma}}_L^{(r)}) \right\rangle^{(r)} = \frac{2}{c^{(r)}}\partial_{\mathbf{M}_0^{(r)}}\widetilde{U}_L. \tag{4.59}$$

In this last relation, the derivatives should be taken with the $\check{\boldsymbol{\sigma}}^{(r)}$ held fixed.

Finally, the stationarity condition (4.53) for the reference stress $\check{\boldsymbol{\sigma}}^{(r)}$ can be used to simplify the expression for the effective potential (4.51) to

$$\widetilde{U}(\overline{\boldsymbol{\sigma}}) = \sum_{r=1}^{N} c^{(r)} \left[u^{(r)}(\overline{\boldsymbol{\sigma}}_L^{(r)}) + \frac{1}{2}\mathbf{C}^{(r)}_{\boldsymbol{\sigma}_L} \cdot \mathbf{M}_t^{(r)}(\overline{\boldsymbol{\sigma}}_L^{(r)}) \right], \tag{4.60}$$

which can be further simplified to

$$\widetilde{U}(\overline{\boldsymbol{\sigma}}) = \sum_{r=1}^{N} c^{(r)} \left[u^{(r)}(\overline{\boldsymbol{\sigma}}_L^{(r)}) + \frac{1}{2}\partial_{\boldsymbol{\sigma}} u^{(r)}(\overline{\boldsymbol{\sigma}}_L^{(r)}) \cdot \left(\overline{\boldsymbol{\sigma}} - \overline{\boldsymbol{\sigma}}_L^{(r)} \right) \right]. \tag{4.61}$$

The estimates (4.38) and (4.51) for the effective potentials can be shown to agree with the exact small-contrast expansion of Suquet & Ponte Castañeda (1993) to second order, hence the name of the method. However, it should be emphasized that, in general, the estimates (4.38) and (4.51) are *not* equivalent, in the sense that they are not Legendre duals of each other. In other words, unlike the

'variational' estimates provided in the previous section, the 'tangent second-order' estimates exhibit a duality gap. In fact, it is known (see Nebozhyn & Ponte Castañeda 1998) that the estimates (4.38) and (4.51) can be *non-convex* in certain cases, and therefore they cannot coincide with their convex envelopes, in general. The source of this duality gap is the lack of stationarity of the estimates (4.38) and (4.51) with respect to the tensors $\mathbf{L}_0^{(r)}$ and $\mathbf{M}_0^{(r)}$. (The reader is referred to Ponte Castañeda (2002a) for a more detailed discussion on this issue.) Also, it is precisely because of this lack of stationarity of the estimates for the effective potentials that the corresponding estimates for the effective stress-strain-rate relation and field statistics are given by those in the LCC plus some 'correction' terms, as described in the next subsection.

4.3.2 Effective behavior and field statistics

The 'tangent second-order' estimates for the effective behavior of the viscoplastic composite are obtained by differentiation of (4.38) and (4.51) with respect to $\overline{\boldsymbol{\varepsilon}}$ and $\overline{\boldsymbol{\sigma}}$, respectively. The 'strain-rate' estimate for the effective behavior is made more explicit in the following result, due to Nebozhyn & Ponte Castañeda (1998) (see also, Ponte Castañeda & Suquet 1998).

Result 4.3.1. *The 'tangent second-order' estimate for the effective stress-strain-rate relation is given by*

$$\overline{\boldsymbol{\sigma}} = \partial_{\overline{\boldsymbol{\varepsilon}}}\widetilde{W}(\overline{\boldsymbol{\varepsilon}}) = \overline{\boldsymbol{\sigma}}_L + \sum_{r=1}^{N} c^{(r)}\boldsymbol{\rho}^{(r)} \cdot \partial_{\overline{\boldsymbol{\varepsilon}}}\overline{\boldsymbol{\varepsilon}}_L^{(r)}, \tag{4.62}$$

where $\overline{\boldsymbol{\sigma}}_L$ denotes the macroscopic stress in the LCC, and the tensors $\boldsymbol{\rho}^{(r)}$ are defined in terms of the phase covariance tensors $\mathbf{C}_{\boldsymbol{\varepsilon}_L}^{(r)}$ of the strain rate in the LCC via

$$\boldsymbol{\rho}^{(r)} = \frac{1}{2}\mathbf{C}_{\boldsymbol{\varepsilon}_L}^{(r)} \cdot \partial_{\boldsymbol{\varepsilon}}\mathbf{L}_t^{(r)}(\overline{\boldsymbol{\varepsilon}}_L^{(r)}). \tag{4.63}$$

In expressions (4.62) and (4.63), the notation $\mathbf{a}\cdot\partial_{\mathbf{c}}\mathbf{b}$ and $\mathbf{A}\cdot\partial_{\mathbf{c}}\mathbf{B}$ has been used to denote second-order tensors with ij^{th} components $a_{kl}\partial b_{kl}/\partial c_{ij}$ and $A_{klmn}\partial B_{klmn}/\partial c_{ij}$.

As in the context of the 'variational' estimates, corresponding 'tangent second-order' estimates for the first and second moments of the local fields are obtained by considering composites with perturbed phase potentials (3.3), (3.9), (3.19) and (3.26), and evaluating the derivatives (3.2), (3.8), (3.17) and (3.25), with $\widetilde{W}_\tau$, $\widetilde{W}_\lambda$, $\widetilde{W}_\eta$ and $\widetilde{W}_\mu$ given by the 'tangent second-order' procedure. The latter are given by expression (4.38), with $\widetilde{W}_L$ replaced by the effective potential of the relevant perturbed LCC, respectively, $\widetilde{W}_{L\tau}$, $\widetilde{W}_{L\lambda}$, $\widetilde{W}_{L\eta}$, and $\widetilde{W}_{L\mu}$. The potentials in phase r of these perturbed LCCs are given by expressions analogous to (4.26), (4.28), (4.29) and (4.30), with $w_L^{(r)}$ given by (4.37). In addition, the modulus tensors $\mathbf{L}_0^{(r)}$ are still given by (4.40), and the reference tensors $\check{\boldsymbol{\varepsilon}}^{(r)}$ follow from the appropriate stationarity condition (with $\mathbf{L}_0^{(r)}$ held fixed). In the results below, the symbols $\overline{\boldsymbol{\varepsilon}}_{L\tau}^{(r)}$, $\overline{\boldsymbol{\varepsilon}}_{L\eta}^{(r)}$, $\overline{\boldsymbol{\varepsilon}}_{L\lambda}^{(r)}$ and $\overline{\boldsymbol{\varepsilon}}_{L\mu}^{(r)}$ denote the phase averages in the perturbed LCCs.

Result 4.3.2. *The 'tangent second-order' estimates for the first and second moments of the local*

fields are given by

$$\overline{\boldsymbol{\varepsilon}}^{(r)} = \overline{\boldsymbol{\varepsilon}}_L^{(r)} + \sum_{s=1}^{N} \frac{c^{(s)}}{c^{(r)}}\, \boldsymbol{\rho}^{(s)} \cdot \partial_{\boldsymbol{\tau}^{(r)}} \overline{\boldsymbol{\varepsilon}}_{L\tau}^{(s)}\Big|_{\boldsymbol{\tau}^{(r)}=\mathbf{0}}, \tag{4.64}$$

$$\langle \boldsymbol{\varepsilon} \otimes \boldsymbol{\varepsilon} \rangle^{(r)} = \langle \boldsymbol{\varepsilon}_L \otimes \boldsymbol{\varepsilon}_L \rangle^{(r)} + 2 \sum_{s=1}^{N} \frac{c^{(s)}}{c^{(r)}}\, \boldsymbol{\rho}^{(s)} \cdot \partial_{\boldsymbol{\lambda}^{(r)}} \overline{\boldsymbol{\varepsilon}}_{L\lambda}^{(s)}\Big|_{\boldsymbol{\lambda}^{(r)}=\mathbf{0}}, \tag{4.65}$$

$$\overline{\boldsymbol{\sigma}}^{(r)} = \overline{\boldsymbol{\sigma}}_L^{(r)} + \boldsymbol{\rho}^{(r)} - \sum_{s=1}^{N} \frac{c^{(s)}}{c^{(r)}}\, \boldsymbol{\rho}^{(s)} \cdot \partial_{\boldsymbol{\eta}^{(r)}} \overline{\boldsymbol{\varepsilon}}_{L\eta}^{(s)}\Big|_{\boldsymbol{\eta}^{(r)}=\mathbf{0}}, \tag{4.66}$$

$$\langle \boldsymbol{\sigma} \otimes \boldsymbol{\sigma} \rangle^{(r)} = \langle \boldsymbol{\sigma}_L \otimes \boldsymbol{\sigma}_L \rangle^{(r)} + 2\overline{\boldsymbol{\sigma}}_L^{(r)} \otimes_s \boldsymbol{\rho}^{(r)} - 2 \sum_{s=1}^{N} \frac{c^{(s)}}{c^{(r)}}\, \boldsymbol{\rho}^{(s)} \cdot \partial_{\boldsymbol{\mu}^{(r)}} \overline{\boldsymbol{\varepsilon}}_{L\mu}^{(s)}\Big|_{\boldsymbol{\mu}^{(r)}=\mathbf{0}}, \tag{4.67}$$

where the symbol $\otimes_s$ denotes symmetrized tensor product, and the subscript L has been used to denote, once again, quantities in the LCC.

Proof. We begin by proving the identity (4.64) for the phase averages of the strain rate. In order to make use of proposition 3.2.1, we consider a composite with perturbed local potential (3.3). Thus, phase r in this composite is characterized by (4.24). Making use of the identity (4.36) for the unperturbed potential $w^{(r)}$, we can write the perturbed potential as

$$w_\tau^{(r)}(\boldsymbol{\varepsilon}) = \operatorname*{stat}_{\check{\boldsymbol{\varepsilon}}^{(r)}} \left\{ w_{L\tau}^{(r)}(\boldsymbol{\varepsilon}; \check{\boldsymbol{\varepsilon}}^{(r)}, \mathbf{L}_0^{(r)}) \right\}, \tag{4.68}$$

where $w_{L\tau}^{(r)}$ denotes the phase potential of the perturbed LCC, given in terms of (4.37) by (4.26). The 'tangent second-order' estimate for the perturbed effective potential $\widetilde{W}_\tau$ is thus given by (4.38), with $\widetilde{W}_L$ replaced by $\widetilde{W}_{L\tau}$, the effective potential of the perturbed LCC with phase r characterized by $w_{L\tau}^{(r)}$. The optimal tensors $\check{\boldsymbol{\varepsilon}}^{(r)}$ and $\mathbf{L}_0^{(r)}$ in the perturbed problem are given by (4.39) and (4.40) , with $\overline{\boldsymbol{\varepsilon}}_L^{(r)}$ replaced by $\overline{\boldsymbol{\varepsilon}}_{L\tau}^{(r)}$, the phase averages of the strain rate in the perturbed LCC. Then, recalling that the 'tangent second-order' estimate for $\widetilde{W}_\tau$ is stationary with respect to the variables $\check{\boldsymbol{\varepsilon}}^{(r)}$, but not with respect to the variables $\mathbf{L}_0^{(r)}$, and noting that the latter depend on $\boldsymbol{\tau}^{(r)}$ only through the tensors $\check{\boldsymbol{\varepsilon}}^{(r)}$, we have that

$$\begin{aligned} \partial_{\boldsymbol{\tau}^{(r)}} \widetilde{W}_\tau\Big|_{\boldsymbol{\tau}^{(r)}=\mathbf{0}} &= \partial_{\boldsymbol{\tau}^{(r)}} \widetilde{W}_{L\tau}\Big|_{\boldsymbol{\tau}^{(r)}=\mathbf{0}} + \sum_{s=1}^{N} \left(\partial_{\check{\boldsymbol{\varepsilon}}^{(s)}} \mathbf{L}_0^{(s)} \cdot \partial_{\mathbf{L}_0^{(s)}} \widetilde{W}_L \right) \cdot \partial_{\boldsymbol{\tau}^{(r)}} \check{\boldsymbol{\varepsilon}}^{(s)}\Big|_{\boldsymbol{\tau}^{(r)}=\mathbf{0}} \\ &= c^{(r)} \overline{\boldsymbol{\varepsilon}}_L^{(r)} + \sum_{s=1}^{N} c^{(s)} \boldsymbol{\rho}^{(s)} \cdot \partial_{\boldsymbol{\tau}^{(r)}} \overline{\boldsymbol{\varepsilon}}_{L\tau}^{(s)}\Big|_{\boldsymbol{\tau}^{(r)}=\mathbf{0}}, \end{aligned} \tag{4.69}$$

where the derivative of $\widetilde{W}_{L\tau}$ is taken with the $\mathbf{L}_0^{(r)}$ held fixed. In the last equality, use has been made of proposition 3.2.1 in the first term, and (4.40), (4.63) and (4.50) in the second term. Finally, the identity (4.64) follows from proposition 3.2.1 with (4.69). The identity (4.65) can be derived in an analogous manner, making use of corollary 3.2.3.

Next, we prove the identity (4.66). In order to make use of proposition 3.2.7, we consider a composite with perturbed local potential (3.18). Thus, phase r in this composite is characterized by $w_\eta^{(r)} = (u_\eta^{(r)})^*$, where

$$u_\eta^{(r)}(\boldsymbol{\sigma}) = u^{(r)}(\boldsymbol{\sigma}) + \boldsymbol{\eta}^{(r)} \cdot \boldsymbol{\sigma}, \tag{4.70}$$

with $u^{(r)} = (w^{(r)})^*$. Making use of the dual version of the identity (4.36) for $u^{(r)}$, we can write (4.70) as

$$u_\eta^{(r)}(\boldsymbol{\sigma}) = \underset{\check{\boldsymbol{\sigma}}^{(r)}}{\operatorname{stat}} \left\{ u_L^{(r)}(\boldsymbol{\sigma}; \check{\boldsymbol{\sigma}}^{(r)}, \mathbf{M}_0^{(r)}) + \boldsymbol{\eta}^{(r)} \cdot \boldsymbol{\sigma} \right\}. \tag{4.71}$$

Performing the change of variables (see Ponte Castañeda 2002a)

$$\mathbf{L}_0^{(r)} = \left(\mathbf{M}_0^{(r)} \right)^{-1}, \quad \check{\boldsymbol{\varepsilon}}^{(r)} = \frac{\partial u^{(r)}}{\partial \boldsymbol{\sigma}}(\check{\boldsymbol{\sigma}}^{(r)}), \tag{4.72}$$

the Legendre transform of (4.71) can be written as

$$w_\eta^{(r)}(\boldsymbol{\varepsilon}) = \underset{\check{\boldsymbol{\varepsilon}}^{(r)}}{\operatorname{stat}} \left\{ w_{L\eta}^{(r)}(\boldsymbol{\varepsilon}; \check{\boldsymbol{\varepsilon}}^{(r)}, \mathbf{L}_0^{(r)}) \right\}, \tag{4.73}$$

where $w_{L\eta}^{(r)}$ is given by (4.29) with $w_L^{(r)}$ given by (4.37). The 'tangent second-order' estimate for the perturbed effective potential $\widetilde{W}_\eta$ is thus given by (4.38) with $\widetilde{W}_L$ replaced by $\widetilde{W}_{L\eta}$, the effective potential of a perturbed LCC with phase r characterized by (4.73). The optimal tensors $\check{\boldsymbol{\varepsilon}}^{(r)}$ in the perturbed problem are then

$$\check{\boldsymbol{\varepsilon}}^{(r)} = \overline{\boldsymbol{\varepsilon}}_{L\eta}^{(r)} - \boldsymbol{\eta}^{(r)}, \tag{4.74}$$

and the tensors $\mathbf{L}_0^{(r)}$ are related to $\check{\boldsymbol{\varepsilon}}^{(r)}$ by (4.40). Then, recalling that the 'tangent second-order' estimate for $\widetilde{W}_\eta$ is stationary with respect to the variables $\check{\boldsymbol{\varepsilon}}^{(r)}$ but not with respect to the variables $\mathbf{L}_0^{(r)}$, and noting that the latter depend on $\boldsymbol{\eta}^{(r)}$ only through the tensors $\check{\boldsymbol{\varepsilon}}^{(r)}$, we have that

$$\begin{aligned} \partial_{\boldsymbol{\eta}^{(r)}} \widetilde{W}_\eta \Big|_{\boldsymbol{\eta}^{(r)}=\mathbf{0}} &= \partial_{\boldsymbol{\eta}^{(r)}} \widetilde{W}_{L\eta} \Big|_{\boldsymbol{\eta}^{(r)}=\mathbf{0}} + \sum_{s=1}^{N} \left(\partial_{\check{\boldsymbol{\varepsilon}}^{(s)}} \mathbf{L}_0^{(s)} \cdot \partial_{\mathbf{L}_0^{(s)}} \widetilde{W}_L \right) \cdot \partial_{\boldsymbol{\eta}^{(r)}} \check{\boldsymbol{\varepsilon}}^{(s)} \Big|_{\boldsymbol{\eta}^{(r)}=\mathbf{0}} \\ &= -c^{(r)} \overline{\boldsymbol{\sigma}}_L^{(r)} - c^{(r)} \boldsymbol{\rho}^{(r)} + \sum_{s=1}^{N} c^{(s)} \boldsymbol{\rho}^{(s)} \cdot \partial_{\boldsymbol{\eta}^{(r)}} \overline{\boldsymbol{\varepsilon}}_{L\eta}^{(s)} \Big|_{\boldsymbol{\eta}^{(r)}=\mathbf{0}}, \end{aligned} \tag{4.75}$$

where the derivative of $\widetilde{W}_{L\eta}$ is taken with the $\mathbf{L}_0^{(r)}$ held fixed. In the last equality, use has been made of proposition 3.2.7 in the first term, and (4.40), (4.63), (4.50) and (4.74) in the second term. Finally, the identity (4.66) follows from proposition 3.2.7 with (4.75). The identity (4.67) can be derived in an analogous manner, making use of corollary 3.2.10.

□

Several observations are relevant in the context of result 4.3.2. First, it can be shown that the estimates (4.64) and (4.66) for the phase averages are consistent with the corresponding estimates (4.62) for the effective behavior, in the sense that they satisfy relations (3.27). This implies that the derivatives appearing in (4.64) and (4.66) satisfy the constraints

$$\sum_{r=1}^{N} \sum_{s=1}^{N} c^{(s)} \boldsymbol{\rho}^{(s)} \cdot \partial_{\boldsymbol{\tau}^{(r)}} \overline{\boldsymbol{\varepsilon}}_{L\tau}^{(s)} \Big|_{\boldsymbol{\tau}^{(r)}=\mathbf{0}} = \mathbf{0}, \tag{4.76}$$

$$\sum_{r=1}^{N} \sum_{s=1}^{N} c^{(s)} \boldsymbol{\rho}^{(s)} \cdot \partial_{\boldsymbol{\eta}^{(r)}} \overline{\boldsymbol{\varepsilon}}_{L\eta}^{(s)} \Big|_{\boldsymbol{\eta}^{(r)}=\mathbf{0}} = \sum_{r=1}^{N} c^{(r)} \left[\boldsymbol{\rho}^{(r)} - \boldsymbol{\rho}^{(r)} \cdot \partial_{\overline{\boldsymbol{\varepsilon}}} \overline{\boldsymbol{\varepsilon}}_L^{(r)} \right]. \tag{4.77}$$

It can also be shown that the estimates (4.64) to (4.67) are exact to first order in the heterogeneity contrast, which follows from the fact that the estimate (4.38) for $\widetilde{W}$ is exact to second order. Third,

it is interesting to note that the terms 'correcting' the LCC quantities (effective behavior and field statistics) depend explicitly on the intraphase field fluctuations, through the tensors $\mathbf{C}^{(r)}_{\boldsymbol{\varepsilon}_L}$, and on the degree of nonlinearity of the local potential, through the tensors $\partial_{\boldsymbol{\varepsilon}}\mathbf{L}^{(r)}_t$ (which vanish in the linear case). Moreover, the 'correction' of a nonlinear quantity in phase r depends explicitly, in general, on the properties of all other phases. It is worth mentioning that the derivatives appearing in expressions (4.64)-(4.67) can be expressed in terms of the unperturbed phase averages $\overline{\boldsymbol{\varepsilon}}^{(r)}_L$, by differentiating the perturbed system of nonlinear equations $(4.48)_1$ with respect to the perturbation parameter, setting the parameter equal to zero, and inverting the resulting system of *linear* equations for the derivatives. Finally, it is noted that the 'affine' formulation of Masson *et al.* (2000) for nonlinear composites amounts to dropping the 'correction' terms in expressions (4.62) and (4.64)-(4.67), thus taking the effective behavior and field statistics in the LCC directly as the corresponding nonlinear estimates. Unfortunately, even though this approximation simplifies the computations, the 'correction' terms are usually not negligible, and may even be several times larger than the terms arising from the LCC for sufficiently strong nonlinearities.

Of course, analogous expressions can also be derived from the dual formulation, for the effective stress-strain-rate relation, and the first and second moments of the local fields. These formulas are spelled out in the following result, where the symbols $\overline{\boldsymbol{\sigma}}^{(r)}_{L\tau}$, $\overline{\boldsymbol{\sigma}}^{(r)}_{L\eta}$, $\overline{\boldsymbol{\sigma}}^{(r)}_{L\lambda}$ and $\overline{\boldsymbol{\sigma}}^{(r)}_{L\mu}$ denote the phase averages in the relevant, perturbed LCCs.

Result 4.3.3. *The 'tangent second-order' estimate arising from the stress version, for the effective stress-strain-rate relation is given by*

$$\overline{\boldsymbol{\varepsilon}} = \partial_{\overline{\boldsymbol{\sigma}}}\widetilde{U}(\overline{\boldsymbol{\sigma}}) = \overline{\boldsymbol{\varepsilon}}_L + \sum_{r=1}^{N} c^{(r)}\boldsymbol{\gamma}^{(r)} \cdot \partial_{\overline{\boldsymbol{\sigma}}}\overline{\boldsymbol{\sigma}}^{(r)}_L, \tag{4.78}$$

and the corresponding estimates for first and second moments of the local fields are given by

$$\overline{\boldsymbol{\sigma}}^{(r)} = \overline{\boldsymbol{\sigma}}^{(r)}_L + \sum_{s=1}^{N} \frac{c^{(s)}}{c^{(r)}}\, \boldsymbol{\gamma}^{(s)} \cdot \partial_{\boldsymbol{\eta}^{(r)}}\overline{\boldsymbol{\sigma}}^{(s)}_{L\eta}\Big|_{\boldsymbol{\eta}^{(r)}=\mathbf{0}}, \tag{4.79}$$

$$\langle \boldsymbol{\sigma}\otimes\boldsymbol{\sigma}\rangle^{(r)} = \langle \boldsymbol{\sigma}_L\otimes\boldsymbol{\sigma}_L\rangle^{(r)} + 2\sum_{s=1}^{N} \frac{c^{(s)}}{c^{(r)}}\, \boldsymbol{\gamma}^{(s)} \cdot \partial_{\boldsymbol{\mu}^{(r)}}\overline{\boldsymbol{\sigma}}^{(s)}_{L\mu}\Big|_{\boldsymbol{\mu}^{(r)}=\mathbf{0}}, \tag{4.80}$$

$$\overline{\boldsymbol{\varepsilon}}^{(r)} = \overline{\boldsymbol{\varepsilon}}^{(r)}_L + \boldsymbol{\gamma}^{(r)} - \sum_{s=1}^{N} \frac{c^{(s)}}{c^{(r)}}\, \boldsymbol{\gamma}^{(s)} \cdot \partial_{\boldsymbol{\tau}^{(r)}}\overline{\boldsymbol{\sigma}}^{(s)}_{L\tau}\Big|_{\boldsymbol{\tau}^{(r)}=\mathbf{0}}, \tag{4.81}$$

$$\langle \boldsymbol{\varepsilon}\otimes\boldsymbol{\varepsilon}\rangle^{(r)} = \langle \boldsymbol{\varepsilon}_L\otimes\boldsymbol{\varepsilon}_L\rangle^{(r)} + 2\overline{\boldsymbol{\varepsilon}}^{(r)}_L \otimes_s \boldsymbol{\gamma}^{(r)} - 2\sum_{s=1}^{N} \frac{c^{(s)}}{c^{(r)}}\, \boldsymbol{\gamma}^{(s)} \cdot \partial_{\boldsymbol{\tau}^{(r)}}\overline{\boldsymbol{\sigma}}^{(s)}_{L\lambda}\Big|_{\boldsymbol{\lambda}^{(r)}=\mathbf{0}}. \tag{4.82}$$

In these expressions, the subscript L has been used to denote quantities in the LCC, and the tensors $\boldsymbol{\gamma}^{(r)}$ *are defined in terms of the phase covariance tensors* $\mathbf{C}^{(r)}_{\boldsymbol{\sigma}_L}$ *of the stress in the LCC via*

$$\boldsymbol{\gamma}^{(r)} = \frac{1}{2}\mathbf{C}^{(r)}_{\boldsymbol{\sigma}_L} \cdot \partial_{\boldsymbol{\sigma}}\mathbf{M}^{(r)}_t(\overline{\boldsymbol{\sigma}}^{(r)}_L). \tag{4.83}$$

It should be emphasized that, since the 'tangent second-order' method exhibits a duality gap, these estimates are not equivalent to those arising from the strain-rate formulation.

4.4 'Second-order' estimates

Motivated by the limitations associated with the 'tangent second-order' method, Ponte Castañeda (2002a) has recently introduced an improved version of the method, here referred to as the 'second-order' method, which incorporates information about the field fluctuations in the linearization scheme, and has been found to deliver estimates that are, in general, more accurate than the ones given in the previous sections (see for example Ponte Castañeda 2002b). It should be mentioned, however, that, unlike the 'variational' and 'tangent second-order' methods discussed above, this method has not been fully optimized yet, and is being suject of on-going research. Part of this work has been concerned with this issue, as will be explained below.

4.4.1 Effective potentials

Like the earlier 'tangent second-order' estimates, the 'second-order' estimates also make use of a thermoelastic LCC with phase potentials $w_L^{(r)}$ given in terms of reference, traceless tensors $\check{\boldsymbol{\varepsilon}}^{(r)}$ and viscosity tensors $\mathbf{L}_0^{(r)}$ by (4.37). However, in this case, the tensors $\mathbf{L}_0^{(r)}$ are not identified with the tangent tensors of moduli (4.40). For composites with isotropic constituents characterized by potentials of the form (4.1), Ponte Castañeda (2002a) proposed the use of anisotropic tensors of the form

$$\mathbf{L}_0^{(r)} = 3\kappa^{(r)}\mathbf{J} + 2\lambda_0^{(r)}\mathbf{E}^{(r)} + 2\mu_0^{(r)}\mathbf{F}^{(r)}, \tag{4.84}$$

with $\mathbf{E}^{(r)}$ and $\mathbf{F}^{(r)}$ denoting the projection tensors (4.42). Then, the following identity for the local potentials holds:

$$w^{(r)}(\boldsymbol{\varepsilon}) = \underset{\lambda_0^{(r)},\ \mu_0^{(r)}}{\text{stat}} \left\{ w_L^{(r)}(\boldsymbol{\varepsilon}; \check{\boldsymbol{\varepsilon}}^{(r)}, \mathbf{L}_0^{(r)}) + V^{(r)}(\check{\boldsymbol{\varepsilon}}^{(r)}, \mathbf{L}_0^{(r)}) \right\}, \tag{4.85}$$

where the functions $V^{(r)}$ are defined as

$$V^{(r)}(\check{\boldsymbol{\varepsilon}}^{(r)}, \mathbf{L}_0^{(r)}) = \underset{\boldsymbol{\varepsilon}^{(r)}}{\text{stat}} \left\{ w^{(r)}(\boldsymbol{\varepsilon}^{(r)}) - w_L^{(r)}(\boldsymbol{\varepsilon}^{(r)}; \check{\boldsymbol{\varepsilon}}^{(r)}, \mathbf{L}_0^{(r)}) \right\}. \tag{4.86}$$

To see this, it is convenient to introduce two components (or projections) of the tensor $\boldsymbol{\varepsilon}^{(r)}$ in this expression, that are 'parallel' and 'perpendicular' to the reference tensor $\check{\boldsymbol{\varepsilon}}^{(r)}$, respectively,

$$\varepsilon_{\parallel}^{(r)} = \sqrt{\frac{2}{3}\boldsymbol{\varepsilon}^{(r)} \cdot \mathbf{E}^{(r)}\boldsymbol{\varepsilon}^{(r)}} \quad \text{and} \quad \varepsilon_{\perp}^{(r)} = \sqrt{\frac{2}{3}\boldsymbol{\varepsilon}^{(r)} \cdot \mathbf{F}^{(r)}\boldsymbol{\varepsilon}^{(r)}}, \tag{4.87}$$

which are such that $(\varepsilon_e^{(r)})^2 = (\varepsilon_{\parallel}^{(r)})^2 + (\varepsilon_{\perp}^{(r)})^2$. Then, the stationarity conditions in (4.86), given by the so-called 'generalized-secant' conditions

$$\partial_{\boldsymbol{\varepsilon}} w^{(r)}(\hat{\boldsymbol{\varepsilon}}^{(r)}) - \partial_{\boldsymbol{\varepsilon}} w^{(r)}(\check{\boldsymbol{\varepsilon}}^{(r)}) = \mathbf{L}_0^{(r)}(\hat{\boldsymbol{\varepsilon}}^{(r)} - \check{\boldsymbol{\varepsilon}}^{(r)}), \tag{4.88}$$

can written as

$$\phi^{(r)\prime}(\hat{\varepsilon}_e^{(r)}) \frac{\hat{\varepsilon}_{\parallel}^{(r)}}{\hat{\varepsilon}_e^{(r)}} - \phi^{(r)\prime}(\check{\varepsilon}_e^{(r)}) = 3\lambda_0^{(r)} \left(\hat{\varepsilon}_{\parallel}^{(r)} - \check{\varepsilon}_e^{(r)} \right), \quad \frac{\phi^{(r)\prime}(\hat{\varepsilon}_e^{(r)})}{\hat{\varepsilon}_e^{(r)}} = 3\mu_0^{(r)}, \tag{4.89}$$

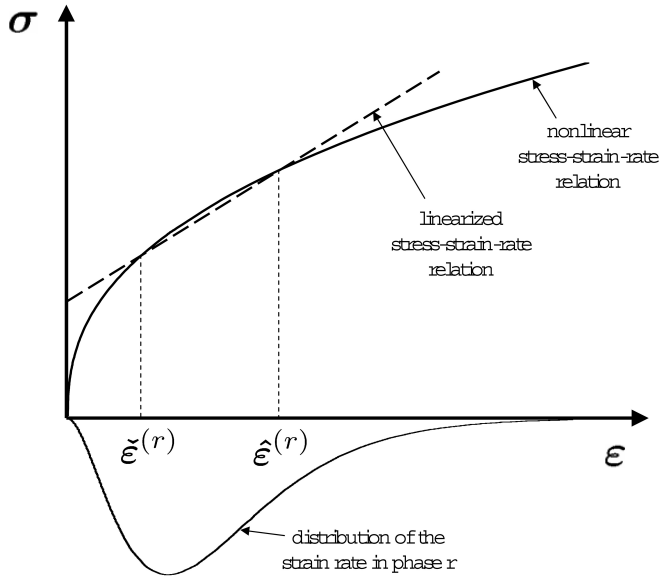

Figure 4.3: One-dimensional sketch of the nonlinear stress-strain-rate relation and the 'generalized-secant' linearization used by the 'second-order' method.

where $\hat{\boldsymbol{\varepsilon}}^{(r)}$ denotes the optimal value of $\boldsymbol{\varepsilon}^{(r)}$ in (4.86). In addition, the stationarity conditions in (4.85) are given by

$$\left(\hat{\varepsilon}_{\parallel}^{(r)} - \check{\varepsilon}_{e}^{(r)}\right)^2 = \frac{2}{3}\partial_{\lambda_0^{(r)}} w_L^{(r)}(\boldsymbol{\varepsilon}; \check{\boldsymbol{\varepsilon}}^{(r)}, \mathbf{L}_0^{(r)}) = \left(\varepsilon_{\parallel} - \check{\varepsilon}_{e}^{(r)}\right)^2, \tag{4.90}$$

$$\left(\hat{\varepsilon}_{\perp}^{(r)}\right)^2 = \frac{2}{3}\partial_{\mu_0^{(r)}} w_L(\boldsymbol{\varepsilon}; \check{\boldsymbol{\varepsilon}}^{(r)}, \mathbf{L}_0^{(r)}) = \varepsilon_{\perp}^2, \tag{4.91}$$

where $\varepsilon_{\parallel}$ and $\varepsilon_{\perp}$ are the 'parallel' and 'perpendicular' components of the strain-rate tensor $\boldsymbol{\varepsilon}$. For given $\boldsymbol{\varepsilon}$ and $\check{\boldsymbol{\varepsilon}}^{(r)}$, the conditions (4.89)-(4.91) constitute a system of four nonlinear, algebraic equations for the variables $\hat{\varepsilon}_{\parallel}^{(r)}$, $\hat{\varepsilon}_{\perp}^{(r)}$, $\lambda_0^{(r)}$, and $\mu_0^{(r)}$. It is easy to see that one solution to this system of equations is such that $\hat{\varepsilon}_{\parallel}^{(r)} = \varepsilon_{\parallel}$ and $\hat{\varepsilon}_{\perp}^{(r)} = \varepsilon_{\perp}$, with $\lambda_0^{(r)}$ and $\mu_0^{(r)}$ being given by relations (4.89). Finally, evaluating the term inside curly brackets in (4.85) at this solution, it can be verified that the potential $w^{(r)}$ is recovered. It should be emphasized that the identity (4.85) is valid for *any* $\check{\boldsymbol{\varepsilon}}^{(r)}$.

The 'second-order' estimates for the effective strain-rate potential are obtained by inserting (4.85) into (2.3), interchanging the optimization operations over $\boldsymbol{\varepsilon}(\mathbf{x})$ and the viscosities $\lambda_0^{(r)}$ and $\mu_0^{(r)}$, and restricting the latter to be constant per phase. The result is the variational approximation (Ponte Castañeda 2002a)

$$\widetilde{W}(\overline{\boldsymbol{\varepsilon}}) = \underset{\lambda_0^{(s)},\ \mu_0^{(s)}}{\text{stat}} \left\{ \widetilde{W}_L(\overline{\boldsymbol{\varepsilon}}; \check{\boldsymbol{\varepsilon}}^{(s)}, \mathbf{L}_0^{(s)}) + \sum_{r=1}^{N} c^{(r)}\, V^{(r)}(\check{\boldsymbol{\varepsilon}}^{(r)}, \mathbf{L}_0^{(r)}) \right\}, \tag{4.92}$$

where $\widetilde{W}_L$ is the effective potential of the LCC with phase potentials given by (4.37), and the reference tensors $\check{\boldsymbol{\varepsilon}}^{(r)}$ remain to be specified. The stationary operation in this expression leads to the following

conditions for the phase viscosities $\lambda_0^{(r)}$ and $\mu_0^{(r)}$:

$$\hat{\varepsilon}_{\parallel}^{(r)} - \check{\varepsilon}_e^{(r)} = \pm\sqrt{\frac{1}{c^{(r)}}\frac{2}{3}\partial_{\lambda_0^{(r)}}\widetilde{W}_L} = \pm\sqrt{\frac{2}{3}\left\langle(\boldsymbol{\varepsilon}_L - \check{\boldsymbol{\varepsilon}}^{(r)})\cdot\mathbf{E}^{(r)}(\boldsymbol{\varepsilon}_L - \check{\boldsymbol{\varepsilon}}^{(r)})\right\rangle^{(r)}}, \tag{4.93}$$

$$\hat{\varepsilon}_{\perp}^{(r)} = \pm\sqrt{\frac{1}{c^{(r)}}\frac{2}{3}\partial_{\mu_0^{(r)}}\widetilde{W}_L} = \pm\sqrt{\frac{2}{3}\left\langle\boldsymbol{\varepsilon}_L\cdot\mathbf{F}^{(r)}\boldsymbol{\varepsilon}_L\right\rangle^{(r)}}, \tag{4.94}$$

where $\boldsymbol{\varepsilon}_L$ has been used to denote the strain-rate field in the LCC. The sign of the square roots in these expressions should be taken to be positive if $\check{\varepsilon}_e^{(r)} \leq \overline{\varepsilon}_{Le}^{(r)}$, and negative otherwise, for consistency of (4.92) with the case of uniform fields (e.g., laminate, homogeneous limit). It is worth noting that the right-hand sides of these relations depend on certain projections of the phase covariance tensors $\mathbf{C}_{\boldsymbol{\varepsilon}_L}^{(r)}$ of the strain rate in the LCC. Then, from relations (4.89) and (4.93)-(4.94), it is seen that the viscosity tensors $\mathbf{L}_0^{(r)}$ correspond to 'generalized-secant' linearizations of the nonlinear stress-strain-rate relations in each phase r, which depends on the intraphase field fluctuations in the LCC. This is depicted graphically in figure 4.3, which should be compared with figures 4.1 and 4.2.

Finally, taking the hydrostatic part of the tensors $\hat{\boldsymbol{\varepsilon}}^{(r)}$ to be given by

$$\hat{\varepsilon}_m^{(r)} = \sqrt{\frac{1}{c^{(r)}}\frac{2}{9}\partial_{\kappa^{(r)}}\widetilde{W}_L} = \sqrt{\langle\varepsilon_{Lm}^2\rangle^{(r)}}, \tag{4.95}$$

it follows from the stationarity conditions (4.93)-(4.94) that the expression (4.92) for the effective potential can be simplified to

$$\widetilde{W}(\overline{\boldsymbol{\varepsilon}}) = \sum_{r=1}^{N} c^{(r)}\left[w^{(r)}(\hat{\boldsymbol{\varepsilon}}^{(r)}) - \partial_{\boldsymbol{\varepsilon}}w^{(r)}(\check{\boldsymbol{\varepsilon}}^{(r)})\cdot\left(\hat{\boldsymbol{\varepsilon}}^{(r)} - \overline{\boldsymbol{\varepsilon}}_L^{(r)}\right)\right], \tag{4.96}$$

where $\overline{\boldsymbol{\varepsilon}}_L^{(r)}$ the average of the strain-rate field in phase r of the LCC.

'Second-order' estimates for the dual potential $\widetilde{U}$ follow from exactly analogous expressions in terms of stress potentials $(4.1)_2$. In this case, the phase potentials in the LCC are given by (4.52), where the phase compliances $\mathbf{M}_0^{(r)}$ are taken to be of the form

$$\mathbf{M}_0^{(r)} = \frac{1}{3\kappa^{(r)}}\mathbf{J} + \frac{1}{2\lambda_0^{(r)}}\mathbf{E}^{(r)} + \frac{1}{2\mu_0^{(r)}}\mathbf{F}^{(r)}, \tag{4.97}$$

with the projection tensors $\mathbf{E}^{(r)}$ and $\mathbf{F}^{(r)}$ given by (4.56). The result is the variational approximation for the effective stress potential (Ponte Castañeda 2002a)

$$\widetilde{U}(\overline{\boldsymbol{\sigma}}) = \underset{\lambda_0^{(s)},\ \mu_0^{(s)}}{\text{stat}}\left\{\widetilde{U}_L(\overline{\boldsymbol{\sigma}};\check{\boldsymbol{\sigma}}^{(s)},\mathbf{M}_0^{(s)}) - \sum_{r=1}^{N} c^{(r)}\,V^{(r)}(\check{\boldsymbol{\sigma}}^{(r)},\mathbf{M}_0^{(r)})\right\}, \tag{4.98}$$

where $\widetilde{U}_L$ is the effective potential of the LCC, and

$$V^{(r)}(\check{\boldsymbol{\sigma}}^{(r)},\mathbf{M}_0^{(r)}) = \underset{\boldsymbol{\sigma}^{(r)}}{\text{stat}}\left\{u_L^{(r)}(\boldsymbol{\sigma}^{(r)};\check{\boldsymbol{\sigma}}^{(r)},\mathbf{M}_0^{(r)}) - u^{(r)}(\boldsymbol{\sigma}^{(r)})\right\}. \tag{4.99}$$

Introducing two components of the tensors $\boldsymbol{\sigma}^{(r)}$ that are 'parallel' and 'perpendicular' to the reference tensors $\check{\boldsymbol{\sigma}}^{(r)}$, respectively,

$$\sigma_{\parallel}^{(r)} = \sqrt{\frac{3}{2}\boldsymbol{\sigma}^{(r)}\cdot\mathbf{E}^{(r)}\boldsymbol{\sigma}^{(r)}} \quad\text{and}\quad \sigma_{\perp}^{(r)} = \sqrt{\frac{3}{2}\boldsymbol{\sigma}^{(r)}\cdot\mathbf{F}^{(r)}\boldsymbol{\sigma}^{(r)}}, \tag{4.100}$$

the stationarity conditions in (4.99) can be written as

$$\psi^{(r)\prime}(\hat{\sigma}_e^{(r)})\frac{\hat{\sigma}_\parallel^{(r)}}{\hat{\sigma}_e^{(r)}} - \psi^{(r)\prime}(\check{\sigma}_e^{(r)}) = \frac{1}{3\lambda_0^{(r)}}\ \left(\hat{\sigma}_\parallel^{(r)} - \check{\sigma}_e^{(r)}\right), \quad \frac{\psi^{(r)\prime}(\hat{\sigma}_e^{(r)})}{\hat{\sigma}_e^{(r)}} = \frac{1}{3\mu_0^{(r)}}, \tag{4.101}$$

where $\hat{\boldsymbol{\sigma}}^{(r)}$ denotes the optimal value of $\boldsymbol{\sigma}^{(r)}$ in (4.99). In addition, the stationarity conditions in (4.98) for the phase viscosities $\lambda_0^{(r)}$ and $\mu_0^{(r)}$ are given by

$$\hat{\sigma}_\parallel^{(r)} - \check{\sigma}_e^{(r)} = \pm\sqrt{\frac{1}{c^{(r)}}\frac{3}{2}\partial_{(\lambda_0^{(r)})^{-1}}\widetilde{U}_L} = \pm\sqrt{\frac{3}{2}\left\langle(\boldsymbol{\sigma}_L - \check{\boldsymbol{\sigma}}^{(r)})\cdot\mathbf{E}^{(r)}(\boldsymbol{\sigma}_L - \check{\boldsymbol{\sigma}}^{(r)})\right\rangle^{(r)}}, \tag{4.102}$$

$$\hat{\sigma}_\perp^{(r)} = \pm\sqrt{\frac{1}{c^{(r)}}\frac{3}{2}\partial_{(\mu_0^{(r)})^{-1}}\widetilde{U}_L} = \pm\sqrt{\frac{3}{2}\left\langle\boldsymbol{\sigma}_L\cdot\mathbf{F}^{(r)}\boldsymbol{\sigma}_L\right\rangle^{(r)}}, \tag{4.103}$$

where $\boldsymbol{\sigma}_L$ has been used to denote the stress field in the LCC. Once again, the sign of the square roots in these expressions should be taken to be positive if $\check{\sigma}_e^{(r)} \leq \overline{\sigma}_{Le}^{(r)}$, and negative otherwise, for consistency of (4.98) with the case of uniform fields.

Finally, taking the hydrostatic part of the tensors $\hat{\boldsymbol{\sigma}}^{(r)}$ to be given by

$$\hat{\sigma}_m^{(r)} = \sqrt{\frac{2}{c^{(r)}}\partial_{(\kappa^{(r)})^{-1}}\widetilde{U}_L} = \sqrt{\langle\sigma_{Lm}^2\rangle^{(r)}}, \tag{4.104}$$

it follows from the stationarity conditions (4.102)-(4.103) that the expression (4.98) for the effective potential can be simplified to

$$\widetilde{U}(\overline{\boldsymbol{\sigma}}) = \sum_{r=1}^{N} c^{(r)}\left[u^{(r)}(\hat{\boldsymbol{\sigma}}^{(r)}) - \partial_{\boldsymbol{\sigma}}u^{(r)}(\check{\boldsymbol{\sigma}}^{(r)})\cdot\left(\hat{\boldsymbol{\sigma}}^{(r)} - \overline{\boldsymbol{\sigma}}_L^{(r)}\right)\right], \tag{4.105}$$

where $\overline{\boldsymbol{\sigma}}_L^{(r)}$ the average of the stress field in phase r of the LCC.

The estimates (4.96) and (4.105) require a prescription for the set of reference tensors $\check{\boldsymbol{\varepsilon}}^{(r)}$ and $\check{\boldsymbol{\sigma}}^{(r)}$. In order for these estimates to be in agreement with the small-contrast expansion of Suquet & Ponte Castañeda (1993) to second order, the reference tensors should reduce to the macroscopic averages $\overline{\boldsymbol{\varepsilon}}$ and $\overline{\boldsymbol{\sigma}}$ to zeroth order in that expansion. In general, however, the 'optimal' references are expected to deviate from these values and to depend on the constitutive behavior of the nonlinear phases.

Initially, Ponte Castañeda (2002a) proposed enforcing stationarity of the functionals in (4.92) and (4.98) with respect to the reference tensors, so that the resulting estimates would be fully stationary with respect to the properties of the LCC. A desirable consequence of this, is that the estimates (4.92) and (4.98) would be Legendre transforms of each other, *i.e.*, they would exhibit no duality gap (see section 6 in Ponte Castañeda 2002a). However, this prescription leads to certain conditions that cannot be satisfied in conjuction with the other stationarity conditions, and therefore had to be abandoned. As an approximation, Ponte Castañeda (2002a) proposed identifying the reference tensors with the phase averages of the local fields in the LCC, *i.e.*,

$$\check{\boldsymbol{\varepsilon}}^{(r)} = \overline{\boldsymbol{\varepsilon}}_{Ld}^{(r)} \quad \text{and} \quad \check{\boldsymbol{\sigma}}^{(r)} = \overline{\boldsymbol{\sigma}}_{Ld}^{(r)}, \tag{4.106}$$

where the subscript d denotes deviatoric part. The phase averages $\overline{\boldsymbol{\varepsilon}}_L^{(r)}$ (resp. $\overline{\boldsymbol{\sigma}}_L^{(r)}$) in the LCC are given by expressions (4.48) (resp. (4.49)), which, together with the conditions (4.89), (4.93) and (4.94)

(resp. (4.101), (4.102) and (4.103)), constitute a system of algebraic, nonlinear equations. In addition to being physically appealing, this choice renders the effective potentials of the LCCs stationary, thus partially satisfying the requirement of full stationarity of the functionals (4.92) and (4.98). Of course, the phase averages reduce to the macroscopic averages to zeroth order in the heterogeneity contrast, and therefore, the resulting estimates are exact to second order. This prescription was employed to obtain the first 'second-order' estimates in the context of two-phase composites with isotropic constituents (Ponte Castañeda 2002b, Appendix A), which were found to improve, in general, on the earlier 'variational' and 'tangent second-order' estimates. As expected from the lack of full stationarity, the estimates (4.96) and (4.105) resulting from this prescription are not equivalent, although the duality gap was found to be relatively small, in general, and even vanished in certain strongly nonlinear cases. However, it was later found (see Appendix B) that, by making use of this prescription, the optimal viscosity/compliance tensors in the LCC may lose strong ellipticity in certain cases at sufficiently strong nonlinearities. Motivated by these findings, several alternative choices for the 'reference' tensors were explored in this work. The simplest prescription corresponds in fact to identifying these tensors with the macroscopic averages themselves, i.e.,

$$\check{\boldsymbol{\varepsilon}}^{(r)} = \overline{\boldsymbol{\varepsilon}}_d \quad \text{and} \quad \check{\boldsymbol{\sigma}}^{(r)} = \overline{\boldsymbol{\sigma}}_d. \tag{4.107}$$

This prescription has been found to give sensible results that improve, in general, on those resulting from the prescription (4.106), and exhibit a smaller duality gap (see Appendices B and D). In addition, this prescription has the advantage of simplicity. Indeed, as will be seen in the next subsection, this choice of reference tensors leads to the simplest possible 'second-order' estimates for the effective behavior and field statistics. For these reasons, the prescription (4.107) is preferred over the earlier choice (4.106), at least in the context of composites with isotropic phases. It should be emphasized, however, that the 'optimal' choice for these parameters remains an open problem requiring further investigation. It is worth mentioning, however, that the lack of an optimality condition for the reference tensors suggests the possibility of employing them as 'fitting' parameters in the 'second-order' estimates, which could be used to account for available information on the specific system considered, as in Danas *et al.* (2006).

Finally, an alternative formulation of the 'second-order' method has been provided by Lahellec & Suquet (2004), which is fully stationary with respect to the properties of the LCC, but still exhibits a duality gap, and gives predictions similar to those of the less accurate 'tangent second-order' method (see also Rekik *et al.* 2005).

4.4.2 Effective behavior and field statistics

'Second-order' estimates for the effective behavior and field statistics in viscoplastic composites follow from differentiation of the effective potentials (4.92) and (4.98) with respect to appropriate parameters. In this subsection, expressions for these estimates are first provided with the reference tensors left unspecified, and they are specialized later for particular prescription (4.107). Like the 'tangent

second-order' estimates of the previous section, the 'second-order' estimates for the effective potentials are not fully stationary with respect to the properties of the LCC, and consequently, the corresponding estimates for the effective behavior and field statistics are given by those in the LCC plus certain 'correction' terms. In fact, their form is similar to that of the 'tangent second-order' estimates, as can be seen in the following results.

Result 4.4.1. *The 'second-order' estimates for the effective behavior are given by*

$$\overline{\boldsymbol{\sigma}} = \partial_{\overline{\boldsymbol{\varepsilon}}}\widetilde{W}(\overline{\boldsymbol{\varepsilon}}) = \overline{\boldsymbol{\sigma}}_L + \sum_{r=1}^{N} c^{(r)} \boldsymbol{\rho}^{(r)} \cdot \partial_{\overline{\boldsymbol{\varepsilon}}} \check{\boldsymbol{\varepsilon}}^{(r)}, \tag{4.108}$$

where $\overline{\boldsymbol{\sigma}}_L$ denotes the macroscopic stress in the LCC, and the tensors $\boldsymbol{\rho}^{(r)}$ are

$$\begin{aligned} \boldsymbol{\rho}^{(r)} \quad = \quad & \left[\mathbf{L}_0^{(r)} - \mathbf{L}_t^{(r)}(\check{\boldsymbol{\varepsilon}}^{(r)})\right](\hat{\boldsymbol{\varepsilon}}^{(r)} - \overline{\boldsymbol{\varepsilon}}_L^{(r)}) + \frac{4}{3}\frac{\lambda_0^{(r)} - \mu_0^{(r)}}{(\check{\varepsilon}_e^{(r)})^2} \times \\ & \left[\left\langle (\boldsymbol{\varepsilon}_{d_L} - \check{\boldsymbol{\varepsilon}}_d^{(r)}) \otimes (\boldsymbol{\varepsilon}_{d_L} - \check{\boldsymbol{\varepsilon}}_d^{(r)}) \right\rangle^{(r)} - (\hat{\boldsymbol{\varepsilon}}_d^{(r)} - \check{\boldsymbol{\varepsilon}}_d^{(r)}) \otimes (\hat{\boldsymbol{\varepsilon}}_d^{(r)} - \check{\boldsymbol{\varepsilon}}_d^{(r)}) \right] \check{\boldsymbol{\varepsilon}}_d^{(r)}. \end{aligned} \tag{4.109}$$

In this last expression, the subscript L denotes quantities in the LCC associated with the estimate (4.92), the subscript d denotes deviatoric parts, and $\mathbf{L}_t^{(r)}$ is the tangent viscosity tensor defined by expression (4.40).

Proof. Recalling that the 'second-order' estimate (4.92) for $\widetilde{W}$ is stationary with respect to the variables $\lambda_0^{(r)}$ and $\mu_0^{(r)}$, but not with respect to the $\check{\boldsymbol{\varepsilon}}^{(r)}$, and noting that the functions $V^{(r)}$ do not depend explicitly on $\overline{\boldsymbol{\varepsilon}}$, we have that

$$\partial_{\overline{\boldsymbol{\varepsilon}}}\widetilde{W} = \partial_{\overline{\boldsymbol{\varepsilon}}}\widetilde{W}_L + \sum_{r=1}^{N} \partial_{\check{\boldsymbol{\varepsilon}}^{(r)}} \left(\widetilde{W}_L + c^{(r)}V^{(r)}\right) \cdot \partial_{\overline{\boldsymbol{\varepsilon}}}\check{\boldsymbol{\varepsilon}}^{(r)}, \tag{4.110}$$

where the arguments of the functions have been omitted for ease of notation. The derivative in the first term is taken with the $\check{\boldsymbol{\varepsilon}}^{(r)}$ held fixed, while the derivatives in the second term are taken with $\overline{\boldsymbol{\varepsilon}}$ held fixed. The first term is nothing more than the macroscopic stress in the LCC, $\overline{\boldsymbol{\sigma}}_L = \widetilde{\mathbf{L}}_0\overline{\boldsymbol{\varepsilon}} + \widetilde{\boldsymbol{\tau}}_0$. Now, noting that, while stationary with respect to the $\lambda_0^{(r)}$ and $\mu_0^{(r)}$, the estimate (4.92) is not stationary with respect to the projection tensors $\mathbf{E}^{(r)}$ (taking $\mathbf{F}^{(r)} = \mathbf{K} - \mathbf{E}^{(r)}$), which depend on the reference tensors $\check{\boldsymbol{\varepsilon}}^{(r)}$ as dictated by their definition $(4.42)_1$, and recalling that the functions $V^{(r)}$ are stationary with respect to the $\hat{\boldsymbol{\varepsilon}}^{(r)}$, we have that the second-order tensors appearing in the second term of (4.110) are given by

$$\begin{aligned} \partial_{\check{\boldsymbol{\varepsilon}}^{(r)}} \left(\widetilde{W}_L + c^{(r)}V^{(r)}\right) \quad = \quad & c^{(r)} \left[\mathbf{L}_0^{(s)} - \mathbf{L}_t^{(r)}(\check{\boldsymbol{\varepsilon}}^{(r)})\right] \left(\hat{\boldsymbol{\varepsilon}}^{(r)} - \overline{\boldsymbol{\varepsilon}}_L^{(r)}\right) + ... \\ & ... + \partial_{\mathbf{E}^{(r)}}(\widetilde{W}_L + c^{(r)}V^{(r)}) \cdot \partial_{\check{\boldsymbol{\varepsilon}}^{(r)}}\mathbf{E}^{(r)}. \end{aligned} \tag{4.111}$$

In turn, the derivatives appearing in the second term of this expression are given by

$$\begin{aligned} \partial_{\mathbf{E}^{(r)}} \left(\widetilde{W}_L + c^{(r)}V^{(r)}\right) \quad = \quad & c^{(r)} \ (\lambda_0^{(r)} - \mu_0^{(r)}) \ \left[\left\langle (\boldsymbol{\varepsilon}_L - \check{\boldsymbol{\varepsilon}}^{(r)}) \otimes (\boldsymbol{\varepsilon}_L - \check{\boldsymbol{\varepsilon}}^{(r)}) \right\rangle^{(r)} - ... \right. \\ & \left. ... - (\hat{\boldsymbol{\varepsilon}}^{(r)} - \check{\boldsymbol{\varepsilon}}^{(r)}) \otimes (\hat{\boldsymbol{\varepsilon}}^{(r)} - \check{\boldsymbol{\varepsilon}}^{(r)}) \right], \end{aligned} \tag{4.112}$$

$$\partial_{\check{\varepsilon}_{mn}^{(r)}} E_{ijkl}^{(r)} \quad = \quad \frac{4}{3}\frac{1}{(\check{\varepsilon}_e^{(r)})^2} \left[K_{ijmn}\check{\varepsilon}_{kl}^{(r)}\Big|_{ij,kl} - E_{ijkl}^{(r)} \ \check{\varepsilon}_{mn}^{(r)} \right], \tag{4.113}$$

where the subscript ij, kl has been used to denote symmetrization with respect to the index pairs ij and kl. Recalling the stationarity conditions (4.93), we have that the product between the tensors (4.112) and (4.113) that appears in expression (4.111) is given by

$$\partial_{\mathbf{E}^{(r)}}(\widetilde{W}_L + c^{(r)}V^{(r)}) \cdot \partial_{\check{\boldsymbol{\varepsilon}}^{(r)}}\mathbf{E}^{(r)} = c^{(r)}\ \boldsymbol{\rho}^{(r)}, \tag{4.114}$$

where the the tensor $\boldsymbol{\rho}^{(r)}$ is defined by (4.109). Relations (4.110), (4.111) and (4.114) imply the result (4.108). □

Result 4.4.2. *The 'second-order' estimates for the first and second moments of the local fields are given by*

$$\overline{\boldsymbol{\varepsilon}}^{(r)} = \overline{\boldsymbol{\varepsilon}}_L^{(r)} + \sum_{s=1}^{N} \frac{c^{(s)}}{c^{(r)}}\ \boldsymbol{\rho}^{(s)} \cdot \partial_{\boldsymbol{\tau}^{(r)}} \check{\boldsymbol{\varepsilon}}_\tau^{(s)}\Big|_{\boldsymbol{\tau}^{(r)}=\mathbf{0}}, \tag{4.115}$$

$$\langle \boldsymbol{\varepsilon} \otimes \boldsymbol{\varepsilon} \rangle^{(r)} = \langle \boldsymbol{\varepsilon}_L \otimes \boldsymbol{\varepsilon}_L \rangle^{(r)} + 2\sum_{s=1}^{N} \frac{c^{(s)}}{c^{(r)}}\ \boldsymbol{\rho}^{(s)} \cdot \partial_{\boldsymbol{\lambda}^{(r)}} \check{\boldsymbol{\varepsilon}}_\lambda^{(s)}\Big|_{\boldsymbol{\lambda}^{(r)}=\mathbf{0}}, \tag{4.116}$$

$$\overline{\boldsymbol{\sigma}}^{(r)} = \overline{\boldsymbol{\sigma}}_L^{(r)} + \boldsymbol{\rho}^{(r)} - \sum_{s=1}^{N} \frac{c^{(s)}}{c^{(r)}}\ \boldsymbol{\rho}^{(s)} \cdot \partial_{\boldsymbol{\eta}^{(r)}} \check{\boldsymbol{\varepsilon}}_\eta^{(s)}\Big|_{\boldsymbol{\eta}^{(r)}=\mathbf{0}}, \tag{4.117}$$

$$\langle \boldsymbol{\sigma} \otimes \boldsymbol{\sigma} \rangle^{(r)} = \langle \boldsymbol{\sigma}_L \otimes \boldsymbol{\sigma}_L \rangle^{(r)} + 2\check{\boldsymbol{\sigma}}^{(r)} \otimes_s \boldsymbol{\rho}^{(r)} - 2\sum_{s=1}^{N} \frac{c^{(s)}}{c^{(r)}}\ \boldsymbol{\rho}^{(s)} \cdot \partial_{\boldsymbol{\mu}^{(r)}} \check{\boldsymbol{\varepsilon}}_\mu^{(s)}\Big|_{\boldsymbol{\mu}^{(r)}=\mathbf{0}}, \tag{4.118}$$

where $\check{\boldsymbol{\sigma}}^{(r)} = \partial_{\boldsymbol{\varepsilon}} w^{(r)}(\check{\boldsymbol{\varepsilon}}^{(r)})$, the symbol $\otimes_s$ denotes symmetrized tensor product, the subscript L denotes quantities in the LCC, and $\check{\boldsymbol{\varepsilon}}_\tau^{(s)}$, $\check{\boldsymbol{\varepsilon}}_\lambda^{(s)}$, $\check{\boldsymbol{\varepsilon}}_\eta^{(s)}$ and $\check{\boldsymbol{\varepsilon}}_\mu^{(s)}$ denote the relevant perturbed reference strain rates.

Proof. We begin by proving the identity (4.115) for the phase averages of the strain rate. In order to make use of proposition 3.2.1, we consider a composite with perturbed local potential (3.3). Thus, phase r in this composite is characterized by (4.24). Making use of the identity (4.85) for the unperturbed potential $w^{(r)}$, we can write the perturbed potential as

$$w_\tau^{(r)}(\boldsymbol{\varepsilon}) = \underset{\lambda_0^{(r)},\ \mu_0^{(r)}}{\text{stat}} \left\{ w_{L\tau}^{(r)}(\boldsymbol{\varepsilon}; \check{\boldsymbol{\varepsilon}}^{(r)}, \mathbf{L}_0^{(r)}) + V^{(r)}(\check{\boldsymbol{\varepsilon}}^{(r)}, \mathbf{L}_0^{(r)}) \right\}, \tag{4.119}$$

where $w_{L\tau}^{(r)}$ denotes the phase potential of the perturbed LCC, given in terms of (4.37) by (4.26). The 'second-order' estimate for the perturbed effective potential $\widetilde{W}_\tau$ is thus given by (4.92), with $\widetilde{W}_L$ replaced by $\widetilde{W}_{L\tau}$, the effective potential of the perturbed LCC with phase r characterized by $w_{L\tau}^{(r)}$. The optimal $\lambda_0^{(r)}$ and $\mu_0^{(r)}$ in the perturbed problem are given by (4.93) and (4.94), with $\boldsymbol{\varepsilon}_L$ replaced by $\boldsymbol{\varepsilon}_{L\tau}^{(r)}$, the strain-rate field in the perturbed LCC. Then, recalling that the 'second-order' estimate for $\widetilde{W}_\tau$ is stationary with respect to the variables $\lambda_0^{(r)}$ and $\mu_0^{(r)}$, but not with respect to the variables $\check{\boldsymbol{\varepsilon}}^{(r)}$, and noting that the latter will depend on $\boldsymbol{\tau}^{(r)}$, in general, we have that

$$\begin{aligned} \partial_{\boldsymbol{\tau}^{(r)}} \widetilde{W}\Big|_{\boldsymbol{\tau}^{(r)}=\mathbf{0}} &= \partial_{\boldsymbol{\tau}^{(r)}} \widetilde{W}_{L\tau}\Big|_{\boldsymbol{\tau}^{(r)}=\mathbf{0}} + \sum_{s=1}^{N} \partial_{\check{\boldsymbol{\varepsilon}}^{(s)}} \left(\widetilde{W}_{L\tau} + c^{(s)}V^{(s)} \right) \cdot \partial_{\boldsymbol{\tau}^{(r)}} \check{\boldsymbol{\varepsilon}}^{(s)}\Big|_{\boldsymbol{\tau}^{(r)}=\mathbf{0}}, \\ &= c^{(r)}\overline{\boldsymbol{\varepsilon}}_L^{(r)} + \sum_{s=1}^{N} c^{(s)}\boldsymbol{\rho}^{(s)} \cdot \partial_{\boldsymbol{\tau}^{(r)}} \check{\boldsymbol{\varepsilon}}^{(s)}, \end{aligned} \tag{4.120}$$

In the last equality, use has been made of proposition 3.2.1 in the first term, and (4.110)-(4.120) in the second term. Finally, the identity (4.115) follows from proposition 3.2.1 with (4.120). The identity (4.116) can be derived in an analogous manner, making use of corollary 3.2.3.

Next, we prove the identity (4.117). In order to make use of proposition 3.2.7, we consider a composite with perturbed local potential (3.18). Thus, phase r in this composite is characterized by $w_\eta^{(r)} = (u_\eta^{(r)})^*$, where

$$u_\eta^{(r)}(\boldsymbol{\sigma}) = u^{(r)}(\boldsymbol{\sigma}) + \boldsymbol{\eta}^{(r)} \cdot \boldsymbol{\sigma}, \tag{4.121}$$

with $u^{(r)} = (w^{(r)})^*$. Thus, the perturbed potential $w_\eta^{(r)}$ is given by

$$w_\eta^{(r)}(\boldsymbol{\varepsilon}) = w^{(r)}(\boldsymbol{\varepsilon} - \boldsymbol{\eta}^{(r)}). \tag{4.122}$$

Then, making use of the identity (4.85) for $w^{(r)}$, we can write (4.122) as

$$w_\eta^{(r)}(\boldsymbol{\varepsilon}) = \underset{\lambda_0^{(r)},\ \mu_0^{(r)}}{\text{stat}} \left\{ w_{L\eta}^{(r)}(\boldsymbol{\varepsilon}; \check{\boldsymbol{\varepsilon}}_\eta^{(r)}, \mathbf{L}_0^{(r)}) + V^{(r)}(\check{\boldsymbol{\varepsilon}}_\eta^{(r)}, \mathbf{L}_0^{(r)}) \right\}. \tag{4.123}$$

where $w_{L\eta}^{(r)}$ is given by (4.29) with $w_L^{(r)}$ given by (4.37), and $\check{\boldsymbol{\varepsilon}}_\eta^{(r)} = \check{\boldsymbol{\varepsilon}}^{(r)} - \boldsymbol{\eta}^{(r)}$. The 'second-order' estimate for the perturbed effective potential $\widetilde{W}_\eta$ is thus given by (4.92) with $\widetilde{W}_L$ replaced by $\widetilde{W}_{L\eta}$, the effective potential of a perturbed LCC with phase r characterized by $w_{L\eta}^{(r)}$. Then, recalling that the 'second-order' estimate for $\widetilde{W}_\eta$ is stationary with respect to the variables $\lambda_0^{(r)}$ and $\mu_0^{(r)}$, but not with respect to the variables $\check{\boldsymbol{\varepsilon}}^{(r)}$, we have that

$$\begin{aligned} \partial_{\boldsymbol{\eta}^{(r)}} \widetilde{W}_\eta \Big|_{\boldsymbol{\eta}^{(r)}=\mathbf{0}} &= \partial_{\boldsymbol{\eta}^{(r)}} \widetilde{W}_{L\eta} \Big|_{\boldsymbol{\eta}^{(r)}=\mathbf{0}} + \sum_{s=1}^{N} \partial_{\check{\boldsymbol{\varepsilon}}_\eta^{(s)}} \left(\widetilde{W}_{L\eta} + c^{(s)} V^{(s)} \right) \cdot \partial_{\boldsymbol{\eta}^{(r)}} \check{\boldsymbol{\varepsilon}}_\eta^{(s)} \Big|_{\boldsymbol{\eta}^{(r)}=\mathbf{0}} \\ &= -c^{(r)} \overline{\boldsymbol{\sigma}}_L^{(r)} - c^{(r)} \boldsymbol{\rho}^{(r)} + \sum_{s=1}^{N} c^{(s)} \boldsymbol{\rho}^{(s)} \cdot \partial_{\boldsymbol{\eta}^{(r)}} \check{\boldsymbol{\varepsilon}}^{(s)} \Big|_{\boldsymbol{\eta}^{(r)}=\mathbf{0}}, \end{aligned} \tag{4.124}$$

In the last equality, use has been made of proposition 3.2.7 in the first term, and (4.110)-(4.120) in the second term. Finally, the identity (4.117) follows from proposition 3.2.7 with (4.124). The identity (4.118) can be derived in an analogous manner, making use of corollary 3.2.10.

□

An important observation in the context of this result is that, like the 'tangent second-order' estimates, the 'second-order' estimates (4.115) and (4.117) for the phase averages can be shown to be consistent with the corresponding estimates for the effective stress-strain-rate relation (4.108). Thus, this implies that the terms involving derivatives of the reference tensors in (4.115) and (4.117) satisfy constraints analogous to (4.76) and (4.77).

The results given above are valid for general reference tensors $\check{\boldsymbol{\varepsilon}}^{(r)}$. When the simple prescription $(4.107)_1$ is used for these tensors, the derivatives in expressions (4.108)-(4.118) become trivial. Thus, in the expression for the effective behavior we have that $\partial_{\overline{\boldsymbol{\varepsilon}}} \check{\boldsymbol{\varepsilon}}^{(r)} = \mathbf{K}$, and all derivatives of the perturbed reference tensors with respect to the various perturbation parameters in (4.115)-(4.117) become zero, since they are taken with $\overline{\boldsymbol{\varepsilon}}$ held fixed. The simplified expressions are provided in the following result.

Result 4.4.3. *The 'second-order' estimates for the effective behavior, with prescription (4.107), are given by*

$$\overline{\boldsymbol{\sigma}} = \partial_{\overline{\boldsymbol{\varepsilon}}}\widetilde{W}(\overline{\boldsymbol{\varepsilon}}) = \overline{\boldsymbol{\sigma}}_L + \sum_{r=1}^{N} c^{(r)}\boldsymbol{\rho}^{(r)}, \tag{4.125}$$

and the corresponding estimates for the field statistics are given by

$$\overline{\boldsymbol{\varepsilon}}^{(r)} = \overline{\boldsymbol{\varepsilon}}_L^{(r)}, \qquad \langle \boldsymbol{\varepsilon}\otimes\boldsymbol{\varepsilon}\rangle^{(r)} = \langle \boldsymbol{\varepsilon}_L\otimes\boldsymbol{\varepsilon}_L\rangle^{(r)}, \tag{4.126}$$

$$\overline{\boldsymbol{\sigma}}^{(r)} = \overline{\boldsymbol{\sigma}}_L^{(r)} + \boldsymbol{\rho}^{(r)}, \quad \langle \boldsymbol{\sigma}\otimes\boldsymbol{\sigma}\rangle^{(r)} = \langle \boldsymbol{\sigma}_L\otimes\boldsymbol{\sigma}_L\rangle^{(r)} + 2\check{\boldsymbol{\sigma}}^{(r)}\otimes_s\boldsymbol{\rho}^{(r)}. \tag{4.127}$$

where $\check{\boldsymbol{\sigma}}^{(r)} = \partial_{\boldsymbol{\varepsilon}} w^{(r)}(\overline{\boldsymbol{\varepsilon}})$*, and the tensors* $\boldsymbol{\rho}^{(r)}$ *are defined by (4.109) with (4.107).*

In this case, the 'second-order' estimates for the phase averages and second moments of the strain rate (arising from the strain-rate version) *coincide* with those in the LCC, while the corresponding estimates for the stress quantities still exhibit certain 'correction' terms. It is easy to see for prescription (4.107) that the constraints (4.76) to (4.77) are indeed satisfied.

Analogous expressions can be derived from the stress formulation of the 'second-order' method, which are summerized in the following result.

Result 4.4.4. *The dual 'second-order' estimates for the effective behavior are given by*

$$\overline{\boldsymbol{\varepsilon}} = \partial_{\overline{\boldsymbol{\sigma}}}\widetilde{U}(\overline{\boldsymbol{\sigma}}) = \overline{\boldsymbol{\sigma}}_L + \sum_{r=1}^{N} c^{(r)}\boldsymbol{\gamma}^{(r)}\cdot\partial_{\overline{\boldsymbol{\sigma}}}\check{\boldsymbol{\sigma}}^{(r)}, \tag{4.128}$$

where $\overline{\boldsymbol{\varepsilon}}_L$ *denotes the macroscopic stress in the LCC, and the tensors* $\boldsymbol{\gamma}^{(r)}$ *are*

$$\begin{aligned}\boldsymbol{\gamma}^{(r)} = {} & \left[\mathbf{M}_0^{(r)} - \mathbf{M}_t^{(r)}(\check{\boldsymbol{\sigma}}^{(r)})\right](\hat{\boldsymbol{\sigma}}^{(r)} - \overline{\boldsymbol{\sigma}}_L^{(r)}) + \frac{3}{4}\frac{(\lambda_0^{(r)})^{-1} - (\mu_0^{(r)})^{-1}}{(\check{\sigma}_e^{(r)})^2}\times \\ & \left[\left\langle(\boldsymbol{\sigma}_{d_L} - \check{\boldsymbol{\sigma}}_d^{(r)})\otimes(\boldsymbol{\sigma}_{d_L} - \check{\boldsymbol{\sigma}}_d^{(r)})\right\rangle^{(r)} - (\hat{\boldsymbol{\sigma}}_d^{(r)} - \check{\boldsymbol{\sigma}}_d^{(r)})\otimes(\hat{\boldsymbol{\sigma}}_d^{(r)} - \check{\boldsymbol{\sigma}}_d^{(r)})\right]\check{\boldsymbol{\sigma}}_d^{(r)}.\end{aligned} \tag{4.129}$$

In this last expression, the subscript L denotes quantities in the LCC associated with the estimate (4.98), the subscript d denotes deviatoric parts, and $\mathbf{M}_t^{(r)}$ *is the tangent compliance tensor defined by expression (4.54). The corresponding estimates for the first and second moments of the local fields are given by*

$$\overline{\boldsymbol{\sigma}}^{(r)} = \overline{\boldsymbol{\sigma}}_L^{(r)} + \sum_{s=1}^{N}\frac{c^{(s)}}{c^{(r)}}\,\boldsymbol{\gamma}^{(s)}\cdot\partial_{\boldsymbol{\eta}^{(r)}}\check{\boldsymbol{\sigma}}_\eta^{(s)}\Big|_{\boldsymbol{\eta}^{(r)}=\mathbf{0}}, \tag{4.130}$$

$$\langle\boldsymbol{\sigma}\otimes\boldsymbol{\sigma}\rangle^{(r)} = \langle\boldsymbol{\sigma}_L\otimes\boldsymbol{\sigma}_L\rangle^{(r)} + 2\sum_{s=1}^{N}\frac{c^{(s)}}{c^{(r)}}\,\boldsymbol{\gamma}^{(s)}\cdot\partial_{\boldsymbol{\mu}^{(r)}}\check{\boldsymbol{\sigma}}_\mu^{(s)}\Big|_{\boldsymbol{\mu}^{(r)}=\mathbf{0}}, \tag{4.131}$$

$$\overline{\boldsymbol{\varepsilon}}^{(r)} = \overline{\boldsymbol{\varepsilon}}_L^{(r)} + \boldsymbol{\gamma}^{(r)} - \sum_{s=1}^{N}\frac{c^{(s)}}{c^{(r)}}\,\boldsymbol{\gamma}^{(s)}\cdot\partial_{\boldsymbol{\tau}^{(r)}}\check{\boldsymbol{\sigma}}_\tau^{(s)}\Big|_{\boldsymbol{\tau}^{(r)}=\mathbf{0}}, \tag{4.132}$$

$$\langle\boldsymbol{\varepsilon}\otimes\boldsymbol{\varepsilon}\rangle^{(r)} = \langle\boldsymbol{\varepsilon}_L\otimes\boldsymbol{\varepsilon}_L\rangle^{(r)} + 2\check{\boldsymbol{\varepsilon}}^{(r)}\otimes_s\boldsymbol{\gamma}^{(r)} - 2\sum_{s=1}^{N}\frac{c^{(s)}}{c^{(r)}}\,\boldsymbol{\gamma}^{(s)}\cdot\partial_{\boldsymbol{\lambda}^{(r)}}\check{\boldsymbol{\varepsilon}}_\lambda^{(s)}\Big|_{\boldsymbol{\lambda}^{(r)}=\mathbf{0}}, \tag{4.133}$$

where $\check{\boldsymbol{\varepsilon}}^{(r)} = \partial_{\boldsymbol{\sigma}} u^{(r)}(\check{\boldsymbol{\sigma}}^{(r)})$*, the symbol* $\otimes_s$ *denotes symmetrized tensor product, the subscript L denotes quantities in the LCC, and* $\check{\boldsymbol{\sigma}}_\tau^{(s)}$*,* $\check{\boldsymbol{\sigma}}_\lambda^{(s)}$*,* $\check{\boldsymbol{\sigma}}_\eta^{(s)}$ *and* $\check{\boldsymbol{\sigma}}_\mu^{(s)}$ *denote the relevant perturbed reference stresses.*

In general, the 'second-order' estimates arising from the strain-rate and stress formulations are *not* equivalent, i.e. they exhibit a duality gap, which depends on the prescriptions used for the reference tensors in both versions. Finally, these estimates simplify considerably when the prescription $(4.107)_2$ is utilized for the reference stress tensors $\check{\boldsymbol{\sigma}}^{(r)}$, as given in the next result.

Result 4.4.5. *The dual 'second-order' estimates for the effective behavior, with prescription (4.107), are given by*

$$\overline{\boldsymbol{\varepsilon}} = \partial_{\overline{\boldsymbol{\sigma}}} \widetilde{U}(\overline{\boldsymbol{\sigma}}) = \overline{\boldsymbol{\varepsilon}}_L + \sum_{r=1}^{N} c^{(r)} \boldsymbol{\gamma}^{(r)}, \tag{4.134}$$

and the corresponding estimates for the field statistics are given by

$$\overline{\boldsymbol{\sigma}}^{(r)} = \overline{\boldsymbol{\sigma}}_L^{(r)}, \qquad \langle \boldsymbol{\sigma} \otimes \boldsymbol{\sigma} \rangle^{(r)} = \langle \boldsymbol{\sigma}_L \otimes \boldsymbol{\sigma}_L \rangle^{(r)}, \tag{4.135}$$

$$\overline{\boldsymbol{\varepsilon}}^{(r)} = \overline{\boldsymbol{\varepsilon}}_L^{(r)} + \boldsymbol{\gamma}^{(r)}, \quad \langle \boldsymbol{\varepsilon} \otimes \boldsymbol{\varepsilon} \rangle^{(r)} = \langle \boldsymbol{\varepsilon}_L \otimes \boldsymbol{\varepsilon}_L \rangle^{(r)} + 2\check{\boldsymbol{\varepsilon}}^{(r)} \otimes_s \boldsymbol{\gamma}^{(r)}. \tag{4.136}$$

where $\check{\boldsymbol{\varepsilon}}^{(r)} = \partial_{\boldsymbol{\sigma}} u^{(r)}(\overline{\boldsymbol{\sigma}})$*, and the tensors* $\boldsymbol{\gamma}^{(r)}$ *are defined by (4.129) with (4.107).*

In this case, the 'second-order' estimates for the phase averages and second moments of the stress *coincide* with those in the LCC, while the corresponding estimates for the strain-rate quantities still exhibit certain 'correction' terms.

Chapter 5

Application to two-phase composites

5.1 Introduction

In this chapter, the LCC-based homogenization methods are applied to two-phase composites with *random* 'particulate' microstructures, with clearly defined 'matrix' (1) and 'inclusion' (2) phases. Both phases are assumed to be isotropic, *incompressible* materials characterized by power-law potentials of the form

$$\phi^{(r)}(\varepsilon_e) = \frac{\varepsilon_0 \sigma_0^{(r)}}{1+m}\left(\frac{\varepsilon_e}{\varepsilon_0}\right)^{1+m}, \quad \psi^{(r)}(\sigma_e) = \frac{\varepsilon_0 \sigma_0^{(r)}}{1+n}\left(\frac{\sigma_e}{\sigma_0^{(r)}}\right)^{1+n}, \tag{5.1}$$

where $m = 1/n$ is the strain-rate sensitivity, such that $0 \le m \le 1$, $\sigma_0^{(r)}$ is the flow stress of phase r, and ε_0 is a reference strain rate. Note that the limiting values, $m = 1$ and $m = 0$, correspond to linear and rigid-ideally plastic behaviors, respectively. For simplicity, both phases are assumed to have the same exponent m and reference strain rate ε_0. Then, from the homogeneity of the local potentials (5.1), it follows that the effective potentials can be written as

$$\widetilde{W}(\overline{\boldsymbol{\varepsilon}}) = \frac{\varepsilon_0 \widetilde{\sigma}_0}{1+m}\left(\frac{\overline{\varepsilon}_e}{\varepsilon_0}\right)^{1+m}, \quad \widetilde{U}(\overline{\boldsymbol{\sigma}}) = \frac{\varepsilon_0 \widetilde{\sigma}_0}{1+n}\left(\frac{\overline{\sigma}_e}{\widetilde{\sigma}_0}\right)^{1+n}, \tag{5.2}$$

where $\widetilde{\sigma}_0$ is the *effective flow stress* of the composite, and $\overline{\varepsilon}_e$ and $\overline{\sigma}_e$ are the equivalent macroscopic strain rate and stress.

Two different classes of composites are considered in this work. The first one corresponds to fibrous composites with transversely isotropic microstructures, subjected to isochoric, in-plane loadings. In this case, the effective flow stress $\widetilde{\sigma}_0$ is a function of the strain-rate sensitivity, the heterogeneity contrast, and the inclusion concentration. The second one corresponds to isotropic composites, in which case the flow stress $\widetilde{\sigma}_0$ exhibits additional dependence on the macroscopic strain-rate invariant θ, defined by $\cos(3\theta) = 4\det(\overline{\boldsymbol{\varepsilon}}_d/\overline{\varepsilon}_e)$ (see Ponte Castañeda 1996).

It can be shown for this particular class of nonlinear composites that the local stress and strain-rate fields are homogeneous functions of degree 1 in $\overline{\sigma}_e$ and $\overline{\varepsilon}_e$, respectively. In addition, in transversely isotropic composites subjected to in-plane loadings, it is expected that the phase averages be co-axial with the macroscopic averages. It is also expected that the phase covariance tensors be 'aligned'

with the macroscopic averages, in the sense that one of their eigentensors is co-axial with $\overline{\boldsymbol{\sigma}}$ and $\overline{\boldsymbol{\varepsilon}}$. Then, under incompressible plane-strain conditions, the local stress and strain-rate deviator fields in transversely isotropic composites are vectorial in character, thus co-axiality implies proportionality, and so their phase averages can be written as

$$\overline{\boldsymbol{\sigma}}_d^{(r)} = \frac{\overline{\sigma}_e^{(r)}}{\overline{\sigma}_e}\overline{\boldsymbol{\sigma}}_d \quad \text{and} \quad \overline{\boldsymbol{\varepsilon}}_d^{(r)} = \frac{\overline{\varepsilon}_e^{(r)}}{\overline{\varepsilon}_e}\overline{\boldsymbol{\varepsilon}}_d, \tag{5.3}$$

where the ratios $\overline{\sigma}_e^{(r)}/\overline{\sigma}_e$ and $\overline{\varepsilon}_e^{(r)}/\overline{\varepsilon}_e$ depend only on material parameters. It is also natural to identify two 'components' of the strain-rate (resp. stress) tensor which represent its projections 'parallel', $\varepsilon_\parallel$ (resp. $\sigma_\parallel$), and 'perpendicular', $\varepsilon_\perp$ (resp. $\sigma_\perp$), to the macroscopic strain rate (resp. stress). These components can be determined (up to a sign) by the two orthogonal fourth-order projection tensors $\mathbf{E}$ and $\mathbf{F}$ as given by expressions (4.42) with $\check{\boldsymbol{\varepsilon}}_d^{(r)} = \overline{\boldsymbol{\varepsilon}}_d$, through the following relations:

$$\varepsilon_\parallel^2 = \frac{2}{3}\,\boldsymbol{\varepsilon}\cdot\mathbf{E}\boldsymbol{\varepsilon}, \quad \varepsilon_\perp^2 = \frac{2}{3}\,\boldsymbol{\varepsilon}\cdot\mathbf{F}\boldsymbol{\varepsilon}, \tag{5.4}$$

$$\sigma_\parallel^2 = \frac{3}{2}\,\boldsymbol{\sigma}\cdot\mathbf{E}\boldsymbol{\sigma}, \quad \sigma_\perp^2 = \frac{3}{2}\,\boldsymbol{\sigma}\cdot\mathbf{F}\boldsymbol{\sigma}. \tag{5.5}$$

They are such that $\varepsilon_e^2 = \varepsilon_\parallel^2 + \varepsilon_\perp^2$ and $\sigma_e^2 = \sigma_\parallel^2 + \sigma_\perp^2$. The phase averages of these components correspond to certain traces of the second-moment (fourth-order) tensors in the given phase. In addition, the standard deviations of the spatial distribution within each phase ($SD^{(r)}(\cdot) = \sqrt{\langle(\cdot)^2\rangle^{(r)} - (\langle\cdot\rangle^{(r)})^2}$) of these components provide a convenient measure for the *intraphase* field fluctuations, and are given in terms of the covariance tensors by

$$SD^{(r)}(\varepsilon_\parallel) = \sqrt{\frac{2}{3}\,\mathbf{E}\cdot\mathbf{C}_{\boldsymbol{\varepsilon}}^{(r)}}, \quad SD^{(r)}(\varepsilon_\perp) = \sqrt{\frac{2}{3}\,\mathbf{F}\cdot\mathbf{C}_{\boldsymbol{\varepsilon}}^{(r)}}, \tag{5.6}$$

$$SD^{(r)}(\sigma_\parallel) = \sqrt{\frac{3}{2}\,\mathbf{E}\cdot\mathbf{C}_{\boldsymbol{\sigma}}^{(r)}}, \quad SD^{(r)}(\sigma_\perp) = \sqrt{\frac{3}{2}\,\mathbf{F}\cdot\mathbf{C}_{\boldsymbol{\sigma}}^{(r)}}. \tag{5.7}$$

From the homogeneity of the local fields in $\overline{\sigma}_e$ and $\overline{\varepsilon}_e$, it follows that the ratios $SD^{(r)}(\sigma)/\overline{\sigma}_e$ and $SD^{(r)}(\varepsilon)/\overline{\varepsilon}_e$ depend only on the material parameters.

Similar observations apply to isotropic composites, but because of the tensorial character of the strain-rate and stress tensors, co-axiality does not imply proportionality in the more general three-dimensional case, and therefore relations (5.3) are do not hold under general loading conditions (i.e., arbitrary θ). However, at least in the context of the homogenization estimates (see Nebozhyn & Ponte Castañeda 1999) and sequential laminates (up to numerical accuracy) considered below, proportionality does hold for the extreme cases of axisymmetric ($\theta = 0$) and simple shear ($\theta = \pi/6$) loadings, and so in those cases we can write the phase averages in the form (5.3), where the ratios $(\overline{\varepsilon}_e^{(r)}/\overline{\varepsilon}_e)$ and $(\overline{\sigma}_e^{(r)}/\overline{\sigma}_e)$ depend on material and microstructural parameters, and the particular value of θ.

The nonlinear homogenization methods described in the previous chapter require the use of estimates for the effective behavior of linear elastic and linear thermoelastic composites with phases characterized by a modulus tensor $\mathbf{L}_0^{(r)}$, a 'thermal stress' $\boldsymbol{\tau}_0^{(r)}$, and a 'specific heat' $f_0^{(r)}$ (see expressions (4.45)-(4.47)). In this work, use is made of the generalized Hashin-Shtrikman (HS) estimates of

Willis (1977, 1981), which are provided in Section 2.4. It is recalled that these estimates are known to be quite accurate for composites with 'particulate' microstructures, up to moderate concentrations of the inclusion phase.

In order to assess the accuracy of the nonlinear homogenization estimates, *exact* results have been generated for power-law composites with a special type of 'particulate' microstructures called multiple-rank sequential laminates, following the procedure described in Appendix E. deBotton & Hariton (2002) have shown that there are (2D) lamination sequences for which the macroscopic behavior tends to be more transversely isotropic as the rank increases. In fact, making use of a differential scheme as in deBotton (2005), it can be shown analytically that the macroscopic behavior of these composites does become transversely isotropic in the limit of infinite rank. Similarly, (3D) lamination sequences can also be found such that in the limit of infinite rank, the macroscopic behavior becomes isotropic (see Appendix E). The interest in composites with this class of (transversely) isotropic microstructures is that, in the *linear* case, they reproduce *exactly* the effective behavior of the above-mentioned HS estimates, for *any* values of the modulus tensors of the phases, which follows from the symmetry of the microstructure and the fact that in these composites, the exact solution corresponds to uniform fields in the inclusion phase (Milton 2002). For this reason, homogenization estimates of the HS type, like the ones considered here for the LCC, are particularly appropriate for *nonlinear* composites with this class of microstructures, since the effective behavior of the LCC is being computed exactly in that case, and therefore there is only one level of approximation involved, namely, at the linearization stage. In addition, since this property holds for any type of linearization scheme, this class of nonlinear composites provide an ideal test case to compare LCC-based homogenization methods making use of different linearization schemes. It is relevant to emphasize that the sequentially laminated microstructures are intrinsically different from the 'composite cylinder assemblage' (CCA) microstructures considered by Moulinec & Suquet (2003, 2004) also for two-phase, power-law composites with transversely isotropic symmetry. While these two very different types of microstructures are found to exhibit very similar in-plane behaviors when the phases are linear, their behaviors become progressively more different as the nonlinearity increases, the difference being most notable for the case of an ideally plastic matrix containing weaker inclusions. In this case, the most striking difference is the fact that the strain-rate fluctuations in the inclusion phase are infinite in CCA composites, but identically zero in sequential laminates. Because the HS-type nonlinear homogenization estimates are consistent with zero fluctuations in the inclusion phase, in this work, we have chosen to compare these nonlinear estimates with the corresponding laminate results, instead of the CCA results, as in Appendix C.

In the sections to follow, comparisons are provided between the exact results for power-law laminates (LAM), and the 'variational' (VAR), 'tangent second-order' (TSO) and 'second-order' (SO) estimates described in the previous chapter, for fiber-reinforced ($\sigma_0^{(2)}/\sigma_0^{(1)} = 5$) and fiber-weakened

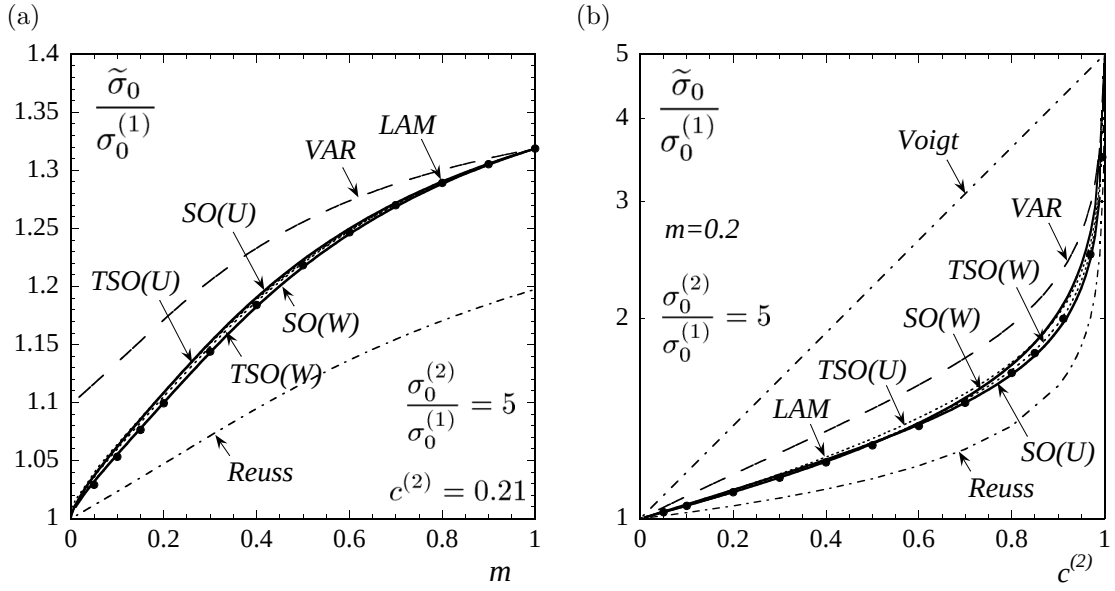

Figure 5.1: Effective flow stress $\widetilde{\sigma}_0$, normalized by the flow stress of the matrix $\sigma_0^{(1)}$, for power-law, fiber-reinforced ($\sigma_0^{(2)}/\sigma_0^{(1)} = 5$) composites subjected to in-plane shear: (a) as a function of the strain-rate sensitivity m, for a given concentration of fibers ($c^{(2)} = 0.21$), (b) as a function of fiber concentration $c^{(2)}$, for a given strain-rate sensitivity ($m = 0.2$). Comparisons between the 'second-order' (SO), 'tangent second-order' (TSO) and 'variational' (VAR) estimates of the Hashin-Shtrikman type, and exact results for power-law laminates (LAM).

($\sigma_0^{(2)}/\sigma_0^{(1)} = 0.2$) composites, as well as for isotropic, rigidly reinforced and porous composites. It is recalled that the SO and TSO estimates exhibit a duality gap, and so two sets of these estimates corresponding to the strain-rate (W) and stress (U) formulations are shown. It should also be mentioned that the SO estimates provided in this work make use of $\overline{\boldsymbol{\varepsilon}}$ and $\overline{\boldsymbol{\sigma}}$ as the 'reference' strain-rate and stress tensors (see Chapter 4). Finally, the classical bounds of Voigt (1889) and Reuss (1929) for the effective behavior are also included for comparison purposes.

5.2 Transversely isotropic, fiber-reinforced composites

Effective behavior. In figure 5.1, plots are provided for the effective flow stress $\widetilde{\sigma}_0$ of a fiber-reinforced composite, normalized by the flow stress of the matrix phase $\sigma_0^{(1)}$. Part (a) shows plots as a function of the strain-rate sensitivity m. Several observations are relevant in the context of this figure. First, all homogenization estimates of the HS type coincide for $m = 1$ with the linear HS estimates and the LAM results, but give different predictions for other values of m. The main observation, however, is that both versions (W and U) of the SO and TSO estimates are in very good agreement with the exact LAM results, for all values of the strain-rate sensitivity m. In particular, the agreement is excellent for the $SO(W)$ estimates. Thus, both methods yield a decreasing $\widetilde{\sigma}_0$ with decreasing values of m (*i.e.*, increasing nonlinearity), and in the perfectly plastic limit ($m \to 0$) they predict no reinforcement effect due to the stronger fibers, *i.e.* $\widetilde{\sigma}_0 = \sigma_0^{(1)}$, which seems to be the case for the LAM results as well (for numerical reasons it was not possible to reach $m = 0$). In fact, as pointed out by

Drucker (1966), this is the correct limit if the arrangement of fibers allows for a shear plane passing through the matrix. Furthermore, this coincides with the Reuss lower bound, which is known to be optimal in this limit (Suquet 2005). The VAR estimates, on the other hand, are seen to overestimate the LAM results for all values of m different than 1, which is not suprising given the fact that the former are known to provide rigorous bounds for the latter. It is also observed that the strain-rate (W) and stress (U) versions of the SO and TSO estimates give slightly different predictions, i.e. they exhibit a duality gap, as anticipated. However, this gap can be shown to vanish not only in the linear case, but also in the rigid-ideally plastic ($m = 0$).

Part (b) shows plots as a function of the fiber concentration, for a moderate nonlinearity ($m = 0.2$). The main observation is again the good accord of the SO and TSO estimates with the LAM results, even at high fiber concentrations. It is also interesting to note that the $SO(W)$ estimates are more accurate than the $SO(U)$ estimates for low to moderate values of $c^{(2)}$, while the converse is true for high values of $c^{(2)}$.

First moments of the local fields. In figure 5.2, results are given for the corresponding first moments (phase averages) of the local fields. Parts (a) & (b) show plots for the equivalent part of the average strain rates in each phase $\overline{\varepsilon}_e^{(r)}$, normalized by the equivalent macroscopic strain rate $\overline{\varepsilon}_e$. It can be seen that all homogenization estimates are in excellent agreement with the LAM results, for all values of m and $c^{(2)}$. Thus, it is found in part (a) that the strain rate in the fibers decreases with increasing nonlinearity (decreasing m) until it vanishes in the ideally plastic limit, meaning that the fibers behave like rigid inclusions in this strongly nonlinear limit, even though they are not rigid, and all the macroscopic deformation is carried by the matrix phase. Part (b) shows that, for a moderate nonlinearity ($m = 0.2$), the strain rate in the fibers remains very small for most values of $c^{(2)}$, and hence the average strain rate in the matrix is $\overline{\varepsilon}_e^{(1)} \approx \overline{\varepsilon}_e / c^{(1)}$.

The corresponding results for the average stresses in each phase $\overline{\sigma}_e^{(r)}$ are shown in parts (c) & (d), normalized by the equivalent macroscopic stress $\overline{\sigma}_e$. Part (c) shows plots as a function of m. Once again, it is seen that the SO and TSO estimates are in good agreement with the LAM results for all values of m, while the VAR estimates are rather inaccurate. In particular, the agreement is found to be excellent for the $SO(W)$ estimates. Thus, these estimates predict a higher average stress in the (stronger) fibers than in the matrix phase, as expected, but as the nonlinearity increases this difference becomes smaller and finally vanishes as $m \to 0$, so that $\overline{\sigma}_e^{(1)} = \overline{\sigma}_e^{(2)} = \overline{\sigma}_e$ in this limit. This is consistent with a stress field becoming uniform throughout the composite in the ideally plastic limit, which in turn is consistent with the effective behavior being given by the Reuss lower bound (see figure 5.1(a)). Part (d) shows that the relative merits of the different homogenization estimates for the average stresses in fact change with fiber concentration. Thus, while the $SO(W)$ estimates are seen to be the most accurate ones for fiber concentrations below 0.5, they deteriorate significantly at higher concentrations. This deterioration can be traced to the use of $\overline{\boldsymbol{\varepsilon}}$ as the reference strain rate, which suggests that this choice is not good for very large concentrations. In contrast, the use of $\overline{\boldsymbol{\sigma}}$ as

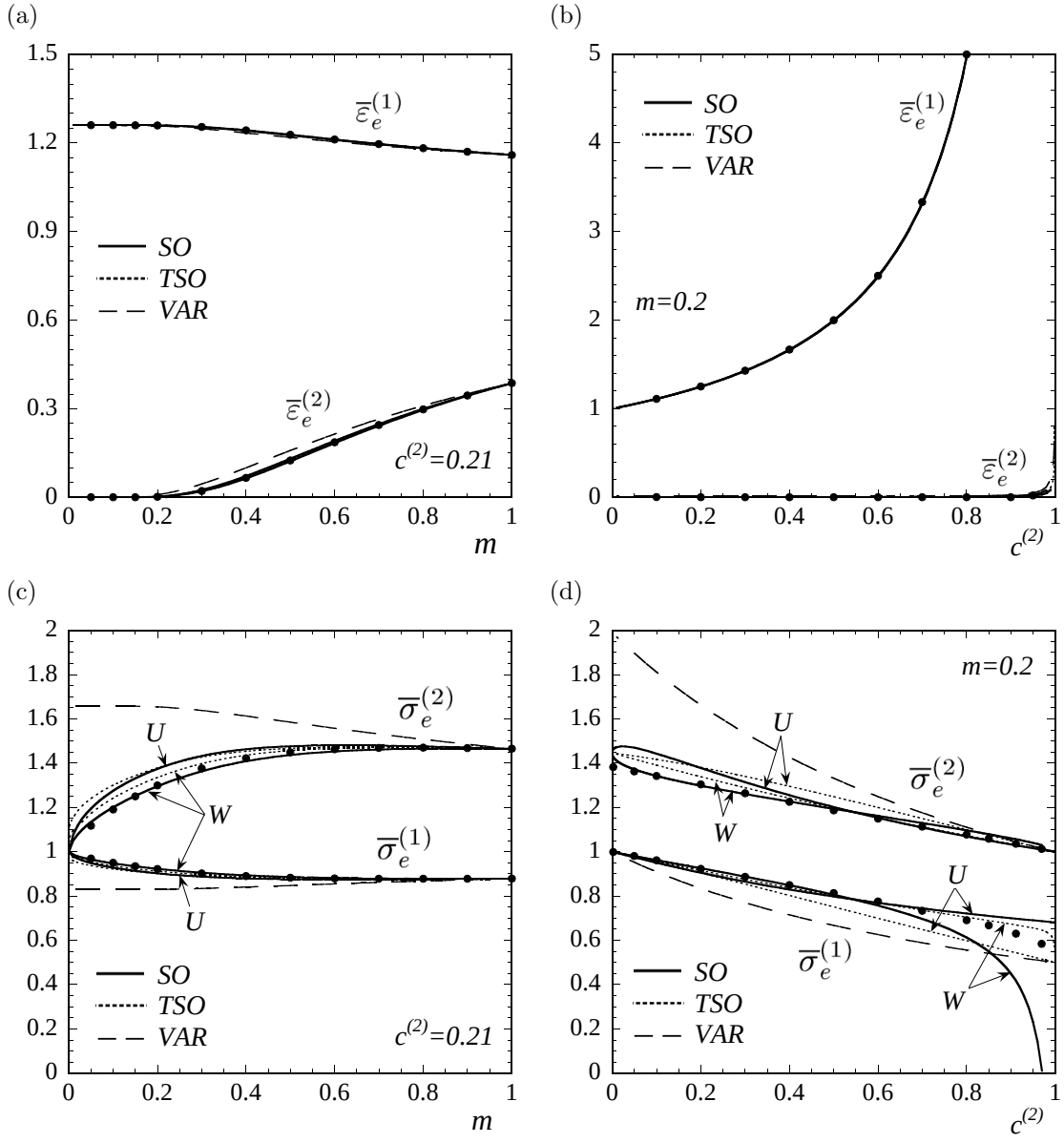

Figure 5.2: First moments (phase averages) of the local fields in fiber-reinforced composites. Equivalent average strain rate $\overline{\varepsilon}_e^{(r)}$ and stress $\overline{\sigma}_e^{(r)}$ in each phase, normalized by the macroscopic equivalent strain rate $\overline{\varepsilon}_e$ and stress $\overline{\sigma}_e$, respectively.

the reference stress in the context of the $SO(U)$ estimates is seen to lead to better behaved, albeit sometimes less accurate, estimates for all values of $c^{(2)}$.

Second moments of the local fields. Plots for the corresponding second moments of the strain-rate field are given in figure 5.3, normalized by $\overline{\varepsilon}_e^2$. Part (a) shows plots for the second moments of the 'parallel' component of the strain rate in each phase, as a function of m. It can be seen in this figure that, in the matrix phase, the LAM results increase significantly with increasing nonlinearity, and tend to become unbounded as $m \to 0$, unlike the first moments of the strain rate, which remain finite in this limit (see figure 5.2(a)). This implies that the spatial distribution of the strain rate in the matrix phase becomes significantly more heterogeneous with increasing nonlinearity. On the other hand, part (c) shows that the LAM results for the second moments of $\varepsilon_\perp$ in the matrix exhibit a slight increase for weak nonlinearities, but drop to zero as $m \to 0$, meaning that in this limit the strain-rate field becomes 'aligned' with the macroscopic strain rate throughout the composite. In addition, for a finite value of m, the second moments of both components are seen in parts (b) & (d) to increase monotonically, and significantly, in the matrix phase, with increasing concentration of fibers, becoming unbounded as $c^{(2)} \to 1$. Both versions of the SO and TSO estimates are found to be consistent with these observations, being in good qualitative agreement with the LAM results for all values of m and $c^{(2)}$. On the other hand, the VAR estimates are found, once again, to be the least accurate among the nonlinear homogenization estimates. Finally, it is recalled that the local fields in the *inclusion* phase of the power-law laminates are *uniform*, for any value of the material parameters. Thus, the LAM results in the inclusion phase are such that $\overline{\sigma}_e^{(2)}/\sigma_0^{(2)} = (\overline{\varepsilon}_e^{(2)}/\varepsilon_0)^m$, $\langle \varepsilon_\parallel^2 \rangle^{(2)} = (\overline{\varepsilon}_e^{(2)})^2$ and $\langle \varepsilon_\perp^2 \rangle^{(2)} = 0$. In this connection, it is noted that, while the SO and VAR estimates satistfy these relations, thus being consistent with uniform fields in the fibers, the TSO estimates do not satisfy the first two. In fact, the TSO estimates for $\langle \varepsilon_e^2 \rangle^{(2)}$ are found to be slightly less than those for $(\overline{\varepsilon}_e^{(2)})^2$, and therefore violate the rigorous inequality $\langle \varepsilon_e^2 \rangle^{(2)} \geq (\overline{\varepsilon}_e^{(2)})^2$. This inconsistency demonstrates that the TSO estimates are less good than the SO estimates.

Plots for the corresponding second moments of the 'parallel' $\sigma_\parallel$ and 'perpendicular' $\sigma_\perp$ components of the stress, normalized by $\overline{\sigma}_e^2$, are given in figure 5.4. Parts (a) & (c) show plots as a function of m. The LAM results show that the second moments of the stress remain bounded as $m \to 0$, unlike those of the strain rate, and seem to be consistent with vanishing fluctuations in the ideally plastic limit. It can be seen that SO and TSO estimates are in good qualitative agreement with the LAM results, for all values of m, and predict no stress fluctuations in the ideally plastic limit, which is consistent with the fact that the corresponding estimates for $\widetilde{\sigma}_0$ attain the Reuss lower bound in this limit. In particular, the agreement is seen to be excellent for the $SO(W)$ estimates, at least for this moderate value of fiber concentration ($c^{(2)} = 0.21$). Parts (b) & (d) show that the $SO(W)$ remain the most accurate among the homogenization estimates up to fairly large fiber concentrations. However, as $c^{(2)}$ becomes larger, the $SO(W)$ estimates for the second moments of $\sigma_\parallel$ in the matrix deteriorate significantly, while the $SO(U)$ estimates remain well-behaved, which is consistent with the

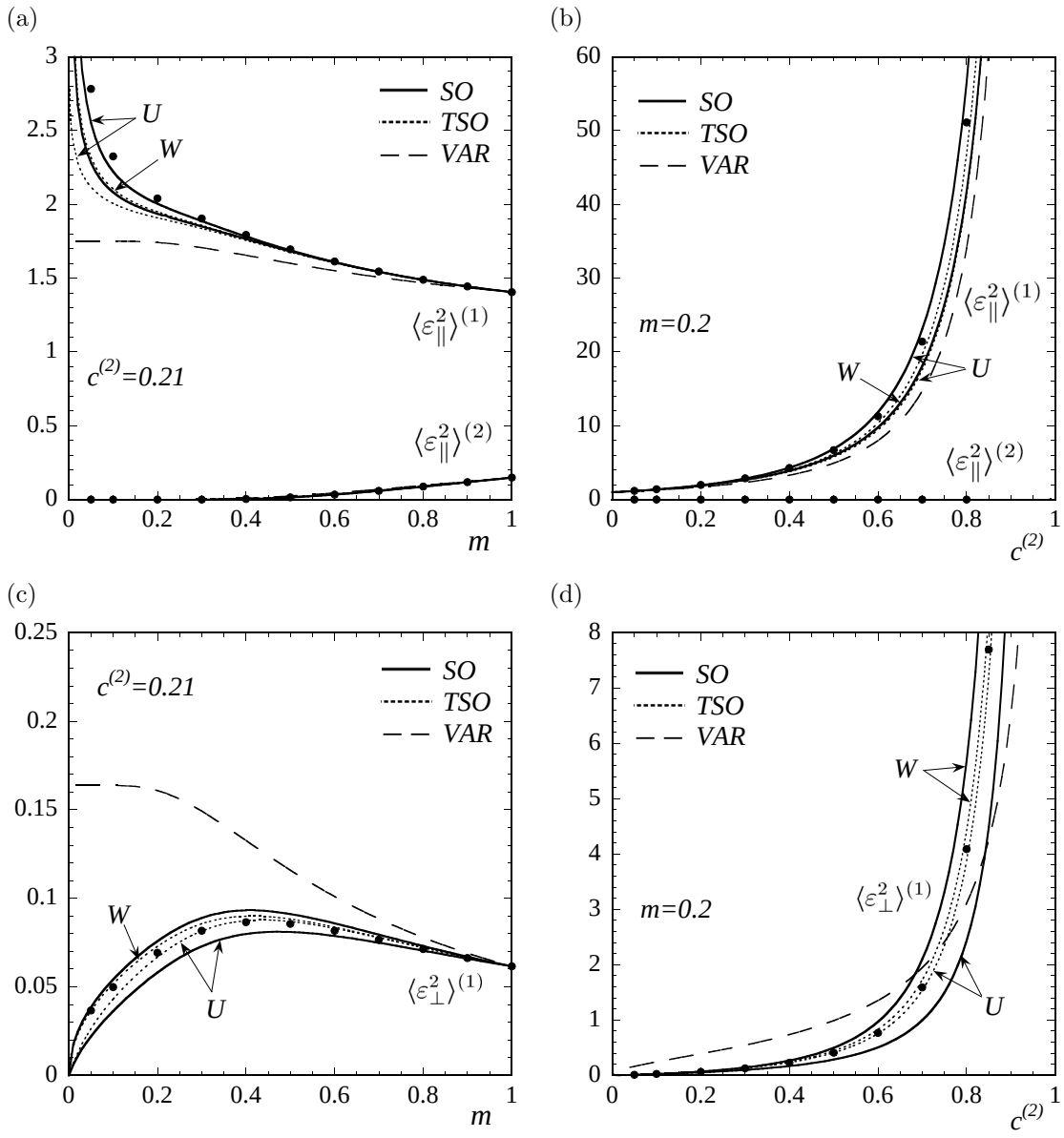

Figure 5.3: Second moments of the strain-rate field in fiber-reinforced composites. 'Parallel' $\varepsilon_{\|}$ and 'perpendicular' $\varepsilon_{\perp}$ components, normalized by $\overline{\varepsilon}_e^2$.

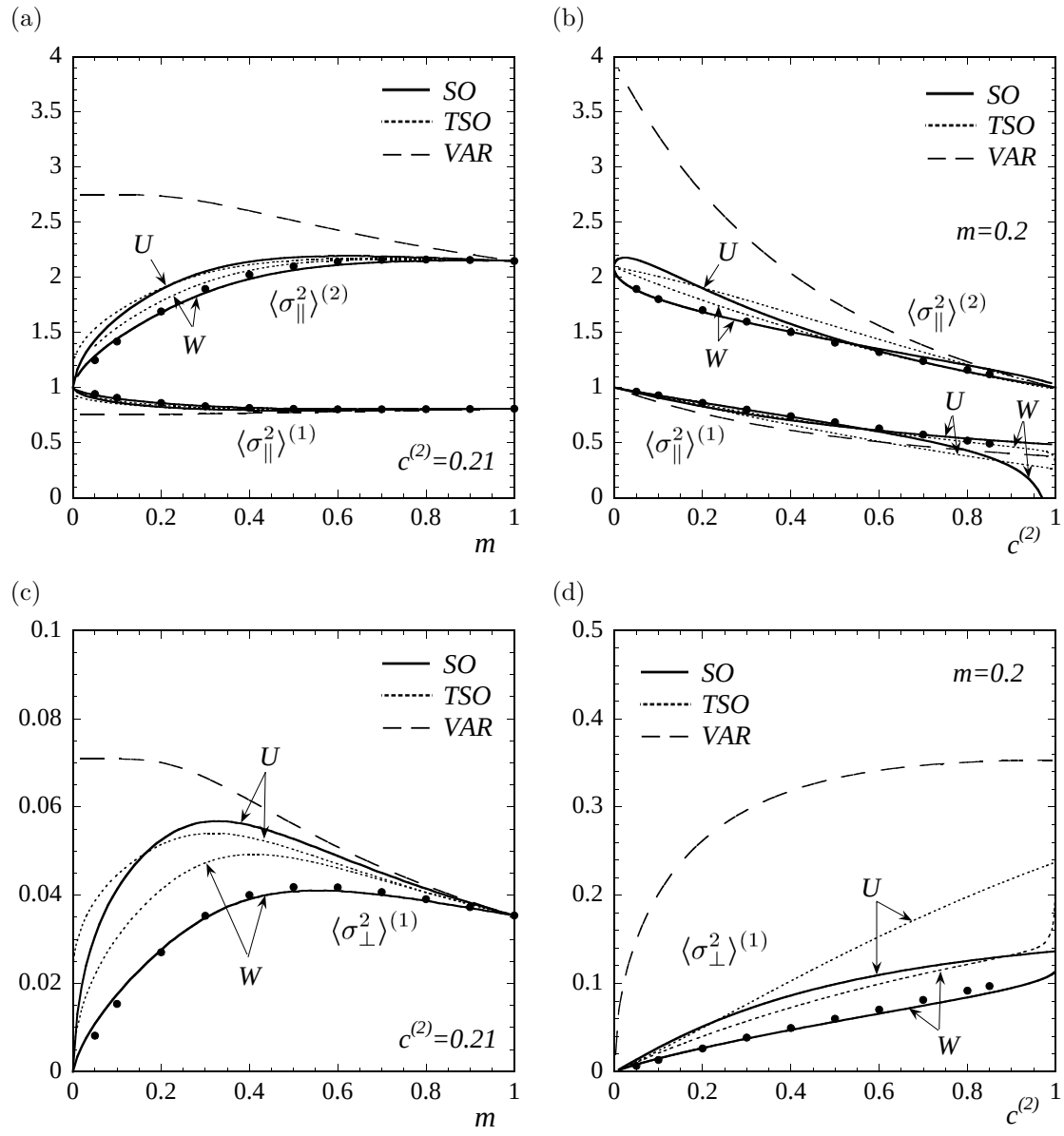

Figure 5.4: Second moments of the strain-rate field in fiber-reinforced composites. 'Parallel' $\sigma_{\parallel}$ and 'perpendicular' $\sigma_{\perp}$ components, normalized by $\overline{\sigma}_e^2$.

observations made in the context of figure 5.2(d). Finally, as has already been noted in the context of figure 5.3, it should be mentioned that, while the SO and VAR estimates are consistent with uniform fields in the inclusion phase, in agreement with the LAM results, both versions of the TSO estimates for the average and second moments of the stress in the inclusion phase are not so and violate the inequality $\langle \sigma_e^2 \rangle^{(2)} \geq (\overline{\sigma}_e^{(r)})^{(2)}$. Again, this suggests that the TSO estimates should be less reliable, in general, than the SO estimates, as expected.

Fluctuations of the local fields. More insight on the distributions of the local fields can be gained by looking at the standard deviations (SD) of the 'parallel' and 'perpendicular' components of the fields rather than the second moments. Figure 5.5 provides plots for these quantities in the matrix phase as a function of the strain-rate sensitivity m and reinforcement concentration $c^{(2)}$. The main observation in the context of this figure is that the field fluctuations in the sequential laminates, while *isotropic* in the linear case (i.e., $SD^{(1)}(\varepsilon_{\parallel}) = SD^{(1)}(\varepsilon_{\perp})$ and $SD^{(1)}(\sigma_{\parallel}) = SD^{(1)}(\sigma_{\perp})$), they become progressively more *anisotropic* with increasing nonlinearity. Thus, the 'parallel' fluctuations of the strain rate increase monotonically with increasing nonlinearity, and blow up as $m \to 0$, whereas the 'perpendicular' fluctuations exhibit a non-monotonic dependence on m, and are found to vanish as $m \to 0$. It was originally conjectured (see Appendix A) and later found by means of full field simulations (see Appendix C) that this highly anisotropic dependence of the strain-rate fluctuations on nonlinearity is a manifestation of the fact that the strain-rate field localizes in bands which become progressively thinner as the nonlinearity increases. These bands run across the specimen avoiding the (stronger) inclusions, remaining at the same time as 'parallel' as possible to the directions of maximum macroscopic shear. Thus, by allowing strain-rate localization, nonlinearity not only increases significantly the strain-rate fluctuations, but also induces anisotropy on them, even though the phases and their spatial distribution are isotropic. In the ideally plastic limit, the localization bands can turn into shear bands, across which the tangential component of the velocity field is discontinuous (Suquet 1981). Then, the fluctuations of certain components of the strain rate may become unbounded, as is the case in the problem here considered. (In ideal plasticity, the strain-rate tensor $\boldsymbol{\varepsilon}$ is a bounded measure on Ω, and therefore, its integral is finite but its L^2 norm may become unbounded (Suquet 1981).) In contrast, the stress fluctuations are seen to remain bounded for all values of m, and to vanish in the ideally plastic limit. It is interesting to note that, while the 'parallel' fluctuations of the strain rate are larger than the corresponding 'perpendicular' ones, the opposite is true for the stress fluctuations. Finally, both the strain-rate and stress fluctuations are seen to increase with increasing reinforcement concentration, but the effect is found to be more dramatic for the strain-rate fluctuations, which, unlike the stress fluctuations, blow up as $c^{(2)} \to 1$.

It can be seen that the SO and TSO estimates are in good qualitative agreement with the LAM results, for all values of m, and up to moderate values of $c^{(2)}$. Thus, these estimates are able to capture the strong anisotropy of the fluctuations that develops in strongly nonlinear reinforced composites. In contrast, the VAR estimates predict isotropic fluctuations for all values of m, and are therefore

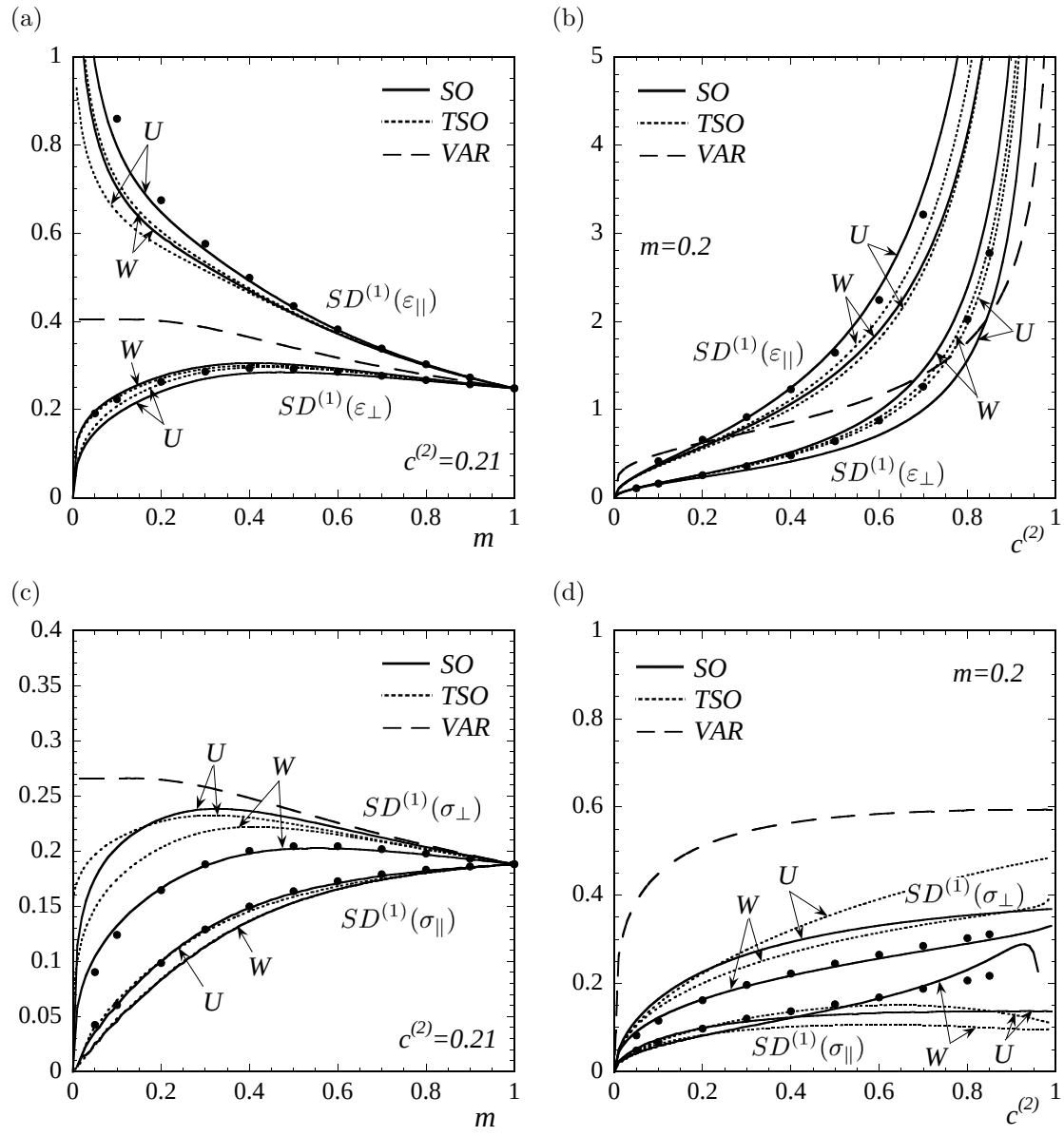

Figure 5.5: Standard deviations (SD) of the 'parallel' and 'perpendicular' components of the strain-rate and stress fields in fiber-reinforced composites, normalized by $\overline{\varepsilon}_e$ and $\overline{\sigma}_e$, respectively.

qualitatively incorrect.

Statistics of the local fields in the LCC. Because earlier approaches amount to extract field statistics directly from the LCC, it is of interest to assess the importance of the 'correction' terms arising in the context of the 'second-order' and 'tangent second-order' methods. Figures 5.6 and 5.7 show 'second-order' and 'tangent second-order' estimates for first- and second-order field statistics, together with the corresponding quantities in the associated LCCs, normalized by the equivalent parts of the (nonlinear) macroscopic fields. The 'correction' terms correspond to the difference between nonlinear estimate and the corresponding quantity in the LCC. It is noted that, because of the particular choice of 'reference' tensors and the fact that the HS estimates are consistent with uniform fields in the inclusion phase of the LCC, the 'second-order' estimates only exhibit 'correction' terms for the statistics of the dual field in the matrix phase (i.e., strain-rate statistics from the stress version, and *vice versa*), while the 'tangent second-order' estimates exhibit 'correction' terms for all quantities. Thus, the main observation in the context of these figures is that, in most cases, the 'correction' terms have a beneficial effect over the field statistics in the LCC, in the sense that the nonlinear estimates lie closer to the exact LAM results. Moreover, for sufficiently strong nonlinearities, the 'correction' terms can be several orders of magnitude larger than the corresponding quantity in the LCC, and they can even amount to the totality of the nonlinear estimate in the ideally plastic limit, as may be seen in parts (a) & (b) of figures 5.6 & 5.7. Thus, these terms cannot be neglected in general, even in first-order statistics.

5.3 Transversely isotropic, fiber-weakened composites

Effective behavior. In figure 5.8, plots are provided for the effective flow stress $\widetilde{\sigma}_0$ of a fiber-weakened composite, normalized by the flow stress of the matrix phase $\sigma_0^{(1)}$. Part (a) shows plots as a function of the strain-rate sensitivity m. The main observation in the context of this figure is that both versions of the SO estimates are found to be in very good agreement with the LAM results not only for weak nonlinearities but, more importantly, also for strong nonlinearities. In contrast, the TSO estimates are seen to be in very good agreement with the exact LAM results for weak to moderate nonlinearities, but, unlike in the case of stronger fibers, they are seen to deteriorate and deviate significantly from each other (large duality gap) for strong nonlinearities. In this connection, it is observed that, as $m \to 0$ the $TSO(W)$ estimates rapidly decrease to a finite value well below the LAM results, while the $TSO(U)$ estimates tend to the Voigt upper bound, violating the sharper bound provided by the VAR estimates. Part (b) shows plots of $\widetilde{\sigma}_0$ as a function of the fiber concentration $c^{(2)}$, for a strong nonlinearity ($m = 0.1$). It can be seen that the SO estimates are in very good agreement with the LAM results for all values of the fiber concentration.

First moments of the local fields. Plots for the corresponding phase averages of the local fields are provided in figure 5.9. Part (a) shows the equivalent average strain rates $\overline{\overline{\varepsilon}}_e^{(r)}$ in each phase,

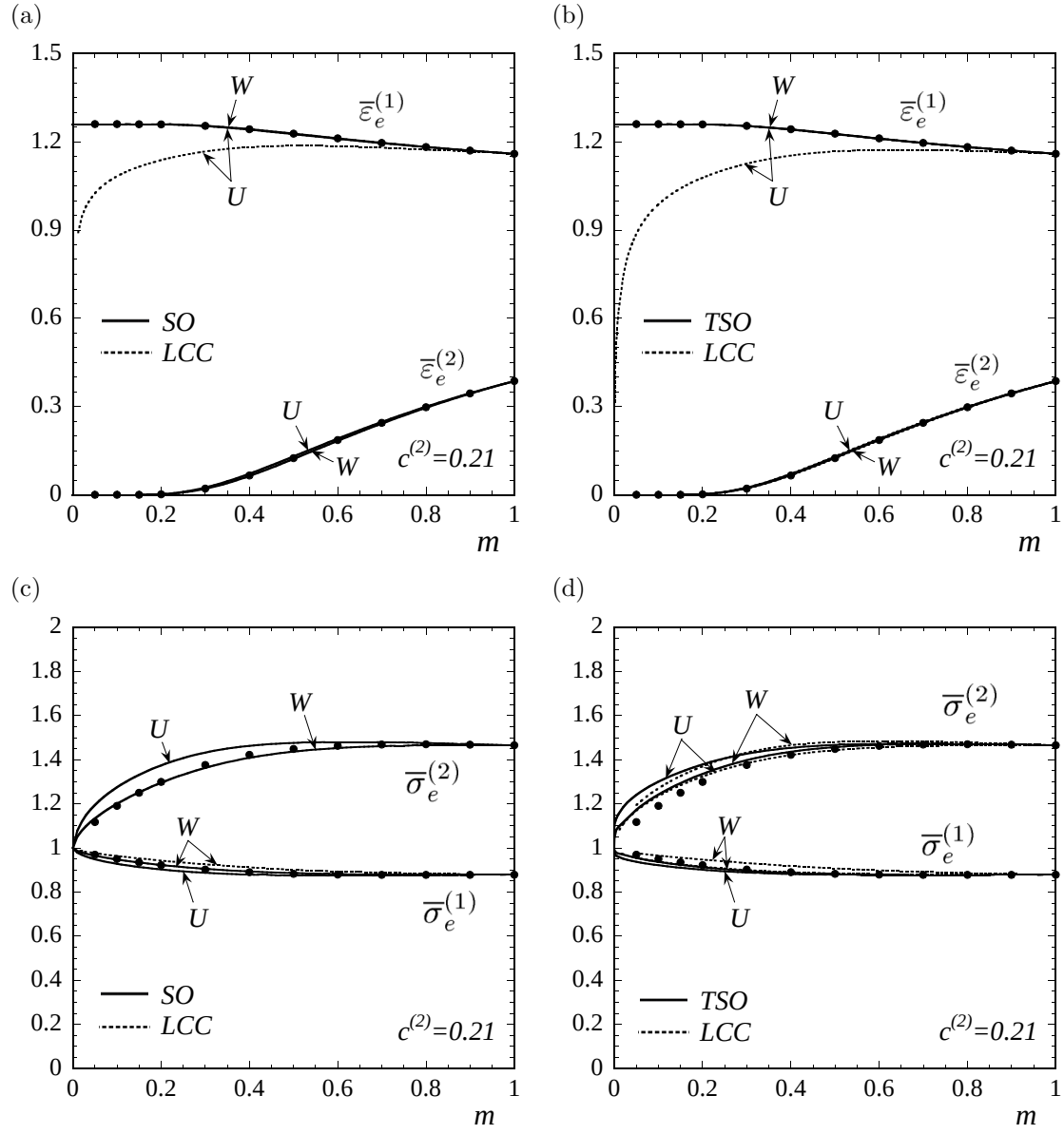

Figure 5.6: First moments (phase averages) of the local fields in fiber-reinforced composites. Equivalent average strain rate $\overline{\varepsilon}_e^{(r)}$ and stress $\overline{\sigma}_e^{(r)}$ in each phase of the nonlinear composite and corresponding LCC, normalized by the (nonlinear) macroscopic equivalent strain rate $\overline{\varepsilon}_e$ and stress $\overline{\sigma}_e$, respectively.

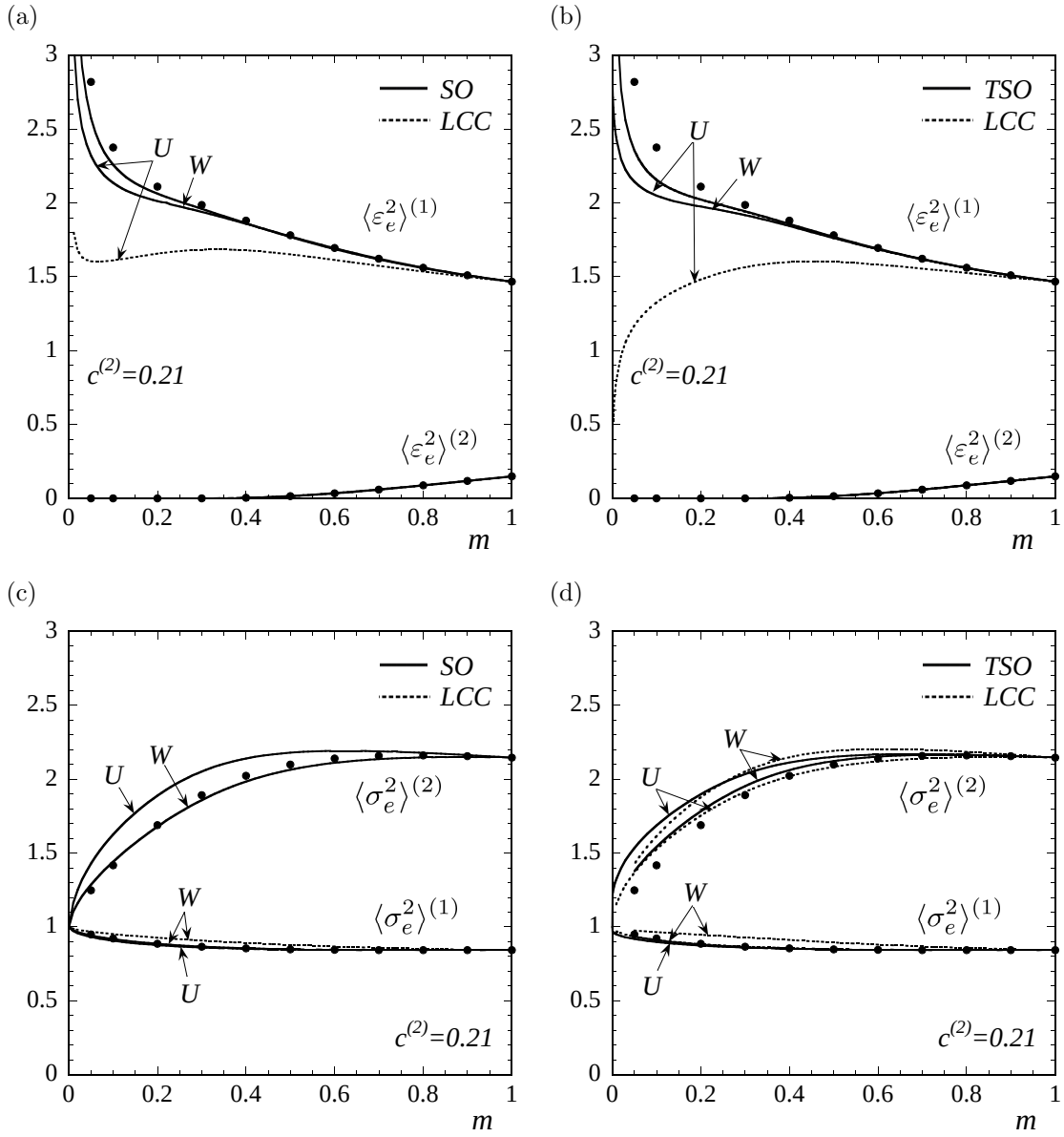

Figure 5.7: Second moments of the equivalent part of the local fields in fiber-reinforced, nonlinear composites and corresponding LCC, normalized by the (nonlinear) macroscopic equivalent strain rate $\overline{\varepsilon}_e^2$ and stress $\overline{\sigma}_e^2$, respectively.

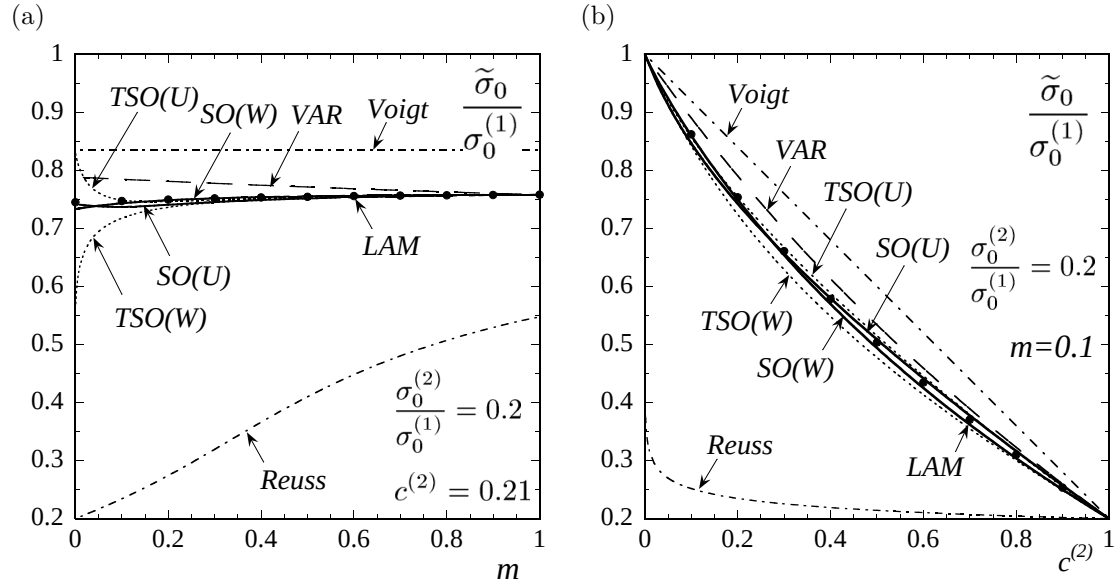

Figure 5.8: Effective flow stress $\widetilde{\sigma}_0$, normalized by the flow stress of the matrix $\sigma_0^{(1)}$, for power-law, fiber-weakened ($\sigma_0^{(2)}/\sigma_0^{(1)} = 0.2$) composites subjected to in-plane shear: (a) as a function of the strain-rate sensitivity m, for a given concentration of fibers ($c^{(2)} = 0.21$), (b) as a function of fiber concentration $c^{(2)}$, for a given strain-rate sensitivity ($m = 0.1$). Comparisons between the 'second-order' (SO), 'tangent second-order' (TSO) and 'variational' (VAR) estimates of the Hashin-Shtrikman type, and exact results for power-law laminates (LAM).

normalized by $\overline{\varepsilon}_e$, as a function of m. It can be seen in this figure that the LAM results show an average deformation that is higher in the (weaker) fibers than in the matrix, as expected, and that increases with increasing nonlinearity. The $SO(W)$ estimates are found to be in excellent agreement with the LAM results for all values of m, while the agreement is less good for the $SO(U)$ estimates, which exhibit a peculiar, non-monotonic behavior close to the ideally plastic limit. On the other hand, the TSO estimates are in very good agreement with the LAM results up to moderate nonlinearities, but deteriorate significantly as $m \to 0$. In particular, the $TSO(U)$ estimates give $\overline{\varepsilon}_e^{(1)} = \overline{\varepsilon}_e^{(2)} = \overline{\varepsilon}_e$, which is consistent with the $TSO(U)$ estimates for $\widetilde{\sigma}_0$ being given by the Voigt bound (see figure 5.8(a)). Finally, the VAR estimates are seen to capture the right trends, even if they underestimate significantly the deformation of the inclusion phase for strong nonlinearities. Part (b) of this figure shows that the $SO(W)$ estimates remain the most accurate for all values of the fiber concentration. These estimates agree with the LAM results in that the deformation in the inclusion phase increases with decreasing fiber concentrations, and that this trend is significantly enhanced by nonlinearity.

Parts (c) & (d) show plots for the equivalent average stresses $\overline{\sigma}_e^{(r)}$ in each phase. We begin by noting that the LAM results show an average stress that is lower in the (weaker) fibers than in the matrix, as expected, and that decreases with increasing nonlinearity. The main observation in the context of these figures, however, is that all homogenization estimates are in very good agreement with the LAM results, for all values of m and $c^{(2)}$. This is not surprising, for in the limit of void fibers ($\sigma_0^{(2)} = 0$) all the estimates predict the correct ratios $\overline{\sigma}_e^{(r)}/\overline{\sigma}_e$. However, it is observed in part

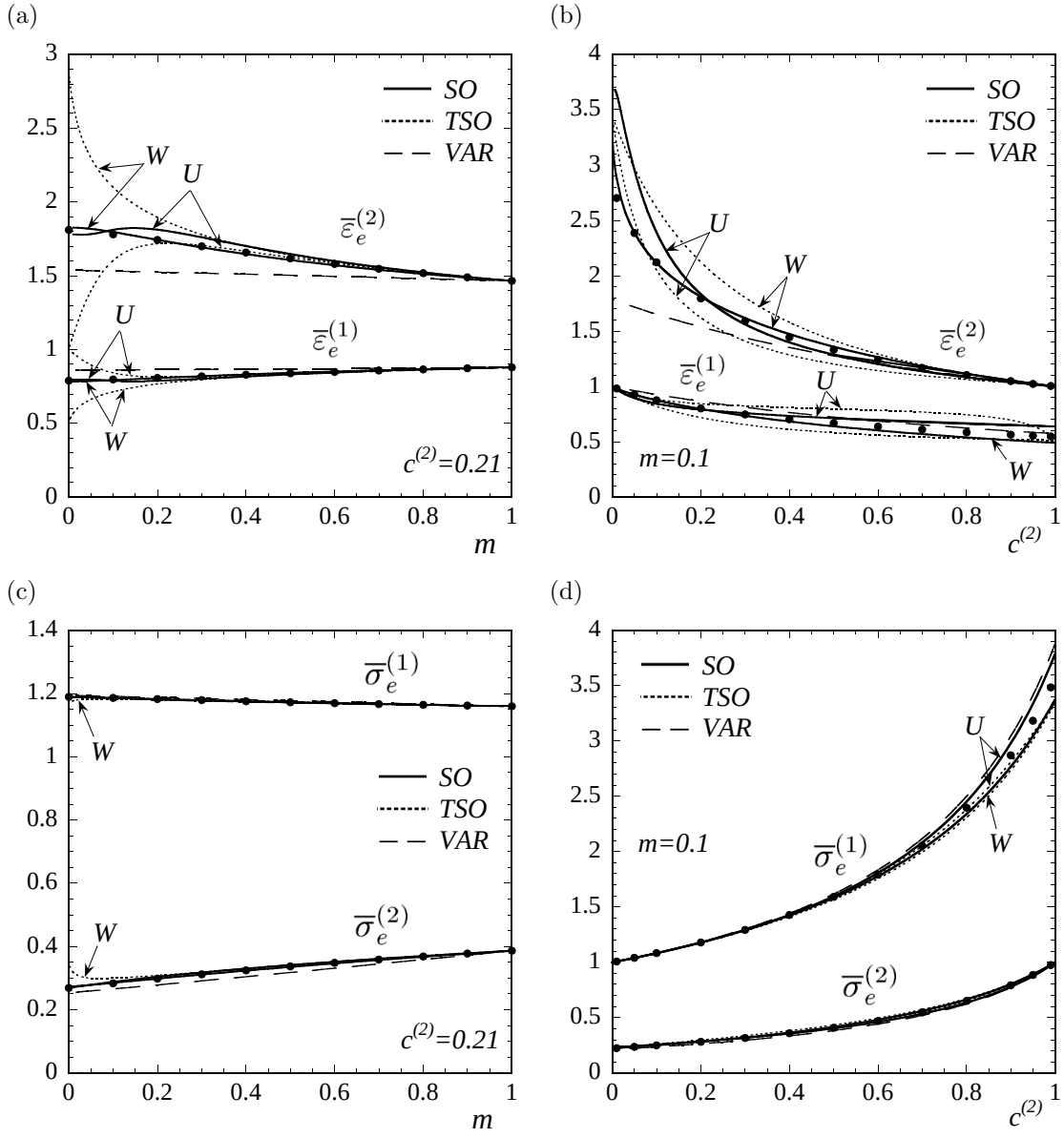

Figure 5.9: First moments (phase averages) of the local fields in fiber-weakened composites. Equivalent average strain rate $\overline{\varepsilon}_e^{(r)}$ and stress $\overline{\sigma}_e^{(r)}$ in each phase, normalized by the macroscopic equivalent strain rate $\overline{\varepsilon}_e$ and stress $\overline{\sigma}_e$, respectively.

(c) that, as $m \to 0$, the $TSO(W)$ estimates exhibit a peculiar behavior, deviating from the exact LAM results and thus becoming less accurate than the other estimates in this strongly nonlinear limit.

Second moments of the local fields. Figure 5.10 shows plots for the second moments of the 'parallel' $\varepsilon_{\parallel}$ and 'perpendicular' $\varepsilon_{\perp}$ components of the strain rate in each phase, as a function of m (parts (a) & (c)) and fiber concentration (parts (b) & (d)). We begin by noting that the general agreement between the exact LAM results and the different homogenization estimates is less good than that found for the first moments of the strain rate (see figures 5.9(a)-(b)). Of all the homogenization estimates, the $SO(U)$ estimates seem to be the most consistent with the LAM results, in general, even though they exhibit the peculiar behavior for strong nonlinearities already observed in the context of figure 5.9(a). On the other hand, while better for the second moments of the strain rate in the inclusion phase, in the matrix phase the $SO(W)$ estimates underestimate considerably the second moments of $\varepsilon_{\perp}$. However, both versions of the SO estimates are consistent with uniform fields in the inclusion phase, in agreement with the exact LAM results. In contrast, both versions of the TSO estimates are relatively good for weak to moderate nonlinearities, but become meaningless for sufficiently strong nonlinearities, violating, once again, the rigorous inequality $\langle \varepsilon_e^2 \rangle^{(r)} \geq (\overline{\varepsilon}_e^{(r)})^2$ in the inclusion phase ($r = 2$) and sometimes even in the matrix phase ($r = 1$). It should be noted that, in the limit $m \to 0$, the $TSO(U)$ estimates for $\widetilde{U}$ deviate from the Voigt bound when the perturbation parameters $\boldsymbol{\lambda}^{(r)}$ (see Chapter 4) are non-zero, and therefore the $TSO(U)$ estimates for the second moments of the strain rate do not agree with uniform strain-rate fields, unlike those for the phase averages.

Figure 5.11 shows plots for the second moments of the 'parallel' $\sigma_{\parallel}$ and 'perpendicular' $\sigma_{\perp}$ components of the stress in each phase, as a function of m (parts (a) & (c)) and fiber concentration (parts (b) & (d)). Once again, it is noted that the general agreement between the exact LAM results and the different homogenization estimates is less good than that found for the first moments of the stress (see figures 5.9(c)-(d)), even though the stress statistics are less sensitive than the corresponding strain-rate statistics in the case of weaker fibers. Of all homogenization estimates, the $SO(W)$ seem to do best for the second moments of the stress, as opposed to the $SO(U)$ estimates for the corresponding strain-rate quantities, the agreement with the LAM results being good for all values of m and $c^{(2)}$. In contrast, both versions of the TSO estimates are found to be in good agreement with the LAM results for weak to moderate nonlinearities, but deteriorate significantly as $m \to 0$, where they violate the inequality $\langle \sigma_e^2 \rangle^{(2)} \geq (\overline{\sigma}_e^{(2)})^2$. In particular, the TSO estimates for the second moments of $\sigma_{\perp}$ in the matrix phase are seen to blow up in this limit, which is at odds with the exact LAM results.

Noting that the plots for the stress statistics provided in figures 5.9 & 5.11 are appropriately normalized by $\overline{\sigma}_e$, which should be set equal to $\widetilde{\sigma}_0$ in the ideally plastic limit for the composite to flow, it is inferred that, as $m \to 0$, the exact LAM results for the second moments of the equivalent stress in the matrix phase $\sqrt{\langle \sigma_e^2 \rangle^{(1)}}$ tend to the flow stress $\sigma_0^{(1)}$, while those for $\overline{\sigma}_e^{(1)}$ remain below

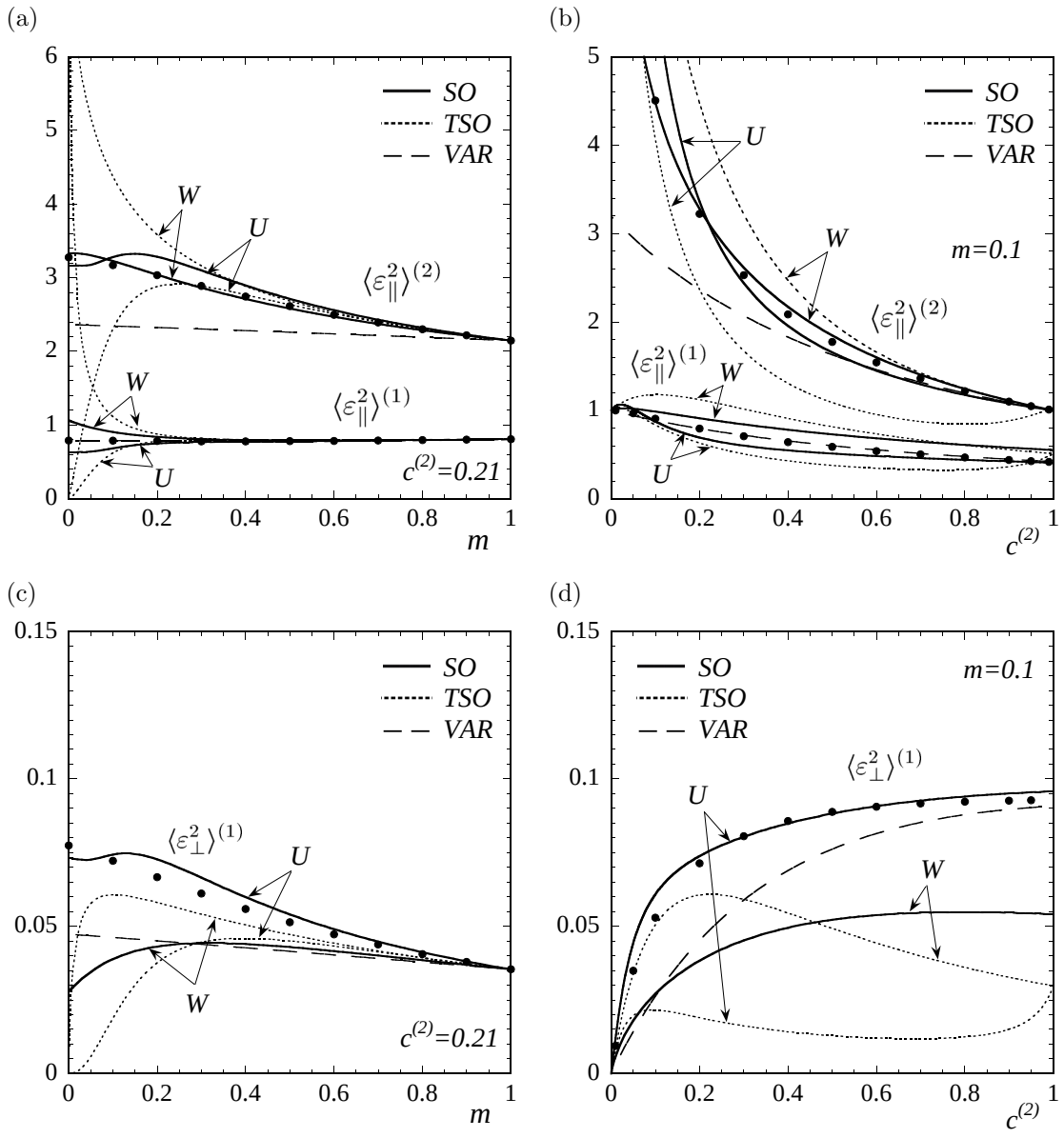

Figure 5.10: Second moments of the strain-rate field in fiber-weakened composites. 'Parallel' $\varepsilon_{\parallel}$ and 'perpendicular' $\varepsilon_{\perp}$ components, normalized by $\overline{\varepsilon}_e^2$.

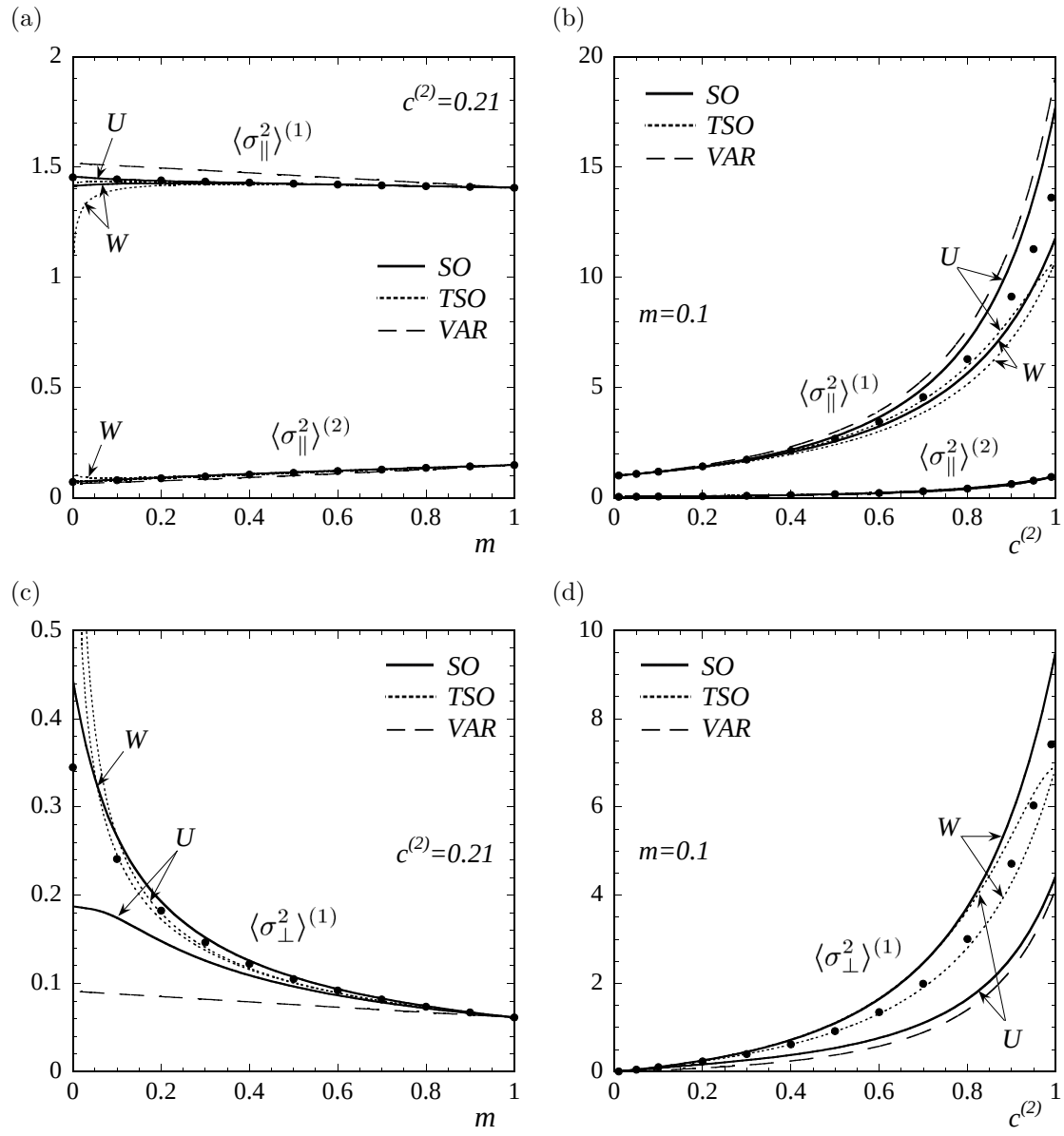

Figure 5.11: Second moments of the strain-rate field in fiber-weakened composites. 'Parallel' $\sigma_{\parallel}$ and 'perpendicular' $\sigma_{\perp}$ components, normalized by $\overline{\sigma}_e^2$.

$\sigma_0^{(1)}$. In addition, the LAM results for these quantities in the (weaker) inclusion phase tend to the flow stress $\sigma_0^{(2)}$ in this limit. This means that in ideally plastic, sequential laminates like those considered here, every point is at yield in both phases. However, in the matrix phase, the 'direction' of the stress tensor varies with position, thus giving rise to intraphase stress fluctuations even though $\sigma_e = \sigma_0^{(1)}$ everywhere. This is a very special behavior that would not be expected to happen in more realistic microstructures, as, for example, in those considered in Appendix C. It should be emphasized, nevertheless, that, independently of the microstructure, the stress statistics in ideally plastic composites are such that $\overline{\sigma}_e^{(r)} \leq \sqrt{\langle \sigma_e^2 \rangle^{(r)}} \leq \sigma_0^{(r)}$, and therefore accurate estimates should satisfy these inequalities. Even though not shown here, it is noted that the SO and VAR estimates do satisfy these inequalities in the ideally plastic limit, but the TSO estimates sometimes violate them. In this connection, it is recalled that the so-called 'affine' method, which amounts to obtaining the estimates directly from the LCC of the TSO method and therefore delivers estimates even less accurate than the TSO estimates, is already known to predict second moments of the 'resolved' shear stresses that are larger than the flow stress of the slip system in the context of viscoplastic polycrystals (see Brenner *et al.* 2004).

Fluctuations of the local fields. Figure 5.12 shows plots for the standard deviations (SD) of the 'parallel' and 'perpendicular' components of the local fields in the matrix phase. It can be seen in parts (a) & (c) that, as already observed in the case of stronger inclusions, the field fluctuations in the sequential laminates are isotropic in the linear case, but become progressively more anisotropic with increasing nonlinearity. However, unlike in the case of stronger inclusions, in this case the strain-rate fluctuations are seen to remain bounded in the ideally plastic limit. A possible explanation for this is that, if the strain-rate field were to localize into shear bands running through the specimen, energetic considerations would dictate that the bands should *seek* out the weaker inclusions, remaining at the same time as 'parallel' as possible to the directions of maximum macroscopic shear, as has been observed, for instance, in nonlinear composites with CCA microstructures (see Appendix C). However, it has already been pointed out that a peculiarity of the sequential laminated microstructures is that the fields inside the inclusions are always uniform, what precludes the presence of shear bands running across them. Thus, there may be other deformation mechanisms in these sequential laminates that are energetically more favourable than shear bands running entirely through the (hard) matrix, which, being more 'diffuse' than shear bands, would involve finite strain-rate fluctuations. In any event, it can be seen that the SO estimates, and to a lesser extent the TSO estimates, are in good agreement with the LAM results for weak to moderate nonlinearities, but deteriorate significantly for sufficiently strong nonlinearities, despite the fact that these estimates are fairly accurate for the first and second moments separately (cf. figures 5.9 & 5.11). In contrast, the VAR estimates are inaccurate for all values of m different than 1, and are unable to capture the anisotropy of the fluctuations induced by nonlinearity. Finally, it can be seen in parts (b) & (d) that most predictions for the field fluctuations worsen with increasing inclusion concentration.

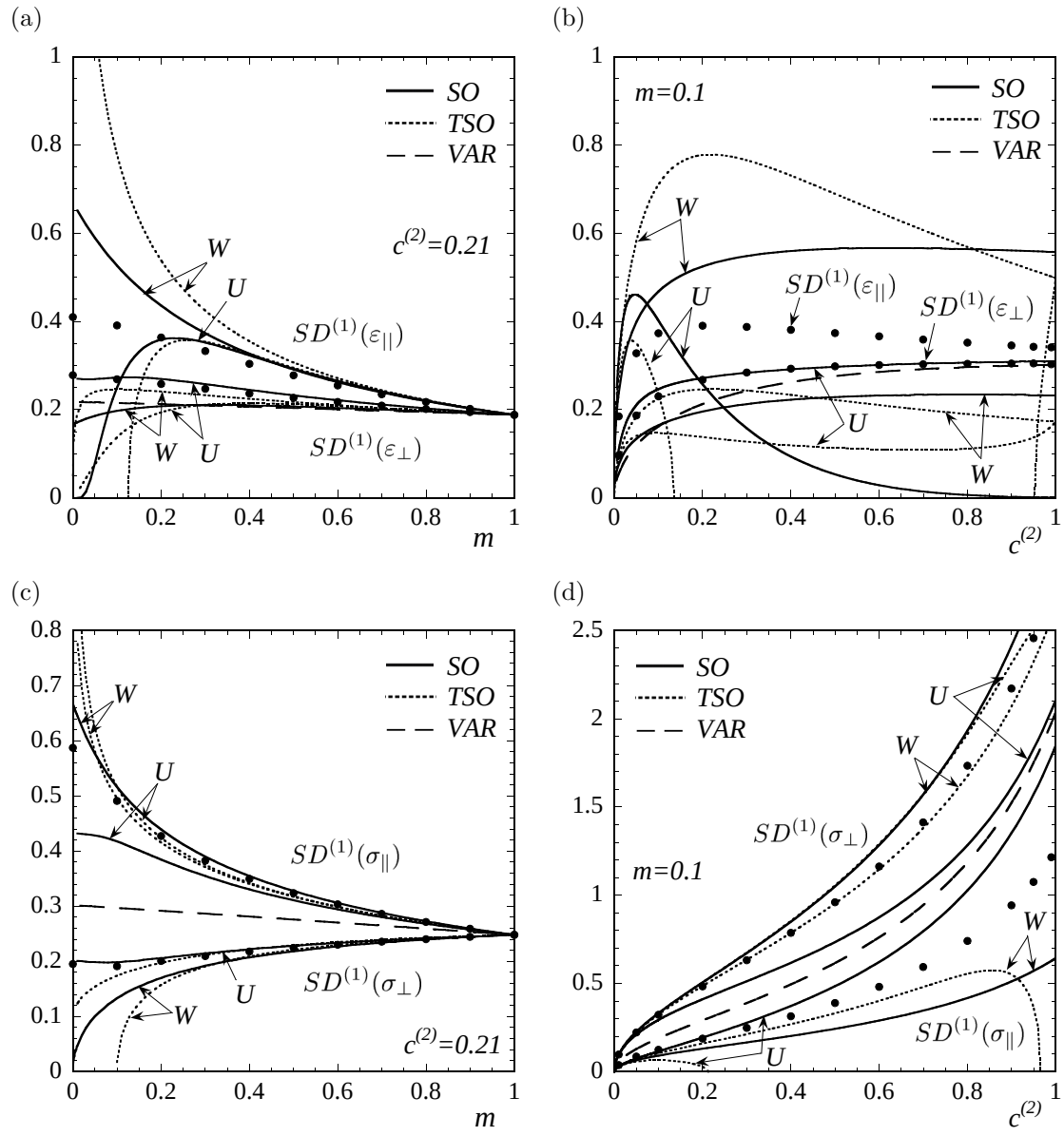

Figure 5.12: Standard deviations (SD) of the 'parallel' and 'perpendicular' components of the strain-rate and stress fields in fiber-weakened composites, normalized by $\overline{\varepsilon}_e$ and $\overline{\sigma}_e$, respectively.

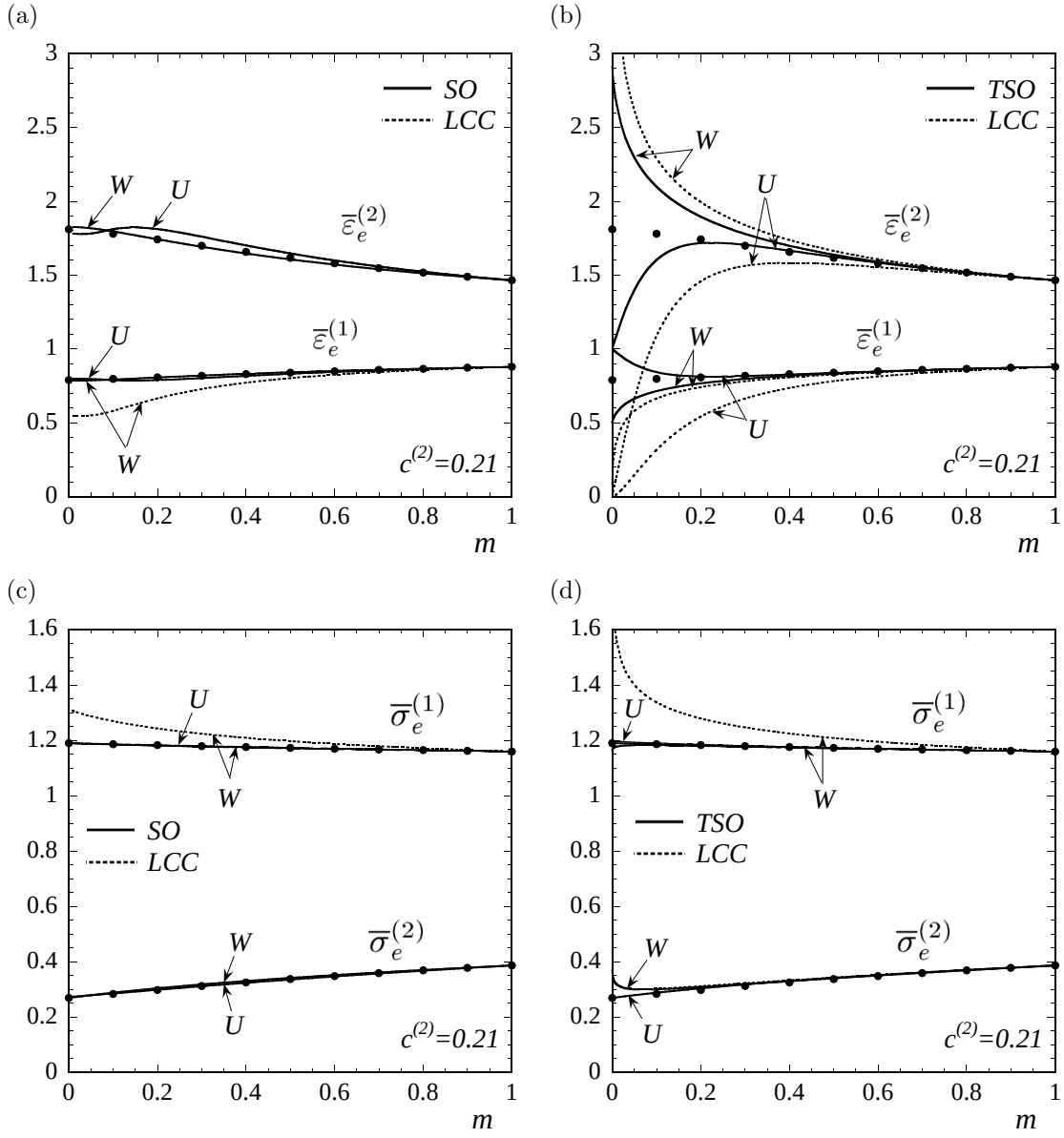

Figure 5.13: First moments (phase averages) of the local fields in fiber-weakened composites. Equivalent average strain rate $\overline{\varepsilon}_e^{(r)}$ and stress $\overline{\sigma}_e^{(r)}$ in each phase of the nonlinear composite and corresponding LCC, normalized by the (nonlinear) macroscopic equivalent strain rate $\overline{\varepsilon}_e$ and stress $\overline{\sigma}_e$, respectively.

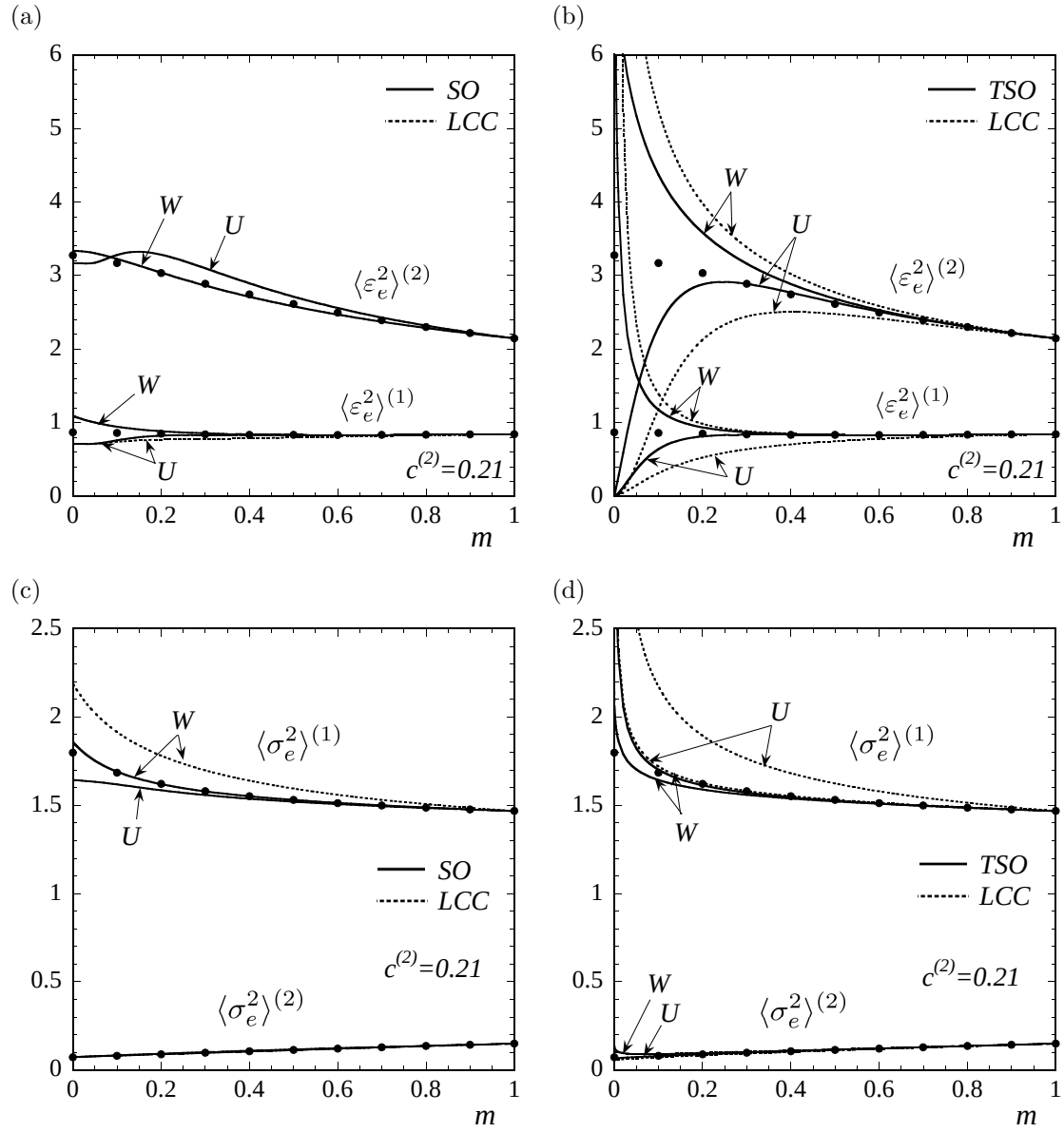

Figure 5.14: Second moments of the equivalent part of the local fields in fiber-weakened, nonlinear composites and corresponding LCC, normalized by the (nonlinear) macroscopic equivalent strain rate $\overline{\varepsilon}_e^2$ and stress $\overline{\sigma}_e^2$, respectively.

Statistics of the local fields in the LCC. In figures 5.13 & 5.14, the TSO and SO estimates for the field statistics are compared with the corresponding quantities in the associated LCC. It is recalled that the differences between the nonlinear estimates and the corresponding quantities in the LCC amount to the 'correction' terms derived in Chapter 4. Thus, it can be seen that accounting for the terms 'correcting' the statistics of the fields in the LCC always have a beneficial effect, in the sense that the nonlinear estimates lie closer to the exact LAM results than the corresponding quantities in the LCC. Moreover, the 'correction' terms can be much larger than the corresponding quantities in the LCC, and may even constitute the totality of the nonlinear estimates for some quantities in the ideally plastic limit (see figure 5.13). It is also worth noting that the 'correction' terms are, in general, larger in the context of the 'tangent second-order' method than in context of the 'second-order' method. In this connection, it is recalled that the so-called 'affine' estimates of Masson *et al.* (2000) amount to taking the strain-rate and stress statistics directly from the LCCs associated with the strain-rate and stress versions of the 'tangent second-order' estimates, respectively, thus neglecting the 'correction' terms and consequently being less accurate.

5.4 Isotropic, rigidly reinforced composites

In this section, results are provided for the effective behavior and statistics of the local fields in isotropic power-law composites with rigid inclusions. It is recalled that in three dimensions, the behavior depends on the third invariant θ of the macroscopic loading. Rather than giving a detailed analysis as in the two-dimensional case, the intention here is to provide some preliminary results which show salient features associated with the three-dimensional case. Thus, we consider only the extreme values of θ, which correspond to axisymmetric shear ($\theta = 0$) and simple shear ($\theta = \pi/6$) loadings, and TSO estimates are provided only for the effective behavior.

Effective behavior. In figure 5.15, plots are provided for the effective flow stress $\widetilde{\sigma}_0$, normalized by the flow stress of the matrix phase $\sigma_0^{(1)}$, as a function of the strain-rate sensitivity m and reinforcement concentration $c^{(2)}$. The main observation in the context of this figure is that the SO estimates are found to be the most accurate among the nonlinear homogenization estimates, for all values of m and $c^{(2)}$, and both loading conditions. Thus, these estimates are able to capture the right dependence on the third invariant θ exhibited by the exact LAM results. In the ideally plastic limit ($m \to 0$), the SO estimates predict a finite reinforcement effect under axisymmetric shear, while no reinforcement effect under simple shear (see parts (a) & (c)). Even though reliable LAM results could not be obtained in this limit, the trend exhibited by the LAM results for finite m seem to be in agreement with such predictions. It is also worth noting that the duality gap exhibited by the SO estimates is found to be small, and it even vanishes as $m \to 0$ for the case of simple shear loading (but not for axisymmetric shear). As in the case of fiber-reinforced composites (see figure 5.1(b)), it is seen that for low to moderate values of $c^{(2)}$, the $SO(W)$ estimates are closer to the exact LAM results than the $SO(U)$ estimates, while for large values of $c^{(2)}$ the converse is true. It can be seen that the

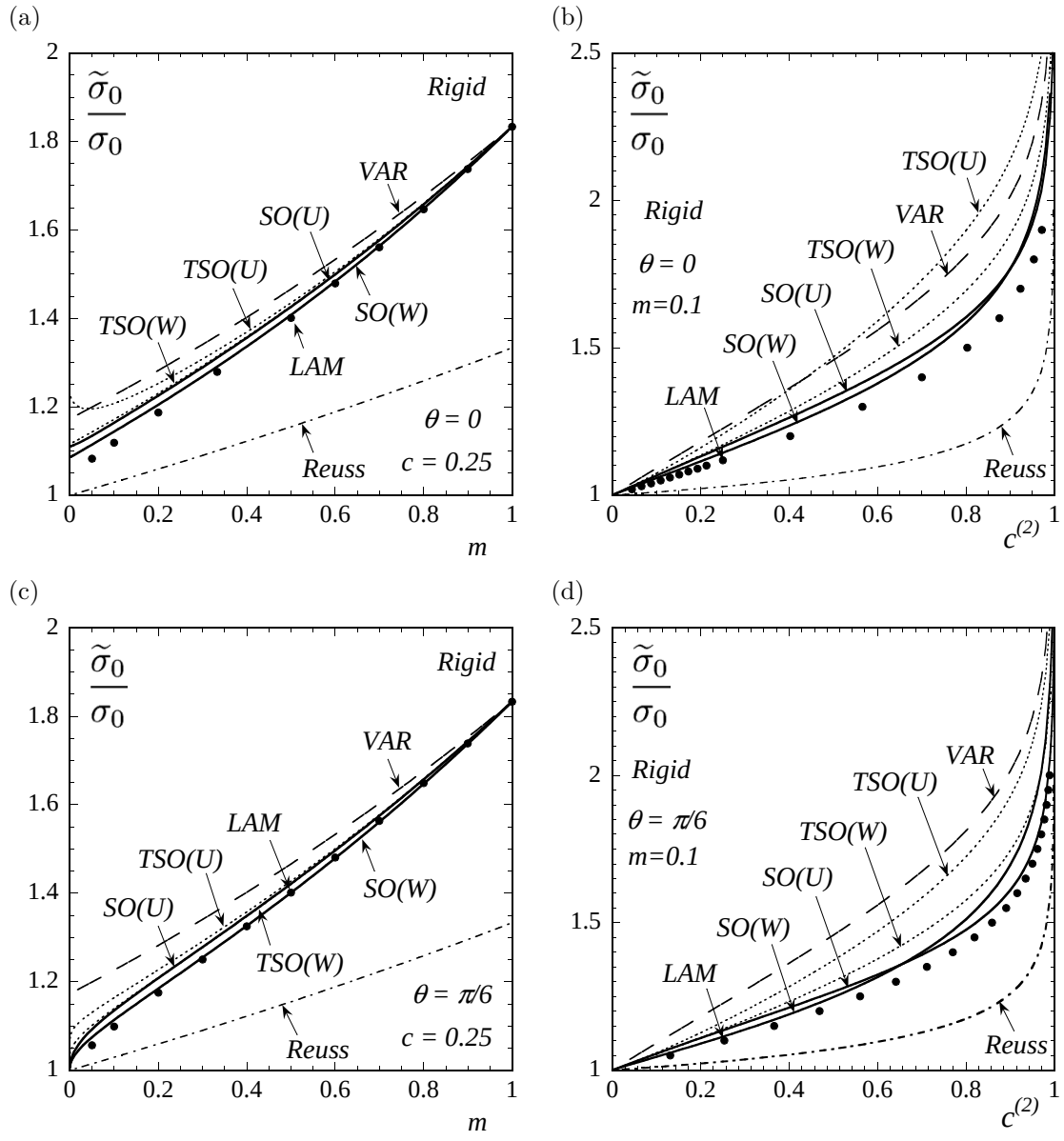

Figure 5.15: Estimates and exact results for power-law rigidly reinforced composites, subjected to axisymmetric ($\theta = 0$) and simple ($\theta = \pi/6$) shear. Effective flow stress $\widetilde{\sigma}_0$, normalized by the flow stress of the matrix $\sigma_0^{(1)}$, (a) & (c) as a function of the strain-rate sensitivity m, for a given reinforcement concentration ($c^{(2)} = 0.25$), and (b) & (d) as a function of reinforcement concentration $c^{(2)}$, for a given strain-rate sensitivity ($m = 0.1$). Comparisons between the 'second-order' (SO), 'tangent second-order' (TSO) and 'variational' (VAR) estimates of the Hashin-Shtrikman type, and exact results for power-law laminates (LAM).

TSO estimates are also able to capture the effect of the third invariant θ on $\widetilde{\sigma}_0$, but they are found to be less accurate than the SO estimates, with the stress version even violating the rigorous bound provided by the VAR estimates (see part (a)). In contrast, the VAR estimates are insensible to the third invariant θ, and are seen to overestimate, sometimes significantly, the effective flow stress, which is not surprising in view of their upper bound character.

First moments of the local fields. It is recalled that, since the inclusions are rigid, the phase averages of the strain rate are trivial in this case, namely $\overline{\boldsymbol{\varepsilon}}^{(2)} = \mathbf{0}$ and $\overline{\boldsymbol{\varepsilon}}^{(1)} = \overline{\boldsymbol{\varepsilon}}/c^{(1)}$, and all homogenization estimates agree with this fact.

The corresponding average stresses are shown in figure 5.16. Parts (a) & (c) show plots as a function of the strain-rate sensitivity m. It can be seen that the SO estimates are, in general, in good qualitative agreement with the LAM results for all values of m. Thus, these estimates predict a higher stress in the (rigid) inclusion phase than in the matrix phase, as expected, but these difference becomes smaller as the nonlinearity increases. In the ideally plastic limit, the SO estimates are such that in simple shear $\overline{\boldsymbol{\sigma}}^{(1)} = \overline{\boldsymbol{\sigma}}^{(2)} = \overline{\boldsymbol{\sigma}}$, which is consistent with a uniform stress distribution throughout the composite, while in axisymmetric shear they are consistent with a hetergeneous distribution of the stress field. In turn, this is consistent with the effective flow stress being in agreement with the Reuss lower bound in the former case and not in the latter case (see figure 5.15). However, while the SO estimates are able to capture the right dependence on θ, they are found to overestimate $\overline{\sigma}_e^{(2)}$ for dilute reinforcement concentrations (see parts (b) & (d)). Again, it is observed that, for low to moderate values of $c^{(2)}$, the $SO(W)$ estimates are in better agreement with the LAM results than the $SO(U)$ estimates, while the opposite is true at large $c^{(2)}$. In this connection, the $SO(W)$ estimates for $\overline{\sigma}_e^{(1)}$ deteriorate significantly as $c^{(2)} \to 1$, which, as already noted in the case of fiber-reinforced composites, should be related to the non-optimal choice of reference tensors. Finally, the VAR estimates for the statistics of the stress field are insensitive not only to the third invariant θ, like the corresponding estimates for $\widetilde{\sigma}_0$, but also to the strain-rate sensitivity m. This is because the VAR estimates for the statistics of the local fields correspond to those quantities in the associated LCC. These quantities can depend on m only through the heterogeneity contrast in the LCC, which in the case of rigid inclusions is infinite and therefore independent of m.

Fluctuations of the local fields. Figure 5.17 shows plots for the standard deviations (SD) of the 'parallel' and 'perpendicular' components of the strain-rate field in the matrix phase, normalized by the macroscopic equivalent strain rate $\overline{\varepsilon}_e$. We begin by noting that the strain-rate fluctuations exhibited by the LAM results increase significantly with increasing nonlinearity, and seem to be consistent with unbounded fluctuations as $m \to 0$ (see parts (a) & (c)). However, it is interesting to note that, while in the case of simple shear it is only the 'parallel' fluctuations that seem to become unbounded, in the case of axisymmetric shear it is both the 'parallel' and 'perpendicular' fluctuations. This suggests that, in ideally plastic sequential laminates, the macroscopic deformation is accommodated by shear planes running through the matrix phase, which are 'aligned' with the

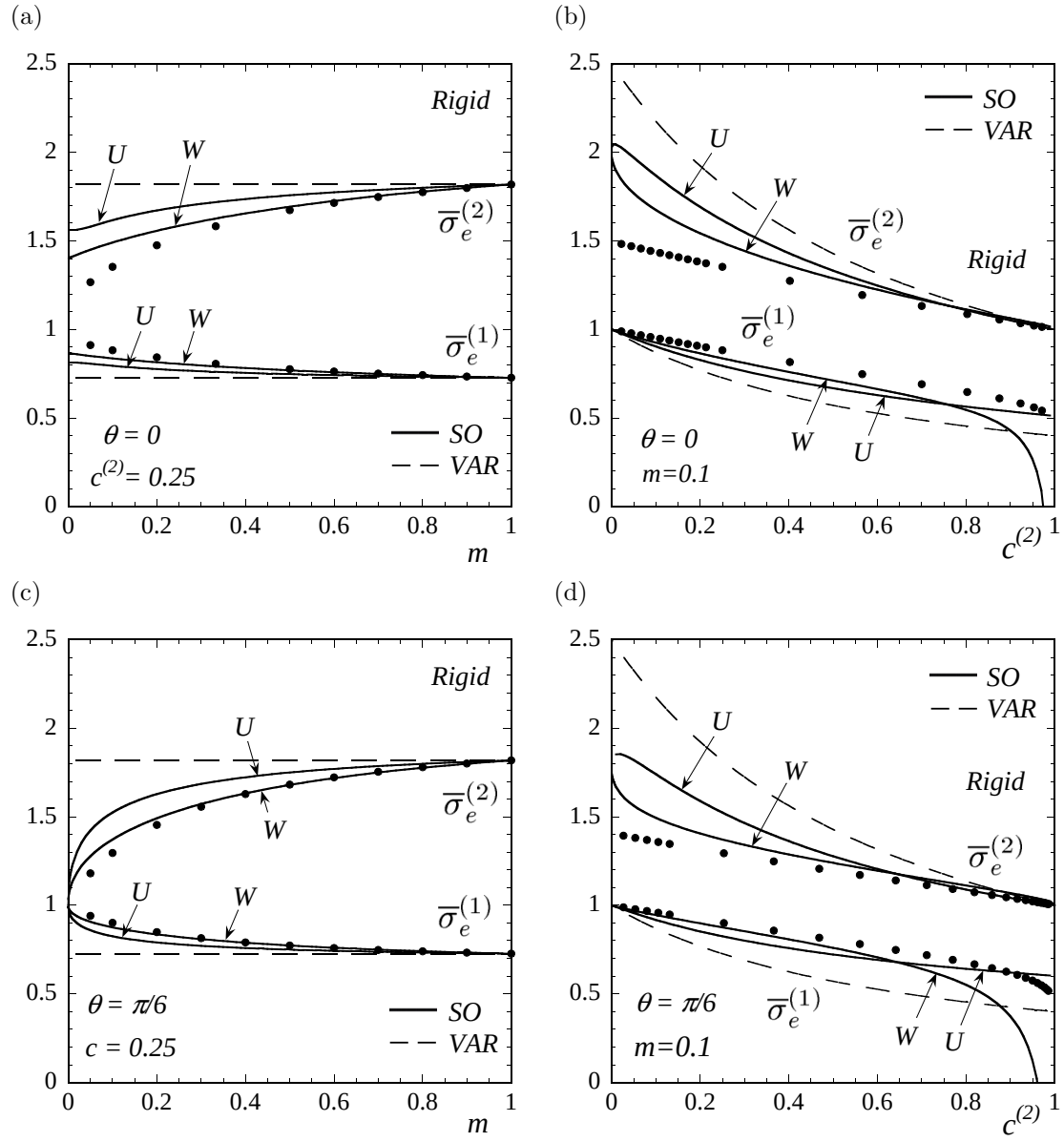

Figure 5.16: Equivalent part of the phase averages of the stress field ($\overline{\sigma}_e^{(r)}$) in rigidly-reinforced composites, normalized by the equivalent macroscopic stress $\overline{\sigma}_e$.

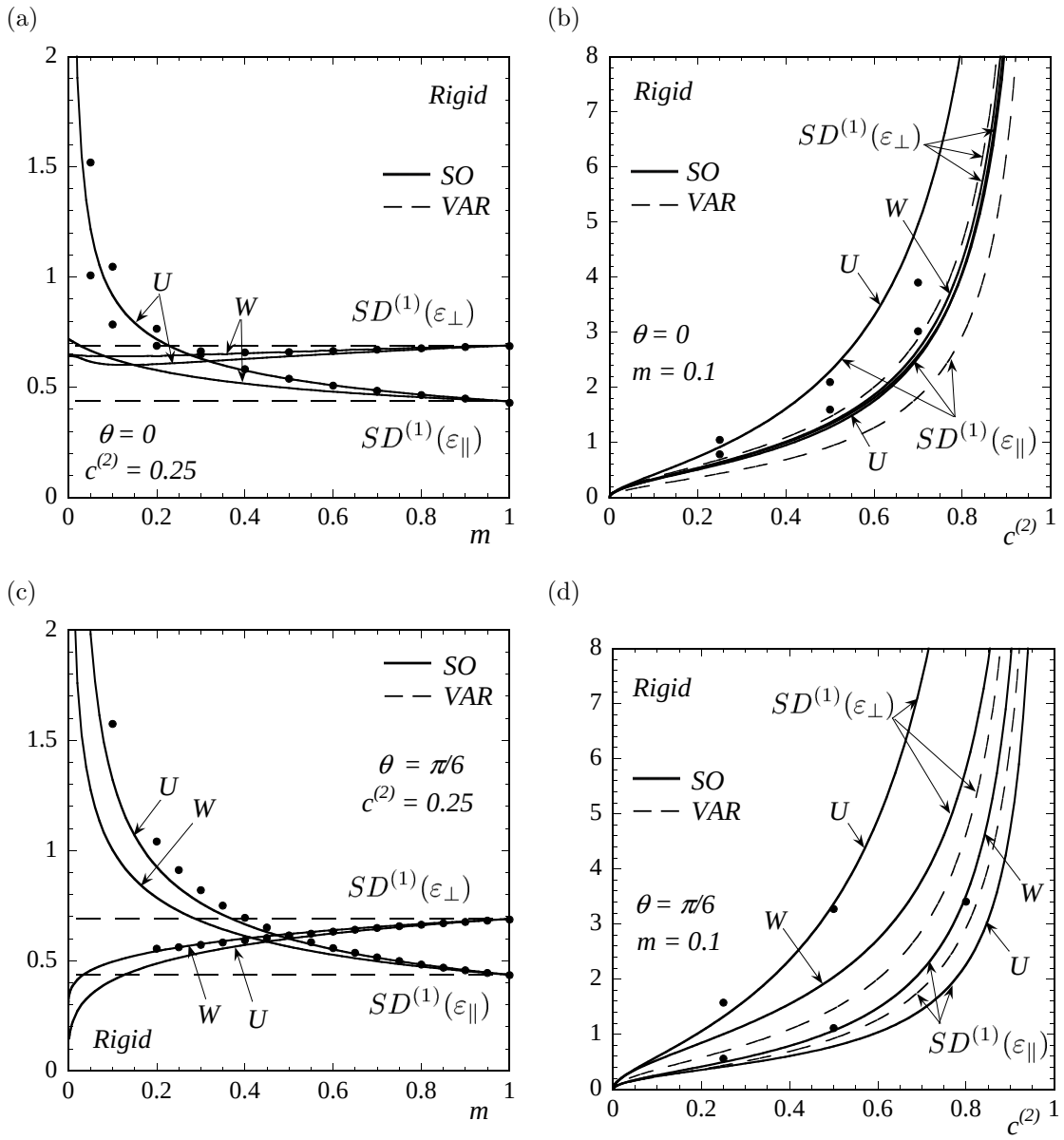

Figure 5.17: Standard deviations (SD) of the 'parallel' and 'perpendicular' components of the strain-rate field in rigidly reinforced materials, normalized by the equivalent macroscopic strain rate $\overline{\varepsilon}_e$.

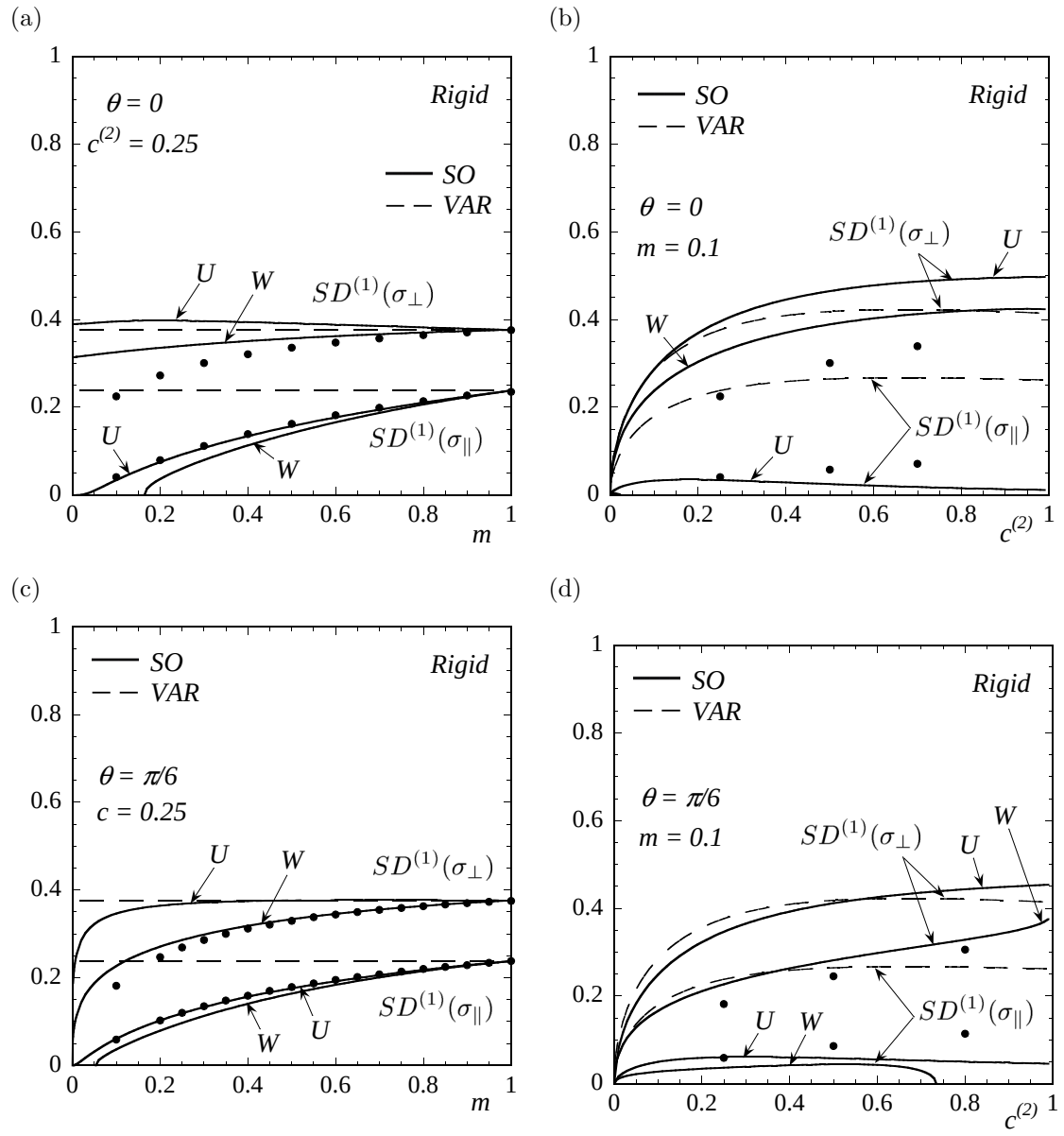

Figure 5.18: Standard deviations (SD) of the 'parallel' and 'perpendicular' components of the stress field in rigidly reinforced materials, normalized by the equivalent macroscopic stress $\overline{\sigma}_e$.

direction of maximum macroscopic shear in the case of simple shear but not in the case of axisymmetric shear loadings. Further improvements of the computer program utilized for the computation of the LAM results are necessary to obtain reliable results for smaller strain-rate sensitivities, which will clarify this point. In any event, the SO estimates for simple shear loadings (part (c)) are found to be in good agreement with the LAM results for all values of m, while those for axisymmetric shear are accurate for weak to moderate nonlinearities, but only the $SO(U)$ estimates are able to capture the blow up of the 'parallel' fluctuations as $m \to 0$. It should be emphasized, however, that the SO estimates are seen to provide a significant improvement over the earlier VAR estimates, which, as already mentioned, are insensible to m and θ. Figure 5.18 shows plots for the standard deviations (SD) of the 'parallel' and 'perpendicular' components of the stress field in the matrix phase, normalized by the macroscopic equivalent stress $\overline{\sigma}_e$. It can be seen that the SO estimates are in good qualitative agreement with the LAM results in general, and are remarkably accurate in some particular cases, even at strong nonlinearities (e.g., $SO(U)$ estimates for the 'parallel' fluctuations of the stress, see parts (a) & (c)). However, the $SO(W)$ estimates for the second moments of σ_e become smaller than the corresponding estimates for $\overline{\sigma}_e^{(1)}$ at sufficiently strong nonlinearities (i.e., $m < 0.2$), thus violating a strict inequality. This is related to the fact that the 'optimal' LCC associated with those $SO(W)$ estimates involves an $\mathbf{L}_0^{(1)}$ that is not strongly elliptic. The fact that this negative feature is manifested in this 'extreme' case is surely related to the non-optimal choice of the reference tensor $\breve{\boldsymbol{\varepsilon}}^{(1)}$, which has been set equal to $\overline{\boldsymbol{\varepsilon}}$ in this work (see Chapter 4). However, in practise, it does not seem to have a big effect on the predictions for the effective behavior and phase averages. Finally, it can be seen that the SO estimates constitute, once again, a significant improvement over the earlier VAR estimates.

5.5 Isotropic, porous materials

In this section, results are provided for the effective behavior and statistics of the local fields in isotropic, porous materials with incompressible pores, subjected to axisymmetric shear ($\theta = 0$) and simple shear ($\theta = \pi/6$) loadings.

Effective behavior. In figure 5.19, plots are given for the effective flow stress $\widetilde{\sigma}_0$, normalized by the flow stress of the matrix phase $\sigma_0^{(1)}$, as a function of the strain-rate sensitivity m and porosity $c^{(2)}$. The main observation in the context of this figure is that both versions of the SO estimates are found to be in excellent agreement with the exact LAM results, for all values of m and $c^{(2)}$, and both types of loading conditions. Thus, as in the case of stronger particles, these estimates are able to capture the right dependence on θ, which happens to be subtle in this case, and they are seen to exhibit a very small duality gap. The TSO estimates, on the other hand, are found to be, once again, very accurate for weak to moderate nonlinearities, but in the ideally plastic limit, the $TSO(U)$ estimates for both loading conditions tend to the Voigt upper bound, thus violating the sharper VAR bounds, while the $TSO(W)$ estimates for simple shear loadings underestimates significantly the LAM results.

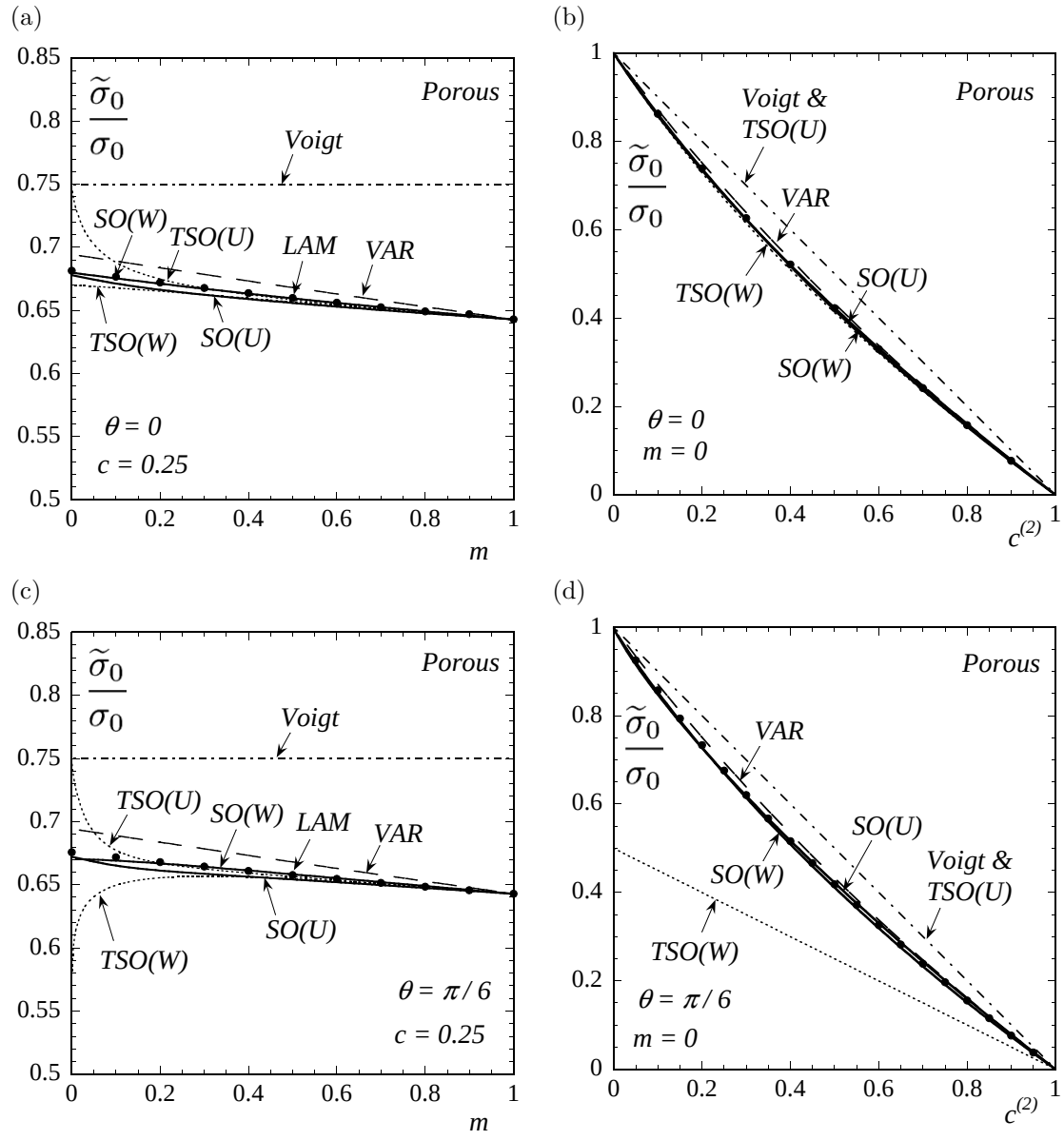

Figure 5.19: Estimates and exact results for power-law porous materials, subjected to axisymmetric ($\theta = 0$) and simple ($\theta = \pi/6$) shear. Effective flow stress $\widetilde{\sigma}_0$, normalized by the flow stress of the matrix $\sigma_0^{(1)}$, (a) & (c) as a function of the strain-rate sensitivity m, for a given reinforcement concentration ($c^{(2)} = 0.25$), and (b) & (d) as a function of reinforcement concentration $c^{(2)}$, for a given strain-rate sensitivity ($m = 0.1$). Comparisons between the 'second-order' (SO), 'tangent second-order' (TSO) and 'variational' (VAR) estimates of the Hashin-Shtrikman type, and exact results for power-law laminates (LAM).

Finally, the VAR estimates, even though insensitive to θ, are in relatively good agreement with the LAM results in this case.

First moments of the local fields. It is recalled that, since the inclusions are incompressible pores, the deviatoric parts of the average stresses in each phase are trivial in this case, namely $\overline{\boldsymbol{\sigma}}_d^{(2)} = \mathbf{0}$ and $\overline{\boldsymbol{\sigma}}_d^{(1)} = \overline{\boldsymbol{\sigma}}_d / c^{(1)}$.

The corresponding phase averages of the strain rate are shown in figure 5.20. It is seen that, as for the effective behavior, the SO estimates are in very good agreement with the LAM results for all values of m and $c^{(2)}$, under both loading conditions. While the improvement in the predictions for the effective behavior of the SO estimates over the VAR estimates was found to be relatively modest, the corresponding improvement in the phase averages of the strain rate in the pores can be quite significant. This is especially the case of an ideally plastic matrix with small concentrations of porosity, where huge differences in the predictions may be observed. In this connection, it is interesting to note that, as $c^{(2)} \to 0$, the SO estimates predict that the average strain rate in the pores remains finite in axisymmetric shear (see part (b)), but blow up in simple shear (see part (d)). Even though the available LAM results are not conclusive in this respect, they do suggest that these predictions might indeed be correct, which, if true, would constitute a remarkable result. In contrast, the VAR estimates are found to underestimate the average strain rate in the pores for low values of the porosity, in addition of being insensitive to θ and m. It is worth emphasizing that accurate predictions for the average strain rate in the porous phase of viscoplastic, porous materials are very important, since they may affect significantly the evolution of the microstructure, which in turn can have a significant effect on the macroscopic response.

Fluctuations of the local fields. In figure 5.21, plots are given for the standard deviations (SD) of the 'parallel' and 'perpendicular' components of the strain-rate field in the matrix phase, normalized by the macroscopic equivalent strain rate $\overline{\varepsilon}_e$. It can be seen that, while being fairly accurate for weak to moderate nonlinearities, no single set of SO estimates give accurate predictions at sufficiently strong nonlinearities for both 'parallel' and 'perpendicular' fluctuations, and both loading conditions. Thus, the $SO(W)$ estimates are in good qualitative agreement with the LAM results for axisymmetric shear, but not for simple shear, while the $SO(U)$ estimates for the 'parallel' fluctuations tend to zero as $m \to 0$, at odds with the LAM results. Unlike in the two-dimensional case, in this case the VAR estimates are seen to be qualitatively good, because the strain-rate fluctuations in the sequential laminates do not exhibit a strong dependence on nonlinearity. The corresponding standard deviations (SD) of the 'parallel' and 'perpendicular' components of the stress field in the matrix phase are provided in figure 5.22, normalized by the macroscopic equivalent stress $\overline{\sigma}_e$. It can be seen that the $SO(U)$ estimates are in good qualitative agreement with the LAM results for all values of m and $c^{(2)}$, and both loading conditions. The $SO(W)$ estimates, on the other hand, while accurate for the 'perpendicular' fluctuations, they predict vanishing 'parallel' fluctuations in the ideally plastic limit, which is inconsistent with the LAM results. In conclusion, the SO estimates for the fluctuations of

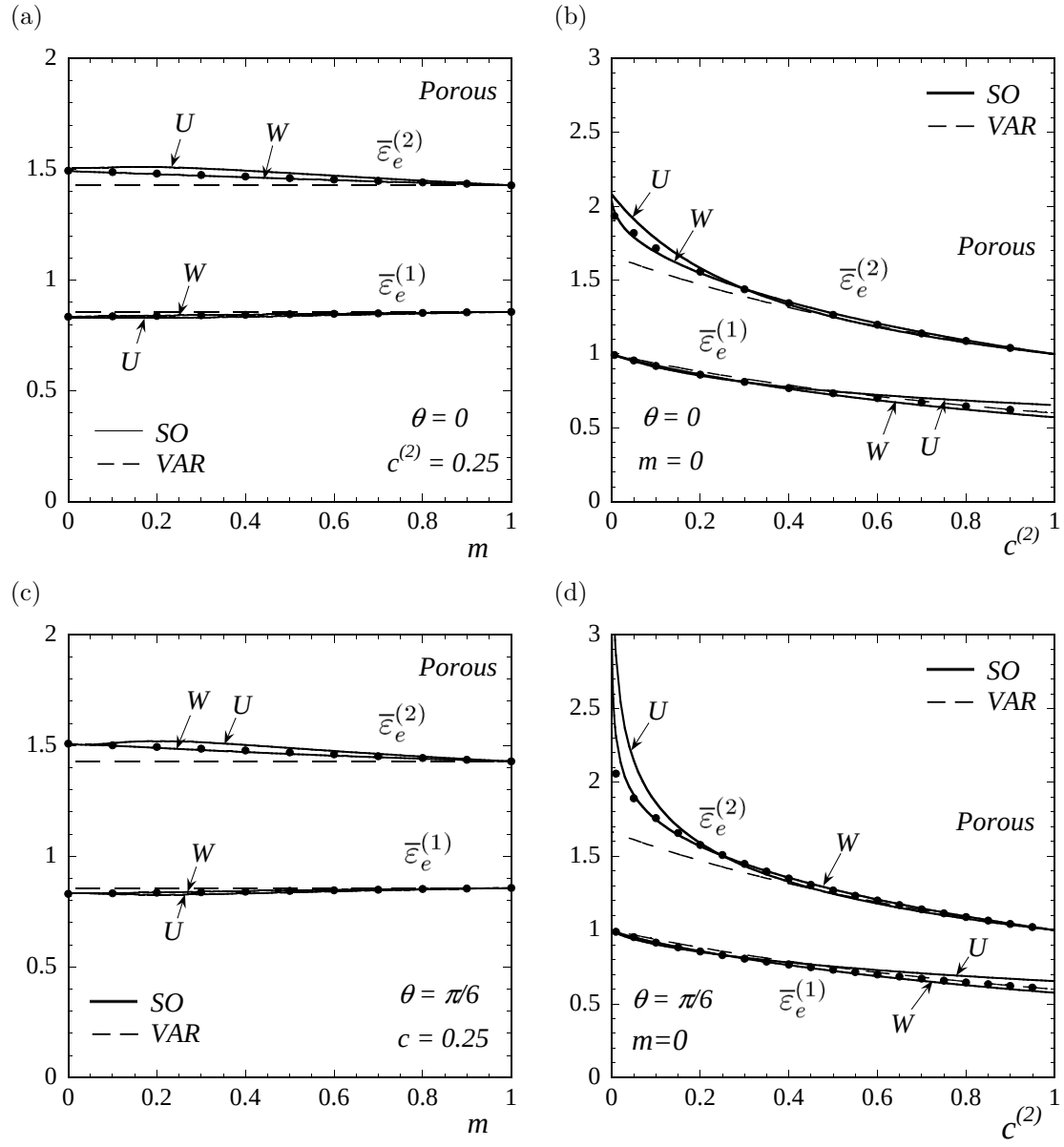

Figure 5.20: Equivalent part of the phase averages of the strain-rate field ($\overline{\varepsilon}_e^{(r)}$) in porous materials, normalized by the equivalent macroscopic strain rate $\overline{\varepsilon}_e$.

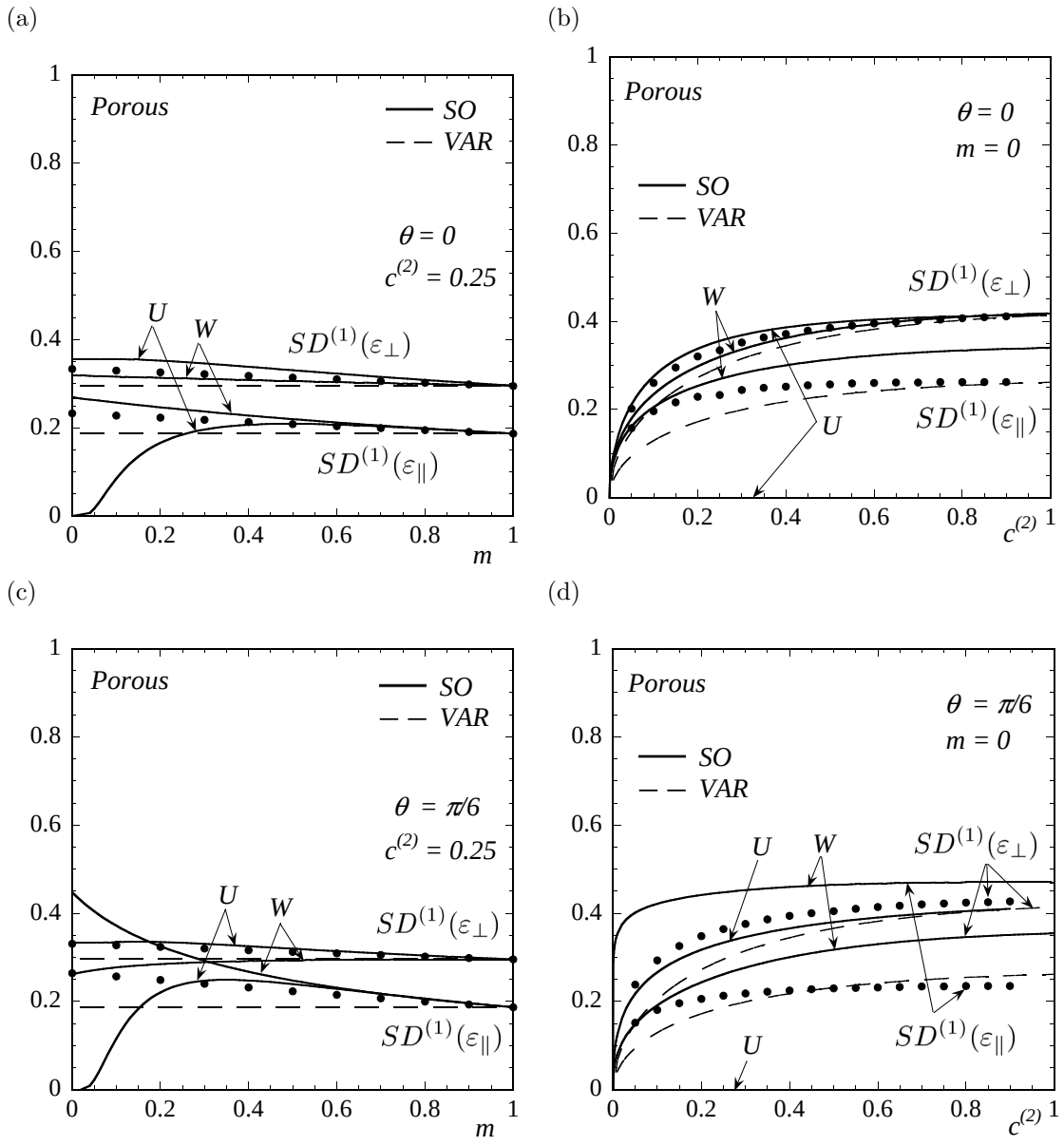

Figure 5.21: Standard deviations (SD) of the 'parallel' and 'perpendicular' components of the strain-rate field in porous materials, normalized by the equivalent macroscopic strain rate $\overline{\varepsilon}_e$.

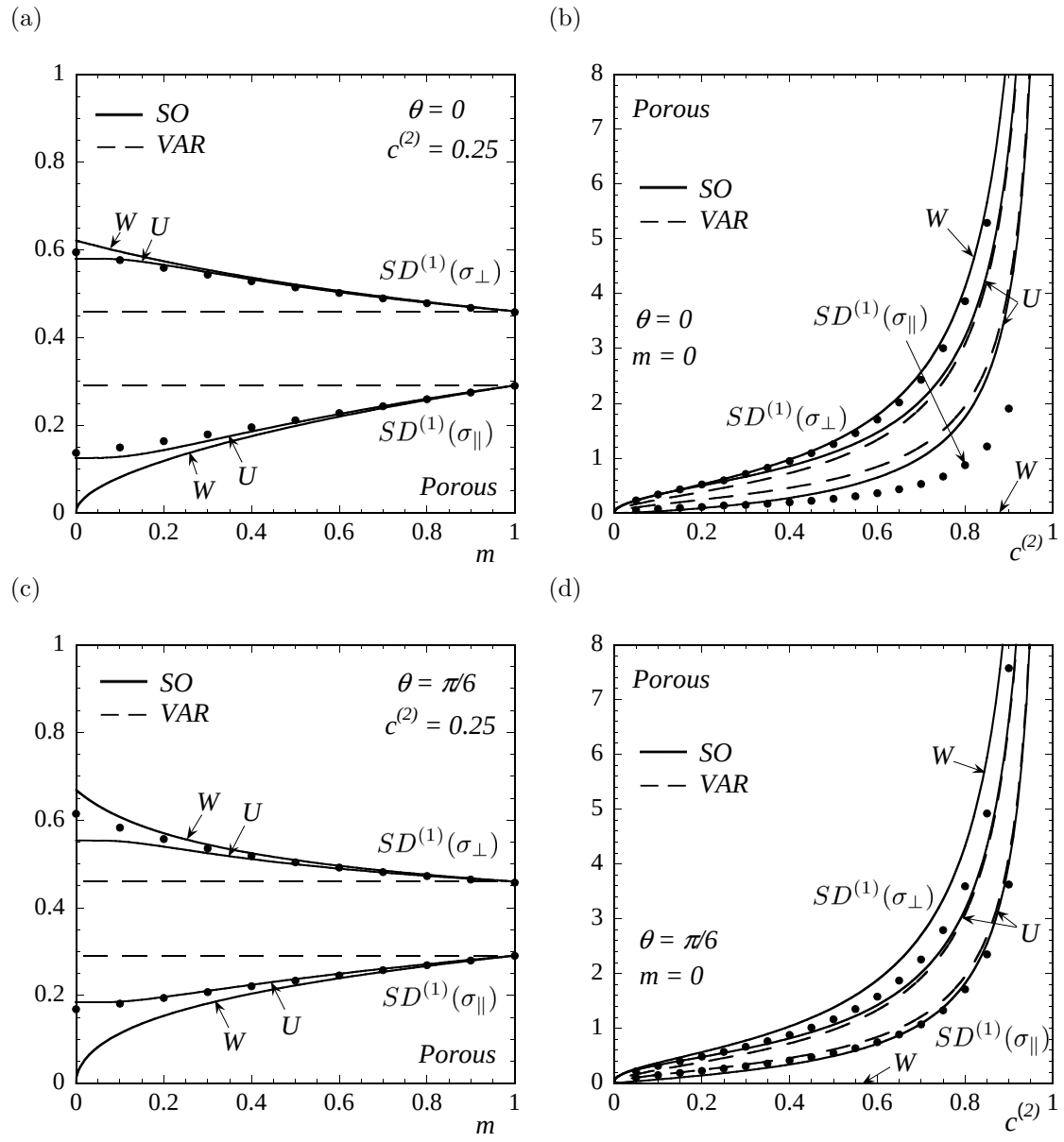

Figure 5.22: Standard deviations (SD) of the 'parallel' and 'perpendicular' components of the stress field in porous materials, normalized by the equivalent macroscopic stress $\overline{\sigma}_e$.

the local fields in porous materials are quite accurate for weak to moderate nonlinearities, but may become unreliable for sufficiently strong nonlinearities, especially in the ideally plastic limit. It is worth recalling, however, that the standard deviations correspond to sensitive statistical information, more so than the first and second moments separately. For this reason, the SO estimates for these quantities may degrade more than the corresponding estimates for the effective behavior when the choice of 'reference' tensors is not 'optimal', as in this work.

5.6 Concluding remarks

The nonlinear homogenization estimates for the effective behavior and field statistics proposed in Chapter 4 of this work have been applied to the specific cases of two-phase, power-law composites with isotropic and transversely isotropic microstructures, and have been compared with corresponding exact results for composites with sequentially laminated microstructures. The main findings are as follows:

Globally, the 'second-order' estimates are found to be superior to the 'tangent second-order' and 'variational' estimates, which can lead to inconsistent predictions in some cases. In particular, the TSO estimates have been found to give predictions for the second moments of the stress that are inconsistent with inequalities of the type $\langle \sigma_e^2 \rangle^{(r)} \geq (\overline{\sigma}_e^{(r)})^2$, for sufficiently strong nonlinearities. In addition, it was found that for low to moderate inclusion concentrations, the strain-rate formulation of the 'second-order' method leads to more accurate estimates than the stress formulation, whereas the converse is true for high inclusion concentrations.

More specifically, for the case of reinforced composites, both versions of the 'second-order' and 'tangent second-order' estimates for the effective behavior, as well as for the field statistics, were found to be in fairly good agreement with the exact results for all values of the nonlinearity. All these estimates (SO and TSO) are able to capture the anisotropic character of the field fluctuations and the fact that certain components of the strain-rate fluctuations in the matrix become unbounded in the strongly nonlinear ideally plastic limit. In contrast, the 'variational' estimates were found to significantly overestimate the effective behavior, in agreement with their upper bound character, and to give qualitatively incorrect predictions for the field statistics, failing to capture the strong anisotropy of the strain-rate fluctuations at high nonlinearities.

For the cases of fiber-weakened and porous composites, which are more 'demanding' than those of reinforced composites, the 'second-order' estimates for the effective behavior and first moments of the local fields were found to be in good agreement with the exact results even for strong nonlinearities. In general, the accuracy of the corresponding estimates for the second moments of the fields was found to be less good, which is not surprising in view of the fact that they correspond to more sensitive information. However, these estimates agree with the exact results in that, unlike in the case of reinforced composites, the second moments of the strain rate remain bounded in the ideally plastic limit, thus capturing the relative differences between the deformation patterns in the weaker-

and stronger-particle cases. On the other hand, the 'tangent second-order' estimates were found to be fairly accurate for weak to moderate nonlinearities, but deteriorate significantly for strong nonlinearites. In turn, the 'variational' estimates were found to be relatively good for the effective behavior, but qualitatively incorrect for the field statistics.

It is worth mentioning that accounting for the 'correction' terms derived in Chapter 4 in the context of the 'second-order' and 'tangent second-order' estimates for the field statistics almost always had a beneficial effect, in that they improve the predictions arising from the sole use of the LCC. This improvement can be quite significant at strong nonlinearities, especially for the statistics of the dual field (i.e., the strain-rate statistics arising from the stress formulation of the methods, and *vice versa*). Finally, it is emphasized that even though the 'optimal' choice of the 'reference tensors' in the context of the 'second-order' estimates remains an open question, the results provided in this work show that accurate estimates can be obtained by making use of the simplest possible prescriptions for these tensors, namely, the macroscopic fields themselves. In addition, these choices have been shown (see Chapter 4) to lead to relatively simple analytical estimates for the first and second moments of the strain-rate and stress fields.

Chapter 6

Homogenization estimates for viscoplastic composites with anisotropic constituents

6.1 Introduction

Chapters 4 and 5 were concerned with nonlinear composites made up of *isotropic* constituents. However, a wide range of natural and man-made heterogeneous materials are intrinsically *anisotropic*. This is the case, especially, of polycrystalline materials, such as metals, ice, and many rocks. In fact, most of the work already alluded to in the Introduction has been driven by the need to understand plastic flow in polycrystals. The present chapter is concerned with an extension of the 'variational' method of Ponte Castañeda (1991, 1992a) to composites with nonlinear (viscoplastic) anisotropic phases. It will be shown that this generalization has the capability to give improved bounds relative to the earlier generalization provided by deBotton & Ponte Castañeda (1995) in the specific context of viscoplastic polycrystals, and the further generalization of Suquet (see Ponte Castañeda & Suquet 1998) for more general anisotropies.

For simplicity, this chapter has been written in the context of nonlinear, infinitesimal elasticity, so that $\boldsymbol{\varepsilon}$ and $\boldsymbol{\sigma}$ represent the infinitesimal strain and stress, respectively. However, it is recalled that the results apply *mutatis mutandis* to the case of finite viscous deformations, in which case $\boldsymbol{\varepsilon}$ and $\boldsymbol{\sigma}$ represent the Eulerian strain-rate and Cauchy stress tensors, respectively.

6.2 Linear comparison materials

Consider a *linear-elastic comparison* material with positive-definite, fully symmetric stiffness tensor $\mathbf{L}_0$, such that its strain potential is given by

$$w_0(\mathbf{x}, \boldsymbol{\varepsilon}) = \frac{1}{2}\boldsymbol{\varepsilon} \cdot \mathbf{L}_0(\mathbf{x})\boldsymbol{\varepsilon}. \tag{6.1}$$

Assuming that $w^{(r)}$ has 'weaker-than-quadratic' growth at infinity, implying that $\left(w^{(r)} - w_0\right) \to -\infty$ as $|\boldsymbol{\varepsilon}| \to \infty$ (for fixed $\mathbf{x}$), suggests the following definition.

Definition 6.2.1. *Let $v^{(r)}$ be the phase 'corrector' function, serving as a measure of the nonlinearity in the original material with strain potential $w^{(r)}$, and given by*

$$v^{(r)}(\mathbf{L}_0) = \sup_{\boldsymbol{\varepsilon}} \left\{ w^{(r)}(\boldsymbol{\varepsilon}) - \frac{1}{2}\boldsymbol{\varepsilon} \cdot \mathbf{L}_0 \boldsymbol{\varepsilon} \right\}. \tag{6.2}$$

Remark 6.2.2. The definition (6.2) is still valid when the stiffness tensor $\mathbf{L}_0$ is *not* positive definite, but in this case $v^{(r)}$ takes on infinite values. This is easy to see, because choosing $\boldsymbol{\varepsilon}$ to be proportional to the eigentensor corresponding to any zero, or negative eigenvalue of $\mathbf{L}_0$ leads to an infinite value for the supremum in expression (6.2). In fact, $v^{(r)}$ tends to infinity, when any eigenvalue of (a positive-definite) $\mathbf{L}_0$ tends to zero. Also, note that, by definition, $v^{(r)}(\mathbf{L}_0) \geq w^{(r)}(\mathbf{0}) = 0$, and so $v^{(r)}$ is a *non-negative* function. In addition, being the pointwise supremum of a collection of affine functions of $\mathbf{L}_0$, $v^{(r)}$ is a *convex* function of $\mathbf{L}_0$. Furthermore, assuming smoothness of the functions $w^{(r)}$, the solutions of the *non-concave* optimization problem defined by (6.2) are normally given by the *stationarity* conditions

$$\mathbf{L}_0 \hat{\boldsymbol{\varepsilon}}^{(r)}_{(m)} = \partial_{\boldsymbol{\varepsilon}} w^{(r)} \left(\hat{\boldsymbol{\varepsilon}}^{(r)}_{(m)} \right), \tag{6.3}$$

where the $\hat{\boldsymbol{\varepsilon}}^{(r)}_{(m)}$, $m = 1, ..., M^{(r)}$, denote *all* the strain tensors for which the maximum is attained in (6.2) for a given $\mathbf{L}_0$. (Note that $M^{(r)}$ can be infinite in some instances, such as when the potential $w^{(r)}$ and $\mathbf{L}_0$ are both isotropic.)

It follows from the definition (6.2) that

$$w^{(r)}(\boldsymbol{\varepsilon}) \leq \frac{1}{2}\boldsymbol{\varepsilon} \cdot \mathbf{L}_0 \boldsymbol{\varepsilon} + v^{(r)}(\mathbf{L}_0), \tag{6.4}$$

for any $\mathbf{L}_0$, and hence that

$$w^{(r)}(\boldsymbol{\varepsilon}) \leq \inf_{\mathbf{L}_0} \left\{ \frac{1}{2}\boldsymbol{\varepsilon} \cdot \mathbf{L}_0 \boldsymbol{\varepsilon} + v^{(r)}(\mathbf{L}_0) \right\}. \tag{6.5}$$

But, as has been pointed out earlier, the function $v^{(r)}$ is infinite if $\mathbf{L}_0$ is *not* positive definite, and therefore, the expression (6.5) can be equivalently written as

$$w^{(r)}(\boldsymbol{\varepsilon}) \leq \inf_{\mathbf{L}_0 > 0} \left\{ \frac{1}{2}\boldsymbol{\varepsilon} \cdot \mathbf{L}_0 \boldsymbol{\varepsilon} + v^{(r)}(\mathbf{L}_0) \right\}, \tag{6.6}$$

where the notation $\mathbf{L}_0 > 0$ has been used to signify that $\mathbf{L}_0$ is positive definite.

In general, the inequality in expression (6.6) will hold. However, there may be classes of nonlinear materials, for which the equality would hold. Noting that the right-hand side of the expression (6.6) is concave in the variable $\boldsymbol{\varepsilon} \otimes \boldsymbol{\varepsilon}$ (because it is the pointwise infimum of a set of affine functions in this variable) suggests that in order for equality to hold in expression (6.6), the potential w must be concave in the variable $\boldsymbol{\varepsilon} \otimes \boldsymbol{\varepsilon}$. Accordingly, it will be assumed that the potentials w of interest here satisfy the following 'square concavity' hypothesis.

Hypothesis 6.2.3. *It is assumed that there exist functions $f^{(r)}$ that are concave in the space of fourth-order tensors, $\mathbf{e}$, possessing the usual symmetry properties of elasticity tensors, and satisfying the properties: (i) $f^{(r)}(\mathbb{O}) = 0$, and (ii) $f^{(r)} \to \infty$ as $|\mathbf{e}| \to \infty$, such that the phase potentials $w^{(r)}$ may be expressed as*

$$w^{(r)}(\boldsymbol{\varepsilon}) = f^{(r)} \left(\frac{1}{2}\boldsymbol{\varepsilon} \otimes \boldsymbol{\varepsilon} \right). \tag{6.7}$$

This hypothesis was introduced by Ponte Castañeda (1992a) for isotropic materials, and generalized as described above for anisotropic materials by Suquet (see Ponte Castañeda & Suquet 1998). It should be emphasized that the functions $f^{(r)}$ are not uniquely determined. Also, a consequence of the above hypothesis is that the potentials $w^{(r)}$, as defined by relation (6.7), should satisfy the relation: $w^{(r)}(-\boldsymbol{\varepsilon}) = w^{(r)}(\boldsymbol{\varepsilon})$. In addition, it should be noted that this hypothesis is consistent with the earlier assumption that the potentials $w^{(r)}$ exhibit *weaker-than-quadratic* growth on the strain $\boldsymbol{\varepsilon}$. It is shown next that the equality holds strictly in expression (6.6) when the stronger 'square concavity' hypothesis is made.

Lemma 6.2.4. *Consider a composite with 'square concave' phase potentials $w^{(r)}$, as defined in Hypothesis 6.2.3. It then follows that*

$$w^{(r)}(\boldsymbol{\varepsilon}) = \inf_{\mathbf{L}_0>0} \left\{ \frac{1}{2}\boldsymbol{\varepsilon}\cdot\mathbf{L}_0\boldsymbol{\varepsilon} + v^{(r)}(\mathbf{L}_0) \right\}, \tag{6.8}$$

where the 'corrector' functions $v^{(r)}$ have been defined by relations (6.2). It also follows that

$$w(\mathbf{x},\boldsymbol{\varepsilon}) = \inf_{\mathbf{L}_0>0} \left\{ w_0(\mathbf{x},\boldsymbol{\varepsilon}) + v(\mathbf{x},\mathbf{L}_0) \right\}, \tag{6.9}$$

where w_0 is given by (6.1), and v is the function defined by

$$v(\mathbf{x},\mathbf{L}_0) = \sup_{\boldsymbol{\varepsilon}} \left\{ w(\mathbf{x},\boldsymbol{\varepsilon}) - w_0(\mathbf{x},\boldsymbol{\varepsilon}) \right\}. \tag{6.10}$$

Proof. The concave Legendre-Fenchel transform of $f^{(r)}$ is defined as:

$$f_*^{(r)}(\mathbf{L}_0) = \inf_{\mathbf{e}} \left\{ \mathbf{L}_0\cdot\mathbf{e} - f^{(r)}(\mathbf{e}) \right\}. \tag{6.11}$$

Note that $f_*^{(r)}$ is a non-positive, concave function of $\mathbf{L}_0$, such that $f_*^{(r)}(\mathbf{L}_0) = -\infty$ when $\mathbf{L}_0$ is not positive definite. It then follows from the assumed concavity of $f^{(r)}$ that

$$f^{(r)}(\mathbf{e}) = \inf_{\mathbf{L}_0>0} \left\{ \mathbf{L}_0\cdot\mathbf{e} - f_*^{(r)}(\mathbf{L}_0) \right\}, \tag{6.12}$$

where the restriction to positive definite $\mathbf{L}_0$ has been made since, otherwise, the right-hand side would be infinite.

Using (6.7), it is concluded from (6.12) that

$$w^{(r)}(\boldsymbol{\varepsilon}) = \inf_{\mathbf{L}_0>0} \left\{ \frac{1}{2}\boldsymbol{\varepsilon}\cdot\mathbf{L}_0\boldsymbol{\varepsilon} - f_*^{(r)}(\mathbf{L}_0) \right\}. \tag{6.13}$$

It should be emphasized that this result, first given in Ponte Castañeda & Suquet (1998), is valid for any 'concave extension' $f^{(r)}$ of the phase potential $w^{(r)}$, as provided by Hypothesis 6.2.3.

Now, it follows from (6.11) that

$$\begin{aligned} f_*^{(r)}(\mathbf{L}_0) &\leq \inf_{\mathbf{e}=\frac{1}{2}\boldsymbol{\varepsilon}\otimes\boldsymbol{\varepsilon}} \left\{ \mathbf{L}_0\cdot\mathbf{e} - f^{(r)}(\mathbf{e}) \right\} \\ &= \inf_{\boldsymbol{\varepsilon}} \left\{ \frac{1}{2}\boldsymbol{\varepsilon}\cdot\mathbf{L}_0\boldsymbol{\varepsilon} - w^{(r)}(\boldsymbol{\varepsilon}) \right\}, \end{aligned} \tag{6.14}$$

and, hence that

$$-f_*^{(r)}(\mathbf{L}_0) \geq v^{(r)}(\mathbf{L}_0), \tag{6.15}$$

where $v^{(r)}$ is the phase corrector function, as defined by (6.2). (It is important to emphasize that, in general, the functions $v^{(r)}$ cannot be identified with the functions $-f_*^{(r)}$.) Therefore, from expression (6.13), it is concluded that

$$w^{(r)}(\boldsymbol{\varepsilon}) \geq \inf_{\mathbf{L}_0>0} \left\{ \frac{1}{2}\boldsymbol{\varepsilon}\cdot\mathbf{L}_0\boldsymbol{\varepsilon} + v^{(r)}(\mathbf{L}_0) \right\}. \tag{6.16}$$

But this expression, together with (6.6), which is itself independent of any concavity hypothesis, indeed implies that the identity (6.8) holds under the above 'square concavity' hypothesis.

Next, recalling that w is defined in terms of the phase potentials $w^{(r)}$ by relation (2.2), and defining v similarly in terms of the functions $v^{(r)}$ by

$$v(\mathbf{x},\mathbf{L}_0) = \sum_{r=1}^{N} \chi^{(r)}(\mathbf{x})\; v^{(r)}(\mathbf{L}_0), \tag{6.17}$$

it is concluded that relations (6.9) and (6.10) also hold true, where use has been made of relation (6.1).

□

Remark 6.2.5. On account of the convexity of $v^{(r)}$ on $\mathbf{L}_0$, and of the fact that the restriction to positive definite $\mathbf{L}_0$ simply corresponds to the domain of $v^{(r)}$, the optimality condition in expression (6.8) for $w^{(r)}$ is given by the condition that zero should be included in the subdifferential of the terms in curly brackets, which may also be written as

$$-\frac{1}{2}\boldsymbol{\varepsilon}\otimes\boldsymbol{\varepsilon} \in \partial_{\mathbf{L}_0} v^{(r)}(\hat{\mathbf{L}}_0), \tag{6.18}$$

where $\hat{\mathbf{L}}_0$ is the optimal value of $\mathbf{L}_0$, and $\partial_{\mathbf{L}_0} v^{(r)}$ is the subdifferential of the function $v^{(r)}$. In this connection, it should be emphasized that the functions $v^{(r)}$ are not smooth, even when the $w^{(r)}$ are. (This is essentially because the optimal solutions (6.3) in expressions (6.2) for the functions $v^{(r)}$ can change abruptly with changes in $\mathbf{L}_0$, leading to 'corners' and 'edges' in the $v^{(r)}$.) As a consequence, the eigendirections of $\hat{\mathbf{L}}_0$ may be determined by these sharp edges, leaving the corresponding eigenvalues to be determined by appropriate stationarity conditions. In this connection, it is useful to note that the subdifferential of $v^{(r)}$, which is, by definition, a 'max-function,' may be expressed as (see, for instance, Exercise 10 in section 6.1 of Borwein & Lewis 2000):

$$\partial_{\mathbf{L}_0} v^{(r)}\left(\mathbf{L}_0\right) = \left\{ \mathbf{e} | \mathbf{e} = -\frac{1}{2}\sum_{m=1}^{M^{(r)}} a_m^{(r)} \left(\hat{\boldsymbol{\varepsilon}}_{(m)}^{(r)} \otimes \hat{\boldsymbol{\varepsilon}}_{(m)}^{(r)} \right),\; a_m^{(r)} \geq 0,\; \sum_{m=1}^{M^{(r)}} a_m^{(r)} = 1 \right\}, \tag{6.19}$$

where $\hat{\boldsymbol{\varepsilon}}_{(m)}^{(r)}$, $m = 1, ..., M^{(r)}$, denote *all* the strain vectors for which the maximum in (6.2) is attained for a given $\mathbf{L}_0$ (see also the optimality relations (6.3)). In words, the subdifferential (6.19) of the function $v^{(r)}$ is the set of all convex combinations of the rank-one tensors $(-1/2)\,\hat{\boldsymbol{\varepsilon}}_{(m)}^{(r)} \otimes \hat{\boldsymbol{\varepsilon}}_{(m)}^{(r)}$, formed by the optimal strain vectors $\hat{\boldsymbol{\varepsilon}}_{(m)}^{(r)}$ in expressions (6.2) for the functions $v^{(r)}$.

Result 6.2.6. *The stress-strain relation associated with the strain potential $w^{(r)}$, as determined by expression (6.8), is given by*

$$\boldsymbol{\sigma} = \partial_{\boldsymbol{\varepsilon}} w^{(r)}(\boldsymbol{\varepsilon}) = \hat{\mathbf{L}}_0(\boldsymbol{\varepsilon})\,\boldsymbol{\varepsilon}, \tag{6.20}$$

where $\hat{\mathbf{L}}_0(\boldsymbol{\varepsilon})$ *is the optimal value of* $\mathbf{L}_0$ *in expression (6.8), evaluated at* $\boldsymbol{\varepsilon}$*.*

Proof. Given the convexity of $w^{(r)}$ and the fact that the optimality condition in expression (6.8) is not a simple stationarity condition, it is best to work here with the subdifferential. Now, if $\boldsymbol{\sigma} \in \partial_{\boldsymbol{\varepsilon}} w^{(r)}(\boldsymbol{\varepsilon})$, then

$$\boldsymbol{\sigma} \cdot (\boldsymbol{\varepsilon}' - \boldsymbol{\varepsilon}) \leq w^{(r)}(\boldsymbol{\varepsilon}') - w^{(r)}(\boldsymbol{\varepsilon}), \quad \text{for all } \boldsymbol{\varepsilon}', \tag{6.21}$$

or, using expression (6.8) for $w^{(r)}$,

$$\begin{aligned} \boldsymbol{\sigma} \cdot (\boldsymbol{\varepsilon}' - \boldsymbol{\varepsilon}) &\leq \inf_{\mathbf{L}_0 > 0} \left\{ \frac{1}{2} \boldsymbol{\varepsilon}' \cdot \mathbf{L}_0 \boldsymbol{\varepsilon}' + v^{(r)}(\mathbf{L}_0) \right\} - \inf_{\mathbf{L}_0 > 0} \left\{ \frac{1}{2} \boldsymbol{\varepsilon} \cdot \mathbf{L}_0 \boldsymbol{\varepsilon} + v^{(r)}(\mathbf{L}_0) \right\} \\ &\leq \frac{1}{2} \boldsymbol{\varepsilon}' \cdot \mathbf{L}_0' \boldsymbol{\varepsilon}' + v^{(r)}(\mathbf{L}_0') - \frac{1}{2} \boldsymbol{\varepsilon} \cdot \hat{\mathbf{L}}_0 \boldsymbol{\varepsilon} + v^{(r)}(\hat{\mathbf{L}}_0), \quad \text{for all } \boldsymbol{\varepsilon}', \mathbf{L}_0', \end{aligned}$$

where $\hat{\mathbf{L}}_0$ is the optimal value of $\mathbf{L}_0$ evaluated at $\boldsymbol{\varepsilon}$. In particular, for $\mathbf{L}_0' = \hat{\mathbf{L}}_0(\boldsymbol{\varepsilon})$, it follows that

$$\boldsymbol{\sigma} \cdot (\boldsymbol{\varepsilon}' - \boldsymbol{\varepsilon}) \leq \frac{1}{2} \boldsymbol{\varepsilon}' \cdot \hat{\mathbf{L}}_0(\boldsymbol{\varepsilon}) \boldsymbol{\varepsilon}' - \frac{1}{2} \boldsymbol{\varepsilon} \cdot \hat{\mathbf{L}}_0(\boldsymbol{\varepsilon}) \boldsymbol{\varepsilon}, \quad \text{for all } \boldsymbol{\varepsilon}', \tag{6.22}$$

which means that $\boldsymbol{\sigma} \in \partial_{\boldsymbol{\varepsilon}} w_0$, where $w_0 = \frac{1}{2} \boldsymbol{\varepsilon} \cdot \hat{\mathbf{L}}_0 \boldsymbol{\varepsilon}$, with $\hat{\mathbf{L}}_0$ fixed. But w_0 is differentiable, with derivative $\hat{\mathbf{L}}_0 \boldsymbol{\varepsilon}$, and so, $\partial_{\boldsymbol{\varepsilon}} w_0(\boldsymbol{\varepsilon}) = \{\hat{\mathbf{L}}_0(\boldsymbol{\varepsilon}) \boldsymbol{\varepsilon}\}$. In conclusion, it has been shown that if $\boldsymbol{\sigma} \in \partial_{\boldsymbol{\varepsilon}} w^{(r)}(\boldsymbol{\varepsilon})$, then $\boldsymbol{\sigma} = \hat{\mathbf{L}}_0(\boldsymbol{\varepsilon}) \boldsymbol{\varepsilon}$, which is the desired result.

□

Remark 6.2.7. The result (6.20) should not be confused with the optimality condition (6.3), which is only a prescription for the optimal $\hat{\boldsymbol{\varepsilon}}_{(m)}^{(r)}$, for some given $\mathbf{L}_0$, in the definition of the corrector function $v^{(r)}$. Interestingly, although the expression (6.3) is commonly used to define (in a non-unique fashion) the *secant modulus* tensor (see, for example, Ponte Castañeda & Suquet 1998), it follows from Result 6.2.6, that, in fact, a *better* definition of the secant modulus, in the general anisotropic case, is provided by the optimal $\hat{\mathbf{L}}_0$ in expression (6.8). This leads to a well-defined prescription that can be shown to be consistent with the standard prescription in the isotropic case.

It is also possible to obtain an alternative representation starting from the local stress potentials (2.6). To accomplish this, note that (6.2) can be re-expressed as

$$\begin{aligned} v^{(r)}(\mathbf{L}_0) &= \sup_{\boldsymbol{\varepsilon}} \left\{ \sup_{\boldsymbol{\sigma}} \left\{ \boldsymbol{\varepsilon} \cdot \boldsymbol{\sigma} - u^{(r)}(\boldsymbol{\sigma}) \right\} - \frac{1}{2} \boldsymbol{\varepsilon} \cdot \mathbf{L}_0 \boldsymbol{\varepsilon} \right\} \\ &= \sup_{\boldsymbol{\sigma}} \left\{ \sup_{\boldsymbol{\varepsilon}} \left\{ \boldsymbol{\varepsilon} \cdot \boldsymbol{\sigma} - \frac{1}{2} \boldsymbol{\varepsilon} \cdot \mathbf{L}_0 \boldsymbol{\varepsilon} \right\} - u^{(r)}(\boldsymbol{\sigma}) \right\} \\ &= \sup_{\boldsymbol{\sigma}} \left\{ \frac{1}{2} \boldsymbol{\sigma} \cdot (\mathbf{L}_0)^{-1} \boldsymbol{\sigma} - u^{(r)}(\boldsymbol{\sigma}) \right\}, \end{aligned} \tag{6.23}$$

where use has been made of the fact that $w^{(r)} = u^{(r)^*}$ and of the positive definiteness of $\mathbf{L}_0$, as well as of the fact that the order of suprema can be interchanged. This allows the definition of a new function $\check{v}^{(r)}(\mathbf{M}_0) = v^{(r)}(\mathbf{L}_0 = \mathbf{M}_0^{-1})$, as follows.

Definition 6.2.8. *The phase 'corrector' functions can alternatively be expressed in terms of the phase compliance tensors* $\mathbf{M}_0$ *via the relations*

$$\check{v}^{(r)}(\mathbf{M}_0) = \sup_{\boldsymbol{\sigma}} \left\{ \frac{1}{2} \boldsymbol{\sigma} \cdot \mathbf{M}_0 \boldsymbol{\sigma} - u^{(r)}(\boldsymbol{\sigma}) \right\}. \tag{6.24}$$

Remark 6.2.9. $\check{v}^{(r)}$ is a convex, non-negative function of $\mathbf{M}_0 \left(= \mathbf{L}_0^{-1}\right)$, such that $\check{v}^{(r)} = 0$ when $\mathbf{M}_0 \leq 0$. Note that in the following there will be no risk of confusion, and, for simplicity, no attempt will be made to distinguish between $\check{v}^{(r)}$ and $v^{(r)}$, henceforth writing simply $v^{(r)}(\mathbf{M}_0)$. Also, assuming smoothness of the functions $u^{(r)}$, the solutions of the *non-concave* optimization problem defined by (6.24) are normally given by the *stationarity* conditions

$$\mathbf{M}_0 \hat{\boldsymbol{\sigma}}_{(m)}^{(r)} = \partial_{\boldsymbol{\sigma}} u^{(r)} \left(\hat{\boldsymbol{\sigma}}_{(m)}^{(r)} \right), \tag{6.25}$$

where the $\hat{\boldsymbol{\sigma}}_{(m)}^{(r)}$, $m = 1, ..., N^{(r)}$, denote *all* the stress tensors for which the maximum is attained in (6.24) for a given $\mathbf{M}_0$.

Then, introducing the stress potential of the linear comparison material via

$$u_0(\mathbf{x}, \boldsymbol{\sigma}) = \frac{1}{2} \boldsymbol{\sigma} \cdot \mathbf{M}_0(\mathbf{x}) \boldsymbol{\sigma}, \tag{6.26}$$

it is also possible to define the local 'corrector' function:

$$v(\mathbf{x}, \mathbf{M}_0) = \sup_{\boldsymbol{\sigma}} \left\{ u_0(\mathbf{x}, \boldsymbol{\sigma}) - u(\mathbf{x}, \boldsymbol{\sigma}) \right\}. \tag{6.27}$$

From these definitions, the next result follows.

Lemma 6.2.10. *Consider a composite with phase stress potential $u^{(r)} = w^{(r)^*}$, as defined by relation (2.6), where the $w^{(r)}$ are 'square concave' (see Hypothesis 6.2.3). Then, the $u^{(r)}$ are 'square convex' and*

$$u^{(r)}(\boldsymbol{\sigma}) = \sup_{\mathbf{M}_0 \geq 0} \left\{ \frac{1}{2} \boldsymbol{\sigma} \cdot \mathbf{M}_0 \boldsymbol{\sigma} - v^{(r)}(\mathbf{M}_0) \right\}, \tag{6.28}$$

where the functions $v^{(r)} = \check{v}^{(r)}$ are defined by (6.24). Similarly, the local stress potential $u = w^*$, as defined by relation (2.7)$_2$, is given by

$$u(\mathbf{x}, \boldsymbol{\sigma}) = \sup_{\mathbf{M}_0 \geq 0} \left\{ u_0(\mathbf{x}, \boldsymbol{\sigma}) - v(\mathbf{x}, \mathbf{M}_0) \right\}, \tag{6.29}$$

where u_0 and v are the functions defined by (6.26) and (6.27), respectively.

Proof. On account of (6.8), it follows that

$$\begin{aligned} u^{(r)}(\boldsymbol{\sigma}) &= \sup_{\boldsymbol{\varepsilon}} \left\{ \boldsymbol{\varepsilon} \cdot \boldsymbol{\sigma} - \inf_{\mathbf{L}_0 > 0} \left\{ \frac{1}{2} \boldsymbol{\varepsilon} \cdot \mathbf{L}_0 \boldsymbol{\varepsilon} + v^{(r)}(\mathbf{L}_0) \right\} \right\} \\ &= \sup_{\mathbf{L}_0 > 0} \left\{ \sup_{\boldsymbol{\varepsilon}} \left\{ \boldsymbol{\varepsilon} \cdot \boldsymbol{\sigma} - \frac{1}{2} \boldsymbol{\varepsilon} \cdot \mathbf{L}_0 \boldsymbol{\varepsilon} \right\} - v^{(r)}(\mathbf{L}_0) \right\} \\ &= \sup_{\mathbf{L}_0 > 0} \left\{ \frac{1}{2} \boldsymbol{\sigma} \cdot (\mathbf{L}_0)^{-1} \boldsymbol{\sigma} - v^{(r)}(\mathbf{L}_0) \right\}, \end{aligned} \tag{6.30}$$

which leads to the result (6.28) upon setting $\mathbf{M}_0 = \mathbf{L}_0^{-1}$ (recall that $\mathbf{L}_0 > 0$). This result also demonstrates the existence of a *convex* function $g^{(r)}$ (in the space of fully symmetric, fourth-order tensors), such that

$$u^{(r)}(\boldsymbol{\sigma}) = g^{(r)} \left(\frac{1}{2} \boldsymbol{\sigma} \otimes \boldsymbol{\sigma} \right). \tag{6.31}$$

Thus, 'square concavity' for $w^{(r)}$ implies 'square convexity' for $u^{(r)}$. Note also that 'square convexity' is consistent with 'super-quadratic' growth for the $u^{(r)}$. The derivation of (6.29) is now straightforward in view of (2.7)$_2$, (6.17) and (6.26).

□

6.3 Variational principles for anisotropic materials

In this section, use is made of the above expressions for the local potentials w and u in terms of linear comparison materials to derive alternative variational representations that are equivalent to (2.3) and (2.8), but that can be used to generate improved bounds — relative to the classical bounds of Voigt and Reuss — for the effective potentials.

Proposition 6.3.1. *Under the 'square concavity' Hypothesis 6.2.3, the effective potential $\widetilde{W}$ defined by (2.3) admits the alternative representation*

$$\widetilde{W}(\overline{\boldsymbol{\varepsilon}}) = \inf_{\mathbf{L}_0(\mathbf{x})>0} \left\{ \widetilde{W}_0(\overline{\boldsymbol{\varepsilon}}) + \mathcal{V}(\mathbf{L}_0) \right\}, \tag{6.32}$$

where $\mathcal{V}(\mathbf{L}_0) = \langle v(\mathbf{x}, \mathbf{L}_0(\mathbf{x})) \rangle$, with v given by (6.10), and where $\widetilde{W}_0$ denotes the effective potential of the linear comparison material with local potential (6.1), i.e.*,*

$$\widetilde{W}_0(\overline{\boldsymbol{\varepsilon}}) \;=\; \inf_{\boldsymbol{\varepsilon} \in \mathcal{K}(\overline{\boldsymbol{\varepsilon}})} \langle w_0(\mathbf{x}, \boldsymbol{\varepsilon}(\mathbf{v})) \rangle \,. \tag{6.33}$$

Proof. Lemma 6.2.4 is used together with the expression (2.3) to deduce the following result for the effective strain-energy density:

$$\widetilde{W}(\overline{\boldsymbol{\varepsilon}}) = \inf_{\boldsymbol{\varepsilon} \in \mathcal{K}(\overline{\boldsymbol{\varepsilon}})} \inf_{\mathbf{L}_0(\mathbf{x})>0} \left\{ \langle w_0(\mathbf{x}, \boldsymbol{\varepsilon}) \rangle + \langle v(\mathbf{x}, \mathbf{L}_0(\mathbf{x})) \rangle \right\}, \tag{6.34}$$

where the infimum over $\mathbf{L}_0$ has been taken out of the volume integral implied by the triangular brackets. (Note that $\mathbf{L}_0$ is now function of position $\mathbf{x}$.) But the order of infima can be interchanged, and hence,

$$\widetilde{W}(\overline{\boldsymbol{\varepsilon}}) = \inf_{\mathbf{L}_0(\mathbf{x})>0} \inf_{\boldsymbol{\varepsilon} \in \mathcal{K}(\overline{\boldsymbol{\varepsilon}})} \left\{ \langle w_0(\mathbf{x}, \boldsymbol{\varepsilon}) \rangle + \langle v(\mathbf{x}, \mathbf{L}_0(\mathbf{x})) \rangle \right\}. \tag{6.35}$$

Noticing that the inner infimum over $\boldsymbol{\varepsilon}$ affects only the first term inside the curly brackets, and that $\mathcal{V}(\mathbf{L}_0) = \langle v(\mathbf{x}, \mathbf{L}_0(\mathbf{x})) \rangle$, one arrives at the desired result. □

Remark 6.3.2. The variational representation (6.32) generalizes a corresponding variational representation for nonlinear composites with isotropic phases first given by Ponte Castañeda (1992a). It expresses the effective properties of the nonlinear composite (through its potential $\widetilde{W}$) in terms of two functionals. The functional $\widetilde{W}_0$ is the elastic energy of a *fictitious linear heterogeneous solid*, called the linear comparison material, made up of phases with stiffness $\mathbf{L}_0(\mathbf{x})$ at point $\mathbf{x}$, whose properties are determined by the solution of the variational representation (6.32) itself. The functional $\mathcal{V}$ depends on the phase 'corrector' functions $v^{(r)}$, and thus provides a measure of the nonlinearity of the actual material. The representation (6.32) is exact and strictly equivalent to the variational characterization of $\widetilde{W}$ given in (2.3). But it requires the exact solution of the optimization problem (6.33), which is a difficult task in view of the fact that it corresponds to a linear composite material with infinitely many phases. However, as will be seen in the next section, this variational representation can be used to generate estimates for $\widetilde{W}$, by making use of suitable trial fields for the moduli tensor $\mathbf{L}_0$ of the linear comparison material.

Remark 6.3.3. The representation (6.32) also provides an interpretation of the strain field in the actual nonlinear composite as the strain field in the *optimal* linear comparison solid. Indeed, although the strain field $\boldsymbol{\varepsilon}_0$ associated with the minimizer in the linear comparison problem (6.33) depends on $\mathbf{L}_0$, and is therefore different, in general, from the strain field $\boldsymbol{\varepsilon}$ associated with the original nonlinear problem (2.3), under the hypothesis of 'square concavity' of w, it follows from (6.32) that the 'linear' minimizer $\boldsymbol{\varepsilon}_0$ arising from the optimal choice of $\mathbf{L}_0$ is precisely the nonlinear minimizer $\boldsymbol{\varepsilon}$.

It is also possible to start from the identity (6.29) for the local stress potential u to generate a corresponding representation for the effective stress potential $\widetilde{U}$.

Proposition 6.3.4. *Assuming 'square convexity' of the local stress potential u (or 'square concavity' of the corresponding strain potential w), the effective stress potential $\widetilde{U}$ defined by (2.8)$_2$ admits the alternative representation*

$$\widetilde{U}(\overline{\boldsymbol{\sigma}}) = \sup_{\mathbf{M}_0(\mathbf{x})\geq 0} \left\{ \widetilde{U}_0(\overline{\boldsymbol{\sigma}}) - \mathcal{V}(\mathbf{M}_0) \right\}, \tag{6.36}$$

where $\mathcal{V}(\mathbf{M}_0) = \langle v(\mathbf{x}, \mathbf{M}_0(\mathbf{x}))\rangle$, with v given by (6.27), and where $\widetilde{U}_0$ denotes the effective potential of the linear comparison material with local potential (6.26), i.e.*,*

$$\widetilde{U}_0(\overline{\boldsymbol{\sigma}}) \;=\; \inf_{\boldsymbol{\sigma}\in\mathcal{S}(\overline{\boldsymbol{\sigma}})} \langle u_0(\mathbf{x}, \boldsymbol{\sigma})\rangle \,. \tag{6.37}$$

Proof. Lemma 6.2.10 is used together with the expression (2.8)$_2$ to deduce the following result for the effective stress potential:

$$\widetilde{U}(\overline{\boldsymbol{\sigma}}) = \inf_{\boldsymbol{\sigma}\in\mathcal{S}(\overline{\boldsymbol{\sigma}})} \sup_{\mathbf{M}_0(\mathbf{x})\geq 0} \left\{ \langle u_0(\mathbf{x}, \boldsymbol{\sigma})\rangle - \langle v(\mathbf{x}, \mathbf{M}_0(\mathbf{x}))\rangle \right\}, \tag{6.38}$$

where the supremum over $\mathbf{M}_0$ has been taken out of the triangular brackets. But u_0 is convex in $\boldsymbol{\sigma}$ and $-v$ is concave in $\mathbf{M}_0$, and therefore, by the Saddle Point Theorem (Ekeland & Teman 1999), the order of the infimum and supremum can be interchanged, and hence,

$$\widetilde{U}(\overline{\boldsymbol{\sigma}}) = \sup_{\mathbf{M}_0(\mathbf{x})\geq 0} \inf_{\boldsymbol{\sigma}\in\mathcal{S}(\overline{\boldsymbol{\sigma}})} \left\{ \langle u_0(\mathbf{x}, \boldsymbol{\sigma})\rangle - \langle v(\mathbf{x}, \mathbf{M}_0(\mathbf{x}))\rangle \right\}, \tag{6.39}$$

which leads to the desired result. □

Remark 6.3.5. It can be shown directly that the two versions of the variational representation, (6.32) and (6.36), are exactly equivalent, under the given hypothesis on the potentials w and u, respectively. (In other words, the result (6.36) for $\widetilde{U}$ can be shown to follow directly from the result (6.32) for $\widetilde{W}$ by using the fact that $\widetilde{U} = \widetilde{W}^*$.) It should also be emphasized that the variational principles (6.32) and (6.36) for composites with anisotropic phases are entirely consistent with the earlier variational representations (Ponte Castañeda 1992a) for composites with isotropic phases. Indeed, it can be shown that, for nonlinear composites with phases characterized by potentials of the form (4.1), the optimal choice for the comparison elasticity and compliance tensors in the context of the general anisotropic forms (6.32) and (6.36) is provided by isotropic fourth-order tensors. To see this, note that any tensor field $\mathbf{L}_0(\mathbf{x})$ can be decomposed into isotropic and anisotropic parts like

$$\mathbf{L}_0(\mathbf{x}) = \mathbf{L}_{iso}(\mathbf{x}) + \mathbf{L}'_0(\mathbf{x}), \quad \mathbf{L}_{iso}(\mathbf{x}) = 3\kappa(\mathbf{x})\ \mathbf{J} + 2\mu_m(\mathbf{x})\ \mathbf{K}, \tag{6.40}$$

where $\kappa(\mathbf{x})$ coincides with the $\kappa^{(r)}$ of each nonlinear phase, and μ_m denotes the minimum shear eigenvalue of the tensor $\mathbf{L}_0$. Then, noting that $\mathbf{L}_0' = \mathbf{L}_0 - \mathbf{L}_{iso}$ is a positive semi-definite tensor, and that $w(\mathbf{x}, \boldsymbol{\varepsilon}) - (1/2)\ \boldsymbol{\varepsilon} \cdot \mathbf{L}_{iso}\boldsymbol{\varepsilon}$ is an isotropic function of $\boldsymbol{\varepsilon}$, we have that

$$\begin{aligned} \mathcal{V}(\mathbf{L}_0) &= \sup_{\boldsymbol{\varepsilon}(\mathbf{x})} \left\langle w\left(\mathbf{x}, \boldsymbol{\varepsilon}(\mathbf{x})\right) - \frac{1}{2}\boldsymbol{\varepsilon}(\mathbf{x}) \cdot \mathbf{L}_{iso}(\mathbf{x})\ \boldsymbol{\varepsilon}(\mathbf{x}) - \frac{1}{2}\boldsymbol{\varepsilon}(\mathbf{x}) \cdot \mathbf{L}_0'(\mathbf{x})\ \boldsymbol{\varepsilon}(\mathbf{x}) \right\rangle \\ &= \sup_{\boldsymbol{\varepsilon}(\mathbf{x})} \left\langle w\left(\mathbf{x}, \boldsymbol{\varepsilon}(\mathbf{x})\right) - \frac{1}{2}\boldsymbol{\varepsilon}(\mathbf{x}) \cdot \mathbf{L}_{iso}(\mathbf{x})\ \boldsymbol{\varepsilon}(\mathbf{x}) \right\rangle = \mathcal{V}(\mathbf{L}_{iso}). \end{aligned} \tag{6.41}$$

In addition, the local inequality $\boldsymbol{\varepsilon} \cdot \mathbf{L}_{iso}\boldsymbol{\varepsilon} \leq \boldsymbol{\varepsilon} \cdot \mathbf{L}_0\boldsymbol{\varepsilon}$ implies that

$$\widetilde{W}_0(\overline{\boldsymbol{\varepsilon}}; \mathbf{L}_{iso}) \leq \widetilde{W}_0(\overline{\boldsymbol{\varepsilon}}; \mathbf{L}_0). \tag{6.42}$$

It follows immediately from (6.41) and (6.42) that the minimum in (6.32) is attained at isotropic elasticity tensors. Analogous arguments apply to the dual version.

Remark 6.3.6. Finally, it is noted that an alternative version of the variational representations (6.32) and (6.36) for composites with anisotropic phases was presented in Ponte Castañeda & Suquet (1998), generalizing earlier estimates for the special case of crystalline plasticity by deBotton & Ponte Castañeda (1995). These variational principles have a form identical to the representations (6.32) and (6.36), except that the function $v^{(r)}$ are defined differently. Essentially, the $v^{(r)}$ are identified with the functions $-f_*^{(r)}$ introduced in expressions (6.11), which, as has already been observed (see eqns. (6.15)), are different, in general, from the functions $v^{(r)}$, as defined by relations (6.2). However, because of these differences, it will be argued below that the variational representations developed here are more powerful, and can lead to sharper bounds, in general.

6.4 Bounds and estimates via piecewise constant moduli

6.4.1 Effective potentials

Unlike the stress and strain trial fields in the context of the classical variational representations (2.3) and $(2.8)_2$, the trial fields of stiffnesses and compliances in the variational representations (6.32) and (6.36) can be chosen to be constant in each phase (not necessarily the same constant). Thus, the optimization over the elasticity moduli $\mathbf{L}_0(\mathbf{x})$ can be restricted to the set of piecewise constant moduli

$$\mathbf{L}_0(\mathbf{x}) = \sum_{r=1}^{N} \chi^{(r)}(\mathbf{x})\mathbf{L}_0^{(r)}, \tag{6.43}$$

where the tensors $\mathbf{L}_0^{(r)}$ are taken to be constant. Making use of this trial field in the variational statement (6.32) for $\widetilde{W}$ then leads to the following bound, which is a generalization for composites with anisotropic phases of bounds that were first given for composites with isotropic phases by Ponte Castañeda (1991).

Result 6.4.1. *The effective strain potential* $\widetilde{W}$ *of the nonlinear composite is bounded above by:*

$$\widetilde{W}_+(\overline{\boldsymbol{\varepsilon}}) = \inf_{\substack{\mathbf{L}_0^{(r)} > 0 \\ r=1,...,N}} \left\{ \widetilde{W}_0(\overline{\boldsymbol{\varepsilon}}) + \sum_{r=1}^{N} c^{(r)} v^{(r)}(\mathbf{L}_0^{(r)}) \right\}, \tag{6.44}$$

where the functions $v^{(r)}$ *are defined by relations (6.2), and where*

$$\widetilde{W}_0(\overline{\boldsymbol{\varepsilon}}) \;=\; \frac{1}{2}\overline{\boldsymbol{\varepsilon}} \cdot \widetilde{\mathbf{L}}_0 \left(\mathbf{L}_0^{(s)}\right) \overline{\boldsymbol{\varepsilon}} \tag{6.45}$$

is now the effective strain potential (6.33) of a linear comparison composite (LCC) with uniform stiffness tensors $\mathbf{L}_0^{(r)}$ *in each of the phases* ($r = 1, ..., N$)*—and, hence, the same microstructure as the nonlinear composite—and with effective stiffness tensor* $\widetilde{\mathbf{L}}_0$*.*

Remark 6.4.2. The form (6.44) for the bound $\widetilde{W}_+(\overline{\boldsymbol{\varepsilon}})$ involves a *convex optimization* problem for the stiffness tensors $\mathbf{L}_0^{(r)}$. This follows, for example, from Lemma 2.1 of Ekeland & Temam (1999), because the terms inside the curly brackets may be written as the infimum (over the variables $\boldsymbol{\varepsilon} \in \mathcal{K}(\overline{\boldsymbol{\varepsilon}})$) of a *convex* function in the arguments $\boldsymbol{\varepsilon}$ *and* $\mathbf{L}_0^{(r)}$ (refer to eqn. (6.34)). In this connection, it is important to recall that the tensors $\mathbf{L}_0^{(r)}$ need not be restricted to be positive definite (*cf.*, the passage from relations (6.5) to (6.6)); it is simply that the infimum cannot occur for $\mathbf{L}_0^{(r)}$ that are not positive definite, since the value of the functions $v^{(r)}$ would be infinite in that case. Thus, given that the optimization problem for the bound $\widetilde{W}_+$ is convex for the whole space of stiffness tensors $\mathbf{L}_0^{(r)}$—and the fact that the functions $v^{(r)}$ need not be smooth—a necessary and sufficient condition for the minimum to be attained is that zero be included in the subdifferential of the terms inside the curly brackets in eqn. (6.44) above, for the optimal stiffness tensors $\widehat{\mathbf{L}}_0^{(r)}$. Now, since $\widetilde{W}_0$ is differentiable (with respect to the $\mathbf{L}_0^{(r)}$), this optimality condition can also be written as:

$$-\frac{1}{2c^{(r)}} \partial_{\mathbf{L}_0^{(r)}} \left(\overline{\boldsymbol{\varepsilon}} \cdot \widetilde{\mathbf{L}}_0 \overline{\boldsymbol{\varepsilon}} \right) \in \partial_{\mathbf{L}_0} v^{(r)} \left(\widehat{\mathbf{L}}_0^{(r)} \right). \tag{6.46}$$

Then, making use of the following identity for linear composites (see Chapter 2)

$$\langle \boldsymbol{\varepsilon}_L \otimes \boldsymbol{\varepsilon}_L \rangle^{(r)} = \frac{1}{c^{(r)}} \partial_{\mathbf{L}_0^{(r)}} \left(\overline{\boldsymbol{\varepsilon}} \cdot \widetilde{\mathbf{L}}_0 \overline{\boldsymbol{\varepsilon}} \right), \tag{6.47}$$

where $\boldsymbol{\varepsilon}_L$ is the local strain field in the LCC, as well as of the expression (6.19) for the subdifferential of the $v^{(r)}$, the optimality conditions (6.46) for the $\mathbf{L}_0^{(r)}$ may also be expressed as: Do there exist an integer $M^{(r)}$ and constants $a_m^{(r)}$ ($m = 1, \cdots, M^{(r)}$), satisfying the conditions $a_m^{(r)} \geq 0$, $\sum_{m=1}^{M^{(r)}} a_m^{(r)} = 1$, such that the identity

$$\langle \boldsymbol{\varepsilon}_L \otimes \boldsymbol{\varepsilon}_L \rangle^{(r)} = \sum_{m=1}^{M^{(r)}} a_m^{(r)} \left(\hat{\boldsymbol{\varepsilon}}_{(m)}^{(r)} \otimes \hat{\boldsymbol{\varepsilon}}_{(m)}^{(r)} \right), \tag{6.48}$$

is satisfied? Thus, it is seen here too that the optimal values $\hat{\mathbf{L}}_0^{(r)}$ may be related to the second moments $\langle \boldsymbol{\varepsilon}_L \otimes \boldsymbol{\varepsilon}_L \rangle^{(r)}$ of the strain field in the LCC, as has been shown by Suquet (1995) and Hu (1996) for the special case of composites with isotropic phases. In general, the tensor of the second moments of the strain is of full rank, and consequently, the optimality conditions (6.48) require that

the $\widehat{\mathbf{L}}_0^{(r)}$ be such that the maximum in the function $v^{(r)}$ be attained simultaneously at several strains $\hat{\boldsymbol{\varepsilon}}_{(m)}^{(r)}$ (*i.e.*, $M^{(r)}$ should be sufficiently large), so that the fourth-order tensors on the two sides of (6.48) have the same rank. In turn, this implies that the optimal $\widehat{\mathbf{L}}_0^{(r)}$ should be precisely in regions where the functions $v^{(r)}$ are *not* differentiable ($M^{(r)} > 1$). Thus, the fact that the functions $v^{(r)}$ have sharp edges implies that the optimal tensors $\widehat{\mathbf{L}}_0^{(r)}$ have certain preferred orientations, depending on the anisotropy of the functions $w^{(r)}$, and correspondingly depend only on certain traces of the second moment strain tensor $\langle \boldsymbol{\varepsilon}_L \otimes \boldsymbol{\varepsilon}_L \rangle^{(r)}$.

Remark 6.4.3. It is also possible to make use of expressions (6.2) for the functions $v^{(r)}$ in expression (6.44) for $\widetilde{W}_+$, to rewrite the problem as an inf-sup optimization. (Note that this problem is not concave in the variables $\boldsymbol{\varepsilon}$, and therefore the order of the inf and the sup cannot be interchanged in general.) Then, using the optimality conditions (6.48), it can be shown that the bound $\widetilde{W}_+$ can be formally written in the form

$$\widetilde{W}_+(\overline{\boldsymbol{\varepsilon}}) = \sum_{r=1}^{N} \sum_{m=1}^{M^{(r)}} c^{(r)}\, a_m^{(r)}\, w^{(r)} \left(\hat{\boldsymbol{\varepsilon}}_{(m)}^{(r)} \right), \tag{6.49}$$

where the $\hat{\boldsymbol{\varepsilon}}_{(m)}^{(r)}$ are the optimal solutions of the problem (6.2) for the functions $v^{(r)}$, satisfying the secant condition (6.3), and evaluated at the optimal values of the $\widehat{\mathbf{L}}_0^{(r)}$, as determined by relation (6.44). This form generalizes the form proposed by Suquet (1995) for composites with isotropic phases, but it should be emphasized that in the more general case of anisotropic phases the (difficult) inf-sup problem must be solved anyway to determine the correct choice for the $\hat{\boldsymbol{\varepsilon}}_{(m)}^{(r)}$. (Recall that there are several possible stationary points in the definition (6.2) for the functions $v^{(r)}$, only some of which are the optimal $\hat{\boldsymbol{\varepsilon}}_{(m)}^{(r)}$.) Expression (6.49) states that the optimal bound for $\widetilde{W}_+$ is given by a convex sum of the phase potentials evaluated at certain traces of the second moments of the strain field in the LCC.

A bound that is equivalent to (6.44) can be obtained by considering the stress potential $\widetilde{U}$ and its variational representation (6.36). Thus, restricting the optimization in (6.36) to piecewise constant compliances $\mathbf{M}_0^{(r)}$ in the variational representation (6.36) leads to a lower bound for $\widetilde{U}$.

Result 6.4.4. *The effective stress potential $\widetilde{U}$ of the nonlinear composite is bounded below by:*

$$\widetilde{U}_-(\overline{\boldsymbol{\sigma}}) = \sup_{\substack{\mathbf{M}_0^{(r)} \geq 0 \\ r=1,...,N}} \left\{ \widetilde{U}_0(\overline{\boldsymbol{\sigma}}) - \sum_{r=1}^{N} c^{(r)} v^{(r)} \left(\mathbf{M}_0^{(r)} \right) \right\}, \tag{6.50}$$

where the functions $v^{(r)}$ have been defined by relations (6.24), and where

$$\widetilde{U}_0(\overline{\boldsymbol{\sigma}}) \;=\; \frac{1}{2} \overline{\boldsymbol{\sigma}} \cdot \widetilde{\mathbf{M}}_0 \left(\mathbf{M}_0^{(s)} \right) \overline{\boldsymbol{\sigma}} \tag{6.51}$$

is now the effective stress potential of a linear comparison composite (LCC) with uniform compliance tensors $\mathbf{M}_0^{(r)}$ in each of the phases ($r = 1, ..., N$), and effective compliance tensor $\widetilde{\mathbf{M}}_0$.

Remark 6.4.5. The expression (6.50) for the bound $\widetilde{U}_-$ involves a *concave optimization* problem for the compliance tensors $\mathbf{M}_0^{(r)}$. This follows from the facts that the functions $v^{(r)}$ are convex in the tensors $\mathbf{M}_0^{(r)}$, while the term arising from $\widetilde{U}_0$ is, on the other hand, *concave* in the tensors $\mathbf{M}_0^{(r)}$. (This last observation is easy to show making use of the definition (6.37) and of the fact that the infimum of the sum is greater than the sum of the infima.) Then, the analysis carried out in the context of Remarks 6.4.2 and 6.4.3 can be repeated step by step, with results completely analogous to expressions (6.46), (6.48), and (6.49). Thus, the optimality conditions in (6.50) lead to the requirement that

$$\langle \boldsymbol{\sigma}_L \otimes \boldsymbol{\sigma}_L \rangle^{(r)} = \sum_{m=1}^{N^{(r)}} b_m^{(r)} \left(\hat{\boldsymbol{\sigma}}_{(m)}^{(r)} \otimes \hat{\boldsymbol{\sigma}}_{(m)}^{(r)} \right), \tag{6.52}$$

where $\boldsymbol{\sigma}_L$ is the local stress field in the LCC, $\hat{\boldsymbol{\sigma}}_{(m)}^{(r)}$, $m = 1, ..., N^{(r)}$, denote *all* the stress vectors at which the maximum in (6.24) is attained when $\mathbf{M}_0 = \hat{\mathbf{M}}_0^{(r)}$, and the coefficients $b_m^{(r)}$ satisfy the constraints $b_m^{(r)} \geq 0$, $\sum_{m=1}^{N^{(r)}} b_m^{(r)} = 1$. It then follows that the optimal bound (6.50) for $\widetilde{U}_-$ may be written in the form

$$\widetilde{U}_-(\overline{\boldsymbol{\sigma}}) = \sum_{r=1}^{N} \sum_{m=1}^{N^{(r)}} c^{(r)}\, b_m^{(r)}\, u^{(r)} \left(\hat{\boldsymbol{\sigma}}_{(m)}^{(r)} \right), \tag{6.53}$$

which states that the optimal bound is given by a convex combination of the local potentials evaluated at certain traces of the second moments of the stress field in the LCC.

Remark 6.4.6. The 'variational' estimates (6.44) and (6.50) are completely equivalent, in the sense that they are Legendre transforms of each other. This can be shown directly from the Legendre-Fenchel transform of the estimate (6.44):

$$\begin{aligned}
(\widetilde{W}_+)^*(\overline{\boldsymbol{\sigma}}) &= \sup_{\overline{\boldsymbol{\varepsilon}}} \left[\overline{\boldsymbol{\sigma}} \cdot \overline{\boldsymbol{\varepsilon}} - \widetilde{W}_+(\overline{\boldsymbol{\varepsilon}}) \right] \\
&= \sup_{\overline{\boldsymbol{\varepsilon}}} \left[\overline{\boldsymbol{\sigma}} \cdot \overline{\boldsymbol{\varepsilon}} - \inf_{\mathbf{L}_0^{(r)} > 0} \left[\widetilde{W}_0(\overline{\boldsymbol{\varepsilon}}; \mathbf{L}_0^{(s)}) + \sum_{s=1}^{N} c^{(s)} v^{(s)}(\mathbf{L}_0^{(s)}) \right] \right] \\
&= \sup_{\mathbf{L}_0^{(r)} > 0} \left[\sup_{\overline{\boldsymbol{\varepsilon}}} \left[\overline{\boldsymbol{\sigma}} \cdot \overline{\boldsymbol{\varepsilon}} - \widetilde{W}_0(\overline{\boldsymbol{\varepsilon}}; \mathbf{L}_0^{(s)}) \right] - \sum_{s=1}^{N} c^{(s)} v^{(s)}(\mathbf{L}_0^{(s)}) \right] \\
&= \sup_{\mathbf{M}_0^{(r)} \geq 0} \left[\widetilde{U}_0(\overline{\boldsymbol{\sigma}}; \mathbf{M}_0^{(s)}) - \sum_{s=1}^{N} c^{(s)} v^{(s)}(\mathbf{M}_0^{(s)}) \right] = \widetilde{U}_-(\overline{\boldsymbol{\sigma}}),
\end{aligned} \tag{6.54}$$

where use has been made of (6.23). In turn, this implies that the estimates are convex functions of the macroscopic fields, in agreement with the exact solution.

Special results for power-law materials

The above bounds for the effective potential may be given simpler, alternative forms for *power-law* composites by exploiting the homogeneity of the relevant potentials and corrector functions. Such results generalize earlier results for composites with isotropic phases by Suquet (1993), who made use of Hölder's inequality for their derivation. Thus, when phase r is of the (incompressible) power-law type with exponent m, such that $0 \leq m \leq 1$, the strain potential $w^{(r)}$ is positively homogeneous of

degree $m+1$:

$$w^{(r)}(\lambda\boldsymbol{\varepsilon}) = \lambda^{m+1}\, w^{(r)}(\boldsymbol{\varepsilon}), \quad \forall\lambda \geq 0. \tag{6.55}$$

Replacing $\boldsymbol{\varepsilon}$ by $\lambda\boldsymbol{\varepsilon}$ in expression (6.2), using the property (6.55), and optimizing with respect to λ, the function $v^{(r)}$ can be written in the form

$$v^{(r)}(\mathbf{L}_0) = \frac{1}{2}\frac{1-m}{1+m}\sup_{\boldsymbol{\varepsilon}}\left\{\frac{\left[(1+m)w^{(r)}(\boldsymbol{\varepsilon})\right]^{\frac{2}{1-m}}}{\left[\boldsymbol{\varepsilon}\cdot\mathbf{L}_0\boldsymbol{\varepsilon}\right]^{\frac{1+m}{1-m}}}\right\}, \tag{6.56}$$

where the optimization variables $\boldsymbol{\varepsilon}$ can now be chosen to have magnitude 1 (and therefore belong to a bounded space). Note that it follows from this expression that $v^{(r)}$ is a homogeneous function of degree $(m+1)/(m-1)$ in the variable $\mathbf{L}_0$.

When all the phases in a composite are made of (incompressible) power-law materials with the same exponent m, the composite is itself an (incompressible) power-law material (Ponte Castañeda & Suquet 1998). In other words, the effective potential $\widetilde{W}$ is also homogeneous of degree $m+1$. Then, letting $\mathbf{L}_0(\mathbf{x}) = t\mathbf{L}_0(\mathbf{x})$, for arbitrary positive t, noting that $\widetilde{W}_0$ and $v^{(r)}$, as defined by relations (6.45) and (6.56), are homogeneous functions of degrees 1 and $\frac{m+1}{m-1}$ in $\mathbf{L}_0$, respectively, and optimizing with respect to t, the following, alternative representation for the bound $\widetilde{W}_+$ is obtained.

Result 6.4.7. *The effective strain potential $\widetilde{W}$ for power-law composites is bounded above by*

$$\widetilde{W}_+(\overline{\boldsymbol{\varepsilon}}) = \frac{2}{m+1}\inf_{\substack{\mathbf{L}_0^{(r)}>0\\ r=1,...,N}}\left\{\left[\widetilde{W}_0\left(\overline{\boldsymbol{\varepsilon}}\right)\right]^{\frac{m+1}{2}}\left[\frac{1+m}{1-m}\sum_{r=1}^{N}c^{(r)}v^{(r)}(\mathbf{L}_0^{(r)})\right]^{\frac{1-m}{2}}\right\}, \tag{6.57}$$

where the $v^{(r)}$ are given by (6.56).

A corresponding representation can be given for the lower bound $\widetilde{U}_-$ when all the individual phases are power-law materials with the same exponent $n = 1/m$. The details are omitted here for brevity, but the result is as follows.

Result 6.4.8. *The effective stress potential $\widetilde{U}$ for power-law composites is bounded below by*

$$\widetilde{U}_-(\overline{\boldsymbol{\sigma}}) = \frac{2}{n+1}\sup_{\substack{\mathbf{M}_0^{(r)}>0\\ r=1,...,N}}\left\{\left[\widetilde{U}_0\left(\overline{\boldsymbol{\sigma}}\right)\right]^{\frac{n+1}{2}}\left[\frac{n+1}{n-1}\sum_{r=1}^{N}c^{(r)}v^{(r)}(\mathbf{M}_0^{(r)})\right]^{\frac{1-n}{2}}\right\}, \tag{6.58}$$

where

$$v^{(r)}(\mathbf{M}_0) = \frac{1}{2}\frac{n-1}{n+1}\sup_{\boldsymbol{\sigma}}\left\{\frac{\left[\boldsymbol{\sigma}\cdot\mathbf{M}_0\boldsymbol{\sigma}\right]^{\frac{n+1}{n-1}}}{\left[(n+1)u^{(r)}(\boldsymbol{\sigma})\right]^{\frac{2}{n-1}}}\right\}. \tag{6.59}$$

Special results for rigid-ideally plastic materials

Even though simpler than the general form of the bounds, the alternative forms of the bounds (6.57) and (6.58) for power-law composites still require the solution of difficult *non-concave* problems (6.56)

and (6.59) for the functions $v^{(r)}$. In the limiting case of ideal plasticity ($n \to \infty$), however, this problem simplifies considerably. This is because, in that case, the functions $v^{(r)}$, defined by (6.24), can be written in the form

$$v^{(r)}(\mathbf{M}_0) = \sup_{\boldsymbol{\sigma} \in P^{(r)}} \left\{ \frac{1}{2}\boldsymbol{\sigma} \cdot \mathbf{M}_0 \boldsymbol{\sigma} \right\}, \tag{6.60}$$

where $P^{(r)}$ is the *strength domain* of phase r, defined by the conditions $u^{(r)}(\boldsymbol{\sigma}) = 0$ if $\boldsymbol{\sigma} \in P^{(r)}$, and ∞, otherwise. Note that $P^{(r)}$ is the closed, convex set of stress tensors bounded by the yield surface of phase r. The advantage of rewriting the functions $v^{(r)}$ in this way is that its computation reduces to the well-studied problem of finding the maximum of a convex function relative to a convex set. Indeed, it can be shown (see Corollary 32.3.2 in Rockafellar 1970) that the maximum in (6.60) is attained at one or more of the *extreme points* of the set $P^{(r)}$, which means that the optimal $\hat{\boldsymbol{\sigma}}^{(r)}_{(m)}$ are necessarily on the yield surface of phase r. Furthermore, in many cases, such as that of crystalline phases considered in the next chapter, the number of extreme points of $P^{(r)}$ is finite, and so the function $v^{(r)}$ can be written as

$$v^{(r)}\left(\mathbf{M}_0\right) = \max_{k=1,..,K_e^{(r)}} \left\{ \frac{1}{2}\boldsymbol{\sigma}^{(r)}_{(k)} \cdot \mathbf{M}_0 \boldsymbol{\sigma}^{(r)}_{(k)} \right\}, \tag{6.61}$$

where $K_e^{(r)}$ is the total number of extreme points of $P^{(r)}$, and $\boldsymbol{\sigma}^{(r)}_{(k)}$ denotes the stress vector associated with the k^{th} extreme point. For a given $\mathbf{M}_0$, this expression is very simple to evaluate. Finally, considering the limit as $n \to \infty$ in expression (6.58) for $\widetilde{U}_-$, the following result is obtained for the effective strength domain $\widetilde{P}$ of the ideally plastic composite, which is defined by the conditions $\widetilde{U}(\overline{\boldsymbol{\sigma}}) = 0$ if $\overline{\boldsymbol{\sigma}} \in \widetilde{P}$, and ∞, otherwise.

Result 6.4.9. *The effective strength domain $\widetilde{P}$ of the ideally plastic composite is bounded from the outside by*

$$\widetilde{P}_+ = \left\{ \overline{\boldsymbol{\sigma}} \,|\, \widetilde{U}_0(\overline{\boldsymbol{\sigma}}) \leq \sum_{r=1}^{N} c^{(r)} v^{(r)}(\mathbf{M}_0^{(r)}),\, \forall\, \mathbf{M}_0^{(r)} \geq 0 \right\}. \tag{6.62}$$

Note that this set corresponds to the intersection of all quadratic functions of the average stress $\overline{\boldsymbol{\sigma}}$, which are defined by the conditions $\widetilde{U}_0(\overline{\boldsymbol{\sigma}}) \leq \sum_{r=1}^{N} c^{(r)} v^{(r)}(\mathbf{M}_0^{(r)})$, for each possible choice of the compliance tensors $\mathbf{M}_0^{(r)} \geq 0$ of the LCC.

Remark 6.4.10. The bound (6.62) was first given by Olson (1994).

6.4.2 Effective behavior and field statistics

In general, the estimate (6.44) for $\widetilde{W}$ requires numerical treatment, and therefore to determine the effective behavior and field statistics directly from this expression, the relevant derivatives would have to be computed numerically. However, the following results avoid this complication.

Result 6.4.11. *The 'variational' estimate for the effective stress-strain relation of the nonlinear composite is given by*

$$\overline{\boldsymbol{\sigma}} = \partial_{\overline{\boldsymbol{\varepsilon}}} \widetilde{W}_+(\overline{\boldsymbol{\varepsilon}}) = \widetilde{\mathbf{L}}_0 \left(\widehat{\mathbf{L}}_0^{(s)} \right) \overline{\boldsymbol{\varepsilon}}, \tag{6.63}$$

where the $\widehat{\mathbf{L}}_0^{(s)}$ are the stiffness tensors satisfying the optimality conditions in (6.44).

Remark 6.4.12. The demonstration of this result is analogous to the derivation of Result 6.2.6, and will not be detailed further here for conciseness. It should be emphasized, however, that the relation (6.63) is an *approximation* to the exact stress-strain relation of the nonlinear composite. This relation is a generalization of a result first given in the context of composites with isotropic phases by deBotton & Ponte Castañeda (1993). In spite of its appearance, this effective stress-strain relation is nonlinear, due to the nonlinear dependence of the optimal $\widehat{\mathbf{L}}_0^{(r)}$ on the average strain $\overline{\boldsymbol{\varepsilon}}$. In fact, in parallel with Remark 6.2.7 concerning the interpretation of the $\widehat{\mathbf{L}}_0^{(s)}$ as the secant moduli tensors of the phases, relation (6.63) suggests that $\widetilde{\mathbf{L}}_0$ can be interpreted as the secant modulus tensor of the nonlinear composite, generalizing earlier interpretations for the isotropic case by Suquet (1995) and Hu (1996).

Result 6.4.13. *The 'variational' estimates for the first and second moments of the local fields in the nonlinear composite are given by*

$$\overline{\boldsymbol{\varepsilon}}^{(r)} = \overline{\boldsymbol{\varepsilon}}_L^{(r)}, \qquad \langle \boldsymbol{\varepsilon} \otimes \boldsymbol{\varepsilon} \rangle^{(r)} = \langle \boldsymbol{\varepsilon}_L \otimes \boldsymbol{\varepsilon}_L \rangle^{(r)}, \tag{6.64}$$

$$\overline{\boldsymbol{\sigma}}^{(r)} = \overline{\boldsymbol{\sigma}}_L^{(r)}, \qquad \langle \boldsymbol{\sigma} \otimes \boldsymbol{\sigma} \rangle^{(r)} = \langle \boldsymbol{\sigma}_L \otimes \boldsymbol{\sigma}_L \rangle^{(r)}, \tag{6.65}$$

whenever the effective potential (6.44) is differentiable with respect to the relevant perturbation parameters. In these expressions, the subscript L has been used to denote quantities in the LCC associated with the 'variational' estimate (6.44).

Proof. We begin by proving the identity $(6.64)_1$ for the phase averages of the strain. In order to make use of proposition 3.2.1, we consider a composite with perturbed local potential (3.3), where $w^{(s)}$ denote the unperturbed phase potentials. Thus, phase r in this composite is characterized by

$$w_\tau^{(r)}(\boldsymbol{\varepsilon}) = w^{(r)}(\boldsymbol{\varepsilon}) + \boldsymbol{\tau}^{(r)} \cdot \boldsymbol{\varepsilon}. \tag{6.66}$$

Making use of the identity (6.8) for $w^{(r)}$, this potential can be written as

$$w_\tau^{(r)}(\boldsymbol{\varepsilon}) = \inf_{\mathbf{L}_0^{(r)} > 0} \left\{ w_{0\tau}^{(r)}(\boldsymbol{\varepsilon}; \mathbf{L}_0^{(r)}) + V^{(r)}(\mathbf{L}_0^{(r)}) \right\}. \tag{6.67}$$

where $w_{0\tau}^{(r)}$ denotes the phase potential of a perturbed LCC, given by

$$w_{0\tau}^{(r)}(\boldsymbol{\varepsilon}; \mathbf{L}_0^{(r)}) = \frac{1}{2} \boldsymbol{\varepsilon} \cdot \mathbf{L}_0^{(r)} \boldsymbol{\varepsilon} + \boldsymbol{\tau}^{(r)} \cdot \boldsymbol{\varepsilon}. \tag{6.68}$$

The 'variational' estimate for the perturbed effective potential $\widetilde{W}_\tau$ is then obtained by following the procedure described in the context of expression (6.44). The resulting expression for $\widetilde{W}_\tau$ is in fact (6.44), but with $\widetilde{W}_0$ replaced by $\widetilde{W}_{0\tau}$, the effective potential of the perturbed LCC with phase r characterized by (6.68). The function $\widetilde{W}_{0\tau}$ being differentiable with respect to $\boldsymbol{\tau}^{(r)}$, the phase average of the strain in phase r of the unperturbed LCC is given by (see Chapter 2)

$$\overline{\boldsymbol{\varepsilon}}_L^{(r)} = \frac{1}{c^{(r)}} \, \partial_{\boldsymbol{\tau}^{(r)}} \widetilde{W}_{0\tau} \Big|_{\boldsymbol{\tau}^{(r)} = \mathbf{0}}. \tag{6.69}$$

Now, the function $\widetilde{W}_{0\tau}$ is an infimum of a collection of affine functions of $\boldsymbol{\tau}^{(r)}$, and therefore it is concave in this variable. Then, from the definition of its subgradient (at $\boldsymbol{\tau}^{(r)} = \mathbf{0}$), it follows that

the tensor $\overline{\boldsymbol{\varepsilon}}_L^{(r)}$ satisfies the inequality

$$c^{(r)}\overline{\boldsymbol{\varepsilon}}_L^{(r)} \cdot \boldsymbol{\tau}' \geq \widetilde{W}_{0\tau}\left(\overline{\boldsymbol{\varepsilon}}; \widehat{\mathbf{L}}_0^{(s)}, \boldsymbol{\tau}'\right) - \widetilde{W}_0\left(\overline{\boldsymbol{\varepsilon}}; \widehat{\mathbf{L}}_0^{(s)}\right), \quad \text{for all } \boldsymbol{\tau}', \tag{6.70}$$

where the $\widehat{\mathbf{L}}_0^{(s)}$ denote the optimal stiffness tensors in the unperturbed problem (6.44), and use has been made of the fact that $\widetilde{W}_{0\tau}(\overline{\boldsymbol{\varepsilon}}; \widehat{\mathbf{L}}_0^{(s)}, \mathbf{0}) = \widetilde{W}_0(\overline{\boldsymbol{\varepsilon}}; \widehat{\mathbf{L}}_0^{(s)})$. Then, denoting by $\widehat{\mathbf{L}}_0^{(s)'}$ the optimal stiffness tensor associated with the perturbed 'variational' estimates with $\boldsymbol{\tau}'$, we have that

$$\begin{aligned}
c^{(r)}\overline{\boldsymbol{\varepsilon}}_L^{(r)} \cdot \boldsymbol{\tau}' &\geq \widetilde{W}_{0\tau}\left(\overline{\boldsymbol{\varepsilon}}; \widehat{\mathbf{L}}_0^{(s)}, \boldsymbol{\tau}'\right) + \sum_{s=1}^{N} c^{(s)} v^{(s)}(\widehat{\mathbf{L}}_0^{(s)}) - \widetilde{W}_0\left(\overline{\boldsymbol{\varepsilon}}; \widehat{\mathbf{L}}_0^{(s)}\right) - \sum_{s=1}^{N} c^{(s)} v^{(s)}(\widehat{\mathbf{L}}_0^{(s)}) \\
&\geq \widetilde{W}_{0\tau}\left(\overline{\boldsymbol{\varepsilon}}; \widehat{\mathbf{L}}_0^{(s)'}, \boldsymbol{\tau}'\right) + \sum_{s=1}^{N} c^{(s)} v^{(s)}(\widehat{\mathbf{L}}_0^{(s)'}) - \widetilde{W}_0\left(\overline{\boldsymbol{\varepsilon}}; \widehat{\mathbf{L}}_0^{(s)}\right) - \sum_{s=1}^{N} c^{(s)} v^{(s)}(\widehat{\mathbf{L}}_0^{(s)}) \\
&= \widetilde{W}_{\tau}\left(\overline{\boldsymbol{\varepsilon}}; \boldsymbol{\tau}'\right) - \widetilde{W}_{\tau}\left(\overline{\boldsymbol{\varepsilon}}; \mathbf{0}\right), \quad \text{for all } \boldsymbol{\tau}',
\end{aligned}$$

where the second inequality follows from the fact that the first two terms on the right-hand side are minimum at $\widehat{\mathbf{L}}_0^{(s)'}$. This implies that $c^{(r)}\overline{\boldsymbol{\varepsilon}}_L^{(r)}$ belongs to the subdifferential of the perturbed 'variational' estimate $\widetilde{W}_\tau$, at $\boldsymbol{\tau}^{(r)} = \mathbf{0}$. Therefore, if the latter is differentiable at $\boldsymbol{\tau}^{(r)} = \mathbf{0}$, we have that

$$\frac{1}{c^{(r)}}\, \partial_{\boldsymbol{\tau}^{(r)}} \widetilde{W}_\tau \Big|_{\boldsymbol{\tau}^{(r)}=\mathbf{0}} = \overline{\boldsymbol{\varepsilon}}_L^{(r)}, \tag{6.71}$$

which, by proposition (3.2.1), implies the identity $(6.64)_1$. The identity $(6.64)_2$ for the second moments of the strain field can be proved in a completely analogous fashion, making use of corollary (3.2.3).

Next, we prove the identity $(6.65)_1$ for the phase averages of the stress. In order to make use of proposition 3.2.7, we consider a composite with perturbed local potential (3.19), where $w^{(s)}$ denote the unperturbed phase potentials. Thus, phase r in this composite is characterized by

$$w_\eta^{(r)}(\boldsymbol{\varepsilon}) = w^{(r)}(\boldsymbol{\varepsilon} - \boldsymbol{\eta}^{(r)}). \tag{6.72}$$

Making use of the identity (6.8) for $w^{(r)}$, this potential can be written as

$$w_\eta^{(r)}(\boldsymbol{\varepsilon}) = \inf_{\mathbf{L}_0^{(r)} > 0} \left\{ w_{0\eta}^{(r)}(\boldsymbol{\varepsilon}; \mathbf{L}_0^{(r)}) + V^{(r)}(\mathbf{L}_0^{(r)}) \right\}. \tag{6.73}$$

where $w_{0\eta}^{(r)}$ denotes the phase potential of a perturbed LCC, given by

$$w_{0\eta}^{(r)}(\boldsymbol{\varepsilon}; \mathbf{L}_0^{(r)}) = \frac{1}{2}(\boldsymbol{\varepsilon} - \boldsymbol{\eta}^{(r)}) \cdot \mathbf{L}_0^{(r)}(\boldsymbol{\varepsilon} - \boldsymbol{\eta}^{(r)}). \tag{6.74}$$

The 'variational' estimate for the perturbed effective potential $\widetilde{W}_\eta$ is then obtained by following the procedure described in the context of expression (6.44). The resulting expression for $\widetilde{W}_\eta$ is in fact (6.44), but with $\widetilde{W}_0$ replaced by $\widetilde{W}_{0\eta}$, the effective potential of the perturbed LCC with phase r characterized by (6.74). The potential $\widetilde{W}_{0\eta}$ is convex in $\boldsymbol{\eta}^{(r)}$, since it is the infimum of a collection of affine functions in this variable. Then, for $c^{(r)}\overline{\boldsymbol{\sigma}}^{(r)}$ to be a subgradient of this potential at $\boldsymbol{\eta}^{(r)} = \mathbf{0}$, it must satisfy the inequality

$$c^{(r)}\overline{\boldsymbol{\sigma}}^{(r)} \cdot \boldsymbol{\eta}' \leq \widetilde{W}_\eta(\overline{\boldsymbol{\varepsilon}}; \boldsymbol{\eta}') - \widetilde{W}_\eta(\overline{\boldsymbol{\varepsilon}}; \mathbf{0}), \quad \text{for all } \boldsymbol{\eta}'. \tag{6.75}$$

Letting $\hat{\mathbf{L}}_0^{(s)}$ and $\hat{\mathbf{L}}_0^{(s)'}$ denote the optimal stiffness tensors associated with the perturbed estimates at $\boldsymbol{\eta}^{(r)} = \mathbf{0}$ and $\boldsymbol{\eta}^{(r)} = \boldsymbol{\eta}'$, respectively, the inequality (6.75) can be written as

$$\begin{aligned} c^{(r)}\overline{\boldsymbol{\sigma}}^{(r)} \cdot \boldsymbol{\eta}' &\leq \widetilde{W}_{0\eta}(\overline{\boldsymbol{\varepsilon}}; \hat{\mathbf{L}}_0^{(s)'}, \boldsymbol{\eta}') + \sum_{s=1}^{N} c^{(s)} v^{(s)}(\hat{\mathbf{L}}_0^{(s)'}) - \widetilde{W}_0(\overline{\boldsymbol{\varepsilon}}; \hat{\mathbf{L}}_0^{(s)}) - \sum_{s=1}^{N} c^{(s)} v^{(s)}(\hat{\mathbf{L}}_0^{(s)}), \\ &\leq \widetilde{W}_{0\eta}(\overline{\boldsymbol{\varepsilon}}; \hat{\mathbf{L}}_0^{(s)}, \boldsymbol{\eta}') - \widetilde{W}_0(\overline{\boldsymbol{\varepsilon}}; \hat{\mathbf{L}}_0^{(s)}), \quad \text{for all } \boldsymbol{\eta}'. \end{aligned} \tag{6.76}$$

Since the effective potential $\widetilde{W}_{0\eta}$ of the perturbed LCC is differentiable with respect to $\boldsymbol{\eta}^{(r)}$, this inequality implies that

$$c^{(r)}\overline{\boldsymbol{\sigma}}^{(r)} = \partial_{\boldsymbol{\eta}^{(r)}} \widetilde{W}_{0\eta}\Big|_{\boldsymbol{\eta}^{(r)}=\mathbf{0}} = c^{(r)}\overline{\boldsymbol{\sigma}}_L^{(r)}, \tag{6.77}$$

what proves the identity $(6.65)_1$. The identity $(6.65)_2$ for the second moments of the stress field can be proved in a completely analogous fashion, making use of corollary 3.2.10. □

Remark 6.4.14. It should be noted that, while the identities (6.65) for the stress statistics always hold, the identities for the strain statistics (6.64) follow from the additional requirement that the estimate for the perturbed effective potential be differentiable with respect to the relevant perturbation parameter. Otherwise, the equality (6.71) does not hold, and we are left with the inclusion $c^{(r)}\overline{\boldsymbol{\varepsilon}}_L^{(r)} \in \partial_{\boldsymbol{\tau}^{(r)}} \widetilde{W}_{\tau}\Big|_{\boldsymbol{\tau}^{(r)}=\mathbf{0}}$. This is related to the fact that this result applies to composites with phase potentials $w^{(r)}$ that are not necessarily strictly convex, in which case, the strain field may not be unique. However, it is expected that when the potentials $w^{(r)}$ are strictly convex, the 'variational' estimates for the perturbed effective potentials should be differentiable with respect to the perturbation parameters, in which case the 'variational' estimates for the first and second moments of the local fields *coincide* with those of the associated LCC, in agreement with the conjecture of Ponte Castañeda & Zaidman (1994).

Completely analogous expressions can be derived from the effective stress potential (6.50). Thus, the first and second moments of the local fields concide with those of the associated LCC, while the effective behavior is given in the next result.

Result 6.4.15. *The dual 'variational' estimate for the effective stress-strain relation of the nonlinear composite is given by*

$$\overline{\boldsymbol{\varepsilon}} = \partial_{\overline{\boldsymbol{\sigma}}} \widetilde{U}_{-}(\overline{\boldsymbol{\sigma}}) = \widetilde{\mathbf{M}}_0 \left(\widehat{\mathbf{M}}_0^{(s)} \right) \overline{\boldsymbol{\sigma}}, \tag{6.78}$$

where the $\widehat{\mathbf{M}}_0^{(s)}$ *are the optimal values of the* $\mathbf{M}_0^{(s)}$ *in expression (6.50).*

6.5 Concluding remarks

In Section 6.4, bounds have been derived for nonlinear composites with anisotropic phases, including special forms for power-law and ideally plastic composites, making use of the variational representations derived in section 3. As already noted (Remark 6.3.6), alternative forms for the variational

representations have been proposed in Ponte Castañeda & Suquet (1998). These alternative representations for $\widetilde{W}$ and $\widetilde{U}$ can be used to generate bounds that exhibit precisely the same forms as bounds (6.44) and (6.50) for general 'square concave' and 'square convex' phase potentials $w^{(r)}$ and $u^{(r)}$, respectively, except that the functions $v^{(r)}$, as defined by relations (6.2) (or (6.24)), must be replaced by the functions $-f_*^{(r)}$, as defined in expression (6.11). Similarly, special forms of the bounds may be derived for power-law and ideally plastic composites that correspond exactly to the forms (6.57), (6.58) and (6.62), but with the same caveat for the functions $v^{(r)}$.

Now, it follows trivially from the inequalities (6.15), $v^{(r)} \leq -f_*^{(r)}$, that the bounds proposed in this work are at least as good as the corresponding bounds given in Ponte Castañeda & Suquet (1998). The question of interest, however, is whether the bounds given in this work are actually better, in general, as suggested by the above-mentioned inequality. This question will be answered in the next chapter in the context of composites with crystalline phases. This is an important example because it corresponds to the (visco)plastic behavior of single crystals, which is known to characterize the behavior of metals and minerals in their single-crystal state, and can be used to deduce the effective response of polycrystalline aggregates of such materials. In fact, for the specific class of crystalline materials, there is an earlier, alternative form of the bounds due to deBotton & Ponte Castañeda (1995), which has already been shown to be exactly equivalent to the more general bounds of Ponte Castañeda & Suquet (1998). Thus, it will be shown in the next chapter that the new bounds derived here are sharper, in general, than the bounds of deBotton & Ponte Castañeda (1995) for crystalline materials, and therefore than the bounds of Ponte Castañeda & Suquet (1998) for more general classes of anisotropies.

It should be emphasized, however, that the earlier bounds have a significant advantage over the new bounds proposed in this work in terms of computational efficiency. Indeed, the corrector functions $v^{(r)}$ needed in the computation of the new bounds require solving a non-concave (non-convex) problem, while the corresponding functions $-f_*^{(r)}$ in the earlier bounds require the solution of a concave problem (in an enlarged space). This additional structure, which makes the problem for the bounds concave in one set of variables and convex in the other, allows the use of the Saddle Point Theorem to simplify the computation of the earlier bounds. In particular, the form of the bounds corresponding to expression (6.49) depends directly on the second moments of the strain in the linear comparison composite. (On the other hand, the earlier bounds could depend on the 'concave extension' $f^{(r)}$ of the phase potentials $w^{(r)}$, while the new ones, given in this work, depend only on the actual potentials $w^{(r)}$.) Thus, in conclusion, the new bounds developed in this work can give improved results, relative to the earlier bounds, but any improvement will come at an increased computational cost.

Chapter 7

Application to crystalline materials

In the present chapter, the 'variational' (linear comparison) bounds derived in the previous chapter are specialized to nonlinear composites with crystalline constituents, including polycrystals, which is perhaps the most common type of composite material with anisotropic constituents.

7.1 Crystalline phases and polycrystals

We consider a reference *single crystal* which is capable of undergoing viscoplastic deformation on a set of K preferred crystallographic slip systems. These systems are characterized by the second-order tensors $\boldsymbol{\mu}_{(k)}$, $k = 1, \cdots, K$, defined by:

$$\boldsymbol{\mu}_{(k)} = \frac{1}{2}(\mathbf{n}_{(k)} \otimes \mathbf{m}_{(k)} + \mathbf{m}_{(k)} \otimes \mathbf{n}_{(k)}), \tag{7.1}$$

where $\mathbf{n}_{(k)}$ and $\mathbf{m}_{(k)}$ are the unit vectors normal to the slip plane and along the slip direction in the kth system, respectively. When the crystal is subjected to an applied stress $\boldsymbol{\sigma}$, the resolved shear stress acting on the kth slip system is given by $\tau_{(k)} = \boldsymbol{\sigma} \cdot \boldsymbol{\mu}_{(k)}$, and the strain (rate) $\boldsymbol{\varepsilon}$ in the crystal is the superposition of the strain (rates) $\gamma_{(k)}$ on each slip system k ($k = 1, \cdots, K$). They are assumed to depend on the resolved shear stress $\tau_{(k)}$, through a slip potential $\psi_{(k)}$, such that $\gamma_{(k)} = \psi'_{(k)}(\tau_{(k)})$. For consistency with the hypothesis of 'square convexity' introduced in the previous chapter, the potentials $\psi_{(k)}$ will be assumed here to be *convex* in the variable $\tau^2_{(k)}$ (and are therefore also convex in $\tau_{(k)}$). A commonly used form for the slip potentials $\psi_{(k)}$ is the power-law form:

$$\psi_{(k)}(\tau) = \frac{\gamma_0 \, (\tau_0)_{(k)}}{n+1} \left(\frac{|\tau|}{(\tau_0)_{(k)}} \right)^{n+1}, \tag{7.2}$$

where $m = 1/n$ ($0 \leq m \leq 1$) and $(\tau_0)_{(k)}$ are, respectively, the strain-rate sensitivity and flow stress of the kth slip system, and γ_0 is a reference strain rate. Note that the limiting values of the exponent $m = 1$ and $m = 0$ correspond to linear and rigid-ideally plastic behaviors, respectively. In this connection, it is recalled that, even though the slip potentials $\psi_{(k)}$ are not differentiable in the rigid-ideally plastic case, it is still possible to relate $\gamma_{(k)}$ and $\tau_{(k)}$ via the subdifferential of convex analysis.

Because the phases in a composite made of such crystalline materials may also exhibit different orientations, it is useful to introduce a set of rotation tensors $\boldsymbol{R}^{(r)}$ $(r = 1, ..., N)$. Then, defining phase r as the region occupied by all crystals of a given type and orientation $\boldsymbol{R}^{(r)}$, its constitutive behavior is characterized by the stress potential

$$u^{(r)}(\boldsymbol{\sigma}) = \sum_{k=1}^{K^{(r)}} \psi_{(k)}^{(r)} \left(\tau_{(k)}^{(r)} \right), \tag{7.3}$$

where the functions $\psi_{(k)}^{(r)}$ characterize the constitutive response of the slip systems of all the crystals associated with phase r, and

$$\tau_{(k)}^{(r)} = \boldsymbol{\sigma} \cdot \left({\boldsymbol{R}^{(r)}}^T \boldsymbol{\mu}_{(k)}^{(r)} \boldsymbol{R}^{(r)} \right) \tag{7.4}$$

It is recalled that a *polycrystal* is an aggregate of a large number of *identical* single crystals with different orientations. This special case is included in expression (7.3), provided that all the phase slip systems and potentials be taken identical to each other ($\boldsymbol{\mu}_{(k)}^{(r)} = \boldsymbol{\mu}_{(k)}$ and $\psi_{(k)}^{(r)} = \psi_{(k)}$). But the definition (7.3) is general enough to include multi-phase polycrystals, as well as composites with crystalline phases, such as the porous, crystalline materials considered in the next section.

7.1.1 Variational bounds

Because the phase stress potentials (7.3) have been assumed to be 'square convex,' the 'variational' bound given in Result 6.4.4 holds and can be used for the above-defined class of composites with crystalline phases.

Result 7.1.1. *The effective stress potential $\widetilde{u}$ of an N-phase nonlinear composite (or polycrystal) with crystalline phase potentials (7.3) is bounded below by:*

$$\widetilde{u}_-(\overline{\boldsymbol{\sigma}}) = \sup_{\substack{\mathbf{M}_0^{(r)} \geq 0 \\ r = 1, ..., N}} \left\{ \widetilde{u}_0(\overline{\boldsymbol{\sigma}}) - \sum_{r=1}^{N} c^{(r)} v^{(r)} \left(\mathbf{M}_0^{(r)} \right) \right\}, \tag{7.5}$$

where the corrector functions $v^{(r)}$ are given by

$$v^{(r)}(\mathbf{M}_0^{(r)}) = \sup_{\boldsymbol{\sigma}} \left\{ \frac{1}{2} \boldsymbol{\sigma} \cdot \mathbf{M}^{(r)} \boldsymbol{\sigma} - u^{(r)}(\boldsymbol{\sigma}) \right\}, \tag{7.6}$$

and where

$$\widetilde{u}_0(\overline{\boldsymbol{\sigma}}) \;=\; \frac{1}{2} \overline{\boldsymbol{\sigma}} \cdot \widetilde{\mathbf{M}}_0 \left(\mathbf{M}_0^{(s)} \right) \overline{\boldsymbol{\sigma}} \tag{7.7}$$

is the effective stress potential of a linear comparison composite (LCC) with uniform compliance tensors $\mathbf{M}_0^{(r)}$ in each of the phases ($r = 1, ..., N$), and effective compliance tensor $\widetilde{\mathbf{M}}_0$.

As discussed in Remark 6.4.5, the bound (7.5) involves a *nonsmooth, concave* optimization problem for the variables $\mathbf{M}_0^{(r)}$, which can be solved by making use of appropriate numerical methods. However, as will be seen in the context of the model problem considered below, the main difficulty in the determination of this bound lies in the computation of the 'corrector' functions $v^{(r)}$, which involve

a *non-concave* optimization problem that must be solved making use of more sensitive numerical algorithms.

If the slip potentials $\psi_{(k)}^{(r)}$ are all of the power-law type (7.2) with the same exponent n, as in the model problem considered in the next section, the bound (7.5) admits the following alternative representation, as can be deduced from Result 6.4.8.

Result 7.1.2. *The effective stress potential $\widetilde{u}$ of an N-phase, power-law composite (or polycrystal) with crystalline phase potentials given by (7.3), together with (7.2), is bounded below by*

$$\widetilde{u}_-(\overline{\boldsymbol{\sigma}}) = \frac{2}{n+1} \sup_{\substack{\mathbf{M}_0^{(r)} \geq 0 \\ r=1,...,N}} \left\{ \left[\widetilde{u}_0\left(\overline{\boldsymbol{\sigma}}\right)\right]^{\frac{n+1}{2}} \left[\frac{n+1}{n-1} \sum_{r=1}^{N} c^{(r)} v^{(r)}(\mathbf{M}_0^{(r)})\right]^{\frac{1-n}{2}} \right\}, \tag{7.8}$$

where $\widetilde{u}_0$ is given by (7.7), and

$$v^{(r)}(\mathbf{M}_0) = \frac{1}{2}\frac{n-1}{n+1} \sup_{||\boldsymbol{\sigma}||=1} \left\{ \frac{\left[\boldsymbol{\sigma} \cdot \mathbf{M}_0 \boldsymbol{\sigma}\right]^{\frac{n+1}{n-1}}}{\left[(n+1)\ u^{(r)}(\boldsymbol{\sigma})\right]^{\frac{2}{n-1}}} \right\}. \tag{7.9}$$

The main advantage of this special representation for power-law composites is that, even though the functions $v^{(r)}$ as given by (7.9) still require the solution of a non-concave optimization problem, this optimization is now over a bounded domain ($||\boldsymbol{\sigma}|| = 1$). In addition, expression (7.8) is well behaved for large values of the nonlinearity n, which facilitates the numerical resolution of the problem. In general, further simplifications are not possible for potentials $u^{(r)}$ of the form (7.3), and the solution strategies must be adapted to the specific system of interest.

However, considerable simplification is possible for ideally plastic composites. It is then convenient to introduce the strength domain $P^{(r)}$ of each phase r, defined by the conditions $u^{(r)}(\boldsymbol{\sigma}) = 0$ if $\boldsymbol{\sigma} \in P^{(r)}$, and ∞ otherwise. For crystalline phases characterized by ideally plastic slip potentials of the form (7.2) with $n \to \infty$, the sets $P^{(r)}$ are *polyhedral*, and therefore, the extreme points of those sets are given by their finitely many *vertices* (see Rockafellar 1970). This fact allows the following, further specialization of Result 6.4.9, for the effective strength domain $\widetilde{P}$ of an ideally plastic composite with crystalline phases.

Result 7.1.3. *The effective strength domain $\widetilde{P}$ of an N-phase composite (or polycrystal) with crystalline, rigid-ideally plastic phases is bounded from the outside by*

$$\widetilde{P}_+ = \left\{ \overline{\boldsymbol{\sigma}} \,|\, \widetilde{U}_0(\overline{\boldsymbol{\sigma}}) \leq \sum_{r=1}^{N} c^{(r)} v^{(r)}\left(\mathbf{M}_0^{(r)}\right), \forall\, \mathbf{M}_0^{(r)} \geq 0 \right\}, \tag{7.10}$$

where $\widetilde{U}_0$ is given by (7.7), and the functions $v^{(r)}$ are given by

$$v^{(r)}\left(\mathbf{M}_0^{(r)}\right) = \max_{k=1,..,K_v^{(r)}} \left\{ \frac{1}{2} \boldsymbol{\sigma}_{(k)}^{(r)} \cdot \mathbf{M}_0^{(r)} \boldsymbol{\sigma}_{(k)}^{(r)} \right\}, \tag{7.11}$$

where $K_v^{(r)}$ is the total number of vertices of $P^{(r)}$, and $\boldsymbol{\sigma}_{(k)}^{(r)}$ denotes the stress vector associated with the k^{th} vertex.

Thus, in the case of ideally plastic, crystalline phases, evaluation of the functions $v^{(r)}$ as given by (7.11) is very simple, requiring only knowledge of the vertex stress vectors $\boldsymbol{\sigma}_{(k)}$ of the crystal in question. Such geometric information on the yield surface is already available for common crystal symmetries, such as FCC (Bishop 1955, Kocks *et al.* 1983) and HCP crystals (Tomé & Kocks 1985), since it is required in applications of the classical Taylor theory of polycrystal plasticity.

7.1.2 Relaxed variational bounds

As already mentioned in the previous chapter, there is an alternative version of the 'variational' bound for general anisotropic phases due to Suquet (see Ponte Castañeda & Suquet 1998), which is easier to compute, because it makes use of a relaxation of the corrector functions $v^{(r)}$. When applied to composites with crystalline phase potentials of the form (7.3), this bound can be shown (see Ponte Castañeda & Suquet 1998) to agree exactly with the earlier bound introduced by deBotton & Ponte Castañeda (1995), specifically for that class of nonlinear composites. With the objective of establishing a relationship between the new bound (7.5) and this earlier version, the rest of this section is devoted to a derivation of the bound of deBotton & Ponte Castañeda (1995) directly from (7.5).

Let the compliance tensors $\mathbf{M}_0^{(r)}$ in (7.5) take the special form

$$\mathbf{M}_0^{(r)} = 2\sum_{k=1}^{K} \alpha_{(k)}^{(r)}\, \boldsymbol{\mu}_{(k)}^{(r)} \otimes \boldsymbol{\mu}_{(k)}^{(r)}, \quad \alpha_{(k)}^{(r)} \geq 0, \tag{7.12}$$

where the $\boldsymbol{\mu}_{(k)}^{(r)}$ are those of the nonlinear crystalline phase r. Then, recalling the definition (7.6) of the functions $v^{(r)}$, it follows that

$$\begin{aligned} v^{(r)}(\mathbf{M}_0^{(r)}) &= \sup_{\boldsymbol{\sigma}} \left\{ \frac{1}{2}\boldsymbol{\sigma}\cdot\mathbf{M}_0^{(r)}\boldsymbol{\sigma} - u^{(r)}(\boldsymbol{\sigma}) \right\} \\ &= \sup_{\boldsymbol{\sigma}} \sum_{k=1}^{K} \left\{ \alpha_{(k)}^{(r)} \left(\boldsymbol{\sigma}\cdot\boldsymbol{\mu}_{(k)}^{(r)} \right)^2 - \psi_{(k)}^{(r)} \left(\boldsymbol{\sigma}\cdot\boldsymbol{\mu}_{(k)}^{(r)} \right) \right\} \\ &\leq \sum_{k=1}^{K} \sup_{\tau_{(k)}^{(r)}} \left\{ \alpha_{(k)}^{(r)} \left(\tau_{(k)}^{(r)} \right)^2 - \psi_{(k)}^{(r)} \left(\tau_{(k)}^{(r)} \right) \right\}, \end{aligned} \tag{7.13}$$

and therefore

$$v^{(r)}(\mathbf{M}_0^{(r)}) \leq \sum_{k=1}^{K} v_{(k)}^{(r)} \left(\alpha_{(k)}^{(r)} \right), \tag{7.14}$$

where

$$v_{(k)}^{(r)} \left(\alpha_{(k)}^{(r)} \right) = \sup_{\tau} \left\{ \alpha_{(k)}^{(r)} \tau^2 - \psi_{(k)}^{(r)}(\tau) \right\}. \tag{7.15}$$

In view of the 'square convexity' hypothesis for the slip potentials $\psi_{(k)}^{(r)}$, the expression inside the curly brackets in (7.15) is concave in τ^2, and so the computation of the functions $v_{(k)}^{(r)}$ is straightforward, as opposed to that of the functions $v^{(r)}$, which as already stated requires, in general, the solution of a non-concave optimization problem. For this reason, the bound of deBotton & Ponte Castañeda (1995), which follows from (7.14) and is detailed in the next result, is much simpler to compute.

Result 7.1.4. *The lower bound (7.5) for the effective stress potential $\widetilde{u}$ of an N-phase nonlinear composite with crystalline phase potentials (7.3) is bounded below by:*

$$\widetilde{u}_{R-}(\overline{\boldsymbol{\sigma}}) = \sup_{\substack{\alpha_{(k)}^{(r)} \geq 0 \\ r=1,...,N \\ k=1,...,K}} \left\{ \widetilde{U}_0(\overline{\boldsymbol{\sigma}}) - \sum_{r=1}^{N}\sum_{k=1}^{K} c^{(r)} v_{(k)}^{(r)}\left(\alpha_{(k)}^{(r)}\right) \right\}, \tag{7.16}$$

where $\widetilde{U}_0$ is the effective stress potential of an LCC, defined by (7.7), with phase compliance tensors $\mathbf{M}_0^{(s)}$, as given by (7.12) in terms of the slip compliances $\alpha_{(k)}^{(s)}$, and the functions $v_{(k)}^{(r)}$ are determined by relations (7.15).

Because of its derivation here, the bound (7.16) will be referred to as the 'relaxed variational' (linear comparison) bound, as opposed to the bound (7.5), which will be plainly called the 'variational' (linear comparison) bound.

For power-law and ideally plastic crystalline phases, the functions $v_{(k)}^{(r)}$ can be computed explicitly, and the 'relaxed' bounds can be simplified further. The results are quoted below (Ponte Castañeda & Suquet 1998), for completeness.

Result 7.1.5. *For N-phase composites with power-law, crystalline phases, the 'relaxed variational' bound (7.16) can be rewritten as*

$$\widetilde{u}_{R-}(\overline{\boldsymbol{\sigma}}) = \frac{\gamma_0}{n+1} \sup_{\substack{\alpha_{(k)}^{(r)} \geq 0 \\ r=1,...,N, \\ k=1,...,K}} \left\{ \left[\widetilde{U}_0(\overline{\boldsymbol{\sigma}})\right]^{\frac{n+1}{2}} \left[\sum_{r=1}^{N}\sum_{k=1}^{K} c^{(r)} (\alpha_{(k)}^{(r)})^{\frac{1+n}{n-1}} \left((\tau_0)_{(k)}^{(r)}\right)^{\frac{2n}{n-1}} \right]^{\frac{1-n}{2}} \right\}. \tag{7.17}$$

Also, the effective strength domain $\widetilde{P}$ of an N-phase composite with rigid-ideally plastic ($n \to \infty$), crystalline phases is bounded from the outside by

$$\widetilde{P}_{R+} = \left\{ \overline{\boldsymbol{\sigma}} \,|\, \widetilde{U}_0(\overline{\boldsymbol{\sigma}}) \leq \sum_{r=1}^{N}\sum_{k=1}^{K} c^{(r)}\ \alpha_{(k)}^{(r)} \left((\tau_0)_{(k)}^{(r)}\right)^2, \forall\, \alpha_{(k)}^{(r)} \geq 0 \right\}. \tag{7.18}$$

It is worth noting that equality in (7.14) holds if the set of K tensors $\boldsymbol{\mu}_{(k)}^{(r)}$ form a basis for the space of stress tensors, since in that case, the scalar quantities $\tau_{(k)}^{(r)}$ represent the components of a stress tensor relative to that basis. This suggests that the 'relaxed variational' bound (7.16) coincides with the 'variational' bound (7.5) when this is the case and the optimal $\widehat{\mathbf{M}}_0^{(r)}$ in the context of the latter are of the form (7.12). This is precisely what happens in the model problem to be discussed below. Unfortunately, it is not representative of what happens in practice, since for most cases, including FCC, BCC and HCP crystals, the number of available slip systems is larger than the dimension of the relevant stress space.

7.2 Application to a model, porous crystal

In this section, the focus is on a special class of porous materials with 'particulate' microstructures, consisting of aligned cylindrical pores ($r = 2$) that are distributed *randomly* and *isotropically* in a viscoplastic *single-crystal* phase ($r = 1$) . It is assumed that the symmetry axes of the crystalline matrix and the cylindrical pores are aligned with the x_3 axis. It is further assumed that the behavior of the crystalline matrix is characterized by an *incompressible* stress potential $u^{(1)}$ of the form (7.3), where the slip potentials $\psi^{(1)}_{(k)}$ are of the power-law type (7.2), and the Schmid tensors $\boldsymbol{\mu}_{(k)}$ are taken to be of the form

$$\boldsymbol{\mu}_{(k)} = \frac{1}{2}(\mathbf{n}_{(k)} \otimes \mathbf{e}_3 + \mathbf{e}_3 \otimes \mathbf{n}_{(k)}). \tag{7.19}$$

Here, $\mathbf{e}_3$ is parallel to the slip direction, and

$$\mathbf{n}_{(k)} = \cos\theta_{(k)}\mathbf{e}_1 + \sin\theta_{(k)}\mathbf{e}_2 \tag{7.20}$$

denotes the unit vector normal to the slip plane of the kth system, relative to a laboratory frame of reference $\mathbf{e}_i$ (in the sequel, components are always referred to this basis). The porous material is subjected to *anti-plane* loadings, and the relevant viscoplastic boundary value problem becomes a vectorial, two-dimensional problem, where the non-zero components of the stress and strain-rate vectors, namely, σ_{13}, σ_{23}, ε_{13} and ε_{23}, are functions of x_1 and x_2 only. (This problem is mathematically equivalent to 2D conductivity.)

For simplicity, it will be assumed initially that all slip systems have the same flow stress, i.e., $(\tau_0)_{(k)} = \tau_0$ for all k. Of particular interest here are three different types of anisotropy, characterized by the sets of angles $\theta_{(k)}$ given by $\{0, \pi/2\}$, $\{0, \pm\pi/3\}$, and $\{0, \pm\pi/4, \pi/2\}$, which correspond to square ($K = 2$), hexagonal ($K = 3$), and octagonal ($K = 4$) symmetry, respectively. In the linear case, the potential $u^{(1)}$ is in fact isotropic for these three types of anisotropies. In the nonlinear case, however, the potential $u^{(1)}$ is, in general, anisotropic, and in the ideally plastic limit, it defines an anisotropic, polygonal yield surface in the σ_{13}-σ_{23} stress space, as depicted in figure 7.1. Note that as the number of slip systems K increases, the potential approaches an isotropic yield surface with flow stress τ_0.

From the homogeneity of the potential (7.3) and the symmetry of the problem, it follows that, under anti-plane conditions, the effective stress potential can be written as

$$\widetilde{U}(\overline{\boldsymbol{\sigma}}) = \frac{\widetilde{\tau}_0\dot{\gamma}_0}{1+n}\left(\frac{\overline{\tau}_e}{\widetilde{\tau}_0}\right)^{1+n}, \tag{7.21}$$

where $\overline{\tau}_e = \sqrt{(1/2)\,\overline{\boldsymbol{\sigma}}_d \cdot \overline{\boldsymbol{\sigma}}_d} = (\overline{\sigma}^2_{13}+\overline{\sigma}^2_{23})^{1/2}$ is the macroscopic equivalent stress, and $\widetilde{\tau}_0$ is the *effective flow stress*, which depends on the porosity $f = c^{(2)}$ and the direction of loading $\overline{\theta} = \tan^{-1}(\overline{\sigma}_{23}/\overline{\sigma}_{13})$, and completely characterizes the effective response of the porous material. It is noted that, for the particular class of composites considered here, the potential $\widetilde{U}$ exhibits the same symmetries as the matrix potential $u^{(1)}$, and therefore $\widetilde{\tau}_0$ is a periodic function of $\overline{\theta}$ with period π/K. Thus, it suffices to restrict attention to loading directions in the range $|\overline{\theta}| \le \pi/(2K)$. Note that the values $\overline{\theta} = 0$ and

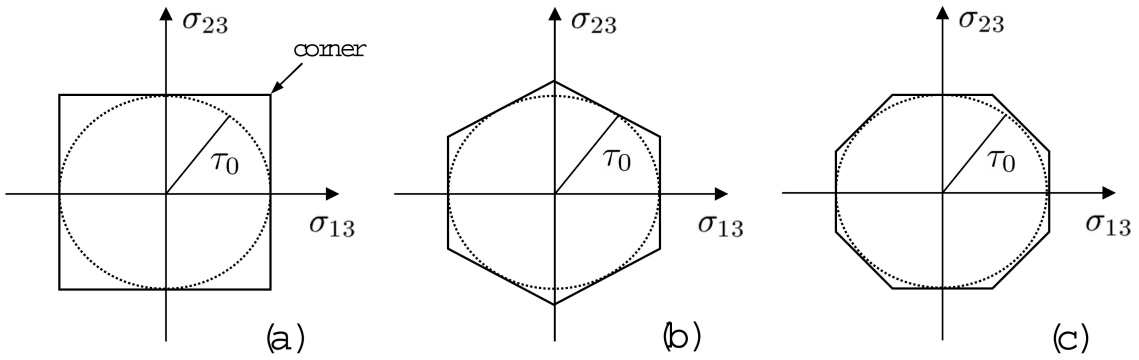

Figure 7.1: Yield surfaces in σ_{13}-σ_{23} space for (a) square ($K = 2$), (b) hexagonal ($K = 3$), and (c) octagonal ($K = 4$) symmetries.

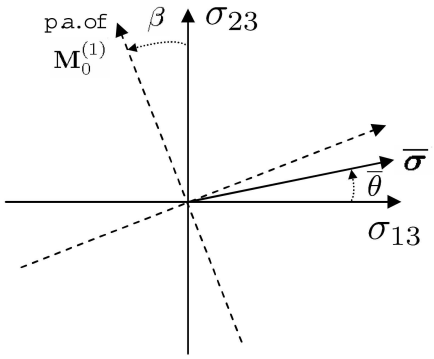

Figure 7.2: Angles in σ_{13}-σ_{23} space: β denotes the orientation of the principal axes (p.a.) of the compliance tensor $\mathbf{M}_0^{(1)}$, and $\overline{\theta}$ denotes the direction of the macroscopic stress $\overline{\boldsymbol{\sigma}}$.

$\overline{\theta} = \pm\pi/(2K)$ correspond, respectively, to loadings directed along a slip system and a 'corner' of the matrix phase (see figures 7.1 & 7.2).

7.2.1 Variational bounds

In this subsection, the 'variational' bounds described in Result 7.1.2 are specialized to the model porous material introduced in the previous subsection. Thus, from the lower bound (7.8) for the effective stress potential of a power-law composite, we obtain the following upper bound for the effective flow stress of the model porous material:

$$\widetilde{\tau}_0\left(\overline{\theta}\right) = \left(\frac{\gamma_0}{2}\right)^{1/n} \inf_{\mathbf{M}_0^{(1)} \geq 0} \left\{ \left[\widetilde{U}_0(\overline{\boldsymbol{\sigma}}/\overline{\tau}_e)\right]^{-\frac{n+1}{2n}} \left[(1-f)\,\frac{n+1}{n-1}\,v^{(1)}(\mathbf{M}_0^{(1)})\right]^{\frac{n-1}{2n}} \right\}, \tag{7.22}$$

where $\widetilde{U}_0$ and $v^{(1)}$ are defined by (7.7) and (7.6), respectively.

For the problem at hand, it suffices to restrict the optimization over the compliance tensors $\mathbf{M}_0^{(1)}$ to the out-of-plane components $S_{0\,(i3)(j3)}^{(1)}$, $i, j = 1, 2$. It is then convenient to write these tensors in the spectral form

$$\mathbf{M}_0^{(1)} = \frac{1}{2\lambda_0}\mathbf{E} + \frac{1}{2\mu_0}\mathbf{F}, \tag{7.23}$$

where $\mathbf{E}$ and $\mathbf{F}$ are eigentensors given by $\mathbf{E} = \boldsymbol{\mu}_0 \otimes \boldsymbol{\mu}_0$ and $\mathbf{F} = \mathbf{K} - \mathbf{E}$, with $\boldsymbol{\mu}_0 = \frac{1}{\sqrt{2}}(\mathbf{n} \otimes \mathbf{e}_3 + \mathbf{e}_3 \otimes \mathbf{n})$, $\mathbf{n} = \cos\beta\, \mathbf{e}_1 + \sin\beta\, \mathbf{e}_2$, and $\mathbf{K}$ denoting the out-of-plane projection of the fourth-order identity tensor. Thus, the tensors $\mathbf{M}_0^{(1)}$ are completely specified by two positive moduli λ_0 and μ_0 (eigenvalues), and the orientation of their principal axes β, given by $\tan 2\beta = 2S^{(1)}_{0\,1323}/(S^{(1)}_{0\,1313} - S^{(1)}_{0\,2323})$. Note that the degree of anisotropy of these compliance tensors is characterized by the ratio $k_0 = \lambda_0/\mu_0$, which takes the value 1 for isotropic tensors, and 0 or infinity, for strongly anisotropic tensors.

The 'variational' bounds (7.22) require the use of appropriate bounds for the effective potential $\widetilde{U}_0$ of *linearly* viscous, porous materials with matrix compliances of the form (7.23). In this work, use is made of the generalized Hashin-Shtrikman (HS) bounds of Willis (1977), which are provided in Section 2.4. Thus, the effective compliance tensor can be written as

$$\widetilde{\mathbf{M}}_0 = \mathbf{M}_0^{(1)} + \frac{f}{1-f}(\mathbf{Q}^{(1)})^{-1}, \tag{7.24}$$

where $\mathbf{Q}^{(1)}$ is given by $\mathbf{Q}^{(1)} = \mathbf{L}_0^{(1)} - \mathbf{L}_0^{(1)}\mathbf{P}^{(1)}\mathbf{L}_0^{(1)}$. Here, $\mathbf{L}_0^{(1)} = \mathbf{M}_0^{(1)^{-1}}$, and the out-of-plane projection of the microstructural tensor $\mathbf{P}^{(1)}$ can be written as (see Ponte Castañeda & Nebozhyn 1997)

$$\mathbf{P}^{(1)} = \frac{\sqrt{k_0}}{1+\sqrt{k_0}}\frac{1}{2\lambda_0}\mathbf{E} + \frac{1}{1+\sqrt{k_0}}\frac{1}{2\mu_0}\mathbf{F}, \tag{7.25}$$

where the tensors $\mathbf{E}$ and $\mathbf{F}$ have been defined in the context of expression (7.23). The resulting effective compliance tensor $\widetilde{\mathbf{M}}_0$ has the same form as the compliance tensor of the matrix phase (7.23), but with effective moduli given by

$$\widetilde{\lambda}_0 = \frac{1-f}{1+f\sqrt{k_0}}\,\lambda_0, \quad \widetilde{\mu}_0 = \frac{1-f}{1+f/\sqrt{k_0}}\,\mu_0. \tag{7.26}$$

Note that the compliance tensors $\widetilde{\mathbf{M}}_0$ and $\mathbf{M}_0^{(1)}$ are therefore co-axial, i.e., they have the same principal directions, which is a consequence of the assumed isotropy of the microstructure.

In addition, the bound (7.22) requires the evaluation of the 'corrector' function $v^{(1)}$. This actually constitutes the main difficulty in the computation of the 'variational' bound, for the optimization with respect to $\check{\boldsymbol{\sigma}}^{(1)}$ in (7.6) is a non-convex global optimization problem. In general, this optimization has to be carried out numerically, using, for instance, methods based on genetic algorithms, such as the differential evolution algorithm of Storn & Price (1997). In this connection, it should be emphasized that such optimization methods cannot, in general, guarantee that the result obtained is indeed the global optimum. However, in the context of the model problem considered here, the optimization in (7.6) involves only one variable in a bounded domain, namely the orientation angle of the stress vector $\check{\boldsymbol{\sigma}}^{(1)}$, and is therefore a fairly simple one for these methods, which have been developed to deal with high dimensional optimizations. (Note that even in the most general, three-dimensional case, the optimization in (7.6) would involve only five variables, and incompressibility even reduces this number to four.) Finally, the optimization of the bound (7.22) with respect to the compliance tensor $\mathbf{M}_0^{(1)}$ should be carried out numerically, in general, making use of an appropriate method for nonsmooth optimization, since the 'corrector' function $v^{(1)}$ is not differentiable in its entire domain.

Rigid-ideally plastic matrix. It has been shown that the computation of the 'variational' bound simplifies considerably in the case of ideal plasticity. Indeed, in this case, the 'variational' bounds for the model problem considered here can be computed analytically. First, note that in the ideally plastic limit ($n \to \infty$), the 'variational' bound (7.22) for $\widetilde{\tau}_0$ simplifies to

$$\widetilde{\tau}_0\left(\overline{\theta}\right) = \inf_{\mathbf{M}_0^{(1)} \geq 0} \left\{ \frac{\widetilde{U}_0(\overline{\boldsymbol{\sigma}}/\overline{\tau}_e)}{(1-f)\, v^{(1)}(\mathbf{M}_0^{(1)})} \right\}^{-1/2}, \tag{7.27}$$

which defines a bound from the outside for the macroscopic yield surface of the ideally plastic, porous material. The most important simplification, however, comes from the fact that, in this case, the function $v^{(1)}$ can be written in the form (7.11), with $\boldsymbol{\sigma}_{(k)}^{(1)}$ being the stress vectors corresponding to the $2K$ vertices, or 'corners', of the matrix yield surface (see figure 7.1). Then, the following explicit expressions for $v^{(1)}$ may be derived by routine analysis:

$$K = 2: \quad v^{(1)}(\mathbf{M}_0) = (\tau_0^2/2)\left\{\lambda_0^{-1} + \mu_0^{-1} + |\lambda_0^{-1} - \mu_0^{-1}|\, \sin\left(|2\beta|\right)\right\},$$

$$K = 3: \quad v^{(1)}(\mathbf{M}_0) = (\tau_0^2/3)\left\{\lambda_0^{-1} + \mu_0^{-1} + |\lambda_0^{-1} - \mu_0^{-1}|\, \cos\left[|2\beta| - \tfrac{\pi}{3} H(1-k_0)\right]\right\},$$

$$K = 4: \quad v^{(1)}(\mathbf{M}_0) = (\tau_0^2/4)\sec^2(\pi/8)\left\{\lambda_0^{-1} + \mu_0^{-1} + |\lambda_0^{-1} - \mu_0^{-1}|\, \cos\left[|2\beta| - \tfrac{\pi}{4} + \pi H(k_0-1)\right]\right\},$$

where H denotes the Heaviside function, and it is recalled that $k_0 = \lambda_0/\mu_0$. These expressions are valid for $|\beta| \leq \pi/(2K)$, but use can be made of the fact that the functions $v^{(1)}$ are even and periodic in β, with period π/K, to obtain corresponding expressions that are valid outside this range. It is emphasized that these functions are differentiable everywhere except at $\beta = 0$ and $\lambda_0 = \mu_0$.

The optimization with respect to $\mathbf{M}_0^{(1)}$ in (7.27) can then be carried out analytically, leading to the following explicit bound for the effective flow stress:

$$\widetilde{\tau}_0(\overline{\theta}) = \tau_0\, \sec\theta_c\, (1-f)\left[1 + \frac{f}{2}\frac{1+k_0}{\sqrt{k_0}}\right]^{-1/2}, \tag{7.28}$$

where $\theta_c = \pi/(2K)$, and the anisotropy ratio k_0 is a periodic function of $\overline{\theta}$, with period $2\theta_c$, given by

$$\sqrt{k_0} = \begin{cases} \dfrac{\sqrt{(\cos 2\overline{\theta} - \cos 2\theta_c)^2 + f^2 \sin^2 2\theta_c} - (\cos 2\overline{\theta} - \cos 2\theta_c)}{(1 - \cos 2\theta_c)\, f} & |\overline{\theta}| < \overline{\theta}_c, \\ 1 & \overline{\theta}_c \leq |\overline{\theta}| \leq \theta_c, \end{cases} \tag{7.29}$$

with the angle $\overline{\theta}_c$ given by $\cos 2\overline{\theta}_c = \min\{(1+f)\cos 2\theta_c, 1\}$. It is noted that, even though k_0 is *not* smooth at $\overline{\theta} = \overline{\theta}_c$, the effective flow stress (7.28) turns out to be a smooth function of $\overline{\theta}$.

Statistics of the local fields. The 'variational' estimates for the field statistics are given by those quantities in the LCC. Being a porous material, the phase averages of the stress are trivial, i.e. $\overline{\boldsymbol{\sigma}}^{(1)} = \overline{\boldsymbol{\sigma}}/c^{(1)}$ and $\overline{\boldsymbol{\sigma}}^{(2)} = \mathbf{0}$, while those of the strain are given by the HS estimates provided in Section 2.4, with the tensors $\mathbf{M}^{(1)}$ and $\mathbf{P}^{(1)}$ given by (7.23) and (7.25). Also provided in Section 2.4 are the HS estimates for the second moments of the strain and stress field in each phase. These

estimates take on a very simple form when the macroscopic loading is directed along a slip system of the matrix phase, e.g. $\overline{\theta} = 0$. In that case, the optimal $\mathbf{M}_0^{(1)}$ is such that $\beta = 0$, and so it can be verified that

$$\frac{\overline{\varepsilon}_e^{(1)}}{\overline{\varepsilon}_e} = \frac{1}{1 + f\ \sqrt{k_0}}, \quad \frac{\overline{\varepsilon}_e^{(2)}}{\overline{\varepsilon}_e} = \frac{1 + \sqrt{k_0}}{1 + f\ \sqrt{k_0}}, \tag{7.30}$$

where k_0 is the optimal anisotropy ratio associated with the estimate (7.22). In addition, introducing two components of the local fields that are 'parallel' and 'perpendicular' to the applied fields (which are aligned in this case), defined by

$$\varepsilon_{\parallel}^2 = \boldsymbol{\varepsilon} \cdot \mathbf{E}\boldsymbol{\varepsilon}, \quad \varepsilon_{\perp}^2 = \boldsymbol{\varepsilon} \cdot \mathbf{F}\boldsymbol{\varepsilon}, \quad \text{and} \quad \tau_{\parallel}^2 = \boldsymbol{\sigma} \cdot \mathbf{E}\boldsymbol{\sigma}, \quad \tau_{\perp}^2 = \boldsymbol{\sigma} \cdot \mathbf{F}\boldsymbol{\sigma}, \tag{7.31}$$

the HS estimates for the second moments are such that the standard deviations (SD) of these quantities in the matrix phase are given by

$$\frac{SD^{(1)}(\varepsilon_{\parallel})}{\overline{\varepsilon}_e^{(1)}} = \frac{SD^{(1)}(\tau_{\parallel})}{\overline{\tau}_e^{(1)}} = \sqrt{\frac{c}{2}}\ k_0^{1/4}, \quad \frac{SD^{(1)}(\varepsilon_{\perp})}{\overline{\varepsilon}_e^{(1)}} = k_0\ \frac{SD^{(1)}(\tau_{\perp})}{\overline{\tau}_e^{(1)}} = \sqrt{\frac{c}{2}}\ k_0^{3/4}, \tag{7.32}$$

while in the inclusion phase, the HS estimates predict uniform fields.

7.2.2 Relaxed variational bounds

In this subsection, the 'relaxed variational' bounds of deBotton & Ponte Castañeda (1995) recalled in Result 2.5 are specialized for the above-described model problem. Thus, from the lower bound (7.17) for the effective stress potential, we obtain the following upper bound for the effective flow stress of the model porous material:

$$\widetilde{\tau}_0\left(\overline{\theta}\right) = \tau_0 \inf_{\alpha_{(k)} \geq 0} \left\{ \left[\widetilde{U}_0(\overline{\boldsymbol{\sigma}}/\overline{\tau}_e)\right]^{-\frac{n+1}{2n}} \left[(1-f)\sum_{k=1}^{K} (\alpha_{(k)})^{\frac{n+1}{n-1}}\right]^{\frac{n-1}{2n}} \right\}, \tag{7.33}$$

where $\widetilde{U}_0$ is the effective potential of a linear, porous material with matrix compliance tensor

$$\mathbf{M}_0^{(1)} = 2\sum_{k=1}^{K} \alpha_{(k)} \boldsymbol{\mu}_{(k)} \otimes \boldsymbol{\mu}_{(k)}, \tag{7.34}$$

with the $\boldsymbol{\mu}_{(k)}$ given by (7.19). The tensor (7.34) can be written in the form (7.23), where the tensors $\mathbf{E}$ and $\mathbf{F}$ depend on the orientation of the principal axes of (7.34), β, and the moduli λ_0 and μ_0 are given by

$$\frac{1}{2\lambda_0} = 2\sum_{k=1}^{K} \alpha_{(k)} (\boldsymbol{\mu}_{(k)} \cdot \mathbf{E}\boldsymbol{\mu}_{(k)}), \quad \frac{1}{2\mu_0} = 2\sum_{k=1}^{K} \alpha_{(k)} (\boldsymbol{\mu}_{(k)} \cdot \mathbf{F}\boldsymbol{\mu}_{(k)}). \tag{7.35}$$

Then, the linear Hashin-Shtrikman bounds for the effective stress potential $\widetilde{U}_0$ of the LCC in (7.33) are given by expressions (7.24)-(7.26), with λ_0, μ_0, $\mathbf{E}$ and $\mathbf{F}$ being those associated with the compliance tensor (7.34).

Finally, the optimization with respect to the variables $\alpha_{(k)}$ in (7.33) should be carried out numerically using a smooth optimization method.

Ideally plastic matrix. In the ideally plastic limit, the 'relaxed variational' bound (7.33) for $\widetilde{\tau}_0$ can be shown to reduce to

$$\widetilde{\tau}_0\left(\overline{\theta}\right) = \sqrt{2}\,\tau_0\,(1-f)\,\inf_{\alpha_{(k)}\geq 0}\left\{1+\frac{1-k_0}{1+k_0}\cos\left[2(\overline{\theta}-\beta)\right]+\frac{2\sqrt{k_0}}{1+k_0}f\right\}^{-1/2}. \tag{7.36}$$

In this expression, k_0 and β depend on the slip compliances $\alpha_{(k)}$ and the symmetry of the matrix potential through the relations

$$k_0 = \frac{\sum_{k=1}^{K}\alpha_{(k)}(1-\cos\left[2(\theta_{(k)}-\beta)\right])}{\sum_{k=1}^{K}\alpha_{(k)}(1+\cos\left[2(\theta_{(k)}-\beta)\right])}, \quad \tan 2\beta = \frac{\sum_{k=1}^{K}\alpha_{(k)}\sin 2\theta_{(k)}}{\sum_{k=1}^{K}\alpha_{(k)}\cos 2\theta_{(k)}}. \tag{7.37}$$

In general, the optimization in (7.36) still has to be carried out numerically. However, for macroscopic loadings directed along a slip system (i.e., $\overline{\theta}=\theta_{(k)}$, see expression (7.20)), the symmetry of the problem requires the optimal $\alpha_{(k)}$'s to be such that $\beta=\overline{\theta}$. Then, the optimization in (7.36) reduces to a one-dimensional minimization with respect to k_0, which yields $\sqrt{k_0}=(\sqrt{1+f^2}-1)/f$, and so the bound (7.36) becomes

$$\widetilde{\tau}_0 = \sqrt{2}\,\tau_0\,\frac{1-f}{f}\,\left(\sqrt{1+f^2}-1\right)^{1/2}, \tag{7.38}$$

which is independent of the number of slip systems K.

Statistics of the local fields. It can be shown that the 'relaxed variational' estimates for the field statistics are given by those quantities in the LCC. Thus, the first and second moments of the local fields in each phase are given by the expressions provided in Section 2.4, with $\mathbf{M}^{(1)}$ given by (7.34). When the applied fields are directed along a slip system of the matrix phase, e.g. $\overline{\theta}=0$, the the first moments and standard deviations of the fields are given by expressions (7.30)-(7.32), with k_0 denoting the optimal anisotropy ratio associated with the estimate (7.33).

7.2.3 Results and discussion

This subsection presents comparisons between the 'variational' (VAR) and 'relaxed variational' ($RVAR$) bounds of the Hashin-Shtrikman type, as well as the classical Voigt bounds, for the above-described model problem .

Figure 7.3 provides comparisons among the various bounds for porous, power-law materials with square ($K=2$), hexagonal ($K=3$) and octagonal ($K=4$) symmetries, subjected to a macroscopic stress $\overline{\boldsymbol{\sigma}}$ directed along a slip system of the matrix phase ($\overline{\theta}=0$). In this figure, plots are shown for the effective flow stress $\widetilde{\tau}_0$, normalized by the flow stress of the matrix τ_0, as a function of the strain-rate sensitivity m, for a moderate value of the porosity ($f=0.25$). We begin by noting that, independently of K, the VAR and the $RVAR$ bounds coincide for $m=1$ with the linear Hashin-Shtrikman bounds, as they should, and they are seen to improve on the Voigt bound for all values of the strain-rate sensitivity, even though the improvement is less significant in the ideally plastic limit ($m=0$). The main observation in the context of this figure, however, is that, while the VAR and $RVAR$ bounds agree exactly in the case of a matrix with two slip systems (see part (a)), the VAR bounds become progressively sharper than the $RVAR$ bounds as the number of slip systems increases,

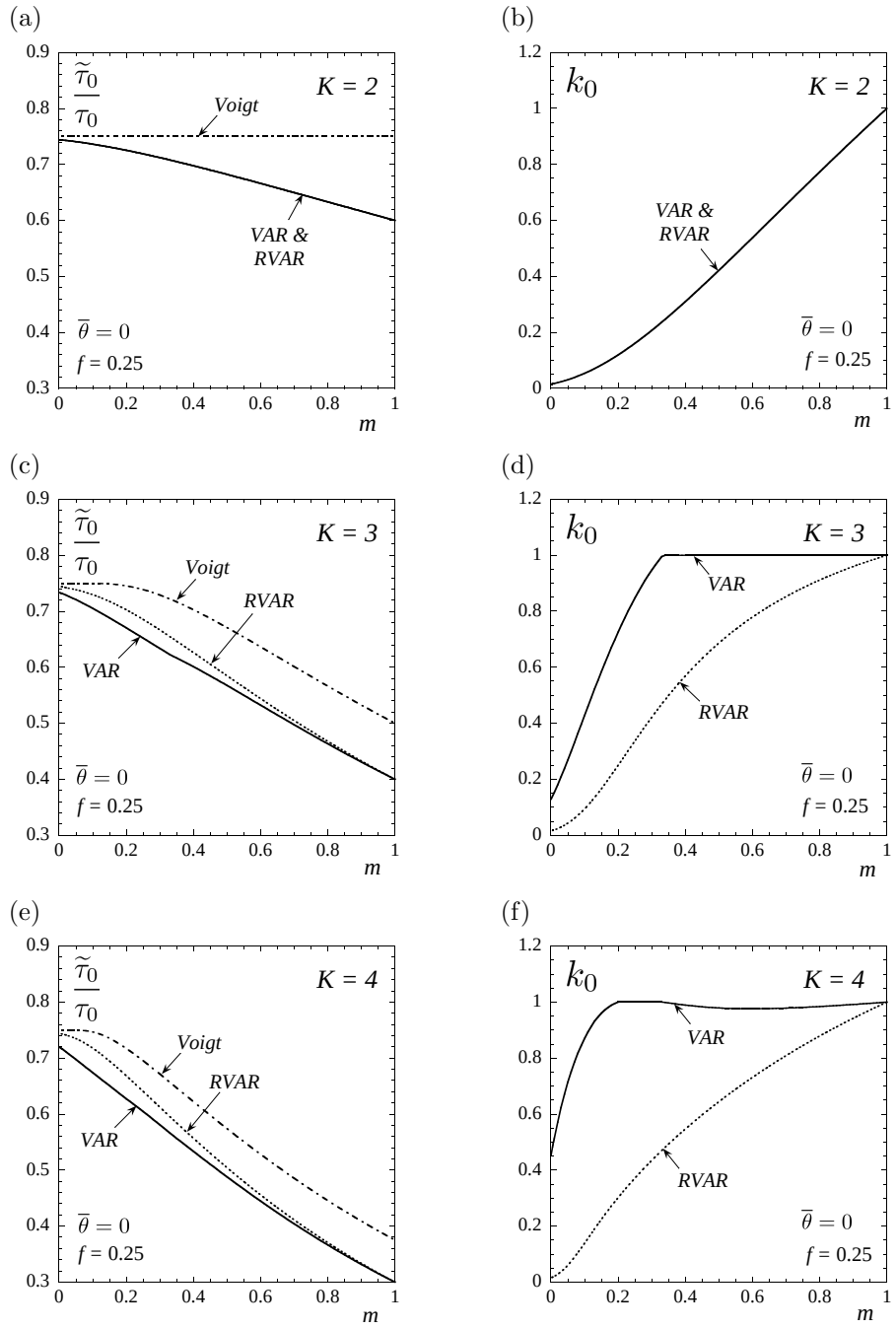

Figure 7.3: Effective flow stress $\widetilde{\tau}_0$, normalized by the flow stress of the matrix τ_0, and corresponding anisotropy ratios k, as a function of the strain-rate sensitivity m, for power-law, porous materials with square, hexagonal, and octagonal symmetry, and a given porosity ($f = 0.25$). The macroscopic stress is directed along a slip system ($\overline{\theta} = 0$). Comparisons between the 'variational' (VAR) and 'relaxed variational' ($RVAR$) bounds of the Hashin-Shtrikman type, and the Voigt bound.

for all values of the strain-rate sensitivity different than 1 (see parts (c) & (e)). In fact, in the ideally plastic limit, the $RVAR$ bounds are found to be insensitive to K for this particular loading direction ($\overline{\theta} = 0$), while the corresponding VAR bounds decrease monotonically with increasing K. The largest difference between these two sets of bounds is found to be approximately 6% in the case of $K = 4$. Finally, it is noted that the fact that the VAR and $RVAR$ bounds coincide for $K = 2$, but not more generally, is because, in that case, the optimal compliances $\widehat{\mathbf{M}}_0^{(1)}$ associated with both sets of bounds can be written as (7.34), with the tensors $\boldsymbol{\mu}_{(k)}$ forming a basis for the relevant (two-dimensional) stress space, so that equality holds in the relaxation of the function $v^{(1)}$ (see expression (7.13)).

Also shown in figure 7.3 are plots for the anisotropy ratio $k_0 = \lambda_0/\mu_0$ of the optimal compliances $\widehat{\mathbf{M}}_0^{(1)}$ associated with the VAR and $RVAR$ bounds. It is recalled that $k_0 = 1$ and $k_0 = 0$ correspond to isotropic and strongly anisotropic compliance tensors, respectively. Thus, it is observed that, in general, the optimal $\widehat{\mathbf{M}}_0^{(1)}$ associated with the VAR bounds tends to be more isotropic as the number of slip systems in the matrix (and therefore the symmetry of the potential $u^{(1)}$) increases. In fact, in the case of $K = 3$, the potential $u^{(1)}$ is isotropic not only for $m = 1$, but also for $m = 1/3$, and in the case of $K = 4$, it is also isotropic for $m = 1/5$, and so are the optimal $\widehat{\mathbf{M}}_0^{(1)}$ associated with the corresponding VAR bounds. (Note that the latter are also isotropic for other values of m, for which the potential $u^{(1)}$ is anisotropic.) In contrast, the optimal $\widehat{\mathbf{M}}_0^{(1)}$ associated with the $RVAR$ bounds are always found to be anisotropic for strain-rate sensitivities different than 1, even if the potential $u^{(1)}$ is isotropic. This is consistent with the fact that, while in the context of the VAR bounds, the tensors $\widehat{\mathbf{M}}_0^{(r)}$ are identified with secant compliances of the phase potentials, which are known to be isotropic if the potentials are isotropic, in the context of the $RVAR$, the tensors $\widehat{\mathbf{M}}_0^{(r)}$ are constructed by summing slip secant compliances, and do not correspond to secant compliances of the phase potentials. Finally, it is worth noting that the optimal compliances $\widehat{\mathbf{M}}_0^{(1)}$ associated with both, the VAR and $RVAR$ bounds of figure 7.3, have principal axes that are 'aligned' with the symmetry axes of the potential $u^{(1)}$ and the macroscopic stress vector $\overline{\boldsymbol{\sigma}}$ (i.e., $\beta = \overline{\theta} = 0$), as expected from the symmetry of the problem. It should be emphasized, however, that in the context of the VAR bounds, the optimal orientation of the tensor $\widehat{\mathbf{M}}_0^{(1)}$ does not follow from a stationarity condition, since the function $v^{(1)}$, as given by (7.6), is nonsmooth precisely at $\beta = 0$.

The differences in the optimal anisotropy ratio k_0 identified above lead to qualitative differences in the predictions for the statistics of the strain field, as can be seen in figure 7.4, which in turn, can lead to significantly different preditions for the evolution of the microstructure in a finite-deformation process. It is not evident, however, which set of estimates is better, and only comparisons with exact results will elucidate this point.

Figure 7.5 provides comparisons between the various bounds for the yield surfaces of porous, ideally plastic materials with square ($K = 2$), hexagonal ($K = 3$) and octagonal ($K = 4$) symmetries, for a given value of the porosity ($f = 0.25$). The yield surfaces are symmetric about the σ_{13}- and σ_{23}-axes. We begin by noting that, in all three cases, the VAR and $RVAR$ bounds improve on the Voigt bounds for all directions of the macroscopic stress vector $\overline{\boldsymbol{\sigma}}$. The main observation in the

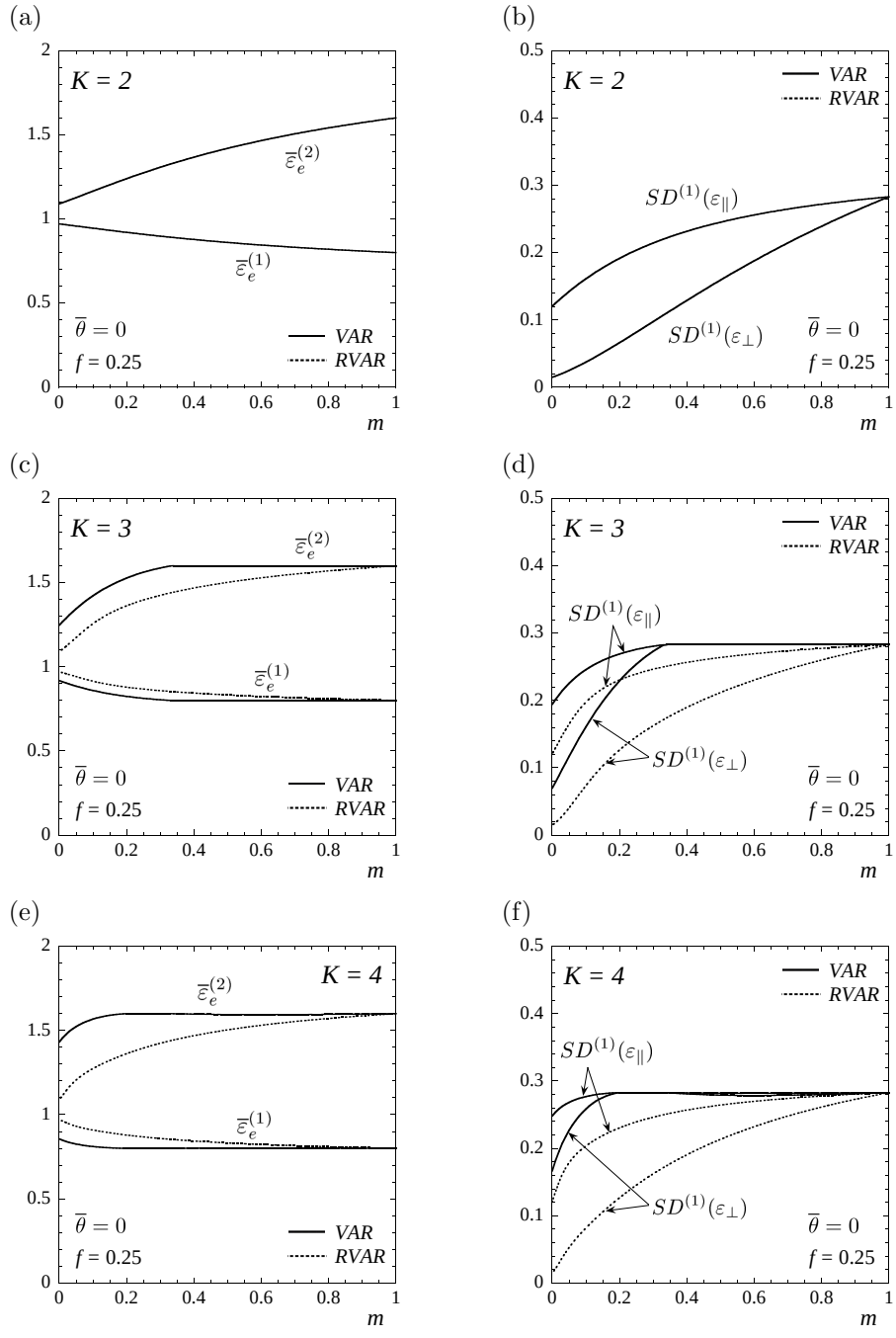

Figure 7.4: Statistics of the strain field, normalized by the equivalent macroscopic strain $\overline{\varepsilon}_e$, as a function of the strain-rate sensitivity m, for power-law, porous materials with square, hexagonal, and octagonal symmetry, and a given porosity ($f = 0.25$). The macroscopic stress is directed along a slip system ($\overline{\theta} = 0$). Comparisons between the 'variational' (VAR) and 'relaxed variational' ($RVAR$) estimates of the Hashin-Shtrikman type.

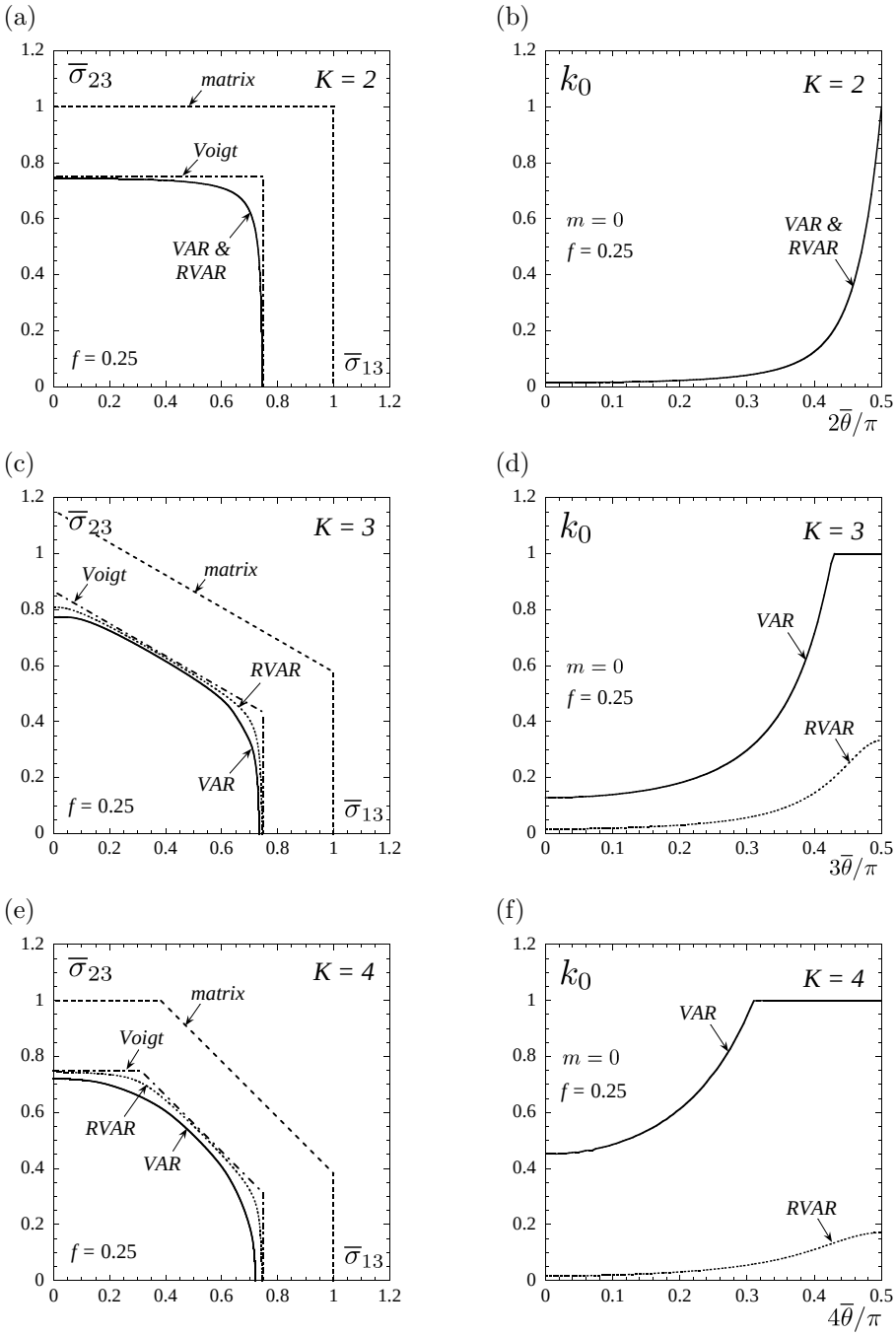

Figure 7.5: Yield surfaces, normalized by the flow stress of the matrix τ_0, and corresponding anisotropy ratios k_0, for porous, ideally plastic materials with square, hexagonal, and octagonal symmetry, and a given porosity ($f = 0.25$). Comparisons between the 'variational' (VAR) and 'relaxed variational' ($RVAR$) bounds of the Hashin-Shtrikman type, and the Voigt bound.

context of this figure, however, is that, once again, the VAR and $RVAR$ bounds agree exactly in the case of a matrix phase with two slip systems (see part (a)), but as the number of slip systems increases, the VAR bounds become progressively sharper than the $RVAR$ bounds, for all directions of the macroscopic stress vector $\overline{\boldsymbol{\sigma}}$ (see parts (c) & (e)), the largest difference being of the order of 6% in the case of a matrix phase with four slip systems. In addition, it is interesting to note that, while the macroscopic yield surfaces predicted by the Voigt bounds are simply rescaled versions of the yield surface of the corresponding matrix phase, and therefore exhibit homologous corners, the macroscopic yield surfaces predicted by the VAR and $RVAR$ bounds are smooth, and exhibit a more complicated dependence on the loading direction.

Also shown in figure 7.5 are plots for the anisotropy ratio k_0 of the optimal $\widehat{\mathbf{M}}_0^{(1)}$ associated with the VAR and $RVAR$ bounds, as a function of the loading angle $\overline{\theta}$. Given the symmetries of the problem, it is sufficient to restrict attention to values of $\overline{\theta}$ between 0 and $\pi/(2K)$, which correspond to loadings along a slip system and a 'corner' of the matrix phase, respectively. It can be seen that the optimal $\widehat{\mathbf{M}}_0^{(1)}$ associated with the VAR bounds are, in general, anisotropic ($k_0 < 1$), but become isotropic ($k_0 \to 1$) as the loading direction approaches that of a 'corner' of the matrix phase ($\overline{\theta} \to \pi/(2K)$). On the other hand, the principal axes of $\widehat{\mathbf{M}}_0^{(1)}$, always in the context of the VAR bounds, remain aligned with the symmetry axes of $u^{(1)}$ (i.e., $\beta = 0$) for all loading directions in this range. It follows from the symmetry of the problem that, as the loading direction varies from one slip system to an adjacent one, the principal directions of $\widehat{\mathbf{M}}_0^{(1)}$ 'switch' from one set of symmetry axes of $u^{(1)}$ to another by becoming isotropic in between. Thus, it is found that the principal directions of the optimal $\widehat{\mathbf{M}}_0^{(1)}$ depend on the direction of loading, as expected, but in such a way that they always coincide with symmetry axes of the phase potential $u^{(1)}$. This fact, if also true in higher dimensions, could be exploited to simplify the computations of the 'variational' bounds in the context of more complex materials with phase potentials exhibiting certain symmetries, such as polycrystals. In contrast, the optimal compliances $\widehat{\mathbf{M}}_0^{(1)}$ associated with the $RVAR$ bounds for $K = 3$ and $K = 4$ are seen to remain anisotropic for all loading directions (see parts (d) & (f)), and their principal directions are found to vary smoothly with $\overline{\theta}$, being aligned with the macroscopic stress vector whenever the latter is directed along a symmetry axis of $u^{(1)}$, as expected.

The results provided hitherto correspond to matrix phases with the same flow stress for all slip systems. It is also of interest, however, to consider the effect of contrast between the different slip systems on the various bounds. Figure 7.6 provides comparisons between the various bounds for the effective behavior of porous, ideally plastic materials with 'anisotropic' hexagonal and octagonal symmetry, with one slip system being harder than the others. Part (a) shows plots for the effective flow stress $\widetilde{\tau}_0$, normalized by the flow stress of the soft slip system $(\tau_0)_{(2)}$, of a hexagonal material loaded along the hard slip system ($\overline{\theta} = 0$), as a function of the contrast $(\tau_0)_{(1)}/(\tau_0)_{(2)}$, for a given porosity ($f = 0.25$). The main observation in the context of this figure is that, while the differences between the VAR and $RVAR$ bounds are relatively small for low values of the contrast, the VAR bounds become progressively sharper than the $RVAR$ bounds as the contrast increases. However,

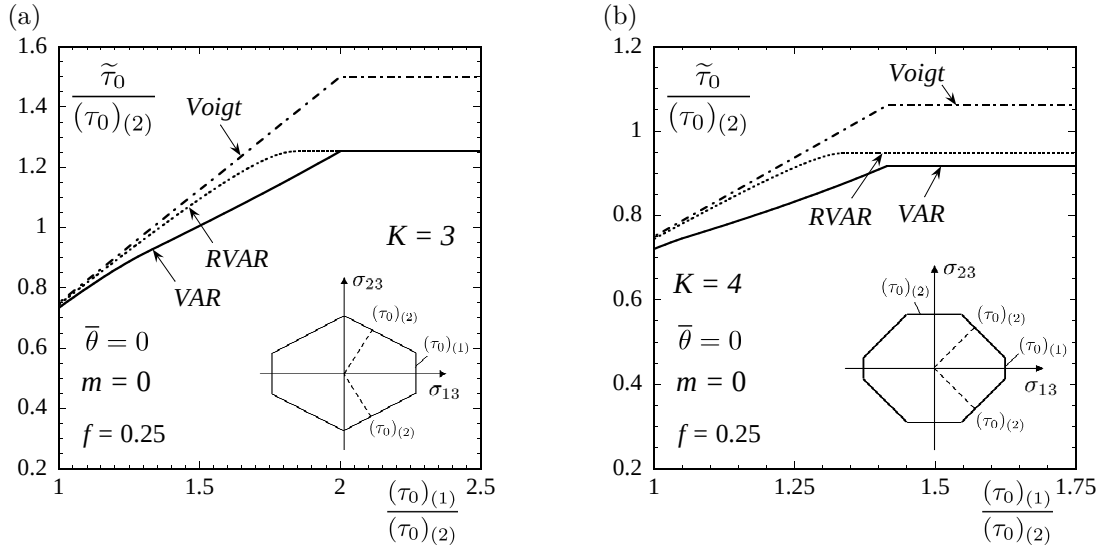

Figure 7.6: Effective flow stress $\widetilde{\tau}_0$ of a porous, ideally plastic material with 'anisotropic' (a) hexagonal and (b) octagonal symmetry, loaded along the hard slip system ($\overline{\theta} = 0$). Comparisons between the 'variational' (VAR) and 'relaxed variational' ($RVAR$) bounds of the Hashin-Shtrikman type, as a function of the contrast $(\tau_0)_{(1)}/(\tau_0)_{(2)}$, for a given porosity ($f = 0.25$). Plots are normalized by the flow stress of the soft slip system $(\tau_0)_{(2)}$.

for values of the contrast larger than 2, the hard slip system ceases to play any role, and since the number of active slip systems coincides with the dimension of the stress space (two), the VAR and $RVAR$ bounds agree exactly. (Note that the matrix symmetry is not square but rhomboidal in that case.) Thus, the largest difference between the VAR and $RVAR$ bounds occurs at an intermediate value of the contrast, approximately 1.7 at this particular porosity and loading direction, and it is of the order of 10%. It is also worth noting that these bounds significantly improve on the Voigt bound for large values of the contrast. Part (b) shows similar plots for an octagonal matrix. Like in the previous case, it is observed that the differences between the VAR and $RVAR$ bounds increase with increasing values of the contrast, the largest difference being of the order of 10%. However, for values of the contrast larger than $\sqrt{2}$, the number of active slip systems reduces from four to three, which is larger than the dimension of the stress space, and consequently the VAR bounds remain sharper than the $RVAR$ bounds in this case.

7.3 Application to isotropic, porous materials

7.3.1 Power-law, porous materials

It has been found in the previous section that the differences between the 'variational' and 'relaxed variational' bounds become more significant as the number of slip systems in the matrix phase increases. In this section, the limiting case of a power-law matrix phase with an *infinite* number of slip systems is considered. To that end, it is convenient to consider first the following variant of the

matrix potential (7.3) with a finite number of slip systems:

$$u^{(1)}(\boldsymbol{\sigma}) = \frac{2\pi}{K}\sum_{k=1}^{K}\overline{\psi}\left(\boldsymbol{\sigma}\cdot\boldsymbol{\mu}_{(k)}\right), \quad \overline{\psi}(\tau) = \varrho(n)\,\frac{\gamma_0\,\tau_0}{n+1}\left|\frac{\tau}{\tau_0}\right|^{n+1}. \tag{7.39}$$

In this expression, the Schmid tensors $\boldsymbol{\mu}_{(k)}$ are given by (7.19), with $\mathbf{n}_{(k)}$ denoting unit vectors (7.20) normal to the slip planes defined by the angles $\theta_{(k)} = \pi\,(k-1)/K$, and ϱ is defined as

$$\varrho(n) = \frac{n+1}{2n}\frac{\Gamma(\frac{n+1}{2})}{\sqrt{\pi}\,\Gamma(\frac{n}{2})}, \tag{7.40}$$

where Γ denotes the Euler gamma function. Then, in the limit $K\to\infty$, the potential (7.39) becomes

$$\lim_{K\to\infty} u^{(1)}(\boldsymbol{\sigma}) = \int_0^{2\pi}\overline{\psi}\,(\boldsymbol{\sigma}\cdot\boldsymbol{\mu}(\theta))\;d\theta = \frac{\tau_0\gamma_0}{n+1}\left(\frac{\tau_e}{\tau_0}\right)^{n+1} = \psi(\tau_e), \tag{7.41}$$

where $\tau_e = \sqrt{(1/2)\,\boldsymbol{\sigma}_d\cdot\boldsymbol{\sigma}_d} = (\sigma_{13}^2+\sigma_{23}^2)^{1/2}$ is the equivalent stress. Thus, the potential (7.39) tends to an *isotropic*, power-law potential ψ, as the number of slip systems tends to infinity. In fact, (7.41) is nothing more than the plane-wave decomposition of the isotropic potential ψ (see for example Gel'fand & Shilov 1964). This decomposition makes it possible to apply the 'relaxed variational' method of deBotton & Ponte Castañeda (1995), which is specifically designed for potentials of the form (7.3), to composites made up of isotropic, power-law phases. In addition, it allows us to compare the 'variational' and 'relaxed variational' bounds, in the limiting case of an infinite number of slip systems, where the differences between them are expected to be most significant.

It is recalled that under anti-plane conditions, the effective stress potential $\widetilde{U}$ of a porous material with a matrix potential (7.39) can be written as (7.21), where the effective flow stress $\widetilde{\tau}_0$ is a function of the loading direction $\overline{\theta}$, except in the limit $K\to\infty$, where the material becomes isotropic and, therefore $\widetilde{\tau}_0$, independent of $\overline{\theta}$.

Finally, it is recalled that in the previous section only the *stress* formulations of the 'variational' and 'relaxed variational' bounds were considered. The reason for this is that the Legendre transform of potentials of the form (7.3) cannot be written as a sum of slip potentials[1], and therefore a strain-rate version of the 'relaxed variational' bounds of deBotton & Ponte Castañeda (1995) is not available in that case, except for the case of an infinite number of slip systems, when the Legendre transform of (7.41), ψ^*, can in fact be written as an infinite sum of slip potentials, again, by making use of the plane-wave decomposition. More explicitly,

$$\varphi(\varepsilon_e) = \frac{\tau_0\gamma_0}{1+m}\left(\frac{\varepsilon_e}{\gamma_0}\right)^{1+m} = \int_0^{2\pi}\overline{\varphi}\,(2\,\boldsymbol{\varepsilon}\cdot\boldsymbol{\mu}(\theta))\;d\theta, \quad \overline{\varphi}(\gamma) = \varrho(m)\frac{\gamma_0\,\tau_0}{1+m}\left|\frac{\gamma}{\gamma_0}\right|^{1+m}. \tag{7.42}$$

where $\varepsilon_e = \sqrt{2\,\boldsymbol{\varepsilon}_d\cdot\boldsymbol{\varepsilon}_d} = 2\,(\varepsilon_{13}^2+\varepsilon_{23}^2)^{1/2}$ is the equivalent strain-rate, and $\varrho(m)$ is given by (7.40) evaluated at m instead of n. This last result will be used below to obtain an alternate 'relaxed variational' bound for porous materials with an isotropic, power-law matrix. On the other hand, there is no point in making use of the dual form (strain-rate version) of the 'variational' bound, since we know from the general theory that it would lead to precisely the same bounds.

[1] The Legendre transform of a sum of convex potentials is the inf-convolution of the sum of their Legendre transforms, and not simply the sum of their Legendre transforms (see, for example, Theorem 16.4 in Rockafellar 1970)

7.3.2 Variational bounds

The 'variational' bounds of the Hashin-Shtrikman type for the effective behavior of a porous material with a matrix potential (7.39), with finite number of slip systems, can be derived as already discussed in the previous section. However, in the limiting case of infinitely many slip systems, the matrix potential becomes isotropic, and the optimal compliance tensors $\widehat{\mathbf{M}}_0^{(1)}$ can be shown to be isotropic, *i.e.*, $\lambda_0 = \mu_0$ in (7.23) and $k_0 = 1$. Then, the function $v^{(1)}$ can be easily computed, and the optimization with respect to the single modulus μ_0 can be carried out analytically. The resulting 'variational' bound for the effective flow stress is given by

$$\frac{\widetilde{\tau}_0}{\tau_0} = \frac{1-f}{(1+f)^{\frac{1+m}{2}}}. \tag{7.43}$$

This result is in exact agreement with the bound for porous, power-law materials first obtained by Ponte Castañeda (1991) by means of the 'variational' method initially proposed for composites with *isotropic* phases.

7.3.3 Relaxed variational bounds

The 'relaxed variational' bounds of the Hashin-Shtrikman type for the effective behavior of a porous material with a matrix potential (7.39), with finite number of slip systems, are computed in the manner described in the previous section. Although the matrix potential becomes isotropic for infinitely many slip systems (with the same flow stress), the optimal compliance tensors $\widehat{\mathbf{M}}_0^{(1)}$ are found to remain anisotropic (i.e., $k_0 \neq 1$) in this case. But, from the symmetry of the problem, it follows that the principal axes of $\widehat{\mathbf{M}}_0^{(1)}$ should be such that $\beta = \overline{\theta}$. Then, the optimality conditions with respect to the slip compliances simplify, and the 'relaxed variational' bounds for the effective flow stress arising from the *stress* formulation can be written as

$$\frac{\widetilde{\tau}_0}{\tau_0} = \frac{1-f}{\left[1+\frac{f}{2}\left(\sqrt{k_0}+\frac{1}{\sqrt{k_0}}\right)\right]^{\frac{1+m}{2}}} \left\{ \frac{\varrho(n)}{2^{(n+1)/2}} \int_0^{2\pi} \left| 1 + \frac{\sqrt{k_0} - (f/2)(1-k_0)}{\sqrt{k_0} + (f/2)(1+k_0)} \cos 2\theta \right|^{\frac{n+1}{2}} \mathrm{d}\theta \right\}^{-m}, \tag{7.44}$$

where k_0 is the solution to

$$\int_0^{\frac{\pi}{2}} \left| 1 + \frac{\sqrt{k_0} - (f/2)(1-k_0)}{\sqrt{k_0} + (f/2)(1+k_0)} \cos 2\theta \right|^{\frac{n-1}{2}} \left(\cos 2\theta - \frac{1-k_0}{1+k_0} \right) \mathrm{d}\theta = 0. \tag{7.45}$$

In the ideally plastic limit ($n \to \infty$), equation (7.45) yields $\sqrt{k_0} = (\sqrt{1+f^2} - 1)/f$, and expression (7.44) reduces to (7.38). Also, as already stated above, a dual (strain-rate) version of the bound (7.44) can be obtained in a completely analogous fashion. The resulting expression for the effective flow stress is

$$\begin{aligned} \frac{\widetilde{\tau}_0}{\tau_0} \;=\; & (1-f) \left[\frac{1 + \frac{f}{2}\sqrt{k_0}(1+k_0)}{(1+f\sqrt{k_0})^2} \right]^{\frac{1+m}{2}} \times \\ & \left\{ \frac{\varrho(m)}{2^{(m+1)/2}} \int_0^{2\pi} \left| 1 + \frac{1 + (f/2)\sqrt{k_0}(1-k_0)}{1 + (f/2)\sqrt{k_0}(1+k_0)} \cos 2\theta \right|^{\frac{m+1}{2}} \mathrm{d}\theta \right\}, \end{aligned} \tag{7.46}$$

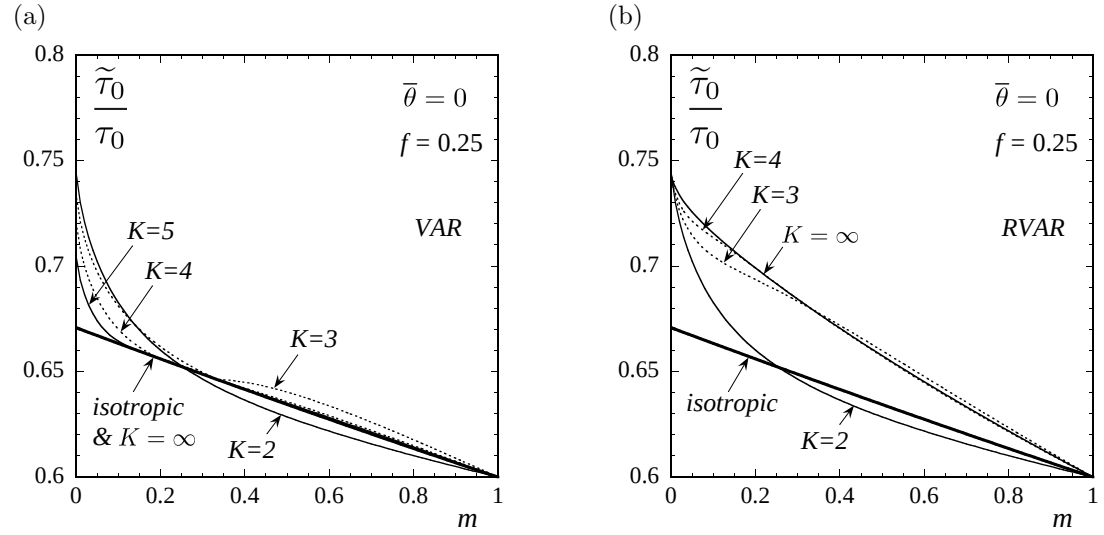

Figure 7.7: Effective flow stress $\widetilde{\tau}_0$, normalized by the flow stress of the matrix τ_0, of power-law, porous materials, as a function of the strain-rate sensitivity m, for several numbers of slip systems K, and a given porosity ($f = 0.25$). The macroscopic stress is directed along a slip system ($\overline{\theta} = 0$). Comparisons between the (a) 'variational' (VAR) and (b) 'relaxed variational' ($RVAR$) bounds with the 'variational' bound for isotropic phases.

where k_0 is the solution to

$$\int_0^{\frac{\pi}{2}} \left| 1 + \frac{1 + (f/2)\sqrt{k_0}(1 - k_0)}{1 + (f/2)\sqrt{k_0}(1 + k_0)} \cos 2\theta \right|^{\frac{m-1}{2}} \left(\cos 2\theta + \frac{1 - k_0}{1 + k_0} \right) \mathrm{d}\theta = 0. \tag{7.47}$$

In the ideally plastic limit ($m \to 0$), expression (7.46) simplifies to

$$\frac{\widetilde{\tau}_0}{\tau_0} = (1 - f) \frac{\sqrt{f/2}\, k_0^{3/4}}{1 + f\sqrt{k_0}} \, \mathrm{E}\left(- \frac{1 + (f/2)\sqrt{k_0}(1 - k_0)}{(f/2)k^{3/2}} \right), \tag{7.48}$$

where k_0 is the solution to (7.47) with $m = 0$, and E denotes the complete elliptic integral of the second kind.

7.3.4 Results and discussion

In figure 7.7, results are provided for porous, power-law materials with a matrix potential (7.39), loaded along a slip system ($\overline{\theta} = 0$), for several values of K (number of slip systems). Parts (a) & (b) show plots for the stress versions of the 'variational' (VAR) and 'relaxed variational' ($RVAR$) upper bounds, respectively, for the effective flow stress $\widetilde{\tau}_0$, normalized by the flow stress of the matrix phase τ_0, as a function of the strain-rate sensitivity m, for a moderate value of the porosity ($f = 0.25$). Also shown in this figure are the corresponding 'variational' upper bounds for an isotropic matrix, given by (7.43). The key observation in the context of this figure is that, while the VAR bounds tend to the 'isotropic' bounds as K tends to infinity, the $RVAR$ bounds tend to a *different* limit, given by (7.44), well above the 'isotropic' bounds, for all values of the strain-rate sensitivity different than 1. In the ideally plastic limit, the difference between the $RVAR$ and the 'isotropic' bounds is of the order of 10% for this particular value of the porosity. It is recalled that, unlike what is

found here, Ponte Castañeda & Suquet (1998) have shown that the 'relaxed variational' bounds do recover the bound of Ponte Castañeda (1991) when the constituents are isotropic. This apparent contradiction is simply a consequence of the (undesired) fact that, as mentioned in the previous chapter, the 'relaxed variational' bounds depend on an *arbitrary* convex/concave extension of the phase potentials (defined in certain subset of rank-one, fourth-order tensors) to the space of fully symmetric, fourth-order tensors. Thus, the 'extended' isotropic potential used in Ponte Castañeda & Suquet (1998) does *not* coincide with the 'crystalline' isotropic potential considered here for general fourth-order tensors, and consequently the corresponding 'relaxed variational' bounds are different.

Direct comparisons between the VAR and $RVAR$ bounds for $K = \infty$ are provided in figure 7.8, as a function of the strain-rate sensitivity m. Note that both, the stress (U) and strain-rate (W) versions of the $RVAR$ bounds have been included in this figure. The main observation is that, unlike the dual versions of the VAR bounds, the stress and strain-rate versions of the $RVAR$ bounds are *not* equivalent to each other, for all values of m different than 1 (see part (a)). In other words, the $RVAR$ bounds exhibit a *duality gap*, which is seen to increase with increasing nonlinearity. Furthermore, of the two versions of the $RVAR$ bounds, the $RVAR(W)$ bounds are found to be sharper than the $RVAR(U)$ bounds, lying roughly midway between the VAR and $RVAR(U)$ bounds in the ideally plastic limit. The reason for the duality gap in the $RVAR$ bounds, even though they are fully stationary with respect to the properties of the associated LCC, is that the functions $\overline{\psi}$ and $\overline{\phi}$ in the plane-wave decompositions of (7.41) and (7.42) are *not* Legendre duals of each other, except for $n = 1/m = 1$. Finally, part (b) provides plots for the optimal anisotropy ratios k_0 associated with the bounds shown in part (a). It can be seen that, as already mentioned, the optimal compliance tensor $\widehat{\mathbf{M}}_0^{(1)}$ associated with the VAR bounds is isotropic (i.e., $k_0 = 1$) for all values of m, whereas those associated with the $RVAR(U)$ and $RVAR(W)$ bounds are anisotropic for all values of m different than 1.

7.4 Concluding remarks

The 'variational' bounds proposed in the previous chapter for composites with anisotropic phases have been specialized for composites with crystalline phases, and computed for a model porous material with a power-law, crystalline matrix phase. It was found that the new 'variational' bounds improve, in general, on the earlier 'relaxed variational' bounds of deBotton & Ponte Castañeda (1995). The improvement was found to become more significant with increasing nonlinearity and with an increasing number of slip systems, being as much as 10% in some extreme cases. Although these findings were made in the context of a model system, they are expected to be representative of what would happen for more general material systems, including the very important case of polycrystalline aggregates. In this connection, it is recalled that the 'relaxed variational' bounds of the Hashin-Shtrikman type for viscoplastic FCC polycrystals, where the crystals have a large number of slip systems, become virtually indistinguishable from the Taylor bound, especially for large nonlinearities (deBotton &

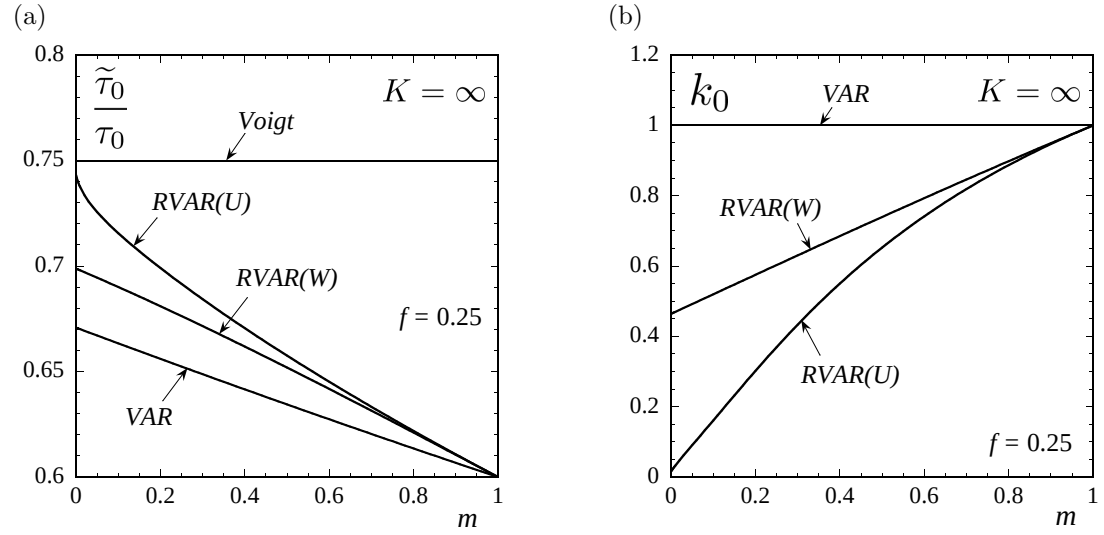

Figure 7.8: Effective flow stress $\widetilde{\tau}_0$, normalized by the flow stress of the matrix τ_0, and corresponding anisotropy ratio k_0, for isotropic, power-law, porous materials, as a function of the strain-rate sensitivity m, for a given porosity ($f = 0.25$). Comparisons between the 'variational' (VAR) and 'relaxed variational' ($RVAR$) bounds.

Ponte Castañeda 1995), in spite of incorporating additional microstructural information. The results provided in this work suggest that this fact could be due, in part, to the relaxation of the 'corrector' functions, and that the 'variational' bounds proposed in here should lead to improved bounds that are sharper than the Taylor bound for such polycrystals. This observation could also be relevant for the bounds of Dendievel *et al.* (1991), which make use of a similar relaxation to avoid non-convex optimizations in the context of the Talbot-Willis approach (see Willis 1994). While the computation of 'variational' bounds for general types of viscoplastic polycrystals might be a difficult task due to the non-convex optimizations involved, it should be relatively simple at least in the strongly nonlinear limit of rigid-ideally plastic behavior, which is actually the case where the observations mentioned above should be most relevant. Applications to such polycrystalline systems will be pursued in future work.

Chapter 8

Closure

In this work, new homogenization estimates have been proposed for the effective behavior and statistics of the local fields in viscoplastic composites. These estimates are based on rigorous variational methods (Ponte Castañeda 1991, 1996, 2002a), making use of the notion of 'linear comparison composite' (LCC), which allows direct conversion of successful linear estimates into corresponding estimates for nonlinear composites. The estimates for the field statistics follow from a novel procedure based on suitably perturbed effective potentials, which, unlike earlier approaches, is not restricted to first and second moments, but may also be used to estimate phase averages of more general convex functions of the local fields.

In the context of viscoplastic composites with *isotropic* constituents, it was found that, while the 'variational' estimates for the first and second moments of the local fields over a given phase agree with those in the associated LCC, as had been previously conjectured (Ponte Castañeda & Zaidman 1994), the 'tangent second-order' and 'second-order' estimates exhibit certain 'correction' terms, which arise due to the lack of full stationarity of the relevant functionals with respect to the properties of the LCC. These 'correction' terms are such that the estimates for the first moments are entirely consistent with the corresponding estimates for the macroscopic behavior. These estimates have been applied to two-phase, power-law composites with random, 'particulate' microstructures exhibiting overall transversely isotropic and isotropic symmetry, and their accuracy has been assessed by confronting them with corresponding exact results for sequential laminates. Based on these comparisons, the following conclusions have been drawn:

1. Among the nonlinear homogenization methods considered, the recent 'second-order' method gives, globally, the most accurate predictions for the effective behavior and field statistics in viscoplastic composites, especially for large nonlinearity and heterogeneity contrast.

2. For the case of reinforced composites, both (strain-rate and stress) versions of the 'second-order' (SO) and 'tangent second-order' (TSO) estimates for the effective behaviour, as well as for the field statistics, were found to be in fairly good agreement with the exact results for all values of the nonlinearity. All these estimates (SO and TSO) are able to capture the anisotropic character of the field fluctuations and the fact that certain components of the strain-rate fluctuations in

the matrix become unbounded in the strongly nonlinear ideally plastic limit. In contrast, the 'variational' estimates were found to significantly overestimate the effective behaviour, in agreement with their upper bound character, and to give qualitatively incorrect predictions for the field statistics, failing to capture the strong anisotropy of the strain-rate fluctuations at high nonlinearities.

3. For the cases of fiber-weakened and porous composites, which are more 'demanding' than those of reinforced composites, the SO estimates for the effective behaviour and first moments of the local fields were found to be in good agreement with the exact results even for strong nonlinearities. In general, the accuracy of the corresponding estimates for the second moments of the fields was found to be less good, which is not surprising in view of the fact that they correspond to more sensitive information. However, these estimates agree with the exact results in that, unlike in the case of reinforced composites, the second moments of the strain rate remain bounded in the ideally plastic limit, thus capturing the relative differences between the deformation patterns in the weaker- and stronger-particle cases. On the other hand, the TSO estimates were found to be fairly accurate for weak to moderate nonlinearities, but deteriorate significantly for strong nonlinearites. In turn, the 'variational' estimates were found to be relatively good for the effective behaviour, but qualitatively incorrect for the field statistics.

4. In general, it has been found that accurate estimates for the field statistics of order higher than one require highly accurate estimates for the effective potentials.

It should be emphasized that, unlike the 'variational' and 'tangent second-order' methods, the 'second-order' method has not been fully optimized yet, and part of this work was concerned with this issue. Thus, it was found that, although giving sensible estimates for most situations, the use of the phase averages as 'reference' tensors, like originally proposed in Ponte Castañeda (2002a), can lead to inconsistent results for sufficiently strong nonlinearities. An alternative prescription for these tensors was proposed, consisting in the use of the macroscopic averages, which not only leads to more accurate estimates, at least in the cases considered, but also has the advantage of simplicity. However, it is emphasized that the 'optimal' choice for these 'reference' tensors remains an open question, which requires further investigation.

In the context of viscoplastic composites with *anisotropic* constituents, a generalization of the 'variational' method of Ponte Castañeda (1991), originally developed for isotropic constituents, has been proposed. This generalization, which is more closely tied to the original formulation, has the capability of delivering improved bounds relative to the earlier generalizations provided by deBotton & Ponte Castañeda (1995) for polycrystalline materials, and by Suquet (Ponte Castañeda & Suquet 1998) for more general anisotropies. The bounds can be expressed in terms of a convex (concave) optimization problem, requiring the computation of certain 'corrector' functions that, in turn, depend on the solution of a non-concave/non-convex optimization problem. In general, the main difficulty

in computation of the bounds lies precisely in the solution of this non-convex optimization problem, which requires the use of appropriate numerical schemes, such as those based on genetic algorithms. In fact, the earlier generalizations avoid this complication by relaxing a constraint so that this non-concave/non-convex optimization becomes concave/convex. It is worth noting, however, that the non-concave/non-convex optimization simplifies dramatically in the strongly nonlinear case of ideal plasticity. The 'variational' bounds were studied and compared with the earlier bounds in the context of a model, two-dimensional porous composite with a viscoplastic, crystalline matrix phase. From these comparisons, the following conclusions have been drawn:

1. The new 'variational' bounds do improve on the earlier 'relaxed variational' bounds, the former becoming progressively sharper than the latter with increasing number of slip systems of the crystalline matrix phase. In the context of the model problem considered, the improvement on the effective flow stress was found to be as much as 10%.

2. Even larger differences were observed in the corresponding estimates for the statistics of the strain-rate field, which, in turn, could lead to significant differences in the predictions for the evolution of the microstructure.

3. Unlike the 'relaxed' bounds, the new bounds do not depend on arbitrary 'extensions' of the phase potentials, they reduce to the bounds of Ponte Castañeda (1991) in the case of isotropic phases, and they do not exhibit a duality gap.

While the computation of 'variational' bounds for general types of viscoplastic polycrystals might be a difficult task due to the non-convex optimizations involved, it should be relatively simple at least in the strongly nonlinear limit of rigid-ideally plastic behavior. Applications to FCC and HCP ideally plastic polycrystals will be pursued in future work, making use of the linear Hashin-Shtrikman bounds as well as the self-consistent estimates. It will also be interesting to apply these new bounds to porous polycrystals under general loadings, where the improvements over the earlier bounds might be even more significant, especially at large triaxialities.

To conclude, we would like to discuss possible directions for future work, in addition to those mentioned above, motivated by the present dissertation. First, it is noted that the procedure proposed in this work to compute field statistics opens up the possibility of incorporating to homogenization estimates the effects of a wide variety of local processes taking place in viscoplastic composites.

For instance, statistics of the strain-rate field, other than the phase averages, should be useful in developing improved descriptions for the evolution of the microstructure, including both, phase morphology and distribution. This is particularly important to accurately predict texture evolution in viscoplastic polycrystals undergoing finite deformations. However, even though such additional information on the strain-rate statistics may now be obtained, it is not clear yet what is the best way of incorporating it into the models, and further research along these lines is required. In addition, a rigorous derivation must be given for the statistics of the vorticity field (anti-symmetric part of the

velocity gradient), which are needed to incorporate the effect of finite rotations (see, for example, Kailasam & Ponte Castañeda 1998).

Castelnau *et al.* (2006) have recently shown that the effect of strain heterogeneity on the work hardening, resulting from the progressive increase of the resistance to dislocation motion by slip, can be important to accurately predict the effective behavior of viscoplastic polycrystals. These authors have noted that, even when the classical description of Mandel (1965) and Hill (1966) for the strain hardening is adopted in its simplest form, the first moment of the slip rate along a given slip system is not adequate to describe the heterogeneous evolution of the corresponding reference resolved shear stress, and averages of other functions of the slip rate, such as the absolute value, may be more appropriate. The procedure proposed in this work should allow direct computation of such averaged quantities from homogenization estimates, thus avoiding additional approximations as those introduced in that work.

It will also be interesting to consider the problem of incorporating higher order statistics of the stress field into stochastic models of damage nucleation and evolution. For instance, interface debonding in reinforced composites is sometimes represented by means of probability distributions for the volume fraction of debonded reinforcements, depending only on the first moments of the stress in a given phase (*e.g.*, González & LLorca 2000, Dvorak & Zhang 2001). It is reasonable to expect, however, that more accurate predictions should result from the use of appropriate measures of the second moments, which constitute better estimates for maximum stress values.

While in this work composite materials have been assumed to exhibit a purely viscous (nonlinear) behavior, a more accurate description of their mechanical behavior would require the incorporation of elastic effects. This can now be accomplished by means of the variational procedure recently proposed by Lahellec & Suquet (2003, 2006), which allows to extend any of the methodologies considered in this work to composites exhibiting an elasto-viscoplastic behavior. Encouraging results have been obtained by those authors for fiber-reinforced composites with an elasto-viscoplastic matrix, subjected to complex loading histories. The use of this procedure in the context of elasto-viscoplastic polycrystals subjected to non-monotonic loadings could help developing new micromechanics-based models for metal fatigue, which should be useful in estimating the life-time of metallic components and structures.

At the more theoretical end, it is noted that, while sequential laminates have lead to many important developments in the context of *linear* composites (see, for instance, Milton 2002), very little seems to have been done in the *nonlinear* context. In this work, infinite-rank sequential laminates have only been used as a reference against which approximate estimates could be compared. However, the formulae provided in Appendix E should be useful in exploring some theoretical aspects of two-phase nonlinear composites. Could these microstructures be 'optimal' as in the linear case? If not in general, at least to second order in the contrast, thus constituting second-order bounds? In addition, it will be interesting to obtain exact results for two-phase sequential laminates with phase potentials other than isotropic, power-law (*e.g.*, anisotropic potentials). The scarcity of exact results for hyperelastic

composites should make sequential laminates extremely attractive in that context as well.

Finally, it is emphasized that the applicability of the methodologies considered in this work is not restricted to the study of the mechanical properties of composites, and can be well extended to study other physical properties of nonlinear heterogeneous media, such as electrical, thermal and optical properties, as well as the coupling among them. Thus, these methodologies constitute a powerful tool for achieving an overall understanding of the mechanics and physics of solids.

Appendix A

Field fluctuations and macroscopic properties for nonlinear composites[1]

M. I. Idiart, P. Ponte Castañeda

Department of Mechanical Engineering and Applied Mechanics, University of Pennsylvania, Philadelphia, PA 19104-6315, U.S.A.

Abstract — A recently introduced nonlinear homogenization method (*Ponte Castañeda, P., 2002, J. Mech. Phys. Solids* **50**, 737–757) is used to estimate the effective behavior and the associated strain and stress fluctuations in a fibrous composite with power-law phases subjected to anti-plane strain or in-plane strain loading. Using the Hashin-Shtrikman estimates for the relevant "linear comparison composite," results are generated for two-phase systems, including fiber-reinforced and fiber-weakened composites. These results, which are known to be exact to second-order in the heterogeneity contrast, are found to satisfy all known bounds. Explicit analytical expressions are obtained for the special case of rigid-ideally plastic composites, including results for arbitrary contrast and fiber concentration. The effective properties, as well as the phase averages and fluctuations predicted for these strongly nonlinear composites appear to be consistent with deformation mechanisms involving shear bands. More specifically, in the case where the fibers are stronger than the matrix, the bands tend to avoid the fibers, and in the opposite case they become attracted to the fibers.

A.1 Introduction

This paper is concerned with the application of the recently developed "second-order" homogenization method of Ponte Castañeda (2002a) to two-phase power-law composites with arbitrary heterogeneity contrast. One of the interesting aspects of this new method is that, unlike the previous version (Ponte

[1]This chapter appeared in *Int. J. Sol. Struct.* **40** (2003) 7015–7033.

Castañeda 1996), it incorporates information about the fluctuations of the relevant fields, providing nonlinear estimates that are exact to second order in the heterogeneity contrast and that do not violate rigorous bounds.

For completeness and later reference, it is recalled here that bounds of the Hashin-Shtrikman type for nonlinear composites were first given by Talbot and Willis (1985), using a generalization of the variational principles of Hashin and Shtrikman (1962) for nonlinear media. More general types of bounds, including three-point bounds, were obtained by Ponte Castañeda (1991) by means of new variational principles (Ponte Castañeda 1992a) involving "linear comparison composites." Equivalent bounds for the special class of power-law composites were generated by Suquet (1993) using linear comparison composites and Hölder-type inequalities. For more comprehensive reviews of the nonlinear homogenization literature, the reader is referred to Ponte Castañeda and Suquet (1998) and Willis (2000). Field fluctuations in composites with linear elastic properties have been studied by Kreher and Pompe (1985) and Bobeth and Diener (1987), among others. Corresponding studies have apparently not yet been carried out for nonlinear composites in the mechanical context, although a start along this direction was given in Ponte Castañeda (2002a,2002b). There are also some recent results for weakly nonlinear composites (Pellegrini, 2000), as well as some theoretical results for strongly nonlinear composites (Pellegrini, 2001, Ponte Castañeda, 2001) in the context of conductivity.

A.2 Effective behavior

The assumption is made here that the material is composed of N different phases, which are *randomly* distributed in a specimen occupying a volume Ω, at a length scale that is much smaller than the size of the specimen and scale of variation of the loading conditions. The constitutive behavior of the nonlinear phases is characterized by *convex strain potentials* $w^{(r)}$ $(r = 1, ..., N)$, such that the local stress-strain relation is determined by:

$$\boldsymbol{\sigma} = \frac{\partial w^{(r)}}{\partial \boldsymbol{\varepsilon}}(\boldsymbol{\varepsilon}), \quad w(\mathbf{x}, \boldsymbol{\varepsilon}) = \sum_{r=1}^{N} \chi^{(r)}(\mathbf{x})\ w^{(r)}(\boldsymbol{\varepsilon}), \tag{A.1}$$

where the characteristic functions $\chi^{(r)}$ are 1 if the position vector $\mathbf{x}$ is in phase r and 0 otherwise. The effective behavior of the composite is characterized by the *effective strain potential*. Using the minimum potential energy principle it can be written as:

$$\widetilde{W}(\overline{\boldsymbol{\varepsilon}}) = \min_{\boldsymbol{\varepsilon} \in \mathcal{K}(\overline{\boldsymbol{\varepsilon}})} \langle w(\mathbf{x}, \boldsymbol{\varepsilon}) \rangle = \min_{\boldsymbol{\varepsilon} \in \mathcal{K}(\overline{\boldsymbol{\varepsilon}})} \sum_{r=1}^{N} c^{(r)}\ \langle w^{(r)}(\boldsymbol{\varepsilon}) \rangle^{(r)}, \tag{A.2}$$

where angular brackets $\langle . \rangle$ and $\langle . \rangle^r$ are used to denote volume averages over the composite (Ω) and over the phase r, respectively, $c^{(r)}$ are the volume fractions of the phases, and $\mathcal{K}(\overline{\boldsymbol{\varepsilon}})$ denotes the set of kinematically admissible strain fields, given by:

$$\mathcal{K}(\overline{\boldsymbol{\varepsilon}}) = \{\boldsymbol{\varepsilon} \mid \text{there is } \mathbf{u} \text{ with } \boldsymbol{\varepsilon} = \frac{1}{2}\left[\nabla\mathbf{u} + (\nabla\mathbf{u})^T\right] \text{ in } \Omega,\ \mathbf{u} = \overline{\boldsymbol{\varepsilon}}\mathbf{x} \text{ on } \partial\Omega\}, \tag{A.3}$$

where $\mathbf{u}$ is the displacement field and $\overline{\boldsymbol{\varepsilon}}$ is a constant second order tensor. Note that, in this case, $\mathbf{u}$ is such that the average strain is simply $\langle\boldsymbol{\varepsilon}\rangle = \overline{\boldsymbol{\varepsilon}}$.

Alternatively, the behavior of the phases can be characterized by *stress potentials*, $u^{(r)}$, which are dual to the $w^{(r)}$, such that the local strain-stress relation is determined by:

$$\boldsymbol{\varepsilon} = \frac{\partial u^{(r)}}{\partial \boldsymbol{\sigma}}(\boldsymbol{\sigma}), \quad u(\mathbf{x}, \boldsymbol{\sigma}) = \sum_{r=1}^{N} \chi^{(r)}(\mathbf{x})\ u^{(r)}(\boldsymbol{\sigma}). \tag{A.4}$$

According to the minimum complementary energy principle, the *effective stress potential*, $\tilde{U}$, can be written as:

$$\widetilde{U}(\overline{\boldsymbol{\sigma}}) = \min_{\boldsymbol{\sigma}\in\mathcal{S}(\overline{\boldsymbol{\sigma}})} \langle u(\mathbf{x}, \boldsymbol{\sigma})\rangle = \min_{\boldsymbol{\sigma}\in\mathcal{S}(\overline{\boldsymbol{\sigma}})} \sum_{r=1}^{N} c^{(r)}\ \langle u^{(r)}(\boldsymbol{\sigma})\rangle^{(r)}, \tag{A.5}$$

where $\mathcal{S}(\overline{\boldsymbol{\sigma}})$ is the set of self-equilibrated stresses that are consistent with the average stress condition $\langle\boldsymbol{\sigma}\rangle = \overline{\boldsymbol{\sigma}}$.

It can be shown (see, for example, Ponte Castañeda and Suquet, 1998) that the average stress in the composite, $\overline{\boldsymbol{\sigma}}$, is related to the average strain, $\overline{\boldsymbol{\varepsilon}}$, through the relations:

$$\overline{\boldsymbol{\sigma}} = \frac{\partial\widetilde{W}}{\partial\overline{\boldsymbol{\varepsilon}}}(\overline{\boldsymbol{\varepsilon}}) \quad \text{and} \quad \overline{\boldsymbol{\varepsilon}} = \frac{\partial\widetilde{U}}{\partial\overline{\boldsymbol{\sigma}}}(\overline{\boldsymbol{\sigma}}), \tag{A.6}$$

which provide the macroscopic constitutive relation for the composite. Thus, if we know the effective energy functions, we can obtain the stress-strain relation for the nonlinear composite. Note that these functions are very difficult to compute, in general, since they correspond to the solution of a set of nonlinear partial differential equations with randomly oscillating coefficients. In the next section the new variational principles are used to generate estimates for $\widetilde{W}$ and $\widetilde{U}$.

A.3 Second-order homogenization estimates

In this section an outline of the second-order homogenization method of Ponte Castañeda (2002a) is given. The idea is to construct a *linear comparison composite* whose effective potential can be used to estimate the effective potential of the *nonlinear composite*. The homogenization is thus carried out for a *linear* heterogeneous medium, for which many accurate estimates are already available (see, for example, Milton, 2002, Torquato, 2001). Let the comparison composite have a strain potential of the form:

$$w_T(\mathbf{x}, \boldsymbol{\varepsilon}) = \sum_{r=1}^{N} \chi^{(r)}(\mathbf{x})\ w_T^{(r)}(\boldsymbol{\varepsilon}), \tag{A.7}$$

where the $\chi^{(r)}$ are the same characteristic functions as the nonlinear composite's (i.e. both composites have the same microstructure), and the phase potentials $w_T^{(r)}$ are second-order Taylor-type expressions:

$$w_T^{(r)}(\boldsymbol{\varepsilon}) = w^{(r)}(\boldsymbol{\varepsilon}^{(r)}) + \frac{\partial w^{(r)}}{\partial \boldsymbol{\varepsilon}}(\boldsymbol{\varepsilon}^{(r)}) \cdot (\boldsymbol{\varepsilon} - \boldsymbol{\varepsilon}^{(r)}) + \frac{1}{2}(\boldsymbol{\varepsilon} - \boldsymbol{\varepsilon}^{(r)}) \cdot \mathbf{L}_0^{(r)}(\boldsymbol{\varepsilon} - \boldsymbol{\varepsilon}^{(r)}). \tag{A.8}$$

In these last expressions, $\boldsymbol{\varepsilon}^{(r)}$ is a uniform reference strain, $\mathbf{L}_0^{(r)}$ is a symmetric, constant fourth-order tensor, and $w^{(r)}$ is the nonlinear potential of phase r. Differentiating this potential gives a stress-strain relation:

$$\boldsymbol{\sigma} = \frac{\partial w^{(r)}}{\partial \boldsymbol{\varepsilon}}(\boldsymbol{\varepsilon}^{(r)}) + \mathbf{L}_0^{(r)}(\boldsymbol{\varepsilon} - \boldsymbol{\varepsilon}^{(r)}) = \boldsymbol{\tau}^{(r)} + \mathbf{L}_0^{(r)}\boldsymbol{\varepsilon}, \tag{A.9}$$

where the stress polarization tensors $\boldsymbol{\tau}^{(r)} = \partial w^{(r)}/\partial \boldsymbol{\varepsilon}(\boldsymbol{\varepsilon}^{(r)}) - \mathbf{L}_0^{(r)}\boldsymbol{\varepsilon}^{(r)}$ are mathematically equivalent to thermal stress tensors, since they are independent of the strain. Also note that $\mathbf{L}_0^{(r)}$ corresponds to the modulus tensor of the linear phase. The effective potential associated with the linear comparison composite with local potential given by (A.7) and (A.8) can be written as (Laws 1973, Willis 1981):

$$\widetilde{W}_T(\overline{\boldsymbol{\varepsilon}}) = \min_{\boldsymbol{\varepsilon} \in \mathcal{K}(\overline{\boldsymbol{\varepsilon}})} \langle w_T(\mathbf{x}, \boldsymbol{\varepsilon}) \rangle = \tilde{f} + \widetilde{\boldsymbol{\tau}} \cdot \overline{\boldsymbol{\varepsilon}} + \frac{1}{2}\overline{\boldsymbol{\varepsilon}} \cdot \widetilde{\mathbf{L}}_0 \overline{\boldsymbol{\varepsilon}}, \tag{A.10}$$

where $\tilde{f}$, $\widetilde{\boldsymbol{\tau}}$ and $\widetilde{\mathbf{L}}_0$ are the relevant effective energy at zero applied strain, the effective polarization, and effective modulus tensor, respectively.

The idea of the second-order procedure is to choose, within certain simplifying assumptions, the reference strains and modulus tensors of the above-defined linear comparison composite, in such a way as to generate the best possible estimates for the nonlinear potential $\widetilde{W}$ through known estimates for the linear potential $\widetilde{W}_T$. This optimization procedure, which involves some approximations, is not repeated here for brevity (see Ponte Castañeda, 2002a for details). In any event, the optimal values of the variables $\boldsymbol{\varepsilon}^{(r)}$ and $\mathbf{L}_0^{(r)}$ are given by:

$$\boldsymbol{\varepsilon}^{(r)} = \overline{\boldsymbol{\varepsilon}}^{(r)}, \quad \text{and} \quad \frac{\partial w^{(r)}}{\partial \boldsymbol{\varepsilon}}(\hat{\boldsymbol{\varepsilon}}^{(r)}) - \frac{\partial w^{(r)}}{\partial \boldsymbol{\varepsilon}}(\overline{\boldsymbol{\varepsilon}}^{(r)}) = \mathbf{L}_0^{(r)}(\hat{\boldsymbol{\varepsilon}}^{(r)} - \overline{\boldsymbol{\varepsilon}}^{(r)}), \tag{A.11}$$

where the $\hat{\boldsymbol{\varepsilon}}^{(r)}$ are constant second-order tensors, arising from the introduction of suitable error measures (Ponte Castañeda 2002a), that depend on the second moments of the fluctuations of the strain through appropriate *traces* of the relations:

$$(\hat{\boldsymbol{\varepsilon}}^{(r)} - \overline{\boldsymbol{\varepsilon}}^{(r)}) \otimes (\hat{\boldsymbol{\varepsilon}}^{(r)} - \overline{\boldsymbol{\varepsilon}}^{(r)}) = \langle (\boldsymbol{\varepsilon} - \overline{\boldsymbol{\varepsilon}}^{(r)}) \otimes (\boldsymbol{\varepsilon} - \overline{\boldsymbol{\varepsilon}}^{(r)}) \rangle^{(r)} \doteq \mathbf{C}_{\boldsymbol{\varepsilon}}^{(r)}, \tag{A.12}$$

where $\mathbf{C}_{\boldsymbol{\varepsilon}}^{(r)}$ serves to denote the covariance tensor of the strain field in phase r of the linear comparison composite. It should be emphasized that, in general, the equality cannot be enforced for all components of the tensorial relation (A.12), and that is why only certain traces of this relation are used.

Thus, the reference strains $\boldsymbol{\varepsilon}^{(r)}$ are identified with the phase averages of the strain, and the modulus tensors $\mathbf{L}_0^{(r)}$ follow from the so-called "generalized secant condition" (A.11b). Fig. A.1

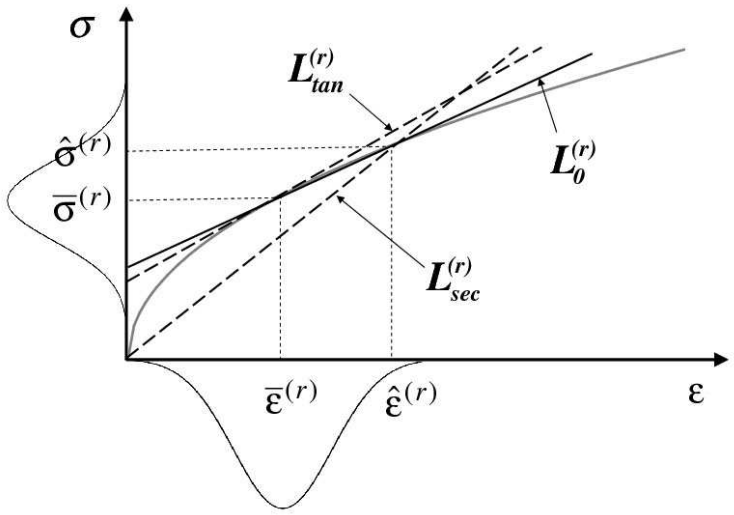

Figure A.1: One-dimensional sketch of the nonlinear stress-strain relation and different types of linearizations: $\mathbf{L}_0^{(r)}$, $\mathbf{L}_{sec}^{(r)}$ and $\mathbf{L}_{tan}^{(r)}$ refer to the new "generalized secant", secant, and tangent modulus, respectively.

shows a one-dimensional graphical representation of this condition. Note that, if the strain field in a phase is quite homogeneous, i.e. the fluctuations are small, the modulus tensor of the corresponding linearized phase in the comparison composite will be close to the tangent modulus tensor. But if the field has a heterogeneous distribution, the new method will result in a less stiff modulus tensor.

The average strains and the strain covariance tensors of the actual strain field may be computed "self-consistently" from the linear comparison composite using the following identities (Ponte Castañeda and Suquet, 1998):

$$\overline{\boldsymbol{\varepsilon}}^{(r)} = \frac{1}{c^{(r)}} \frac{\partial(\widetilde{W}_T - \bar{f})}{\partial \boldsymbol{\tau}^{(r)}}, \quad \text{and} \quad \mathbf{C}_{\boldsymbol{\varepsilon}}^{(r)} = \frac{2}{c^{(r)}} \frac{\partial \widetilde{W}_T}{\partial \mathbf{L}_0^{(r)}}. \tag{A.13}$$

In the first relation, $\bar{f} = \sum_{r=1}^{N} c^{(r)}\ f^{(r)}$, $f^{(r)} = w^{(r)}(\overline{\boldsymbol{\varepsilon}}^{(r)}) - \boldsymbol{\tau}^{(r)} \cdot \overline{\boldsymbol{\varepsilon}}^{(r)} - \frac{1}{2}\overline{\boldsymbol{\varepsilon}}^{(r)} \cdot \mathbf{L}_0^{(r)} \overline{\boldsymbol{\varepsilon}}^{(r)}$ and the $\mathbf{L}_0^{(r)}$ are held fixed, while in the second, the $\overline{\boldsymbol{\varepsilon}}^{(r)}$ are held fixed.

Finally, the effective potential of the nonlinear composite (A.2) may be re-expressed only in terms of the variables $\overline{\boldsymbol{\varepsilon}}^{(r)}$ and $\hat{\boldsymbol{\varepsilon}}^{(r)}$ via the relation (Ponte Castañeda, 2002a):

$$\widetilde{W}(\overline{\boldsymbol{\varepsilon}}) = \sum_{r=1}^{N} c^{(r)} \left[w^{(r)}(\hat{\boldsymbol{\varepsilon}}^{(r)}) - \frac{\partial w^{(r)}}{\partial \boldsymbol{\varepsilon}}(\overline{\boldsymbol{\varepsilon}}^{(r)}) \cdot (\hat{\boldsymbol{\varepsilon}}^{(r)} - \overline{\boldsymbol{\varepsilon}}^{(r)}) \right]. \tag{A.14}$$

Knowing the effective potential $\widetilde{W}_T$ of the linear comparison composite as a function of the phase moduli $\mathbf{L}_0^{(r)}$, and the polarizations $\boldsymbol{\tau}^{(r)}$, the variables $\overline{\boldsymbol{\varepsilon}}^{(r)}$ and $\hat{\boldsymbol{\varepsilon}}^{(r)}$ can then be computed using (A.13), and an estimate for the nonlinear potential may be obtained via (A.14). Several methods are available to estimate and bound the effective potential of a linear composite, such as the Hashin-Shtrikman and self-consistent methods. If the method used is exact to second order in the heterogeneity contrast, it

can be shown that the estimate (A.14) is also exact to second order, and therefore in agreement with the small-contrast expansion of Suquet and Ponte Castañeda (1993).

Next, consider the case of isotropic, incompressible phases with $w^{(r)}(\boldsymbol{\varepsilon}) = \phi^{(r)}(\varepsilon_e)$, where $\boldsymbol{\varepsilon}$ is assumed to be traceless, and ε_e is the von Mises equivalent strain, defined in terms of the strain deviatoric tensor $\boldsymbol{\varepsilon}_d$ by $\varepsilon_e = \sqrt{(2/3)\boldsymbol{\varepsilon}_d \cdot \boldsymbol{\varepsilon}_d}$. For this broad class of potentials, Ponte Castañeda (2002b) proposed, as an approximation, (incompressible) tensors $\mathbf{L}_0^{(r)}$ with principal axes aligned with the average strain, such that:

$$\mathbf{L}_0^{(r)} = 2\lambda_0^{(r)}\mathbf{E}^{(r)} + 2\mu_0^{(r)}\mathbf{F}^{(r)}. \tag{A.15}$$

Here, $\mathbf{E}^{(r)}$ and $\mathbf{F}^{(r)}$ are fourth-order projection tensors (Ponte Castañeda, 1996) defined by $\mathbf{E}^{(r)} = (2/3)\breve{\boldsymbol{\varepsilon}}_d^{(r)} \otimes \breve{\boldsymbol{\varepsilon}}_d^{(r)}$, $\mathbf{E}^{(r)} + \mathbf{F}^{(r)} = \mathbf{K}$, with $\breve{\boldsymbol{\varepsilon}}^{(r)} = \overline{\boldsymbol{\varepsilon}}^{(r)}/\overline{\varepsilon}_e^{(r)}$, such that $\mathbf{E}^{(r)}\mathbf{E}^{(r)} = \mathbf{E}^{(r)}, \mathbf{F}^{(r)}\mathbf{F}^{(r)} = \mathbf{F}^{(r)}, \mathbf{E}^{(r)}\mathbf{F}^{(r)} = \mathbf{F}^{(r)}\mathbf{E}^{(r)} = \mathbf{0}$. Also, $\mathbf{K}$ is the standard fourth order isotropic shear projection tensor. Note that although the nonlinear phases are isotropic, the phases of the linear comparison composite are anisotropic. With this choice of $\mathbf{L}_0^{(r)}$, it follows from (A.11b) that the traceless tensors $\hat{\boldsymbol{\varepsilon}}^{(r)}$ have components "parallel" and "perpendicular" to the average fields, which, from (A.12), are given by:

$$\hat{\varepsilon}_{\parallel}^{(r)} = \overline{\varepsilon}_e{}^{(r)} + \sqrt{\frac{2}{3}\mathbf{E}^{(r)} \cdot \mathbf{C}_{\boldsymbol{\varepsilon}}^{(r)}}, \quad \hat{\varepsilon}_{\perp}^{(r)} = \sqrt{\frac{2}{3}\mathbf{F}^{(r)} \cdot \mathbf{C}_{\boldsymbol{\varepsilon}}^{(r)}}, \tag{A.16}$$

where $\hat{\varepsilon}_{\parallel}^{(r)} = \left(\frac{2}{3}\hat{\boldsymbol{\varepsilon}}^{(r)} \cdot \mathbf{E}^{(r)}\hat{\boldsymbol{\varepsilon}}^{(r)}\right)^{\frac{1}{2}}$ and $\hat{\varepsilon}_{\perp}^{(r)} = \left(\frac{2}{3}\hat{\boldsymbol{\varepsilon}}^{(r)} \cdot \mathbf{F}^{(r)}\hat{\boldsymbol{\varepsilon}}^{(r)}\right)^{\frac{1}{2}}$, so that $(\hat{\varepsilon}_e^{(r)})^2 = (\hat{\varepsilon}_{\parallel}^{(r)})^2 + (\hat{\varepsilon}_{\perp}^{(r)})^2$. The "generalized secant" conditions (A.11b) reduce to:

$$3\lambda_0^{(r)}\left(\hat{\varepsilon}_{\parallel}^{(r)} - \overline{\varepsilon}_e^{(r)}\right) = {\phi^{(r)}}'(\hat{\varepsilon}_e^{(r)})\,\frac{\hat{\varepsilon}_{\parallel}^{(r)}}{\hat{\varepsilon}_e^{(r)}} - {\phi^{(r)}}'\left(\overline{\varepsilon}_e^{(r)}\right), \quad 3\mu_0^{(r)} = \frac{{\phi^{(r)}}'(\hat{\varepsilon}_e^{(r)})}{\hat{\varepsilon}_e^{(r)}}. \tag{A.17}$$

Finally, expression (A.14) for $\widetilde{W}$ simplifies to:

$$\widetilde{W}(\overline{\boldsymbol{\varepsilon}}) = \sum_{r=1}^{N} c^{(r)}\left[\phi^{(r)}(\hat{\varepsilon}_e^{(r)}) - {\phi^{(r)}}'\left(\overline{\varepsilon}_e^{(r)}\right)\left(\hat{\varepsilon}_{\parallel}^{(r)} - \overline{\varepsilon}_e^{(r)}\right)\right]. \tag{A.18}$$

Proceeding in a completely analogous fashion, estimates for $\widetilde{U}$ can be obtained using the stress potentials $u^{(r)}$ and their corresponding second-order Taylor-type expressions $u_T^{(r)}$:

$$\widetilde{U}(\overline{\boldsymbol{\sigma}}) = \sum_{r=1}^{N} c^{(r)}\left[u^{(r)}(\hat{\boldsymbol{\sigma}}^{(r)}) - \frac{\partial u^{(r)}}{\partial \boldsymbol{\sigma}}(\overline{\boldsymbol{\sigma}}^{(r)}) \cdot (\hat{\boldsymbol{\sigma}}^{(r)} - \overline{\boldsymbol{\sigma}}^{(r)})\right], \tag{A.19}$$

where the uniform reference stresses $\boldsymbol{\sigma}^{(r)}$ have been identified with the average stresses in each phase $\overline{\boldsymbol{\sigma}}^{(r)}$, and $\hat{\boldsymbol{\sigma}}^{(r)}$ are constant tensors that depend on the stress fluctuations through appropriate *traces* of the relations:

$$(\hat{\boldsymbol{\sigma}}^{(r)} - \overline{\boldsymbol{\sigma}}^{(r)}) \otimes (\hat{\boldsymbol{\sigma}}^{(r)} - \overline{\boldsymbol{\sigma}}^{(r)}) = \langle(\boldsymbol{\sigma} - \overline{\boldsymbol{\sigma}}^{(r)}) \otimes (\boldsymbol{\sigma} - \overline{\boldsymbol{\sigma}}^{(r)})\rangle^{(r)} \doteq \mathbf{C}_{\boldsymbol{\sigma}}^{(r)}, \tag{A.20}$$

where $\mathbf{C}_{\boldsymbol{\sigma}}^{(r)}$ is the covariance tensor of the stress field in phase r. The phases of the linear thermoelastic comparison composite have strain polarizations $\boldsymbol{\eta}^{(r)} = \partial u^{(r)}/\partial\boldsymbol{\sigma}(\overline{\boldsymbol{\sigma}}^{(r)}) - \mathbf{M}_0^{(r)}\overline{\boldsymbol{\sigma}}^{(r)}$, and compliances $\mathbf{M}_0^{(r)}$ given by the secant-type condition:

$$\frac{\partial u^{(r)}}{\partial \boldsymbol{\sigma}}(\hat{\boldsymbol{\sigma}}^{(r)}) - \frac{\partial u^{(r)}}{\partial \boldsymbol{\sigma}}(\overline{\boldsymbol{\sigma}}^{(r)}) = \mathbf{M}_0^{(r)}(\hat{\boldsymbol{\sigma}}^{(r)} - \overline{\boldsymbol{\sigma}}^{(r)}). \tag{A.21}$$

Again, consider the case of isotropic, incompressible phases with $u^{(r)}(\boldsymbol{\sigma}) = \psi^{(r)}(\sigma_e)$, where σ_e is the von Mises equivalent stress, defined in terms of the stress deviatoric tensor $\boldsymbol{\sigma}_d$ by $\sigma_e = \sqrt{(2/3)\boldsymbol{\sigma}_d \cdot \boldsymbol{\sigma}_d}$. As in the strain formulation, for this class of potentials, we restrict attention to (incompressible) compliance tensors whose principal axes are aligned with the average stress:

$$\mathbf{M}_0^{(r)} = \frac{1}{2\lambda_0^{(r)}}\mathbf{E}^{(r)} + \frac{1}{2\mu_0^{(r)}}\mathbf{F}^{(r)}, \tag{A.22}$$

where $\mathbf{E}^{(r)} = (3/2)\check{\boldsymbol{\sigma}}_d^{(r)} \otimes \check{\boldsymbol{\sigma}}_d^{(r)}$, $\mathbf{E}^{(r)} + \mathbf{F}^{(r)} = \mathbf{K}$, with $\check{\boldsymbol{\sigma}}^{(r)} = \overline{\boldsymbol{\sigma}}^{(r)}/\overline{\sigma}_e^{(r)}$, are the appropriate projection tensors in this case. From (A.20) and (A.21) it follows that:

$$\hat{\sigma}_{\parallel}^{(r)} = \overline{\sigma}_e{}^{(r)} + \sqrt{\frac{3}{2}\mathbf{E}^{(r)} \cdot \mathbf{C}_{\boldsymbol{\sigma}}^{(r)}}, \quad \hat{\sigma}_{\perp}^{(r)} = \sqrt{\frac{3}{2}\mathbf{F}^{(r)} \cdot \mathbf{C}_{\boldsymbol{\sigma}}^{(r)}}, \tag{A.23}$$

where $\hat{\sigma}_{\parallel}^{(r)} = \left(\frac{3}{2}\hat{\boldsymbol{\sigma}}^{(r)} \cdot \mathbf{E}^{(r)}\hat{\boldsymbol{\sigma}}^{(r)}\right)^{\frac{1}{2}}$ and $\hat{\sigma}_{\perp}^{(r)} = \left(\frac{3}{2}\hat{\boldsymbol{\sigma}}^{(r)} \cdot \mathbf{F}^{(r)}\hat{\boldsymbol{\sigma}}^{(r)}\right)^{\frac{1}{2}}$, are the "parallel" and "perpendicular" components of the traceless tensors $\hat{\boldsymbol{\sigma}}^{(r)}$, respectively. The "generalized secant conditions" (A.21) reduce to:

$$\frac{1}{3\lambda_0^{(r)}}\left(\hat{\sigma}_{\parallel}^{(r)} - \overline{\sigma}_e^{(r)}\right) = \psi^{(r)\prime}(\hat{\sigma}_e^{(r)})\frac{\hat{\sigma}_{\parallel}^{(r)}}{\hat{\sigma}_e^{(r)}} - \psi^{(r)\prime}\left(\overline{\sigma}_e^{(r)}\right), \quad \frac{1}{3\mu_0^{(r)}} = \frac{\psi^{(r)\prime}(\hat{\sigma}_e^{(r)})}{\hat{\sigma}_e^{(r)}}. \tag{A.24}$$

Finally, expression (A.19) can be written as:

$$\widetilde{U}(\overline{\boldsymbol{\sigma}}) = \sum_{r=1}^{N} c^{(r)}\left[\psi^{(r)}(\hat{\sigma_e}^{(r)}) - \psi^{(r)\prime}\left(\overline{\sigma}_e^{(r)}\right)\left(\hat{\sigma}_{\parallel}^{(r)} - \overline{\sigma}_e^{(r)}\right)\right]. \tag{A.25}$$

Relations (A.14) and (A.19) provide two different ways to estimate the effective behavior of the nonlinear composites. However, it is important to emphasize that, because of the approximations introduced in the optimization procedure, these estimates are not exactly equivalent (see Ponte Castañeda, 2002a), and a small *duality gap* is expected, in general.

A *third* way to approximate the constitutive behavior of the nonlinear composite is to use, directly, the constitutive relations of the associated linear comparison composite, as given by (Laws, 1973):

$$\overline{\boldsymbol{\sigma}} = \tilde{\boldsymbol{\tau}} + \widetilde{\mathbf{L}}_0\overline{\boldsymbol{\varepsilon}}, \quad \overline{\boldsymbol{\varepsilon}} = \tilde{\boldsymbol{\eta}} + \widetilde{\mathbf{M}}_0\overline{\boldsymbol{\sigma}}. \tag{A.26}$$

Making use of well-known expressions for the modulus and compliance tensors $\widetilde{\mathbf{L}}_0$ and $\widetilde{\mathbf{M}}_0$, and the stress and strain polarizations $\tilde{\boldsymbol{\tau}}$ and $\tilde{\boldsymbol{\eta}}$, together with the expressions for the phase polarizations $\boldsymbol{\tau}^{(r)}$ and $\boldsymbol{\eta}^{(r)}$ in terms of the phase averages $\overline{\boldsymbol{\varepsilon}}^{(r)}$ and $\overline{\boldsymbol{\sigma}}^{(r)}$, and modulus tensors $\mathbf{L}_0^{(r)}$ and $\mathbf{M}_0^{(r)}$, these expressions may be re-written more explicitly as (Ponte Castañeda, 2002a):

$$\overline{\boldsymbol{\sigma}} = \sum_{r=1}^{N} c^{(r)}\frac{\partial w^{(r)}}{\partial \boldsymbol{\varepsilon}}(\overline{\boldsymbol{\varepsilon}}^{(r)}), \quad \text{and} \quad \overline{\boldsymbol{\varepsilon}} = \sum_{r=1}^{N} c^{(r)}\frac{\partial u^{(r)}}{\partial \boldsymbol{\sigma}}(\overline{\boldsymbol{\sigma}}^{(r)}). \tag{A.27}$$

These two stress-strain relations for the nonlinear composite are exactly equivalent to each other, because there is *no* duality gap for the linear comparison composite. However, again for reasons related to the approximations mentioned above, they can be shown to be *different* from the corresponding relations for the nonlinear composite generated by direct derivation (A.6) of the second-order estimates (A.14) and (A.19). They can be thought of as improved versions of the "affine" estimates of Masson et al. (2000), in the same sense as the second-order estimates of Ponte Castañeda (2002a) are improved versions of the earlier second-order estimates of Ponte Castañeda (1996). Unfortunately, these new "affine" estimates are not exact to second-order in the contrast, and are expected to be less accurate than the corresponding estimates (A.14) and (A.19).

Finally, since the linear phase potentials $w_T^{(r)}$ and $u_T^{(r)}$ are dual to each other, it is worth noting that the following duality relations hold between the strain/moduli variables in (A.14) and stress/compliance variables in (A.19):

$$\begin{aligned}
\overline{\boldsymbol{\sigma}}^{(r)} &= \frac{\partial w^{(r)}}{\partial \boldsymbol{\varepsilon}}(\overline{\boldsymbol{\varepsilon}}^{(r)}), \quad \overline{\boldsymbol{\varepsilon}}^{(r)} = \tfrac{\partial u^{(r)}}{\partial \boldsymbol{\sigma}}(\overline{\boldsymbol{\sigma}}^{(r)}),\\
\hat{\boldsymbol{\sigma}}^{(r)} &= \frac{\partial w^{(r)}}{\partial \boldsymbol{\varepsilon}}(\hat{\boldsymbol{\varepsilon}}^{(r)}), \quad \hat{\boldsymbol{\varepsilon}}^{(r)} = \tfrac{\partial u^{(r)}}{\partial \boldsymbol{\sigma}}(\hat{\boldsymbol{\sigma}}^{(r)}),\\
\mathbf{M}_0^{(r)} &= \left(\mathbf{L}_0^{(r)}\right)^{-1},
\end{aligned} \tag{A.28}$$

provided $\overline{\boldsymbol{\varepsilon}}$ and $\overline{\boldsymbol{\sigma}}$ are taken to be related by expression (A.26), or equivalently, by expression (A.27).

A.4 Two-phase, power-law fibrous composites under anti-plane or in-plane loading

In this section we consider fibrous composites with incompressible power-law phases subject to anti-plane or in-plane loading. The phase strain and stress potentials are given by:

$$w^{(r)}(\boldsymbol{\varepsilon}) = \frac{\varepsilon_0 \sigma_0^{(r)}}{1+m}\left(\frac{\varepsilon_e}{\varepsilon_0}\right)^{1+m}, \quad u^{(r)}(\boldsymbol{\sigma}) = \frac{\varepsilon_0 \sigma_0^{(r)}}{1+n}\left(\frac{\sigma_e}{\sigma_0^{(r)}}\right)^{1+n}, \tag{A.29}$$

respectively. In these expressions, m is the strain-hardening parameter, such that $0 \leq m \leq 1$, $n = 1/m$ is the corresponding nonlinearity exponent, $\sigma_0^{(r)}$ is the flow stress of phase r, ε_0 is a reference strain, and the ε_e and σ_e are the von Mises equivalent strain and stress, already introduced in the previous section. The stress-strain relation for such a material is given by:

$$\boldsymbol{\sigma} = \frac{\partial w}{\partial \boldsymbol{\varepsilon}}(\boldsymbol{\varepsilon}) = -p\mathbf{I} + \frac{2}{3}\frac{\sigma_0}{\varepsilon_0}\left(\frac{\varepsilon_e}{\varepsilon_0}\right)^{m-1}\boldsymbol{\varepsilon}_d, \tag{A.30}$$

where $p = -\mathrm{tr}(\boldsymbol{\sigma})/3$ is the indeterminate, hydrostatic stress associated with the incompressibility condition $\mathrm{tr}(\boldsymbol{\varepsilon}) = 0$. Note that $m = 1$ and $m = 0$ represent linear and rigid-perfectly plastic behavior, respectively. This model is commonly used to characterize time-independent plastic deformation of metals, as well as their time-dependent viscous deformation (e.g. high temperature creep). In the

first case, the deformations are infinitesimal and $\boldsymbol{\sigma}$ and $\boldsymbol{\varepsilon}$ represent the infinitesimal stress and strain tensors, respectively. In the second case, the deformations are finite and $\boldsymbol{\sigma}$ and $\boldsymbol{\varepsilon}$ are identified with the Cauchy stress and Eulerian strain-rate, respectively. Then, m becomes a strain-rate sensitivity parameter. Although we will continue to use only infinitesimal stresses and strains below, reference will also be made to the rate-sensitivity case, without further clarification.

The infinitely long fibers are assumed to be aligned and perfectly bonded to the matrix, and to have circular cross section with diameter much smaller than the dimensions of the specimen. The distribution of the fibers in the transverse plane is assumed *random* and *isotropic*, so the composite is transversely isotropic. Furthermore, from the homogeneity of the potentials (A.29) in their corresponding fields, it follows that a transversely isotropic composite, made up of power-law phases with the same exponent m and the same reference strain ε_0, subject to anti-plane or in-plane loading, has effective potentials of the form (A.29). They can be written as:

$$\widetilde{W}(\overline{\boldsymbol{\varepsilon}}) = \frac{\varepsilon_0\tilde{\sigma}_0}{1+m}\left(\frac{\overline{\varepsilon}_e}{\varepsilon_0}\right)^{1+m}, \quad \widetilde{U}(\overline{\boldsymbol{\sigma}}) = \frac{\varepsilon_0\tilde{\sigma}_0}{1+n}\left(\frac{\overline{\sigma}_e}{\tilde{\sigma}_0}\right)^{1+n}, \tag{A.31}$$

where $\overline{\varepsilon}_e$ and $\overline{\sigma}_e$ are the equivalent average strain and stress, respectively. For anti-plane loading along the 3-direction they reduce to $\overline{\varepsilon}_e = (2/\sqrt{3})\sqrt{\overline{\varepsilon}_{13}^2 + \overline{\varepsilon}_{23}^2}$ and $\overline{\sigma}_e = (\sqrt{3})\sqrt{\overline{\sigma}_{13}^2 + \overline{\sigma}_{23}^2}$, and for in-plane loading they reduce to $\overline{\varepsilon}_e = (2/\sqrt{3})\sqrt{\overline{\varepsilon}_{12}^2 + \frac{1}{4}(\overline{\varepsilon}_{11} - \overline{\varepsilon}_{22})^2}$ and $\overline{\sigma}_e = (\sqrt{3})\sqrt{\overline{\sigma}_{12}^2 + \frac{1}{4}(\overline{\sigma}_{11} - \overline{\sigma}_{22})^2}$. The effective flow stress $\tilde{\sigma}_0$ is a function of the nonlinearity, the contrast, and concentration of fibers, and it completely characterizes the effective behavior.

Before proceeding to the computation of the effective potentials (A.31) for the fibrous composites, we note that the effective energy (A.10) of the N-phase thermoelastic comparison composite simplifies greatly when the composite has only two phases. In this case, the Levin relations (Levin, 1967) can be used to obtain the effective thermal stress tensor in terms of the effective elastic tensor. The effective energy then takes the form:

$$\begin{aligned}\widetilde{W}_T(\overline{\boldsymbol{\varepsilon}}) = \bar{f} + \bar{\boldsymbol{\tau}}\cdot\overline{\boldsymbol{\varepsilon}} + \frac{1}{2}\overline{\boldsymbol{\varepsilon}}\cdot\bar{\mathbf{L}}_0\overline{\boldsymbol{\varepsilon}} + ... \\ ... + \frac{1}{2}\left[\overline{\boldsymbol{\varepsilon}} + (\triangle\mathbf{L}_0)^{-1}(\triangle\boldsymbol{\tau})\right]\cdot(\widetilde{\mathbf{L}}_0 - \bar{\mathbf{L}}_0)\left[\overline{\boldsymbol{\varepsilon}} + (\triangle\mathbf{L}_0)^{-1}(\triangle\boldsymbol{\tau})\right],\end{aligned} \tag{A.32}$$

where the overbar denotes volume averages, $\triangle\mathbf{L}_0 = \mathbf{L}_0^{(1)} - \mathbf{L}_0^{(2)}$ and $\triangle\boldsymbol{\tau} = \boldsymbol{\tau}^{(1)} - \boldsymbol{\tau}^{(2)}$. Note that the only non-explicit term in this expression is the tensor of effective moduli $\tilde{\mathbf{L}}_0$ for a two-phase, linear-elastic composite. Estimates of the Hashin-Shtrikman type for such linear composites with particulate-type microstructures (i.e., inclusions of phase 2 dispersed in a matrix of phase 1) have been given by Willis (1977, 1978) and Ponte Castañeda and Willis (1995). The relevant expression for the effective modulus tensor is:

$$\widetilde{\mathbf{L}}_0 = \sum_{r=1}^{2} c^{(r)}\mathbf{L}_0^{(r)}\left[\mathbf{I} + \mathbf{P}^{(0)}(\mathbf{L}_0^{(r)} - \mathbf{L}^{(0)})\right]^{-1}\left\{\sum_{s=1}^{2} c^{(s)}\left[\mathbf{I} + \mathbf{P}^{(0)}(\mathbf{L}_0^{(s)} - \mathbf{L}^{(0)})\right]^{-1}\right\}^{-1}, \tag{A.33}$$

where the modulus tensor $\mathbf{L}^{(0)}$ of the homogeneous reference medium in the Hashin-Shtrikman approximation must be identified with the modulus tensor of the matrix phase ($\mathbf{L}_0^{(1)}$, in this case), and $\mathbf{P}^{(0)}$ is a microstructural tensor, related to the Eshelby tensor, which depends on $\mathbf{L}^{(0)}$, the shape and orientation of the particles, as well as on the shape and orientation of the two-point correlation functions for their distribution in space. These estimates are known to be exact to first order in the volume fraction of the particles and to second order in the heterogeneity contrast. They tend to underestimate the interaction between particles, but can give fairly accurate estimates for small to intermediate concentrations.

Since the nonlinear phases are isotropic, and are isotropically distributed in the transverse plane, under the assumptions of anti-plane or in-plane strain loading, it is reasonable to assume that the average strain field in the phases is aligned with the average strain, i.e. $\check{\boldsymbol{\varepsilon}}^{(r)} = \check{\boldsymbol{\varepsilon}} = \overline{\boldsymbol{\varepsilon}}/\overline{\varepsilon}_e$ for all r, such that the projection tensors become $\mathbf{E} = (2/3)\check{\boldsymbol{\varepsilon}} \otimes \check{\boldsymbol{\varepsilon}}$ and $\mathbf{F} = \mathbf{K} - \mathbf{E}$. Then, using the fact that $\mathbf{L}^{(0)}$ has the form (A.15), and making use of the long-fiber limit in the appropriate expressions for the tensor $\mathbf{P}^{(0)}$, it can be shown (see Ponte Castañeda, 1996) that under in-plane and anti-plane loading, the in-plane and anti-plane components of the tensor $\mathbf{P}^{(0)}$, respectively, may be written in the form:

$$\mathbf{P}^{(0)} = \frac{\sqrt{k}}{2(1+\sqrt{k})\lambda^{(0)}}\mathbf{E} + \frac{1}{2(1+\sqrt{k})\mu^{(0)}}\mathbf{F}, \tag{A.34}$$

where $k = \lambda^{(0)}/\mu^{(0)}$ is the anisotropy ratio of the homogeneous reference medium, and the projection tensors have to be suitably interpreted.

With expressions (A.32), (A.33) and (A.34) defining explicitly the effective energy of the relevant linear comparison composite, we have everything required to compute the effective energies of the power-law fibrous composites. Thus, introducing (A.29a) and (A.31a) into (A.18), we arrive at the following expression for the normalized effective flow stress:

$$\begin{aligned}\frac{\tilde{\sigma}_0}{\sigma_0^{(1)}} &= c^{(1)}\left[\left(\frac{\hat{\varepsilon_e}^{(1)}}{\overline{\varepsilon}_e}\right)^{1+m} - (1+m)\left(\frac{\overline{\varepsilon}_e^{(1)}}{\overline{\varepsilon}_e}\right)^{m}\left(\frac{\hat{\varepsilon}_{\parallel}^{(1)}}{\overline{\varepsilon}_e} - \frac{\overline{\varepsilon}_e^{(1)}}{\overline{\varepsilon}_e}\right)\right] \\ &\quad + c^{(2)}\frac{\sigma_0^{(2)}}{\sigma_0^{(1)}}\left(\frac{\overline{\varepsilon}_e^{(2)}}{\overline{\varepsilon}_e}\right)^{1+m},\end{aligned} \tag{A.35}$$

where it is recalled that the labels 1 and 2 has been used to identify the matrix and fiber phases, respectively. Note that $\overline{\varepsilon}_e^{(2)}$ can be eliminated in favor of $\overline{\varepsilon}_e^{(1)}$ using the average strain condition, i.e. $\overline{\varepsilon}_e^{(2)} = (\overline{\varepsilon}_e - c^{(1)}\overline{\varepsilon}_e^{(1)})/c^{(2)}$, and that the variables $\hat{\varepsilon}_{\parallel}^{(2)}$ and $\hat{\varepsilon}_{\perp}^{(2)}$ do not appear in (A.35) because there are no fluctuations in phase 2. This last result is associated with the Hashin-Shtrikman approximation and can be verified by noting that the tensor $\mathbf{P}$ is independent of $\mathbf{L}_0^{(2)}$ in this case. Expression (A.35) allows the computation of $\tilde{\sigma}_0$ as a function of the rate-sensitivity m, the fiber concentration $c^{(2)}$, and the contrast $\sigma_0^{(2)}/\sigma_0^{(1)}$ in terms of the variables $\overline{\varepsilon}_e^{(1)}$, $\hat{\varepsilon}_{\parallel}^{(1)}$ and $\hat{\varepsilon}_{\perp}^{(1)}$, which, in turn, must be determined from a set of three algebraic nonlinear equations in these unknowns arising from expressions (A.13), together with (A.32), (A.33) and (A.34), as well as relations (A.17) and (A.16).

The stress potential (A.29b) can be used as the starting point to generate alternative estimates for $\tilde{\sigma}_0$. In this case, the effective stress potential of the linear comparison composite is given in terms of the compliances and strain polarizations by an expression analogous to (A.32). In turn, the effective compliance tensor $\widetilde{\mathbf{M}}_0$ is given in terms of the compliances by an expression analogous to (A.33), where the relevant microstructural tensor is related to the P-tensor (A.34) by $\mathbf{Q}^{(0)} = \left(\mathbf{M}^{(0)}\right)^{-1} - \left(\mathbf{M}^{(0)}\right)^{-1} \mathbf{P}^{(0)} \left(\mathbf{M}^{(0)}\right)^{-1}$. From (A.25), the normalized effective flow stress may be expressed in terms of the stress variables via:

$$\frac{\tilde{\sigma}_0}{\sigma_0^{(1)}} = \left\{ c^{(1)} \left[\left(\frac{\hat{\sigma_e}^{(1)}}{\overline{\sigma}_e} \right)^{1+n} - (1+n) \left(\frac{\overline{\sigma}_e^{(1)}}{\overline{\sigma}_e} \right)^{n} \left(\frac{\hat{\sigma}_{\parallel}^{(1)}}{\overline{\sigma}_e} - \frac{\overline{\sigma}_e^{(1)}}{\overline{\sigma}_e} \right) \right] + c^{(2)} \left(\frac{\sigma_0^{(2)}}{\sigma_0^{(1)}} \right)^{-n} \left(\frac{\overline{\sigma}_e{}^{(2)}}{\overline{\sigma}_e} \right)^{1+n} \right\}^{-1/n}, \tag{A.36}$$

where the variables $\overline{\sigma}_e^{(1)}$, $\hat{\sigma}_{\parallel}^{(1)}$, and $\hat{\sigma}_{\perp}^{(1)}$ may be obtained from expressions completely analogous to the above-mentioned expressions in the context of the variables $\overline{\varepsilon}_e^{(1)}$, $\hat{\varepsilon}_{\parallel}^{(1)}$ and $\hat{\varepsilon}_{\perp}^{(1)}$. However, they may also be computed with the help of the duality relations (A.28).

Finally, a third expression for $\tilde{\sigma}_0$ is obtained by making use of the affine version of the estimates, as specified by relations (A.27). For example, the first of them gives the expression:

$$\frac{\tilde{\sigma}_0}{\sigma_0^{(1)}} = c^{(1)} \left(\frac{\overline{\varepsilon}_e^{(1)}}{\overline{\varepsilon}_e} \right)^{m} + c^{(2)} \frac{\sigma_0^{(2)}}{\sigma_0^{(1)}} \left(\frac{\overline{\varepsilon}_e^{(2)}}{\overline{\varepsilon}_e} \right)^{m}. \tag{A.37}$$

Expressions (A.35), (A.36) and (A.37) generalize corresponding expressions for the extreme cases of rigid particles and voids (infinite contrast) given by Ponte Castañeda (2002b). This author also gave estimates of the self-consistent type for these special case, where the fluctuations in both phases do not vanish in general. As a consequence of the duality gap, these three expressions are expected to give slightly different predictions for $\tilde{\sigma}_0$ for any m different from 1 (the linear limit). However, as verified in the next section, these expressions all agree also in the ideally plastic (rate-insensitive) limit (m tends to zero).

It is emphasized that all the results presented in this section are valid for anti-plane as well as in-plane loading, although the stress and strain fields in those two cases are obviously different.

A.4.1 Hashin-Shtrikman estimates for rigid-perfectly plastic phases

The above expressions simplify considerably for the special case of rigid-perfectly plastic behavior, which corresponds to a potential (A.29) with $m = 0$. When taking the limit $m \to 0$, we must consider two cases separately.

If the fibers are *stronger* than the matrix ($\sigma_0^{(2)}/\sigma_0^{(1)} \geq 1$) the solution can be shown to reduce to that for rigid particles, regardless of the contrast. In this case, the average strain in the particles is zero, and in the matrix we have $\overline{\varepsilon}_e^{(1)} = \overline{\varepsilon}_e / c^{(1)}$, $\hat{\varepsilon}_{\parallel}^{(1)} \to \infty$, and $\hat{\varepsilon}_{\perp}^{(1)} = 0$. The average stress in the

matrix is the flow stress, i.e. $\overline{\sigma}_e^{(1)} = \sigma_0^{(1)}$, and the stress fluctuations are such that $\hat{\sigma}_{\parallel}^{(1)} = \sigma_0^{(1)}$ and $\hat{\sigma}_{\perp}^{(1)} = 0$, respectively. All three of the above expressions for the effective flow stress, (A.35), (A.36) and (A.37), reduce to the result:

$$\tilde{\sigma}_0/\sigma_0^{(1)} = 1. \tag{A.38}$$

If the fibers are *weaker* than the matrix ($\sigma_0^{(2)}/\sigma_0^{(1)} < 1$), it is important to realize that when $m \to 0$, the average strain in the matrix goes to zero exponentially, $\overline{\varepsilon}_e^{(1)} \approx e^{-\alpha(k)/m}$, in such a way that the average stress in this phase, which is proportional to $\left(\overline{\varepsilon}_e^{(1)}\right)^m$, is below $\sigma_0^{(1)}$. Thus, in the matrix $\overline{\varepsilon}_e^{(1)} = 0$, so that $\overline{\varepsilon}_e^{(2)} = \overline{\varepsilon}_e/c^{(2)}$, and from relations (A.16):

$$\frac{\hat{\varepsilon}_{\parallel}^{(1)}}{\overline{\varepsilon}_e} = \frac{1}{\sqrt{2c^{(2)}}}\frac{1}{k^{1/4}}, \quad \frac{\hat{\varepsilon}_{\perp}^{(1)}}{\overline{\varepsilon}_e} = \frac{1}{\sqrt{2c^{(2)}}}k^{1/4},$$

where the anisotropy ratio k is determined as a function of the contrast and concentration from:

$$\frac{k^{3/4}}{1-k} = \sqrt{\frac{c^{(2)}}{2}}\left(1 - \frac{\sigma_0^{(2)}}{\sigma_0^{(1)}}\frac{\sqrt{1+k}}{1-k}\right), \tag{A.39}$$

which follows from the generalized secant condition (A.17) in phase 1.

The corresponding phase average and fluctuations of the stress can be deduced from (A.28). They are given in terms of the anisotropy ratio by:

$$\frac{\overline{\sigma}_e^{(1)}}{\sigma_0^{(1)}} = \frac{1-k}{\sqrt{1+k}}, \quad \frac{\hat{\sigma}_{\parallel}^{(1)}}{\sigma_0^{(1)}} = \frac{1}{\sqrt{1+k}}, \quad \frac{\hat{\sigma}_{\perp}^{(1)}}{\sigma_0^{(1)}} = \frac{\sqrt{k}}{\sqrt{1+k}}.$$

Finally, expressions (A.35), (A.36) and (A.37) for the normalized effective flow stress all simplify to:

$$\frac{\tilde{\sigma}_0}{\sigma_0^{(1)}} = c^{(2)}\frac{\sigma_0^{(2)}}{\sigma_0^{(1)}} + (1-c^{(2)})\frac{1-k}{\sqrt{1+k}}. \tag{A.40}$$

When $\sigma_0^{(2)}/\sigma_0^{(1)} \to 0$, these expressions reduce to the results of Ponte Castañeda (2002b) for the special case of aligned cylindrical voids distributed isotropically in a rigid-perfectly plastic matrix with zero hydrostatic strain.

A.4.2 Small contrast expansion

As already mentioned, estimates (A.35) and (A.36) are exact to second order in the heterogeneity contrast, that is, they both agree with the exact second-order asymptotic expansion of Ponte Castañeda and Suquet (1995), which for this case can be written as:

$$\tilde{\sigma}_0 = \langle\sigma_0\rangle - \frac{1}{2}\frac{1+m}{\sqrt{m}+m}\frac{\langle\sigma_0^2\rangle - \langle\sigma_0\rangle^2}{\langle\sigma_0\rangle}. \tag{A.41}$$

The first term in this expansion corresponds to the Voigt upper bound. Note that the range of validity of (A.41) vanishes as $m \to 0$. In fact, the estimate for the rigid-perfectly plastic limit ($m = 0$) has an

expansion of a different form, which actually depends on whether the fibers are stronger or weaker than the matrix. Thus, for $\sigma_0^{(2)}/\sigma_0^{(1)} \geq 1$ the result is independent of the contrast, i.e. $\tilde{\sigma}_0 = \sigma_0^{(1)}$, while for $\sigma_0^{(2)}/\sigma_0^{(1)} < 1$ it is given by:

$$\tilde{\sigma}_0 = \langle \sigma_0 \rangle - \frac{3}{2}\left(1 - c^{(2)}\right)^{1/3} \left(\frac{\langle \sigma_0^2 \rangle - \langle \sigma_0 \rangle^2}{\langle \sigma_0 \rangle} \right)^{2/3}, \tag{A.42}$$

which is the small-contrast expansion of expression (A.40).

On the other hand, the affine estimate (A.37), which is known not to be exact to second order in the contrast, has an expansion of the form:

$$\tilde{\sigma}_0 = \langle \sigma_0 \rangle - \frac{1}{2} \frac{\langle \sigma_0^2 \rangle - \langle \sigma_0 \rangle^2}{\langle \sigma_0 \rangle}, \tag{A.43}$$

which does not agree with (A.41) except, of course, for $m = 1$. Moreover, it is independent of the nonlinearity, which first appears in the next order term. Interestingly, this expression coincides with the second-order expansion of the variational estimate of Ponte Castañeda (1991), which is a rigorous upper bound for $\tilde{\sigma}_0$.

A.5 Results and discussion

Here, results from Section A.4 for anti-plane and in-plane loading are presented as a function of the strain-rate-sensitivity m and fiber concentration $c^{(2)}$, for two values of the heterogeneity contrast—one corresponding to stronger fibers ($\sigma_0^{(2)}/\sigma_0^{(1)} = 5$) and the other to weaker fibers ($\sigma_0^{(2)}/\sigma_0^{(1)} = 0.2$). The new "second-order" estimates for the effective flow stress are compared with rigorous bounds and other linearization schemes. For brevity, they will be denoted by the labels $SOE(W)$, $SOE(U)$ and $SOE(A)$, corresponding respectively to the strain-potential formulation (A.35), the stress-potential formulation (A.36), and the constitutive-relation (affine) formulation (A.37). The corresponding "old" second-order estimates of Ponte Castañeda (1996) will be denoted by $OSOE(W)$, $OSOE(U)$ and $OSOE(A)$. Recall that these estimates make use of a similar linear comparison composite except that it uses the tangent moduli of the phases evaluated at the phase averages. The "variational" Hashin-Shtrikman estimates of Ponte Castañeda (1991) provide rigorous upper bounds for all other nonlinear Hashin-Shtrikman estimates, and, in particular, for the second-order estimates. These bounds make use of the secant moduli of the phases evaluated at the second moments of the fields (Suquet, 1995). The Voigt and Reuss estimates are rigorous, microstructure-independent upper and lower bounds, which are obtained from uniform strain and stress trial fields, respectively.

A.5.1 Fibers stronger than the matrix

Figure A.2a shows various estimates of the Hashin-Shtrikman type for the effective flow stress of a fiber-reinforced composite, normalized by the flow stress of the matrix, $\tilde{\sigma}_0/\sigma_0^{(1)}$, as a function of the strain-rate-sensitivity m, for a given contrast ($\sigma_0^{(2)}/\sigma_0^{(1)} = 5$) and concentration of fibers ($c^{(2)}$ =25%).

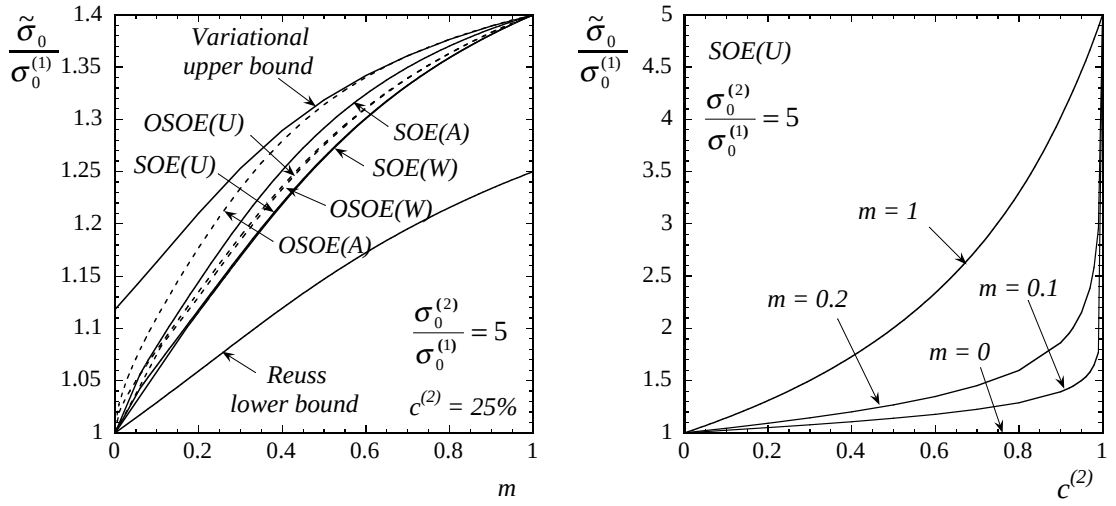

(a) (b)

Figure A.2: Effective flow stress normalized by the flow stress of the matrix for a contrast of 5: (a) as a function of the strain-rate-sensitivity for a concentration of 25 %; (b) as a function of the fiber concentration for several values of m. Labels 1 and 2 refer to the matrix and fibers, respectively.

It is observed that the new (SOE) estimates lie between the variational upper and Reuss lower bounds for all values of m. The $OSOE(A)$ violates the variational upper bound for some values of m close to 1. Note that the new estimates are *weaker* than the corresponding old ones. Also, the W- and U-type estimates are different for the new as well as the old second-order method. As already mentioned, this *duality gap* arises from the approximations made in the optimization procedure, and it gives an idea of the error introduced. In this case, we see that it is very small except for some small values of m. Moreover, it vanishes in the linear case, $m = 1$, where both estimates go to the variational upper bound, and in the extremely nonlinear rigid-perfectly plastic case, $m = 0$, where both versions go to the Reuss lower bound. Note that as the nonlinearity $n = 1/m$ increases, the reinforcement effect becomes smaller and finally vanishes in the rigid-perfectly plastic limit. Figure A.2b shows the $SOE(U)$ estimates for the normalized effective flow stress as a function of fiber concentration $c^{(2)}$ for several values of the strain-rate-sensitivity ($m = 0, 0.2, 0.1, 1$). Recall that the Hashin-Shtrikman estimates used for the linear comparison composite are exact only to first order in the concentration. For very high concentrations, i.e. $c^{(2)} \to 1$, the estimates become more steep as m decreases, and in the limiting case $m = 0$ the estimate presents a jump from 0 to 5.

The phase averages and fluctuations of the strains associated with the new estimates are shown in fig. A.3a, normalized by the equivalent applied strain $\overline{\varepsilon}_e$. The average strain in the fibers (the stronger phase) can be shown to decay exponentially as $m \to 0$, $\overline{\varepsilon}_e^{(2)} \approx e^{-\alpha/m}$, so that in the ideally plastic limit the average stress in this phase, $\overline{\sigma}_e^{(2)}/\sigma_0^{(2)} \approx \left(\overline{\varepsilon}_e^{(2)}\right)^m \sim O(1)$, remains below the flow stress $\sigma_0^{(2)}$. Recall that the fields were assumed constant inside the fibers, hence there are no fluctuations in phase 2, so that the modulus tensor in the linearized phase is the tangent moduli. The fluctuations in the matrix are seen to increase with the nonlinearity, meaning the strain field becomes more heterogeneous. Note also that these fluctuations are isotropic in the linear case, but become

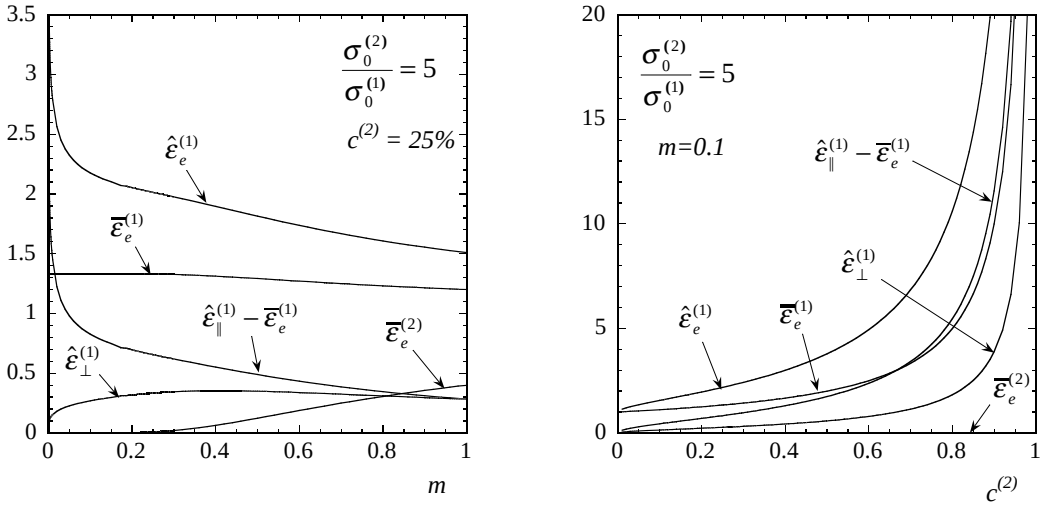

Figure A.3: Phase averages and fluctuations of the strain, normalized by the equivalent applied strain $\overline{\varepsilon}_e$, for a contrast of 5: (a) as a function of the strain-rate-sensitivity for a concentration of 25 %; (b) as a function of the fiber concentration for several values of m. Labels 1 and 2 refer to the matrix and fibers, respectively.

anisotropic as the nonlinearity increases, and they are always higher in the parallel direction. When $m = 0$, the stress-strain curve is "flat", the variables $\overline{\boldsymbol{\varepsilon}}^{(1)}$ and $\hat{\boldsymbol{\varepsilon}}^{(1)}$ become aligned, and since neither of them vanishes, the modulus tensor in the linearized matrix tends to the tangent moduli (which has zero *parallel* component). This is why the new and the old versions of the estimate coincide in this case. The phase averages and fluctuations of the strain for $m = 0.1$ are shown in fig. A.3b as a function of the fiber concentration. For this and smaller values of m, the average strain inside the fibers is almost negligible, except as $c^{(2)} \to 1$, when $\overline{\varepsilon}_e^{(2)}/\overline{\varepsilon}_e \to 1$. Since the fibers practically do not deform, the average strain in the matrix is approximately $\overline{\varepsilon}_e^{(1)}/\overline{\varepsilon}_e \approx 1/c^{(1)}$, which goes to infinity as $c^{(2)} \to 1$. As expected, there are no fluctuations for $c^{(2)} = 0$, since the composite is actually a homogeneous material (the matrix) and hence the fields are constant. As the concentration of fibers increases, the strain field becomes more heterogeneous and thus the fluctuations are higher, and they are seen to blow up when $c^{(2)} \to 1$. But when normalized with the phase average $\overline{\varepsilon}_e^{(1)}$, it can be shown that $\hat{\varepsilon}_\parallel^{(1)}/\overline{\varepsilon}_e^{(1)} \to const.$ and $\hat{\varepsilon}_\perp^{(1)}/\overline{\varepsilon}_e^{(1)} \to const.$ in this limit.

Fig. A.4a shows the corresponding phase averages and fluctuations of the stress normalized by the flow stresses of the phases, as a function of m. The equivalent applied stress has been set equal to the flow stress of the matrix, i.e. $\overline{\sigma}_e = \sigma_0^{(1)}$, and it is related to $\overline{\varepsilon}_e$ through (A.37). Since the stress-strain curve "flattens" as m decreases, and the strain in the matrix does not vanish (see fig. A.3a), the stress fluctuations become smaller, meaning the stress field becomes more homogeneous. Note that, unlike the strain field, the stress field has higher fluctuations in the perpendicular direction. Again, the stress fluctuations are isotropic in the linear case and anisotropic for general values of m, but they vanish when $m = 0$, i.e. the stress field becomes constant. The variables $\overline{\boldsymbol{\sigma}}^{(1)}$ and $\hat{\boldsymbol{\sigma}}^{(1)}$ are the same in this limit, and so the compliance tensor of the linearized matrix becomes the tangent compliance. As

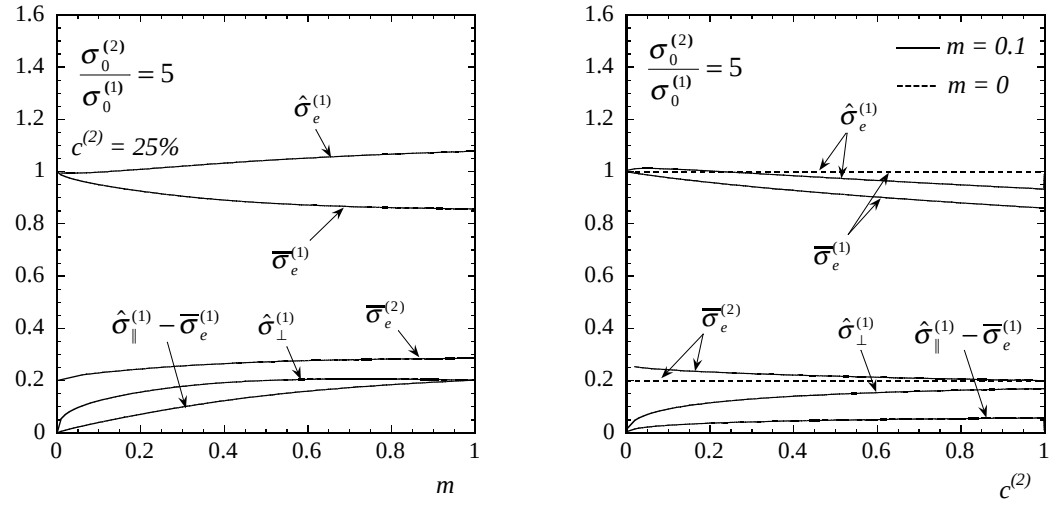

Figure A.4: Phase averages and fluctuations of the stress, normalized by the flow stress $\sigma_0^{(r)}$ of the corresponding phase, for a contrast of 5: (a) as a function of the strain-rate-sensitivity for a concentration of 25 %; (b) as a function of the fiber concentration for several values of m. The equivalent applied stress $\overline{\sigma}_e$ has been set equal to the value of $\widetilde{\sigma}_0$ at $m = 0$. Labels 1 and 2 refer to the matrix and fibers, respectively.

already mentioned, the average stress in the fibers (the stronger phase) remains below the flow stress $\sigma_0^{(2)}$ for all values of m. The phase averages and fluctuations of the stress for $m = 0.1$ (continuous lines) can be seen in fig. A.4b, as a function of the fiber concentration. When $c^{(2)} = 0$ there are no stress fluctuations in the matrix, and they are seen to increase with concentration in both directions. Note that the average stresses remain below the corresponding flow stresses, except when $c^{(2)} = 0$, where the average stress in the matrix (weaker phase) reaches the flow stress.

At this point, some comments about the rigid-perfectly plastic limit ($m = 0$) are appropriate. First, there is no duality gap in this limit. Both, $SOE(W)$ and $SOE(U)$ estimates give no reinforcement effect due to the presence of stronger fibers (see fig. A.2), except when $c^{(2)} \to 1$. The solution actually reduces to that of rigid particles, regardless of the heterogeneity contrast. It is known from the work of Drucker (1966) that in this case the exact solution corresponds to straight shear bands passing through the matrix, the weaker phase, at least at low concentrations of fibers (see fig. A.5a). The deformation is localized in these bands, which correspond to discontinuities in the displacement field. Note that the results of fig. A.3a, which shows that the average strain in the fibers is zero when $m = 0$, are consistent with such a deformation mechanism. This means that the average stress in the fibers is below their flow stress, i.e. $\overline{\sigma}_e^{(2)} < \sigma_0^{(2)}$, whereas in the matrix, in order to deform, the average stress should be the flow stress, i.e. $\overline{\sigma}_e^{(1)} = \sigma_0^{(1)}$ (see fig. A.4b). Vanishing strain fluctuations in the perpendicular direction are also consistent with the fact that the shear bands are straight, though it is not clear yet what are the implications of infinite strain fluctuations in the parallel direction (see fig. A.3a). It might be related to the presence of not one but an infinite number of bands: one for every "parallel" straight path free of inclusions. Anyway, they do not appear in the simplified

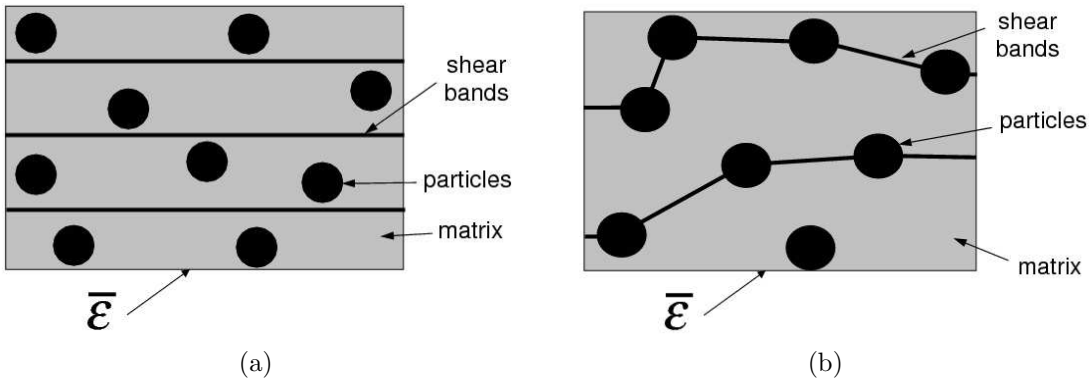

Figure A.5: Rigid-perfectly plastic composite subject to antiplane shear in the vertical direction: (a) when the fibers are stronger than the matrix the shear bands go through the matrix; (b) when the fibers are weaker than the matrix the shear bands go through the fibers.

expression for the effective flow stress. Vanishing stress fluctuations in the perpendicular direction (see fig. A.4a) means that the field is constant in this direction, namely zero since the fields are aligned with the applied stress, and so the load is entirely carried by the parallel component of the stress, which is also constant and equal to the flow stress.

The shear band scheme in fig. A.5a becomes unrealistic for large concentrations, since it turns difficult to find a straight path between fibers. In fact, when $c^{(2)} = 1$ the estimate for the effective property has a discontinuity, and it jumps from 1 to 5 (see fig. A.2b). This may be related to the special microstructure associated with Hashin-Shtrikman estimates. Indeed, Ponte Castañeda (2002b) found a non-vanishing strengthening effect for non-zero values of the concentration, when the self-consistent estimate is used for the linear comparison composite.

A.5.2 Fibers weaker than the matrix

Estimates of the Hashin-Shtrikman type for a fiber-weakened composite are shown in fig. A.6a as a function of the strain-rate-sensitivity, for a given contrast ($\sigma_0^{(2)}/\sigma_0^{(1)} = 0.2$) and concentration of fibers ($c^{(2)}$ =25%). The new second-order estimates lie between the bounds for all values of m here as well. On the other hand, the old $OSOE(U)$ estimate violates the variational upper bound for sufficiently small values of m, and it tends to the Voigt upper bound in the rigid-perfectly plastic limit. Note also that the $OSOE(A)$ estimate violates the variational upper bound for all values of $m < 1$. Moreover, unlike the old $OSOE(W)$ and $OSOE(U)$ estimates, which diverged in the rigid-perfectly plastic limit, the new $SOE(W)$, $SOE(U)$ and $SOE(A)$ estimates coincide: there is no duality gap in this highly nonlinear limit, for *any* contrast and concentration of fibers. This was already noted in the case of voids by Ponte Castañeda (2002b). However, the SOE estimates still exhibit a non-negligible duality gap for small, non-zero values of m. Of the three possible types of estimates, the stress-potential-type estimates $SOE(U)$ appear to give the best overall predictions. Figure A.6b shows $SOE(U)$ estimates for the normalized effective flow stress as a function of fiber concentration, for several values of the strain-rate-sensitivity ($m = 1, 0.2, 0$). The new estimate for the rigid-perfectly plastic limit is given

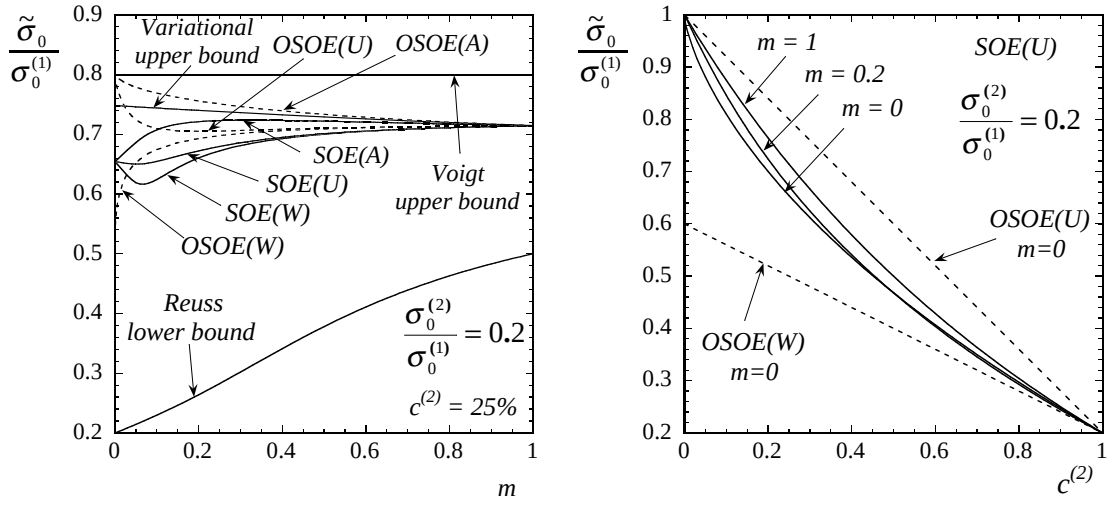

Figure A.6: Effective flow stress normalized by the flow stress of the matrix for a contrast of 0.2: (a) as a function of the strain-rate-sensitivity for a concentration of 25 %; (b) as a function of the fiber concentration for several values of m. Labels 1 and 2 refer to the matrix and fibers, respectively.

by expression (A.40). Note that the old second-order estimates $OSOE(W)$ and $OSOE(U)$ for $m = 0$ (dashed lines) depend linearly on $c^{(2)}$, and they are considerably different. On the other hand, the new estimates $SOE(U)$ and $SOE(W)$ are equivalent for $m = 0$, and they exhibit a more complex, nonlinear dependence on $c^{(2)}$.

The associated phase averages and fluctuations of the strain, normalized by the applied equivalent strain $\overline{\varepsilon}_e$, are shown in fig. A.7a as a function of the strain-rate-sensitivity. The fields were assumed constant inside the inclusions, so there are no fluctuations in phase 2. As in the previous case, the average strain in the stronger phase, now the matrix, goes to zero exponentially as $m \to 0$, $\overline{\varepsilon}_e^{(1)} \approx e^{-\alpha/m}$, such that the average stress in that phase, $\overline{\sigma}_e^{(1)}/\sigma_0^{(1)} \approx \left(\overline{\varepsilon}_e^{(1)}\right)^m \sim O(1)$ in the rigid-perfectly plastic limit. The fluctuations in both directions go up with decreasing m, but they saturate, reaching a maximum value for $m = 0$. They are isotropic for the linear case, becoming more anisotropic with increasing nonlinearity $n = 1/m$, with the parallel strain fluctuations always higher than the perpendicular ones. Fig. A.7b shows the normalized phase averages and fluctuations of the strain as a function of concentration, for two values of m (0, 0.1). When $m = 0.1$ (continuous lines), the average strain in the matrix decreases monotonically with increasing concentration of fibers, but in the fibers the average strain has a maximum for some small value of $c^{(2)}$. The fluctuations in the matrix vanish when $c^{(2)} = 0$ as they should, since the composite is actually a homogeneous material (the matrix) in this case. Notice that the fluctuations reach a maximum value and then decrease with increasing fiber concentration. It is interesting to note that they actually increase monotonically when normalized with the phase average $\overline{\varepsilon}_e^{(1)}$. But for $m = 0$ (dashed lines), the fluctuations in the matrix are seen to decrease monotonically with concentration of fibers, and blow up in the dilute limit, i.e. $c^{(2)} \to 0$.

Figure A.8a shows the corresponding phase averages and fluctuations of the stress normalized by

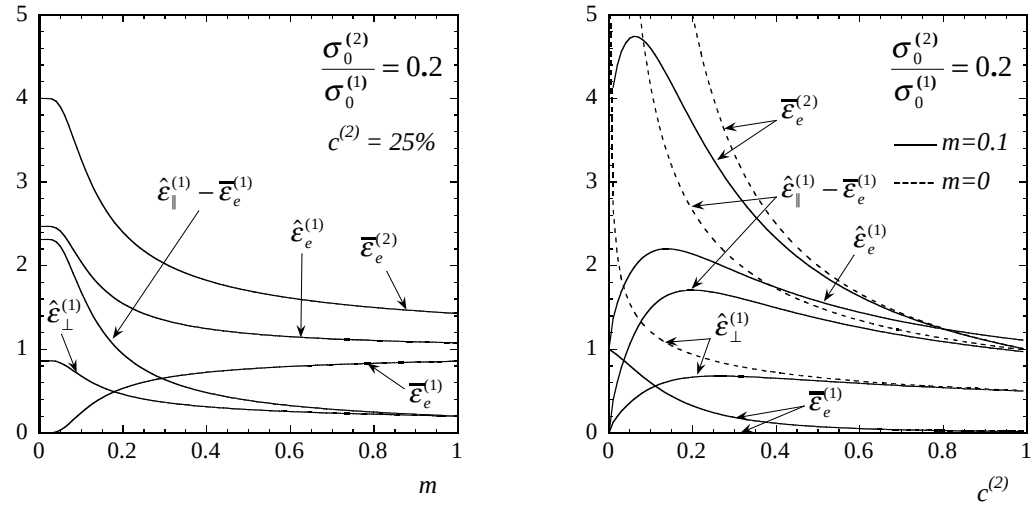

Figure A.7: Phase averages and fluctuations of the strain, normalized by the equivalent applied strain $\overline{\varepsilon}_e$, for a contrast of 5: (a) as a function of the strain-rate-sensitivity for a concentration of 25 %; (b) as a function of the fiber concentration for several values of m. Labels 1 and 2 refer to the matrix and fibers, respectively.

the flow stress of the phases, as a function of the strain-rate-sensitivity. The equivalent applied stress has been set equal to the effective flow stress for the rigid-perfectly plastic case, i.e. $\overline{\sigma}_e = \tilde{\sigma}_0$, where $\tilde{\sigma}_0$ is given by (A.40). As before, the stress fluctuations are isotropic for the linear case, and the anisotropy increases with decreasing m, though this time they do not vanish for $m = 0$. Note that they are higher in the perpendicular direction for all values of m. The average stress in the matrix is always below the flow stress $\sigma_0^{(1)}$, whereas the average stress in the fibers is always above the flow stress $\sigma_0^{(2)}$, except for $m = 0$ where $\overline{\sigma}_e^{(2)} = \sigma_0^{(2)}$. In fig. A.8b we can see the stresses as a function of the concentration, for two values of m (0, 0.1). Again, we observe that the stress fluctuations vanish when $c^{(2)} = 0$, and they increase monotonically (in both directions) with the concentration of fibers.

Some interesting observations can be made for the rigid-perfectly plastic limit ($m = 0$). As in the case of stronger fibers, there is no duality gap in this limit, for any contrast and concentration of fibers. Since now it is the average strain in the matrix that goes to zero, the stress in this phase can take any value from zero to the flow stress, $\sigma_0^{(1)}$, and so we should expect a more complicated stress field than in the case of stronger fibers. Moreover, since $\hat{\boldsymbol{\varepsilon}}^{(1)} \neq \overline{\boldsymbol{\varepsilon}}^{(1)}$, the moduli tensor of the linearized matrix is not the tangent moduli, i.e. $\mathbf{L}_0^{(1)} \neq \mathbf{L}_t^{(1)}$, and that is why the new and the old second-order estimates do not coincide in this case. Although the average strain in the matrix is zero, the matrix does deform—through the strain fluctuations!

Figure A.6b shows that there is a weakening effect due to weaker fibers. Note that the effective flow has an infinite slope at zero fiber concentration. In fact, the dilute expansion of expression (A.40) can be shown to be:

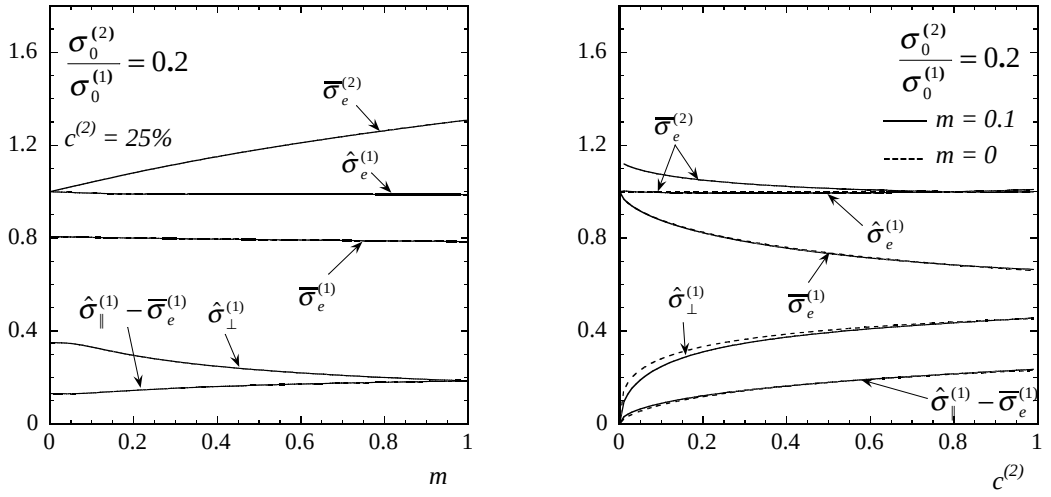

Figure A.8: Phase averages and fluctuations of the stress, normalized by the flow stress $\sigma_0^{(r)}$ of the corresponding phase, for a contrast of 5: (a) as a function of the strain-rate-sensitivity for a concentration of 25 %; (b) as a function of the fiber concentration for several values of m. The equivalent applied stress $\overline{\sigma}_e$ has been set equal to the value of $\widetilde{\sigma}_0$ at $m = 0$. Labels 1 and 2 refer to the matrix and fibers, respectively.

$$\frac{\tilde{\sigma}_0}{\sigma_0^{(1)}} = 1 - \frac{3}{2}\left(1 - \frac{\sigma_0^{(2)}}{\sigma_0^{(1)}}\right)^{4/3}\left(\frac{c^{(2)}}{2}\right)^{2/3},$$

which has an infinite derivative at $c^{(2)} = 0$. As first suggested by Drucker (1966), when the inclusions are weaker than the matrix the shear bands tend to go through the inclusions (see fig. A.5b). This deformation mechanism for a *periodic three-dimensional* porous medium with a dilute concentration of spherical pores leads to a prediction for the effective flow stress proportional to $1-\alpha\left(c^{(2)}\right)^{(2/3)}$. On the other hand, for *periodic two-dimensional* porous media with dilute concentrations of cylindrical pores, Drucker obtained a similar expression, but with an exponent of 1/2, instead of 2/3. The second-order estimates generated in this work predict an exponent of 2/3 for the case of *randomly* distributed cylindrical voids. This is different from Drucker's prediction, but it is not clear at this stage what the effect of randomness versus periodicity of the microstructure is on this exponent. However, recent numerical simulations of porous media based on limit analysis, suggest that the exponent should be between 1/2 and 2/3 (Pastor et. al., 2002). These simulations consist of finite element discretizations of a hollow cylinder, a commonly used model for porous media, subject to two different types of boundary conditions. Results corresponding to uniform stress lead to the lower exponent, whereas uniform strain results seem to be consistent with a 2/3 exponent. In any event, the important thing to realize is that the exponent would be expected to be less than 1, because of the strong interactions between inclusions, due to the shear bands, even at very low concentrations.

Furthermore, the stress and strain fields exhibit peculiar behaviors in this limit. Figure A.8b shows that not only in the weaker phase but also in the stronger phase, the average stress goes to the corresponding flow stress as $c^{(2)} \to 0$. Since the stress cannot be higher than the flow stress for

$m = 0$, this implies that the stress fields become uniform. In fact, the stress fluctuations go to zero like $\left(c^{(2)}\right)^{2/3}$ and $\left(c^{(2)}\right)^{1/3}$, in the parallel and perpendicular directions, respectively. On the other hand, figure A.7b shows that the strain fluctuations blow up as $c^{(2)} \to 0$, which is unexpected. The question arises as to whether the fluctuations really go to infinity when the material is actually more and more homogeneous, or if it is an artifact of the approximation. This interesting limit, which will be pursued in future work, may be linked to the strong interactions among the inclusions in the dilute limit.

A.6 Concluding remarks

The new second-order method of Ponte Castañeda (2002a) was used to estimate the effective behavior of a power-law fibrous composite with arbitrary heterogeneity contrast subject to antiplane shear. Estimates of the Hashin-Shtrikman type along with their corresponding strain and stress fluctuations were presented and discussed. They improve on earlier estimates in two ways. First, the estimates, which are exact to second order in the heterogeneity contrast, were found to satisfy rigorous bounds, namely the variational upper bound and the Reuss lower bound. Second, although there is still a difference between the strain and stress-based estimates, the so-called duality gap, it is smaller than in the previous estimates and, more interestingly, it vanishes for the rigid-perfectly plastic case, for any contrast and concentration of fibers. This is a remarkable improvement over the old second-order method, which did not take into account field fluctuations. The fluctuations are isotropic when the materials are linear, but they were found to become more anisotropic as the nonlinearity increases.

Simple expressions for the extremely nonlinear rigid-perfectly plastic limit were derived and studied in detail. Results seem to be consistent with a deformation mechanism involving shear bands. In the fiber-reinforced case, this translated into no reinforcement effect, and infinite strain fluctuations were predicted in the matrix. In the case of weaker fibers, the dilute limit shows a dependence of the effective property on the concentration of fibers of the type $\tilde{\sigma}_0/\sigma_0^{(1)} \approx 1 - \alpha \left(c^{(2)}\right)^{2/3}$, which is not in exact agreement with Drucker's results for periodic media, but it is closer and more realistic than previous estimates. This is a sensitive limit where both phases are at yield, and the strain fluctuations in the matrix blow up. The question remains as to what are the implications of this result.

The effect of tension along the fibers will be considered in future work in an attempt to generate the yield surface for general loading conditions. The use of self-consistent estimates for the linear comparison composite would allow the incorporation of information about the fluctuations in both phases, and the corresponding nonlinear estimates would be expected to be more accurate for high concentration of inclusions, at least for certain types of symmetric microstructures. This problem will also be addressed in future work.

Acknowledgments

This work was supported by NSF grants CMS-99-72234 and CMS-02-01454.

Appendix B

Second-order estimates for nonlinear isotropic composites with spherical pores and rigid particles[1]

M.I. Idiart[a,b], P. Ponte Castañeda[a,b]

[a] Laboratoire de Mécanique des Solides, C.N.R.S. UMR 7649, Département de Mécanique, École Polytechnique, 91128 Palaiseau Cedex, France.

[b] Department of Mechanical Engineering and Applied Mechanics, University of Pennsylvania, Philadelphia, PA 19104-6315, U.S.A.

Abstract — The "second-order" nonlinear homogenization method (Ponte Castañeda, J. Mech. Phys. Solids 50 (2002) 737–757) is used to generate estimates of the Hashin-Shtrikman-type for the effective behavior of viscoplastic materials with isotropically distributed spherical pores or rigid particles. In the limiting case of an ideally plastic matrix with a dilute concentration of pores, the resulting estimates were found to exhibit a linear dependence on the porosity when the material is subjected to axisymmetric shear, but this dependece becomes singular for simple shear. In the process of this work, an alternative prescription for certain reference tensors used in the method is proposed, and shown to lead to more consistent estimates for the effective behavior than the earlier prescription.

Résumé — On utilise la méthode d'homogénéisation non linéaire proposée par Ponte Castañeda (J. Mech. Phys. Solids 50 (2002) 737–757), dite du second ordre, pour générer des estimations du type Hashin-Shtrikman pour le comportement effectif des matériaux viscoplastiques contenant des pores et des particules rigides sphériques. Dans le cas limite d'une matrice parfaitement plastique à faible concentration de pores, les estimations trouvées présentent une dépendance linéaire de la porosité sous un chargement de cisaillement axisymmétrique ; cependant cette dépendance devient singulière sous cisaillement

[1] This chapter appeared in *C. R. Mecanique* **333** (2005) 147–154.

simple. Lors de ce travail, certaines limites de la formulation de la méthode initialement proposée dans la référence ci-dessus ont été identifiées. En conséquence, des alternatives ont été testées.

B.1 Introduction

Much effort is still being devoted to developing methods capable of accurately estimating the effective behavior of nonlinear heterogeneous media (Ponte Castañeda & Suquet 1998). A fairly general homogenization method has been introduced by Ponte Castañeda (2002a), which delivers estimates that are exact to second-order in the heterogeneity contrast and that do not violate rigorous bounds. This "second-order" method, based on a variational principle, reduces to finding a set of constants that renders a certain functional stationary. To simplify the calculations, it was proposed, as an approximation in Ponte Castañeda (2002a), to replace some of these (full) stationarity conditions by a set of partial stationarity conditions. In this Note, the method is used to generate estimates for the effective behavior of nonlinear composites with spherical pores or rigid particles. In the process of this work, some limitations of the approximation mentioned above were identified, and some alternatives were evaluated.

We consider composite materials made of N different homogeneous constituents, or *phases*, which are assumed to be *randomly* distributed in a specimen occupying a volume Ω, at a length scale that is much smaller than the size of Ω and the scale of variation of the loading conditions. The constitutive behavior of each phase is characterized by a *convex* potential function $u^{(r)}$ $(r = 1, ..., N)$, such that the stress $\boldsymbol{\sigma}$ and strain $\boldsymbol{\varepsilon}$ tensors are related by

$$\boldsymbol{\varepsilon} = \frac{\partial u^{(r)}}{\partial \boldsymbol{\sigma}}(\boldsymbol{\sigma}). \tag{B.1}$$

This constitutive relation can be used within the context of the deformation theory of plasticity, where $\boldsymbol{\sigma}$ and $\boldsymbol{\varepsilon}$ represent the infinitesimal stress and strain, respectively. Relation (B.1) applies equally well to viscoplastic materials, in which case $\boldsymbol{\sigma}$ and $\boldsymbol{\varepsilon}$ represent the Cauchy stress and Eulerian strain rate, respectively.

We are concerned with the problem of finding the effective behavior of the composite, which is defined as the relation between the average stress $\overline{\boldsymbol{\sigma}} = \langle \boldsymbol{\sigma} \rangle$ and the average strain $\overline{\boldsymbol{\varepsilon}} = \langle \boldsymbol{\varepsilon} \rangle$, and can also be characterized (Ponte Castañeda & Suquet 1998) by an effective potential $\widetilde{U}$, such that

$$\overline{\boldsymbol{\varepsilon}} = \frac{\partial \widetilde{U}}{\partial \overline{\boldsymbol{\varepsilon}}}(\overline{\boldsymbol{\sigma}}), \quad \widetilde{U}(\overline{\boldsymbol{\sigma}}) = \min_{\boldsymbol{\sigma} \in \mathcal{K}(\overline{\boldsymbol{\sigma}})} \sum_{r=1}^{N} c^{(r)} \left\langle u^{(r)}(\boldsymbol{\sigma}) \right\rangle^{(r)}. \tag{B.2}$$

Here, $\langle \cdot \rangle$ and $\langle \cdot \rangle^{(r)}$ denote the volume averages over the composite (Ω) and over phase r ($\Omega^{(r)}$), respectively, $c^{(r)}$ is the volume fraction of phase r, and $\mathcal{K}(\overline{\boldsymbol{\sigma}}) = \{\boldsymbol{\sigma}, \mathrm{div}\boldsymbol{\sigma} = \mathbf{0} \text{ in } \Omega, \langle \boldsymbol{\sigma} \rangle = \overline{\boldsymbol{\sigma}}\}$ is the set of statically admissible stresses. Thus, the problem of estimating the effective behavior of the composite is equivalent to that of estimating the function $\widetilde{U}$.

B.2 Second-order homogenization estimates

The second-order method (Ponte Castañeda 2002a) delivers the following estimate for the effective potential of a general N-phase composite:

$$\widetilde{U}(\overline{\boldsymbol{\sigma}}) = \underset{\mathbf{M}_0^{(s)}}{\text{stat}} \left\{ \widetilde{U}_T(\overline{\boldsymbol{\sigma}}; \check{\boldsymbol{\sigma}}^{(s)}, \mathbf{M}_0^{(s)}) - \sum_{r=1}^{N} c^{(r)}\, V^{(r)}(\check{\boldsymbol{\sigma}}^{(r)}, \mathbf{M}_0^{(r)}) \right\}, \tag{B.3}$$

where the stat*ionary* operation consists in setting the partial derivative of the argument with respect to the variable equal to zero. In this expression, $\widetilde{U}_T$ is the effective potential of a *linear* comparison composite (LCC) with the same microstructure as the nonlinear composite, and phase potentials $u_T^{(r)}$ given by

$$u_T^{(r)}(\boldsymbol{\sigma}; \check{\boldsymbol{\sigma}}^{(r)}, \mathbf{M}_0^{(r)}) = u^{(r)}(\check{\boldsymbol{\sigma}}^{(r)}) + \frac{\partial u^{(r)}}{\partial \boldsymbol{\sigma}}(\check{\boldsymbol{\sigma}}^{(r)}) \cdot (\boldsymbol{\sigma} - \check{\boldsymbol{\sigma}}^{(r)}) + \frac{1}{2}(\boldsymbol{\sigma} - \check{\boldsymbol{\sigma}}^{(r)}) \cdot \mathbf{M}_0^{(r)}(\boldsymbol{\sigma} - \check{\boldsymbol{\sigma}}^{(r)}), \tag{B.4}$$

where the $\check{\boldsymbol{\sigma}}^{(r)}$ are uniform reference stresses, and $\mathbf{M}_0^{(r)}$, symmetric, constant, fourth-order tensors (of compliances). The "error functions" $V^{(r)}$ are defined as

$$V^{(r)}(\check{\boldsymbol{\sigma}}^{(r)}, \mathbf{M}_0^{(r)}) = \underset{\hat{\boldsymbol{\sigma}}^{(r)}}{\text{stat}} \left\{ u_T^{(r)}(\hat{\boldsymbol{\sigma}}^{(r)}; \check{\boldsymbol{\sigma}}^{(r)}, \mathbf{M}_0^{(r)}) - u^{(r)}(\hat{\boldsymbol{\sigma}}^{(r)}) \right\}, \tag{B.5}$$

where the $\hat{\boldsymbol{\sigma}}^{(r)}$ are uniform (stress) tensors in each phase, which are determined by the stationary condition in (B.5):

$$\frac{\partial u^{(r)}}{\partial \boldsymbol{\sigma}}(\hat{\boldsymbol{\sigma}}^{(r)}) - \frac{\partial u^{(r)}}{\partial \boldsymbol{\sigma}}(\check{\boldsymbol{\sigma}}^{(r)}) = \mathbf{M}_0^{(r)}\,(\hat{\boldsymbol{\sigma}}^{(r)} - \check{\boldsymbol{\sigma}}^{(r)}). \tag{B.6}$$

Note that the compliance tensors $\mathbf{M}_0^{(r)}$ correspond to "generalized secant" approximations to the nonlinear stress-strain relations.

In turn, the stationary operation in (B.3) leads to additional conditions in each phase r, given by

$$(\hat{\boldsymbol{\sigma}}^{(r)} - \check{\boldsymbol{\sigma}}^{(r)}) \otimes (\hat{\boldsymbol{\sigma}}^{(r)} - \check{\boldsymbol{\sigma}}^{(r)}) = \frac{2}{c^{(r)}} \frac{\partial \widetilde{U}_T}{\partial \mathbf{M}_0^{(r)}} = \left\langle (\boldsymbol{\sigma} - \check{\boldsymbol{\sigma}}^{(r)}) \otimes (\boldsymbol{\sigma} - \check{\boldsymbol{\sigma}}^{(r)}) \right\rangle^{(r)}, \tag{B.7}$$

which relate the variables $\hat{\boldsymbol{\sigma}}^{(r)}$ to the variables $\check{\boldsymbol{\sigma}}^{(r)}$ and $\mathbf{M}_0^{(r)}$ through the (intraphase) field fluctuations (about the references $\check{\boldsymbol{\sigma}}^{(r)}$) in the LCC.

Then, using the fact that (B.3) and (B.5) are stationary with respect to the tensors $\mathbf{M}_0^{(r)}$ and $\hat{\boldsymbol{\sigma}}^{(r)}$, respectively, we can rewrite the estimate (B.3) as:

$$\widetilde{U}(\overline{\boldsymbol{\sigma}}) = \sum_{r=1}^{N} c^{(r)} \left[u^{(r)}(\hat{\boldsymbol{\sigma}}^{(r)}) - \frac{\partial u^{(r)}}{\partial \boldsymbol{\sigma}}(\check{\boldsymbol{\sigma}}^{(r)}) \cdot (\hat{\boldsymbol{\sigma}}^{(r)} - \overline{\boldsymbol{\sigma}}^{(r)}) \right], \tag{B.8}$$

where $\overline{\boldsymbol{\sigma}}^{(r)} = \langle \boldsymbol{\sigma} \rangle^{(r)}$ is the average of the stress over phase r in the LCC. Equations (B.6) and (B.7) determine the variables $\hat{\boldsymbol{\sigma}}^{(r)}$ and $\mathbf{M}_0^{(r)}$ for any choice of the reference tensors $\check{\boldsymbol{\sigma}}^{(r)}$, which remain to be specified.

Completely analogous expressions may be developed (Ponte Castañeda 2002a) starting from the dual formulation for the strain potentials $w^{(r)}$, which are the Legendre transforms of $u^{(r)}$ (so that $\boldsymbol{\sigma} = \partial w^{(r)}/\partial \boldsymbol{\varepsilon}(\boldsymbol{\varepsilon})$). This formulation involves a LCC with phase potentials $w_T^{(r)}$, given by second-order Taylor approximations to $w^{(r)}$ of the same form as (B.4), in terms of reference strains $\check{\boldsymbol{\varepsilon}}^{(r)}$ and tensors of moduli $\mathbf{L}_0^{(r)}$, and generates the following estimate for the effective strain potential

$$\widetilde{W}(\overline{\boldsymbol{\varepsilon}}) = \sum_{r=1}^{N} c^{(r)} \left[w^{(r)}(\hat{\boldsymbol{\varepsilon}}^{(r)}) - \frac{\partial w^{(r)}}{\partial \boldsymbol{\varepsilon}}(\check{\boldsymbol{\varepsilon}}^{(r)}) \cdot (\hat{\boldsymbol{\varepsilon}}^{(r)} - \overline{\boldsymbol{\varepsilon}}^{(r)}) \right], \tag{B.9}$$

where $\overline{\boldsymbol{\varepsilon}}^{(r)} = \langle \boldsymbol{\varepsilon} \rangle^{(r)}$ in the LCC, and the tensors $\hat{\boldsymbol{\varepsilon}}^{(r)}$ and $\mathbf{L}_0^{(r)}$ depend on the reference tensors $\check{\boldsymbol{\varepsilon}}^{(r)}$ and the second moments of the strain fluctuations (in the LCC) through equations analogous to (B.6) and (B.7).

Choice of reference tensors. Ideally, the estimates (B.8) and (B.9) for $\widetilde{U}$ and $\widetilde{W}$ should be Legendre duals of each other (i.e., no *duality gap*). These estimates would indeed satisfy this requirement if they were stationary with respect to the reference tensors $\check{\boldsymbol{\sigma}}^{(r)}$ and $\check{\boldsymbol{\varepsilon}}^{(r)}$, respectively (see Section 6 in (Ponte Castañeda 2002a) for details). In addition, this prescription for the references would lead to potentials $u_T^{(r)}$ and $w_T^{(r)}$ that would also be Legendre duals of each other, and the effective stress-strain relation of this LCC would coincide with that obtained by differentiation of (B.8) and (B.9). Unfortunately, it has not yet been possible to find a satisfactory solution to the resulting system of equations.

For this reason, it was suggested, as an approximation in Ponte Castañeda (2002a), the use of the phase averages in the LCC as references, that is

$$\check{\boldsymbol{\sigma}}^{(r)} = \overline{\boldsymbol{\sigma}}^{(r)} \quad \text{and} \quad \check{\boldsymbol{\varepsilon}}^{(r)} = \overline{\boldsymbol{\varepsilon}}^{(r)}. \tag{B.10}$$

This choice is physically appealing, for the right-hand side in (B.7) becomes the covariance tensor of the field fluctuations in phase r. Besides, this choice can be shown to render $\widetilde{U}_T$ and $\widetilde{W}_T$ stationary, thus *partially* satisfing the stationarity condition with respect to the references (see expression (B.3)). However, this approximation leads to estimates for $\widetilde{U}$ and $\widetilde{W}$ that are *not* Legendre duals of each other, i.e., there is a *duality gap*. But it should be noted that the phase potentials $u_T^{(r)}$ and $w_T^{(r)}$ of the LCC's are still Legendre duals of each other (Ponte Castañeda 2002a), provided $\overline{\boldsymbol{\sigma}}$ in (B.8) and $\overline{\boldsymbol{\varepsilon}}$ in (B.9) are taken to be related by the effective stress-strain relation of the LCC. As will be seen in the next section, the choice (B.10) can lead to inconsistencies in certain cases, and therefore, other prescriptions need to be considered.

A simple alternative consists in the choices

$$\check{\boldsymbol{\sigma}}^{(r)} = \overline{\boldsymbol{\sigma}} \quad \text{and} \quad \check{\boldsymbol{\varepsilon}}^{(r)} = \frac{\partial u^{(r)}}{\partial \boldsymbol{\sigma}}(\overline{\boldsymbol{\sigma}}), \tag{B.11}$$

where $\overline{\boldsymbol{\sigma}}$ is the overall stress in the LCC. Note that the requirement $(B.11)_2$ implies that the $\check{\boldsymbol{\varepsilon}}^{(r)}$ are not equal to $\overline{\boldsymbol{\varepsilon}}$, but it does imply that $u_T^{(r)}$ and $w_T^{(r)}$ remain Legendre duals of each other (in the sense mentioned above).

For a given choice of reference tensors, the estimates (B.8) and (B.9) require the computation of the effective potentials $\widetilde{U}_T$ and $\widetilde{W}_T$, which can be obtained using any *linear* homogenization method appropriate for composites with local potentials $u_T^{(r)}$ and $w_T^{(r)}$, and the same microstructure as the nonlinear composite. It can be verified that expressions (B.8) and (B.9), together with (B.10), as well as with (B.11), are exact to second order in the heterogenity contrast, and therefore in agreement with the small-contrast expansion of Suquet & Ponte Castañeda (1993). It should be mentioned that Lahellec & Suquet (2004) have provided an alternative formulation of the second-order method, which has some advantages relative to the original formulation (Ponte Castañeda 1996), but still does not resolve the duality problem.

Choice of compliance tensors. The left-hand side of relation (B.7) is a rank-one tensor, whereas the right-hand side is, in general, of full rank. Therefore, equality cannot be enforced for all components of the tensorial relation, and only certain traces of it can be used. Consequently, the number of *independent* components of the tensors $\mathbf{M}_0^{(r)}$ can be at most equal to the number of components of $\hat{\boldsymbol{\sigma}}^{(r)}$. Thus, the estimates (B.8) cannot be fully stationary with respect to the variables $\mathbf{M}_0^{(r)}$.

For *isotropic*, incompressible phases with potentials depending only on the Von Mises equivalent stress σ_e, it was proposed in Ponte Castañeda (2002a) the use of *anisotropic*, incompressible tensors of the form

$$\mathbf{M}_0^{(r)} = (2\lambda_0^{(r)})^{-1}\mathbf{E}^{(r)} + (2\mu_0^{(r)})^{-1}\mathbf{F}^{(r)}, \tag{B.12}$$

where $\mathbf{E}^{(r)}$ and $\mathbf{F}^{(r)}$ are projection tensors with principal axes aligned with the reference stresses $\check{\boldsymbol{\sigma}}^{(r)}$. Then, expression (B.7) reduces to

$$\hat{\sigma}_{\parallel}^{(r)} = \check{\sigma}_e^{(r)} \pm \sqrt{\frac{3}{2}\left\langle(\boldsymbol{\sigma}-\check{\boldsymbol{\sigma}}^{(r)})\cdot\mathbf{E}^{(r)}(\boldsymbol{\sigma}-\check{\boldsymbol{\sigma}}^{(r)})\right\rangle^{(r)}}, \quad \hat{\sigma}_{\perp}^{(r)} = \pm\sqrt{\frac{3}{2}\left\langle\boldsymbol{\sigma}\cdot\mathbf{F}^{(r)}\boldsymbol{\sigma}\right\rangle^{(r)}}, \tag{B.13}$$

where $\hat{\sigma}_{\parallel}^{(r)} = \left(\frac{3}{2}\hat{\boldsymbol{\sigma}}^{(r)}\cdot\mathbf{E}^{(r)}\hat{\boldsymbol{\sigma}}^{(r)}\right)^{\frac{1}{2}}$ and $\hat{\sigma}_{\perp}^{(r)} = \left(\frac{3}{2}\hat{\boldsymbol{\sigma}}^{(r)}\cdot\mathbf{F}^{(r)}\hat{\boldsymbol{\sigma}}^{(r)}\right)^{\frac{1}{2}}$ are the "parallel" and "perpendicular" components of the traceless tensors $\hat{\boldsymbol{\sigma}}^{(r)}$, respectively. The sign of the square roots in (B.13) should be positive if $\check{\sigma}_e^{(r)} \leq \overline{\sigma}_e^{(r)}$, and negative otherwise, for consistency of (B.8) with the case of uniform fields (e.g., laminate, homogeneous limit). These same observations apply to the tensors $\mathbf{L}_0^{(r)}$ and $\hat{\boldsymbol{\varepsilon}}^{(r)}$ in the dual version.

B.3 Power-law composites

In this section we consider composite materials with phases characterized by isotropic, incompressible power-law potentials

$$u^{(r)}(\boldsymbol{\sigma}) = \frac{\varepsilon_0\sigma_0^{(r)}}{1+n}\left(\frac{\sigma_e}{\sigma_0^{(r)}}\right)^{1+n}, \quad n = 1/m, \tag{B.14}$$

where $\sigma_0^{(r)}$ is the flow stress of phase r, m is such that $0 \leq m \leq 1$, ε_0 is a reference strain, and σ_e is the von Mises equivalent stress. Note that $m = 1$ and $m = 0$ correspond to linear and rigid-ideally plastic behaviors, respectively. For simplicity, we consider statistically isotropic microstructures, and phase potentials (B.14) with the same exponent m. It then follows that the effective potential can be written as

$$\widetilde{U}(\overline{\boldsymbol{\sigma}}) = \frac{\varepsilon_0 \widetilde{\sigma}_0}{1+n} \left(\frac{\overline{\sigma}_e}{\widetilde{\sigma}_0} \right)^{1+n}, \tag{B.15}$$

where $\widetilde{\sigma}_0$ is the effective flow stress, completely characterizing the effective behavior. In two-dimensional problems, such as transverse shear of a matrix with aligned fibers, $\widetilde{\sigma}_0$ is a function of m, $\sigma_0^{(r)}$, and the volume fractions of the phases. In three dimensions, $\widetilde{\sigma}_0$ also depends on the plastic phase angle θ, which in turn is related to the two invariants of the deviatoric stress $\overline{\boldsymbol{\sigma}}_d$ through $\cos(3\theta) = 4 \det(\overline{\boldsymbol{\sigma}}_d)/\overline{\sigma}_e^3$.

The extreme cases of infinite contrast are of particular interest. The results given in the following subsections correspond to a matrix (phase 1) with flow stress $\sigma_0^{(1)} = \sigma_0$, with randomly distributed spherical pores or rigid particles (phase 2) at volume fraction $c^{(2)} = c$. Only the case of axisymmetric shear ($\theta = 0$) is considered in some detail. The Hashin-Shtrikman (HS) estimates of Willis (1977) are used to estimate the effective behavior of the associated LCC. These estimates are known to be appropriate for (linear) particulate media at low to moderate concentrations, and are exact to second-order in the heterogeneity contrast. Both, the stress (U) and the strain (W) versions of the second-order (SO) estimates of the previous section are provided for two different choices of reference tensors. We denote by I the estimates associated with (B.10), whereas those associated with (B.11) are denoted by II. These estimates are compared with the "original" HS second-order (OSO) estimates of Ponte Castañeda (1996), which do not make use of the field fluctuations in the linearization, as well as the corresponding "variational" HS estimates of Ponte Castañeda (1991). The latter are actually rigorous upper bounds for all other nonlinear HS estimates, and, in particular, for the second-order estimates. They all coincide, of course, for $m = 1$, where they reduce to the linear HS estimates. Also included for comparison purposes are the classical upper and lower bounds of Voigt and Reuss.

B.3.1 Porous materials

Figure B.1 provides upper bounds and estimates for the effective flow stress $\widetilde{\sigma}_0$ for the porous case. We begin by noting that, unlike the OSO estimates (dashed lines), the SO-I estimates satisfy the HS variational bound (long-dashed lines) for all values of the nonlinearity exponent m (see fig. B.1a). Furthermore, the duality gap is found to vanish for $m = 0$, and it is negligible for most values of m, except in a small interval around $m^* \approx 0.15$. At this value of the nonlinearity exponent, the W-version presents a kink. This is related to the fact that, as will be explained shortly, the choice $(\text{B.10})_2$ cannot be enforced for $m < m^*$ in this particular case. In contrast, both versions of the

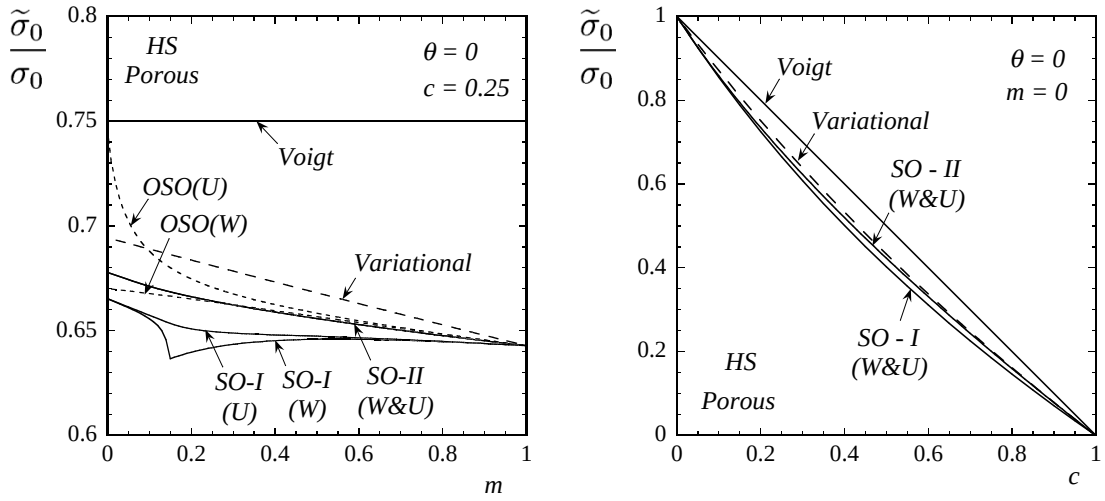

Figure B.1: Upper bounds and estimates of the Hashin-Shtrikman (HS) type for the effective flow stress $\widetilde{\sigma}_0$ of a power-law porous material subject to axisymmetric shear ($\theta = 0$): a) as a function of the nonlinearity exponent m with a given concentration of pores ($c = 0.25$); b) as a function of the pore concentration c with a rigid-ideally plastic matrix ($m = 0$).

SO-II estimates are found to be smooth functions of the nonlinearity exponent, since choice (B.11) is consistent for all values of m. These estimates lie closer to the variational bound than the SO-I, still satisfing it for all m, and present a duality gap which is negligible for all m and even vanishes in the ideally-plastic limit ($m = 0$). It should be noted that the differences between the SO-I and SO-II estimates are not as significant as the enlarged scale in this figure might suggest. A fairer comparison is provided in fig. B.1b, where estimates for the limiting case $m = 0$ are shown as a function of the concentration of pores c. The SO-II estimates are found to lie between the SO-I and the variational bound for all c, the differences being small. In fact, the SO-I & II estimates can be shown to agree in the dilute limit, for any m, with the OSO(W) estimates, as given by the first-order expansion of expression (5.4) of Ponte Castañeda (1996) with $\theta = 0$, for small concentrations of pores.

Figure B.2a shows the "anisotropy" ratio $k = \lambda_0/\mu_0$ of elastic moduli (see expression (B.12)) in the matrix of the LCC's associated with the second-order estimates of fig. B.1a. The OSO estimates make use of a tangent compliance tensor, which for potentials (B.14) takes the form (B.12) with $k = m$, whereas the anisotropy of the more general compliance tensors used by the SO estimates depends not only on m but also on c. In the linear case ($m = 1$), these tensors are isotropic, so that $k = 1$, and as the nonlinearity increases they become progressively more anisotropic. The main observation in the context of this figure is that when prescription (B.10) is used, the associated k-I vanishes at a finite value m^* (already introduced in the context of fig. B.1a). In fact, for $m < m^*$, insisting on the prescription (B.10) for the references would lead to negative values of k, which is unacceptable since this implies a matrix with a negative definite compliance tensor in the LCC. The SO-I estimates provided in this Note were obtained by initially assuming an arbitrary $\check{\boldsymbol{\sigma}}^{(1)}$, with the corresponding reference strain given by $\check{\boldsymbol{\varepsilon}}^{(1)} = \partial u^{(1)}/\partial \boldsymbol{\sigma}(\check{\boldsymbol{\sigma}}^{(1)})$, and then taking the limit $\check{\boldsymbol{\sigma}}^{(1)} \to \overline{\boldsymbol{\sigma}}^{(1)}$.

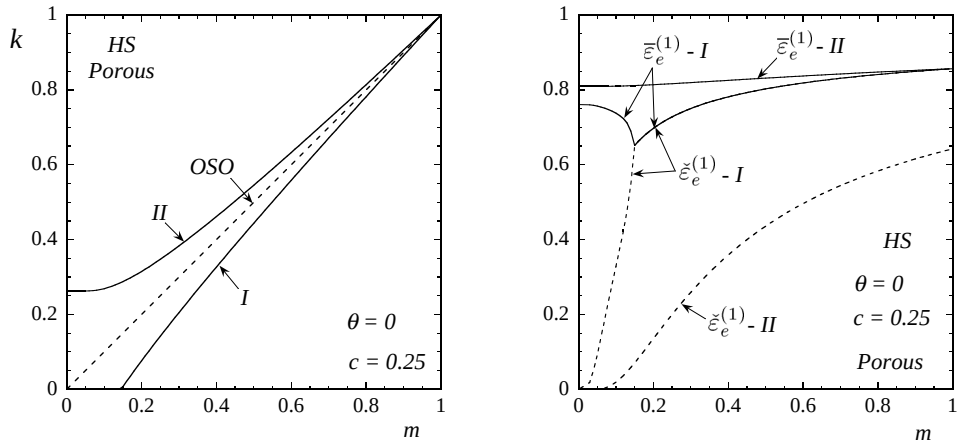

Figure B.2: a) Anisotropy ratio $k = \lambda_0/\mu_0$ of the matrix in the LCC, and b) equivalent average strain $\overline{\varepsilon}_e^{(1)}$ (continuous lines) and reference $\breve{\varepsilon}_e^{(1)}$ (dashed lines) in the matrix of the LCC, normalized by the equivalent applied strain $\overline{\varepsilon}_e$, as a function of the nonlinearity exponent m, for a power-law porous material with a given concentration of pores ($c = 0.25$), subject to axisymmetric shear ($\theta = 0$).

As can be seen in fig. B.2b, the resulting $\breve{\varepsilon}_e^{(1)}$-$I$ and $\overline{\varepsilon}_e^{(1)}$-$I$ coincide for $m \geq m^*$, in accordance with $(\text{B.10})_2$, but for $m < m^*$ we have that $k = 0$ and the relation between $\breve{\boldsymbol{\varepsilon}}^{(1)}$ and $\breve{\boldsymbol{\sigma}}^{(1)}$ mentioned above no longer implies $(\text{B.10})_2$. On the other hand, the alternative choice (B.11) leads to a well-behaved k-II that tends to some finite value, dependent on c, in the ideally-plastic limit. Moreover, $\overline{\boldsymbol{\varepsilon}}^{(1)}$-$II$ is different from $\breve{\boldsymbol{\varepsilon}}^{(1)}$-$II$ for all values of m, and exhibits a smooth behavior even at high nonlinearities (see fig. B.2b).

In view of the smaller duality gap and the smoother behavior of the corresponding LCC, the prescription (B.11) is to be preferred to the earlier prescription (B.10). However, only comparisons with exact results will allow corroboration of this choice.

B.3.2 Rigidly-reinforced materials

Figure B.3 provides bounds and estimates for the effective flow stress $\widetilde{\sigma}_0$ for the case of rigid reinforcement. The SO-I estimates are not shown for brevity, but it is worth mentioning that the associated k behaves similarly to the k-I shown in fig. B.2a, for the reasons described above. Here, the SO-II estimates, unlike the OSO ones, are found to satisfy the bounds for all values of m, and exhibit essentially no duality gap (see fig. B.3a). Fig. B.3b shows that the SO-II estimates lie below the corresponding OSO(W) estimates for all c, although the differences are small. In fact, they can be shown to agree in the dilute limit, as given by expression (5.3) of Ponte Castañeda (1996) with $\theta = 0$, for any m.

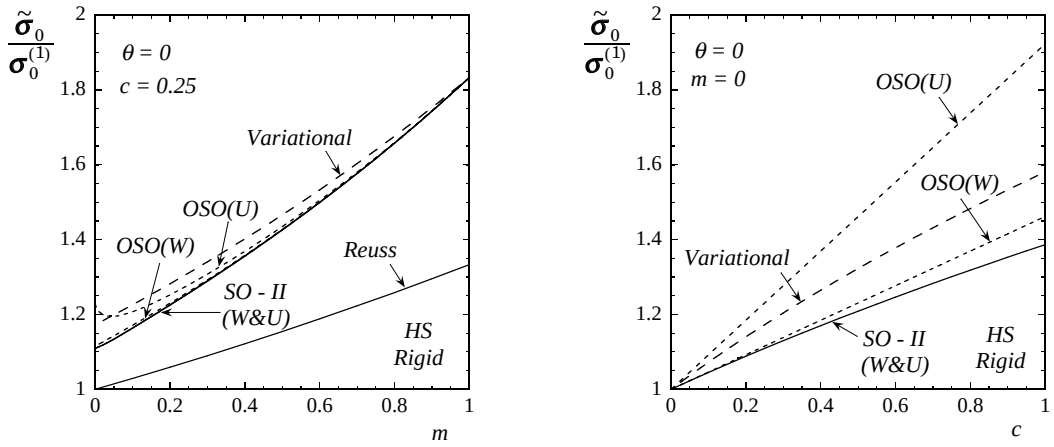

Figure B.3: Bounds and estimates of the Hashin-Shtrikman (HS) type for the effective flow stress $\widetilde{\sigma}_0$ of a rigidly-reinforced power-law material subject to axisymmetric shear ($\theta = 0$): a) as a function of the nonlinearity exponent m with a given concentration of particles ($c = 0.25$); b) as a function of the particle concentration c for the case of a rigid-ideally plastic matrix ($m = 0$).

B.4 Final comments

Estimates of the HS type have also been obtained for the case of simple shear ($\theta = \pi/6$). The trends for $\widetilde{\sigma}_0$ were found to be similar to those given in (Ponte Castañeda 2002b) for the in-plane shearing of $2D$ random fiber composites. Interestingly, for a dilute concentration of (cylindrical) pores in a rigid-ideally plastic matrix subject to simple shear, it was found in (Ponte Castañeda 2002b) that

$$\frac{\widetilde{\sigma}_0}{\sigma_0} \sim 1 - \frac{3}{2}\left(\frac{c}{2}\right)^{2/3},$$

which is non-analytic at $c = 0$. For simple shear of ($3D$) spherical pores in a rigid-ideally plastic matrix, the corresponding dilute limit is found to be

$$\frac{\widetilde{\sigma}_0}{\sigma_0} \sim 1 - \frac{1}{4}\, c|\ln c|,$$

which is also non-analytic at $c = 0$, but with a *weaker* singularity. Weaker singularities in $3D$ than in $2D$ have already been found by Drucker (1966) for the case of *periodic* arrays of pores. The question remains as to whether the singularities predicted by the second-order method for the random case may be indeed correct. That this might be the case is suggested by the comparisons with numerical results provided by Pastor & Ponte Castañeda (2002). In any case, the mere fact that the second-order method can capture some signature of the strongly nonlinear fields associated with ideally-plastic composites is already a positive result, as no other method to date seems to able to do so.

We conclude by emphasizing that the issue of the best choice for the reference tensors $\check{\boldsymbol{\sigma}}^{(r)}$ and $\check{\boldsymbol{\varepsilon}}^{(r)}$ in the context of the second-order method remains largely open. Nonetheless, the results provided in this Note suggest that the identification of $\check{\boldsymbol{\sigma}}^{(r)}$ with the macroscopic average $\overline{\boldsymbol{\sigma}}$ appears to give reasonable estimates. Although giving sensible estimates for most situations, the earlier choice for

these variables (i.e., the phase averages $\overline{\boldsymbol{\sigma}}^{(r)}$) suggested in Ponte Castañeda (2002a) can lead to inconsistent results for strong nonlinearities, if care is not taken to ensure that the LCC remains strongly elliptic. To avoid this complication, the use of the prescription (B.11) is recommended.

Acknowledgments

This work was supported by NSF grant CMS-02-01454.

Appendix C

Macroscopic behavior and field fluctuations in viscoplastic composites: second-order estimates versus full-field simulations[1]

M.I. Idiart[a,b], H. Moulinec[c], P. Ponte Castañeda[a,b], P. Suquet[c]

[a] Laboratoire de Mécanique des Solides, C.N.R.S. UMR7649, Département de Mécanique, École Polytechnique, 91128 Palaiseau Cedex, France.

[b] Department of Mechanical Engineering and Applied Mechanics, University of Pennsylvania, Philadelphia, PA 19104-6315, U.S.A.

[c] L.M.A./C.N.R.S., 31 Chemin Joseph Aiguier, 13402 Marseille Cedex 20, France.

Abstract — This work presents a combined numerical and theoretical study of the effective behavior and statistics of the local fields in random viscoplastic composites. The full-field numerical simulations make use of a method based on the fast Fourier transform (FFT) algorithm (Moulinec & Suquet, C.R. Acad. Sci. Paris II 318 (1994) 1417), while the theoretical estimates follow from the so-called "second-order" procedure (Ponte Castañeda, J. Mech. Phys. Solids 50 (2002) 737). Two-phase fiber composites with power-law phases are considered in detail, for two different heterogeneity contrasts corresponding to fiber-reinforced and fiber-weakened composites. In both cases, the FFT simulations show strain-rate fluctuations that increase significantly and become progressively more anisotropic as the nonlinearity increases. Furthermore, the strain-rate fluctuations tend to become unbounded in the perfectly plastic limit. This is found to be related to localization of the strain field into bands running through the composite with certain preferential directions determined by the loading conditions. The bands tend to

[1]This chapter appeared in *J. Mech. Phys. Solids* **54** (2006) 1029–1063

avoid the fibers when these are stronger than the matrix, and to pass through the fibers when these are weaker than the matrix. In general, the "second-order" estimates are found to be in good agreement with the FFT simulations, even for high nonlinearities, improving—often in qualitative terms—on earlier nonlinear homogenization estimates for both the macroscopic behavior and the first two moments of the local fields. In addition, it is shown that the "second-order" method can be used to extract useful information about the anisotropic distribution of the local fields in these nonlinear composites.

C.1 Introduction

Homogenization methods for nonlinear heterogeneous media have come a long way since the early work of Taylor (1938) to estimate the effective behavior of viscoplastic polycrystals. Following the development of rigorous bounds by Talbot and Willis (1985), who made use of an extension of the Hashin-Shtrikman variational principles for nonlinear media (Willis, 1983), a novel "variational" method was proposed by Ponte Castañeda (1991) to generate more general types of estimates for the effective behavior of nonlinear composites in terms of suitably optimized *linear comparison composites* (LCCs). Closely related methods have been developed by Suquet (1993) for the special cases of power-law composites. Suquet (1995) and Hu (1996) have shown that the "variational" method of Ponte Castañeda (1991) could be given an alternative interpretation as a "modified secant" approach, thus establishing a link with the second moments of the local fields in the LCC. In an attempt to improve on these "variational" estimates, and in particular, to generate estimates that are exact to second order in the heterogeneity contrast, and therefore agree with the perturbation expansions of Suquet and Ponte Castañeda (1993) for weakly inhomogeneous nonlinear composites, Ponte Castañeda (1996) proposed a "second-order" method, which made use of an LCC with elastic moduli given by the tangent moduli of the nonlinear phases evaluated at the phase averages of the fields in the LCC. However, this method may violate the rigorous bounds provided by the earlier "variational" method when the field fluctuations are large, as is the case near the percolation limit. Motivated by this finding, Ponte Castañeda (2002a) proposed an improved "second-order" method that makes use of a "generalized secant" interpolation of the nonlinear constitutive relations, incorporating dependence on both the first and second moments of the relevant fields in the LCCs.

In parallel developments, methods have also been developed for computing numerically the effective behavior of nonlinear composites. One of these methods that is particularly well suited to strongly nonlinear composites, such as viscoplastic materials with low strain-rate sensitivity, or in the limit, ideally plastic materials, is the Fast Fourier Transform (FFT) method first proposed by Moulinec and Suquet (1994, 1998), and developed further by Michel, Moulinec and Suquet (2001). Such accurate numerical simulations allow for, among other things, comparisons with the above-mentioned theoretical approaches with the objective of assessing the accuracy of the latter. Comparisons of this type

have already been carried out (Moulinec and Suquet 2003, 2004) in the context of the earlier "variational" method showing that, while more accurate in general than earlier methods, the "variational" method can lead to inaccurate predictions for large values of the heterogeneity parameter and strong nonlinearities. One of the goals of this study is to investigate the accuracy of the "second-order" estimates, particularly with reference to the earlier variational approach.

In the development of the "second-order" method, it was recognized (Ponte Castañeda, 2002a) that this method could not only be used to generate estimates for the effective behavior of the nonlinear composite, but also to extract estimates for the covariance of the field fluctuations in the phases of the nonlinear composite. Such information could be useful for obtaining improved descriptions of microstructure evolution in composite materials and polycrystals that are subjected to finite-deformation processes, as well as for developing statistical theories of damage nucleation and evolution in heterogeneous material systems. Field fluctuations in *linear* composites have been studied by Bobeth and Diener (1987), Parton and Buryachenko (1990), and Cheng and Torquato (1997), among others. A combined experimental and theoretical study of field fluctuations in two-phase elastoplastic solids was given by Bornert et al. (1994). In the context of conductivity, Pellegrini (2000) conjectured that the distribution of the local fields in the constituent phases of composites with linear constitutive behavior is Gaussian, and suggested that this could also be a good approximation for composites with nonlinear constitutive behavior (Pellegrini, 2001). Another objective of this work is to investigate this point further.

In connection with applications of the "second-order" method to porous and two-phase power-law composites, Ponte Castañeda (2002b) and Idiart and Ponte Castañeda (2003) found that the covariance of the field fluctuations generally increase and become highly anisotropic with increasing nonlinearity. The conjecture was then made in these works that the developing anisotropy of the field fluctuations with nonlinearity could be correlated with the known fact that the strain fields become localized and preferentially oriented for strongly nonlinear composites (*e.g.*, Moulinec and Suquet, 1998). Of course, the numerical simulations allow for the characterization of the full fields in the composite, and it is natural to compute, in particular, the covariance of the field fluctuations in the phases of the nonlinear composite, and to compare them with the theoretical predictions, in an attempt to assess whether the homogenization theories can be used to reliably extract information about the field fluctuations. A preliminary study of such comparisons has been carried out recently by Moulinec and Suquet (2003, 2004) in the context of the isotropic "variational" method, and it has been shown there that the predictions of this method for the second moments of the fields are not accurate.

In the present work, comparisons will be made between the theoretical predictions of the "second-order" method for the averages and standard deviations of the fields in the phases of a certain class of nonlinear composites with particulate microstructure, and the corresponding results from the full-field numerical simulations. The objective will be to see how accurate the "second-order" predictions for these first- and second-order statistics of the fields are, and whether such statistics can be used to

gain *a priori* insight into the actual distribution of the fields in the physical space. More generally, the full distributions of the fields will be computed in order to assess the relative importance of the higher moments (higher than second) of the fields, as well as their implication for the homogenization methods based on the use of linear comparison composites.

C.2 Preliminaries on viscoplastic composites

We consider composite materials made of N different homogeneous constituents, or *phases*, which are assumed to be *randomly* distributed in a specimen occupying a volume Ω, with boundary $\partial\Omega$, at a length scale that is much smaller than the size of Ω and the scale of variation of the the loading conditions. The constitutive behavior of the viscoplastic phases is characterized by *convex* dissipation (or strain-rate) potentials $w^{(r)}$ $(r = 1, ..., N)$, such that the Cauchy stress $\boldsymbol{\sigma}$ and Eulerian strain rate $\boldsymbol{\varepsilon}$ are related by

$$\boldsymbol{\sigma} = \frac{\partial w}{\partial \boldsymbol{\varepsilon}}(\mathbf{x}, \boldsymbol{\varepsilon}), \quad w(\mathbf{x}, \boldsymbol{\varepsilon}) = \sum_{r=1}^{N} \chi^{(r)}(\mathbf{x})\ w^{(r)}(\boldsymbol{\varepsilon}), \tag{C.1}$$

where the characteristic functions $\chi^{(r)}$ serve to describe the microstructure, being 1 if the position vector $\mathbf{x}$ is in phase r, and 0 otherwise. These relations can also be used to represent nonlinear elastic behavior within the context of small deformations, $\boldsymbol{\sigma}$ and $\boldsymbol{\varepsilon}$ being identified with the infinitesimal stress and strain, respectively. In turn, that problem is mathematically equivalent to the deformation theory of plasticity.

Let $\langle\cdot\rangle$ and $\langle\cdot\rangle^{(r)}$ denote the volume averages over the composite (Ω) and over phase r $(\Omega^{(r)})$, respectively. We are concerned with the problem of finding the *effective behavior* of the composite, which is defined as the relation between the average stress $\overline{\boldsymbol{\sigma}} = \langle\boldsymbol{\sigma}\rangle$ and the average strain rate $\overline{\boldsymbol{\varepsilon}} = \langle\boldsymbol{\varepsilon}\rangle$. The procedure which relates $\overline{\boldsymbol{\sigma}}$ and $\overline{\boldsymbol{\varepsilon}}$ by means of the local constitutive behavior is called homogenization. A rigorous derivation of the mathematical theory of homogenization has been given by Marcellini (1978) for composites with strictly convex local potentials $w(\mathbf{x}, \boldsymbol{\varepsilon})$ with a appropriate growth in $\boldsymbol{\varepsilon}$ at infinity. The limiting case of rigid-perfectly plastic composites, for which the potentials are convex but not strictly convex, requires special treatment as in Bouchitte and Suquet (1991). (In that case, the derivatives in relations (C.1) and (2.7) are to be understood in the sense of subdifferentials.)

The effective behavior can be determined from the *effective strain-rate potential*, which, using the minimum dissipation principle, can be written as

$$\widetilde{W}(\overline{\boldsymbol{\varepsilon}}) = \inf_{\boldsymbol{\varepsilon}\in\mathcal{K}(\overline{\boldsymbol{\varepsilon}})} \langle w(\mathbf{x}, \boldsymbol{\varepsilon})\rangle = \inf_{\boldsymbol{\varepsilon}\in\mathcal{K}(\overline{\boldsymbol{\varepsilon}})} \sum_{r=1}^{N} c^{(r)}\ \langle w^{(r)}(\boldsymbol{\varepsilon})\rangle^{(r)}, \tag{C.2}$$

where $c^{(r)}$ denotes the volume fraction of phase r, and $\mathcal{K}(\overline{\boldsymbol{\varepsilon}})$ is the set of kinematically admissible strain-rate fields, such that there is a velocity field $\mathbf{v}$ satisfying $\boldsymbol{\varepsilon} = \left[\nabla\mathbf{v} + (\nabla\mathbf{v})^T\right]/2$ in Ω, and $\mathbf{v} = \overline{\boldsymbol{\varepsilon}}\,\mathbf{x}$ on $\partial\Omega$. Under the given hypothesis, the above formula can be simplified for periodic microstructures,

as discussed in more detail in section C.4.1. Physically, $\widetilde{W}$ corresponds to the energy dissipated in the composite when subjected to affine velocities on the boundary, with prescribed strain rate $\overline{\boldsymbol{\varepsilon}} = \langle \boldsymbol{\varepsilon} \rangle$.

Alternatively, the behavior of the phases can be characterized by *convex* stress potentials $u^{(r)}$, which are the Legendre transforms of $w^{(r)}$, that is

$$u^{(r)}(\boldsymbol{\sigma}) = \operatorname*{stat}_{\boldsymbol{\varepsilon}} \left\{ \boldsymbol{\sigma} \cdot \boldsymbol{\varepsilon} - w^{(r)}(\boldsymbol{\varepsilon}) \right\} \doteq (w^{(r)})^*(\boldsymbol{\sigma}). \tag{C.3}$$

The stat*ionary* operation consists in setting the partial derivative of the argument with respect to the variable equal to zero, solving for the variable, and substituting the result back into the argument. Then, the local stress and strain-rate tensors are related by

$$\boldsymbol{\varepsilon} = \frac{\partial u}{\partial \boldsymbol{\sigma}}(\boldsymbol{\sigma}), \quad u(\mathbf{x}, \boldsymbol{\sigma}) = \sum_{r=1}^{N} \chi^{(r)}(\mathbf{x})\ u^{(r)}(\boldsymbol{\sigma}), \tag{C.4}$$

and the effective behavior can be described in terms of the *effective stress potential*, which, using the minimum complementary-energy principle, can be written as

$$\widetilde{U}(\overline{\boldsymbol{\sigma}}) = \inf_{\boldsymbol{\sigma} \in \mathcal{S}(\overline{\boldsymbol{\sigma}})} \langle u(\mathbf{x}, \boldsymbol{\sigma}) \rangle = \inf_{\boldsymbol{\sigma} \in \mathcal{S}(\overline{\boldsymbol{\sigma}})} \sum_{r=1}^{N} c^{(r)}\ \langle u^{(r)}(\boldsymbol{\sigma}) \rangle^{(r)}, \tag{C.5}$$

where $\mathcal{S}(\overline{\boldsymbol{\sigma}})$ is the set of self-equilibrated stresses such that $\overline{\boldsymbol{\sigma}} = \langle \boldsymbol{\sigma} \rangle$.

Given the definitions (C.2) and (C.5) for the effective potentials, it can be shown (see, for example, Ponte Castañeda and Suquet, 1998) that the average strain-rate and average stress are related by

$$\overline{\boldsymbol{\sigma}} = \frac{\partial \widetilde{W}}{\partial \overline{\boldsymbol{\varepsilon}}}(\overline{\boldsymbol{\varepsilon}}) \quad \text{and} \quad \overline{\boldsymbol{\varepsilon}} = \frac{\partial \widetilde{U}}{\partial \overline{\boldsymbol{\sigma}}}(\overline{\boldsymbol{\sigma}}). \tag{C.6}$$

These relations provide the macroscopic constitutive relations for the composite. The variational formulations (C.2) and (C.5) can be shown to be completely equivalent, in the sense that the functions $\widetilde{W}$ and $\widetilde{U}$ are Legendre duals of each other. In general, these functions are very difficult to compute, since they require the solution to sets of nonlinear partial differential equations with randomly oscillating coefficients. In the next section we describe a variational method for estimating these effective potentials.

C.3 Second-order variational estimates

In this section, an outline is given of the "second-order" homogenization method introduced by Ponte Castañeda (2002a). Like earlier nonlinear homogenization methods, it is based on the construction of a *linear comparison composite* (LCC), with the same microstructure as the nonlinear composite, whose constituent phases are identified with appropriate linearizations of the given nonlinear phases. This allows the use of the many different methods already available to bound and estimate the effective behavior of *linear* composites to generate corresponding estimates for the effective behavior of *nonlinear* heterogeneous media.

C.3.1 Estimates for the effective behavior

The second-order method can be formulated using either strain-rate or stress potentials. We begin here by considering the stress formulation. In this case, a LCC is introduced with a stress potential given by

$$u_T(\mathbf{x},\boldsymbol{\sigma}) = \sum_{r=1}^{N} \chi^{(r)}(\mathbf{x})\; u_T^{(r)}(\boldsymbol{\sigma}), \tag{C.7}$$

where the characteristic functions $\chi^{(r)}$ are the same as those for the nonlinear composite, and the phase potentials $u_T^{(r)}$ are given by second-order Taylor approximations to the corresponding stress potentials $u^{(r)}$,

$$u_T^{(r)}(\boldsymbol{\sigma}) = u^{(r)}(\check{\boldsymbol{\sigma}}^{(r)}) + \frac{\partial u^{(r)}}{\partial \boldsymbol{\sigma}}(\check{\boldsymbol{\sigma}}^{(r)}) \cdot (\boldsymbol{\sigma} - \check{\boldsymbol{\sigma}}^{(r)}) + \frac{1}{2}(\boldsymbol{\sigma} - \check{\boldsymbol{\sigma}}^{(r)}) \cdot \mathbf{M}^{(r)}(\boldsymbol{\sigma} - \check{\boldsymbol{\sigma}}^{(r)}), \tag{C.8}$$

where $\check{\boldsymbol{\sigma}}^{(r)}$ are uniform reference stresses, and $\mathbf{M}^{(r)}$ are uniform, symmetric, fourth-order tensors (viscous compliances). Note that the stress-strain-rate relations associated with (C.8) correspond to that of a "thermoelastic" material, given by $\boldsymbol{\varepsilon} = \mathbf{M}^{(r)}\boldsymbol{\sigma} + \boldsymbol{\eta}^{(r)}$, where $\boldsymbol{\eta}^{(r)} = \partial u^{(r)}/\partial \boldsymbol{\sigma}(\check{\boldsymbol{\sigma}}^{(r)}) - \mathbf{M}^{(r)}\check{\boldsymbol{\sigma}}^{(r)}$ are uniform strain-rate polarization tensors. The effective stress potential $\widetilde{U}_T$ associated with this LCC can be written as (Laws, 1973; Willis, 1981)

$$\widetilde{U}_T(\overline{\boldsymbol{\sigma}}; \check{\boldsymbol{\sigma}}^{(s)}, \mathbf{M}^{(s)}) = \inf_{\boldsymbol{\sigma} \in \mathcal{S}(\overline{\boldsymbol{\sigma}})} \langle u_T(\mathbf{x},\boldsymbol{\sigma}) \rangle = \tilde{g} + \widetilde{\boldsymbol{\eta}} \cdot \overline{\boldsymbol{\sigma}} + \frac{1}{2}\overline{\boldsymbol{\sigma}} \cdot \widetilde{\mathbf{M}}\overline{\boldsymbol{\sigma}}, \tag{C.9}$$

where $\tilde{g}$, $\widetilde{\boldsymbol{\eta}}$, and $\widetilde{\mathbf{M}}$ are the relevant effective energy at zero applied stress, the effective polarization, and effective viscous-compliance tensor, respectively.

The central idea of the method is to choose the variables $\check{\boldsymbol{\sigma}}^{(r)}$ and $\mathbf{M}^{(r)}$ in such a way as to generate the best possible estimates for the effective potential $\widetilde{U}$ of the nonlinear composite in terms of corresponding estimates for the effective potential $\widetilde{U}_T$ of the LCC. To that end, a suitably designed variational principle is used, which leads to the following estimate for $\widetilde{U}$ (see Ponte Castañeda, 2002a):

$$\widetilde{U}(\overline{\boldsymbol{\sigma}}) = \operatorname*{stat}_{\mathbf{M}^{(s)}} \left\{ \widetilde{U}_T(\overline{\boldsymbol{\sigma}}; \check{\boldsymbol{\sigma}}^{(s)}, \mathbf{M}^{(s)}) - \sum_{r=1}^{N} c^{(r)}\, V^{(r)}(\check{\boldsymbol{\sigma}}^{(r)}, \mathbf{M}^{(r)}) \right\}, \tag{C.10}$$

where an equality has been used in the sense of a variational approximation. The second term in (C.10) involves "error functions" $V^{(r)}$, which are defined by

$$V^{(r)}(\check{\boldsymbol{\sigma}}^{(r)}, \mathbf{M}^{(r)}) = \operatorname*{stat}_{\hat{\boldsymbol{\sigma}}^{(r)}} \left\{ u_T^{(r)}(\hat{\boldsymbol{\sigma}}^{(r)}) - u^{(r)}(\hat{\boldsymbol{\sigma}}^{(r)}) \right\}, \tag{C.11}$$

where $\hat{\boldsymbol{\sigma}}^{(r)}$ are uniform (stress) tensors in each phase.

The stationary operation in (C.11) leads to the following conditions for the variables $\hat{\boldsymbol{\sigma}}^{(r)}$:

$$\frac{\partial u^{(r)}}{\partial \boldsymbol{\sigma}}(\hat{\boldsymbol{\sigma}}^{(r)}) - \frac{\partial u^{(r)}}{\partial \boldsymbol{\sigma}}(\check{\boldsymbol{\sigma}}^{(r)}) = \mathbf{M}^{(r)}\,(\hat{\boldsymbol{\sigma}}^{(r)} - \check{\boldsymbol{\sigma}}^{(r)}). \tag{C.12}$$

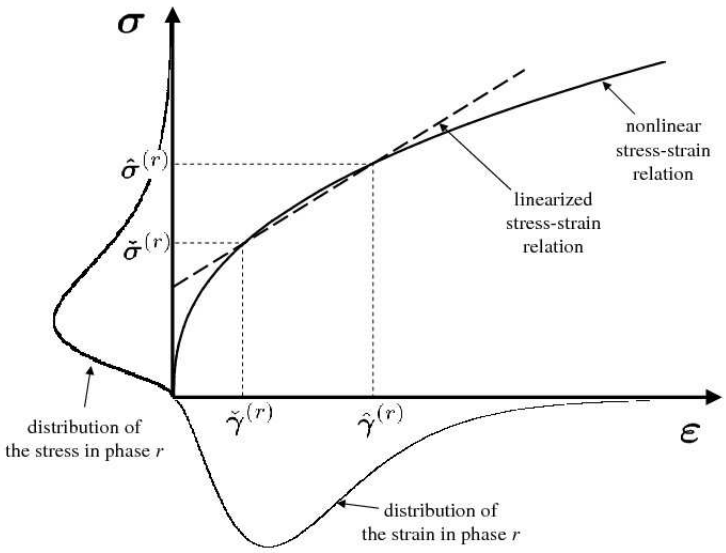

Figure C.1: One-dimensional sketch of the nonlinear stress-strain-rate relation and the "generalized secant" linearization used by the second-order method. The symbols $\check{\boldsymbol{\gamma}}^{(r)}$ and $\hat{\boldsymbol{\gamma}}^{(r)}$ denote the strain rates associated with the stresses $\check{\boldsymbol{\sigma}}^{(r)}$ and $\hat{\boldsymbol{\sigma}}^{(r)}$, respectively.

In turn, the stationary operation with respect to the tensors $\mathbf{M}^{(r)}$ in expression (C.10) leads to the conditions

$$(\hat{\boldsymbol{\sigma}}^{(r)} - \check{\boldsymbol{\sigma}}^{(r)}) \otimes (\hat{\boldsymbol{\sigma}}^{(r)} - \check{\boldsymbol{\sigma}}^{(r)}) = \frac{2}{c^{(r)}} \frac{\partial \widetilde{U}_T}{\partial \mathbf{M}^{(r)}} = \Big\langle (\boldsymbol{\sigma} - \check{\boldsymbol{\sigma}}^{(r)}) \otimes (\boldsymbol{\sigma} - \check{\boldsymbol{\sigma}}^{(r)}) \Big\rangle^{(r)} . \tag{C.13}$$

These last relations can be rewritten as

$$(\hat{\boldsymbol{\sigma}}^{(r)} - \check{\boldsymbol{\sigma}}^{(r)}) \otimes (\hat{\boldsymbol{\sigma}}^{(r)} - \check{\boldsymbol{\sigma}}^{(r)}) = \mathbf{C}_{\boldsymbol{\sigma}}^{(r)} + (\overline{\boldsymbol{\sigma}}^{(r)} - \check{\boldsymbol{\sigma}}^{(r)}) \otimes (\overline{\boldsymbol{\sigma}}^{(r)} - \check{\boldsymbol{\sigma}}^{(r)}), \tag{C.14}$$

where $\overline{\boldsymbol{\sigma}}^{(r)} = \langle \boldsymbol{\sigma} \rangle^{(r)}$ is the average of the stress over phase r, and

$$\mathbf{C}_{\boldsymbol{\sigma}}^{(r)} \doteq \Big\langle (\boldsymbol{\sigma} - \overline{\boldsymbol{\sigma}}^{(r)}) \otimes (\boldsymbol{\sigma} - \overline{\boldsymbol{\sigma}}^{(r)}) \Big\rangle^{(r)} \tag{C.15}$$

denotes the covariance tensor of the stress fluctuations in phase r (Bobeth and Diener, 1987; Parton and Buryachenko, 1990; Kreher, 1990), in the LCC. It should be emphasized that the left-hand side of (C.14) is a rank-one tensor, whereas the right-hand side is, in general, of full rank. Thus equality cannot be enforced for all components of this tensorial relation, and only certain traces of it have to be used, depending on the form of the tensors $\mathbf{M}^{(r)}$ (see Appendix).

From relations (C.12) and (C.13), it is seen that the viscous-compliance tensor $\mathbf{M}^{(r)}$ corresponds to a "generalized secant" linearization of the nonlinear stress-strain-rate relation for phase r, which depends on the second-moments of the (intraphase) fluctuations of the stress field. This is depicted graphically in fig. C.1, where the symbol $\boldsymbol{\gamma}^{(r)}$ has been used to denote $\partial u^{(r)}/\partial \boldsymbol{\sigma}$.

Finally, using the fact that (C.10) and (C.11) are stationary with respect to the tensors $\mathbf{M}^{(r)}$ and $\hat{\boldsymbol{\sigma}}^{(r)}$, respectively, the estimate (C.10) can be shown to reduce to

$$\widetilde{U}(\overline{\boldsymbol{\sigma}}) = \sum_{r=1}^{N} c^{(r)} \left[u^{(r)}(\hat{\boldsymbol{\sigma}}^{(r)}) - \frac{\partial u^{(r)}}{\partial \boldsymbol{\sigma}}(\check{\boldsymbol{\sigma}}^{(r)}) \cdot (\hat{\boldsymbol{\sigma}}^{(r)} - \overline{\boldsymbol{\sigma}}^{(r)}) \right], \tag{C.16}$$

where the reference tensors $\check{\boldsymbol{\sigma}}^{(r)}$ remain to be specified. The work of Ponte Castañeda and Willis (1999) initially suggested that the best possible estimate for $\widetilde{U}$ within this scheme could be obtained by enforcing stationarity of (C.10) with respect to the tensors $\check{\boldsymbol{\sigma}}^{(r)}$. Unfortunately, it has not yet been possible to satisfy the resulting conditions on $\check{\boldsymbol{\sigma}}^{(r)}$. As an approximation, Ponte Castañeda (2002a) proposed the use of the phase averages as reference tensors, *i.e.* $\check{\boldsymbol{\sigma}}^{(r)} = \overline{\boldsymbol{\sigma}}^{(r)}$. This prescription has been used in several works (Ponte Castañeda, 2002b, Idiart and Ponte Castañeda, 2003, among others), leading in general to sensible estimates. However, it has been recently found by Idiart and Ponte Castañeda (2005) that this prescription can lead to inconsistent results for strong nonlinearities. These authors proposed as a simple alternative to set all reference tensors equal to the macroscopic average, *i.e.*

$$\check{\boldsymbol{\sigma}}^{(r)} = \overline{\boldsymbol{\sigma}}. \tag{C.17}$$

This new prescription was found to eliminate the inconsistencies associated with the earlier prescription, and to lead to reasonable estimates, at least in the context of two-phase isotropic composites. Consequently, in this work we make use of prescription (C.17). It should be emphasized, though, that the optimal choice of the reference tensors $\check{\boldsymbol{\sigma}}^{(r)}$ remains an open question.

Thus the estimate (C.16) requires the computation of the effective potential $\widetilde{U}_T$, which can be obtained using any *linear* homogenization method appropriate for composites with local potentials $u_T^{(r)}$ and the same microstructure as the nonlinear composite. Then, relations (C.12) and (C.14) become a system of algebraic nonlinear equations for the variables $\hat{\boldsymbol{\sigma}}^{(r)}$ and $\mathbf{M}^{(r)}$ in each phase. Once these variables are determined, the tensors $\overline{\boldsymbol{\sigma}}^{(r)}$ can be computed from the LCC (see expression (C.20) below), and expression (C.16) gives the desired estimate for the effective potential of the nonlinear composite.

A dual formulation of the method using strain-rate potentials $w^{(r)}$ can be similarly obtained. In this case, a LCC is introduced with phase potentials $w_T^{(r)}$, given by second-order Taylor approximations to the corresponding nonlinear strain-rate potentials $w^{(r)}$ analogous to (C.8), in terms of uniform reference strain rates $\check{\boldsymbol{\varepsilon}}^{(r)}$ and viscosity tensors $\mathbf{L}^{(r)}$. Again, a suitable variational principle is used (see Ponte Castañeda, 2002a) to generate estimates for the nonlinear effective potentials $\widetilde{W}$ in terms of the effective potentials $\widetilde{W}_T$ of the LCC and certain "error functions" analogous to (C.11). These error functions involve stationarity conditions with respect to uniform (strain-rate) tensors $\hat{\boldsymbol{\varepsilon}}^{(r)}$ in each phase, which lead to requirements analogous to (C.12). In turn, the stationary conditions with respect to the tensors $\mathbf{L}^{(r)}$ lead to requirements analogous to (C.14), in terms of the phase averages of the strain rate $\overline{\boldsymbol{\varepsilon}}^{(r)} = \langle \boldsymbol{\varepsilon} \rangle^{(r)}$, and the phase covariance tensors $\mathbf{C}_{\boldsymbol{\varepsilon}}^{(r)}$ of the strain-rate fluctuations,

in the LCC. Finally, the estimate for the nonlinear strain-rate potential is given by

$$\widetilde{W}(\overline{\boldsymbol{\varepsilon}}) = \sum_{r=1}^{N} c^{(r)} \left[w^{(r)}(\hat{\boldsymbol{\varepsilon}}^{(r)}) - \frac{\partial w^{(r)}}{\partial \boldsymbol{\varepsilon}}(\check{\boldsymbol{\varepsilon}}^{(r)}) \cdot (\hat{\boldsymbol{\varepsilon}}^{(r)} - \overline{\boldsymbol{\varepsilon}}^{(r)}) \right], \tag{C.18}$$

for any choice of reference tensors $\check{\boldsymbol{\varepsilon}}^{(r)}$. For reasons that will become evident in the next subsection, in this work it is of interest to have a set of estimates (C.16) and (C.18) which are Legendre duals of each other. One way to do that is to set all reference strain rates $\check{\boldsymbol{\varepsilon}}^{(r)}$ equal to a second-order tensor $\check{\boldsymbol{\varepsilon}}$, and then determine this tensor using the condition

$$\widetilde{U}(\overline{\boldsymbol{\sigma}}; \check{\boldsymbol{\sigma}}) = \widetilde{W}^*(\overline{\boldsymbol{\sigma}}; \check{\boldsymbol{\varepsilon}}), \quad \text{or equivalently,} \quad \widetilde{W}(\overline{\boldsymbol{\varepsilon}}; \check{\boldsymbol{\varepsilon}}) = \widetilde{U}^*(\overline{\boldsymbol{\varepsilon}}; \check{\boldsymbol{\sigma}}), \tag{C.19}$$

where the superscript * stands for Legendre transform as defined in (C.3). Thus the procedure to compute the estimates (C.18) is similar to that required to compute the estimates (C.16), but with an extra equation for the tensor $\check{\boldsymbol{\varepsilon}}$ to ensure complete equivalence.

It can be verified that the estimates (C.16) and (C.18) are exact to second order in the heterogeneity contrast, and therefore in agreement with the small-contrast expansion of Suquet and Ponte Castañeda (1993).

C.3.2 Statistics of the local fields

The local fields in the associated LCC constitute an approximation to the local fields in the nonlinear composite. Although such an approximation is not expected to be very accurate in a pointwise sense, it is reasonable to expect that it may yield accurate estimates for averaged quantities, such as the phase averages and second-moments of the field fluctuations.

Thus the phase averages and phase covariance tensors of the stress can be obtained from the LCC generated by the *stress* version, using the following identities (see for example Laws, 1973; Ponte Castañeda and Suquet, 1998):

$$\overline{\boldsymbol{\sigma}}^{(r)} = \mathbf{B}^{(r)}\, \overline{\boldsymbol{\sigma}} + \mathbf{b}^{(r)}, \tag{C.20}$$

$$\mathbf{C}_{\boldsymbol{\sigma}}^{(r)} = \frac{2}{c^{(r)}} \frac{\partial \widetilde{U}_T}{\partial \mathbf{M}^{(r)}} - \left(\overline{\boldsymbol{\sigma}}^{(r)} - \check{\boldsymbol{\sigma}}^{(r)} \right) \otimes \left(\overline{\boldsymbol{\sigma}}^{(r)} - \check{\boldsymbol{\sigma}}^{(r)} \right). \tag{C.21}$$

In these expressions, $\mathbf{B}^{(r)}$ and $\mathbf{b}^{(r)}$ are concentration tensors that depend on the tensors $\mathbf{M}^{(r)}$ and $\check{\boldsymbol{\sigma}}^{(r)}$ according to the homogenization procedure utilized, $\widetilde{U}_T$ is the effective potential of the LCC as given by expression (C.9), and the derivative should be taken with $\check{\boldsymbol{\sigma}}^{(r)}$ held fixed.

Similarly, the phase averages and phase covariance tensors of the strain-rate can be obtained from the LCC generated by the *strain-rate* version, using analogous identities:

$$\overline{\boldsymbol{\varepsilon}}^{(r)} = \mathbf{A}^{(r)}\, \overline{\boldsymbol{\varepsilon}} + \mathbf{a}^{(r)}, \tag{C.22}$$

$$\mathbf{C}_{\boldsymbol{\varepsilon}}^{(r)} = \frac{2}{c^{(r)}} \frac{\partial \widetilde{W}_T}{\partial \mathbf{L}^{(r)}} - \left(\overline{\boldsymbol{\varepsilon}}^{(r)} - \check{\boldsymbol{\varepsilon}}^{(r)} \right) \otimes \left(\overline{\boldsymbol{\varepsilon}}^{(r)} - \check{\boldsymbol{\varepsilon}}^{(r)} \right), \tag{C.23}$$

where $\mathbf{A}^{(r)}$ and $\mathbf{a}^{(r)}$ are the relevant concentration tensors, which depend on the tensors $\mathbf{L}^{(r)}$ and $\breve{\boldsymbol{\varepsilon}}^{(r)}$, $\widetilde{W}_T$ is the effective potential of the LCC, and the derivative should be taken with $\breve{\boldsymbol{\varepsilon}}^{(r)}$ held fixed.

It should be remarked at this point that, in general, the LCCs generated by the stress and strain-rate versions are not equivalent to each other, in the sense that $u_T^{(r)} \neq (w_T^{(r)})^*$, and therefore the stress quantities (C.20)-(C.21) and the strain-rate quantities (C.22)-(C.23) correspond to different LCCs. However, it is emphasized that the phase averages (C.20) and (C.22) are actually consistent with the stress-strain-rate relation of the *nonlinear* composite arising from the "second-order" estimates, in the sense that

$$\overline{\boldsymbol{\varepsilon}} = \frac{\partial \widetilde{U}}{\partial \overline{\boldsymbol{\sigma}}}(\overline{\boldsymbol{\sigma}}) = \sum_{r=1}^{N} c^{(r)}\, \overline{\boldsymbol{\varepsilon}}^{(r)} \quad \text{and} \quad \overline{\boldsymbol{\sigma}} = \frac{\partial \widetilde{W}}{\partial \overline{\boldsymbol{\varepsilon}}}(\overline{\boldsymbol{\varepsilon}}) = \sum_{r=1}^{N} c^{(r)}\, \overline{\boldsymbol{\sigma}}^{(r)}, \tag{C.24}$$

where $\widetilde{U}$ and $\widetilde{W}$ are the nonlinear estimates (C.16) and (C.18). The reason for this is that the LCC associated with the stress (resp. strain-rate) formulation is subjected to the same macroscopic stress (resp. strain-rate) as the nonlinear composite (*cf.* expression (C.10)). Then, relations (C.24) follow from the fact that the effective potentials generated by both versions are Legendre duals of each other, which in turn follows from the choice (C.19) for the reference strain-rate.

C.4 A numerical method based on the Fast Fourier Transform

The numerical method used in the present work derives from that initially developed in the context of elasto-plasticity by Moulinec and Suquet (1994, 1998), which is based on Fast Fourier Transforms.

For clarity, the notation used in this section is slightly different from that used in the rest of the paper. The strain-rate, denoted by $\boldsymbol{\varepsilon}$ in the rest of the paper, will be denoted here by $\dot{\boldsymbol{\varepsilon}}$, since the constitutive relations which are used for computational purposes involve both the strain $\boldsymbol{\varepsilon}$ and the strain-rate $\dot{\boldsymbol{\varepsilon}}$.

C.4.1 Elasto-viscoplastic problem

The Euler equations associated with the variational problem (C.2) amount to finding a stress field $\boldsymbol{\sigma}$ and a velocity field $\mathbf{v}$ such that

$$\dot{\boldsymbol{\varepsilon}} = \frac{\partial u}{\partial \boldsymbol{\sigma}}(\mathbf{x}, \boldsymbol{\sigma}), \quad \dot{\boldsymbol{\varepsilon}} = \frac{1}{2}\left(\nabla \mathbf{v} + \nabla \mathbf{v}^{\mathrm{T}}\right), \quad \mathrm{div}(\boldsymbol{\sigma}) = 0, \quad \langle \dot{\boldsymbol{\varepsilon}} \rangle = \dot{\overline{\boldsymbol{\varepsilon}}}. \tag{C.25}$$

The problem is closed by imposing periodicity conditions on the boundary of the r.v.e. V:

$$\mathbf{v} - \dot{\overline{\boldsymbol{\varepsilon}}}\,\mathbf{x} \quad \text{periodic}, \quad \boldsymbol{\sigma}\,\mathbf{n} \quad \text{anti} - \text{periodic}. \tag{C.26}$$

The solution of the nonlinear system (C.25) is obtained by incorporating elastic effects in the constitutive equations and then taking the limit as the time t tends to $+\infty$ of the solution of an elasto-viscoplastic problem derived from (C.25) (this procedure is very similar to the approach used

by Moulinec and Suquet (1998) or Michel *et al.* (1999) to determine the extremal surface of rigid-plastic composites from the resolution of elasto-plastic problems).

Each nonlinear viscous constituents is given an elasticity characterized by a fourth-order tensor $\mathbf{L}^{(r)}$, and the following evolution problem with periodic boundary conditions is considered:

$$\left.\begin{array}{c} \dot{\boldsymbol{\sigma}} = \mathbf{L}(\mathbf{x})(\dot{\boldsymbol{\varepsilon}} - \dot{\boldsymbol{\varepsilon}}^{\mathrm{vp}}), \quad \dot{\boldsymbol{\varepsilon}}^{\mathrm{vp}}(\mathbf{x}) = \dfrac{\partial u}{\partial \boldsymbol{\sigma}}(\mathbf{x}, \boldsymbol{\sigma}), \\ \dot{\boldsymbol{\varepsilon}} = \frac{1}{2}\left(\nabla \mathbf{v} + \nabla \mathbf{v}^{\mathrm{T}}\right), \quad \mathrm{div}(\boldsymbol{\sigma}) = 0, \quad \langle \dot{\boldsymbol{\varepsilon}} \rangle = \dot{\overline{\boldsymbol{\varepsilon}}}. \end{array}\right\} \tag{C.27}$$

The system of equations (C.27) is solved incrementally. A constant (time-independent) macroscopic strain-rate $\dot{\overline{\boldsymbol{\varepsilon}}}$ is applied to the unit-cell, and the time-dependent stress and strain fields (with initial conditions identically 0) are determined by a time integration algorithm detailed below. As t tends to $+\infty$ the stress field $\boldsymbol{\sigma}$ and the strain-rate field $\dot{\boldsymbol{\varepsilon}}$ eventually reach an asymptotic state for which $\dot{\boldsymbol{\sigma}} = \mathbf{0}$ and $\dot{\boldsymbol{\varepsilon}} = \dot{\boldsymbol{\varepsilon}}^{\mathrm{vp}}$. These asymptotic fields are solutions of (C.25). The resolution of (C.27) is numerically simpler and less stiff than that of (C.25).

The system (C.27) consists of two different sets of equations. The first set, corresponding to the first line, is an ordinary differential equation expressing the constitutive relations. The second set, corrresponding to the second line in (C.27), consists of the partial differential equations expressing equilibrium and compatibility. The two sets of equations are handled separately.

C.4.2 Time integration of the constitutive relations

The integration in time of the constitutive relations (C.27a) is performed by an implicit step-by step time integration algorithm very similar to the radial-return algorithm used in Moulinec and Suquet (1998).

The time interval $[0, T]$ is discretized into time steps $[t^i, t^{i+1}]$. Assuming that the fields $\boldsymbol{\sigma}^i$ and $\boldsymbol{\varepsilon}^i$ at time $t = t^i$ have been determined, we look for the unknown fields $\boldsymbol{\sigma}^{i+1}$ and $\boldsymbol{\varepsilon}^{i+1}$ at time $t = t^{i+1}$. Replacing time differentiation by a finite difference in (C.27) gives (the dependence on the phase is omitted for simplicity):

$$\boldsymbol{\sigma}^{i+1} - \boldsymbol{\sigma}^i = \mathbf{L}\left(\boldsymbol{\varepsilon}^{i+1} - \boldsymbol{\varepsilon}^i - (\dot{\boldsymbol{\varepsilon}}^{\mathrm{vp}})^{i+1} \times (t^{i+1} - t^i)\right), (\dot{\boldsymbol{\varepsilon}}^{\mathrm{vp}})^{i+1} = \frac{\partial u}{\partial \boldsymbol{\sigma}}(\boldsymbol{\sigma}^{i+1}). \tag{C.28}$$

Assume that a "guess" for $\boldsymbol{\varepsilon}^{i+1}$ is available (from a previous iteration within the present time step). Then, $\boldsymbol{\sigma}^{i+1}$ solves the following nonlinear equation:

$$\boldsymbol{\sigma}^{i+1} + (t^{i+1} - t^i)\,\mathbf{L}\,\frac{\partial u}{\partial \boldsymbol{\sigma}}(\boldsymbol{\sigma}^{i+1}) = \boldsymbol{\sigma}^i + \mathbf{L}\left(\boldsymbol{\varepsilon}^{i+1} - \boldsymbol{\varepsilon}^i\right). \tag{C.29}$$

Introducing the elastic "trial" prediction $\boldsymbol{\sigma}_T^{i+1} = \boldsymbol{\sigma}^i + \mathbf{L}\left(\boldsymbol{\varepsilon}^{i+1} - \boldsymbol{\varepsilon}^i\right)$, the nonlinear equation (C.29) takes the form

$$\boldsymbol{\sigma}^{i+1} + (t^{i+1} - t^i)\,\mathbf{L}\,\frac{\partial u}{\partial \boldsymbol{\sigma}}(\boldsymbol{\sigma}^{i+1}) = \boldsymbol{\sigma}_T^{i+1}. \tag{C.30}$$

The nonlinear equation (C.30) is solved for $\boldsymbol{\sigma}^{i+1}$ by any nonlinear solver. When the phases are isotropic and incompressible, the nonlinear equation (C.30) further reduces to a single nonlinear scalar equation. Note that, in general, the resolution of this nonlinear equation is to be performed at each material point individually, and that $\boldsymbol{\sigma}^{i+1}$ at a given material point $\mathbf{x}$ depends only on quantities $\boldsymbol{\sigma}^{i}$, $\boldsymbol{\varepsilon}^{i}$ and $\boldsymbol{\varepsilon}^{i+1}$ defined at the same point $\mathbf{x}$. Therefore the solution of (C.30) can be expressed symbolically as a nonlinear constitutive relation

$$\boldsymbol{\sigma}^{i+1}(\mathbf{x}) = \mathbf{F}^{i+1}(\mathbf{x}, \boldsymbol{\varepsilon}^{i+1}(\mathbf{x})). \tag{C.31}$$

In addition, $\boldsymbol{\sigma}^{i+1}$ and $\boldsymbol{\varepsilon}^{i+1}$ must also satisfy the equilibrium and compatibility equations. These partial differential equations coupling different material points in the r.v.e. are treated in the next section through a Green's operator approach.

C.4.3 Equilibrium and compatibility

Consider first an auxiliary problem for a homogeneous linear-elastic medium with stiffness $\mathbf{L}^0$, subjected to an arbitrary eigenstress field $\boldsymbol{\tau}$. The periodic Green's operator $\boldsymbol{\Gamma}^0$ for the Navier equations associated with $\mathbf{L}^0$ permits to construct the strain field created by $\boldsymbol{\tau}$ in the homogeneous elastic medium. More specifically, the solution $\boldsymbol{\varepsilon}(\mathbf{u}^*)$ of the problem with periodic conditions:

$$\boldsymbol{\sigma}(\mathbf{x}) = \mathbf{L}^0\,\boldsymbol{\varepsilon}(\mathbf{u}^*(\mathbf{x})) + \boldsymbol{\tau}(\mathbf{x}), \quad \mathrm{div}(\boldsymbol{\sigma}) = 0, \quad \langle \boldsymbol{\varepsilon}(\mathbf{u}^*) \rangle = 0, \tag{C.32}$$

reads as

$$\boldsymbol{\varepsilon}(\mathbf{u}^*) = -\boldsymbol{\Gamma}^0 * \boldsymbol{\tau}, \tag{C.33}$$

where $*$ stands for convolution, and $\boldsymbol{\Gamma}^0$ is the periodic Green's operator of the reference medium. The Fourier transform of $\boldsymbol{\Gamma}^0$ is explicitly known for a general anisotropic $\mathbf{L}^0$. For an isotropic reference medium it reads (see, for example, Moulinec and Suquet, 1998):

$$\hat{\Gamma}^0_{ijkh}(\boldsymbol{\xi}) = \frac{1}{4\mu^0|\boldsymbol{\xi}|^2}(\delta_{ki}\xi_h\xi_j + \delta_{hi}\xi_k\xi_j \ + \delta_{kj}\xi_h\xi_i + \delta_{hj}\xi_k\xi_i) - \frac{\lambda^0+\mu^0}{\mu^0(\lambda^0+2\mu^0)}\,\frac{\xi_i\xi_j\xi_k\xi_h}{|\boldsymbol{\xi}|^4}. \tag{C.34}$$

The solution of the auxiliary problem is used to reduce the local problem for nonlinear materials to a nonlinear integral equation. The nonlinear local problem

$$\boldsymbol{\sigma} = \mathbf{F}(\varepsilon), \quad \boldsymbol{\varepsilon} = \frac{1}{2}\left(\nabla\mathbf{u} + \nabla\mathbf{u}^{\mathrm{T}}\right), \quad \mathrm{div}(\boldsymbol{\sigma}) = 0, \quad \langle \boldsymbol{\varepsilon} \rangle = \overline{\boldsymbol{\varepsilon}}, \tag{C.35}$$

with periodic boundary conditions, can be rewritten in the form (C.32) with

$$\boldsymbol{\tau}(\mathbf{x}) = \delta\mathbf{F}(\mathbf{x}, \boldsymbol{\varepsilon}) + \mathbf{L}^0\overline{\boldsymbol{\varepsilon}}, \quad \delta\mathbf{F}(\mathbf{x}, \boldsymbol{\varepsilon}) = \ \mathbf{F}(\mathbf{x}, \boldsymbol{\varepsilon}) - \mathbf{L}^0\boldsymbol{\varepsilon}. \tag{C.36}$$

Substituting this expression into the relation (C.33) yields a nonlinear integral equation for $\boldsymbol{\varepsilon}$:

$$\boldsymbol{\varepsilon}(\mathbf{u}) = -\boldsymbol{\Gamma}^0 * \delta\mathbf{F}\left(\boldsymbol{\varepsilon}(\mathbf{u})\right) + \overline{\boldsymbol{\varepsilon}}. \tag{C.37}$$

The integral equation (C.37) is solved by iterations:

$$\boldsymbol{\varepsilon}(\mathbf{u}_{\mathrm{k}+1}) = -\boldsymbol{\Gamma}^0 * \delta\mathbf{F}\left(\boldsymbol{\varepsilon}(\mathbf{u}_{\mathrm{k}})\right) + \overline{\boldsymbol{\varepsilon}}, \tag{C.38}$$

which can be further simplified by noting that $\boldsymbol{\Gamma}^0 * \left(\mathbf{L}^0\,\boldsymbol{\varepsilon}(\mathbf{u})\right) = \boldsymbol{\varepsilon}(\mathbf{u}^*)$. The final iterative scheme reads:

$$\boldsymbol{\varepsilon}(\mathbf{u}_{\mathrm{k}+1}) = \boldsymbol{\varepsilon}(\mathbf{u}_{\mathrm{k}}) - \boldsymbol{\Gamma}^0 * \boldsymbol{\sigma}_{\mathrm{k}}, \quad \text{where } \boldsymbol{\sigma}_{\mathrm{k}} = \mathbf{F}\left(\boldsymbol{\varepsilon}(\mathbf{u}_{\mathrm{k}})\right). \tag{C.39}$$

Finally, this iterative scheme is used with $\mathbf{F} = \mathbf{F}^{\mathrm{i}}$.

The final form of the algorithm used to determine the stress and strain fields $\boldsymbol{\sigma}^{i+1}$ and $\boldsymbol{\varepsilon}^{i+1}$ at time t^{i+1}, knowing $\boldsymbol{\sigma}^i$ and $\boldsymbol{\varepsilon}^i$ at time t^i, reads as follows. For simplicity, the superscript $i+1$ is omitted and the subscript k denotes an inner loop within the current time step $[t^i, t^{i+1}]$.

Initialization:

- $\boldsymbol{\varepsilon}_{\mathrm{k}=0}(\mathbf{x})$ is extrapolated linearly from the two preceeding time steps:

$$\boldsymbol{\varepsilon}_{\mathrm{k}=0}(\mathbf{x}) = \boldsymbol{\varepsilon}^{\mathrm{i}}(\mathbf{x}) + \frac{t^{i+1} - t^i}{t^i - t^{i-1}}\left(\boldsymbol{\varepsilon}^{\mathrm{i}}(\mathbf{x}) - \boldsymbol{\varepsilon}^{\mathrm{i}-1}(\mathbf{x})\right) \quad \forall\, \mathbf{x} \in\ V, \tag{C.40}$$

- $\boldsymbol{\sigma}_{\mathrm{k}=0}(\mathbf{x})$ is computed from $\boldsymbol{\varepsilon}_{\mathrm{k}=0}(\mathbf{x})$, $\boldsymbol{\varepsilon}^{\mathrm{i}}(\mathbf{x})$ and $\boldsymbol{\sigma}^{\mathrm{i}}(\mathbf{x})$ by the time integration method of section (C.4.2).

Iterate k+1:

$\boldsymbol{\varepsilon}_{\mathrm{k}}$ and $\boldsymbol{\sigma}_{\mathrm{k}}$ being known, do until convergence:

1) $\hat{\boldsymbol{\sigma}}_{\mathrm{k}} = FT(\boldsymbol{\sigma}_{\mathrm{k}})$,

2) Check equilibrium: $|\mathrm{div}(\boldsymbol{\sigma}_{\mathrm{k}})| = |\hat{\boldsymbol{\sigma}}_{\mathrm{k}}(\boldsymbol{\xi})\boldsymbol{\xi}|$ less than a required precision.

3) $\hat{\varepsilon}_{\mathrm{k}+1}(\boldsymbol{\xi}) = \hat{\varepsilon}_{\mathrm{k}}(\boldsymbol{\xi}) - \hat{\boldsymbol{\Gamma}}^0(\boldsymbol{\xi})\hat{\boldsymbol{\sigma}}_{\mathrm{k}}(\boldsymbol{\xi}) \quad \forall \boldsymbol{\xi} \neq \mathbf{0}$ and $\hat{\varepsilon}_{\mathrm{k}+1}(\mathbf{0}) = \overline{\boldsymbol{\varepsilon}}$,

4) $\boldsymbol{\varepsilon}_{\mathrm{k}+1}(\mathbf{x}) = FT^{-1}(\hat{\varepsilon}_{\mathrm{k}+1}(\boldsymbol{\xi}))$

5) $\boldsymbol{\sigma}_{\mathrm{k}+1}(\mathbf{x})$ is computed from $\boldsymbol{\varepsilon}_{\mathrm{k}+1}(\mathbf{x})$, $\boldsymbol{\varepsilon}^{\mathrm{i}}(\mathbf{x})$ and $\boldsymbol{\sigma}^{\mathrm{i}}(\mathbf{x})$ applying the time integration method of section C.4.2.

FT and FT^{-1} stand for the Fourier transform and its inverse.

The choice of the reference medium has a strong influence on the convergence rate of the method. In the present problem, where the elasticity of the phases is arbitrary and can be set to be the same for all phases, the elasticity of the reference medium coincides with that of the phases.

C.5 Two-phase, power-law, fiber composites

In what follows, the focus will be on two-phase, fiber composites with *random* microstructures exhibiting overall transversely isotropic symmetry. The fibers are assumed to be aligned with the x_3 axis, and will be identified with phase 2, whereas the continuous phase, called the matrix, will be identified with phase 1. The individual phases are assumed to be isotropic, incompressible, viscoplastic materials with a constitutive behavior characterized by power-law potentials

$$w^{(r)}(\boldsymbol{\varepsilon}) = \frac{\varepsilon_0 \sigma_0^{(r)}}{1+m}\left(\frac{\varepsilon_e}{\varepsilon_0}\right)^{1+m}, \quad u^{(r)}(\boldsymbol{\sigma}) = \frac{\varepsilon_0 \sigma_0^{(r)}}{1+n}\left(\frac{\sigma_e}{\sigma_0^{(r)}}\right)^{1+n}, \tag{C.41}$$

where ε_0 is a reference strain rate, m is the strain-rate sensitivity, such that $n = 1/m$ and $0 \leq m \leq 1$, $\sigma_0^{(r)}$ is the flow stress of phase r, and the von Mises equivalent strain rate and stress are respectively given in terms of the deviatoric strain-rate and stress tensors by $\varepsilon_e = \sqrt{(2/3)\,\boldsymbol{\varepsilon}_d \cdot \boldsymbol{\varepsilon}_d}$ and $\sigma_e = \sqrt{(3/2)\,\boldsymbol{\sigma}_d \cdot \boldsymbol{\sigma}_d}$. Note that the limiting values, $m = 1$ and $m = 0$, correspond to linearly viscous and rigid-perfectly plastic (rate-insensitive) behaviors, respectively.

For simplicity, both phases are assumed to have the same exponent m and reference strain rate ε_0. Then, from the homogeneity of the local potentials (C.41), and the fact that the composites are transversely isotropic, it follows that, under isochoric *plane-strain* conditions, the effective potentials can be written as

$$\widetilde{W}(\overline{\boldsymbol{\varepsilon}}) = \frac{\varepsilon_0 \widetilde{\sigma}_0}{1+m}\left(\frac{\overline{\varepsilon}_e}{\varepsilon_0}\right)^{1+m}, \quad \widetilde{U}(\overline{\boldsymbol{\sigma}}) = \frac{\varepsilon_0 \widetilde{\sigma}_0}{1+n}\left(\frac{\overline{\sigma}_e}{\widetilde{\sigma}_0}\right)^{1+n}, \tag{C.42}$$

where $\widetilde{\sigma}_0$ is the *effective flow stress* of the composite, and $\overline{\varepsilon}_e$ and $\overline{\sigma}_e$ are the equivalent macroscopic strain rate and stress, respectively, which are given by $\overline{\varepsilon}_e = (2/\sqrt{3})\sqrt{\overline{\varepsilon}_{12}^2 + \frac{1}{4}(\overline{\varepsilon}_{11} - \overline{\varepsilon}_{22})^2}$ and $\overline{\sigma}_e = (\sqrt{3})\sqrt{\overline{\sigma}_{12}^2 + \frac{1}{4}(\overline{\sigma}_{11} - \overline{\sigma}_{22})^2}$. This is a very special class of nonlinear ($2D$) composites, for which the analytical form of the effective potentials is known *a priori*. The effective behavior is thus completely characterized by $\widetilde{\sigma}_0$, which is a function of the strain-rate sensitivity, the heterogeneity contrast, and the concentration of fibers. It should be emphasized, however, that the methods presented above can account for very general microstructures and constitutive behaviors, and that the choice made in this work is dictated by convenience, while preserving the capability of dealing with strongly nonlinear behavior.

It can also be shown for this particular class of nonlinear composites that the local stress and strain-rate fields are homogeneous functions of degree 1 in $\overline{\sigma}_e$ and $\overline{\varepsilon}_e$, respectively. In addition, since the phases and their distribution are isotropic, it is expected that the phase averages are co-axial with the macroscopic averages. It is also expected that the phase covariance tensors are "aligned" with the macroscopic averages, in the sense that one of their eigentensors is co-axial with $\overline{\boldsymbol{\sigma}}$ and $\overline{\boldsymbol{\varepsilon}}$. (Indeed, this turns out to be the case in the calculations to follow.) Under incompressible plane-strain conditions, the local stress and strain deviator fields are vectorial in character, thus co-axiality implies proportionality, and so their phase averages can be written as

$$\overline{\boldsymbol{\sigma}}_d^{(r)} = \frac{\overline{\sigma}_e^{(r)}}{\overline{\sigma}_e}\overline{\boldsymbol{\sigma}}_d \quad \text{and} \quad \overline{\boldsymbol{\varepsilon}}_d^{(r)} = \frac{\overline{\varepsilon}_e^{(r)}}{\overline{\varepsilon}_e}\overline{\boldsymbol{\varepsilon}}_d, \tag{C.43}$$

where the ratios $\overline{\sigma}_e^{(r)}/\overline{\sigma}_e$ and $\overline{\varepsilon}_e^{(r)}/\overline{\varepsilon}_e$ depend only on material parameters. It is also natural to identify two "components" of the strain-rate (resp. stress) tensor which represent its projections "parallel", $\varepsilon_\parallel$ (resp. $\sigma_\parallel$), and "perpendicular", $\varepsilon_\perp$ (resp. $\sigma_\perp$), to the macroscopic strain rate (resp. stress). These components can be determined (up to a sign) by the two orthogonal fourth-order projection tensors $\mathbf{E}$ and $\mathbf{F}$ given by expressions (56) in Ponte Castañeda 2002a, with $\check{\boldsymbol{\sigma}}^{(r)} = \overline{\boldsymbol{\sigma}}$, through the following relations: $\varepsilon_\parallel^2 = (2/3)\,(\boldsymbol{\varepsilon}\cdot\mathbf{E}\boldsymbol{\varepsilon})$, $\varepsilon_\perp^2 = (2/3)\,(\boldsymbol{\varepsilon}\cdot\mathbf{F}\boldsymbol{\varepsilon})$, $\sigma_\parallel^2 = (3/2)\,(\boldsymbol{\sigma}\cdot\mathbf{E}\boldsymbol{\sigma})$, and $\sigma_\perp^2 = (3/2)\,(\boldsymbol{\sigma}\cdot\mathbf{F}\boldsymbol{\sigma})$. They are such that $\varepsilon_e^2 = \varepsilon_\parallel^2 + \varepsilon_\perp^2$ and $\sigma_e^2 = \sigma_\parallel^2 + \sigma_\perp^2$. For instance, in the numerical simulations to follow, the macroscopic stress will be taken to be

$$\overline{\boldsymbol{\sigma}} = \overline{\sigma}_{12}\,(\mathbf{e}_1 \otimes \mathbf{e}_2 + \mathbf{e}_2 \otimes \mathbf{e}_1), \tag{C.44}$$

so that the corresponding "parallel" and "perpendicular" components of the local fields are

$$\sigma_\parallel = \sqrt{3}\,\sigma_{12}, \quad \sigma_\perp = \sqrt{3}\,\frac{\sigma_{11}-\sigma_{22}}{2}, \quad \varepsilon_\parallel = \frac{2}{\sqrt{3}}\,\varepsilon_{12}, \quad \varepsilon_\perp = \frac{2}{\sqrt{3}}\,\frac{\varepsilon_{11}-\varepsilon_{22}}{2}. \tag{C.45}$$

The standard deviations of the spatial distributions within each phase of the quantities (C.45) ($SD^{(r)}(\cdot) = \sqrt{\langle(\cdot)^2\rangle^{(r)} - (\langle\cdot\rangle^{(r)})^2}$) provide a measure of the intraphase field fluctuations, and are given in terms of the phase covariance tensors by

$$SD^{(r)}(\sigma_\parallel) = \sqrt{\frac{3}{2}\,\mathbf{E}\cdot\mathbf{C}_{\boldsymbol{\sigma}}^{(r)}}, \quad SD^{(r)}(\sigma_\perp) = \sqrt{\frac{3}{2}\,\mathbf{F}\cdot\mathbf{C}_{\boldsymbol{\sigma}}^{(r)}}, \tag{C.46}$$

$$SD^{(r)}(\varepsilon_\parallel) = \sqrt{\frac{2}{3}\,\mathbf{E}\cdot\mathbf{C}_{\boldsymbol{\varepsilon}}^{(r)}}, \quad SD^{(r)}(\varepsilon_\perp) = \sqrt{\frac{2}{3}\,\mathbf{F}\cdot\mathbf{C}_{\boldsymbol{\varepsilon}}^{(r)}}. \tag{C.47}$$

From the homogeneity of the local fields in $\overline{\sigma}_e$ and $\overline{\varepsilon}_e$, it follows that the ratios $SD^{(r)}(\sigma)/\overline{\sigma}_e$ and $SD^{(r)}(\varepsilon)/\overline{\varepsilon}_e$ depend only on the material parameters.

In this work, a special class of random transversely-isotropic microstructures is considered known as the composite cylinder assemblage (CCA), introduced by Hashin and Rosen (1964), in which aligned homothetic composite cylinders of an infinite number of sizes fill the entire space. The interest in this type of microstructures is that, in the *linear* case, their effective behavior is known to be well approximated by the Hashin-Shtrikman (HS) estimates (Hashin and Shtrikman, 1963), at least when the constituent phases are isotropic. Because of this, the "second-order" estimates for *nonlinear* composites with this type of microstructures will be generated by making use of the *linear* HS estimates to determine the homogenized behavior of the associated LCC.

In order to carry out full-field numerical simulations for this class of composites using the FFT method, 20 different configurations of the unit-cell were generated by *randomly* placing in a square cell self-similar non-overlapping composite cylinders of three different sizes, with periodicity conditions for cylinders intersecting the cell boundaries. Figure C.2 shows a typical configuration for the unit cell, containing 490 composite cylinders. Each composite cylinder is composed of a circular core (in

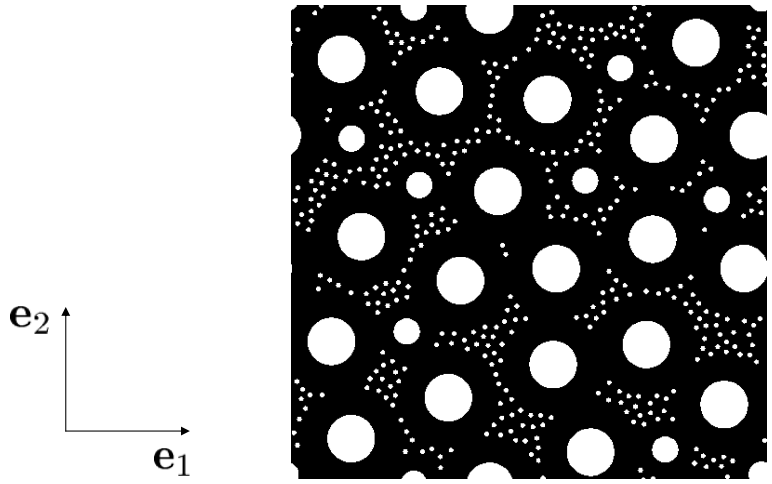

Figure C.2: Typical configuration of the unit cell used in the full-field FFT simulations. It contains 490 composite cylinders of three different sizes, randomly distributed.

white in figure C.2) surrounded by a circular layer of matrix (in black). It is emphasized that these microstructures constitute an approximation to the CCAs described above, since only a finite number of sizes is used for the composite cylinders. As a consequence of using a finite number of sizes for the composite cylinders, as well as a different number of cylinders of a given size from one configuration to another, the fiber concentration in each configuration is not exactly the same, and ranged between 0.203 and 0.210, the average value being 0.20626.

The issues of statistical homogeneity and isotropy for this type of microstructures are briefly discussed in Moulinec and Suquet (2004) (see also Kanit *et al*, 2003, for a related problem). Both the number of composite cylinders per unit-cell and the number of different configurations used in the analysis result from a compromise between several constraints. First, each configuration has to be large enough to ensure that the periodicity conditions play almost no role on the effective properties. Second, by considering large unit-cells containing a large number of inclusions (several hundreds), the scatter in the quantities of interest (effective properties, first and second moments of the fields) is small and only a few configurations are necessary for the ensemble average of these quantities to reach stationarity.

The FFT results provided in the next section for the effective properties, phase averages, and standard deviations of the local fields, are ensemble averages of the computational results over all configurations, and they are taken as approximate values for a fiber concentration of 0.20626. The way these ensemble averages were performed can be found in Moulinec and Suquet (2003, 2004). In addition to the phase averages and covariance tensors, the histograms of the spatial distribution of the local fields can be obtained from the FFT simulations. For any scalar field z, it is convenient to introduce a "density of states per unit volume" or "probability density function", $\mathcal{P}_z^{(r)}(z)$, defined so that $\mathcal{P}_z^{(r)}(z)\,dz$ is the volume fraction of phase r in a given configuration where the variable z takes values in the range z and $z+dz$. (Note that the first and second moments of z are then given by $\langle z^q \rangle^{(r)} = \int_{-\infty}^{\infty} z^q\, \mathcal{P}_z^{(r)}(z)\,dz$ with $q=1$ and $q=2$, respectively.) At a given value z_i, the function $\mathcal{P}_z^{(r)}$

is computed from the numerical simulations by counting the number of pixels $N_i^{(r)}$ out of the total number of pixels $N^{(r)}$ in phase r where the variable z takes values between $z_i \leq z < z_i + \Delta z$. In this work, the following relations have been used:

$$\mathcal{P}_z^{(r)}(z_i) = \frac{1}{\Delta z}\,\frac{N_i^{(r)}}{N^{(r)}}, \quad z_i = z_{min} + i\,\Delta z, \quad \Delta z = \frac{z_{max} - z_{min}}{N_b - 1}, \tag{C.48}$$

where N_b denotes the number of bars in the histogram (200 in this work), z_{min} and z_{max} denote, respectively, the minimum and maximum values that the quantity z takes in a given simulation, and $i = 0, 1, .., N_b - 2$. For the last bar, $N_{N_b-1}^{(r)}$ is set equal to the number of pixels where z takes the value z_{max}.

The unit-cells used in the numerical simulations were discretized into 1024×1024 pixels. They were subjected to an in-plane shear stress (C.44), and the computations were run until the macroscopic strain reached $\overline{\varepsilon}_{12} = 0.5$.

Second-order estimates for rigid-ideally plastic composites. Power-law phases characterized by potentials (C.41) become rigid-ideally plastic in the limit $m \to 0$. For such materials, the flow stress $\sigma_0^{(r)}$ defines a set of admissible stresses given by the Von Mises criterion $|\sigma_e| \leq \sigma_0^{(r)}$. The corresponding effective behavior is also rigid-perfectly plastic, with a set of admissible (overall) stresses given by $|\overline{\sigma}_e| \leq \widetilde{\sigma}_0$.

C.6 Results and discussion

In this section, the "second-order" (SO) estimates of the Hashin-Shtrikman type, described in the previous section, for the effective behavior and statistics of the local fields in the power-law composites are compared with corresponding results generated by FFT full-field simulations. The results are presented as a function of the strain-rate sensitivity m, for a given concentration of fibers ($c^{(2)} = 0.20626$). Two values of the heterogeneity contrast are considered, one corresponding to fiber-reinforced composites ($\sigma_0^{(2)}/\sigma_0^{(1)} = 5$) and the other to fiber-weakened composites ($\sigma_0^{(2)}/\sigma_0^{(1)} = 0.2$). Full-field simulations were carried out for several values of the strain-rate sensitivity ($1/m = n = 1, 2, 3, 10, \infty$). The dark circles representing the FFT results in the plots to follow correspond to ensemble averages over twenty different configurations (like the one shown in fig. C.2), and the "error" bars (where given) correspond to the maximum and minimum values, quantifying the scatter of the numerical results.

In addition, comparisons are also provided with the earlier "variational" (VAR) method of Ponte Castañeda (1991) and Suquet (1993), as well as with the "tangent second-order" (TSO) method of Ponte Castañeda (1996), once again, making use of the HS estimates for the relevant LCC. It is recalled here that these methods arise from considering different linearization schemes. Thus, the "variational" method makes use of a LCC whose phases are identified with the "secant" viscous-compliance/viscosity tensors of the nonlinear phases, evaluated at the second-moments of the local

fields over the phases (Suquet, 1995; Hu, 1996). It is emphasized that since the nonlinear phases are isotropic, the corresponding LCC is also locally isotropic in this model. On the other hand, in the earlier version of the "second-order" method (TSO), the phases of the LCC are identified with the "tangent" viscous-compliance/viscosity tensors of the nonlinear phases, evaluated at the phase averages of the local fields. Therefore, unlike the "second-order" method outlined above, this method does not take into account the field fluctuations in the linearization. It should also be mentioned that the TSO estimates are known to have a duality gap (Ponte Castañeda, 1996), and so two sets of estimates corresponding to the strain-rate (W) and stress (U) versions are shown. Finally, the classical estimates of Voigt and Reuss are also included for comparison purposes. These are rigorous upper and lower bounds, independent of the microstructure, which are obtained by using uniform strain-rate and stress trial fields in the minimum energy principles (C.2) and (C.5), respectively.

Before proceeding with the discussion of the results, it is useful to recall that the nonlinear homogenization methods based on the use of a LCC involve *two* different levels of approximation. The first one consists in the linearization of the behavior of each phase in the nonlinear composite, in order to generate the LCC. Once the LCC is generated, however, its effective behavior needs to be computed. In general, computing exactly the effective behavior of the LCC, which is a random composite, is still a difficult problem, and therefore a second level of approximation is required, which consists in estimating the effective behavior of the LCC, making use of suitable *linear* homogenization estimates. Therefore, any differences between the homogenization results and the numerical simulations shown below could have either one (or both) of two sources: the estimate used for the LCC (in this case, the HS estimates), or the linearization procedure itself (SO, TSO, VAR).

C.6.1 Fiber-weakened composites

Effective behavior. In fig. C.3a, the various bounds and estimates for the effective flow stress $\widetilde{\sigma}_0$ of a fiber-weakened composite, and the corresponding FFT results, are plotted as a function of the strain-rate sensitivity m. (Part (b) will be discussed in the next subsection.) The results are normalized by the flow stress of the matrix $\sigma_0^{(1)}$. It can be observed that the FFT simulations yield a $\widetilde{\sigma}_0$ which decreases slightly with decreasing values of m (*i.e.*, increasing nonlinearity). The main observation, however, is that the SO estimates are found to be in good agreement with the FFT simulations, for weak to moderate nonlinearities ($0.2 \leq m \leq 1$), but the agreement is found to deteriorate close to the perfectly plastic limit ($m \to 0$), where the FFT results keep decreasing with m, while the SO estimates exhibit a slight increase. As explained in more detail below, the reason for such differences as $m \to 0$ could be related to the use of HS estimates for the LCC. It is worth noting though that for $m = 0.1$ the differences are still relatively small (approx. 3.5%). Also included in the figure are both versions of the TSO estimates, as well as the "variational" estimates. The latter are known to provide rigorous upper bounds for the $\widetilde{\sigma}_0$ of the class of composites here considered (see, for example, Ponte Castañeda and Suquet, 1998). Several observations are in order. First, the homogenization estimates all coincide for $m = 1$ with the linear HS estimate, as they should, but give diverging predictions as

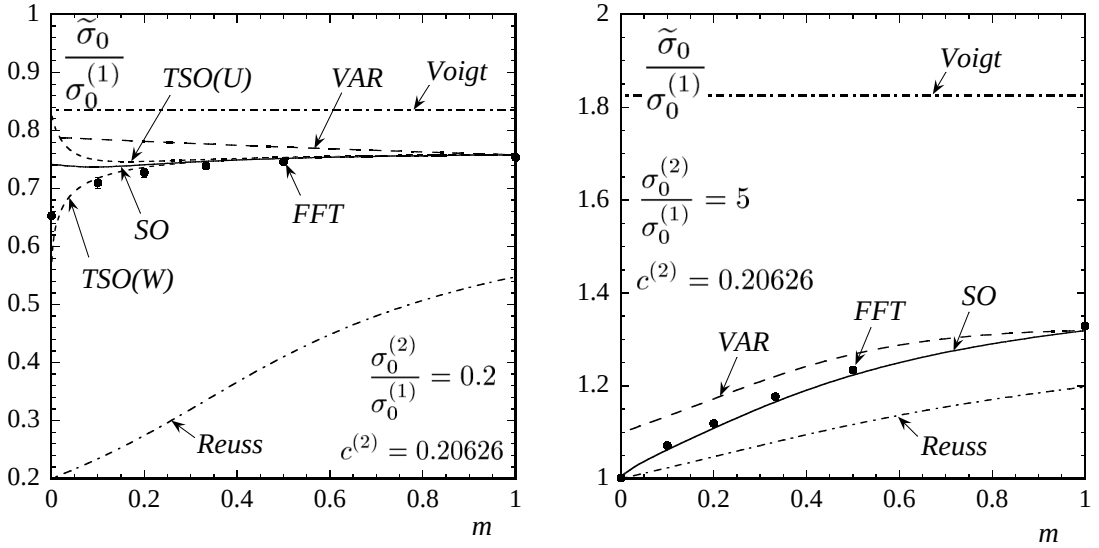

Figure C.3: Effective flow stress $\widetilde{\sigma}_0$, normalized by the flow stress of the matrix $\sigma_0^{(1)}$, for power-law fiber composites subjected to in-plane shear, as a function of the strain-rate sensitivity m, for a given concentration of fibers ($c^{(2)} = 0.20626$). Comparisons between the "second-order" (SO), "tangent second-order" (TSO), and "variational" (VAR) estimates of the Hashin-Shtrikman type, and the FFT results, for the cases of: (a) weaker fibers ($\sigma_0^{(2)}/\sigma_0^{(1)} = 0.2$), (b) stronger fibers ($\sigma_0^{(2)}/\sigma_0^{(1)} = 5$).

m decreases. However, it is seen that the TSO and SO estimates give very close predictions for weak to moderate nonlinearities ($0.3 \leq m \leq 1$), and it is only for strong nonlinearities that they differ significantly. In this connection, it is noted that, as already pointed out by Ponte Castañeda (2002b), the TSO estimates exhibit a large duality gap for small values of m, and in the limit $m \to 0$ the $TSO(U)$ estimates tend to the Voigt bound, thus violating the sharper "variational" upper bound. In contrast, the new SO estimates have no duality gap, and are found to satisfy the "variational" upper bound for all values of m. Finally, it is noted that the scatter exhibited by the FFT results, although barely noticeable in this figure, increases with increasing nonlinearity. This scatter is due to several reasons, such as the finite size of the specimens, as well as the fact that all specimens have slightly different fiber concentrations. In any event, the scatter is found to be very small even for the smaller values of m, suggesting that the quality of the numerical results is good.

Statistics of the local fields. Corresponding estimates for the phase averages and standard deviations of the stress field are given in fig. C.4. In part (a), the equivalent average stresses in each phase $\overline{\sigma}_e^{(r)}$ are shown, normalized by the equivalent macroscopic stress $\overline{\sigma}_e$. It can be seen that all the homogenization estimates are in good agreement with the FFT simulations, for all values of m. This is perhaps not surprising, since for the extreme case of void fibers (*i.e.*, $\sigma_0^{(2)} = 0$) all these methods give the exact result (*i.e.*, $\overline{\sigma}_e^{(1)}/\overline{\sigma}_e = 1/c^{(1)}$ and $\overline{\sigma}_e^{(2)}/\overline{\sigma}_e = 0$). Nonetheless, it is worth mentioning that the SO estimates are the most consistent ones with the FFT results, the agreement being excellent. Part (b) shows the standard deviations of the stress field in the matrix, as given by expressions (C.46), normalized by the equivalent macroscopic stress $\overline{\sigma}_e$. The main observation

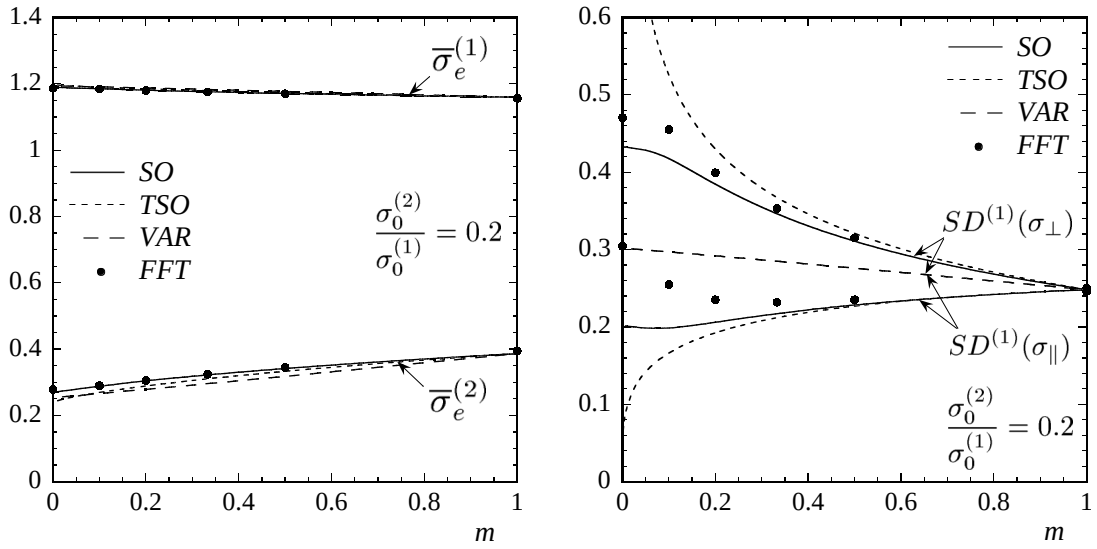

Figure C.4: Statistics of the stress field for the case of weaker fibers. (a) Equivalent average stresses in the matrix ($\overline{\sigma}_e^{(1)}$) and in the fibers ($\overline{\sigma}_e^{(2)}$). (b) Standard deviation (SD) of the "parallel" and "perpendicular" components of the stress field in the matrix. The results are normalized by the equivalent macroscopic stress $\overline{\sigma}_e$.

in the context of this figure is that the FFT simulations show that, while the stress fluctuations are *isotropic* (*i.e.*, $SD^{(1)}(\sigma_\parallel) = SD^{(1)}(\sigma_\perp)$) in the linear case, they become progressively more *anisotropic* as the nonlinearity increases, being larger for the "perpendicular" component than for the "parallel" component. Furthermore, the "perpendicular" fluctuations are found to increase with decreasing m, while the "parallel" fluctuations exhibit a non-monotonic dependence on m. It can be seen in the figure that the SO estimates are consistent with these observations, exhibiting good agreement with the FFT results for weak to moderate nonlinearities ($0.3 \leq m \leq 1$). However, this agreement is seen to deteriorate close to the perfectly plastic limit, where the SO estimates underestimate the stress fluctuations. On the other hand, while for weak to moderate nonlinearities the $TSO(U)$ estimates are very similar to the SO estimates, as $m \to 0$ they give vanishing and infinite fluctuations in the "parallel" and "perpendicular" directions, respectively, which is in disagreement with the FFT results. Finally, the "variational" estimates are seen to predict isotropic stress fluctuations for all values of m, and are thus inconsistent with the FFT simulations.

Figure C.5 provides corresponding estimates for the phase averages and standard deviations of the strain-rate field. Part (a) shows the equivalent average strain rates in each phase $\overline{\varepsilon}_e^{(r)}$, normalized by the equivalent macroscopic strain rate $\overline{\varepsilon}_e$. It can be seen that the FFT simulations yield an average strain rate in the (weaker) fibers which is higher than that in the matrix, as expected, and that the former increases with nonlinearity while the latter decreases. (Note that, in view of relations (C.43), these quantities are related by $c^{(1)}\,(\overline{\varepsilon}_e^{(1)}/\overline{\varepsilon}_e) + c^{(2)}\,(\overline{\varepsilon}_e^{(2)}/\overline{\varepsilon}_e) = 1$.) Among the homogenization estimates, the SO estimates are found to be, once again, the most consistent with the FFT results, the agreement being very good for all values of m. Although the $TSO(W)$ estimates give very similar

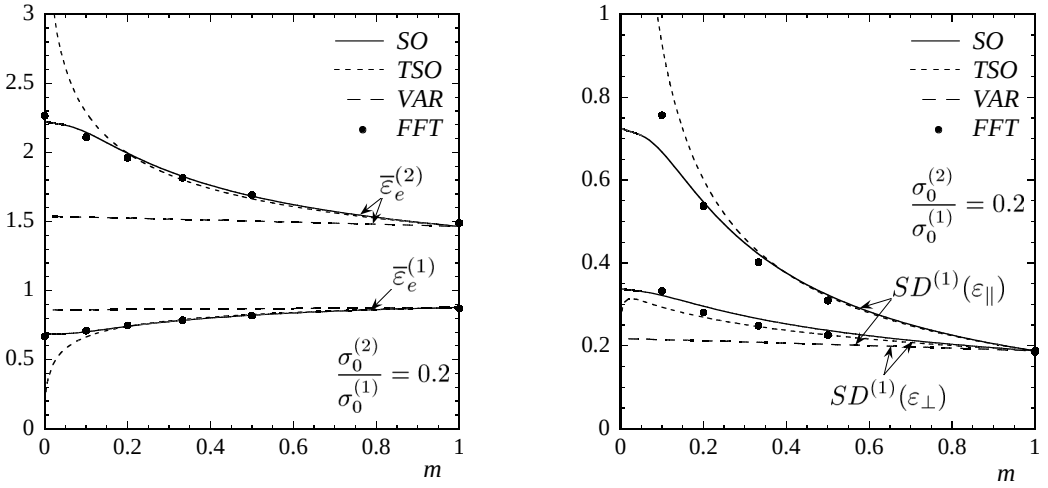

Figure C.5: Statistics of the strain-rate field for the case of weaker fibers. (a) Equivalent average strain rates in the matrix ($\overline{\varepsilon}_e^{(1)}$) and fibers ($\overline{\varepsilon}_e^{(2)}$). (b) Standard deviation (SD) of the "parallel" and "perpendicular" components of the strain-rate field in the matrix. The results are normalized by the equivalent macroscopic strain rate $\overline{\varepsilon}_e$.

predictions in the range $0.2 \leq m \leq 1$, they are seen to deviate significantly as $m \to 0$. In fact, in this limit, they predict a vanishing average strain rate in the matrix, which is inconsistent with the FFT results. In this connection, it is worth mentioning that the SO estimates with reference tensors $\check{\boldsymbol{\sigma}}^{(r)}$ identified with the phase averages predict an average strain rate in the matrix that also vanishes as $m \to 0$ (see Idiart and Ponte Castañeda, 2003, 2005). Thus the alternative prescription (C.17)-(C.19) used in this work is found to give much more reasonable estimates, especially for strong nonlinearities. Finally, it is observed that the "variational" estimates are inconsistent with the FFT simulations, being almost insensitive to m. Part (b) provides plots for the standard deviations of the strain-rate field in the matrix, normalized by the equivalent macroscopic strain rate $\overline{\varepsilon}_e$. The main observation in the context of this figure is that the FFT simulations show that the strain-rate fluctuations, which are *isotropic* in the linear case, increase significantly and become progressively more *anisotropic* as the nonlinearity increases. Furthermore, it is observed that, unlike the stress fluctuations (*cf.* fig. C.4b), the strain-rate fluctuations are larger for the "parallel" component than for the "perpendicular" component. As will be seen in detail shortly, the increase of the strain-rate fluctuations and their anisotropy are consequences of strain localization, which becomes more pronounced with increasing nonlinearity. It can be seen in the figure that the SO estimates are in good agreement with the FFT results for weak to moderate nonlinearities ($0.2 \leq m \leq 1$), but they are found to underestimate the strain-rate fluctuations for small values of m, yielding finite values in the ideally plastic limit, while the FFT results seem to be consistent with unbounded fluctuations in this limit (the FFT results for $m = 0$ yield strain-rate fluctuations that are very large but finite, since the numerical procedure cannot handle infinite quantities). The $TSO(W)$ estimates are seen to give similar predictions to the SO estimates for weak to moderate nonlinearities, but as $m \to 0$ they give

infinite and vanishing fluctuations for the "parallel" and "perpendicular" components, respectively, which is also inconsistent, since the FFT results suggest that the fluctuations blow up for both components. Finally, the "variational" estimates are seen to be almost insensitive to m here as well, and more importantly, they predict isotropic fluctuations for all values of m, which is inconsistent with the FFT simulations.

At this point, it is worth noting that the degree of anisotropy of the stress and strain-rate fluctuations predicted by the different homogenization methods depends strongly on the anisotropy of the compliance/elastic tensors used in the LCC. In fact, for the cases considered here, the compliance/elastic tensors used by these methods are all of the same form, as given by expressions (55) and (44) in Ponte Castañeda (2002a), and it can be verified that the anisotropy of the HS estimates for the stress fluctuations in the matrix is $SD^{(1)}(\sigma_{\parallel})/SD^{(1)}(\sigma_{\perp}) = \sqrt{k}$, while that of the strain-rate fluctuations is $SD^{(1)}(\varepsilon_{\parallel})/SD^{(1)}(\varepsilon_{\perp}) = 1/\sqrt{k}$, where $k = \lambda_0^{(1)}/\mu_0^{(1)}$ is the (anisotropy) ratio of the "parallel" and "perpendicular" shear moduli. Thus, as already mentioned, the "variational" method makes use of isotropic compliance tensors (when the nonlinear phase is isotropic), so $k = 1$, and consequently it predicts isotropic stress and strain-rate fluctuations for all values of m. On the other hand, the TSO estimates make use of the "tangent" compliance tensor, which for a power-law phase is of the form mentioned above with $k = m$. This still constitutes a strong restriction, for the anisotropy of the fluctuations is thus given by the strain-rate sensitivity, and cannot depend, for example, on the microstructure. In contrast, the compliance tensors used by the new SO estimates are somewhat more general (see section C.3), allowing for k to depend not only on m but also on the heterogeneity contrast and concentration of fibers. This is one of the reasons why the "second-order" method is able to give superior predictions over the earlier "tangent second-order" and "variational" methods. Finally, it is noted that, the k associated with the W and U versions of the SO estimates are not equal, thus allowing the anisotropy of the strain-rate and stress fluctuations to be different from each other, which is in agreement with the FFT simulations.

The corresponding standard deviations of the local fields in the fiber phase are shown in fig. C.6a. (Part (b) will be discussed in the next subsection.) It can be seen that the FFT results yield stress fluctuations in the fibers that are small, yet finite, in comparison with those in the matrix phase (*cf.* fig. C.4b), for all values of m. On the other hand, the strain-rate fluctuations are comparable to those in the matrix phase when $m = 1$, and more importantly, they are seen to increase significantly with decreasing m, becoming even larger than those in the matrix phase (*cf.* fig. C.5b). Furthermore, they seem to be consistent with unbounded strain-rate fluctuations in the perfectly plastic limit (the FFT results for $m = 0$ yield very large strain-rate fluctuations in this phase as well). Such an increase of the strain fluctuations in the fiber phase is due to the fact that, as the nonlinearity increases, the strain rate also becomes localized in this (weaker) phase, as is discussed further below. In contrast, the nonlinear homogenization estimates provided in this work require zero field fluctuations in the fibers. The reason for this is that use has been made of the Hashin-Shtrikman estimates to homogenize the associated LCCs, which assume that the local

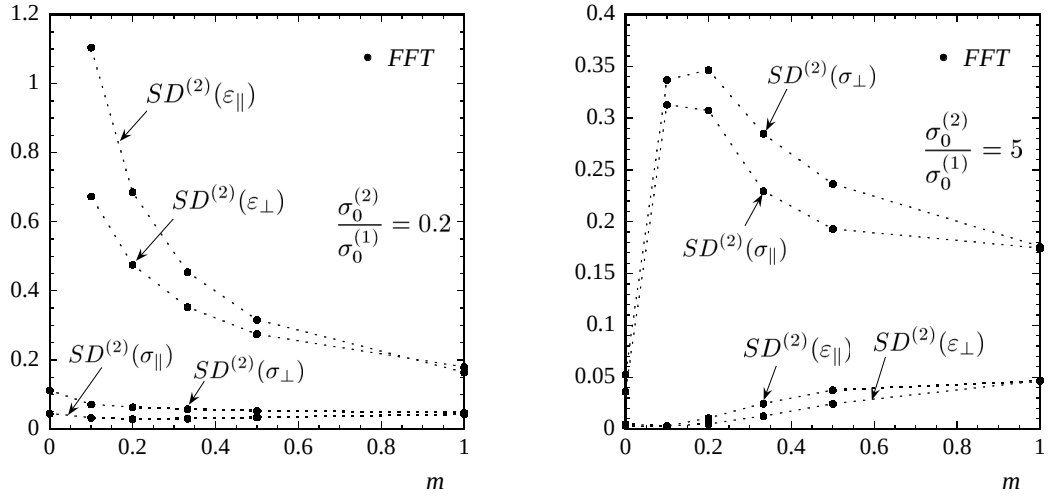

Figure C.6: FFT results for the standard deviations (SD) of the fields in the fibers, for the cases of: (a) weaker fibers ($\sigma_0^{(2)}/\sigma_0^{(1)} = 0.2$), (b) stronger fibers ($\sigma_0^{(2)}/\sigma_0^{(1)} = 5$). The SD of the stress components are normalized by the equivalent macroscopic stress $\overline{\sigma}_e$, while the SD of the strain-rate components are normalized by the equivalent macroscopic strain rate $\overline{\varepsilon}_e$.

fields are uniform and equal inside all the fibers, and this assumption carries over to the nonlinear estimates. It should be emphasized, however, that this is a limitation associated only with the *linear* HS estimates and not with the nonlinear homogenization methods considered here. The fact that the strain-rate fluctuations in the FFT simulations become very large for small values of m suggests that, for the class of microstructures considered here, the linear HS estimates used in the context of the nonlinear homogenization methods may be inappropriate as $m \to 0$. In this connection, it is noted that for strong nonlinearities, the LCC generated by the "second-order" method has highly anisotropic phases, and the linear HS estimates, which are known to be accurate for CCA microstructures with isotropic phases, may not give accurate predictions for composites with CCA microstructures when the phases are that anisotropic, at least for the case of weaker fibers. This could explain why the SO estimates and the FFT results provided in this subsection are generally found to be in very good agreement for weak to moderate nonlinearities, while for strong nonlinearities they are found to exhibit different trends. In particular, the fact that the SO estimates for the effective flow stress become larger than the corresponding FFT results (see fig. C.3a) is consistent with the fact that the requirement of uniform fields in the fiber phase implicit in the HS hypothesis should lead to a stiffer macroscopic behavior, since in a sense, it "prevents" the localization of the strain field in the fibers. In turn, this suggests that a better correlation should be obtained by using the "second-order" method in combination with more appropriate linear homogenization methods, or even by computing numerically the homogenized behavior of the LCC, as has been recently done in combination with the "variational" method by Moulinec and Suquet (2004).

Distribution of local fields. For a fuller understanding of the results discussed above, maps of the local fields were generated from the FFT simulations. The maps provided in this work correspond to

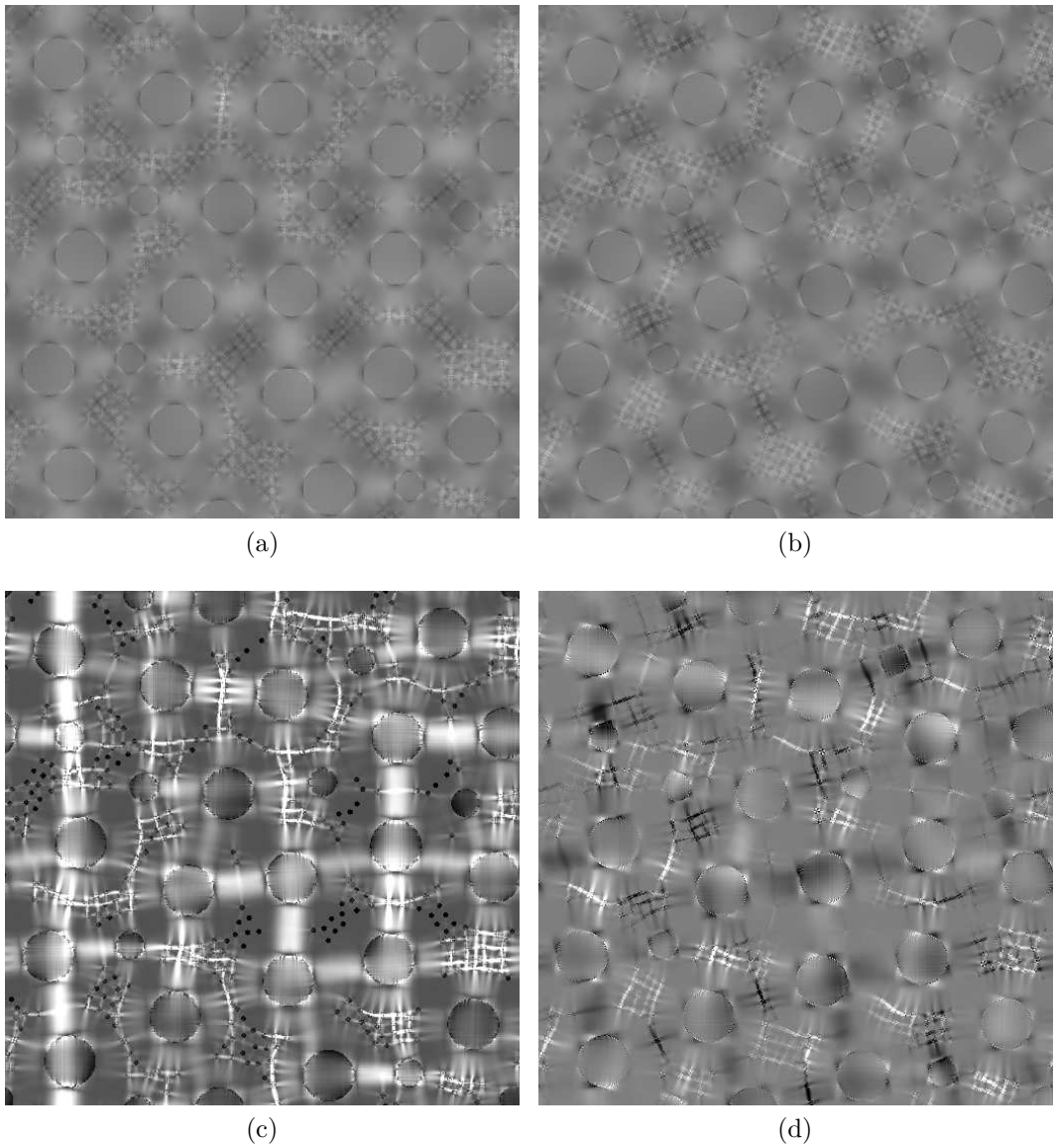

(a) (b)

(c) (d)

Figure C.7: Strain-rate distribution in a power-law composite with weaker fibers ($\sigma_0^{(2)}/\sigma_0^{(1)} = 0.2$), subjected to in-plane shear $\overline{\sigma}_{12}$. The microstructure is the one shown in fig. C.2. Distribution of the "parallel" component $\varepsilon_{12} - \overline{\varepsilon}_{12}^{(r)}$ when: (a) $m = 1$, (c) $m = 0.1$; distribution of the "perpendicular" component $(\varepsilon_{11} - \varepsilon_{22})/2$ when: (b) $m = 1$, (d) $m = 0.1$. Black and white correspond, respectively, to values smaller than -2 and larger than 2. The quantities are normalized by $(\sqrt{3}/2)\,\overline{\varepsilon}_e$.

a composite with the microstructure shown in fig. C.2, subject to in-plane shear (C.44). Thus, in this case the "parallel" and "perpendicular" components of the fields refer to those defined by expressions (C.45).

Figure C.7 provides maps of the components of the strain-rate field. Parts (a) and (c) show the deviation in each phase of the "parallel" component about its phase average, that is $\varepsilon_{12}(\mathbf{x}) - \overline{\varepsilon}_{12}^{(1)}$ in the matrix and $\varepsilon_{12}(\mathbf{x}) - \overline{\varepsilon}_{12}^{(2)}$ in the fibers, while parts (b) and (d) show the "perpendicular" component $(\varepsilon_{11} - \varepsilon_{22})/2$, which fluctuates about zero in both phases. In turn, parts (a) and (b) correspond to the case of linear ($m = 1$) phases, while parts (c) and (d) correspond to the case of highly nonlinear ($m = 0.1$) phases. These maps show the changing character of the spatial distribution of the strain rate with nonlinearity. Thus, in the linear case, the distributions of both components of the strain rate are rather diffuse and exhibit similar degrees of heterogeneity (see parts (a) and (b)). This fact is manifested by the isotropy of the strain-rate fluctuations mentioned in the context of fig. C.5b. In contrast, the distributions of the "parallel" and "perpendicular" components of the strain rate in the nonlinear case are much more heterogeneous and significantly different from each other (see parts (c) and (d)). In this connection, it should be recalled that in nonlinear composites the deformation rate can localize in bands, which may become progressively thinner as the nonlinearity increases (see, for example, Moulinec and Suquet, 1998). Across such bands, the tangential component of the velocity field varies significantly, resulting in large shear strain rate. More precisely, if the vectors $\mathbf{t}$ and $\mathbf{n}$ denote, respectively, the directions tangential and normal to the band, then ε_{tn} increases with decreasing band width, but not $(\varepsilon_{nn} - \varepsilon_{tt})/2$. Indeed, it can be seen in part (c) that the "parallel" component of the strain localizes in (white) bands running across the specimen, which are found to *seek* the (weaker) fibers, remaining at the same time as parallel as possible to the directions of maximum macroscopic shear (0° and 90°). Thus, the macroscopic deformation rate is being accommodated mainly by large deformation rates along these bands, outside of which the deformation rate is relatively small. These localization bands are responsible for the significant increase of $SD^{(r)}(\varepsilon_{\parallel})$ observed in figs. C.5b and C.6a. On the other hand, it can be seen in part (d) that the "perpendicular" component of the strain rate is small wherever the bands observed in part (c) are oriented at 0° and 90°. However, when the bands "bend" in order to accommodate the randomness of the distribution of fibers, this component is also found to be very large, being positive (white) or negative (black) depending on the local orientation of the band. Thus, the fact that all bands are not perfectly "aligned" with the directions of maximum macroscopic shear in this case, explains the significant increase of $SD^{(r)}(\varepsilon_{\perp})$ observed in figs. C.5b and C.6a. Nonetheless, the fluctuations of the "parallel" component of the strain rate are larger than those of the "perpendicular" component as a consequence of the preferred orientation of the bands mentioned above. (In fact, the ratio $SD^{(r)}(\varepsilon_{\perp})/SD^{(r)}(\varepsilon_{\parallel})$ provides a measure of the tortuosity of the bands, for low enough values of m, which is strongly dependent on the concentration of fibers.) Thus, by allowing strain localization, nonlinearity not only increases significantly the strain-rate fluctuations, but also induces anisotropy on them, even though the phases and their spatial distribution are isotropic.

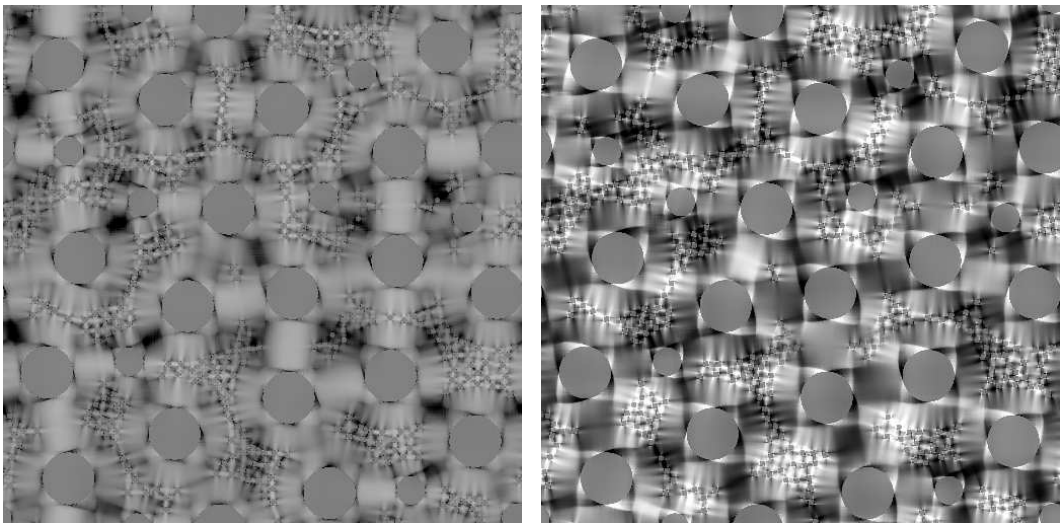

(a) (b)

Figure C.8: Stress distribution in a power-law composite with weaker fibers ($\sigma_0^{(2)}/\sigma_0^{(1)} = 0.2$), subjected to in-plane shear $\overline{\sigma}_{12}$. The microstructure is the one shown in fig. C.2. Distribution for $m = 0.1$ of the: (a) "parallel" component $\sigma_{12} - \overline{\sigma}_{12}^{(r)}$, and (b) "perpendicular" component $(\sigma_{11} - \sigma_{22})/2$. Black and white correspond, respectively, to values smaller than -1 and larger than 1. The quantities are normalized by $\overline{\sigma}_e/\sqrt{3}$.

In the perfectly plastic limit, the localization bands can turn into shear bands, across which the tangential component of the velocity field is discontinuous (Suquet, 1981). In this connection, it is recalled that in the case of perfectly plastic porous composites with periodic microstructures, the exact solution corresponds to shear bands passing through the pores (Drucker, 1966), which is consistent with the localization bands observed in fig. C.7c. In addition, it is noted that in the presence of shear bands, the fluctuations of certain components of the strain rate may become unbounded. (In perfect plasticity, the strain-rate tensor $\boldsymbol{\varepsilon}$ is a bounded measure on Ω, and therefore, its L^1 norm is finite but its L^2 norm may become unbounded (Suquet, 1981).) As already mentioned, the FFT results for the standard deviations of both components of the strain rate shown in figs. C.6b and C.5b are seen to increase at an increasing rate as m decreases. This strongly suggests that indeed the strain-rate fluctuations should blow up in the perfectly plastic limit.

Figure C.8 provides the corresponding maps of the components of the stress field for the case of highly nonlinear ($m = 0.1$) phases. Part (a) shows the deviation in each phase of the "parallel" component about its phase average, that is $\sigma_{12}(\mathbf{x}) - \overline{\sigma}_{12}^{(1)}$ in the matrix and $\sigma_{12}(\mathbf{x}) - \overline{\sigma}_{12}^{(2)}$ in the fibers, while part (b) shows the "perpendicular" component $(\sigma_{11} - \sigma_{22})/2$, which fluctuates about zero in both phases. In the linear case, the stress components are simply equal to the corresponding strain-rate component multiplied by the flow stress (constant within each phase), and so the maps of the stress are very similar to those shown in figs. C.7a and C.7b, and are omitted here. The important point to make, however, is that, in the linear case, the distributions of both components of the stress also exhibit similar degrees of heterogeneity, and this is manifested by the isotropy of the stress fluctuations mentioned in the context of fig. C.4b. When the phases are nonlinear, on

the other hand, the distribution of the "perpendicular" component is seen to be more heterogeneous than the that of the "parallel" component. In addition, the "parallel" component (part (a)) is seen to exhibit, in the matrix, a pattern similar to that of the strain rate observed in fig. C.7c, but much less contrasted, taking the largest values along the localization bands mentioned in the context of that figure. This is not surprising, since in the perfectly plastic limit a necessary (local) condition for the development of a shear band running at 0° or 90° is that $\sigma_{\parallel} = \sigma_0^{(r)}$. Note that while the strain rate is becoming unbounded along these bands, the stress is becoming bounded by the flow stress in each phase, as $m \to 0$. This is why the strain-rate fluctuations shown in figs. C.5b and C.6a blow up as $m \to 0$, whereas the stress fluctuations shown in figs. C.4b and C.6a remain finite.

Histograms. Figure C.9 provides plots for the probability density functions of the components of the local fields in the matrix. The clear and dark circles represent the FFT results corresponding to the specific configuration shown in fig. C.2 (and not to the ensemble averages) with linear ($m = 1$) and highly nonlinear ($m = 0.1$) phases, respectively. In addition, the continuous and dashed lines represent, respectively, Gaussian distributions whose mean and standard deviation are those obtained from the FFT simulations for $m = 1$ and $m = 0.1$, which are included in order to verify the possible Gaussian character of the field distributions.

Parts (a) and (b) show, respectively, the distributions of the "parallel" and "perpendicular" components of the stress normalized by the equivalent macroscopic stress $\overline{\sigma}_e$ (as given by expressions (C.48) with $z = \sigma_{\parallel}/\overline{\sigma}_e$ and $z = \sigma_{\perp}/\overline{\sigma}_e$). We begin by noting that in the linear case (clear circles), the distributions of both components of the stress are in very good agreement with the corresponding Gaussian distributions (continuous lines). (In this connection, it should be mentioned that while the Gaussian distributions vanish only at infinity, the distributions of the local fields vanish at finite values, which correspond to the maximum and minimum values that the fields take in the composite.) In addition, the distributions of both components are seen to be fairly similar to each other, except for a shift in abscissa, which is manifested by the isotropy of the stress fluctuations mentioned in the context of fig. C.4b. In the nonlinear case, on the other hand, while the distribution of the "perpendicular" component remains fairly Gaussian, the distribution of the "parallel" component is seen to become skewed to the right and to drop to zero rather abruptly for values of $\sigma_{\parallel}/\overline{\sigma}_e$ larger than the mean. The latter is a manifestation of the fact that in the limiting case of perfect plasticity ($m \to 0$), the stress components become bounded by the requirement $\sigma_e^2 = \sigma_{\parallel}^2 + \sigma_{\perp}^2 \leq (\sigma_0^{(r)})^2$. Although this restriction applies to both stress components, the fact that only the distribution of the "parallel" component exhibits an abrupt drop follows from the fact that, unlike the "perpendicular" component, its mean value is greater than zero and therefore closer to the bound that develops in the limit $m \to 0$.

Parts (c) and (d) show, respectively, the corresponding distributions of the "parallel" and "perpendicular" components of the strain rate, normalized by the equivalent macroscopic strain rate $\overline{\varepsilon}_e$ (as given by expressions (C.48) with $z = \varepsilon_{\parallel}/\overline{\varepsilon}_e$ and $z = \varepsilon_{\perp}/\overline{\varepsilon}_e$). In the linear case, the distributions

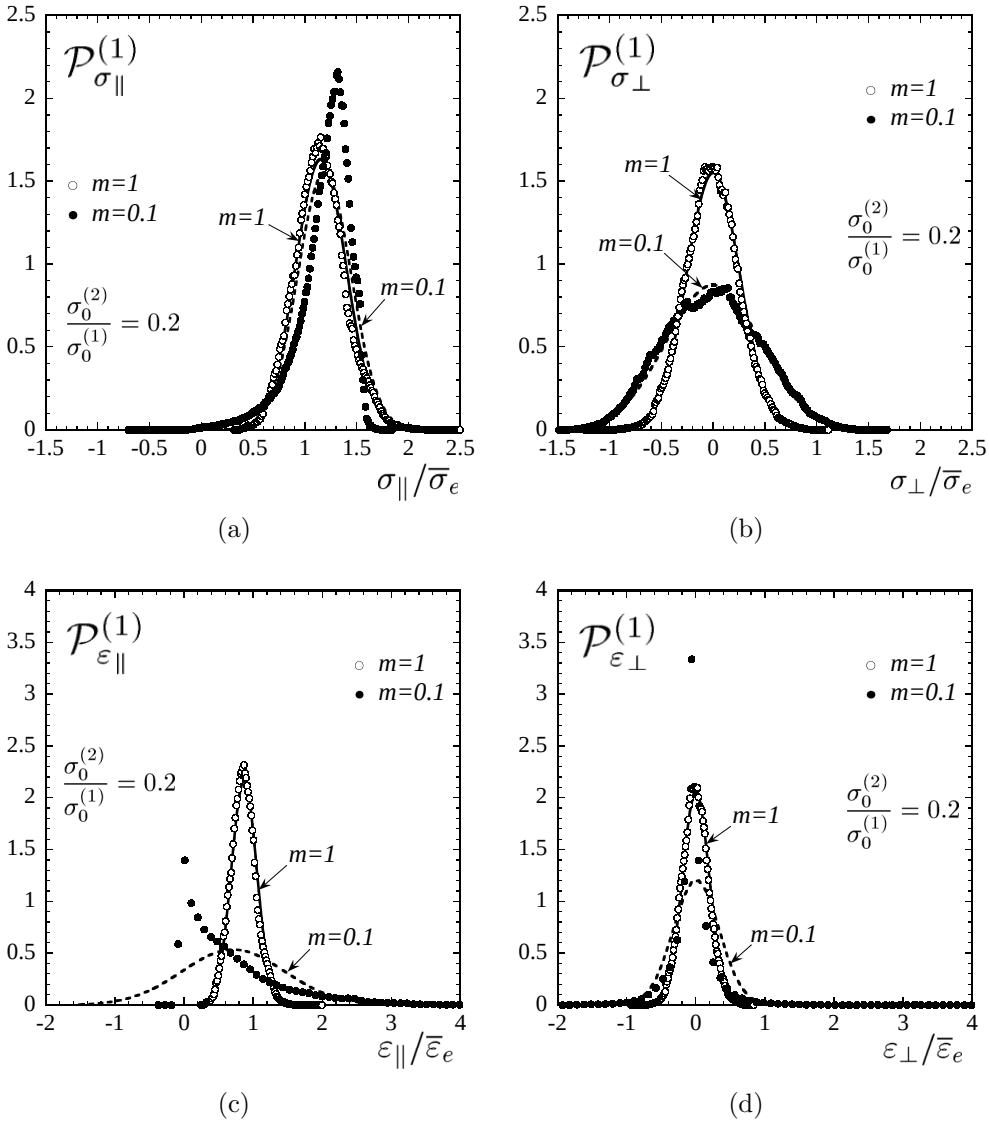

Figure C.9: FFT results for the probability density functions of the local fields for the case of weaker fibers, associated with the microstructure shown in fig. C.2. The clear and dark circles correspond, respectively, to exponents $m = 1$ and $m = 0.1$. The continuous and dashed lines represent, respectively, the Gaussian distributions whose mean and standard deviation are those obtained from the FFT simulations for $m = 1$ and $m = 0.1$. Distributions of: (a) "parallel" ($\sigma_\parallel/\overline{\sigma}_e$) and (b) "perpendicular" ($\sigma_\perp/\overline{\sigma}_e$) components of the stress, (c) "parallel" ($\varepsilon_\parallel/\overline{\varepsilon}_e$) and (d) "perpendicular" ($\varepsilon_\perp/\overline{\varepsilon}_e$) components of the strain rate.

of the strain-rate components are similar to those of the corresponding stress components, and therefore similar observations apply. Thus, the distributions of both strain-rate components (clear circles) are also found to be in good agreement with the corresponding Gaussian distributions (continuous lines). In the nonlinear case, on the other hand, the distributions of the "parallel" and "perpendicular" components (dark circles) are found to be very different from the corresponding Gaussian distributions (dashed lines). In particular, the distribution of the "parallel" component is seen to be highly skewed to the left with respect to its mean, being maximum at $\varepsilon_{\parallel}/\overline{\varepsilon}_e \approx 0$ and exhibiting an abrupt drop for smaller values of $\varepsilon_{\parallel}/\overline{\varepsilon}_e$ (see part (c)). In addition, this distribution is found to develop a tail in the range of large values of $\varepsilon_{\parallel}/\overline{\varepsilon}_e$. In contrast, the distribution of the "perpendicular" component is found to remain symmetric about its mean, but it becomes more concentrated close to $\varepsilon_{\perp}/\overline{\varepsilon}_e = 0$ than in the linear case, and it develops tails in the range of large values of $|\varepsilon_{\perp}/\overline{\varepsilon}_e|$. The tails developed by the strain-rate distributions correspond to the presence of very large strain rates in very small regions, *i.e.* localization bands, and the fact that these distributions are maximum at approximately 0 means that the deformation rate is relatively small for most regions (in the matrix) outside the bands. Thus, as the nonlinearity increases, the strain-rate distributions, especially that of the "parallel" component, progressively deviate further from a Gaussian distribution, due to the development of strain localization. It is worth noting that the reasons why the field distributions become non-Gaussian with nonlinearity are different for the strain rate than for the stress fields, and that the former is seen to be more sensitive in this regard than the latter.

C.6.2 Fiber-reinforced composites

Effective behavior. The various bounds and estimates for the effective flow stress $\widetilde{\sigma}_0$ of a fiber-reinforced composite are plotted in fig. C.3b, together with the FFT results as a function of the strain-rate sensitivity m, normalized by the flow stress of the matrix $\sigma_0^{(1)}$. The main observation in the context of this figure is that the SO estimates are found to be in good agreement with the FFT simulations, even for the smaller values of m. Thus, both methods yield a decreasing $\widetilde{\sigma}_0$ with decreasing values of m (*i.e.*, increasing nonlinearity), and in the perfectly plastic limit ($m \to 0$) they predict no reinforcement effect due to the stronger fibers, *i.e.* $\widetilde{\sigma}_0 = \sigma_0^{(1)}$. As pointed out by Drucker (1966), this is the correct limit if the arrangement of fibers allows for a shear plane passing through the matrix (see below for more details). Furthermore, this coincides with the Reuss lower bound, which is known to be optimal in this limit (see Garroni et al., 2001, Suquet, 2005). Also included in this figure are the "tangent second-order" (TSO) estimates and the"variational" (VAR) estimates. As already mentioned, the latter are rigorous upper bounds for all other nonlinear estimates of the HS type, and in particular for the SO and TSO estimates. Several comments are in order. First, the homogenization estimates all coincide for $m = 1$ with the linear HS estimates, as they should, but give different predictions for other values of m. However, the SO and TSO estimates are found to be very similar for all values of m in this case, and they coincide not only for $m = 1$ but also for $m = 0$. Thus the TSO estimates are also in good agreement with the FFT results in this case.

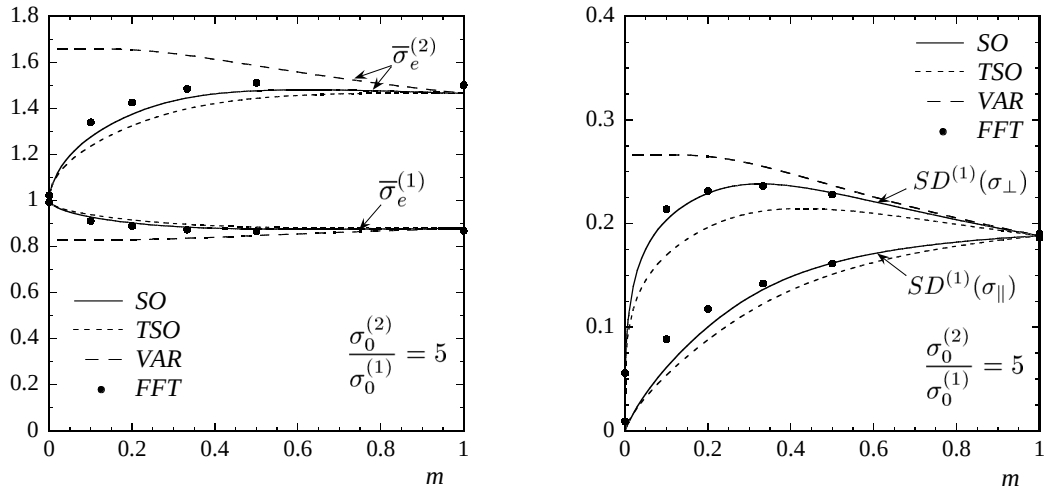

Figure C.10: Statistics of the stress field for the case of stronger fibers. (a) Equivalent average stresses in the matrix ($\overline{\sigma}_e^{(1)}$) and fibers ($\overline{\sigma}_e^{(2)}$). (b) Standard deviation (SD) of the "parallel" and "perpendicular" components of the stress field in the matrix. The results are normalized by $\overline{\sigma}_e$.

The "variational" estimates, on the other hand, are found to overestimate the FFT results for all values of m different than 1, and they even give a finite reinforcement effect in the limit $m \to 0$. It is further observed that, as anticipated, the TSO estimates exhibit a duality gap, but as opposed to what happens in the case of fiber-weakened composites, this gap is seen to be small for all values of m, and even vanishes in the perfectly plastic limit. In contrast, the SO estimates (C.16) and (C.18) are exactly equivalent for all values of m. Finally, it is noted that the scatter exhibited by the FFT results is found to be very small in this case as well.

Statistics of the local fields. Corresponding estimates for the phase averages and standard deviations of the stress field are shown in fig. C.10. Part (a) provides plots for the equivalent average stresses $\overline{\sigma}_e^{(r)}$ in each phase, normalized by the equivalent macroscopic stress $\overline{\sigma}_e$. It can be seen in this figure that the FFT results show an average stress in the (stronger) fibers that is always higher than that in the matrix, as expected. However, the former is seen to decrease with increasing nonlinearity, while the latter is seen to increase, until they both coincide with $\overline{\sigma}_e$ in the perfectly plastic limit. Among the homogenization estimates, the SO estimates are the most consistent ones with the FFT simulations, the agreement being good for all values of m. The $TSO(U)$ estimates are found to give similar predictions, and even coincide with the SO estimates as $m \to 0$, as anticipated in the previous paragraph. In contrast, the trends exhibited by the "variational" estimates are seen to be inconsistent with the FFT results. Part (b) shows plots for the standard deviations of the "parallel" and "perpendicular" components of the stress in the matrix, normalized by the equivalent macroscopic stress $\overline{\sigma}_e$. The main observation in the context of this figure is that, like in the previous subsection, the FFT simulations are found to give stress fluctuations that are isotropic in the linear case and become progressively more anisotropic as the nonlinearity increases, being larger for the "perpendicular" component than for the "parallel" component. However, unlike what happens in a

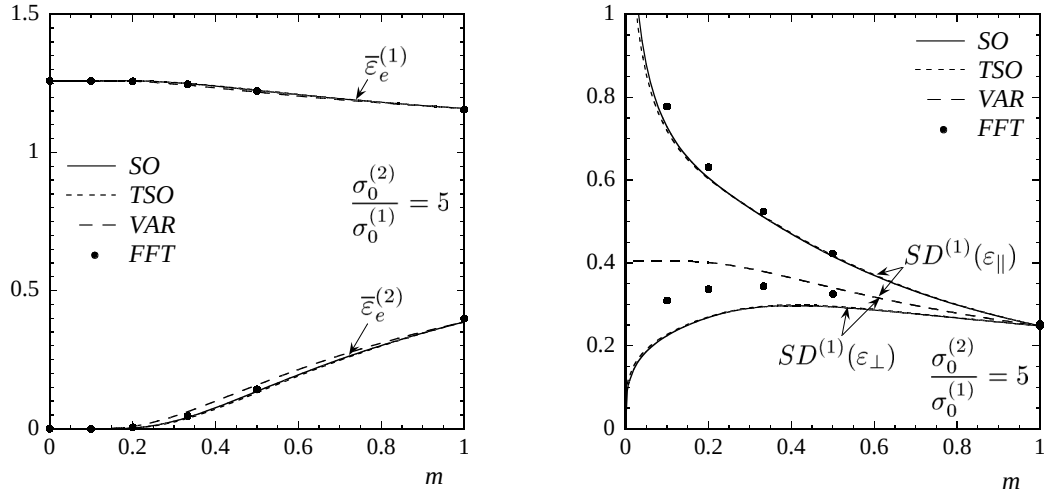

Figure C.11: Statistics of the strain-rate field for the case of stronger fibers. (a) Equivalent average strain rates in the matrix ($\overline{\varepsilon}_e^{(1)}$) and fibers ($\overline{\varepsilon}_e^{(2)}$). (b) Standard deviation (SD) of the "parallel" and "perpendicular" components of the strain-rate field in the matrix. The results are normalized by $\overline{\varepsilon}_e$.

fiber-weakened composite (*cf.* fig. C.4b), both the "parallel" and the "perpendicular" fluctuations are found to decrease for values of m smaller than about 0.3, almost vanishing in the perfectly plastic limit. It can be seen that the SO estimates are consistent with these observations, being in good agreement with the FFT results for all values of m. Note that in the limit $m \to 0$ these estimates predict vanishing fluctuations, which, together with the fact that $\overline{\sigma}_e^{(1)} = \overline{\sigma}_e^{(2)} = \overline{\sigma}_e$ (see part (a)), implies that the stress field tends to become uniform throughout the composite. It is further observed that the $TSO(U)$ estimates exhibit the same trends as the FFT results, but they are not as close in general to them as the SO estimates. Finally, the "variational" estimates are seen to overestimate the stress fluctuations for all values of m different than 1, and more importantly, they predict isotropic stress fluctuations for all values of m, thus being, once again, inconsistent with the FFT simulations.

Figure C.11 provides corresponding estimates for the phase averages and standard deviations of the strain-rate field. In part (a), plots are given for the equivalent average strain rate $\overline{\varepsilon}_e^{(r)}$ in each phase, normalized by the equivalent macroscopic strain rate $\overline{\varepsilon}_e$. It is observed in this figure that all homogenization estimates are in very good agreement with the FFT simulations, for all values of m. Thus, all methods are seen to predict an average strain rate in the (stronger) fibers which is lower than that in the matrix, and that decreases with decreasing m, until it vanishes in the limit $m \to 0$. Thus in this limit, the fibers behave like rigid inclusions. This is related to the well-known fact that nonlinearity enhances the contrast between the phases. In part (b), plots are given for the standard deviations of the strain-rate field in the matrix, normalized by the equivalent macroscopic strain rate $\overline{\varepsilon}_e$. It is observed that, like in the case of fiber-weakened composites, the FFT simulations show strain-rate fluctuations which are isotropic in the linear case, and become progressively more anisotropic as the nonlinearity increases, being larger for the "parallel" component than for the "perpendicular" one. Moreover, the "parallel" fluctuations are seen to increase monotonically with nonlinearity here as

well. However, unlike what happens in fiber-weakened composites, the "perpendicular" fluctuations are found to increase slightly in the range $0.3 \leq m \leq 1$, and decrease for smaller values of m. It can be seen that the SO estimates are consistent with these observations. Furthermore, it is seen that the SO estimates for the "parallel" strain-rate fluctuations are in good agreement with the FFT results for all values of m. On the other hand, the agreement may not be as good for the "perpendicular" strain-rate fluctuations, quantitatively, but the trends exhibited by both sets of results are seen to be fully consistent. It is also noted that, as $m \to 0$, the SO estimates predict infinite and vanishing strain-rate fluctuations in the "parallel" and "perpendicular" directions, respectively, which is consistent with strain localization along straight shear bands, as discussed below. It is further observed that the $TSO(W)$ estimates are almost identical to the SO estimates for all values of m, so that the previous comments apply to these estimates as well. In contrast, the "variational" estimates are found to predict a slight increase of the strain-rate fluctuations with increasing nonlinearity, but more importantly, they predict, once again, isotropic strain-rate fluctuations for all values of m, which is inconsistent with the FFT simulations.

The corresponding standard deviations of the local fields in the fiber phase are shown in fig. C.6b. It can be seen that, unlike for the case of weaker fibers, the FFT simulations give stress fluctuations that are comparable to those in the matrix phase when $m = 1$, and increase with increasing nonlinearity, becoming even larger than the stress fluctuations in the matrix phase for moderate nonlinearities. However, they decrease significantly as $m \to 0$, which together with the FFT results for the stress phase averages and fluctuations in the matrix (*cf.* fig. C.10) indicates that the stress field is quite uniform (and approximately equal to the macroscopic stress) in the perfectly plastic limit throughout the composite. On the other hand, the strain-rate fluctuations in the fiber phase are much smaller than those in the matrix phase (*cf.* fig. C.11b), for all values of m, and decrease with increasing nonlinearity. This is a consequence of the fact that, opposite to what happens in the case of weaker fibers, no strain localization occurs in the fibers when these are stronger than the matrix (see further below). The fact that the fluctuations of the local fields shown in fig. C.6b tend to be relatively small as $m \to 0$ may explain why the SO predictions based on the HS estimates for the LCC are in better agreement with the FFT results in this case than in the case of weaker fibers, where the strain-rate fluctuations in the fiber phase increase significantly for small values of m, and are therefore inconsistent with the HS hypothesis.

Distribution of local fields. Figure C.12 provides maps of the strain-rate field generated from the FFT simulations, for a composite with the microstructure shown in fig. C.2, for the case of highly nonlinear ($m = 0.1$) phases, subjected to in-plane shear (C.44). Part (a) shows the deviation in each phase of the "parallel" component about its phase average, that is $\varepsilon_{12}(\mathbf{x}) - \overline{\varepsilon}_{12}^{(1)}$ in the matrix and $\varepsilon_{12}(\mathbf{x}) - \overline{\varepsilon}_{12}^{(2)}$ in the fibers, while part (b) shows the "perpendicular" component $(\varepsilon_{11} - \varepsilon_{22})/2$, which fluctuates about zero in both phases. The corresponding maps for the linear case ($m = 1$) are, for the purposes of the comparisons of interest here, qualitatively similar to those shown in fig. C.7a,b for fiber-weakened composites, and are therefore omitted for brevity. Several comments are

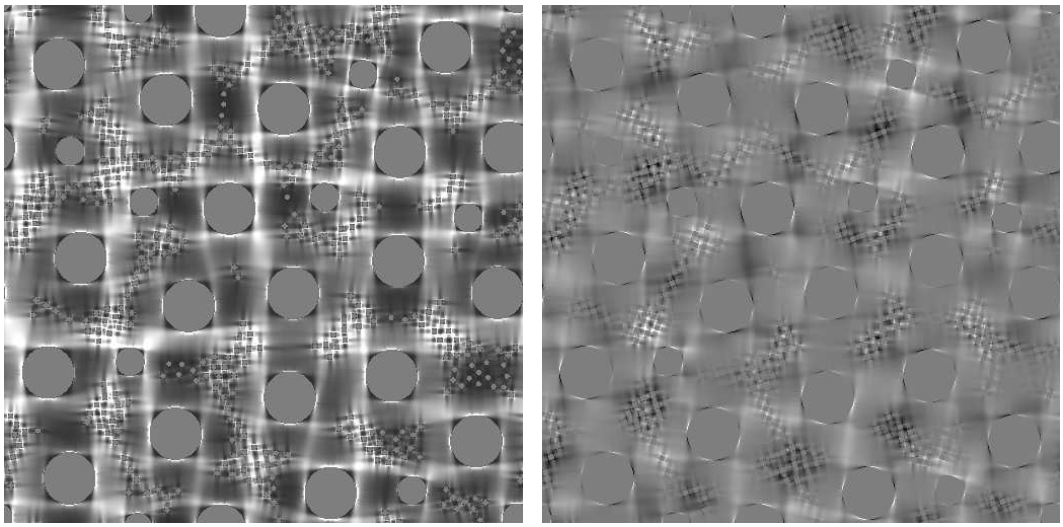

(a) (b)

Figure C.12: Strain-rate distribution in a power-law composite with stronger fibers ($\sigma_0^{(2)}/\sigma_0^{(1)} = 5$), subjected to in-plane shear $\overline{\sigma}_{12}$. The microstructure is the one shown in fig. C.2, and the exponent is $m = 0.1$. Distribution of the: (a) "parallel" component $\varepsilon_{12} - \overline{\varepsilon}_{12}^{(r)}$, and (b) "perpendicular" component $(\varepsilon_{11} - \varepsilon_{22})/2$. Black and white correspond, respectively, to values smaller than -2 and larger than 2. The quantities are normalized by $(\sqrt{3}/2)\,\overline{\varepsilon}_e$.

relevant in the context of this figure. First, as has already been observed in the case of weaker fibers, while in the linear case the distributions of both components of the strain rate are rather diffuse and exhibit similar degrees of heterogeneity, in the nonlinear case the distributions of the "parallel" and "perpendicular" components are much more heterogeneous and significantly different from each other. As already explained in the previous subsection, this is due to the fact that for nonlinear materials the deformation rate tends to localize in thin bands running across the specimen. However, unlike what happens for the case of weaker fibers, these localization bands are found here to *avoid* the (stronger) fibers, remaining at the same time as parallel as possible to the directions of maximum macroscopic shear (0° and 90°). This is the reason why in this case the strain-rate fluctuations, shown in figs. C.11b and C.6b, while increasing in the matrix with increasing nonlinearity, actually decrease in the fibers. In addition, it is observed that, as for the case of weaker fibers, the bands tend to "bend" in order to accommodate the randomness of the distribution of fibers, but they remain straighter than when they seek the fibers (at least at this concentration of fibers). This fact helps explain why the "perpendicular" component shown in fig. C.12b is not as localized as that shown in fig. C.7d. In fact, the trend exhibited by the FFT results for $SD^{(1)}(\varepsilon_\perp)$ shown in fig. C.11b suggests that the fluctuations of the "perpendicular" component of the strain rate in the matrix actually decrease for smaller values of m, unlike in the case of weaker fibers (*cf.* fig. C.6b).

In order to put these results in context, it is useful to recall the following result for ideally plastic materials reinforced by stronger fibers (Drucker, 1966; Suquet, 1993): If the arrangement of the fibers in the composite is such that it is possible to pass (straight) planes through the matrix that are aligned with the shear loading, then the exact result corresponds to straight shear bands along

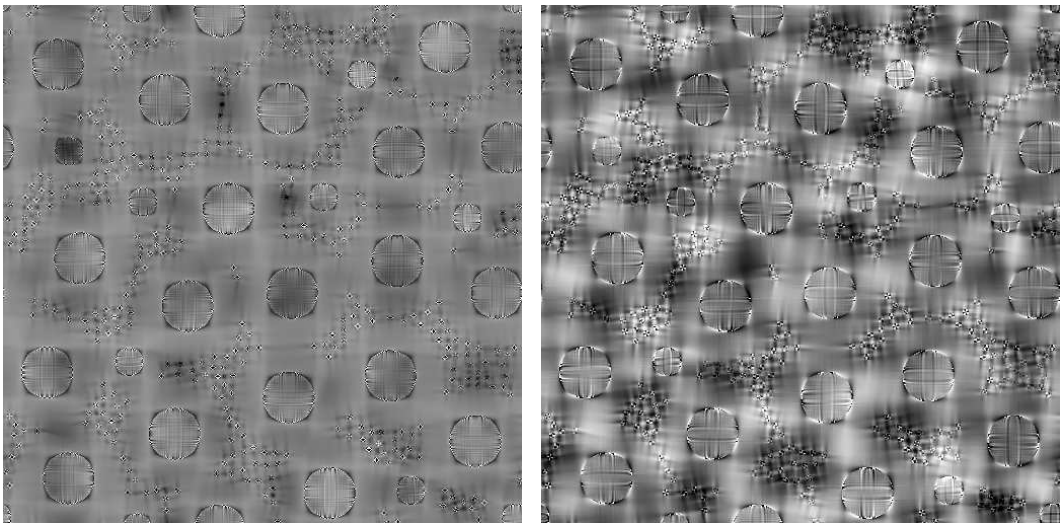

(a) (b)

Figure C.13: Stress distribution in a power-law composite with stronger fibers ($\sigma_0^{(2)}/\sigma_0^{(1)} = 5$), subjected to in-plane shear $\overline{\sigma}_{12}$. The microstructure is the one shown in fig. C.2, and the exponent is $m = 0.1$. Distribution of the: (a) "parallel" component $\sigma_{12} - \overline{\sigma}_{12}^{(r)}$, and (b) "perpendicular" component $(\sigma_{11} - \sigma_{22})/2$. Black and white correspond, respectively, to values smaller than -0.68 and larger than 0.68. The quantities are normalized by $\overline{\sigma}_e/\sqrt{3}$.

these planes. In this case, the effective flow stress $\widetilde{\sigma}_0$ would be exactly that of the matrix, as has already been mentioned. In addition, the corresponding strain-rate fluctuations in the matrix would be such that $SD^{(1)}(\varepsilon_{\parallel}) \to \infty$ and $SD^{(1)}(\varepsilon_{\perp}) \to 0$, while the strain rate in the fibers would be exactly zero. Also, the stress field would be uniform throughout the composite. Now, it is observed that the trends seen for the "second-order" HS predictions in the limit as $m \to 0$ are entirely consistent with this result (regardless of the concentration of fibers). On the other hand, for the specific random microstructures considered in the FFT simulations, the probability of finding such (straight) shear planes is expected to be small at relatively small fiber concentrations, and to vanish at sufficiently high fiber concentrations. Indeed, at the intermediate volume fraction considered here (0.20626), many realizations of the composite do not allow for such straight shear planes, and therefore the above-mentioned results cannot be expected to apply. This is the reason why the FFT results do not agree precisely with the "second-order" HS estimates in the ideally plastic limit. However, the fact that, at this volume fraction, nearly straight bands can develop explains why the FFT results are still in fairly good agreement with the "second-order" HS estimates in this case.

Figure C.13 provides the corresponding maps of the stress field for the case of highly nonlinear ($m = 0.1$) phases. Part (a) shows the deviation of the "parallel" component in each phase about its phase average, that is $\sigma_{12}(\mathbf{x}) - \overline{\sigma}_{12}^{(1)}$ in the matrix and $\sigma_{12}(\mathbf{x}) - \overline{\sigma}_{12}^{(2)}$ in the fibers, while part (b) shows the "perpendicular" component $(\sigma_{11} - \sigma_{22})/2$, which fluctuates about zero in both phases. It is recalled that in the linear case, the maps of the stress are qualitatively similar to those of the strain shown in figs. C.7a and C.7b, and are omitted here. The important point to make, though, is that, when the phases are linear, the distribution of both components of the stress also exhibit similar

degrees of heterogeneity, and this is manifested by the isotropy of the stress fluctuations shown in fig. C.10b. On the other hand, when the phases are nonlinear, the distributions of the "parallel" and "perpendicular" components of the stress are found to be very different from each other. In particular, the "parallel" component shown in part (a) is seen to be quite homogeneous throughout the specimen. In fact, as $m \to 0$ it becomes progressively more homogeneous, tending to the flow stress of the matrix everywhere. Note that this level of stress is large enough to produce localization bands in the matrix, but does not produce any deformation in the (stronger) fibers (*cf.* figs. C.12c and C.12d). In contrast, the distribution of the "perpendicular" component exhibits a much more heterogeneous and complicated pattern, especially in the matrix. We do not have an explanation for such a pattern. In any event, the differences between these distributions is what gives rise to the anisotropy of the stress fluctuations mentioned in the context of fig. C.10b (for $m = 0.1$). Finally, it is also noted that both components of the stress are seen to exhibit a "cross" pattern inside the fibers, but this could be an artifact of the numerical simulations related to the "pixelation" of the fiber boundaries.

Histograms. Figure C.14 provides plots for the probability density functions of the components of the local fields in the matrix. The clear and dark circles represent the FFT results corresponding to the specific configuration shown in fig. C.2 (and not ensemble averages) with linear ($m = 1$) and highly nonlinear ($m = 0.1$) phases, respectively. In addition, the continuous and dashed lines represent, respectively, Gaussian distributions whose mean and standard deviation are those obtained from the FFT simulations for $m = 1$ and $m = 0.1$.

Parts (a) and (b) show, respectively, the distributions of the "parallel" and "perpendicular" components of the stress normalized by the equivalent macroscopic stress $\overline{\sigma}_e$. As in the case of weaker fibers, when the phases are linear, the distributions of both components of the stress (clear circles) are found to be in very good agreement with the corresponding Gaussian distributions (continuous lines). In addition, both distributions are seen to be very similar to each other, which is manifested by the isotropy of the stress fluctuations mentioned in the context of fig. C.10b. When the phases are nonlinear, on the other hand, the distributions of both components of the stress (dark circles) are seen to be very different from each other. Thus, it is observed that, as for the case of weaker fibers, the distribution of the "parallel" component of the stress is in disagreement with the corresponding Gaussian distribution (see part (a)), while the "perpendicular" component remains in good agreement with the corresponding Gaussian distribution (see part (b)). As already mentioned in the context of fig. C.9, this is due to the fact that in the limiting case of perfect plasticity ($m \to 0$), the stress becomes bounded by the requirement $\sigma_e^2 \leq (\sigma_0^{(r)})^2$.

Parts (c) and (d) show, respectively, the corresponding distributions of the "parallel" and "perpendicular" components of the strain rate, normalized by the equivalent macroscopic strain rate $\overline{\varepsilon}_e$. It can be seen that while in the linear case the distributions of the "parallel" and "perpendicular" components of the strain rate are seen to be fairly Gaussian, in the nonlinear case they are found to be very different from the corresponding Gaussian distributions. More specifically, the distribution

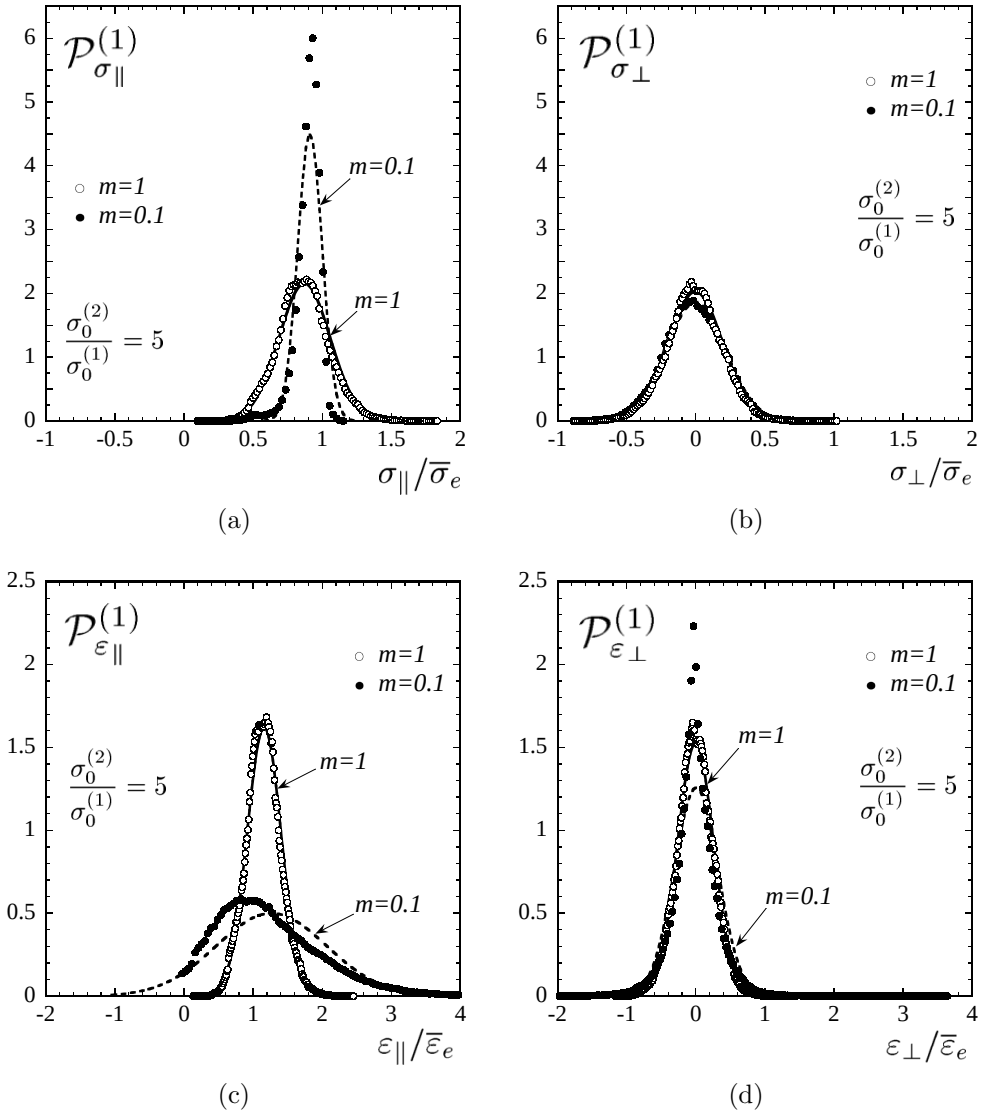

Figure C.14: FFT results for the probability density functions of the local fields for the case of stronger fibers, associated with the microstructure shown in fig. C.2. The clear and dark circles correspond, respectively, to exponents $m = 1$ and $m = 0.1$. The continuous and dashed lines represent, respectively, the Gaussian distributions whose mean and standard deviation are those obtained from the FFT simulations for $m = 1$ and $m = 0.1$. Distributions of: (a) "parallel" ($\sigma_\parallel/\overline{\sigma}_e$) and (b) "perpendicular" ($\sigma_\perp/\overline{\sigma}_e$) components of the stress, (c) "parallel" ($\varepsilon_\parallel/\overline{\varepsilon}_e$) and (d) "perpendicular" ($\varepsilon_\perp/\overline{\varepsilon}_e$) components of the strain rate.

of the "parallel" component is seen to become skewed to the left with respect to its mean, and to develop a tail for large values of $\varepsilon_{\parallel}/\overline{\varepsilon}_e$ (see part (c)). In contrast, the "perpendicular" component is seen to remain fairly symmetric with respect to its mean, becoming more concentrated at $\varepsilon_{\perp}/\overline{\varepsilon}_e = 0$ than in the linear case, and to develop tails in the range of large values of $|\varepsilon_{\perp}/\overline{\varepsilon}_e|$ (see part (d)). As already pointed out in the context of weaker fibers, these tails are due to the presence of strain localization bands, since the bands represent thin regions where the strain rate takes very large values. However, unlike what is observed in the case of weaker fibers, the distribution of the "parallel" component exhibits a maximum at $\varepsilon_{\parallel}/\overline{\varepsilon}_e \approx 1$, as opposed to ≈ 0 (*cf.* fig. C.9c). This means that, while the strain rate in most regions outside the localization bands is relatively small when the fibers are weaker than the matrix, it is approximately equal to the macroscopic strain rate when the fibers are stronger than the matrix, at least at these values of the strain-rate sensitivity and fiber concentration. This may be related to the fact that the localization bands tend to be more uniformly distributed in the matrix phase for the case of stronger fibers than for the case of weaker fibers, where the bands choose fewer paths through the matrix (see figs. C.7c and C.12c). Finally, it is noted that, like in the case of weaker fibers, the strain-rate distributions are seen to be much more sensitive to nonlinearity than the stress distributions, in the sense that they deviate more significantly from the corresponding Gaussian distributions.

C.7 Conclusions

This paper has presented a combined numerical-theoretical study of the macroscopic behavior and local field distributions for a special class of nonlinear composite materials with random "particulate" microstructures. The numerical simulations were carried out using the FFT method developed by Moulinec and Suquet (1994, 1998), and have the advantage of leading to (numerically) exact results, as well as to complete information on the field distributions, at least at the level of one realization of the microstructure. Information on the statistics of the fields were obtained by performing ensemble averages over several different realizations. The theoretical results were obtained by means of the "second-order" homogenization method, proposed by Ponte Castañeda (2002a), making use of suitably chosen estimates for the effective behavior of a *linear comparison composite* (LCC) whose properties are determined by the method itself. The main advantage of the method is that the resulting estimates are analytical, up to some nonlinear algebraic equations, which can be solved numerically with negligible computational effort. On the other hand, the theoretical predictions introduce approximations both at the level of the estimate for the effective behavior of the LCC, as well as at the level of the linearization itself. The main findings of this work are as follows.

The fluctuations of the strain-rate and stress fields, as measured by the standard deviations of these quantities, were found to generally increase and to become anisotropic, with increasing nonlinearity (decreasing values of strain-rate sensitivity m), in agreement with earlier theoretical predictions using the "second-order" method (Ponte Castañeda, 2002b; Idiart and Ponte Castañeda,

2003). More specifically, for the case of softer particles, the FFT simulations show that both the "parallel" and "perpendicular" components of the fluctuations of the strain-rate field tend to increase, with the parallel component increasing faster than the perpendicular component, and tending to become unbounded in the ideally plastic limit ($m = 0$). These results were found to be consistent with the localization of the deformation pattern in the strongly nonlinear composite, where the localization bands "bend" seeking out minimum dissipation paths through the softer inclusions (see fig. C.7). In this case, the fluctuations of the corresponding stress field were also found to increase with increasing nonlinearity, with the difference that this time the perpendicular components of the fluctuations were found to be larger, and that the fluctuations remain bounded in the ideally plastic limit. For the harder-particle case, similar trends were observed for the strain-rate and stress fluctuations, but this time the perpendicular component of the strain-rate, as well as of both components of the stress, tends to become smaller for sufficiently low values of the strain-rate sensitivity parameter. These observations were thought to be related to the fact that, contrary to the softer-particle case, in the harder-particle case, the localized bands tend to avoid the particles and develop in the gaps between the inclusions (see fig. C.12). For the relatively low concentration of fibers considered in this study (approximately 20%), the macroscopic deformation can be accommodated by nearly straight bands, requiring large fluctuations in the parallel component of the strain rate, but relatively smaller fluctuations in the perpendicular component of the strain rate, as well as for both components of the stress.

Even though the "second-order" method, being only a homogenization theory, is not able to capture detailed information about the distribution of the local fields in the composites, it was found that the method gives remarkably accurate predictions not only for the averages of the stress and strain-rate fields in the phases, but also for the standard deviations of the fields in the composite, including the above-mentioned strong dependence of the anisotropy of the fields on the nonlinearity of the material. Even though the "second-order" method could never mimic the highly localized patterns of deformation shown in figs. C.7 and C.12, somehow it is able to capture the signature of these localized fields through fairly accurate predictions for the standard deviations of the fields. Thus, the "second-order" predictions are consistent with the fact that the parallel component of the strain rate localizes more than the corresponding perpendicular component, as well as with the opposite prediction that the perpendicular component of the stress fluctuates more than the corresponding parallel component. The theoretical predictions even reflect the more subtle relative differences between the deformation and stress patterns for the softer- and harder-particle cases.

As already anticipated in an earlier publication (Moulinec and Suquet, 2003), the FFT results (see figs. C.9 and C.14) show that the probability distributions of the fields (in the matrix phase) become progressively distorted away from Gaussian with increasing nonlinearity. This suggests that the "second-order" homogenization theory using a linear comparison composite—and therefore incorporating only information on the first and second moments of the fields—would not be able to capture the higher moments required to explain the strongly non-Gaussian behavior for the higher

nonlinearities. However, the theory somehow does the best it can with the information that it has at its disposal, and it would seem that the higher moments which would be required to capture accurately the non-Gaussian distribution of the fields are perhaps not essential to obtain fairly accurate estimates for the first two moments of the fields (except perhaps in the ideally plastic limit). An additional observation in the context of the probability distributions is that while the distributions of some of the components of the fields become strongly non-Gaussian with increasing nonlinearity, as expected, other components actually remain fairly Gaussian. Thus, the parallel component of the stress becomes skewed to the right, which can be explained by the fact that the stress develops a bound with increasing nonlinearity, while the parallel component of the strain-rate becomes skewed to the left, which can be explained by the fact that the strain-rate field localizes and hence develops a long tail for large values of the strain rate. On the other hand, the perpendicular component of the stress is found to remain fairly Gaussian even for a relatively low value of m (0.1), while the perpendicular component of the strain rate is fairly symmetric, and although strictly not Gaussian, a Gaussian would not be a bad approximation.

As already mentioned, the "second-order" method appears to give fairly accurate estimates for the first and second moments of the stress and strain-rate fields. In addition, the "second-order" estimates for the macroscopic behavior also appear to be quite good. Of course, the agreement is not perfect, especially for the stronger nonlinearities, and it is generally better for the harder-particle case than for the softer-particle case, which appears to be more sensitive. The worse agreement for the softer-particle case than for the harder-particle case is probably related to the fact that the field fluctuations generated by the FFT simulations in the the *inclusion* phase are much larger (in relative terms) for the softer-particle case. This fact is inconsistent with the assumption that the fluctuations are small (in fact, vanish) implicit in the use of the HS estimates to estimate the effective behavior of the LCC (for use with the "second-order" method). Indeed, the fact that the deformation fields localize in bands that tend to go through the inclusion phase in the softer-particle case implies that the fields are forced to fluctuate significantly in the inclusion phase. Therefore, in retrospect, the use of the HS approximation for the LCC in the softer-particle case is probably not fully justified, at least for strong nonlinearities. In this connection, it is important to emphasize that the choice of the HS approximation is strictly appropriate in the context of the composite cylinder assemblage (CCA) microstructure only for linear systems with *isotropic* phases. In fact, the LCC used to estimate the effective behavior of the nonlinear composite has *anisotropic* phases, and so the use of the HS approximation is not necessarily justified *a priori*. On the other hand, the fact that the "second-order" estimates for the harder-particle case, where the HS estimates for the LCC are more appropriate (because the fluctuations in the fibers are smaller in this case), suggest that the "second-order" method itself has the capability of giving good estimates for the effective behavior and field fluctuations in the nonlinear composite, provided that sufficiently accurate estimates are available for the LCC. This suggests that improved "second-order" estimates could be generated for the softer-particle case if use is made of more appropriate estimates for the effective behavior of the

LCC. One possibility, which will be left for future work, is to estimate numerically the exact effective behavior of the LCC, and to generate improved estimates for the effective behavior of the nonlinear composite still using the "second-order" method. This type of comparison is certainly feasible, and has already been attempted in earlier work (Moulinec and Suquet, 2004) in connection with the variational approximation.

Now, if the differences observed between the "second-order" predictions and the FFT simulations at the larger nonlinearities could be largely attributed to inaccuracies associated with the computation of the effective behavior of the LCC, this would suggest that the "second-order" method has the capability to give fairly accurate predictions not only for the first and second moments of the local fields, but also for the macroscopic behavior. Since, in principle, the macroscopic behavior of a nonlinear composite would be expected to also depend on the higher moments of the fields, it would follow that the effective behavior of such nonlinear composite systems is controlled primarily by the first two moments of the fields (which is the only information available to the "second-order" method making use of an LCC). If this observation were confirmed by more careful comparisons between the "second-order" estimates and full-field simulations, it could help explain why the "second-order" estimates for the macroscopic behavior turn out to be so good, at least for this class of microstructures.

Concerning comparisons of the "second-order" estimates with earlier types of estimates, it has been found that the "second-order" estimates are the most accurate in an overall sense. In particular, the variational method (Ponte Castañeda, 1991), or modified secant method (Suquet, 1995) leads to *qualitatively incorrect* predictions for the phase averages and standard deviations of the field fluctuations in the phases. Thus, for example, it gives rather inaccurate predictions for the phase averages of the strain-rate field in the softer-particle case, while it gives inaccurate predictions for the phases averages of the stress field in the harder-particle case. It also misses out the strong dependence of the field fluctuations on nonlinearity, including the pronounced anisotropy of the fluctuations, which can be attributed to the use of a LCC with local isotropic behavior (in the variational method). The variational predictions for the macroscopic behavior are also less accurate than the corresponding "second-order" predictions, although they have the redeeming feature that they provide bounds, while the "second-order" predictions do not. While the earlier "tangent second-order" estimates (Ponte Castañeda, 1996) are only slightly less accurate than the more recent "second-order" estimates (Ponte Castañeda, 2002a) for the harder-particle case, the "tangent second-order" estimates are clearly less accurate for the softer-particle case. Thus, while the "tangent second-order" estimates give very good predictions for weak nonlinearities, they become progressively less accurate, and can also give *qualitatively incorrect* predictions for large values of the nonlinearity. In addition, the "tangent" predictions for the effective behavior exhibit a large duality gap in the ideally plastic limit, which can be associated with the large fluctuations that develop in the fields in this case. It should also be emphasized that the "second-order" estimates derived in this work make use of a different choice for the "reference tensor" than the one proposed originally by Ponte Castañeda (2002a), and used by Idiart and Ponte Castañeda (2003). This new choice for the "reference tensor" appears to give

improved results, in the sense that it gives better overall agreement with the numerical results, but the optimal choice of this variable remains an open problem.

Finally, it should be mentioned that similar comparisons between full-field simulations and homogenization estimates for the macroscopic behavior and field fluctuations in a special class of two-dimensional viscoplastic polycrystals have been carried out recently by Lebensohn, Liu and Ponte Castañeda (2004) (see also Bhattacharya and Suquet, 2004). In that work, use was made of the standard self-consistent approximation for the LCC, which is better suited to "granular" microstructures. However, the conclusions of that work are entirely consistent with the conclusions of the present work, in that it was also found in the polycrystalline work that the "second-order" estimates improved—often in qualitative terms—on earlier types of homogenization estimates, and that these estimates are rather accurate when compared to full-field numerical simulations. Given the fact that the "second-order" method appears to give accurate estimates for these two rather different, but also special types of composites, it is conjectured that the method may also lead to accurate results for even more general types of composites.

Acknowledgments

This research was carried out within the context of an NSF-CNRS international collaboration (NSF Grant No. OISE-0231867). The work of M.I.I. and P.P.C. was supported by NSF grant CMS-02-01454.

Appendix D

Second-order theory for nonlinear composites and application to isotropic constituents [1]

M. I. Idiart[a,b], K. Danas[a,b], P. Ponte Castañeda[a,b]

[a] Laboratoire de Mécanique des Solides, C.N.R.S. UMR 7649, Département de Mécanique, École Polytechnique, 91128 Palaiseau Cedex, France.

[b] Department of Mechanical Engineering and Applied Mechanics, University of Pennsylvania, Philadelphia, PA 19104-6315, U.S.A.

Abstract — New prescriptions are proposed for the "reference" fields in the context of the "second-order" nonlinear homogenization method (Ponte Castañeda, J. Mech. Phys. Solids 50 (2002) 737–757), and are used to generate estimates for the effective behavior and first moments of the local fields in nonlinear composites. The new prescriptions yield simple, analytical expressions not only for the effective potentials, but also for the macroscopic stress-strain relation, as well as for the phase averages of the strain and stress fields. For illustrative purposes, "second-order" estimates of the Hashin-Shtrikman type are provided for two-phase, transversely-isotropic composites with power-law phases, and are compared with exact results available for power-law, multiple-rank, sequential laminates. The agreement is found to be quite good for all ranges of nonlinearities and inclusion concentrations considered.

Abstract — **Méthode du "second ordre" pour les composites non linéaires et applications aux matériaux isotropes** On utilise la méthode d'homogénéisation non linéaire proposée par Ponte Castañeda (J. Mech. Phys. Solids 50 (2002) 737–757), dite du "second ordre", pour générer des estimations pour le comportement effectif et les premiers moments des champs locaux dans des composites non-linéaires. Des expressions

[1] This chapter will appear in *C. R. Mecanique* **334** (2006)

analytiques simples sont données non seulement pour les potentiels effectifs mais également pour la relation contrainte-déformation macroscopique, aussi bien que pour les moyennes par phase des champs de contrainte et de déformation. Des estimations du type de Hashin-Shtrikman sont données pour des composites biphasés, isotropes avec des phases suivant une loi puissance, et sont comparées aux résultats exacts disponibles pour les matériaux laminés. L'accord s'avère bon pour toutes les valeurs de la non-linéarité et de concentration d'inclusion considéreés.

D.1 Introduction

This work is concerned with the problem of estimating the effective (or homogenized) behavior of *nonlinear* composites (Ponte Castañeda & Suquet 1998). The so-called "second-order" homogenization method (Ponte Castañeda 2002a) is used to generate estimates for the effective potentials of nonlinear composites with isotropic constituents. In addition, simple expressions of practical importance are provided for the resulting effective stress-strain relations and the first moments of the local fields in each constituent. The accuracy of these estimates is then assessed by comparing them with exact results available for a special class of nonlinear composites.

We consider composite materials made of N different homogeneous constituents, or *phases*, which are assumed to be *randomly* distributed in a specimen occupying a volume Ω, at a length scale that is much smaller than the size of Ω and the scale of variation of the loading conditions. The constitutive behavior of each phase is characterized by *isotropic* incompressible strain potentials $w^{(r)}$ $(r = 1, ..., N)$ such that

$$\boldsymbol{\sigma} = \partial_{\boldsymbol{\varepsilon}} w^{(r)}(\boldsymbol{\varepsilon}), \quad w^{(r)}(\boldsymbol{\varepsilon}) = \phi^{(r)}(\varepsilon_e), \tag{D.1}$$

where the von Mises equivalent strain is defined in terms of the deviatoric strain tensor by $\varepsilon_e = \sqrt{(2/3)\boldsymbol{\varepsilon}_d \cdot \boldsymbol{\varepsilon}_d}$, $\partial_{\boldsymbol{\varepsilon}}$ denotes differentiation with respect to $\boldsymbol{\varepsilon}$, and $\mathrm{tr}\boldsymbol{\varepsilon} = 0$. This constitutive relation can be used within the context of the deformation theory of plasticity, where $\boldsymbol{\sigma}$ and $\boldsymbol{\varepsilon}$ represent the infinitesimal stress and strain, respectively. Relation (D.1) applies equally well to viscoplastic materials, in which case $\boldsymbol{\sigma}$ and $\boldsymbol{\varepsilon}$ represent the Cauchy stress and Eulerian strain rate, respectively.

We are concerned with the problem of finding the effective behavior of the composite, which is defined as the relation between the average stress $\overline{\boldsymbol{\sigma}} = \langle \boldsymbol{\sigma} \rangle$ and the average strain $\overline{\boldsymbol{\varepsilon}} = \langle \boldsymbol{\varepsilon} \rangle$, and can also be characterized (Ponte Castañeda & Suquet 1998) by an effective strain potential $\widetilde{W}$, such that

$$\overline{\boldsymbol{\sigma}} = \partial_{\overline{\boldsymbol{\varepsilon}}} \widetilde{W}(\overline{\boldsymbol{\varepsilon}}), \quad \widetilde{W}(\overline{\boldsymbol{\varepsilon}}) = \min_{\boldsymbol{\varepsilon} \in \mathcal{K}(\overline{\boldsymbol{\varepsilon}})} \sum_{r=1}^{N} c^{(r)} \left\langle w^{(r)}(\boldsymbol{\varepsilon}) \right\rangle^{(r)}. \tag{D.2}$$

Here, $\langle \cdot \rangle$ and $\langle \cdot \rangle^{(r)}$ denote the volume averages over the composite (Ω) and over phase r ($\Omega^{(r)}$), respectively, $c^{(r)}$ is the volume fraction of phase r, and $\mathcal{K}(\overline{\boldsymbol{\varepsilon}}) = \{\boldsymbol{\varepsilon} \mid$ there is $\mathbf{u}$ such that $\boldsymbol{\varepsilon} = (1/2)\left[\nabla \mathbf{u} + (\nabla \mathbf{u})^T\right]$ in Ω, $\mathbf{u} = \overline{\boldsymbol{\varepsilon}}\mathbf{x}$ on $\partial\Omega\}$ is the set of kinematically admissible strain fields.

A relation completely equivalent to $(D.2)_1$ results from a dual formulation which makes use of stress potentials $u^{(r)}$, such that locally $\boldsymbol{\varepsilon} = \partial_{\boldsymbol{\sigma}} u^{(r)}(\boldsymbol{\sigma})$. For materials characterized by (D.1), the stress potentials are of the form $u^{(r)}(\boldsymbol{\sigma}) = \psi^{(r)}(\sigma_e)$, where the von Mises equivalent stress is $\sigma_e = \sqrt{(3/2)\boldsymbol{\sigma}_d \cdot \boldsymbol{\sigma}_d}$. The effective behavior is then given in terms of an effective stress potential $\widetilde{U}$, such that $\overline{\boldsymbol{\varepsilon}} = \partial_{\overline{\boldsymbol{\sigma}}} \widetilde{U}(\overline{\boldsymbol{\sigma}})$ (see, for instance, Ponte Castañeda & Suquet 1998). Thus, the problem of estimating the effective behavior of the composite reduces to that of estimating the effective potentials $\widetilde{W}$ or $\widetilde{U}$.

D.2 Second-order homogenization method

A fairly general nonlinear homogenization method has been introduced by Ponte Castañeda (2002a), which delivers estimates for the effective potentials $\widetilde{W}$ and $\widetilde{U}$ which are exact to second order in the heterogeneity contrast. The central idea behind this method is the introduction of a *linear comparison composite* (LCC), with the same microstructure as the nonlinear composite, and with phase potentials $w_L^{(r)}$ given by second-order Taylor-type expansions of the nonlinear potentials $w^{(r)}$,

$$w_L^{(r)}(\boldsymbol{\varepsilon}; \check{\boldsymbol{\varepsilon}}^{(r)}, \mathbf{L}_0^{(r)}) = w^{(r)}(\check{\boldsymbol{\varepsilon}}^{(r)}) + \partial_{\boldsymbol{\varepsilon}} w^{(r)}(\check{\boldsymbol{\varepsilon}}^{(r)}) \cdot (\boldsymbol{\varepsilon} - \check{\boldsymbol{\varepsilon}}^{(r)}) + \frac{1}{2}(\boldsymbol{\varepsilon} - \check{\boldsymbol{\varepsilon}}^{(r)}) \cdot \mathbf{L}_0^{(r)} (\boldsymbol{\varepsilon} - \check{\boldsymbol{\varepsilon}}^{(r)}), \tag{D.3}$$

where the $\check{\boldsymbol{\varepsilon}}^{(r)}$ are reference strains, and $\mathbf{L}_0^{(r)}$ are symmetric, fourth-order tensors (of moduli), uniform in each phase. For isotropic, incompressible phases characterized by potentials of the form (D.1), the (anisotropic) tensors $\mathbf{L}_0^{(r)}$ are assumed to be of the form:

$$\mathbf{L}_0^{(r)} = 2\lambda_0^{(r)} \mathbf{E}^{(r)} + 2\mu_0^{(r)} \mathbf{F}^{(r)}, \text{with} \quad \mathbf{E}^{(r)} = \frac{2}{3} \frac{\check{\boldsymbol{\varepsilon}}_d^{(r)}}{\check{\varepsilon}_e^{(r)}} \otimes \frac{\check{\boldsymbol{\varepsilon}}_d^{(r)}}{\check{\varepsilon}_e^{(r)}}, \quad \mathbf{F}^{(r)} = \mathbf{K} - \mathbf{E}^{(r)}, \tag{D.4}$$

where $\mathbf{K}$ denotes the standard, fourth-order, isotropic, shear projection tensor, and the subscript d denotes the deviatoric part. Then, the second-order method delivers the following estimate for the effective strain potential of a general N-phase composite with isotropic constituents:

$$\widetilde{W}(\overline{\boldsymbol{\varepsilon}}) = \underset{\lambda_0^{(s)}, \mu_0^{(s)}}{\text{stat}} \left\{ \widetilde{W}_L(\overline{\boldsymbol{\varepsilon}}; \check{\boldsymbol{\varepsilon}}^{(s)}, \mathbf{L}_0^{(s)}) + \sum_{r=1}^{N} c^{(r)} V^{(r)}(\check{\boldsymbol{\varepsilon}}^{(r)}, \mathbf{L}_0^{(r)}) \right\}, \tag{D.5}$$

where the stat*ionary* operation consists in setting the partial derivative of the argument with respect to the variable equal to zero. In this expression, $\widetilde{W}_L$ is the effective potential of the above mentioned LCC, and the functions $V^{(r)}$ are defined as

$$V^{(r)}(\check{\boldsymbol{\varepsilon}}^{(r)}, \mathbf{L}_0^{(r)}) = \underset{\hat{\boldsymbol{\varepsilon}}^{(r)}}{\text{stat}} \left\{ w^{(r)}(\hat{\boldsymbol{\varepsilon}}^{(r)}) - w_L^{(r)}(\hat{\boldsymbol{\varepsilon}}^{(r)}; \check{\boldsymbol{\varepsilon}}^{(r)}, \mathbf{L}_0^{(r)}) \right\}, \tag{D.6}$$

where the $\hat{\boldsymbol{\varepsilon}}^{(r)}$ are uniform (strain) tensors in each phase. Making use of the symmetry of the tensors $\mathbf{L}_0^{(r)}$, we can define two components of the tensors $\hat{\boldsymbol{\varepsilon}}^{(r)}$ that are "parallel" and "perpendicular" to the corresponding reference tensor $\check{\boldsymbol{\varepsilon}}^{(r)}$, respectively, $\hat{\varepsilon}_{\parallel}^{(r)} = \sqrt{(2/3)\hat{\boldsymbol{\varepsilon}}^{(r)} \cdot \mathbf{E}^{(r)} \hat{\boldsymbol{\varepsilon}}^{(r)}}$ and

$\hat{\varepsilon}_{\perp}^{(r)} = \sqrt{(2/3)\hat{\boldsymbol{\varepsilon}}^{(r)} \cdot \mathbf{F}^{(r)}\hat{\boldsymbol{\varepsilon}}^{(r)}}$. The stationary operation in (D.6) then leads to the following two conditions in each phase:

$$3\lambda_0^{(r)} \left(\hat{\varepsilon}_{\parallel}^{(r)} - \check{\varepsilon}_e^{(r)}\right) = \phi^{(r)\prime}(\hat{\varepsilon}_e^{(r)})\frac{\hat{\varepsilon}_{\parallel}^{(r)}}{\hat{\varepsilon}_e^{(r)}} - \phi^{(r)\prime}(\check{\varepsilon}_e^{(r)}), \quad 3\mu_0^{(r)} = \frac{\phi^{(r)\prime}(\hat{\varepsilon}_e^{(r)})}{\hat{\varepsilon}_e^{(r)}}. \tag{D.7}$$

Relations (D.7) state that the tensors $\mathbf{L}_0^{(r)}$ correspond to "generalized secant" approximations to the nonlinear stress-strain relations. In turn, the stationary operations in (D.5) lead to the conditions

$$\hat{\varepsilon}_{\parallel}^{(r)} - \check{\varepsilon}_e^{(r)} = \pm\sqrt{\frac{2}{3}\frac{1}{c^{(r)}}\frac{\partial\widetilde{W}_L}{\partial\lambda_0^{(r)}}} = \pm\sqrt{\frac{2}{3}\left\langle(\boldsymbol{\varepsilon}_L - \check{\boldsymbol{\varepsilon}}^{(r)}) \cdot \mathbf{E}^{(r)}(\boldsymbol{\varepsilon}_L - \check{\boldsymbol{\varepsilon}}^{(r)})\right\rangle^{(r)}}, \tag{D.8}$$

$$\hat{\varepsilon}_{\perp}^{(r)} = \pm\sqrt{\frac{2}{3}\frac{1}{c^{(r)}}\frac{\partial\widetilde{W}_L}{\partial\mu_0^{(r)}}} = \pm\sqrt{\frac{2}{3}\left\langle\boldsymbol{\varepsilon}_L \cdot \mathbf{F}^{(r)}\boldsymbol{\varepsilon}_L\right\rangle^{(r)}}, \tag{D.9}$$

where $\boldsymbol{\varepsilon}_L$ denotes the strain field in the LCC. The sign of the square roots in these expressions should be taken to be positive if $\check{\varepsilon}_e^{(r)} \leq \overline{\varepsilon}_e^{(r)}$, and negative otherwise, for consistency of (D.10) with the case of uniform fields (e.g., laminate, homogeneous limit). It is worth noting that the right-hand sides of these relations depend on the (intraphase) field fluctuations in the LCC, through certain projections of the phase covariance tensors $\mathbf{C}_{\boldsymbol{\varepsilon}_L}^{(r)} = \langle\boldsymbol{\varepsilon}_L \otimes \boldsymbol{\varepsilon}_L\rangle^{(r)} - \overline{\boldsymbol{\varepsilon}}_L^{(r)} \otimes \overline{\boldsymbol{\varepsilon}}_L^{(r)}$.

Then, using the fact that (D.5) is stationary with respect to the moduli $\lambda_0^{(r)}$ and $\mu_0^{(r)}$, we can rewrite the estimate (D.5) in the simpler form

$$\widetilde{W}(\overline{\boldsymbol{\varepsilon}}) = \sum_{r=1}^{N} c^{(r)}\left[w^{(r)}(\hat{\boldsymbol{\varepsilon}}^{(r)}) - \partial_{\boldsymbol{\varepsilon}}w^{(r)}(\check{\boldsymbol{\varepsilon}}^{(r)}) \cdot (\hat{\boldsymbol{\varepsilon}}^{(r)} - \overline{\boldsymbol{\varepsilon}}_L^{(r)})\right], \tag{D.10}$$

where the $\overline{\boldsymbol{\varepsilon}}_L^{(r)} = \langle\boldsymbol{\varepsilon}_L\rangle^{(r)}$ are the phase averages of the strain in the LCC. Relations (D.7)-(D.9) determine the variables $\hat{\boldsymbol{\varepsilon}}^{(r)}$ and $\mathbf{L}_0^{(r)}$, for any choice of the reference tensors $\check{\boldsymbol{\varepsilon}}^{(r)}$, which remain to be specified. Unfortunately, enforcing stationarity of (D.5) with respect to the tensors $\check{\boldsymbol{\varepsilon}}^{(r)}$, as suggested in Ponte Castañeda (2002a), leads to conditions that cannot be satisfied together with (D.7)-(D.9), in general. Motivated by the findings of Idiart and Ponte Castañeda (2005), we propose here the following prescription:

$$\check{\boldsymbol{\varepsilon}}^{(r)} = \overline{\boldsymbol{\varepsilon}}_d, \quad \text{for all } r, \tag{D.11}$$

where the subscript d has been used to denote deviatoric part. In addition to giving sensible results in the case of isotropic composites, as will be seen in the next section, this prescription has the advantage of simplicity. In fact, with this choice of reference tensors, the 'second-order' estimates for the effective behavior, which follow from differentiation of (D.10), can be shown (Idiart & Ponte Castañeda 2006a) to be given by

$$\overline{\boldsymbol{\sigma}} = \partial_{\overline{\boldsymbol{\varepsilon}}}\widetilde{W}(\overline{\boldsymbol{\varepsilon}}) = \overline{\boldsymbol{\sigma}}_L + \sum_{r=1}^{N} c^{(r)}\boldsymbol{\rho}^{(r)}, \tag{D.12}$$

where $\overline{\boldsymbol{\sigma}}_L$ denotes the macroscopic stress in the LCC, and the (incompressible) tensors $\boldsymbol{\rho}^{(r)}$ are

$$\begin{aligned}\boldsymbol{\rho}^{(r)} &= \left(\mathbf{L}_0^{(r)} - \mathbf{L}_t^{(r)}\right)(\hat{\boldsymbol{\varepsilon}}^{(r)} - \overline{\boldsymbol{\varepsilon}}_L^{(r)}) + \frac{4}{3}\frac{\lambda_0^{(r)} - \mu_0^{(r)}}{\overline{\varepsilon}_e^2} \times \\ &\quad \left[\langle(\boldsymbol{\varepsilon}_{L_d} - \overline{\boldsymbol{\varepsilon}}_d) \otimes (\boldsymbol{\varepsilon}_{L_d} - \overline{\boldsymbol{\varepsilon}}_d)\rangle^{(r)} - (\hat{\boldsymbol{\varepsilon}}_d^{(r)} - \overline{\boldsymbol{\varepsilon}}_d) \otimes (\hat{\boldsymbol{\varepsilon}}_d^{(r)} - \overline{\boldsymbol{\varepsilon}}_d)\right] \overline{\boldsymbol{\varepsilon}}_d.\end{aligned} \tag{D.13}$$

In this last expression, $\mathbf{L}_t^{(r)} = \partial^2_{\boldsymbol{\varepsilon}\boldsymbol{\varepsilon}} w^{(r)}(\overline{\boldsymbol{\varepsilon}})$ are the tangent moduli of the phases, evaluated at $\overline{\boldsymbol{\varepsilon}}$. Thus, while the LCC is subjected to the same macroscopic strain as the nonlinear composite, the macroscopic stress exhibits a 'correction' term due the fact that the estimates (D.5) are not stationary with respect to the variables $\check{\boldsymbol{\varepsilon}}^{(r)}$. In addition, corresponding estimates for the phase averages of the local fields are given by

$$\overline{\boldsymbol{\varepsilon}}^{(r)} = \overline{\boldsymbol{\varepsilon}}_L^{(r)}, \quad \overline{\boldsymbol{\sigma}}^{(r)} = \overline{\boldsymbol{\sigma}}_L^{(r)} + \boldsymbol{\rho}^{(r)}, \tag{D.14}$$

where the subscript L denotes quantities in the LCC. These results follow from the rigorous procedure described in Idiart & Ponte Castañeda (2006a), making use of suitably perturbed phase potentials to extract estimates for the pertinent phase averages via differentiation. Again, while the estimates for $\overline{\boldsymbol{\varepsilon}}^{(r)}$ coincide with those in the associated LCC, the estimates for $\overline{\boldsymbol{\sigma}}^{(r)}$ do not. However, it is emphasized that these estimates are entirely consistent with (D.12), in the sense that they satisfy the relations $\overline{\boldsymbol{\sigma}} = \sum_{r=1}^N c^{(r)} \overline{\boldsymbol{\sigma}}^{(r)}$.

Completely analogous expressions may be developed (Ponte Castañeda 2002a) starting from the dual formulation in terms of the stress potentials $u^{(r)}$. This formulation involves a LCC with phase potentials $u_L^{(r)}$, given by second-order Taylor approximations to $u^{(r)}$ of the same form as (D.3), in terms of reference stresses $\check{\boldsymbol{\sigma}}^{(r)}$ and compliance tensors $\mathbf{M}_0^{(r)}$, and generates the following estimate for the effective stress potential

$$\widetilde{U}(\overline{\boldsymbol{\sigma}}) = \sum_{r=1}^N c^{(r)} \left[u^{(r)}(\hat{\boldsymbol{\sigma}}^{(r)}) - \partial_{\boldsymbol{\sigma}} u^{(r)}(\check{\boldsymbol{\sigma}}^{(r)}) \cdot (\hat{\boldsymbol{\sigma}}^{(r)} - \overline{\boldsymbol{\sigma}}_L^{(r)})\right], \tag{D.15}$$

where $\overline{\boldsymbol{\sigma}}_L^{(r)} = \langle \boldsymbol{\sigma}_L \rangle^{(r)}$ are the phase averages of the stress in the associated LCC, and the tensors $\hat{\boldsymbol{\sigma}}^{(r)}$ and $\mathbf{M}_0^{(r)}$ depend on the reference tensors $\check{\boldsymbol{\sigma}}^{(r)}$ and the second moments of the stress fluctuations (in the LCC) through equations analogous to (D.7)-(D.9). (The same sign convention should also be used for the equivalents of relations (D.8) and (D.9).) Again, the reference stresses $\check{\boldsymbol{\sigma}}^{(r)}$ need to be specified, and the following prescription is proposed (Idiart & Ponte Castañeda 2005):

$$\check{\boldsymbol{\sigma}}^{(r)} = \overline{\boldsymbol{\sigma}}_d, \quad \text{for all } r, \tag{D.16}$$

which is the counterpart of (D.11) in this context. Note that, in spite of the symmetry of the prescriptions (D.11) and (D.16), the corresponding homogenized estimates are not expected to give identical results.

Finally, it is worth emphasizing that nonlinear homogenization methods based on LCCs involve *two* different levels of approximation (Rekik *et al.* 2005; Idiart *et al.* 2006b). The first level consists in

the generation of the LCC by linearizing the behavior of the each phase in the nonlinear composite, while the second level consists in the computation of the effective behavior of the LCC, which in general cannot be done exactly and therefore requires the use of suitable *linear* homogenization estimates.

D.3 Two-phase, power-law composites

We consider here two-phase, fiber composites with *random* microstructures exhibiting overall transversely isotropic symmetry that are loaded in transverse shear. The phases are characterized by isotropic, incompressible, power-law potentials

$$\phi^{(r)}(\varepsilon_e) = \frac{\varepsilon_0 \sigma_0^{(r)}}{1+m}\left(\frac{\varepsilon_e}{\varepsilon_0}\right)^{1+m}, \quad \psi^{(r)}(\sigma_e) = \frac{\varepsilon_0 \sigma_0^{(r)}}{1+n}\left(\frac{\sigma_e}{\sigma_0^{(r)}}\right)^{1+n}, \tag{D.17}$$

where $\sigma_0^{(r)}$ is the flow stress of phase r, m is the strain-rate sensitivity, such that $0 \leq m \leq 1$, ε_0 is a reference strain rate. Note that $m = 1$ and $m = 0$ correspond to linear and rigid-ideally plastic behaviors, respectively. For simplicity, both phases are assumed to have the same exponent m and reference strain ε_0. It then follows that, under isochoric *plane-strain* conditions, the effective potentials can be written as

$$\widetilde{W}(\overline{\boldsymbol{\varepsilon}}) = \frac{\varepsilon_0 \widetilde{\sigma}_0}{1+m}\left(\frac{\overline{\varepsilon}_e}{\varepsilon_0}\right)^{1+m}, \quad \widetilde{U}(\overline{\boldsymbol{\sigma}}) = \frac{\varepsilon_0 \widetilde{\sigma}_0}{1+n}\left(\frac{\overline{\sigma}_e}{\widetilde{\sigma}_0}\right)^{1+n}, \tag{D.18}$$

where $\widetilde{\sigma}_0$ is the *effective flow stress* of the composite, and $\overline{\varepsilon}_e$ and $\overline{\sigma}_e$ are the equivalent macroscopic strain and stress. The effective behavior is thus completely characterized by $\widetilde{\sigma}_0$.

The extreme cases of infinite contrast are of particular interest, and are given in figs. D.1 and D.2 corresponding respectively to porous and rigidly reinforced composites. The matrix phase, labeled 1, has flow stress $\sigma_0^{(1)} = \sigma_0$, and the randomly distributed voids or rigid fibers (phase 2) have circular cross-section, and volume fraction $c^{(2)} = c$. "Second-order" estimates are generated by making use of the Hashin-Shtrikman (HS) estimates of Willis (1977) to determine the effective behavior of the associated LCC. The HS estimates are known to be appropriate for (linear) particulate media at low to moderate concentrations, and are exact to second-order in the heterogeneity contrast. Both the strain (W) and the stress (U) versions of the "second-order" (SO) estimates of the previous section are provided, making use of the simple prescriptions (D.11) and (D.16). In addition, the earlier "variational" (VAR) bounds of Ponte Castañeda (1991), also of the HS type, are included for comparison purposes.

It should be mentioned at this stage that for the cases considered here, i.e. incompressible, transversely isotropic composites under plane-strain loadings, expression (D.13) for the tensor $\boldsymbol{\rho}^{(1)}$ in the matrix phase simplifies to

$$\boldsymbol{\rho}^{(1)} = (2/\overline{\varepsilon}_e)\left(\lambda_0^{(1)} - \lambda_t^{(1)}\right)(\hat{\varepsilon}_{\parallel}^{(1)} - \overline{\varepsilon}_{Le}^{(1)})\overline{\boldsymbol{\varepsilon}}_d, \tag{D.19}$$

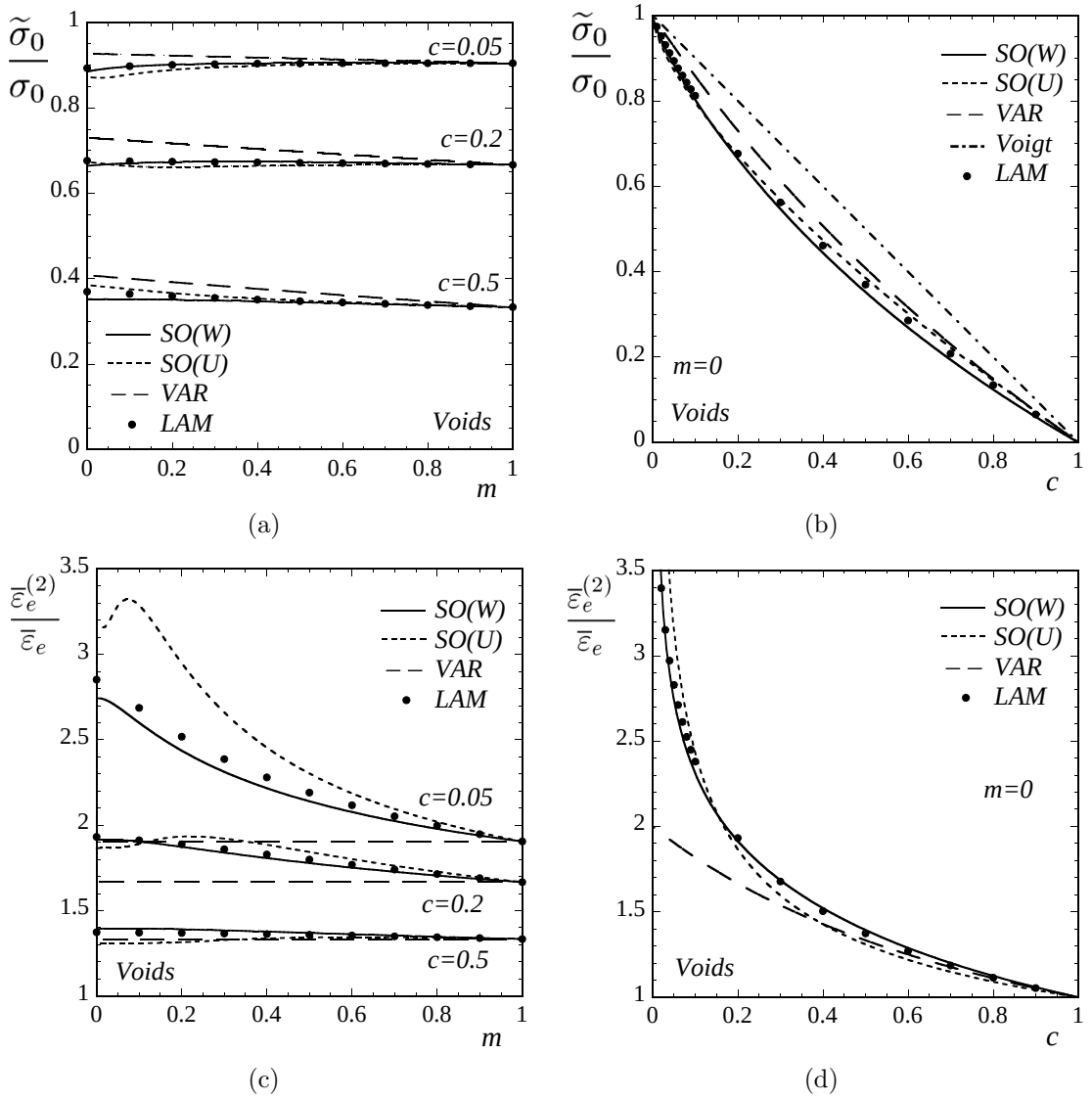

Figure D.1: Estimates and exact results for power-law porous materials subject to in-plane shear. Effective flow stress $\widetilde{\sigma}_0$, normalized by the flow stress of the matrix σ_0, (a) as a function of the power m, for several porosities c, and (b) as a function of the porosity c, in the case of an ideally-plastic matrix. (c) and (d) Corresponding equivalent average strains in the porous phase $\overline{\varepsilon}_e^{(2)}$, normalized by the equivalent macroscopic strain $\overline{\varepsilon}_e$.

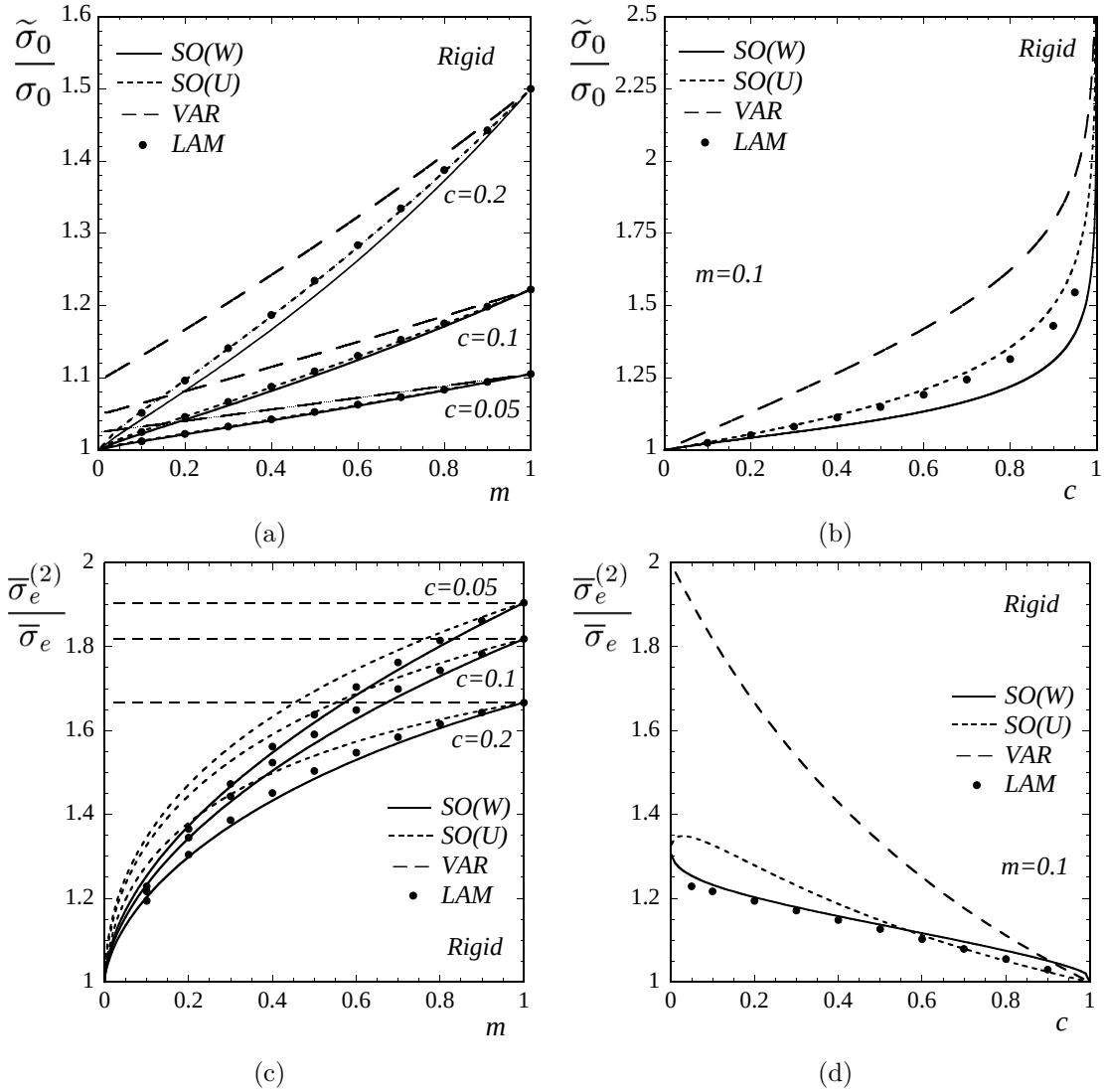

Figure D.2: Estimates and exact results for power-law rigidly-reinforced materials subject to in-plane shear. Effective flow stress $\widetilde{\sigma}_0$, normalized by the flow stress of the matrix σ_0, (a) as a function of the power m, for several fiber concentrations c, and (b) as a function of the fiber concentration c, for a power $m = 0.1$. (c) and (d) Corresponding equivalent average stresses in the rigid phase $\overline{\sigma}_e^{(2)}$, normalized by the equivalent macroscopic stress $\overline{\sigma}_e$.

where $2\lambda_t^{(1)} = \mathbf{E}^{(1)} \cdot \mathbf{L}_t^{(1)} = (2/3)\phi^{(1)\prime\prime}(\overline{\boldsymbol{\varepsilon}})$, while in the inclusion phase, $\boldsymbol{\rho}^{(2)} = \mathbf{0}$. Because the tensor $\boldsymbol{\rho}^{(1)}$ is "aligned" with the macroscopic strain $\overline{\boldsymbol{\varepsilon}}$, so is then the macroscopic stress given by (D.12), as it should be for transversely isotropic composites under in-plane loading.

In order to assess the accuracy of these estimates, *exact* results have been generated for power-law composites with a special class of transversely isotropic, 'particulate' microstructures known as multiple-rank sequential laminates (LAM), following the procedure described by deBotton and Hariton (2002). The rank of these laminates has been set sufficiently high so that the effective behavior exhibits transverse isotropy up to a certain tolerance. The interest in composites with this type of microstructures is that, in the *linear* case, their effective behavior is given *exactly* by the HS estimates, for *any* modulus tensors of the phases. For this reason, LCC-based homogenization estimates of the HS type are particularly appropriate for nonlinear composites with this class of microstructures, since the effective behavior of the LCC is being computed exactly in that case, and therefore there is only one level of approximation involved, namely, in the linearization. In addition, since this holds for any linearization, exact results for nonlinear composites with this class of microstructures provide an ideal test bed to compare different LCC-based homogenization methods. A peculiarity of these nonlinear composites is that, by construction, the fields in the inclusion phase are uniform, independently of the behavior of the phases.

Figures D.1 and D.2 present results for the effective flow stress $\widetilde{\sigma}_0$ as functions of the strain-rate sensitivity m and concentration c, for both the porous and rigidly reinforced composites. They also present results for the averages of the strain $\overline{\varepsilon}_e^{(2)}$ and stress $\overline{\sigma}_e^{(2)}$ over the inclusion phase for the porous and rigidly reinforced composites, respectively. (Note that $\overline{\sigma}_e^{(2)} = 0$ in the pores, and $\overline{\varepsilon}_e^{(2)} = 0$ for rigid particles.) The main observations from these figures are: (*i*) The agreement of the SO estimates—both W and U versions—with the LAM exact results is quite good, and certainly much better than the VAR estimates. (*ii*) Globally speaking, the two versions of the SO estimates perform equally well (sometimes the W version is better, sometimes, the U version is better). (*iii*) While the improvement in the predictions for the effective behavior of the SO estimates over the VAR estimates is relatively modest, the corresponding improvement in the phase averages of the fields in the inclusion phase can be quite significant. This is especially the case for small concentrations of pores or rigid fibers, where huge differences in the predictions are observed. In particular, for the case of a porous materials with an ideally plastic matrix ($m = 0$) (see fig. D.1*d*), the SO predictions and LAM results for the average strain in the pores blow up as the porosity c tends to zero, while the corresponding VAR estimates remain finite. (In fact, the SO estimates behave as $\overline{\varepsilon}_e^{(2)}/\overline{\varepsilon}_e \sim c^{-1/3}$ as $c \to 0$.)

D.4 Concluding remarks

It has been shown that the use of the macroscopic strain and stress as references in the context of the "second-order" homogenization method leads to simple and accurate estimates for the effective response and field averages in the phases of nonlinear composites, even at large heterogeneity contrast

and nonlinearity. One advantage of the new prescription is that the phases averages of both the strain and stress fields can be computed explicitly using only one version (W, or U) of the method. This is in contrast with the methodology proposed recently by Idiart *et al.* (2006b), which requires the computation of both the W and U versions of the second-order estimate (and closing the gap between them) to be able to generate consistent estimates for the phase averages of the stress and strain fields. Although comparisons between these two approaches were not shown here, both approaches give similar predictions, but the new approach is much simpler from a computational point of view.

Acknowledgments

The work of M.I.I. and P.P.C. was supported by NSF Grant CMS-02-01454. K. Danas gratefully acknowledges the support of École Polytechnique through a Monge fellowship.

Appendix E

Nonlinear, sequential laminates

Composite materials whose macroscopic behavior can be computed exactly are extremely valuable from a theoretical point of view, because, among other reasons, they constitute test cases which can be used to assess the accuracy of approximate homogenization methods. A well-known class of composites whose macroscopic behavior can be computed exactly is that of composites with sequentially laminated microstructures, simply called *sequential laminates*, first introduced by Bruggeman (1935) in the context of linear electrostatics. A sequential laminate is an iterative construction obtained by layering laminated materials (which in turn have been obtained from lower-order lamination procedures) with other laminated materials, or directly with the homogeneous phases that make up the composite, in such a way as to produce hierarchical microstructures of increasing complexity. The 'rank' of the laminate refers to the number of layring operations required to reach the final sequential laminate. For the purposes of this work, it suffices to restrict attention to two-phase laminates, even though many results given here can be generalized to N-phase laminates. Thus, a 'rank-1' laminate, also called 'simple' laminate, is obtained by layering two homogeneous phases with a given layering direction $\mathbf{n}^{(1)}$, as shown in figure E.1(a). In turn, a 'rank-2' laminate is constructed by layering the rank-1 laminate with one of the original phases, say $r = 1$, in a different layering direction $\mathbf{n}^{(2)}$, as shown in figure E.1b. N-rank laminates are obtained by iterating this procedure N times (see Milton 2002), layering the $(N-1)$-rank laminate with phase 1. It should be mentioned that in this procedure, it is assumed that the length scale of the embedded laminate is much smaller than the length scale of the embedding laminate, i.e., $\delta_1 << \delta_2$ in figure E.1. This assumption allows to regard the $(N-1)$-rank laminate in the N-rank laminate as a homogeneous phase, what makes the iterative process possible.

Linear-elastic, sequential laminates have been studied by many authors, and relevant references can be found in the recent monograph by Milton (2002). Nonlinear-elastic or viscoplastic sequential laminates, on the other hand, have received much less attention. deBotton & Ponte Castañeda (1992) first obtained an exact expression for the effective potential of simple laminates with nonlinear, isotropic phases, making use of the 'variational' method of Ponte Castañeda (1991). It was shown in that work that nonlinear simple laminates attain the corresponding bounds of Reuss and Voigt. In

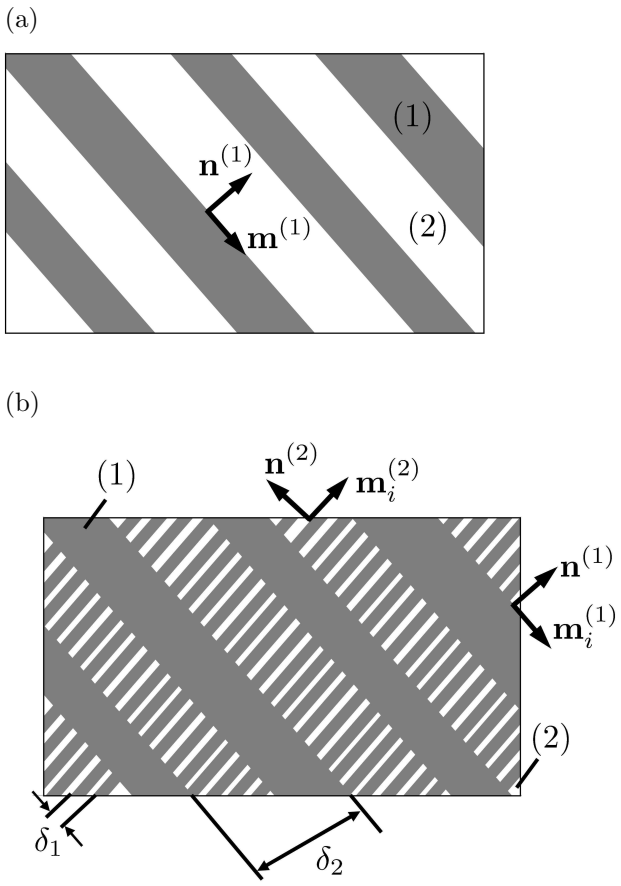

Figure E.1: (a) Rank-one laminate. (b) Rank-two laminate.

the context of nonlinear dielectric composites with isotropic phases, Ponte Castañeda (1992b) provided exact expressions for the effective potential of simple laminates as well as sequential laminates of rank two and three. In that work, low-rank sequential laminates exhibiting overall (transverse) isotropy were generated by considering loading-dependent microstructures, which can be thought of as an approximation to the class of nonlinear (transverse) isotropic microstructures. Later, deBotton & Hariton (2002) made use of the minimum complementary energy principle to obtain an exact expression for the in-plane effective behavior of high-rank sequential laminates with nonlinear, incompressible, isotropic phases, and with microstructures exhibiting cylindrial symmetry. In that work, it was demonstrated, albeit numerically, that the in-plane behavior of such sequential laminates tends to be isotropic for a sufficiently large number of appropriately chosen laminations. Finally, deBotton (2005) derived an exact expression for the effective potential of sequential laminates in the context of finite elasticity, and making use of a 'differential' scheme he was able to evaluate the limit of infinite rank and to obtain explicit results for transversely isotropic sequential laminates with Neo-Hookean phases.

In this Appendix we derive the formulae for the effective strain potential and field statistics in sequential laminates made of general, anisotropic nonlinear phases. We begin by considering the case of a rank-1 laminate, and we then make use of that result to obtain exact expressions for higher

rank laminates. Finally, we consider the limiting case of infinite-rank laminates with microstructures exhibiting overall (transversely) isotropic symmetry, and we obtain analytical expressions for the specific case of power-law phases.

E.1 Rank-one laminate

Consider a two-phase, rank-1 laminate, like the one shown in figure E.1(a), with a volume fraction of phase 1 and 2 given by $(1-f_1)$ and f_1, respectively. Let $\mathbf{n}^{(1)}$ denote the direction of lamination, i.e., $\mathbf{n}^{(1)}$ is a unit vector normal to the laminae, and let $\mathbf{m}_i^{(1)}$, $i=1,2$, be two orthogonal unit vectors lying on the plane of the laminae. The subscript and superscript 1 has been used to emphasize that the quantities correspond to a rank-1 laminate. It is well-known that the exact strain field in a simple laminate, subjected to affine boundary conditions $\mathbf{u}=\overline{\boldsymbol{\varepsilon}}\mathbf{x}$, is uniform per phase. Thus, denoting the uniform strain in phase r by $\overline{\boldsymbol{\varepsilon}}^{(r)}$, compatibility and boundary conditions require that

$$\overline{\boldsymbol{\varepsilon}}^{(1)} - \overline{\boldsymbol{\varepsilon}}^{(2)} = \mathbf{a}^{(1)} \otimes_s \mathbf{n}^{(1)}, \tag{E.1}$$

$$(1-f_1)\,\overline{\boldsymbol{\varepsilon}}^{(1)} + f_1\,\overline{\boldsymbol{\varepsilon}}^{(2)} = \overline{\boldsymbol{\varepsilon}}, \tag{E.2}$$

for some vector $\mathbf{a}^{(1)}$ arbitrarily oriented in the three-dimensional space. The symbol $\otimes_s$ has been used to denote the symmetric part of the tensor product. Solving for the fields $\overline{\boldsymbol{\varepsilon}}^{(r)}$, we obtain

$$\overline{\boldsymbol{\varepsilon}}^{(1)} = \overline{\boldsymbol{\varepsilon}} + f_1\,\mathbf{a}^{(1)} \otimes_s \mathbf{n}^{(1)}, \tag{E.3}$$

$$\overline{\boldsymbol{\varepsilon}}^{(2)} = \overline{\boldsymbol{\varepsilon}} - (1-f_1)\,\mathbf{a}^{(1)} \otimes_s \mathbf{n}^{(1)}. \tag{E.4}$$

Then, from the definition (2.3), it follows that the effective strain potential $\widetilde{w}_1$ of the rank-1 laminate is given by

$$\begin{aligned}\widetilde{w}_1(\overline{\boldsymbol{\varepsilon}}) = \inf_{\mathbf{a}^{(1)}} \Big\{ & f_1\, w^{(1)}\left(\overline{\boldsymbol{\varepsilon}} + f_1\,\mathbf{a}^{(1)} \otimes_s \mathbf{n}^{(1)}\right) + ... \\ & ... + (1-f_1)\, w^{(2)}\left(\overline{\boldsymbol{\varepsilon}} - (1-f_1)\,\mathbf{a}^{(1)} \otimes_s \mathbf{n}^{(1)}\right)\Big\}.\end{aligned} \tag{E.5}$$

Thus, the evaluation of $\widetilde{w}_1$ requires the solution to an optimization with respect to one vector in 3D. This expression was first derived by deBotton & Ponte Castañeda (1992) for the special case of isotropic phases, and by deBotton (2005) for the more general case of anisotropic, hyper-elastic phases.

Once the optimization problem in (E.5) is solved, computing the statistics of the local fields in the simple laminate is a trivial matter. Indeed, since the strain field is constant per phase, the averages of the strain in each phase are given precisely by (E.3) and (E.4), where $\mathbf{a}^{(1)}$ is the optimal one, and the phase averages of the stress follow from the relations $\overline{\boldsymbol{\sigma}}^{(r)} = \partial_{\boldsymbol{\varepsilon}} w^{(r)}(\overline{\boldsymbol{\varepsilon}}^{(r)})$.

E.2 Higher rank laminates

Next, consider a rank-2 laminate, like the one shown in figure E.1(b), made up of a rank-1 laminate and phase 1, in proportions $(1-f_2)$ and f_2, respectively. Note that in this rank-2 laminate, phase 2 can be regarded as an inclusion (discontinuous) phase embeded in a (continuous) matrix made up of phase 1, i.e., it corresponds to a 'particulate' microstructure. Note also that the volume fraction of phase 2 in this rank-2 laminate is given by $c^{(2)} = f_2\, f_1$. Letting $\mathbf{n}^{(2)}$ denote the lamination direction of the rank-2 laminate, and following the argument given in the previous section, the effective strain potential $\widetilde{w}_2$ of the rank-2 laminate can be written as

$$\begin{aligned}\widetilde{w}_2(\overline{\boldsymbol{\varepsilon}}) \;=\; \inf_{\mathbf{a}^{(2)}} \Big\{ & (1-f_2)\, w^{(1)}\left(\overline{\boldsymbol{\varepsilon}} + f_2\, \mathbf{a}^{(2)} \otimes_s \mathbf{n}^{(2)}\right) + ... \\ & ... + f_2\, \widetilde{w}_1\left(\overline{\boldsymbol{\varepsilon}} - (1-f_2)\, \mathbf{a}^{(2)} \otimes_s \mathbf{n}^{(2)}\right)\Big\}. \end{aligned} \tag{E.6}$$

Introducing (E.5) into this expression, we obtain

$$\begin{aligned}\widetilde{w}_2(\overline{\boldsymbol{\varepsilon}}) \;=\; \inf_{\substack{\mathbf{a}^{(i)} \\ i=1,2}} \Big\{ & (1-f_2)\, w^{(1)}\left(\overline{\boldsymbol{\varepsilon}} + f_2\, \mathbf{a}^{(2)} \otimes_s \mathbf{n}^{(2)}\right) + ... \\ & ... + f_2\,(1-f_1)\, w^{(1)}\left(\overline{\boldsymbol{\varepsilon}} - (1-f_2)\, \mathbf{a}^{(2)} \otimes_s \mathbf{n}^{(2)} + f_1\, \mathbf{a}^{(1)} \otimes_s \mathbf{n}^{(1)}\right) + ... \\ & ... + f_2\, f_1\, w^{(2)}\left(\overline{\boldsymbol{\varepsilon}} - (1-f_2)\, \mathbf{a}^{(2)} \otimes_s \mathbf{n}^{(2)} - (1-f_1)\, \mathbf{a}^{(1)} \otimes_s \mathbf{n}^{(1)}\right)\Big\}. \end{aligned} \tag{E.7}$$

Evaluating $\widetilde{w}_2$, thus, requires solving an optimization with respect to two vectors. It should be noted that the expression in curly brackets contains two terms involving the potential $w^{(1)}$, while only one term involving the potential $w^{(2)}$. This is because, as can be deduced from the construction process of the rank-2 laminate described above, the fields are constant in phase 2 but not in phase 1.

Rank-M laminates are obtained by repeating this process M times, always laminating a rank-m laminate with phase 1. The microstructure of the resulting rank-M laminate is characterized by the set of volume fractions f_i and unit vectors $\mathbf{n}^{(i)}$ denoting the directions of lamination. By inspection of the expressions for $\widetilde{w}_2$ and $\widetilde{w}_3$ (not given here), it can be inferred that the effective strain potential $\widetilde{w}_M$ of the rank-M laminate is given by

$$\widetilde{w}_M(\overline{\boldsymbol{\varepsilon}}) \;=\; \inf_{\substack{\mathbf{a}^{(i)} \\ i=1,...,M}} \left\{ c^{(2)}\, w^{(2)}\left(\overline{\boldsymbol{\varepsilon}}^{(2)}\right) + \sum_{i=1}^{M} (1-f_i)\, \hat{f}_i\, w^{(1)}\left(\overline{\boldsymbol{\varepsilon}}_i^{(1)}\right)\right\}, \tag{E.8}$$

where the volume fractions $\hat{f}_i$ and $c^{(2)}$ have been defined as

$$\hat{f}_i = \prod_{j=i+1}^{M} f_j,\; i = 0, ..., (M-1), \quad \hat{f}_M = 1, \quad \text{and} \quad c^{(2)} = \prod_{i=1}^{M} f_i, \tag{E.9}$$

and the strain tensors $\overline{\boldsymbol{\varepsilon}}_i^{(1)}$ and $\overline{\boldsymbol{\varepsilon}}^{(2)}$ are given by

$$\overline{\boldsymbol{\varepsilon}}_i^{(1)} = \overline{\boldsymbol{\varepsilon}} + f_i\,\mathbf{a}^{(i)} \otimes_s \mathbf{n}^{(i)} - \sum_{j=i+1}^{M} (1-f_j)\,\mathbf{a}^{(j)} \otimes_s \mathbf{n}^{(j)}, \tag{E.10}$$

$$\overline{\boldsymbol{\varepsilon}}^{(2)} = \overline{\boldsymbol{\varepsilon}} - \sum_{i=1}^{M} (1-f_i)\,\mathbf{a}^{(i)} \otimes_s \mathbf{n}^{(i)}. \tag{E.11}$$

Note that $c^{(2)}$ is the volume fraction of phase 2, the inclusion phase, in the rank-M laminate. Expression (E.8) was first given by Ponte Castañeda (1992b) in the context of dielectric, nonlinear composites, for sequential laminates with isotropic phases, of rank up to three. Also, an alternative form of expression (E.8) has been derived by deBotton (2005) in the context of hyperelastic composites. However, the form (E.8) is preferred here, for it facilitates the theoretical analysis.

Once the optimization in (E.8) is solved, expressions (E.10)-(E.11) provide the full field distribution in the rank-M laminate, from which field statistics can be readily computed. Indeed, it follows from expression (E.8) that the strain field in the inclusion phase ($r = 2$) is uniform and equal to $\overline{\boldsymbol{\varepsilon}}^{(2)}$, as given by (E.11), while in the matrix phase ($r = 1$) it takes the values $\overline{\boldsymbol{\varepsilon}}_i^{(1)}$, $i = 1, ..., M$, as given by (E.10), in regions occupying a volume fraction $(1 - f_i)\hat{f}_i$. Thus, the k^{th} moments of the strain field in the matrix phase are given by

$$\langle \underbrace{\boldsymbol{\varepsilon} \otimes \boldsymbol{\varepsilon} \otimes ... \otimes \boldsymbol{\varepsilon}}_{K\text{times}} \rangle^{(1)} = \frac{1}{c^{(1)}} \sum_{i=1}^{M} (1-f_i)\ \hat{f}_i\ (\underbrace{\overline{\boldsymbol{\varepsilon}}_i^{(1)} \otimes \overline{\boldsymbol{\varepsilon}}_i^{(1)} \otimes ... \otimes \overline{\boldsymbol{\varepsilon}}_i^{(1)}}_{K\text{times}}). \tag{E.12}$$

In addition, the stress field in the inclusion phase is $\overline{\boldsymbol{\sigma}}^{(2)} = \partial_{\boldsymbol{\varepsilon}} w^{(2)}(\overline{\boldsymbol{\varepsilon}}^{(2)})$, while in the matrix phase, the k^{th} moments of the stress are given by

$$\langle \underbrace{\boldsymbol{\sigma} \otimes \boldsymbol{\sigma} \otimes ... \otimes \boldsymbol{\sigma}}_{K\text{times}} \rangle^{(1)} = \frac{1}{c^{(1)}} \sum_{i=1}^{M} (1-f_i)\ \hat{f}_i\ (\ \underbrace{\partial_{\boldsymbol{\varepsilon}} w^{(1)}(\overline{\boldsymbol{\varepsilon}}_i^{(1)}) \otimes ... \otimes \partial_{\boldsymbol{\varepsilon}} w^{(1)}(\overline{\boldsymbol{\varepsilon}}_i^{(1)})}_{K\text{times}}\ ). \tag{E.13}$$

Thus, the computation of $\widetilde{w}_M$ involves an optimization over M vectors $\mathbf{a}^{(i)}$ in 3D, that must be solved numerically, in general. In the following subsections, we consider some special cases for which this optimization problem can be simplified.

E.2.1 Incompressible matrix

In case of an incompressible matrix phase ($r = 1$), the optimization in (E.8) requires the argument of $w^{(1)}$ to be traceless (see deBotton 2005 for a similar treatment of incompressibility in the context of hyperelastic sequential laminates). This leads to the following constraints on the vectors $\mathbf{a}^{(i)}$:

$$\mathrm{tr}(\overline{\boldsymbol{\varepsilon}}) + f_i\,\mathrm{tr}(\mathbf{a}^{(i)} \otimes_s \mathbf{n}^{(i)}) - \sum_{j=i+1}^{M} (1-f_j)\,\mathrm{tr}(\mathbf{a}^{(j)} \otimes_s \mathbf{n}^{(j)}) = 0, \quad i = 1, ..., M. \tag{E.14}$$

Note that the macroscopic strain $\overline{\boldsymbol{\varepsilon}}$ need not be traceless, since phase 2 is compressible and therefore the composite itself is compressible. Now, for $i = M$, the contraint is given by

$$\mathbf{a}^{(M)} \cdot \mathbf{n}^{(M)} = -\frac{1}{f_M}\,\mathrm{tr}\overline{\boldsymbol{\varepsilon}}, \tag{E.15}$$

where used has been made of the identity $\mathrm{tr}(\mathbf{a}^{(i)} \otimes_s \mathbf{n}^{(i)}) = \mathbf{a}^{(i)} \cdot \mathbf{n}^{(i)}$. Similarly, for $i = M-1$, the constraint is given by

$$\begin{aligned} \mathbf{a}^{(M-1)} \cdot \mathbf{n}^{(M-1)} &= -\frac{1}{f_M}(1-f_M)\,\frac{1}{f_{M-1}}\,\mathrm{tr}\overline{\boldsymbol{\varepsilon}} - \frac{1}{f_{M-1}}\mathrm{tr}\overline{\boldsymbol{\varepsilon}} \\ &= -\frac{1}{f_M\, f_{M-1}}\,\mathrm{tr}\overline{\boldsymbol{\varepsilon}}. \end{aligned} \tag{E.16}$$

In fact, for any i, the constraint (E.15) can be written as

$$\mathbf{a}^{(i)} \cdot \mathbf{n}^{(i)} = -\frac{1}{\hat{f}_{i-1}}\,\mathrm{tr}(\overline{\boldsymbol{\varepsilon}}). \tag{E.17}$$

Then, the vectors $\mathbf{a}^{(i)}$ can be written as

$$\mathbf{a}^{(i)} = -\frac{1}{\hat{f}_{i-1}}\,\mathrm{tr}(\overline{\boldsymbol{\varepsilon}})\,\mathbf{n}^{(i)} + \sqrt{2}\,a_1^{(i)}\mathbf{m}_1^{(i)} + \sqrt{2}\,a_2^{(i)}\mathbf{m}_2^{(i)}, \tag{E.18}$$

where $\sqrt{2}\,a_j^{(i)} = \mathbf{a}^{(i)} \cdot \mathbf{m}_j^{(i)}$ (the reason for the $\sqrt{2}$ will become evident below). Consequently, the effective strain potential of the rank-M laminate simplifies to

$$\widetilde{w}_M(\overline{\boldsymbol{\varepsilon}}) = \inf_{\substack{a_1^{(i)},a_2^{(i)} \\ i=1,\ldots,M}} \left\{ c^{(2)}\, w^{(2)}\left(\overline{\boldsymbol{\varepsilon}}^{(2)}\right) + \sum_{i=1}^{M}(1-f_i)\,\hat{f}_i\, w^{(1)}\left(\overline{\boldsymbol{\varepsilon}}_i^{(1)}\right) \right\}, \tag{E.19}$$

where the strain tensors $\overline{\boldsymbol{\varepsilon}}_i^{(1)}$ and $\overline{\boldsymbol{\varepsilon}}^{(2)}$ are given by

$$\begin{aligned} \overline{\boldsymbol{\varepsilon}}_i^{(1)} &= \overline{\boldsymbol{\varepsilon}} + f_i\left(a_1^{(i)}\mathbf{u}_{nm_1}^{(i)} + a_2^{(i)}\mathbf{u}_{nm_2}^{(i)} - \frac{1}{\hat{f}_{i-1}}\,\mathrm{tr}(\overline{\boldsymbol{\varepsilon}})\,\mathbf{u}_{nn}^{(i)}\right) - \ldots \\ &\qquad \ldots - \sum_{j=i+1}^{M}(1-f_j)\left(a_1^{(j)}\mathbf{u}_{nm_1}^{(j)} + a_2^{(j)}\mathbf{u}_{nm_2}^{(j)} - \frac{1}{\hat{f}_{j-1}}\,\mathrm{tr}(\overline{\boldsymbol{\varepsilon}})\,\mathbf{u}_{nn}^{(j)}\right), \end{aligned} \tag{E.20}$$

$$\overline{\boldsymbol{\varepsilon}}^{(2)} = \overline{\boldsymbol{\varepsilon}} - \sum_{i=1}^{M}(1-f_i)\left(a_1^{(i)}\mathbf{u}_{nm_1}^{(i)} + a_2^{(i)}\mathbf{u}_{nm_2}^{(i)} - \frac{1}{\hat{f}_{i-1}}\mathrm{tr}(\overline{\boldsymbol{\varepsilon}})\,\mathbf{u}_{nn}^{(i)}\right). \tag{E.21}$$

Here, the following second-order tensors have been introduced for convenience:

$$\mathbf{u}_{nn}^{(i)} = \mathbf{n}^{(i)} \otimes \mathbf{n}^{(i)}, \quad \mathbf{u}_{nm_1}^{(i)} = \sqrt{2}\,\mathbf{n}^{(i)} \otimes_s \mathbf{m}_1^{(i)}, \quad \mathbf{u}_{nm_2}^{(i)} = \sqrt{2}\,\mathbf{n}^{(i)} \otimes_s \mathbf{m}_2^{(i)}. \tag{E.22}$$

Note that these tensors are mutually orthogonal and have unit Euclidean norm. Thus, the incompressibility constraint reduces the number of optimization variables required to evaluate $\widetilde{w}_M$ from $3M$ scalars to $2M$ scalars.

Incompressible laminate. If, in addition to the matrix phase, the inclusion phase ($r = 2$) is also incompressible, then the sequential laminate is itself incompressible. In this case, $\mathrm{tr}(\overline{\boldsymbol{\varepsilon}}) = 0$, and the effective strain potential $\widetilde{w}_M$ of the rank-M laminate is given by (E.19), with $\overline{\boldsymbol{\varepsilon}}_i^{(1)}$ and $\overline{\boldsymbol{\varepsilon}}^{(2)}$ given by

$$\overline{\boldsymbol{\varepsilon}}_i^{(1)} = \overline{\boldsymbol{\varepsilon}} + f_i \left(a_1^{(i)} \, \mathbf{u}_{nm_1}^{(i)} + a_2^{(i)} \, \mathbf{u}_{nm_2}^{(i)} \right) - \sum_{j=i+1}^{M} (1 - f_j) \left(a_1^{(j)} \, \mathbf{u}_{nm_1}^{(j)} + a_2^{(j)} \, \mathbf{u}_{nm_2}^{(j)} \right), \tag{E.23}$$

$$\overline{\boldsymbol{\varepsilon}}^{(2)} = \overline{\boldsymbol{\varepsilon}} - \sum_{i=1}^{M} (1 - f_i) \left(a_1^{(i)} \, \mathbf{u}_{nm_1}^{(i)} + a_2^{(i)} \, \mathbf{u}_{nm_2}^{(i)} \right). \tag{E.24}$$

Note that the number of optimization variables remains equal to $2M$.

Plane-strain conditions. Consider sequential laminates whose lamination sequence is such that $\mathbf{m}_2^{(i)} = \mathbf{e}_3$, and therefore such that $\mathbf{n}$ and $\mathbf{m}_1^{(i)}$ lie in the x_1-x_2 plane. These laminates exhibit cylindrical symmetry, with $\mathbf{e}_3$ being the symmetry axis. Under in-plane loading conditions, i.e., $\overline{\varepsilon}_{k3} = 0$, $k = 1, 2, 3$, it follows from the symmetry of the problem that $a_2^{(i)} = 0$ for all i. Let $\mathbf{m}^{(i)} = \mathbf{m}_1^{(i)}$ and $a^{(i)} = a_1^{(i)}$. Then, the effective strain potential is given by (E.19), with $\overline{\boldsymbol{\varepsilon}}_i^{(1)}$ and $\overline{\boldsymbol{\varepsilon}}^{(2)}$ given by

$$\begin{aligned} \overline{\boldsymbol{\varepsilon}}_i^{(1)} = \; & \overline{\boldsymbol{\varepsilon}} + f_i \left(a^{(i)} \, \mathbf{u}_{nm}^{(i)} - \frac{1}{\hat{f}_{i-1}} \, 2\overline{\varepsilon}_m \, \mathbf{u}_{nn}^{(i)} \right) - \ldots \\ & \ldots - \sum_{j=i+1}^{M} (1 - f_j) \left(a^{(j)} \, \mathbf{u}_{nm}^{(j)} - \frac{1}{\hat{f}_{j-1}} \, 2\overline{\varepsilon}_m \, \mathbf{u}_{nn}^{(j)} \right), \end{aligned} \tag{E.25}$$

$$\overline{\boldsymbol{\varepsilon}}^{(2)} = \overline{\boldsymbol{\varepsilon}} - \sum_{i=1}^{M} (1 - f_i) \left(a^{(i)} \, \mathbf{u}_{nm}^{(i)} - \frac{1}{\hat{f}_{i-1}} \, 2\overline{\varepsilon}_m \, \mathbf{u}_{nn}^{(i)} \right), \tag{E.26}$$

where $\overline{\varepsilon}_m = (\overline{\varepsilon}_{11} + \overline{\varepsilon}_{22})/2$ is the in-plane hydrostatic strain. Thus, the number of optimization variables is reduced to M scalars.

Anti-plane strain conditions. Once again, consider sequential laminates whose lamination sequence is such that $\mathbf{m}_2^{(i)} = \mathbf{e}_3$. Under anti-plane loading conditions, i.e., only $\overline{\varepsilon}_{k3} \neq 0$, $k = 1, 2$, it follows from the symmetry of the problem that the local stain field should be such that only $\varepsilon_{k3} \neq 0$, $k = 1, 2$, and therefore $a_1^{(i)} = a_2^{(i)} = 0$. Let $a^{(i)} = a_3^{(i)}$. Then, the effective strain potential is given by (E.19), with $\overline{\boldsymbol{\varepsilon}}_i^{(1)}$ and $\overline{\boldsymbol{\varepsilon}}^{(2)}$ given by

$$\overline{\boldsymbol{\varepsilon}}_i^{(1)} = \overline{\boldsymbol{\varepsilon}} + f_i \, a^{(i)} \, \mathbf{u}_a^{(i)} - \sum_{j=i+1}^{M} (1 - f_j) \, a^{(j)} \, \mathbf{u}_a^{(j)}, \tag{E.27}$$

$$\overline{\boldsymbol{\varepsilon}}^{(2)} = \overline{\boldsymbol{\varepsilon}} - \sum_{i=1}^{M} (1 - f_i) \, a^{(i)} \, \mathbf{u}_a^{(i)}, \tag{E.28}$$

where

$$\mathbf{u}_a^{(i)} = \sqrt{2} \, \mathbf{n}^{(i)} \otimes_s \mathbf{e}_3. \tag{E.29}$$

Thus, the optimization in (E.19) involves M scalars $a^{(i)}$.

E.2.2 Dilute matrix concentration

For reasons that will become evident at the end of this section, it is of interest to consider sequential laminates with a dilute concentration of the matrix phase, i.e., $c^{(1)} << 1$. Following deBotton (2005), we consider rank-M laminates with partial volume fractions given by

$$f_i = 1 - \nu_i\, c^{(1)}, \quad \text{where} \quad 0 < \nu_i < 1, \quad \sum_{i=1}^{M} \nu_i = 1. \tag{E.30}$$

Note that the concentration of phase 2 in the rank-M laminate is therefore

$$c^{(2)} = \prod_{i=1}^{M} f_i = \prod_{i=1}^{M} (1 - \nu_i\, c^{(1)}) = 1 - \sum_{i=1}^{M} \nu_i\, c^{(1)} + O\left((c^{(1)})^2\right) = 1 - c^{(1)} + O\left((c^{(1)})^2\right), \tag{E.31}$$

as it should. Thus, the microstructure of the sequential laminate is specified by the set of constants ν_i and the unit vectors $\mathbf{n}^{(i)}$ denoting the directions of lamination.

We seek to expand the effective potential $\widetilde{w}_M$ of the rank-M laminate, as given by (E.8), to first order in $c^{(1)}$. Assuming the expansion of the optimal $a^{(i)}$ for small $c^{(1)}$ is regular, and expanding the terms inside the curly brackets in (E.8) to first order in $c^{(1)}$, we obtain

$$\begin{aligned} \widetilde{w}_M(\overline{\boldsymbol{\varepsilon}}) \quad = \quad & \inf_{\substack{\mathbf{a}^{(i)} \\ i=1,\ldots,M}} \Big\{ (1 - c^{(1)})\, w^{(2)}(\overline{\boldsymbol{\varepsilon}}) + \ldots \\ & \ldots + c^{(1)} \sum_{i=1}^{M} \nu_i \left[w^{(1)} \left(\overline{\boldsymbol{\varepsilon}} + \mathbf{a}^{(i)} \otimes_s \mathbf{n}^{(i)} \right) - \partial_{\boldsymbol{\varepsilon}} w^{(2)}(\overline{\boldsymbol{\varepsilon}}) \cdot (\mathbf{a}^{(i)} \otimes_s \mathbf{n}^{(i)}) \right] \Big\}. \end{aligned} \tag{E.32}$$

It can be seen that the variables $\mathbf{a}^{(i)}$ are now decoupled, i.e., each $\mathbf{a}^{(i)}$ appears only in one term of the expression inside curly brackets. The optimality conditions for $\mathbf{a}^{(i)}$ follow from setting the derivative of the expression inside curly brackets with respect to each $\mathbf{a}^{(i)}$ equal to zero:

$$\left[\partial_{\boldsymbol{\varepsilon}} w^{(1)} \left(\overline{\boldsymbol{\varepsilon}} + \mathbf{a}^{(i)} \otimes_s \mathbf{n}^{(i)} \right) - \partial_{\boldsymbol{\varepsilon}} w^{(2)}(\overline{\boldsymbol{\varepsilon}}) \right] \mathbf{n}^{(i)} = \mathbf{0}, \tag{E.33}$$

which are, of course, equilibrium conditions involving the traction vectors at the interfaces between the two phases. These equations for $\mathbf{a}^{(i)}$ must be solved numerically, in general, but they can be solved analytically for certain potentials $w^{(r)}$, as will be seen in the next section.

The interest in this limiting case of a dilute matrix stems from the fact that it is very simple to take the limit of expression (E.32) as the rank M tends to infinity. Indeed, in that limit, the set of vectors $\mathbf{a}^{(i)}$ becomes a continuous function of the orientation vector $\mathbf{n}$, and the sum over i in (E.32) becomes an integral over the unit sphere S, with the set of constants ν_i defining a measure over S. Of particular interest in this work is the case of *infinite*-rank laminates with *isotropic* microstructures, which can be constructed by choosing $\nu_i = M^{-1}$ for all i (i.e., all orientations) in (E.32), and taking the limit $M \to \infty$. In this case, the effective strain potential becomes

$$\widetilde{w}_\infty(\overline{\boldsymbol{\varepsilon}}) = (1-c^{(1)})\, w^{(2)}(\overline{\boldsymbol{\varepsilon}}) + c^{(1)} \frac{1}{|S|} \int_S \Big[w^{(1)} \left(\overline{\boldsymbol{\varepsilon}} + \mathbf{a}(\mathbf{n}) \otimes_s \mathbf{n}\right) - \ldots \\ \ldots - \partial_{\boldsymbol{\varepsilon}} w^{(2)}(\overline{\boldsymbol{\varepsilon}}) \cdot (\mathbf{a}(\mathbf{n}) \otimes_s \mathbf{n}) \Big]\, dS(\mathbf{n}), \tag{E.34}$$

where the vector function $\mathbf{a}(\mathbf{n})$ satisfies the optimality condition

$$\Big[\partial_{\boldsymbol{\varepsilon}} w^{(1)} \left(\overline{\boldsymbol{\varepsilon}} + \mathbf{a}(\mathbf{n}) \otimes_s \mathbf{n}\right) - \partial_{\boldsymbol{\varepsilon}} w^{(2)}(\overline{\boldsymbol{\varepsilon}}) \Big]\, \mathbf{n} = \mathbf{0}, \tag{E.35}$$

for every $\mathbf{n}$. Thus, we have obtained an exact, analytical expression (up to a nonlinear, algebraic equation for $\mathbf{a}(\mathbf{n})$) for the effective strain potential of a nonlinear composite with a random 'particulate' microstructure exhibiting overall isotropic symmetry. Even though this result, being valid only for composites with a dilute matrix concentration, may not seem very useful, in fact, it can be used in an iterative process to obtain exact results for composites with *non-dilute* matrix concentrations, as will be seen in the next section.

E.3 Power-law, sequential laminates

In this section, we restrict attention to two-phase, sequential laminates with phases characterized by isotropic, incompressible, power-law potentials of the form

$$w^{(r)}(\boldsymbol{\varepsilon}) = \frac{\varepsilon_0 \sigma_0^{(r)}}{1+m} \left(\frac{\varepsilon_e}{\varepsilon_0} \right)^{1+m}, \tag{E.36}$$

where $\varepsilon_e = \sqrt{(2/3)\boldsymbol{\varepsilon}_d \cdot \boldsymbol{\varepsilon}_d}$ is the von Mises equivalent strain, $m = 1/n$ is the strain-rate sensitivity, such that $0 \leq m \leq 1$, $\sigma_0^{(r)}$ is the flow stress of phase r, and ε_0 is a reference strain rate. For simplicity, both phases are assumed to have the same exponent m and reference strain rate ε_0, so that the effective strain potential of the sequential laminate is itself power-law, with the same exponent m.

We seek to obtain an analytical expression for the effective strain potential of *infinite*-rank, power-law laminates with *arbitrary* phase concentrations, exhibiting overall, isotropic and transversely isotropic symmetry. In those cases, the effective strain potential of the power-law laminate is of the form

$$\widetilde{w}(\overline{\boldsymbol{\varepsilon}}) = \frac{\varepsilon_0 \widetilde{\sigma}_0}{1+m} \left(\frac{\overline{\varepsilon}_e}{\varepsilon_0} \right)^{1+m}, \tag{E.37}$$

where $\overline{\varepsilon}_e = \sqrt{(2/3)\,\overline{\boldsymbol{\varepsilon}}_d \cdot \overline{\boldsymbol{\varepsilon}}_d}$ is the equivalent macroscopic strain, and $\widetilde{\sigma}_0$ is the *effective flow stress*, which completely characterizes the effective response of the laminate. In the case of transversely isotropic laminates, subjected to isochoric in-plane loadings, $\widetilde{\sigma}_0$ is a function of the strain-rate sensitivity, the heterogeneity contrast, and the phase concentrations. In the case of isotropic laminates, $\widetilde{\sigma}_0$ exhibits additional dependence on the macroscopic strain invariant $\overline{\theta}$, defined by

$$\cos(3\overline{\theta}) = 4 \det(\overline{\boldsymbol{\varepsilon}}_d / \overline{\varepsilon}_e). \tag{E.38}$$

Analytical expressions for $\widetilde{\sigma}_0$ are obtained in the next subsections.

E.3.1 Transversely isotropic, power-law laminates

In this subsection, we consider infinite-rank, power-law laminates with transversely isotropic microstructures, subjected to plane-strain conditions. In order to obtain expressions valid for arbitrary phase concentrations, we initially consider laminates with a dilute concentration of the matrix phase, and then make use of an iterative process to reach finite concentrations.

Dilute matrix concentration

Even though expression (E.34) has been derived in the context of isotropic laminates, it remains valid for transversely isotropic laminates under plane-strain conditions, provided the unit vectors $\mathbf{n}$ are constraint to be in the transverse plane. Because of the plane-strain conditions and the symmetry of the laminate, the tensor $\mathbf{a}(\mathbf{n})\otimes_s\mathbf{n}$ is of the form (see *Plane-strain conditions* in the previous section)

$$\mathbf{a}(\mathbf{n})\otimes_s\mathbf{n} = a(\mathbf{n})\,\mathbf{u}_{nm}, \tag{E.39}$$

with $\mathbf{n}$ denoting a unit vector in the transverse plane. Then, expression (E.34) yields the following expression for $\widetilde{\sigma}_0$:

$$\begin{aligned}\frac{\widetilde{\sigma}_0}{\sigma_0^{(1)}} &= \frac{\sigma_0^{(2)}}{\sigma_0^{(1)}} + c^{(1)}\,\frac{1}{|S|}\int_S\left\{\left(\frac{\varepsilon_e}{\overline{\varepsilon}_e}\right)^{1+m} - \ldots\right.\\ &\qquad \left.\ldots - \frac{\sigma_0^{(2)}}{\sigma_0^{(1)}}\left[1+(1+m)\left(\sqrt{\frac{2}{3}}\frac{a(\mathbf{n})}{\overline{\varepsilon}_e}\right)\left(\sqrt{\frac{2}{3}}\frac{\overline{\boldsymbol{\varepsilon}}_d\cdot\mathbf{u}_{nm}}{\overline{\varepsilon}_e}\right)\right]\right\}dS(\mathbf{n}),\end{aligned} \tag{E.40}$$

where the local equivalent strain ε_e is given by

$$\begin{aligned}\left(\frac{\varepsilon_e}{\overline{\varepsilon}_e}\right)^2 &= \frac{2}{3\,\overline{\varepsilon}_e^2}\left[\overline{\boldsymbol{\varepsilon}}_d + \mathbf{a}(\mathbf{n})\otimes_s\mathbf{n}\right]\cdot\left[\overline{\boldsymbol{\varepsilon}}_d + \mathbf{a}(\mathbf{n})\otimes_s\mathbf{n}\right]\\ &= \frac{2}{3\,\overline{\varepsilon}_e^2}\left[\overline{\boldsymbol{\varepsilon}}_d + a(\mathbf{n})\,\mathbf{u}_{nm}\right]\cdot\left[\overline{\boldsymbol{\varepsilon}}_d + a(\mathbf{n})\,\mathbf{u}_{nm}\right]\\ &= 1 + 2\left(\sqrt{\frac{2}{3}}\frac{a(\mathbf{n})}{\overline{\varepsilon}_e}\right)\left(\sqrt{\frac{2}{3}}\frac{\overline{\boldsymbol{\varepsilon}}\cdot\mathbf{u}_{nm}}{\overline{\varepsilon}_e}\right) + \left(\sqrt{\frac{2}{3}}\frac{a(\mathbf{n})}{\overline{\varepsilon}_e}\right)^2,\end{aligned} \tag{E.41}$$

and the function $a(\mathbf{n})$ follows from the optimality condition (E.35). Letting θ denote the angle between the (in-plane) unit vector $\mathbf{n}$ and one of the principal axes of the macroscopic strain $\overline{\boldsymbol{\varepsilon}}$, and introducing a new variable $\breve{a} = (\sqrt{2/3})\,(a(\mathbf{n})/\overline{\varepsilon}_e)$, expression (E.41) can be written as

$$\begin{aligned}\left(\frac{\varepsilon_e}{\overline{\varepsilon}_e}\right)^2 &= 1 + 2\,\breve{a}(\theta)\,\sin(2\theta) + \breve{a}^2(\theta)\\ &= \cos^2(2\theta) + \left[\breve{a}(\theta) + \sin(2\theta)\right]^2.\end{aligned} \tag{E.42}$$

In turn, introducing the function

$$I(z) = \frac{1}{2\pi}\int_0^{2\pi}\left\{\left[\cos^2(2\theta)+\left[\check{a}(\theta)+\sin(2\theta)\right]^2\right]^{\frac{1+m}{2}} - ... \right.$$
$$\left. ... -z\,\left[1+(1+m)\,\check{a}(\theta)\,\sin(2\theta)\right]\right\}\,d\theta, \tag{E.43}$$

expression (E.40) for the effective flow stress can be cast in the simple form

$$\frac{\widetilde{\sigma}_0}{\sigma_0^{(1)}} = \frac{\sigma_0^{(2)}}{\sigma_0^{(1)}} + c^{(1)}\,I\left(\frac{\sigma_0^{(2)}}{\sigma_0^{(1)}}\right). \tag{E.44}$$

The function $\check{a}(\theta)$ in (E.43) follows from the optimality conditions (E.35) for $a(\mathbf{n})$, which can be written as

$$\left[\cos^2(2\theta)+\left(\check{a}(\theta)+\sin(2\theta)\right)^2\right]^{\frac{m-1}{2}}\,\left(\check{a}(\theta)+\sin(2\theta)\right) - z\sin(2\theta) = 0, \tag{E.45}$$

where use has been made of the definition of $\check{a}$ and expression (E.42). This is a nonlinear equation for $\check{a}$, which must be solved numerically at every θ when evaluating the integral in (E.43). For strain-rate sensitivities in the range $0 < m < 1$, equation (E.45) can be written in a simpler form, by introducing a new variable $\hat{a}$ defined by

$$\hat{a}(\theta) = \left(\frac{1+\check{a}(\theta)\,\csc(2\theta)}{z}\right)^{\frac{2}{n-1}}, \tag{E.46}$$

with $n = 1/m$. Then, $\hat{a}(\theta)$ is the solution to

$$\hat{a}^n - z^2\sin^2(2\theta)\,\hat{a}^{n-1} - \cos^2(2\theta) = 0. \tag{E.47}$$

For integer values of the nonlinearity n, this is a polynomial equation in $\hat{a}$, which can be solved analytically in some cases (e.g., $n = 2, 3$). Note that the original variable $\check{a}$ is given in terms of $\hat{a}$ by

$$\check{a}(\theta) = -\sin(2\theta)\,\left(1 - z\,\hat{a}^{\frac{n-1}{2}}\right). \tag{E.48}$$

In summary, the effective flow stress $\widetilde{\sigma}_0$ is given by (E.44), which requires evaluating the integral in (E.43), where the function $\check{a}(\theta)$ is the solution to the nonlinear equation (E.45), or alternatively, (E.47). Thus, we have obtained an analytical expression, up to a nonlinear equation, for the effective strain potential of a transversely isotropic, power-law composite with a *dilute* matrix concentration.

While, in general, equation (E.45) must be solved numerically, it admits closed-form solutions for the extreme values of the strain-rate sensitivity, $m = 1$ and $m = 0$, which correspond, respectively, to composites with linear and ideally plastic phases. Then, in those cases, closed-form expressions for the effective flow stress can be obtained. These expressions are spelled out below.

$m = 1/n = 1$ - *Linear phases.* In this case, the solution to (E.45) is

$$\check{a}(\theta) = (z-1)\,\sin(2\theta), \tag{E.49}$$

and so the function I is given by

$$I(z) = (1-z)\,\frac{1}{2\pi}\int_0^{2\pi}\left\{\cos^2(2\theta) + z\,\sin^2(2\theta)\right\}\,d\theta = \frac{1-z^2}{2}. \tag{E.50}$$

Finally, the effective flow stress is given by

$$\frac{\widetilde{\sigma}_0}{\sigma_0^{(1)}} = \frac{\sigma_0^{(2)}}{\sigma_0^{(1)}} + \frac{c^{(1)}}{2}\left[1 - \left(\frac{\sigma_0^{(2)}}{\sigma_0^{(1)}}\right)^2\right]. \tag{E.51}$$

$m = 1/n = 0$ - *Ideally plastic phases.* In this case, equation (E.45) admits a real solution only for $z \leq 1$, which is given by

$$\breve{a} = \sin(2\theta)\,\left[\sqrt{\frac{z^2\cos^2(2\theta)}{1-z^2\sin^2(2\theta)}} - 1\right], \quad z \leq 1. \tag{E.52}$$

Introducing this solution into (E.43) and integrating over θ, yields the following expression for the function I:

$$I(z) = \frac{1}{\pi}\frac{\arcsin(z)}{z} + \frac{1}{\pi}\sqrt{1-z^2} - \frac{z}{2}. \tag{E.53}$$

Finally, the effective flow stress is given by

$$\frac{\widetilde{\sigma}_0}{\sigma_0^{(1)}} = \frac{\sigma_0^{(2)}}{\sigma_0^{(1)}} + \frac{c^{(1)}}{\pi}\left\{\frac{\arcsin(\sigma_0^{(2)}/\sigma_0^{(1)})}{(\sigma_0^{(2)}/\sigma_0^{(1)})} + \sqrt{1-\left(\frac{\sigma_0^{(2)}}{\sigma_0^{(1)}}\right)^2} - \frac{1}{2}\,\frac{\sigma_0^{(2)}}{\sigma_0^{(1)}}\right\}. \tag{E.54}$$

It is emphasized that this expression is only valid for $\sigma_0^{(2)} \leq \sigma_0^{(1)}$, i.e., for composites with an inclusion phase weaker than the matrix. This is because in the opposite case of stronger inclusions, the range of validity of the expansion (E.34) for $\widetilde{w}_M$, with a correction term being linear in $c^{(1)}$, tends to zero as $m \to 0$.

Arbitrary concentrations

Following deBotton (2005), transversely isotropic composites with a *finite* matrix concentration are constructed by following an iterative process based on a differential scheme. The idea is to consider infinite-rank laminates with a dilute matrix concentration, where the inclusion phase is, in turn, an infinite-rank laminate with a dilute matrix concentration, and so on. Thus, each time, an infinitesimal amount of matrix material is added to the composite, in such a way that, after repeating the process an infinite number of times, a finite concentration of the matrix material is reached. Recalling expression (E.44), the effective flow stress $\widetilde{\sigma}_0^{[i+1]}$ at the $i+1$ iteration is given in terms of the effective flow stress $\widetilde{\sigma}_0^{[i]}$ of the previous iteration (the inclusion phase in the $i+1$ iteration) by

$$\frac{\widetilde{\sigma}_0^{[i+1]}}{\sigma_0^{(1)}} = \frac{\widetilde{\sigma}_0^{[i]}}{\sigma_0^{(1)}} + c^{[i+1]}\,I\left(\frac{\widetilde{\sigma}_0^{[i]}}{\sigma_0^{(1)}}\right), \tag{E.55}$$

where $c^{[i+1]}$ denotes the concentration of matrix material *added* to the composite in the $i+1$ iteration. The *total* concentration $c_{i+1}^{(1)}$ of matrix material in the composite at the $i+1$ iteration is given by

$$c_{i+1}^{(1)} = 1 - \prod_{j=1}^{i+1}(1 - c^{[j]}). \tag{E.56}$$

Then, the increment of total matrix concentration in the composite at each iteration is given by

$$\begin{aligned} c_{i+1}^{(1)} - c_i^{(1)} &= \prod_{j=1}^{i}(1-c^{[j]}) - \prod_{j=1}^{i+1}(1-c^{[j]}) \\ &= \prod_{j=1}^{i}(1-c^{[j]}) - (1-c^{[i+1]}) \prod_{j=1}^{i}(1-c^{[j]}) \\ &= c^{[i+1]} \prod_{j=1}^{i}(1-c^{[j]}) \\ &= c^{[i+1]} (1-c_i^{(1)}). \end{aligned} \tag{E.57}$$

From relations (E.55) and (E.57), it follows that

$$\left[I\left(\frac{\widetilde{\sigma}_0^{[i]}}{\sigma_0^{(1)}} \right) \right]^{-1} \frac{(\widetilde{\sigma}_0^{[i+1]}/\sigma_0^{(1)}) - (\widetilde{\sigma}_0^{[i]}/\sigma_0^{(1)})}{c_{i+1}^{(1)} - c_i^{(1)}} = \frac{1}{1-c_{(i)}^{(1)}}. \tag{E.58}$$

Since the $c^{[i]}$ are infinitesimally small, this relation can be written in differential form,

$$\left[I\left(\widetilde{\sigma}_0/\sigma_0^{(1)} \right) \right]^{-1} \frac{d\left(\widetilde{\sigma}_0/\sigma_0^{(1)} \right)}{dc^{(1)}} = \frac{1}{1-c^{(1)}}. \tag{E.59}$$

This is a differential equation for the effective flow stress $\widetilde{\sigma}_0$, which leads to the following integral equation for $\widetilde{\sigma}_0$:

$$\int_{(\sigma_0^{(2)}/\sigma_0^{(1)})}^{(\widetilde{\sigma}_0/\sigma_0^{(1)})} \frac{dz}{I(z)} = -\ln c^{(2)}, \tag{E.60}$$

where $c^{(2)} = 1 - c^{(1)}$ is the total concentration of the inclusion phase. In general, this equation must be solved numerically for $\widetilde{\sigma}_0$. Thus, we have obtained an analytical expression, up to a nonlinear equation, for the effective flow stress of a transversely isotropic, power-law composite, with finite phase concentrations.

$m = 1/n = 1$ - *Linear phases.* In this case, the function I is given by (E.50), so that equation (E.60) becomes

$$2 \int_{(\sigma_0^{(2)}/\sigma_0^{(1)})}^{(\widetilde{\sigma}_0/\sigma_0^{(1)})} \frac{dz}{1-z^2} = \ln\left(\frac{z+1}{z-1} \right) \Bigg|_{(\sigma_0^{(2)}/\sigma_0^{(1)})}^{(\widetilde{\sigma}_0/\sigma_0^{(1)})} = -\ln c^{(2)}. \tag{E.61}$$

The solution to this equation is given by

$$\frac{\widetilde{\sigma}_0}{\sigma_0^{(1)}} = 1 + c^{(2)} \frac{\left(\frac{\sigma_0^{(2)}}{\sigma_0^{(1)}} - 1 \right)}{1 + \frac{c^{(1)}}{2}\left(\frac{\sigma_0^{(2)}}{\sigma_0^{(1)}} - 1 \right)}. \tag{E.62}$$

This is precisely the expression resulting from the linear Hashin-Shtrikman estimates with the reference elastic tensor chosen to be that of the matrix phase.

$m = 1/n = 0$ - *Ideally plastic phases.* In this case, if $\sigma_0^{(2)} \leq \sigma_0^{(1)}$, the function I is given by (E.53), so that equation (E.60) becomes

$$\int_{(\sigma_0^{(2)}/\sigma_0^{(1)})}^{(\widetilde{\sigma}_0/\sigma_0^{(1)})} \frac{dz}{\frac{1}{\pi}\frac{\arcsin(z)}{z} + \frac{1}{\pi}\sqrt{1-z^2} - \frac{z}{2}} = -\ln c^{(2)}. \tag{E.63}$$

Introducing the variable $v = 2\arcsin z - \pi/2$, and letting

$$v_0 = 2\arcsin\left(\sigma_0^{(2)}/\sigma_0^{(1)}\right) - \frac{\pi}{2} \quad \text{and} \quad \widetilde{v} = 2\arcsin\left(\widetilde{\sigma}_0/\sigma_0^{(1)}\right) - \frac{\pi}{2}, \tag{E.64}$$

equation (E.63) can be written in the equivalent form

$$\frac{\pi}{2}\int_{v_0}^{\widetilde{v}} \frac{\left(\frac{\cos v}{v}\right)}{1 + \left(\frac{\cos v}{v}\right) - \frac{\pi}{2}\left(\frac{\sin v}{v}\right)} dv = -\ln c^{(2)}, \tag{E.65}$$

which is easier to work with. Unfortunately, the integration on the left-hand side is complicated, and it must be solved numerically, in general. However, it is possible to obtain asymptotic results for $\widetilde{\sigma}_0$ that are of particular interest.

Thus, the weak-contrast expansion of $\widetilde{\sigma}_0$ can be obtained by introducing the parameter $\epsilon = 1 - (\sigma_0^{(2)}/\sigma_0^{(2)})$, and expanding the left-hand side of equation (E.65) for small ϵ. The result is:

$$\frac{\widetilde{\sigma}_0}{\sigma_0^{(1)}} = 1 - c^{(2)}\,\epsilon - \frac{8\sqrt{2}}{3\pi}\,c^{(2)}\,\left(1 - \sqrt{c^{(2)}}\right)\,\epsilon^{3/2} + ... \tag{E.66}$$

It can be seen that the first two terms in this expansion coincide with those of the Voigt and Reuss bounds, as expected. More interesting, however, is the fact that the third term in the expansion is of order $\epsilon^{3/2}$, rather than ϵ^2. In this connection, it is recalled that the weak-contrast expansion of Suquet & Ponte Castañeda (1993) yields a quadratic correction (i.e., $\sim \epsilon^2$) to the Voigt and Reuss bounds. However, in the case of power-law composites, the range of validity of that expansion shrinks to zero as $m \to 0$, which signals the transition to correction terms involving non-integer powers of ϵ, precisely as observed in the result (E.66).

Another asymptotic result of interest is that of a dilute concentration of voids (i.e., $c^{(2)} << 1$) in an ideally plastic matrix. Thus, letting $\sigma_0^{(2)} = 0$ (incompressible voids), and $\widetilde{\sigma}_0/\sigma_0^{(1)} = 1 - \delta(c^{(2)})$, with $\delta(c^{(2)}) << 1$, and expanding the left-hand side of equation (E.65) for small δ, we obtain

$$\frac{\widetilde{\sigma}_0}{\sigma_0^{(1)}} = 1 - \beta\,c^{(2)} + ... \tag{E.67}$$

where $\beta \approx 3.0982$. It is interesting to note that the correction term is linear in the porosity $c^{(2)}$.

E.3.2 Isotropic, power-law laminates

In this subsection, we consider infinite-rank, power-law laminates with isotropic microstructures. As in the previous subsection, we initially consider laminates with a dilute concentration of the matrix phase, and then make use of an iterative process to reach finite concentrations.

Dilute matrix concentration

In the case of a dilute matrix concentration, the effective strain potential is given by (E.34), with the tensor $\mathbf{a}(\mathbf{n}) \otimes_s \mathbf{n}$ given by (see *Incompressible laminate* in the previous section)

$$\mathbf{a}(\mathbf{n}) \otimes_s \mathbf{n} = a_1(\mathbf{n})\,\mathbf{u}_{nm_1} + a_2(\mathbf{n})\,\mathbf{u}_{nm_2}. \tag{E.68}$$

Then, following a procedure completely analogous to that of the previous subsection, we can write the effective flow stress as

$$\begin{aligned}\frac{\widetilde{\sigma}_0}{\sigma_0^{(1)}} &= \frac{\sigma_0^{(2)}}{\sigma_0^{(1)}} + c^{(1)}\,\frac{1}{|S|}\int_S \left\{ \left(\frac{\varepsilon_e}{\overline{\varepsilon}_e}\right)^{1+m} - ... \right. \\ &\qquad \left. ... - \frac{\sigma_0^{(2)}}{\sigma_0^{(1)}}\,(1+(1+m)\,[\,\check{a}_1(\mathbf{n})\,u_1(\mathbf{n}) + \check{a}_2(\mathbf{n})\,u_2(\mathbf{n})\,]\,) \right\} dS(\mathbf{n}), \end{aligned} \tag{E.69}$$

where the local equivalent strain ε_e is given by

$$\left(\frac{\varepsilon_e}{\overline{\varepsilon}_e}\right)^2 = 1 - u_1^2(\mathbf{n}) - u_2^2(\mathbf{n}) + [\check{a}_1(\mathbf{n}) + u_1(\mathbf{n})]^2 + [\check{a}_2(\mathbf{n}) + u_2(\mathbf{n})]^2, \tag{E.70}$$

and the quantities $\check{a}_i$ and u_i have been defined as

$$\check{a}_i(\mathbf{n}) = \sqrt{\frac{2}{3}}\frac{a_i(\mathbf{n})}{\overline{\varepsilon}_e}, \quad u_i(\mathbf{n}) = \sqrt{\frac{2}{3}}\frac{\overline{\boldsymbol{\varepsilon}}_d \cdot \mathbf{u}_{nm_i}}{\overline{\varepsilon}_e}, \quad i = 1, 2. \tag{E.71}$$

Expression (E.69) can be put in the simple form

$$\frac{\widetilde{\sigma}_0}{\sigma_0^{(1)}} = \frac{\sigma_0^{(2)}}{\sigma_0^{(1)}} + c^{(1)}\, I\left(\frac{\sigma_0^{(2)}}{\sigma_0^{(1)}}\right), \tag{E.72}$$

where the function I has been defined as

$$\begin{aligned} I(z) &= \frac{1}{|S|}\int_S \left\{ \left[1 - u_1^2(\mathbf{n}) - u_2^2(\mathbf{n}) + [\check{a}_1(\mathbf{n}) + u_1(\mathbf{n})]^2 + [\check{a}_2(\mathbf{n}) + u_2(\mathbf{n})]^2\right]^{\frac{1+m}{2}} - ... \right. \\ &\qquad \left. ... - z\,(1+(1+m)\,[\,\check{a}_1(\mathbf{n})\,u_1(\mathbf{n}) + \check{a}_2(\mathbf{n})\,u_2(\mathbf{n})\,])\right\} dS(\mathbf{n}). \end{aligned} \tag{E.73}$$

It should be noted that, unlike in the case of transverse isotropy, this function I depends on the third invariant $\overline{\theta}$ of $\overline{\boldsymbol{\varepsilon}}_d$, and so does $\widetilde{\sigma}_0$.

The functions $\check{a}_i(\mathbf{n})$ in (E.73) follow from the optimality conditions (E.35) for $a(\mathbf{n})$, which can be written as

$$\begin{aligned} &\left[1 - u_1^2(\mathbf{n}) - u_2^2(\mathbf{n}) + [\check{a}_1(\mathbf{n}) + u_1(\mathbf{n})]^2 + [\check{a}_2(\mathbf{n}) + u_2(\mathbf{n})]^2\right]^{\frac{m-1}{2}} \times ... \\ &\qquad ... \times [\check{a}_i(\mathbf{n}) + u_i(\mathbf{n})] - z\; u_i(\mathbf{n}) = 0, \quad i = 1, 2, \end{aligned} \tag{E.74}$$

where use has been made of the definition of $\check{a}_i$ and expression (E.70). For strain-rate sensitivities in the range $0 < m < 1$, this system of two nonlinear equations for $\check{a}_1$ and $\check{a}_2$ can be combined into the following nonlinear equation:

$$\hat{a}^n - z^2 g(\mathbf{n})\;\hat{a}^{n-1} - (1 - g(\mathbf{n})) = 0, \tag{E.75}$$

where

$$\hat{a}(\mathbf{n}) = \left(\frac{a_i(\mathbf{n})}{z\;u_i(\mathbf{n})}\right)^{\frac{2}{n-1}}, \quad i = 1, 2, \quad \text{and} \quad g(\mathbf{n}) = u_1^2(\mathbf{n}) + u_2^2(\mathbf{n}), \tag{E.76}$$

For integer values of the nonlinearity n, this is a polynomial equation in $\hat{a}$, which can be solved analytically in some cases (e.g., $n = 2, 3$). Note that the original variable $\check{a}$ is given in terms of $\hat{a}$ by

$$\check{a}_i(\mathbf{n}) = u_i(\mathbf{n})\;\left(z\,\hat{a}^{\frac{n-1}{2}} - 1\right). \tag{E.77}$$

The function I can then be written as

$$I(z) = \frac{1}{|S|}\int_S \Big\{ \left[1+\left(z^2\ \hat{a}^{n-1}-1\right)\ g(\mathbf{n})\right]^{\frac{1+m}{2}} - ... \\ ... -z\ \left[1+(1+m)\ \left(z\ \hat{a}^{n-1}-1\right)\ g(\mathbf{n})\right]\Big\}\ dS(\mathbf{n}). \tag{E.78}$$

The integrand in this expression depends on $\mathbf{n}$ only through the function $g(\mathbf{n})$. In order to make this function more explicit, we introduce a set of Euler angles $\{\phi_1, \phi_2, \varphi\}$ to describe the orientation of the orthonormal basis $\{\mathbf{m}_1, \mathbf{m}_2, \mathbf{n}\}$ relative to the principal axes $\mathbf{e}_i$ of $\overline{\boldsymbol{\varepsilon}}_d$, and we express the latter in terms of its third invariant $\overline{\theta}$ (see, for instance, Nebozhyn and Ponte Castañeda 1999):

$$\frac{\overline{\boldsymbol{\varepsilon}}_d}{\overline{\varepsilon}_e} = \mathrm{diag}\left(\frac{\sqrt{3}\sin\overline{\theta}-\cos\overline{\theta}}{2}, -\frac{\sqrt{3}\sin\overline{\theta}+\cos\overline{\theta}}{2}, \cos\overline{\theta}\right). \tag{E.79}$$

Here, the symbol φ has been used to denote the angle between $\mathbf{n}$ and $\mathbf{e}_3$. Then, the function $g(\mathbf{n})$ is given by

$$g(\phi_2,\varphi) = \sin^2\varphi\ \Big\{\sin^2 2\phi_2\ \sin^2\overline{\theta}+\cos^2\varphi\ \Big[3\ \cos^2\overline{\theta}+... \\ ...+\ \cos 2\phi_2\ \left(\cos 2\phi_2\ \sin^2\overline{\theta}-\sqrt{3}\ \sin 2\overline{\theta}\right)\Big]\Big\}. \tag{E.80}$$

It is noted that this special function of $\mathbf{n}$ depends only on *two* of the three Euler angles, as expected from the fact that individual laminae are transversely isotropic, and therefore invariant with respect to rotations about $\mathbf{n}$. The two angles appearing in (E.80) can be used to parametrize the unit sphere S, so that $dS(\mathbf{n}) = \sin\varphi\ d\varphi\ d\phi_2$, and therefore the function I can be written as

$$I(z) = \frac{1}{4\pi}\int_0^{2\pi}\int_0^{\pi} \Big\{ \left[1+\left(z^2\ \hat{a}^{n-1}-1\right)\ g(\phi_2,\varphi)\right]^{\frac{1+m}{2}} - ... \\ ... -z\ \left[1+(1+m)\ \left(z\ \hat{a}^{n-1}-1\right)\ g(\phi_2,\varphi)\right]\Big\}\ \sin\varphi\ d\varphi\ d\phi_2. \tag{E.81}$$

In summary, the effective flow stress $\widetilde{\sigma}_0$ is given by (E.72), which requires evaluating the integral in (E.81), where g is given by (E.80), and the function $\hat{a}$ is the solution to (E.75). Thus, we have obtained an exact, analytical expression, up to a nonlinear equation, for the effective strain potential of an isotropic, power-law composite with a *dilute* matrix concentration. It is emphasized that, unlike in the case of transverse isotropy, in this case, the effective flow stress exhibits a dependence on the third invariant $\overline{\theta}$ of the macroscopic strain, defined by (E.38).

$m = 1/n = 1$ - *Linear phases.* In this case, the solution to (E.74) is

$$\check{a}_i(\theta) = (z-1)\ u_i(\mathbf{n}), \tag{E.82}$$

and so the function I is given by

$$I(z) = (1-z)\left\{1-(1-z)\,\frac{1}{4\pi}\int_0^{2\pi}\int_0^{\pi} g(\phi_2,\varphi)\ \sin\varphi\ d\varphi\ d\phi_2\right\}, \tag{E.83}$$

where g is given by (E.80). The integral in (E.83) can be readily evaluated, so that the function I is given by

$$I(z) = \frac{3}{5}(1-z)\left(1+\frac{2}{3}z\right). \tag{E.84}$$

Finally, the effective flow stress is given by

$$\frac{\widetilde{\sigma}_0}{\sigma_0^{(1)}} = \frac{\sigma_0^{(2)}}{\sigma_0^{(1)}} + \frac{3}{5}c^{(1)} \left(1 - \frac{\sigma_0^{(2)}}{\sigma_0^{(1)}}\right)\left(1 + \frac{2}{3}\frac{\sigma_0^{(2)}}{\sigma_0^{(1)}}\right). \tag{E.85}$$

It should be noted that, in the linear case, the effective flow stress does *not* depend on the third invariant $\overline{\theta}$.

$m = 1/n = 0$ - *Rigid-ideally plastic phases.* In this case, equation (E.74) admits a real solution only for $z \leq 1$, which is given by

$$\check{a}_i(\mathbf{n}) = u_i(\mathbf{n})\left\{z\sqrt{\frac{1 - g(\phi_2,\varphi)}{1 - z^2 g(\phi_2,\varphi)}} - 1\right\}. \tag{E.86}$$

The function I is then given by

$$\begin{aligned} I(z) \;\; = \;\; & \frac{1}{4\pi}\int_0^{2\pi}\int_0^{\pi} \left\{\sqrt{(1 - g(\phi_2,\varphi))\,(1 - z^2\; g(\phi_2,\varphi))} - ... \right. \\ & \left. ... - z\,(1 - g(\phi_2,\varphi))\right\}\; \sin(\varphi)\; d\varphi\; d\phi_2. \end{aligned} \tag{E.87}$$

In general, further simplifications are not possible, and so $\widetilde{\sigma}_0$ is given by (E.72), where the function I must be evaluated numerically. It should be emphasized that, unlike in the linear case, the function I, and therefore $\widetilde{\sigma}_0$, depends on the third invariant $\overline{\theta}$.

Arbitrary concentrations

Isotropic, power-law composites can be constructed in a fashion completely analogous to that employed in the previous subsection for transversely isotropic composites, making use of an iterative process based on a differential scheme. However, an additional complication arises in this case because of the fact that, as already mentioned above, the effective flow stress exhibits a dependence on the third invariant $\overline{\theta}$ of $\overline{\boldsymbol{\varepsilon}}$. Then, at each iteration $i+1$ of the process, the stress-strain relation of the 'inclusion' phase is of the form

$$\partial_{\overline{\boldsymbol{\varepsilon}}}\widetilde{w}^{[i]}(\overline{\boldsymbol{\varepsilon}}) = \frac{2}{3}\;\widetilde{\sigma}_0^{[i]}(\overline{\theta})\;\left(\frac{\overline{\varepsilon}_e}{\varepsilon_0}\right)^m \frac{\overline{\boldsymbol{\varepsilon}}_d}{\overline{\varepsilon}_e} - \frac{\partial\widetilde{\sigma}_0^{[i]}}{\partial\overline{\theta}}(\overline{\theta})\left(\frac{\overline{\varepsilon}_e}{\varepsilon_0}\right)^m \frac{\cot(3\overline{\theta})}{3\;(1+m)}\;\left[\left(\frac{\overline{\boldsymbol{\varepsilon}}_d}{\overline{\varepsilon}_e}\right)^{-1} - 2\;\frac{\overline{\boldsymbol{\varepsilon}}_d}{\overline{\varepsilon}_e}\right], \tag{E.88}$$

which depends not only on $\widetilde{\sigma}_0^{[i]}$, but also on its derivative with respect to $\overline{\theta}$. Therefore, the analogous of expression (E.44) in this case is of the form

$$\frac{\widetilde{\sigma}_0^{[i+1]}}{\sigma_0^{(1)}}(\overline{\theta}, c^{[i+1]}) = \frac{\widetilde{\sigma}_0^{[i]}}{\sigma_0^{(1)}}(\overline{\theta}, c^{[i]}) + c^{[i+1]}\, I\left(\frac{\widetilde{\sigma}_0^{[i]}}{\sigma_0^{(1)}}(\overline{\theta}, c^{[i]}), \frac{\partial}{\partial\overline{\theta}}\frac{\widetilde{\sigma}_0^{[i]}}{\sigma_0^{(1)}}(\overline{\theta}, c^{[i]})\right), \tag{E.89}$$

where the function I is defined by

$$\begin{aligned} I(z,z') \;\; = \;\; & \frac{1}{|S|}\int_S \left\{\left[1 - u_1^2(\mathbf{n}) - u_2^2(\mathbf{n}) + [\check{a}_1(\mathbf{n}) + u_1(\mathbf{n})]^2 + [\check{a}_2(\mathbf{n}) + u_2(\mathbf{n})]^2\right]^{\frac{1+m}{2}} - ... \right. \\ & ... - z\;\left(1 + (1+m)\;[\;\check{a}_1(\mathbf{n})\;u_1(\mathbf{n}) + \check{a}_2(\mathbf{n})\,u_2(\mathbf{n})\;] - z'\;\frac{\cot(3\overline{\theta})}{3}\times \right. \\ & \left. \left. ... \left[\left(\frac{\overline{\boldsymbol{\varepsilon}}_d}{\overline{\varepsilon}_e}\right)^{-1} - 2\frac{\overline{\boldsymbol{\varepsilon}}_d}{\overline{\varepsilon}_e}\right]\cdot[\;a_1(\mathbf{n})\;\mathbf{u}_{nm_1}(\mathbf{n}) + a_2(\mathbf{n})\;\mathbf{u}_{nm_2}(\mathbf{n})\;]\right)\right\}\; dS(\mathbf{n}). \end{aligned} \tag{E.90}$$

Expression (E.89) then leads to the following differential equation:

$$\left(1-c^{(1)}\right)\ \frac{\partial(\widetilde{\sigma}_0/\sigma_0^{(1)})}{\partial c^{(1)}} = I\left((\widetilde{\sigma}_0/\sigma_0^{(1)}), \frac{\partial(\widetilde{\sigma}_0/\sigma_0^{(1)})}{\partial\overline{\theta}}\right). \tag{E.91}$$

This is a nonlinear, hyperbolic, partial differential equation (PDE) for the function $(\widetilde{\sigma}_0/\sigma_0^{(1)})(\overline{\theta}, c^{(1)})$, with $c^{(1)}$ and $\overline{\theta}$ being, respectively, the time- and space-like variables. The initial condition follows from the fact that when $c^{(1)}=0$, the composite is made entirely of phase 2 and therefore $\widetilde{\sigma}_0 = \sigma_0^{(2)}$, while the boundary conditions follow from the fact that the definition (E.38) for $\overline{\theta}$ is periodic in this variable, with period $2\pi/3$. Thus,

$$\frac{\widetilde{\sigma}_0}{\sigma_0^{(1)}}(\overline{\theta},0) = \frac{\sigma_0^{(2)}}{\sigma_0^{(1)}}, \quad \text{and} \quad \frac{\widetilde{\sigma}_0}{\sigma_0^{(1)}}\left(\overline{\theta}, c^{(1)}\right) = \frac{\widetilde{\sigma}_0}{\sigma_0^{(1)}}\left(\overline{\theta}+\frac{2\pi}{3}, c^{(1)}\right). \tag{E.92}$$

In general, this type of PDEs must be solved numerically, using, for instance, the method of lines (see, for instance, Schiesser 1991).

$m = 1/n = 1$ - *Linear phases.* In this case, the function I is given by (E.84), and is therefore independent of its second argument, so that equation (E.91) reduces to the ordinary differential equation

$$\left(1-c^{(1)}\right)\ \frac{d(\widetilde{\sigma}_0/\sigma_0^{(1)})}{dc^{(1)}} = I\left(\widetilde{\sigma}_0/\sigma_0^{(1)}\right). \tag{E.93}$$

Integrating this equation leads to

$$\int_{(\sigma_0^{(2)}/\sigma_0^{(1)})}^{(\widetilde{\sigma}_0/\sigma_0^{(1)})} \frac{dz}{\frac{3}{5}(1-z)\left(1+\frac{2}{3}z\right)} = \ln\left(\frac{2\ z+3}{z-1}\right)\Bigg|_{(\sigma_0^{(2)}/\sigma_0^{(1)})}^{(\widetilde{\sigma}_0/\sigma_0^{(1)})} = -\ln c^{(2)}, \tag{E.94}$$

where $c^{(2)} = 1-c^{(1)}$ is the total concentration of the inclusion phase. Solving this algebraic equation for $\widetilde{\sigma}_0$, we obtain

$$\frac{\widetilde{\sigma}_0}{\sigma_0^{(1)}} = \frac{1+\frac{2}{3}\ \frac{\sigma_0^{(2)}}{\sigma_0^{(1)}} - c^{(2)}\ \left(1-\frac{\sigma_0^{(2)}}{\sigma_0^{(1)}}\right)}{1+\frac{2}{3}\ \frac{\sigma_0^{(2)}}{\sigma_0^{(1)}} + \frac{2}{3}\ c^{(2)}\ \left(1-\frac{\sigma_0^{(2)}}{\sigma_0^{(1)}}\right)}, \tag{E.95}$$

which is precisely the Hashin-Shtrikman estimate with the reference tensor chosen to be that of the matrix phase.

E.3.3 Quasi-isotropic microstructures

While the formulae provided in the previous two subsections constitute precious results for nonlinear isotropic composites, they do not give information about the field statistics, and they can be quite complicated to compute for the general three-dimensional case. An alternative approach is to solve the minimization problem (E.8) numerically, for appropriate lamination sequences and sufficiently large rank M, so that the microstructure exhibits quasi-isotropic symmetry. Once the minimization problem is solved, the entire field distribution is known, and so the field statistics can be computed using relations (E.12)-(E.13).

The microstructure of a rank-M sequential laminate is characterized by the set of unit vectors $\mathbf{n}^{(i)}$ and partial concentrations f_i, $i = 1, ..., M$. This set of variables can be interpreted as a distribution of points over the unit sphere, with masses f_i. By 'appropriate' microstructures, it is meant those that become progressively more (transversely) isotropic with increasing rank M. Thus, an 'appriapriate' choice of partial concentrations f_i is given by (see, for instance, Milton 2002)

$$f_i = \frac{1 - \frac{i}{M}\ c^{(1)}}{1 - \frac{i-1}{M}\ c^{(1)}}, \quad 1 \leq i \leq M, \tag{E.96}$$

where $c^{(1)}$ is the volume fraction of the matrix phase in the rank-M sequential laminate. On the other hand, the 'appropriate' set of vectors $\mathbf{n}^{(i)}$ depends on whether the microstructure should become transversely isotropic or isotropic. These two cases are considered below.

Quasi-transversely isotropic microstructures. In this case, the lamination directions $\mathbf{n}^{(i)}$ should all lie on the same plane, say x_1-x_2, transverse to the axis of cylindrical symmetry of the microstructure. Thus, introducing a basis $\mathbf{e}_i$, we can write

$$\mathbf{n}^{(i)} = \cos\theta_i\ \mathbf{e}_1 + \sin\theta_i\ \mathbf{e}_2, \quad 1 \leq i \leq M, \tag{E.97}$$

the set of perpendicular vectors $\mathbf{m}^{(i)}$ being

$$\mathbf{m}^{(i)} = -\sin\theta_i\ \mathbf{e}_1 + \cos\theta_i\ \mathbf{e}_2, \quad 1 \leq i \leq M. \tag{E.98}$$

In order to obtain a quasi-transversely isotropic microstructure, the lamination angles θ_i must span the unit circle many times (see deBotton & Hariton 2002). Let η denote the number of 'rounds' involved in a given lamination sequence. Then, $M_\eta = M/\eta$ is the number of laminations per round, which should be evenly distributed on the unit circle. Thus, an appropriate set of angles θ_i is given by

$$\theta_{j+kM_\eta} = 2\pi\ \frac{j-1}{M_\eta}, \quad 1 \leq j \leq M_\eta, \quad 0 \leq k \leq \eta - 1. \tag{E.99}$$

A quasi-transversely isotropic microstructure is obtained by considering sufficiently large M *and* η. Accurate results may be obtained, in general, by choosing $M \approx 200$ and $\eta \approx 12$.

Quasi-isotropic microstructures. In this case, the lamination directions $\mathbf{n}^{(i)}$ should lie on the unit sphere. Thus, introducing a basis $\mathbf{e}_i$ and using spherical coordinates, we can write

$$\mathbf{n}^{(i)} = \sin\psi_i \sin\phi_i\ \mathbf{e}_1 + \cos\psi_i \sin\phi_i\ \mathbf{e}_2 + \cos\phi_i\ \mathbf{e}_3, \tag{E.100}$$

$$\mathbf{m}_1^{(i)} = \cos\psi_i\ \mathbf{e}_1 - \sin\psi_i\ \mathbf{e}_2, \tag{E.101}$$

$$\mathbf{m}_2^{(i)} = \sin\psi_i \cos\phi_i\ \mathbf{e}_1 + \cos\psi_i \cos\phi_i\ \mathbf{e}_2 - \sin\phi_i\ \mathbf{e}_3, \tag{E.102}$$

where $\mathbf{m}_\alpha^{(i)}$ denote two vectors perpendicular to $\mathbf{n}^{(i)}$, and the angles ψ_i and ϕ_i are such that $0 \leq \psi_i < 2\pi$, $0 \leq \phi_i \leq \pi$. In order to obtain a quasi-isotropic microstructure, the lamination angles ψ_i and ϕ_i must span the unit sphere many times. Let η denote the number of 'rounds' involved in a given lamination sequence. Then, $M_\eta = M/\eta$ is the number of laminations per round, which should

be evenly distributed on the unit sphere. A possible set of angles satisfying this requirement is given by (see Saff & Kuijlaars 1997)

$$\phi_{j+kM_\eta} = \arccos h_j, \quad h_j = 2\frac{j-1}{M_\eta - 1} - 1, \quad 1 \le j \le M_\eta, \quad 0 \le k \le \eta - 1, \tag{E.103}$$

$$\psi_{j+kM_\eta} = \left(\psi_{j-1} + \frac{3.6}{\sqrt{M_\eta}} \frac{1}{\sqrt{1-h_j^2}} \right) \mod 2\pi,$$
$$2 \le j \le M_\eta - 1, \quad \psi_1 = \psi_{M_\eta} = 0. \tag{E.104}$$

A quasi-isotropic microstructure is obtained by considering sufficiently large M *and* η. Accurate results may be obtained, in general, by choosing $M \approx 1000$ and $\eta \approx 10$.

Bibliography

[1] Allais, L., Bornert, M., Bretheau, T. & Caldemaison, D. (1994) Experimental characterization of the local strain field in a heterogeneous elastoplastic material. *Acta Metall. Mater.* **42**, 3865–3880.

[2] Aravas, N. & Ponte Castañeda, P. (2004) Numerical methods for porous metals with deformation-induced anisotropy. *Comput. Methods Appl. Mech. Engng.* **193**, 3767–3805.

[3] Babout, L., Maire, E., Buffière, J. Y. & Fougères, R. (2001) Characterization by X-ray computed tomography of decohesion, porosity growth and coalescence in model metal matrix composites. *Acta Mater.* **49**, 2055–2063.

[4] Babŭska, I. (1975) Technical note BN-821. Institute of Fluid Dynamics and Applied Mathematics, University of Maryland, College Park, Maryland.

[5] Bensoussan, A., Lions, J.-P. & Papanicolau, G. (1978) *Asymptotic analysis for periodic structures.* Studies in mathematics and its applications **5**, North-Holland Publishing Co., The Netherlands.

[6] Bergman, D. J. (1978) The dielectric constant of a composite material–a problem in classical physics. *Phys. Rep., Phys. Lett.* **43C**, 377–407.

[7] Bhattacharya, K. & Suquet, P. (2005) A model problem concerning recoverable strains in shape memory polycrystals. *Proc. R. Soc. Lond. A* **461**, 2797–2861.

[8] Bishop, J.F.W. (1955) Theory of tensile and compressive textures of face-centered cubic metals. *J. Mech. Phys. Solids* **3**, 130–142.

[9] Bishop, J.F.W. & Hill, R. (1951) A theory of the plastic distortion of a polycrystalline aggregate under combined stresses. *Phil. Mag.* **42**, 414–427.

[10] Bobeth, M. & Diener, G. (1986) Field fluctuations in multicomponent mixtures. *J. Mech. Phys. Solids* **34**, 1–17.

[11] Bobeth, M. & Diener, G. (1987) Static elastic and thermoelastic field fluctuations in multiphase composites. *J. Mech. Phys. Solids* **35**, 37–149.

[12] Bornert, M. (1996) Morphological effects at the local scale in two-phase materials. In: Pineau, A., Zaoui, A. (Eds.), Micromechanics of plasticity and damage of multiphase materials. Kluwer Academic Publishers, Dordrecht, 27–34.

[13] Bornert, M., Hervé E., Stolz C. & Zaoui A. (1994) Self-consistent approaches and strain heterogeneities in two-phase elastoplastic materials. *App. Mech. Rev.* **47**(1), 66–76.

[14] Bornert, M., Masson, R., Ponte Castañeda, P., Zaoui, A. (2001) Second-order estimates for the effective behaviour of viscoplastic polycrystalline materials. *J. Mech. Phys. Solids* **49**, 2737–2764.

[15] Borwein, J. M., Lewis, A. S. (2000) *Convex Analysis and Nonlinear Optimization*. Springer-Verlag, New York.

[16] Bouchitte, G. & Suquet, P. (1991) Homogenization, plasticity and yield design. In Maso, G. D. & Dell'Antonio, G. (eds), *Composite Media and Homogenization Theory*, 107–133. Birkhauser, Boston.

[17] Brenner, R., Castelnau O. & Badea L. (2004) Mechanical field fluctuations in polycrystals estimated by homogenization techniques. *Proc. R. Soc. Lond. A* **460**, 3589–3612.

[18] Briottet, L., Gilormini, P. & Montheillet, F. (1999) Approximate analytical equations for the deformation of an inclusion in a viscoplastic matrix. *Acta Mechanica* **134**, 217–234.

[19] Bruggeman, D. A. G. (1935) Berechnung verschiedener physikalischer Konstanten von heterogenen Substanzen. I. Dielektrizitatskonstanten und Leitfahigkeiten der Mischkorper aus isotropen Substanzen. *Ann. Phys.* **24**, 636–679.

[20] Budiansky, B. (1965) On the elastic moduli of some heterogeneous materials. *J. Mech. Phys. Solids* **13**, 223–227.

[21] Budiansky, B., Hutchinson, J. W. & Slutsky, S. (1982) Void growth and collapse in viscous solids. In: H. G. Hopkins & M. J. Sewell (Eds.), *Mechanics of Solids*, Pergamon Press, Oxford, 13–45.

[22] Buryachenko, V. A. & Kreher, W. S. (1995) Internal residual stresses in heterogeneous solids – A statistical theory for particulate composites. *J. Mech. Phys. Solids* **43**, 1105–1125.

[23] Castelnau, O., Brenner, R. & Lebensohn, R. A. (2006) The effect of strain heterogeneity on the work hardening of polycrystals predicted by mean-field approaches. *Acta Mater.* **54**, 2745–2756.

[24] Castelnau, O., Duval, P., Lebensohn, R. A. & Canova, G. R. (1996) Viscoplastic modeling of texture development in polycrystalline ice with a self-consistent approach: comparison with bound estimates. *J. Geophys. Res.* **101**, 13851–13867.

[25] Castelnau, O., Canova, G. R., Lebensohn, R. A. & Duval, P. (1997) Modelling viscoplastic behavior of anisotropic polycrystalline ice with a self-consistent approach. *Acta Mater.* **45**, 4823–4834.

[26] Chaboche, J., Kanouté, P. & Ross, A. (2005) On the capabilities of mean-field approaches for the description of plasticity in metal matrix composites. *Int. J. Plasticity* **21**, 1409–1434.

[27] Cheng, H. & Torquato, S. (1997) Electric-field fluctuations in random dielectric composites. *Phys. Rev. B* **56**, 8060–8068.

[28] Cule, D. & Torquato, S. (1998) Electric-field distribution in composite media. *Phys. Rev. B* **58**, R11 829–832.

[29] Danas, K., Idiart, M. I. & Ponte Castañeda, P. (2006) Viscoplastic behavior of isotropic, porous materials. In preparation.

[30] Dawson, P. R. & Marin, E. B. (1998) Computational mechanics for metal deformation processes using polycrystal plasticity. *Adv. Appl. Mech.* **34**, 77–169.

[31] Dawson, P. R. & Wenk, H.-R. (2000) Texturing of the upper mantle during convection. *Phil. Mag.* A **80**, 573–598.

[32] De Giorgi, E. (1975) Sulla convergenza di alcune successioni di integrali del tipo dell'area. *Rend. Mat.* **8**, 277–294.

[33] deBotton, G. (2005) Transversely isotropic sequentially laminated composites in finite elasticity. *J. Mech. Phys. Solids* **53**, 1334–1361.

[34] deBotton, G. & Hariton, I. (2002) High-rank nonlinear sequentially laminated composites and their possible tendency towards isotropic behavior. *J. Mech. Phys. Solids* **50**, 2577–2595.

[35] deBotton, G. & Ponte Castañeda, P. (1992) On the ductility of laminated materials. *Int. J. Solids Struct.* **29**, 2329–2353.

[36] deBotton, G. & Ponte Castañeda, P. (1993) Elastoplastic constitutive relations for fiber-reinforced solids. *Int. J. Solids Struct.* **30**, 1865–1890.

[37] deBotton, G. & Ponte Castañeda, P. (1995) Variational estimates for the creep behavior of polycrystals. *Proc. R. Soc. Lond. A* **448**, 121–142.

[38] Dendievel, R., Bonnet, G. & Willis, J.R. (1991) Bounds for the creep behaviour of polycrystalline materials. In: Dvorak, G.J. (Ed.), Inelastic Deformation of Composite Materials. Springer-Verlag, New York, 175–192.

[39] Doghri, I. & Ouaar, A. (2003) Homogenization of two-phase elasto-plastic composite materials and structures. Study of tangent operators, cyclic plasticity and numerical algorithms. *Int. J. Solids Struct.* **40**, 1681–1712.

[40] Doumalin, P., Bornert, M. & Crépin, J. (2003) Characterisation of the strain distribution in heterogeneous materials. *Mécanique & Industries* **4**, 607–617.

[41] Drucker, D. C. (1966) The continuum theory of plasticity on the macroscale and the microscale. *J. Mater.* **1**, 873–910.

[42] Duva, J. M. & Hutchinson, J. W. (1984) Constitutive potentials for dilutely voided nonlinear materials. *Mech. Materials* **3**, 41–54.

[43] Dvorak, G. J. (1992) Transformation field analysis of inelastic composite materials. *Proc. R. Soc. London A* **437**, 31–327.

[44] Dvorak, G. & Bahei-El-Din, Y. (1979) Elastic-plastic behavior of fibrous composites. *J. Mech. Phys. Solids* **27** 51–72.

[45] Dvorak, G. & Madhava Rao, M. S. (1976) Axisymmetric plasticity theory of fibrous composites. *Int. J. Eng. Sci.* **14**, 361–373.

[46] Dvorak, G. & Zhang, J. (2001) Transformation field analysis of damage evolution in composite materials. *J. Mech. Phys. Solids* **49**, 2517–2541.

[47] Dvorak, G., Bahei-El-Din, Y. & Wafa, A. (1994) The modeling of inelastic composite materials with the transformation field analysis. *Model. Simulat. Mater. Sci. Eng.* **2** 571–586.

[48] Ekeland, I. & Temam, R. (1999) *Convex Analysis and Variational Problems*. SIAM, Philadelphia.

[49] Eshelby, J. D. (1957) The determination of the elastic field of an ellipsoidal inclusion, and related problems. *Proc. R. Soc. Lond. A* **241**, 376–396.

[50] Fish, J., Shek, K., Pandheeradi, M. & Shepard, M. (1997) Computational Plasticity for composite structures based on mathematical homogenization: theory and practice. *Comput. Methods Appl. Mech. Eng.* **148**, 53–73.

[51] Fleck, N. A. & Hutchinson, J. W. (1986) Void growth in shear. *Proc. R. Soc. Lond. A* **407**, 435–458.

[52] Garroni, A., Nesi V. & Ponsiglione M. (2001) Dielectric breakdown: optimal bounds. *Proc. R. Soc. Lond. A* **457**, 2317–2335.

[53] Gel'fand, I. M. & Shilov, G. E. (1964) *Generalized functions, Vol. I.* New York: Academic Press Inc.

[54] Gilormini, P. (1995) Insuffisance de l'extension classique du modèle autocohérent au comportement non linéaire. *C. R. Acad. Sci. Paris Ser. IIb* **320**, 115–122.

[55] Gilormini, P. (1996) A critical evaluation of various nonlinear extensions of the self-consistent model. In: Pineau, A., Zaoui, A. (Eds.), Micromechanics of plasticity and damage of multiphase materials. Kluwer Academic Publishers, Dordrecht, 67–74.

[56] Gilormini, P. & Michel, J.-C. (1998) Finite element solution of the problem of a spherical inhomogeneity in an infinite power-law viscous matrix. *Eur. J. Mech. A/Solids* **17**, 725–740.

[57] Gologanu, M., Leblond, J.-B. & Devaux, J. (1993) Approximate models for ductile metals containing non-spherical voids – Case of axisymmetric prolate ellipsoidal cavities. *J. Mech. Phys. Solids* **41**, 1723–1754.

[58] Gologanu, M., Leblond, J.-B. & Devaux, J. (1994) Approximate models for ductile metals containing non-spherical voids – Case of axisymmetric oblate ellipsoidal cavities. *J. Engng. Mater. Tech.* **116**, 290–297.

[59] González, C. & LLorca, J. (2000) A self-consistent approach to the elasto-plastic behaviour of two-phase materials including damage. *J. Mech. Phys. Solids* **48**, 675–692.

[60] Grédiac, M. (2004) The use of full-field measurement methods in composite material characterization: interest and limitations. *Composites A* **35**, 751–761.

[61] Gurson, A. L. (1977) Continuum theory of ductile rupture by void nucleation and growth: Part I – Yield criteria and flow rules for porous ductile media. *J. Engng. Mat. Tech.* **99**, 2–15.

[62] Hashin, Z., Rosen, B. W. (1964) The elastic moduli of fiber-reinforced materials. *J. App. Mech.* **31**, *Trans. ASME E* **86**, 223–232.

[63] Hashin, Z. & Shtrikman, S. (1962) On some variational principles in anisotropic and nonhomogeneous elasticity. *J. Mech. Phys. Solids* **10**, 335–342.

[64] Hashin, Z. & Shtrikman, S. (1963) A variational approach to the theory of the elastic behavior of multiphase materials. *J. Mech. Phys. Solids* **11**, 127–140.

[65] He, M. Y. (1990) On the flow and creep strength of power-law materials containing rigid reinforcements. *Mater. Res. Soc. Symp. Proc.* **194**, 15–22.

[66] Hershey, A. V. (1954) The elasticity of an isotropic aggregate of anisotropic cubic crystals. *ASME J. Appl. Mech.* **21**, 236–240.

[67] Hill, R. (1963) Elastic properties of reinforced solids: Some theoretical principles. *J. Mech. Phys. Solids* **11**, 357–372.

[68] Hill, R. (1965a) Continuum micro-mechanics of elastoplastic polycrystals. *J. Mech. Phys. Solids* **13**, 89–101.

[69] Hill R. (1965b) A self-consistent mechanics of composite materials. *J. Mech. Phys. Solids* **13**, 213–222.

[70] Hill, R. (1966) Generalized constitutive relations for incremental deformation of metal crystals by multislip. *J. Mech. Phys. Solids* **14**, 95–102.

[71] Hill R. (1967) The essential structure of constitutive laws for metal composites and polycrystals. *J. Mech. Phys. Solids* **15**, 79–95.

[72] Hu, G. (1996) A method of plasticity for general aligned spheroidal void of fiber-reinforced composites. *Int. J. Plasticity* **12**, 439–449.

[73] Hutchinson, J. W. (1976) Bounds and self-consistent estimates for creep of polycrystalline materials. *Proc. R. Soc. Lond. A* **348**, 101–127.

[74] Hutchinson, J. W. (1977) Creep and plasticity of hexagonal polycrystals as related to single crystal slip. *Metall. Trans. A* **8**, 1465–1469.

[75] Idiart, M. & Ponte Castañeda, P. (2003) Field fluctuations and macroscopic properties in nonlinear composites. *Int. J. Solids Struct.* **40**, 7015–7033.

[76] Idiart, M. & Ponte Castañeda, P. (2005) Second-order estimates for nonlinear isotropic composites with spherical pores and rigid particles. *C. R. Mecanique* **333**, 147–154.

[77] Idiart, M. I. & Ponte Castañeda P. (2006a) Field statistics in nonlinear composites. I. Theory. *Proc. R. Soc. Lond. A*, in press.

[78] Idiart, M. I. & Ponte Castañeda P. (2006b) Field statistics in nonlinear composites. II. Applications. *Proc. R. Soc. Lond. A*, in press.

[79] Idiart, M. I. & Ponte Castañeda, P. (2006c) Variational linear comparison bounds for nonlinear composites with anisotropic phases. I. General results. *Proc. R. Soc. Lond. A*, submitted for publication.

[80] Idiart, M. I. & Ponte Castañeda, P. (2006d) Variational linear comparison bounds for nonlinear composites with anisotropic phases. II. Crystalline materials. *Proc. R. Soc. Lond. A*, submitted for publication.

[81] Idiart, M. I., Danas, K. & Ponte Castañeda, P. (2006a) Second-order theory for nonlinear composites and application to isotropic constituents. *C. R. Mecanique* **334**, 575–581.

[82] Idiart, M. I., Moulinec H., Ponte Castañeda P. & Suquet P. (2006b) Macroscopic behavior and field fluctuations in viscoplastic composites: second-order estimates vs full-field simulations. *J. Mech. Phys. Solids* **54**, 1029–1063.

[83] Jikov, V. V., Kozlov, S. M. & Oleinik, O. A. (1991) *Homogenization of differential operators and integral functionals*. Springer, Berlin.

[84] Kailasam, M. & Ponte Castañeda, P. (1998) A general constitutive theory for linear and nonlinear particulate media with microstructure evolution. *J. Mech. Phys. Solids* **46**, 427–465.

[85] Kaminński, M. & Figiel, L. (2001) Effective elastoplastic properties of the periodic composites. *Comp. Mat. Sci.* **22**, 221–239.

[86] Kanit, T., Forest S., Galliet, I., Mounoury, V. & Jeulin, D. (2003) Determination of the size of the representative volume element for random composites: statistical and numerical approach. *Int. J. Solids Struct.* **40**, 3647–3679.

[87] Kocks, U.F., Canova, G.R. & Jonas, J.J. 1983 Yield vectors in f.c.c. crystals. *Acta metall.* **31**, 1243–1252.

[88] Kreher, W. (1990) Residual stresses and stored elastic energy of composites and polycrystals. *J. Mech. Phys. Solids* **38**, 115–128.

[89] Kreher, W. & Pompe, W. (1985) Field fluctuations in a heterogeneous elastic material—An information theory approach. *J. Mech. Phys. Solids* **33**, 419–445.

[90] Kröner, E. (1958) Berechnung der elastischen konstanten des vielkristalls aus den konstanten des einkristalls. *Z. Phys.* **151**, 504–518.

[91] Lagoudas, D., Gavazzi, A. C. & Nigam, H. (1991) Elastoplastic behavior of metal matrix composites based on incremental plasticity and the Mori-Tanaka averaging scheme. *Comp. Mech.* **8**, 193–203.

[92] Lahellec, N. & Suquet, P. (2003) Composites non linéaires à deux potentiels: estimations affine et du second-ordre. In: Potier-Ferry, M., Bonnet, M., Bignonnet, A. (Eds.), 6ème Colloque National en Calcul des Structures. Tome 3. CSMA, 49–56.

[93] Lahellec, N. & Suquet, P. (2004) Nonlinear composites: a linearization procedure, exact to second-order in the contrast and for which the strain-energy and affine formulations coincide, *C. R. Mecanique* **332**, 693–700.

[94] Lahellec, N. & Suquet, P. (2006) Effective behavior of linear viscoelastic composites: a time-integration approach. *Int. J. Solids Struct.*, in press.

[95] Laws, N. (1973) On the thermostatics of composite materials. *J. Mech. Phys. Solids* **21**, 9–17.

[96] Lee, B. J. & Mear, M. E. (1992) Effective properties of power-law solids containing elliptical inhomogeneities. Part I: Rigid inclusions. *Mech. Mater.* **13**, 313–335.

[97] Lee, B. J. & Mear, M. E. (1992) Effective properties of power-law solids containing elliptical inhomogeneities. Part II: Voids. *Mech. Mater.* **13**, 337–356.

[98] Lebensohn, R. & Tomé, C. N. (1993) A self-consistent anisotropic approach for the simulation of plastic deformation and texture development of polycrystals: application to zirconium alloys. *Acta Metall. Mater.* **41**, 2611–2624.

[99] Lebensohn, R. A., Liu, Y. & Ponte Castañeda, P. (2004a) Macroscopic properties and field fluctuations in model power-law polycrystals: full-field solutions versus self-consistent estimates. *Proc. R. Soc. Lond. A* **460**, 1381–1405.

[100] Lebensohn, R. A., Liu, Y. & Ponte Castañeda, P. (2004b) On the accuracy of the self-consistent approximation for polycrystals: Comparison with full-field numerical simulations. *Acta Mat.* **52**, 5347–5361.

[101] Leblond, J. B., Perrin, G. & Suquet, P. (1994) Exact results and approximate models for porous viscoplastic solids. *Int. J. Plasticity* **10**, 213–235.

[102] Letouzé, N., Brenner, R., Castelnau, O., Béchade, J. L. & Mathon, M. H. (2002) Residual strain distribution in Zircaloy-4 measured by neutron diffraction and estimated by homogenization techniques. *Scripta Mater.* **47**, 595–599.

[103] Levin, V. M. (1967) Thermal expansion coefficients of heterogeneous materials. *Mekh. Tverd. Tela* **2**, 83–94.

[104] Liu, Y. & Ponte Castañeda, P. (2004a) Second-order theory for the effective behavior and field fluctuations in viscoplastic polycrystals. *J. Mech. Phys. Solids* **52**, 467–495.

[105] Liu, Y. & Ponte Castañeda, P. (2004b) Homogenization estimates for the average behavior and field fluctuations in cubic and hexagonal viscoplastic polycrystals. *J. Mech. Phys. Solids* **52** 1175–1211.

[106] Hutchings, M. T., Withers, P. J., Holden, T. M. & Lorentzen, T. (2005) Introduction to the characterization of residual stress by neutron diffraction. Taylor & Francis, U.S.A.

[107] Maire, E., Bordreuil, C., Babout, L. & Boyer, J. C. (2005) Damage initiation and growth in metals. Comparison between modelling and tomography experiments. *J. Mech. Phys. Solids* **53** 2411–2434.

[108] Mandel, J. (1965) Généralisation de la théorie de plasticité de W. T. Koiter. *Int. J. Solids Struct.* **1**, 273–295.

[109] Marcellini, P. (1978) Periodic solutions and homogenization of non linear variational problems. *Ann. Mat. Pura Appl.* **117**, 139–152.

[110] Masson, R., Bornert, M., Suquet, P. & Zaoui, A. (2000) An affine formulation for the prediction of the effective properties of nonlinear composites and polycrystals *J. Mech. Phys. Solids* **48**, 1203–1227.

[111] Michel, J. & Suquet, P. (2003) Nonuniform transformation field analysis. *Int. J. Solids Struct.* **40**, 6937–6955.

[112] Michel, J., Moulinec, H. & Suquet, P. (2001) A computational scheme for linear and non-linear composites with arbitrarily phase contrast. *Int. J. Numer. Meth. Engng.* **52**, 139-160.

[113] Milton, G. W. (2002) *The Theory of Composites*, Cambridge University Press.

[114] Moulinec, H. & Suquet, P. (1994) A fast numerical method for computing the linear and nonlinear properties of composites. *C. R. Acad. Sci. Paris II* **318**, 1417–1423.

[115] Moulinec, H. & Suquet, P. (1998) A numerical method for computing the overall response of nonlinear composites with complex microstructure. *Comp. Meth. Appl. Mech. Engng.* **157**, 69–94.

[116] Moulinec, H. & Suquet, P. (2003) Intraphase strain heterogeneity in nonlinear composites: a computational approach. *Eur. J. Mech. A* **22**, 751–770.

[117] Moulinec, H. & Suquet, P. (2004) Homogenization for nonlinear composites in the light of numerical simulations. In: Ponte Castañeda, P., et al. (eds.), Nonlinear Homogenization and its Applications to Composites, Polycrystals and Smart Materials. Kluwer Academic Publishers, The Netherlands, pp. 193–223.

[118] Nebozhyn, M. V. & Ponte Castañeda (1999) The second-order procedure: exact vs. approximate results for isotropic, two-phase composites. *J. Mech. Phys. Solids* **47**, 2171–2185.

[119] Nemat-Nasser, S. & Hori, M. (1993) Micromechanics: overall properties of heterogeneous materials. North-Holland Elsevier.

[120] Nemat-Nasser, S. & Obata, M. (1986) Rate-dependent, finite elasto-plastic deformation of polycrystals. *Proc. R. Soc. Lond. A* **407**, 343–375.

[121] Nemat-Nasser, S., Iwakuma, T. & Hejazi, M. (1982) On composites with periodic micrustructure. *Mech. Materials* **1**, 239–267.

[122] Olson, T. (1994) Improvements on Taylor's upper bound for rigid-plastic bodies. *Mater. Sci. Engrg. A* **175**, 15–20.

[123] Parton, V.Z. & Buryachenko, V.A. (1990) Stress fluctuations in elastic composites. *Sov. Phys. Dokl.* **35**, 191–193.

[124] Pastor, J. & Ponte Castañeda, P. (2002) Yield Criteria for porous media in plane strain: second-order estimates versus numerical results. *C. R. Mechanique* **330**, 741–747.

[125] Pellegrini, Y.-P. (2000) Field distributions and effective-medium approximation for weakly nonlinear media. *Phys. Rev. B* **61**, 134–211.

[126] Pellegrini, Y.-P. (2001) Self-consistent effective medium approximation for strongly nonlinear media. *Phys. Rev. B* **61**, 9365–9372.

[127] Pettermann, H., Plankensteiner, A., Böhm, H. & Rammerstorfer, F. (1999) A thermo-elasto-plastic constitutive law for inhomogeneous materials based on an incremental Mori-Tanaka approach. *Comp. Struct.* **71**, 197–214.

[128] Ponte Castañeda, P. (1991) The effective mechanical properties of nonlinear isotropic composites. *J. Mech. Phys. Solids* **39**, 45–71.

[129] Ponte Castañeda, P. (1992a) New variational principles in plasticity and their application to composite materials. *J. Mech. Phys. Solids* **40**, 1757–1788.

[130] Ponte Castañeda, P. (1992b) Bounds and estimates for the properties of nonlinear heterogeneous systems. *Phil. Trans. R. Soc. Lond. A* **340**, 531–567.

[131] Ponte Castañeda, P. (1996) Exact second-order estimates for the effective mechanical properties of nonlinear composite materials. *J. Mech. Phys. Solids* **44**, 827–862.

[132] Ponte Castañeda, P. (2001) Second-order theory for nonlinear composite dielectrics incorporating field fluctuations. *Phys. Rev. B* **64** 214205.

[133] Ponte Castañeda, P. (2002a) Second-order homogenization estimates for nonlinear composites incorporating field fluctuations: I–Theory. *J. Mech. Phys. Solids* **50**, 737–757.

[134] Ponte Castañeda, P. (2002b) Second-order homogenization estimates for nonlinear composites incorporating field fluctuations: II–Applications. *J. Mech. Phys. Solids* **50**, 759–782.

[135] Ponte Castañeda, P. & Nebozhyn, M. V. (1997) Variational estimates of the self-consistent type for the effective behaviour of some model nonlinear polycrystals. *Proc. R. Soc. Lond. A* **453**, 2715–2724.

[136] Ponte Castañeda, P. & Suquet, P. (1995) On the effective mechanical behavior of weakly inhomogeneous nonlinear materials. *Eur. J. Mech. A/Solids* **2**, 205–236.

[137] Ponte Castañeda, P. & Suquet, P. (1998) Nonlinear composites. *Adv. Appl. Mech.* **34**, 171–302.

[138] Ponte Castañeda, P. & Suquet, P. (2001) Nonlinear composites and microstructure evolution. In: Aref, H., Phillips, J. W. (Eds.), *Proceedings of the 20th International Congress of Theoretical and Applied Mechanics* (ICTAM 2000). Kluwer Academic Publishers, Dordrecht, The Netherlands, 253-273.

[139] Ponte Castañeda, P. & Willis, J. R. (1988) On the overall properties of nonlinearly viscous composites. *Proc. R. Soc. Lond. A* **416**, 217–244.

[140] Ponte Castañeda, P. & Willis, J. R. (1995) The effect of spatial distribution on the effective behavior of composite materials and cracked media. *J. Mech. Phys. Solids* **43**, 1919–1951.

[141] Ponte Castañeda, P. & Willis, J. R. (1999) Variational second-order estimates for nonlinear composites. *Proc. R. Soc. London* **455**, 1799–1811.

[142] Ponte Castañeda, P. & Zaidman, M. (1994) Constitutive models for porous materials with evolving microstructure. *J. Mech. Phys. Solids* **42**, 1459–1497.

[143] Rekik, A., Bornert, M., Auslender, F. & Zaoui, A. (2005) A methodology for an accurate evaluation of the linearization procedures in nonlinear mean field homogenization. *C. R. Mecanique* **333**, 789–795.

[144] Reuss, A. (1929) Berechnung der Fliessgrenze von Mischkristallen auf Grund der Plastizitätsbedingung für Einkristalle. *Z. Angew. Math. Mech.* **9**, 49–58.

[145] Rockafellar, T. (1970) *Convex Analysis*. Princeton University Press, Princeton.

[146] Rosen, B. W. & Hashin, Z. (1970) Effective thermal expansion coefficients and specific heats of composite materials. *Int. J. Engng. Sci.* **8**, 157–173.

[147] Saff, E. B. & Kuijlaars, A. B. J. (1997) Distributing many points on a sphere. *The mathematical intelligencer* **19**, 5–11.

[148] Sanchez-Palencia, E. (1970) Solutions périodiques par rapport aux variables d'espace et applications. *C. R. Acad. Sc. Paris* **271**, 1129–1132.

[149] Schiesser, W. E. (1991) *The Numerical Method of Lines: integration of partial differential equations*. Academic Press, U.S.A.

[150] Storn R. & Price K. (1997) Differential evolution – A simple and efficient heuristic for global optimization over continuous spaces. *J. Global Optimization* **11**, 341–359.

[151] Suquet, P. (1981) Sur les équations de la plasticité: existence et régularité des solutions. *J. de Mécanique* **20**, 3–39.

[152] Suquet, P. (1983) Analyse limite et homogénéisation. *C. R. Acad. Sc. Paris II* **296**, 1355–1358.

[153] Suquet, P. (1990) A simplified method for the prediction of homogenized elastic properties of composites with periodic structure. *C.R. Acad. Sci. Paris II* **311**, 769–774.

[154] Suquet, P. (1993) Overall potentials and extremal surfaces of power law or ideally plastic materials. *J. Mech. Phys. Solids* **41**, 981–1002.

[155] Suquet, P. (1995) Overall properties of nonlinear composites: a modified secant moduli theory and its link with Ponte Castañeda's nonlinear variational procedure. *C.R. Acad. Sci. Paris II* **320**, 563–571.

[156] Suquet, P. (1996) Overall properties of nonlinear composites. In: Pineau, A., Zaoui, A. (Eds.), Micromechanics of plasticity and damage of multiphase materials. Kluwer Academic Publishers, Dordrecht, 149–156.

[157] Suquet, P. (1997) Effective properties of nonlinear composites. In: Suquet, P. (Ed.), Continuum Micromechanics. In: *CISM Lecture Notes*, vol. 377. Springer Verlag, New York, 197–264.

[158] Suquet, P. (2005) On the effect of small fluctuations in the volume fraction of constituents on the effective properties of composites. *C. R. Mecanique* **333**, 219–226.

[159] Suquet, P. & Ponte Castañeda, P. (1993) Small-contrast perturbation expansions for the effective properties of nonlinear composites. *C. R. Acad. Sci. Paris II* **317**, 1515–1522.

[160] Taylor, G. I. (1938) Plastic strain in metals. *J. Inst. Metals* **62**, 307–324.

[161] Talbot, D. R. S. & Willis, J. R. (1985) Variational principles for inhomogeneous nonlinear media. *IMA J. Appl. Math.* **35**, 39–54.

[162] Talbot, D.R.S. & Willis, J.R. (1992) Some explicit bounds for the overall behavior of nonlinear composites. *Int. J. Solids Struct.* **29**, 1981–1987.

[163] Tomé, C. & Kocks, U. F. (1985) Yield surface of h.c.p. crystals. *Acta metall.* **33**, 603–621.

[164] Torquato, S. (2001) *Random Heterogeneous Materials.* New York: Springer.

[165] Van Tiel, J. (1984) *Convex Analysis.* Wiley, New York.

[166] Voigt, W. (1889) Ueber die Bezienhung zwischen den beiden Elasticitätsconstanten isotroper Körper. *Ann. Phys.* **38**, 573–587.

[167] Wenk, H.-R., Baumgardner, J. R., Lebensohn, R. A. & Tomé, C. N. (2000) A convection model to explain anisotropy of the inner core. *J. Geophys. Res.* **105**, 5663–5677.

[168] Willis, J. R. (1977) Bounds and self-consistent estimates for the overall moduli of anisotropic composites. *J. Mech. Phys. Solids* **25**, 185–202.

[169] Willis, J. R. (1978) Variational principles and bounds for the overall properties of composites. In *Continuum Models and Discrete Systems (CMDS 2)* (ed. J. Provan), pp 185–215. University of Waterloo Press.

[170] Willis, J. R. (1981) Variational and related methods for the overall properties of composites. *Adv. Appl. Mech.* **21**, 1–78.

[171] Willis, J. R. (1982) Elasticity theory of composites. *Mechanics of Solids*, The Rodney Hill 60th Anniversary Volume, Hopkins, H. G. and Sewell, M. J., eds., Pergamon Press, Oxford, 653–686.

[172] Willis, J. R. (1983) The overall elastic response of composite materials. *J. Appl. Mech.* **50**, 1202–1209.

[173] Willis, J. R. (1991) On methods for bounding the overall properties of nonlinear composites. *J. Mech. Phys. Solids* **39**, 73–86.

[174] Willis, J. R. (1992) On methods for bounding the overall properties of nonlinear composites: correction and addition. *J. Mech. Phys. Solids* **40**, 441–445.

[175] Willis, J. R. (1994) Upper and lower bounds for nonlinear composite behavior. *Mater. Sci. Engrg. A* **175**, 7–14.

[176] Willis, J. R (2000) The overall response of nonlinear composite media. *Eur. J. Mech. A/Solids* **19**, S165–S184.